

CRANFIELD INSTITUTE OF TECHNOLOGY

COLLEGE OF AERONAUTICS

Ph.D. THESIS

H. ALLAHYARI

Application of the Finite Element Method to the  
Post-Buckling Behaviour of Thin Plates  
Containing Imperfections

Supervisor:

A. Rothwell

February, 1978

## SUMMARY

A finite element program, applicable to the pre- and post-buckling behaviour of plates with imperfections, is developed. Suitable incremental stiffness matrices are generated for a plate element with four nodes and twenty degrees of freedom.

Preliminary work, together with a prototype program, is carried out on a simple strut in order to compare various nonlinear solution techniques, both incremental and iterative. The plate program is verified by large deflection calculations for a square plate under lateral pressure, and by comparison with theoretical buckling loads for a perfect plate, closely agreeing with previous theoretical work.

Experimental results in compression, both with and without an artificially introduced imperfection, are used to demonstrate real plate behaviour, and they enable a comparison to be made with computed results. Measurements of deflection are made by the Moire fringe technique, as well as by dial gauges.

The program is used to investigate the effect of buckling on the compressive and shear stiffness of plates with various degrees of imperfection, including the compressive stiffness of a square plate after buckling in shear.

#### ACKNOWLEDGEMENTS

The author wishes to express his gratitude to Mr. A. Rothwell without whose valuable guidance and suggestions this work would not have been possible. Thanks are also due to K. H. Allahyari for typing the manuscript.

## CONTENTS

1	INTRODUCTION	
1.1	NONLINEAR BEHAVIOUR	1
1.1:1	GEOMETRIC NONLINEARITY	1
1.1:2	MATERIAL NONLINEARITY	1
1.2	IMPERFECTION SENSITIVITY	2
1.3	POST-BUCKLING BEHAVIOUR OF PLATES	3
1.4	GENERAL METHODS OF ANALYSIS	3
1.5	CHOICE OF THE FINITE ELEMENT METHOD	4
2	SURVEY OF NONLINEAR METHODS	
2.1	MATERIAL NONLINEARITY	8
2.2	GEOMETRIC NONLINEARITY	9
2.3	"CLASS ONE" TECHNIQUES FOR GEOMETRIC NONLINEARITY	9
2.3:1	INCREMENTAL STIFFNESS PROCEDURE	9
2.3:2	PERTURBATION METHOD	11
2.3:3	INITIAL VALUE APPROACH	12
2.4	"CLASS TWO" TECHNIQUES FOR GEOMETRIC NONLINEARITY	13
2.4:1	ITERATIVE APPROACH	13
2.4:2	SELF CORRECTING FORMULATION	17
3	FINITE ELEMENT METHOD - TECHNIQUES	
3.1	INCREMENTAL PROCEDURE	19
3.2	ITERATIVE METHODS	20
3.2:1	NEWTON-RAPHSON METHOD	22
3.2:2	MODIFIED NEWTON-RAPHSON METHOD	22
3.3	MOVING AND FIXED COORDINATES	23
3.3:1	MOVING AXES	24
3.3:2	FIXED AXES	31
3.4	PROGRAM DEVELOPMENT	39
3.5	PROGRAM DESCRIPTION - MOVING COORDINATE SYSTEM - D67A	41
3.6	PROGRAM DESCRIPTION - FIXED COORDINATE SYSTEM - D67B	43



4	NUMERICAL COMPARISON OF TECHNIQUES	
4.1	USE OF A SIMPLE STRUT AS A MODEL	45
4.2	FINITE ELEMENT REPRESENTATION	49
4.3	COMPARISON BETWEEN ITERATIVE AND INCREMENTAL PROCEDURES	57
4.4	COMPUTER TIME AND ACCURACY	71
4.5	REMARKS AND RECOMMENDATIONS	79
5	FINITE ELEMENT METHOD - APPLICATION TO PLATE PROBLEMS	
5.1	PRE- AND POST-BUCKLING ANALYSIS OF PLATES	82
5.2	NONLINEAR THEORY	84
5.3	FORMULATION OF INCREMENTAL STIFFNESS EQUATION	87
5.4	ELASTIC STIFFNESS MATRIX	93
5.5	INCREMENTAL STIFFNESS MATRICES	97
5.6	THE GAUSS ELIMINATION SOLUTION	118
5.6:1	COMPUTER APPLICATION OF GAUSS ELIMINATION	120
5.7	FRONTAL SOLUTION	121
5.7:1	DESCRIPTION OF FRONTAL SOLUTION	123
5.8	PROGRAM DESCRIPTION - PLATE PROGRAM - D67C	129
5.8:1	DESCRIPTION OF THE SOLUTION ROUTINE	130
5.8:2	SUBROUTINE TRANSFM	133
5.8:3	SUBROUTINE NODFORCE	133
5.8:4	SUBROUTINE STRESS	134
5.8:5	SUBROUTINE ITER	134
6	USE OF PLATE PROGRAM - DEFLECTION	
6.1	INTRODUCTION	136
6.2	LARGE DEFORMATION OF PLATE UNDER LATERAL PRESSURE	138
6.3	DEFORMATION OF PLATE IN COMPRESSION	147
6.4	PERFECTLY FLAT PLATE UNDER COMPRESSION	158
7	USE OF PLATE PROGRAM - STIFFNESS	
7.1	POST-BUCKLED STIFFNESS	163
7.2	PURE COMPRESSION	164

7.3	PURE SHEAR	168
7.4	CHANGE OF MODE SHAPE IN PURE SHEAR	175
7.5	EFFECT OF SHEAR BUCKLING ON COMPRESSIVE STIFFNESS	188
8	THE EXPERIMENTAL PROGRAMME	
8.1	PLATE EXPERIMENT	193
8.2	TEST SPECIMEN	194
8.3	TEST INSTRUMENTATION	195
8.4	THE GRID-SHADOW MOIRE TECHNIQUE	196
8.5	EXPERIMENTAL DESCRIPTION OF THE GRID-SHADOW TECHNIQUE	198
8.6	DESCRIPTION AND OBSERVATION OF TESTS	199
8.7	EXPERIMENTAL RESULTS	201
9	CONCLUSION AND RECOMMENDATION	
9.1	CONCLUSION	233
9.2	RECOMMENDATIONS FOR FURTHER WORK	235
	References	237

APPENDIX A	LISTING OF PROGRAMS	
A-1	NOTATION - PROGRAM D67A AND D67B	246
A-2	INPUT DATA	273
A-3	INPUT DATA PREPARATION	313
APPENDIX B	EXPERIMENTAL RECORD	330
APPENDIX C	DESIGN OF SQUARE TUBE	337

## FIGURES

- 2-1 Demonstration of Newton-Raphson Method
- 2-2 Demonstration of Modified Newton-Raphson Method
- 3-1 Strain Displacement of Beam
- 3-2 Strut Displacements
- 3-3 Distortion of Beam Element
- 3-4 Deformed and Undeformed Position of a Beam
- 4-1 Simple Strut - Convergence of Different Number of Elements
- 4-2 Simple Strut - Comparison of Fixed and Moving Coordinate Systems - Incremental Procedure
- 4-3 Simple Strut - Comparison of Fixed and Moving Coordinate Systems - Incremental with Modified Newton-Raphson Procedure
- 4-4 Simple Strut - Southwell Plot - Moving Coordinate System - Incremental Procedure
- 4-5 Simple Strut - Southwell Plot - Moving Coordinate System - Modified Newton-Raphson Procedure
- 4-6 Simple Strut - Southwell Plot - Fixed Coordinate System - Incremental Procedure
- 4-7 Simple Strut - Southwell Plot - Fixed Coordinate System - Modified Newton-Raphson Procedure
- 4-8 Simple Strut - Comparison of Different Methods with Respect to Computer Time
- 4-9 Simple Strut - Comparison of Different Number of Load Increments
- 4-10 Simple Strut - Error with Respect to Number of Increments at 50%  $P_{cr}$
- 4-11 Simple Strut - Error with Respect to Number of Increments at 70%  $P_{cr}$
- 4-12 Simple Strut - Error with Respect to Number of Increments at 75%  $P_{cr}$

- 4-13 Simple Strut - Improvement on Number of Iterations at 50%  $P_{cr}$
- 4-14 Simple Strut - Improvement on Number of Iterations at 70%  $P_{cr}$
- 4-15 Simple Strut - Improvement on Number of Iterations at 75%  $P_{cr}$
- 4-16 Simple Strut - Comparison of Purely Incremental with Modified Newton-Raphson Procedure for Constant Computer Time
- 5-1 Plate Element
- 5-2 Banded Coefficient Matrix in Frontal Solution
- 5-3 Demonstration of Assembled Stiffness Bandwidth
- 5-4 Demonstration of Frontal Solution Procedure
- 5-5 Demonstration of Frontal Solution Procedure
- 5-6 Demonstration of Frontal Solution Procedure
- 6-1 Demonstration of Plate Behaviour under Pressure
- 6-2 Demonstration of Plate Behaviour under Compression
- 6-3 Plate Program - Convergence to Exact Solution Under Pressure
- 6-4 Plate Program - Convergence to Exact Solution Under Concentrated Load
- 6-5 Plate Program - Deflection Convergence due to Pressure
- 6-6 Normal Pressure Distribution
- 6-7 Plate Program - Central Deflection due to Pressure
- 6-8 Plate Program - Central Stress due to Pressure
- 6-9 Plate Program - Deflection Convergence due to Compression
- 6-10 Plate Program - Southwell Plot - Compressive Load
- 6-11 Plate Program - Central Deflection due to Compression
- 6-12 Plate Program - Central Deflection Due to Compression  
Compression - Unloaded, Edges Free to Wave



- 6-13 Plate Program - Central Deflection Due to  
Compression - Unloaded Edges free to Wave Laterally
- 6-14 Plate Program - Central Deflection Due to  
Compression - Unloaded Edges Not Free to Move  
Laterally
- 6-15 Plate Program - Transverse Stress
- 6-16 Plate Program - Longitudinal Stress
- 6-17 Plate Program - Central Deflection of Perfect  
Plate - Unloaded Edges Free to Wave
- 6-18 Plate Program - Central Deflection of Perfect  
Plate - Unloaded Edges Free to Move Laterally
- 7-1 Plate Program - Compressive Stiffness - Unloaded  
Edges Free to Wave
- 7-2 Plate Program - Compressive Stiffness - Unloaded  
Edges Free to Move Laterally
- 7-3 Plate Program - Coupling Demonstration for Case  
(a), and Case (b)
- 7-4 Plate Program - Shear Tangent Stiffness -  
B. C. Case (a)
- 7-5 Plate Program - Shear Secant Stiffness - B. C.  
Case (a)
- 7-6 Plate Program - Shear Tangent Stiffness - B. C.  
Case (b)
- 7-7 Plate Program - Shear Secant Stiffness - B.C.  
Case (b)
- 7-8 Plate Program - Southwell Plot - Shear Load
- 7-9 Plate Program - Center Deflection Due to Shear  
Load - B. C. Case (a)
- 7-10 Plate Program - Center Deflection Due to Shear  
Load - B. C. Case (b)
- 7-11 Plate Program - Deflection Behaviour Due to Shear  
through Load  
7-13
- 7-14 Plate Program - Contour Plot of Plate Deflection  
through Due to Shear Load  
7-19
- 7-20 Plate Program - Compressive Stiffness Behaviour  
Due to Shear Load

8-1	Buckling Coefficient With Respect to Ratio of Flange to Web
8-2	Buckling Coefficient with Respect to Wave Length
8-3	Buckling Coefficient With Respect to Wave Length
8-4	Basic Dimension of Test Specimen
8-5	Stress - Strain Curve - Tension
8-6	Stress - Strain Curve - Compression
8-7	Initial Imperfection - Test Specimen A
8-8	Initial Imperfection - Test Specimen B
8-9	Reference Points in Finite Element Method
8-10 through 8-21	Fringe Pattern Specimen A
8-22	Deflection Behaviour from Fringe Pattern - Specimen A
8-23	Deflection Behaviour from Fringe Pattern - Specimen A
8-24	Deflection Behaviour by Dial Gauge Readings - Specimen A
8-25	Demonstration of Fringe Readings
8-26 through 8-30	Fringe Pattern - Specimen B
8-31	Deflection Behaviour by Dial Gauge Readings - Specimen B
8-32	Deflection Behaviour by Dial Gauge Readings - Specimen B - With Support Attachments
8-33	Deflection Behaviour by Dial Gauge Readings with Support Attachments - Specimen B
8-34	Computer Result of Experimental Test
8-35	Comparison of Computer Result with Experimental Result
9-1	Assembly of Test Specimen

A-1	Flow Chart - Master Segment - Strut
A-2	Flow Chart - Subroutine SOLV - Strut (Moving Coordinates)
A-3	Flow Chart - Subroutine SOLV - Strut (Fixed Coordinates)
A-4	Flow Chart - Master Segment - Plate
A-5	Flow Chart - Subroutine TRANSFM
A-6	Flow Chart - Master Segment - Subroutine SOLV
A-7	Flow Chart - Master Segment - Subroutine ELIM
A-8	Flow Chart - Master Segment - Subroutine BCKSUB
A-9	Flow Chart - Master Segment - Subroutine ITER
A-10	Plate Idealization
A	
A-11	Plate Idealization
B-1	Square Box - Test Specimen
B-2	Assembly of Square Box - Test Specimen
C-1	Channel Strut - Test Specimen
C-2	Channel Section Support Assembly
C-3	Channel Section Support Detail

## NOTATION

$a$	=	Length of rectangular plate finite element
$A$	=	Area of the beam
$b$	=	Width of rectangular plate finite element
$D$	=	Flexural rigidity of plate
$e$	=	Linear expression for strain
$E$	=	Modulus of elasticity
$I$	=	Moment of inertia of the beam
$[k]$	=	Element stiffness matrix
$[K]$	=	Assembled element stiffness matrix
$[k_G]$	=	Geometric stiffness matrix
$L$	=	Length of the beam, Length of the square tube
$[n_0], [n_1], [n_2]$	=	Zero-, first-, second-order element stiffness matrices, respectively
$\{p\}$	=	Vector of element nodal loads
$P$	=	Applied axial load
$P_{cr}$	=	Critical load
$\{q\}$	=	Vector of net nodal displacements
$\{q_0\}$	=	Vector of element initial displacements
$Q$	=	Shear load
$\{\bar{Q}\}$	=	Normalized or scaled generalized force vector
$\{R\}$	=	Unbalanced loads
$t$	=	Plate thickness
$t'$	=	Equivalent thickness



$u, v, w$	= Displacements in $x, y$ , and $z$ directions, respectively
$U_L$	= Strain energy based on linear strain-displacement relations
$U_{NL}$	= Strain energy contribution due to the inclusion of nonlinearities in the strain-displacement relations
$w$	= Net deflection of plate finite element
$w_0$	= Initial deflection of plate finite element
$W$	= Maximum net deflection of the whole beam or plate
$W_0$	= Maximum initial deflection of the whole beam or plate
$W_T$	= Total deflection
$\beta$	= Initial angle of deformation
$\gamma$	= Shear strain
$\Delta$	= Incremental operator
$\epsilon$	= Strain energy
$\theta$	= Net angle of deformation
$\lambda$	= Half wave length
$[\lambda]$	= Transformation matrix
$\nu$	= Poisson's ratio
$\rho$	= Radius of gyration of corrugated web about centroid axis
$\sigma$	= Axial stress
$\tau$	= Shear stress
$\phi$	= Total angle from global to local coordinate system
$\{ \}$ $[ \ ]$	= Column and row vectors, respectively
$[ \ ]$	= Rectangular matrix

# I N T R O D U C T I O N

## 1.1 NONLINEAR BEHAVIOUR

To deal successfully with nonlinear problems has long been the goal of the engineering analyst, for it is true to say that no structure ever built behaves linearly, and only a very few materials are truly elastic. The ever increasing precision with which we must predict structural response demands that we should account for nonlinearities in the structure's behaviour. Fundamental theory has been developed and directed toward such problems for a considerable period of time.

There are two sources of nonlinearity in structural problems:

- 1) Geometric nonlinearity - deformation large enough to significantly alter the geometry of the structure.
- 2) Material nonlinearity - material properties which cause nonlinear behaviour of the structure.

### 1.1:1 GEOMETRIC NONLINEARITY

Geometric nonlinearity results in two classes of problem that are well known to the structural engineer, the large deflection problem and that of structural stability. Problems falling within the category of large deflection need not have actual deflections which are in the usual sense large; in fact they can be (and often are) as small as those arising in a linear problem. The basic difficulty with geometric nonlinearity is that, since there are significant changes in geometry of the structure, the equations of equilibrium must be formulated for the deformed configuration, which is not known in advance.

### 1.1:2 MATERIAL NONLINEARITY

Material nonlinearity arises from a stress - strain relationship for the material which may be nonlinearly elastic, elasto-plastic, visco-elastic, or some other. Nonlinear problems which have been solved using the finite element procedure are frequently concerned with material nonlinearities, in particular elasto-plastic behaviour. Two general methods have been developed for the elasto-plastic analysis of structures:

- a) The initial strain method
- b) The tangent modulus method

The initial strain method (Ref. 1) treats plastic strains at each incremental load step as initial strains for the next load step.

The tangent modulus method, on the other hand, is based upon the incremental stress - strain laws of plasticity. In this method, plasticity effects are accounted for in the stiffness of the structure, which is updated at each load step.

## 1.2 IMPERFECTION SENSITIVITY

Van der Neut (Ref. 2) has studied the behaviour of thin-walled members under compressive load. He has shown that elastic columns made from thin plates are sometimes highly sensitive to the presence of geometrical imperfections. His study initially was with straight columns containing only local imperfections, but he also studied columns having both local and overall imperfections, and concluded that imperfection of the column axis appears to have only a minor effect on the load carrying capacity. The main reduction stems from initial waviness of the cross-section.

However, Van der Neut (Ref. 3) later re-examined the question of the way in which local and overall imperfections interact to reduce the carrying capacity of a column, and concluded that, in the region of maximum imperfection sensitivity, the effects of local and overall imperfections are comparable.

The effect of imperfections is to merge the pre- and post-buckled behaviour of the structure, so that buckling develops progressively before the theoretical critical load is reached. Thus the loss of stiffness associated, in particular, with local buckling occurs prematurely, causing in some cases a high degree of imperfection sensitivity and a significantly reduced load carrying capacity. The analysis of this loss of stiffness, or more generally the deformation of a plate containing imperfections, requires a large deflection analysis incorporating the geometric nonlinearity associated with buckling.



### 1.3 POST-BUCKLING BEHAVIOUR OF PLATES

Interest in the analysis of instability phenomena for complicated plate structures and shells has intensified recently, due in part to the development of finite element analysis procedures for such structures. It is well known that structures of this type collapse at load levels which are less than those predicted by linear instability theory, because of the role played by initial imperfections.

Koiter (Ref. 4) has presented a comprehensive, higher order theory describing the stability and immediate post-buckling behaviour of structures and the effect of imperfections. His work was extended by Thompson (Ref. 5) and Budiansky and Hutchinson (Ref. 6). The finite element method has been applied to the analysis of large displacement behaviour of structures by considering a higher order incremental theory. Higher order incremental equilibrium equations have also been applied to the large deflection behaviour of different types of structure in the post-buckling region (Ref. 7).

The nature of the post-buckling response of a structure under the influence of specified imperfections yields information on the sensitivity of the structure to jump from the initial state to an adjacent state, at loads below the critical load of the perfect structure. This phenomenon, originally investigated by von Karman and Tsien (Ref. 8) is described mathematically by Koiter (Ref. 4).

In a practical example, a long plate with simply-supported edges under axial compression, buckles principally in the central part of the plate, and an increasingly large proportion of the load is carried by the material close to the supported edges of the plate. Von Karman (Ref. 9) suggested (for aeroplane design) that an effective width of the buckled skin could be included as load carrying material at each stiffener. In a more general situation, it is necessary to define the in-plane stiffness of a plate both after buckling and (in the case of a plate containing imperfections) as pre-buckling deformation takes place.

### 1.4 GENERAL METHODS OF ANALYSIS

Essentially, the solution of a nonlinear problem is reduced to tracing a nonlinear algebraic solution of the differential equations. Accordingly, many different

schemes for solving the governing equations have undergone development. In the procedures developed in recent years, attention has been given primarily to those embodying geometric nonlinearities, for until about 1968, researchers had little choice of solution procedure to solve geometrically nonlinear problems. Before that time, only two solution procedures had been utilized:

- a) incremental stiffness procedure
- b) iteration or successive substitution procedure.

The development and use of these methods was a rather direct extension of linear analysis, and they evolved in a natural manner from the very simple step-by-step linear incremental technique. Recent years, however, have seen an abundance of procedures for attacking the nonlinear equilibrium equations. These include iteration combined with systematic relaxation, perturbation methods, Newton-Raphson procedures, self-correcting incremental forms, incremental procedures combined with Newton-Raphson iteration, initial value formulations, and self-correcting initial-value formulations. With this variety of solution procedures, naturally comes the question of which solution technique is best suited to a particular application. The answer to this question of course hinges upon many factors: the type of problem to be solved, the degree of nonlinearity involved, the accuracy desired, the familiarity of the investigator with nonlinear analysis, the ease of application to automatic computation, the computer time required for a solution, and so on.

## 1.5 CHOICE OF THE FINITE ELEMENT METHOD

The general problem in structural mechanics is that of finding the forces and displacements (or the stresses and strains) in a continuous system. In the finite element method, the system consists of a finite number of elements suitably chosen and joined at selected node points. Each element has a finite number of force and/or displacement parameters at the nodes. Stresses and strains within the element are defined by assumed functions of the nodal parameters. Relations between nodal forces and nodal displacements are obtained by applying a variational principle. Relations for the entire system are obtained by combining individual elements. The most common finite element formulations for an elastic structure are derived from the total



potential energy principle, using assumed displacement functions. Linear response, instability and large-displacement behaviour can all be analysed by such formulations if appropriate terms are included in the strain-displacement relations.

The simplicity and broad application of an organized matrix approach to structural analysis based upon the finite element idealization was made clear in an important paper by Turner, et al (Ref. 10) in 1956. As a consequence, much development took place to realize this potential. Stiffness matrices were sought for elements within diverse classes of structures, and analytical generalizations were proposed to extend the approach to the predictions of different types of behaviour.

Evolution of finite element technology within the theoretical framework of the assumed mode or Ritz approximate variational methods of continuum mechanics has led to a rational, unified approach to representations of finite element characteristics. Element matrices derived in conformity with this governing, theoretical framework are referred to as consistent. Since the structural design of a major portion of aerospace flight hardware components is governed by elastic stability requirements, their relevance to the realistic design situation has provided a strong motivation for the generalization of the powerful finite element analysis techniques to accommodate geometric nonlinearities. Accordingly, many research efforts have been devoted to this objective, and several alternative analyses procedures have emerged. Turner, Dill, et al, (Ref. 11) published the first paper directed towards geometrically nonlinear finite element analysis. Extension of this work was reported subsequently by Turner, Martin and Weikel (Ref. 12). The general approach followed was to introduce nonlinearity by finite grid point displacements.

Gallagher and Padlog (Ref. 13) presented an alternative approach based upon the introduction of nonlinearity from within the finite element model. Extension and application of this work were subsequently reported (Ref. 14).

Argyris (Ref. 15, 16) presented additional work along the lines of the two foregoing approaches, and Martin (Ref. 17) presented a useful review of the work during this period, attempting a clarification.

Considerable literature has since appeared which documents the implementation of finite element eigenvalue buckling analysis capability (Ref. 13, 18, 19).

The more ambitious objective of nonlinear behaviour has been pursued also (Ref. 20, 21). Understandably, linearized, incremental methods have found favour in matrix oriented analyses (Ref. 22, 23). Nonlinear models have provided the means for predicting post-buckling behaviour (Ref. 24, 25). However, the models employed for predicting critical loads and nonlinear behaviour have not experienced the standardization achieved for linear finite element analysis.]

In Reference (17), the finite element theory for geometrically nonlinear problems was established in terms of the Lagrangian strain tensor and the principle of virtual displacements. Theoretical developments since then have occurred along several paths. The development in (Ref. 17) retained quadratic terms in nodal displacements in the expression for the strain energy but discarded higher order terms. Retaining the quadratic terms led to the so-called initial stress (or geometric) stiffness matrix. Although this formulation permitted both large deflection and stability analyses to be undertaken, it left unanswered the question as to the possible importance of the discarded terms. Marcel (Ref. 26) presented an alternative development which retained these higher order terms. This led to a hierarchy of stiffness matrices which Marcel called the initial displacement stiffness matrices.

A second formulation due to Purdy and Przemieniecki (Ref. 27) showed that an alternative formulation was possible which also retained the higher order terms. This formulation leads to the same stiffness matrices as the earlier development based on the quadratic terms; however, an additional generalized load vector is introduced to account for the higher order terms in the strain energy. The choice of whether the higher order terms should be retained or not will obviously have a significant effect on computer programs and computer time.



SURVEY OF NONLINEAR  
METHODS

## 2.1 MATERIAL NONLINEARITY

Among the earlier applications of the finite element method to nonlinear problems were investigations concerned with inelastic behaviour. In 1963, a finite element analysis of a class of two-dimensional nonlinear problems was described by Wilson (Ref. 28) dealing with materially nonlinear structures. Subsequent applications of finite element techniques to problems of creep and elasto-plastic behaviour were published by Argyris, Kelsey, and Kamel (ref. 16), Swedlow and Yang (Ref.29).

More recent investigations have been made of the elasto-plastic problem. Two-dimensional problems were considered by Felippas (Ref. 30), Reyes and Decre (Ref. 31), Marcal and King (Ref. 32), Richard and Blacklock (Ref. 33).

Zienkiewics, Valliappan and King (Ref. 34), along with Marcal (Ref. 32), point out that two main approaches have been used successfully in analyzing elasto-plastic problems. One of these, the so-called "initial strain" approach, involves computing an increase in plastic strain during a load increment and then treating the plastic strain as an initial strain for which the stress distribution is adjusted. This approach fails in the case of ideal, perfectly plastic materials. The second approach is basically a "tangent stiffness" approach in the sense that incremental stiffness relations are derived from incremental stress-strain laws for the material. These stiffness matrices are modified after each load increment in the case of elasto-plastic, work hardening materials.

Zienkiewicz, Valliappan and King (Ref. 34) uses a third method for elasto-plastic problems, termed an "initial stress" approach, wherein total incremental stress-strain relations are used to correct the total value of stress at the end of each load increment.

Further applications of the finite element method to combined geometrically and materially nonlinear structures, and to the analysis of elasto-plastic behaviour of plates and shells, have been investigated. Finite element formulations of the problem of flexure of thin elasto-plastic plates were discussed in the papers of Swedlow and Yang (Ref. 29), Witmer and Kotanchik (Ref. 35), among others.

The paper by Armer, Pifko, and Levine (Ref. 36), which also considers geometrically nonlinear behaviour, points out the difficulties encountered in depicting progressive yielding through the thickness of plates and shells subjected to bending.

## 2.2 GEOMETRIC NONLINEARITY

Many researchers have applied finite element and finite difference methods to geometrically nonlinear problems. From all this work we can classify two solution procedures:

- "Class I"      Methods which are incremental and do not necessarily satisfy equilibrium.
- "Class II"     Methods which are self-correcting and tend to stay on the true equilibrium.

## 2.3 "CLASS ONE" TECHNIQUES FOR GEOMETRIC NONLINEARITY

### 2.3:1 INCREMENTAL STIFFNESS PROCEDURE

In Class I, (historically, the first finite element approach to solving geometrically nonlinear problems), the load is applied in small increments in order to make the structure respond linearly during each increment. Each increment of load produces increments of displacement and corresponding increments of stress. Of course, for each increment, the geometric stiffness matrix has to be taken into account because of the deformed geometry of the structure. It was natural to attempt to handle nonlinearities by calculating corrections to linear solutions. Consequently, most of the work on applications of the finite element method to nonlinear structural problems involve incremental procedures and are confined to problems involving infinitesimal strains.

Turner (Ref. 37) and Argyris (Ref. 38) discussed such incremental procedures as early as 1959, and in 1960 Green (Ref. 39) employed geometric stiffness matrices in an unpublished memorandum dealing with the instability of beam-columns. Similar work was reported by Ortega (Ref. 40).

Geometric stiffness matrices were also used to calculate large displacements of finite element models by Argyris (Ref. 9, Ref. 41) as presented in the first Dayton Conference on matrix methods in structural mechanics in 1965 (Ref. 42). Martin (Ref. 11) reviewed the work on geometrically nonlinear problems up to that time and presented geometric stiffness matrices for a number of structural elements. Martin's paper was published in 1966 along with his summary report on the subject (Ref. 43). General formula for computing geometric stiffness matrices were subsequently presented

by Oden (Ref. 44) and later by Przemieniecki (Ref. 42). Since 1965, numerous investigators have used incremental procedures and geometric stiffness matrices to study both stability and large displacements of complex structures. These include studies of stability of thin plates by Hartz (Ref. 45), Kapur and Hartz (Ref. 46), Anderson, Irons and Zienkiewicz (Ref. 47). Large deflections of plates by Murray and Wilson (Ref. 48, Ref. 49) are also chronicalled in journals.

The incremental approach is clearly popular. This is due to the ease with which the procedure may be applied. However, the procedure has a serious disadvantage in that no real estimate of the solution accuracy is known since, in general, equilibrium is not satisfied at a given load level. This is evidenced by the drifting of the solution from the true solution. Recourse must be made to solving repeatedly the same problem with successively smaller load increments until convergence of two successive solutions can be established. In addition, for structures requiring many degrees of freedom, the updating of the incremental stiffness matrix plus the inversion of the new coefficient matrix at each load step may become excessively time consuming.



## 2.3:2 PERTURBATION METHOD

In another "Class I" procedure, Thompson and Walker (Ref. 50) have applied the perturbation method to non-linear problems. In this procedure, the incremental displacements are expanded in a Taylor series with respect to some incremental load parameter and about some known or assumed equilibrium state. Equations are obtained in the form

$$\{q\}_{i+1} = \{q\}_i + \{\dot{\Delta}q\}_i \Delta \bar{P} + \frac{1}{2} \{\ddot{\Delta}q\}_i \Delta \bar{P}^2 + \dots \quad (2-1)$$

where the dot denotes the derivative with respect to the load parameter  $\bar{P}$ ,  $\{\dot{\Delta}q\}$ ,  $\{\ddot{\Delta}q\}$ , etc., are path derivatives and  $i$  denotes the load increment index. The terms in the Taylor series are obtained through the solution of several sets of the linear equations equal in number to the number of terms retained in the expansion. Once the displacements are obtained at a particular load value, the whole process is repeated to obtain the displacements at the next load value. The procedure may, of course, drift from the true solution since errors will tend to accumulate. The amount of drift is dependent upon the load-step size, and number of terms retained may cause the solution to become time consuming because of the number of evaluations of the path derivatives. This method is also limited to problems where nonlinearities are not too large.

A short review of this technique and its relation to finite element shell stability analysis was well introduced in the paper by Connor and Morin (Ref. 51). Connor and Morin applied the perturbation technique to obtain the nonlinear eigenvalue, i.e., buckling following nonlinear pre-buckling deformations, and also to trace the post-buckling equilibrium path. Lang and Hartz (Ref. 52) presented a matrix formulation for the perturbation of total potential energy and applied it to the analysis of initial post-buckling slope and imperfections sensitivity of flat plates subjected to inplane forces, and shallow arches. Further development of this method is described by Walker (Ref. 53).

### 2.3:3 INITIAL VALUE APPROACH

A final "Class I" procedure is the initial value formulation (Ref. 54). This approach again treats the displacements and loads as a function of some load parameter  $\bar{P}$ , such that  $\{q\} = \bar{P} \{\bar{q}\}$ . By differentiating the equilibrium equations with respect to  $P$ , a set of differential equations is obtained in the form

$$[K] \{dq/d\bar{P}\} = \{\bar{Q}\} \quad (2-2)$$

where  $[K]$  is a nonlinear stiffness matrix dependent upon displacement  $\{q\}$ , and  $\{\bar{Q}\}$  is a vector of scaled or normalized generalized forces. Values of  $\{\bar{Q}\}$  at any load  $\bar{P}$  can be obtained by numerical integration from a known initial displacement state. If the simple Euler method is used for integration, then the incremental approach is obtained. More accurate integration schemes such as the Runge-Kutta method or the Predictor-corrector method may be used to reduce the drifting effect which is so prominent with Euler integration.

## 2.4 "CLASS TWO" TECHNIQUES FOR GEOMETRIC NONLINEARITY

The following solution techniques may all be described as Class II type. The procedures make use of some method by which equilibrium is satisfied at any given point on the load displacement curve. These procedures are perhaps best described as self-correcting.

### 2.4:1 ITERATIVE APPROACH

The iterational approach to solving the governing nonlinear algebraic equations has been used by many investigators (Ref. 16, Ref. 55). This approach is relatively simple to apply. Starting with an initial estimate to the displacement solution, the nonlinear effects are estimated and a set of linearized equations is solved to obtain an improved solution. This solution is back substituted into the equations and the iteration continued until convergence is obtained. The success of the method depends to a large extent upon the accuracy of the initial estimate of the displacements. The load may be applied in increments and various extrapolation procedures utilized to obtain accurate estimates. Relaxation schemes (Ref. 22, Ref. 56) may be used to accelerate convergence. While the iterational method is extremely fast from a computational standpoint, it has a serious disadvantage in that it will converge only for moderately nonlinear problems.

The iterational approach for solving nonlinear problems to give very accurate results and quite rapid convergence for realistic initial estimates of the solution are classified as:

- a) Newton-Raphson Iteration
- b) Modified Newton-Raphson Iteration.

If we take the first-order Taylor series expansion at a Point A, (see Figure 2-1), we obtain

$$\{f(q_A + \Delta q_1)\} = \{f(q_A)\} + \{\Delta q_1\} \left[ \frac{\partial P}{\partial q} \right]_A \quad (2-3)$$

where  $\left[ \frac{\partial P}{\partial q} \right]_A$  is the slope of the curve at point A, the structure tangent stiffness  $[K]_A$ . Since  $\{f(q_A + \Delta q_1)\} = \{P_B\}$  and  $\{f(q_A)\} = \{P_A\}$ , therefore, we can write:

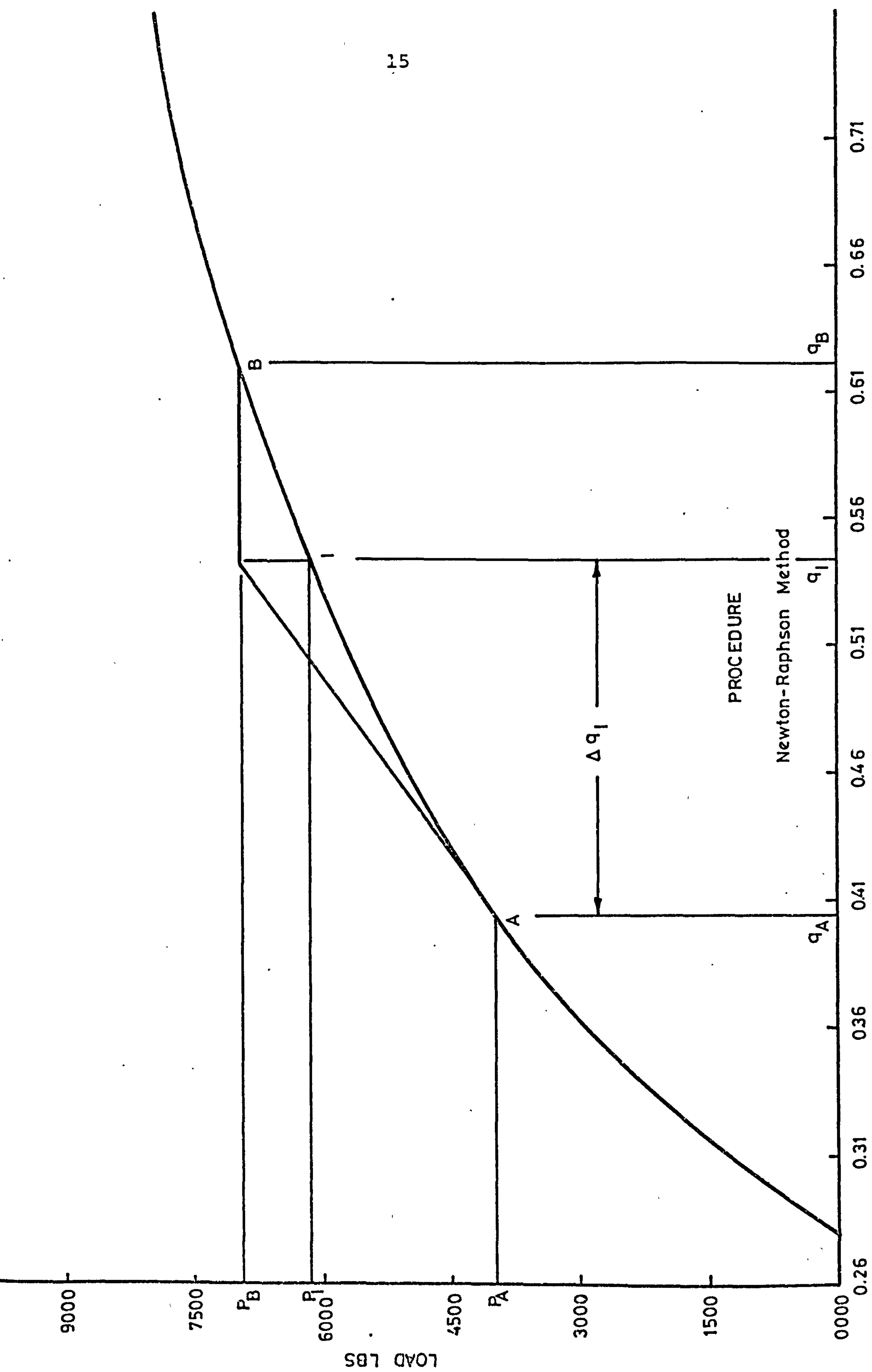
$$[K]_A \{\Delta q_1\} = \{P_B\} - \{P_A\} \quad (2-4)$$

where  $\{q_A + \Delta q_1\}$  is the new estimate of  $q_B$ , which, because the Taylor Series has been truncated, is not exact. In the next iteration, we have the unbalance forces of  $\{P_B\} - \{P_1\}$  with the new slope  $[K_1]$  as the tangent stiffness at Point 1.

By using the Modified Newton-Raphson method, the coefficient matrix is held constant for a number of iterations and then, after the rate of convergence has begun to deteriorate, the matrix is updated on the current displacement. The difference between these two methods is shown graphically. Figure (2-1) and Figure (2-2) are the result of the Newton-Raphson and the Modified Newton-Raphson computer runs. For one step of load, the characteristics of these two methods are demonstrated. These show that the Modified procedure took seven iterations whereas, for the same step load, the Newton-Raphson method took only two iterations to reach a certain accuracy of the solution. In the Modified method, the slope is retained at its value for the first solution (parallel lines). Obviously convergence is now much slower. Since for each iteration by the Newton-Raphson method, the coefficient matrix must be updated, which is time consuming, one might expect to take larger load increments, but it was found this could not be done for the Modified Newton-Raphson method, because of the danger of convergence (see Chapter 4).

Various extrapolation and relaxation procedures again can be incorporated into the iterational cycle to ensure and accelerate convergence.





PROCEDURE  
Newton-Raphson Method

FIGURE 2-1

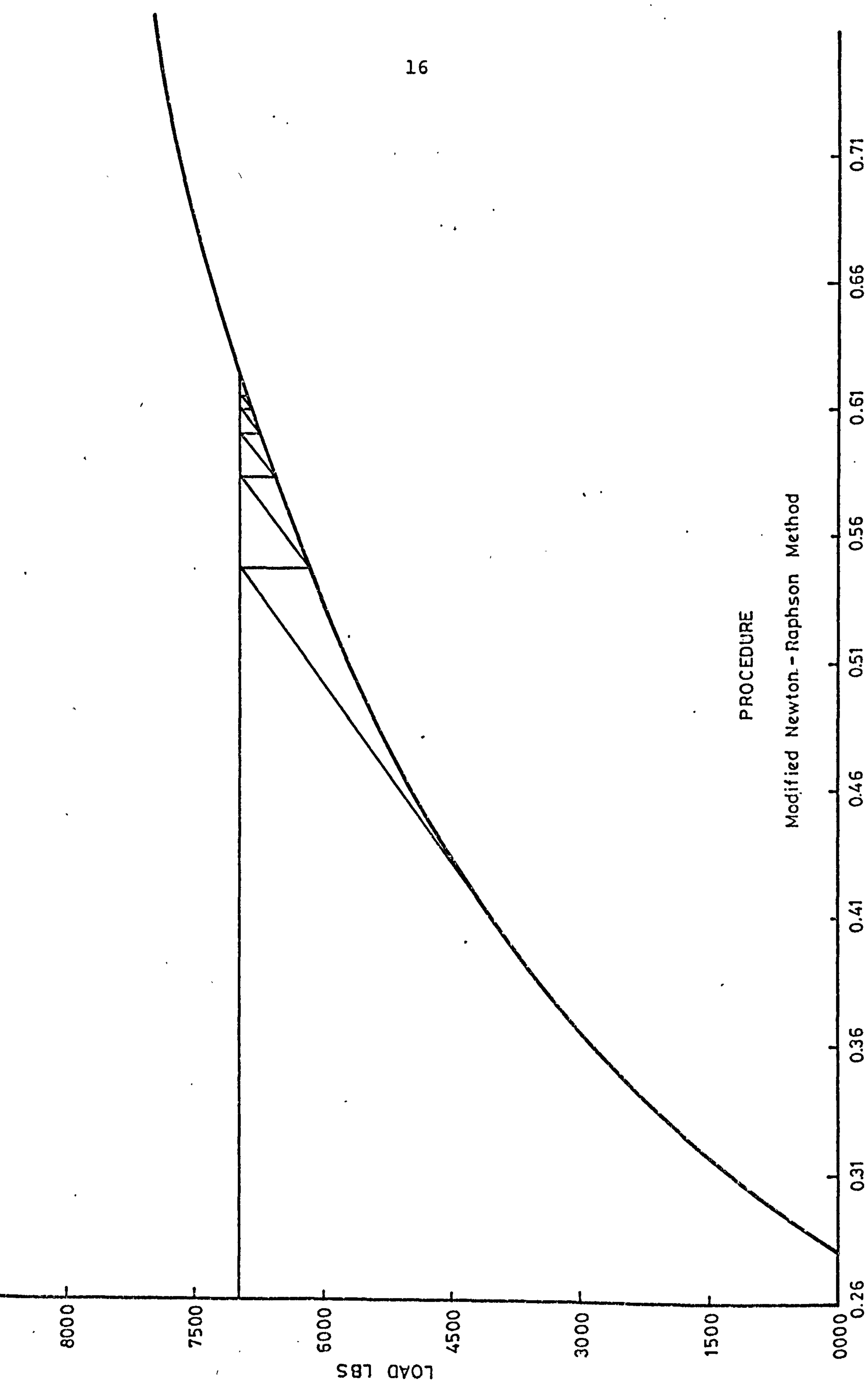


FIGURE 2-2

## 2.4:2 SELF-CORRECTING FORMULATION

Self-Correcting forms of the incremental stiffness procedure have been developed by a number of researchers. Reference (57) describes combined procedures wherein the incremental stiffness procedure is used for a certain number of load steps, and then equilibrium is corrected by applying Newton-Raphson iteration. Self-correcting incremental procedure has the advantage in that it is as easy to apply as the standard incremental procedure but is much more accurate.

A self-correcting initial value formulation was proposed by Stricklin, Haisler and Von Riesenmann (Ref. 58) and Massett and Stricklin (Ref. 59). The procedure applicable to highly nonlinear problems is computationally economical and relatively accurate.

FINITE ELEMENT METHODS  
TECHNIQUES

### 3.1 INCREMENTAL PROCEDURES

In the finite element process, the element incremental stiffness matrix is derived by first formulating the total potential energy of an arbitrary element (plate or beam) and then minimizing the energy on the basis of the minimum potential energy principle. The potential energy expression is derived in terms of the undeformed geometry of the element. The incremental stiffness matrices thus obtained are seen to be simple and easy to apply since they too are written in terms of the geometry of the undeformed element.

The incremental approach consists of a sequence of sufficiently small increment loads so that the structure behaves linearly during each increment. For each increment of load, increments of displacement and corresponding increments of stress and strain are computed. These incremental quantities are used to compute various corrective stiffness matrixes (variously termed geometric, initial stress, and initial strain matrices) which serve to take into account the deformed geometry of the structure. A subsequent increment of load is applied and the process continued until the desired number of load increments has been applied. The net effect is to solve a sequence of linear problems wherein the stiffness properties are recomputed, based on the current geometry prior to each load increment. The solution procedure takes the following form mathematically:

$$[K_E + K_G]_{i-1} \{\Delta q\} = \{\Delta P\} \quad (3-1)$$

where  $[K_E]$  is the elastic stiffness matrix,  $[K_G]$  is the geometric stiffness matrix based on displacements at load step  $i-1$ ;  $\{\Delta q\}$  is the increment of displacement due to the  $i^{\text{th}}$  load increment; and  $\{\Delta P\}$  is the increment of the load applied.

The correct form of the incremental stiffness matrix has been a point of some controversy. Marcal (Ref. 26) separates  $[K_G]$  into initial stress and displacement matrices but neglects quadratic terms of the initial displacement. Some researchers, on the other hand, include these higher order terms.



### 3.2 ITERATIVE METHOD

In the purely incremental approach (as previously discussed), incremental stresses and strains are computed at each step load and are used in the following step load. Although this method is computationally very rapid, it has the disadvantage that equilibrium at any particular load level is not necessarily satisfied. Indeed, no attempt is made to determine whether equilibrium requirements are met. In the iterative method, at the end of each applied load, equilibrium is checked. Oden (Ref. 60) has applied the well known Newton-Raphson technique successfully to nonlinear problems of elasticity. The Newton-Raphson method is one of the oldest techniques for solving systems of nonlinear equations, as well as one of the most reliable. Moreover, it is possible to estimate the rate of convergence, existence of solutions, and to find multiple solutions using this method. Restricting attention to small strains, the equation of equilibrium is obtained as an application of Castigliano's theorem:

$$\left\{ \frac{\partial U}{\partial q} \right\} = \{P\} \quad (3-2)$$

in which,

$$\begin{aligned} U &= \text{the total strain energy,} \\ \{q\} &= \text{generalized displacements,} \\ \{P\} &= \text{generalized forces.} \end{aligned}$$

The strain energy function is a scalar quantity and therefore may be separated into components. It is convenient to separate the strain energy into a contribution due to linear terms,  $U_L$  and one,  $U_{NL}$ , due to the nonlinear terms in the strain-displacement relations. The strain energy due to the linear theory yields a quadratic expression in terms of the generalized displacements and thus

$$[K] \{q\} = \left\{ \frac{\partial U_L}{\partial q} \right\} \quad (3-3)$$

in which,

$$[K] = \text{structural stiffness matrix.}$$

Combining equations (3-2) and (3-3), the complete equations of equilibrium become

$$[K] \{q\} + \left\{ \frac{\partial U_{NL}}{\partial q} \right\} = \{P\} \quad (3-4)$$

Equation (3-4) represents a system of nonlinear algebraic equations which must be solved for any generalized load vector  $\{P\}$ . Two methods of approach will be presented:

- 1) Newton-Raphson Method
- 2) Modified Newton-Raphson Method.

The procedure is used to determine the unbalance in nodal forces at the end of a load increment, and then an iterational approach is used to reduce the unbalance to zero.

### 3.2:1 NEWTON-RAPHSON METHOD

In general, equation (3-4) can not be satisfied with an arbitrary displacement vector  $\{q\}_i$  (subscript denotes the iterational index) and an improved displacement vector  $\{q\}_{i+1}$  is desired. The Newton-Raphson method takes Equation (3-4) and treats it as a function:

$$\{f(q)\} = [K] \{q\} + \left\{ \frac{\partial U}{\partial q} \right\} - \{P\} = \{0\} \quad (3-5)$$

A first order Taylor expansion is used:

$$\left( [K] + \left[ \frac{\partial^2 U_{NL}}{\partial q_i \partial q_j} \right] \right) \{\Delta q\} = - [K] \{q\}_i - \left\{ \frac{\partial U_{NL}}{\partial q} \right\}_i + \{P\} \quad (3-6)$$

in which  $[K]$  is the conventional structural stiffness matrix evaluated on the basis of the undeformed geometry. Equation (3-6) is solved for  $\{\Delta q\}$ . The iterational process is continued until  $\{\Delta q\}$  is sufficiently small, or Equation (3-5) is sufficiently close to zero. If the problem is highly nonlinear, the application of the full load in a single step may cause the solution procedure given by Equation (3-6) to diverge. Consequently, most investigators apply the load in increments and solve for this displacement at all intermediate load steps.

### 3.2:2 MODIFIED NEWTON-RAPHSON METHOD

The standard form of the Newton-Raphson approach given by Equation (3-6) consists of evaluating new coefficients and solving the set of algebraic equations for each iterational cycle. For large order systems, this involves a tremendous amount of computational effort. To reduce the computational effort, a modified Newton-Raphson approach may be used where the coefficient matrix is held constant for a number of load increments and iteration cycles.



### 3.3 MOVING AND FIXED COORDINATES

In addition to the basic choice between incremental or iterative methods, there is a further choice of coordinate systems:

- 1) Moving
- 2) Fixed

The moving coordinate system assumes that the coordinates move with each element. An analysis based on this system requires the use of basic elastic and geometric stiffness. Using the iterative procedure, all displacements, forces, and unbalanced residual forces are found in local system. A particular advantage of using moving coordinates is that large rotations may be accommodated.

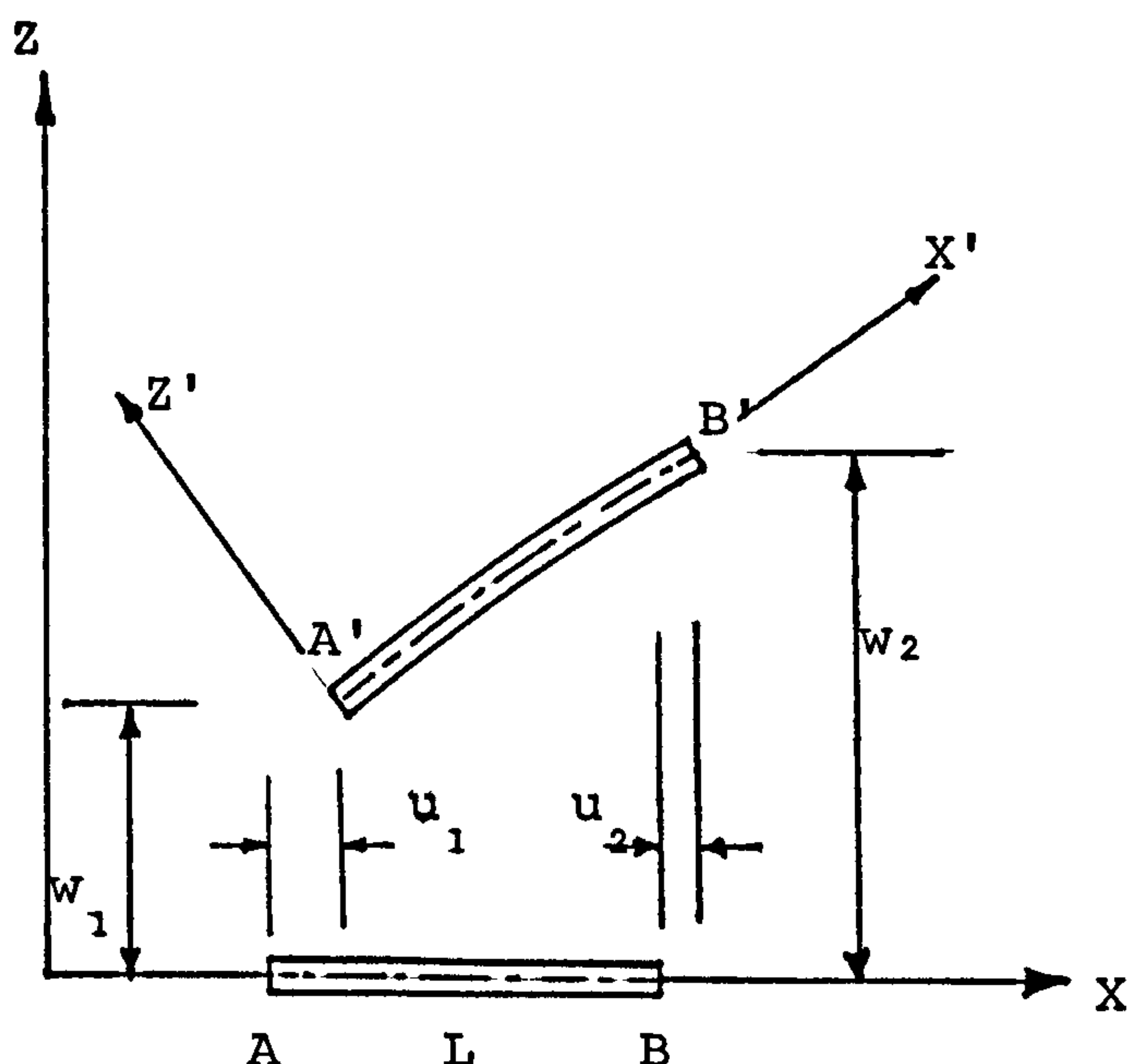
The fixed coordinate system has the advantage of eliminating the need for coordinate transformations between the global and local systems that travel with each element. All displacements, forces and unbalance residual forces refer to the global system.

The beam column is a simple member which embodies all the basic concepts of geometric nonlinearity. It is therefore used here to illustrate the finite element approach to problems such as incremental and iterative procedures in both moving and fixed coordinate systems.

Fixed Coordinates  $X, Z$

Moving Coordinates  $X', Z'$

FIGURE (3-1)



### 3.3:1 MOVING AXES

Under the action of applied load, the beam is displaced from its original locations AB to A'B' as shown in Figure (3-1). Longitudinal strain  $\epsilon_x$  at any point in the beam column is given by

$$\epsilon_x = \frac{\partial u}{\partial x} - z \left( \frac{\partial^2 w}{\partial x^2} \right) + \frac{1}{2} \left( \frac{\partial w}{\partial x} \right)^2, \quad (3-7)$$

where  $u$  and  $w$  are displacements of the point in the  $x$  and  $z$  directions, respectively. The term  $\frac{1}{2} \left( \frac{\partial w}{\partial x} \right)^2$  is only the first term of the series expansion for strain due to large lateral displacements.

The strain energy  $U$  associated with longitudinal strain is

$$U = \int_L \int_A \frac{E}{2} \epsilon_x^2 dA dL, \quad (3-8)$$

where  $L$  and  $A$  are the length and cross-sectional area, respectively, of the beam column, and  $E$  is Young's modulus. Upon substituting (3-7) into (3-8) and integrating over the area, the strain energy becomes a function of four terms in the displacement derivatives:

$$U = \int \left[ \frac{E}{2} \left( \frac{\partial u}{\partial x} \right)^2 + \frac{EI}{2} \left( \frac{\partial^2 w}{\partial x^2} \right)^2 + \frac{EI}{2} \left( \frac{\partial u}{\partial x} \right) \left( \frac{\partial w}{\partial x} \right)^2 + \frac{EA}{8} \left( \frac{\partial w}{\partial x} \right)^4 \right] dL, \quad (3-9)$$

where  $I$  is the moment of inertia of the symmetric cross-section. This expression for strain energy accounts for both linear and nonlinear effects, and it can be used as the basis for several methods of solution. In the stiffness method, the terms involving  $\left( \frac{\partial u}{\partial x} \right)^2$  and  $\left( \frac{\partial^2 w}{\partial x^2} \right)^2$  are associated with the usual constant stiffness of linear analysis, the term  $\left( \frac{\partial u}{\partial x} \right) \left( \frac{\partial w}{\partial x} \right)^2$  is a contribution from nonlinear component of the strain. Using the moving coordinate system, the higher order term  $\left( \frac{\partial w}{\partial x} \right)^4$  can be neglected.

The finite element method involves the selection of assumed functions for the axial and lateral displacement terms in Equation (3-9). Each function has a finite number of components, and the amplitude of each component

is determined by an unknown displacement parameter.  
The displacement distribution for a beam element given  
by Przemieniecki (Ref. 61) would result in the following  
stiffness:

$[K] =$

$\frac{EI}{L^3}$

1	$\frac{AL^2}{I}$					
2	0	12	SYMMETRICAL			
3	0	6L	4L <sup>2</sup>			
4	$-\frac{AL^2}{I}$	0	0	$\frac{AL^2}{I}$		
5	0	-12	-6L	0	12	
6	0	6L	2L <sup>2</sup>	0	-6L	4L <sup>2</sup>
	1	2	3	4	5	6

+

$\frac{P}{L}$

1	0					
2	0	$\frac{6}{5}$	SYMMETRICAL			
3	0	$\frac{L}{10}$	$\frac{2}{15}L^2$			
4	0	0	0	0		
5	0	$-\frac{6}{5}$	$-\frac{L}{10}$	0	$\frac{6}{5}$	
6	0	$\frac{L}{10}$	$-\frac{L^2}{30}$	0	$-\frac{L}{10}$	$\frac{2}{15}L^2$
	1	2	3	4	5	6

where  $P = \frac{EA}{L} (u_4 - u_1) \approx \text{constant}$

$K_E$  is the conventional elastic stiffness matrix and  $K_G$  gives rise to what will be called the "element geometric stiffness" matrix.

If the expression for the slope  $\frac{\partial w}{\partial x}$  is taken as

$$\frac{\partial w}{\partial x} \approx \frac{1}{L} (w_2 - w_1) \quad (3-11)$$

then the nonlinear term in the strain energy expression is simplified. In other words, an average constant slope over the whole length of the element has been assumed; the simplified geometrical stiffness matrix then yields:

$$[K_G] = \frac{P}{L}$$

1	0	SYMMETRICAL									
2	0						1				
3	0						0	0			
4	0						0	0	0		
5	0						-1	0	0	0	
6	0						0	0	0	0	0
	1	2	3	4	5	6					

$$(3-12)$$

If the load is applied to the structure in small increments so that the displacements for any given load application are small, the only effect to be considered will be the change in stiffness due to the axial forces in members:

$$\{\Delta P\} = [K_E + K_G] \{\Delta q\} \quad (3-13)$$



If we take  $[K']$  to be the stiffness matrix of a deformed member  $X' Z'$  and transform this matrix to the undeformed local coordinates  $XZ$  by the standard transformation, we obtain  $[K] = [\lambda]^T [K'] [\lambda]$ ,

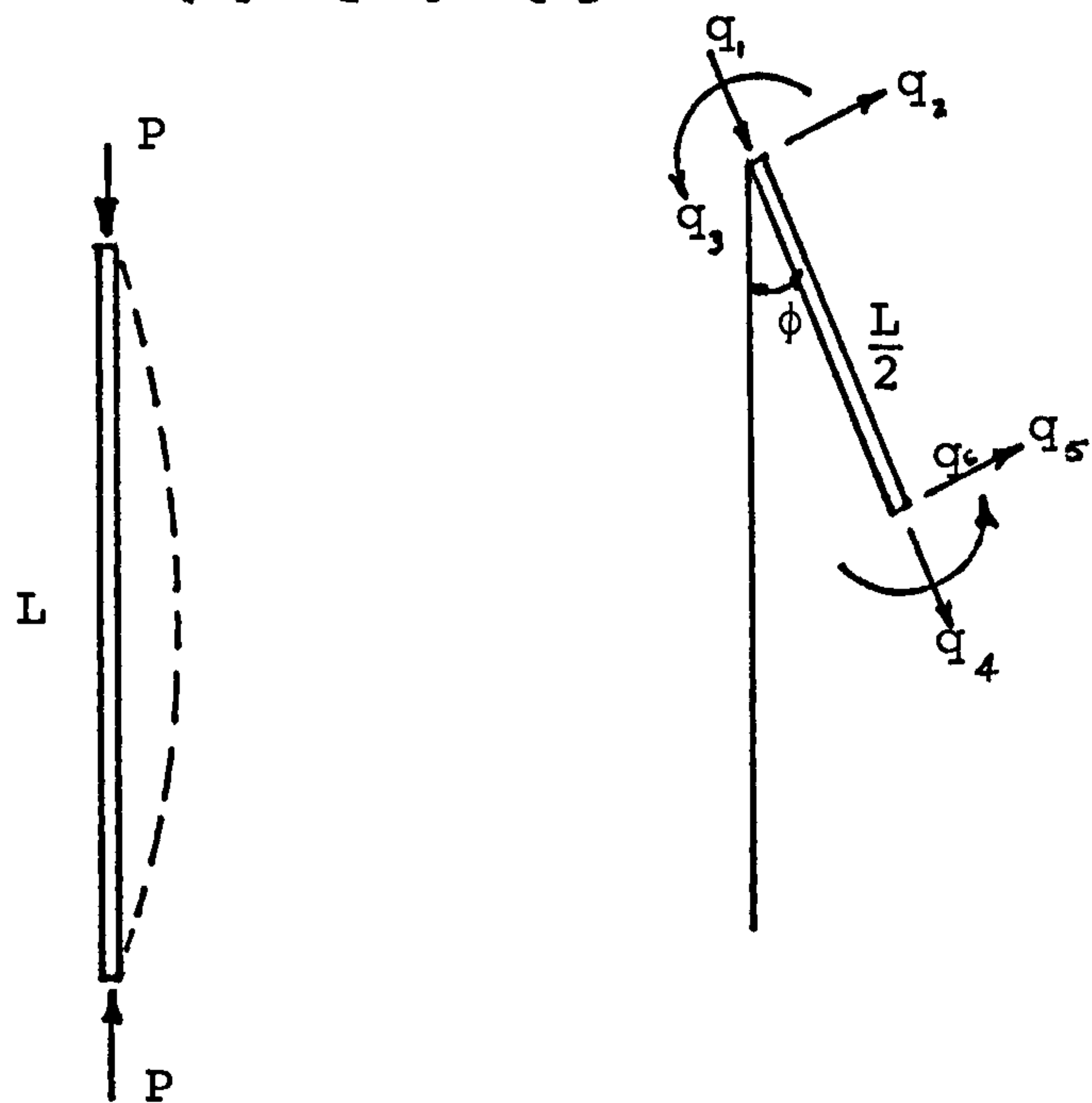


FIGURE (3-2)

where

$[\lambda] =$

1	$\cos\phi$	$\sin\phi$	0	0	0	0
2	$-\sin\phi$	$\cos\phi$	0	0	0	0
3	0	0	1	0	0	0
4	0	0	0	$\cos\phi$	$\sin\phi$	0
5	0	0	0	$-\sin\phi$	$\cos\phi$	0
6	0	0	0	0	0	1
	1	2	3	4	5	6

(3-14)

and, displacements obtained referred to as the global displacements:

$$\{\Delta q\} = [K_E + K_G]^{-1} \{\Delta P\} \quad (3-15)$$

Moving coordinates account for all nonlinear effects. This means that nonlinear effects may be introduced "externally" by means of coordinate rotations as well as by "internally" through the strain-displacement relations.

Distortion of a beam element after load has been applied must be described before the iterative procedure in moving coordinates.

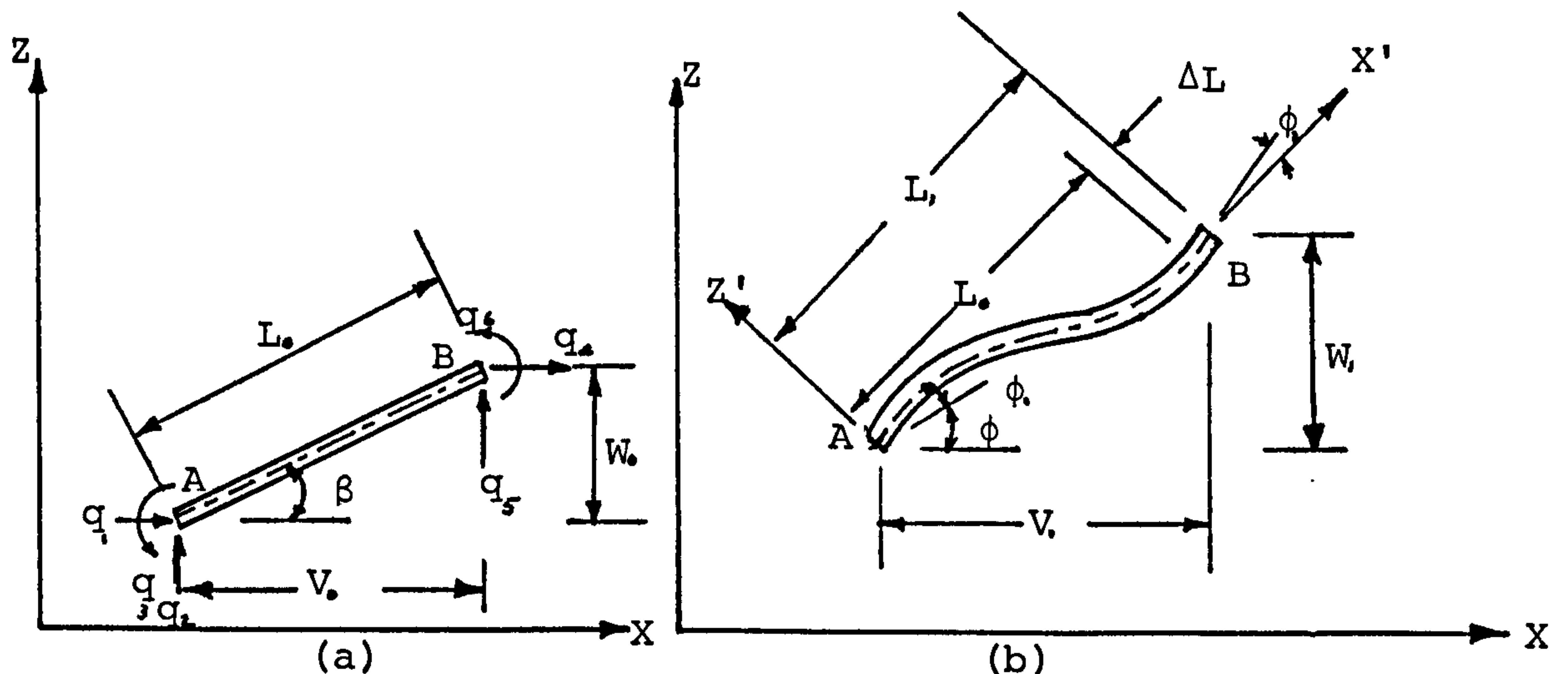


FIGURE (3-3)

In Figure (3-3a), an undeformed beam element is shown in global axis  $XZ$ , where  $V_0$ ,  $w_0$ ,  $L_0$ ,  $\beta$  could be obtained. In terms of the total displacement, the element has both rigid body motion and distortion, and a local axis  $X'$  is established through nodes A and B by subtracting out the rigid body motion:

$$\begin{aligned} V_1 &= V_0 + q_4 - q_1 \\ w_1 &= w_0 + q_5 - q_2 \\ \phi &= \arctan \left( \frac{w_1}{V_1} \right) \end{aligned} \quad (3-16)$$



Also, element distortions in local axis X'Z' are

$$\begin{aligned}\Delta L &= L_1 - L_0 \\ \phi_1 &= q_3 - (\phi - \beta) \\ \phi_2 &= q_6 - (\phi - \beta)\end{aligned}\tag{3-17}$$

The iterative cycle has the following steps under a specified external load for equilibrium.

- 1) Global displacements are used to establish the location and orientation of the displaced local axes.
- 2) Displacements of the nodal points, from an undeformed "reference element" are now determined with reference to the displaced local coordinate axes. These displacements will be referred to as the local displacements.
- 3) Local nodal forces which equilibrate the current local displacements are now determined by premultiplying the local displacements by the element stiffness matrix.
- 4) The element stiffness and equilibrating forces are transformed to global orientation.
- 5) Step 1 through Step 4 are carried out for each element and the equilibrating force and structural stiffness matrix are assembled for the entire structure for the current configuration.
- 6) The difference between the applied forces and the equilibrating forces now form a set of unbalanced loads  $\{\Delta R\}$  acting on the column. The increments in global displacements  $\{\Delta q\}$ , are estimated by solving the incremental equilibrium equations:

$$[K] \{\Delta q\} = \{\Delta R\}\tag{3-18}$$

- 7) Global displacements are incremented by  $\{\Delta q\}$  to form a new estimate of global displacements, and the entire process is repeated from Step 1 until the differences between equilibrating forces and the applied loads become sufficiently small. This indicates that an equilibrium condition has been reached.

- 8) A new load increment may now be applied and the procedure is repeated until equilibrium is established for the new load increment.

Mathematically, the foregoing steps are shown as:

$$\begin{aligned} [K]_i \{\Delta q\}_{i+1} &= \{P\} - \sum [k]_i \{\Delta q\} \\ \{q\}_{i+1} &= \{q\}_i + \{\Delta q\}_{i+1} \end{aligned} \quad (3-19)$$

where  $\{P\}$  represents external loads;  $[k]_i$  and also  $[K]_i$  are based on current displacements  $\{q\}_i$  and are updated every cycle. Some comments on the above procedure for any structure can now be made.

Although displacements and displacement gradients may be large with respect to the global coordinate system, they may be reduced to arbitrarily small quantities with respect to the displaced local coordinate system by refining the subdivision of the structure, providing engineering strains remain small. Essentially, the non-linear strain displacement relationships have been transferred from the strain displacement equations to the geometric transformations required in Step 2. Since the stiffness matrix has been assembled using current geometry, any change of configuration of the structure is included in the equilibrium equations. Since the final configuration is based on an equilibrium balance, between the equilibrating forces and the total applied load, the stiffness used to estimate displacement increments need not be exact. The principal disadvantage of the method is the computational effort involved.

### 3.3:2 FIXED AXES

The axial strain energy for a beam element is given by Equation (3-7) and the corresponding strain energy  $U$  is shown in Equation (3-8). If the higher order terms are not neglected, as was suggested for the moving coordinate system, it is observed that Equation (3-20) consists of two terms, as follows:

$$U = \int \left[ \frac{E}{2} \left( \frac{\partial u}{\partial x} \right)^2 + \frac{EI}{2} \left( \frac{\partial^2 w}{\partial x^2} \right)^2 \right] dL + \int_L \left[ \frac{EI}{2} \left( \frac{\partial u}{\partial x} \right) \left( \frac{\partial w}{\partial x} \right)^2 + \frac{EA}{8} \left( \frac{\partial w}{\partial x} \right)^4 \right] dL \quad (3-20)$$

The first term on the right side of Equation (3-20) is  $U_L$  and the second term is  $U_{NL}$ .  $U_L$  and  $U_{NL}$  are the parts of  $U$  arising from linear and nonlinear strain-displacement expressions respectively. We can show in the following that by including the higher order term  $\left( \frac{\partial w}{\partial x} \right)^4$ , there is no need for ordinary coordinate transformation. But it should be emphasized that, in general, assembly of elements into the structure is accomplished from the undeformed element position, and local coordinates are not established. Taking into account the initial displacements of the deformed structure, the expression for strain can be written as:

$$\epsilon_x = \frac{\partial u}{\partial x} - \frac{\partial^2 w}{\partial x^2} z + \frac{1}{2} \left[ \frac{\partial (w+w_0)}{\partial x} \right]^2 - \frac{1}{2} \left( \frac{\partial w_0}{\partial x} \right)^2, \quad (3-21)$$

or

$$\epsilon_x = e_x - \frac{\partial^2 w}{\partial x^2} z + \frac{1}{2} (\theta + \beta)^2 - \frac{1}{2} \beta^2. \quad (3-22)$$



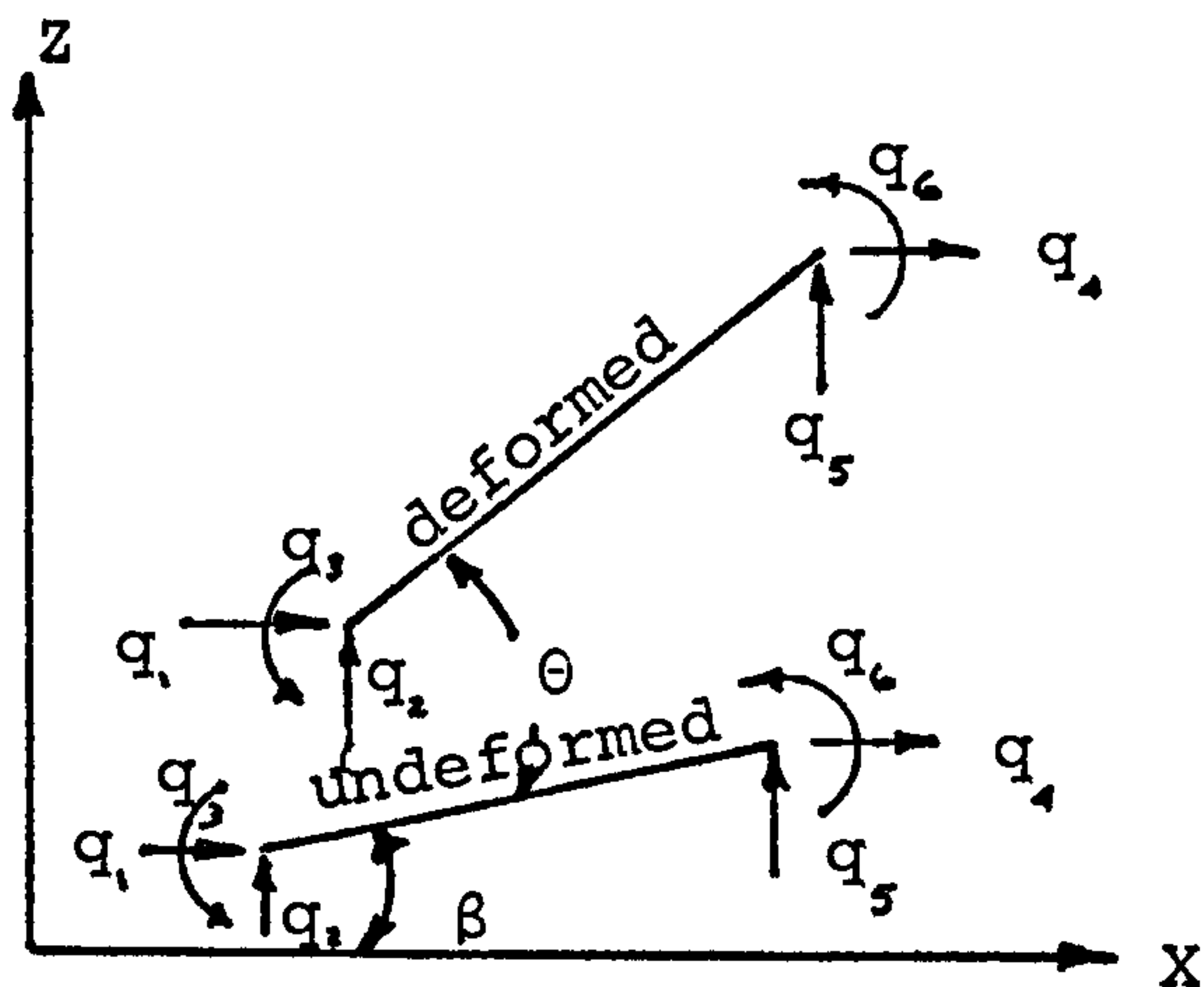


FIGURE (3-4)

where

$$\begin{aligned} e_x &= \text{linear expression for strain,} \\ e_x &= \frac{q_4 - q_1}{L}, \quad \theta = \frac{q_5 - q_2}{L}, \end{aligned} \quad (3-23)$$

$$U = \frac{1}{2} \int E \epsilon_x^2 dx,$$

$$U_L = \frac{AE}{2} \int \left[ e_x^2 + \left( \frac{\partial^2 w}{\partial x^2} \right)^2 z^2 \right] dx, \quad (3-24)$$

$$U_{NL} = \frac{AE}{2} \int (e_x \theta^2 + e_x \beta^2 + 2e_x \theta \beta + \theta^2 \beta^2 + \theta^3 \beta + \frac{\theta^4}{4}) dx.$$

From  $U_L$  we obtain the conventional linear element stiffness matrix  $[K]$ , which is shown by Equation (3-10).  $U_{NL}$  could be broken down to three parts. The effects of initial deflection and large bending on the nonlinear stiffness formulations are characterized by the zero-, first-, and second-order incremental stiffness matrices. The strain energy  $U_0$ , which gives the zero-order incremental stiffness is:

$$U_0 = \frac{AE}{2} \int_0^L (\theta^2 \beta^2 + 2e_x \theta \beta) dx \quad (3-25)$$

or, by differentiation,

$$\frac{\partial U_0}{\partial q_i} = \frac{AE}{2} \int_0^L (2\theta \beta^2 \frac{\partial \theta}{\partial q_i} + 2e_x \beta \frac{\partial \theta}{\partial q_i} + 2\theta \beta \frac{\partial e_x}{\partial q_i}) dx \quad (3-26)$$

where  $i = 1, 6$ .



Substituting  $e_x$  and  $\theta$  from Equation (3-23) in the partial derivatives gives:

$$\left\{ \frac{\partial U_0}{\partial q_i} \right\} = \frac{AE}{2} \begin{Bmatrix} -2\theta\beta \\ -2\theta\beta^2 - 2e_x\beta \\ 0 \\ 2\theta\beta \\ 2\theta\beta^2 + 2e_x\beta \\ 0 \end{Bmatrix} \quad (3-27)$$

Another differentiation and substitution of partial derivatives gives:

$$[N_0] = \frac{\partial^2 U_0}{\partial q_i \partial q_j}$$

$$[N_0] = \frac{AE}{L} \begin{array}{c|cccccc} 1 & 0 & & & & & \\ 2 & \beta & \beta^2 & & & & \\ 3 & 0 & 0 & 0 & & & \\ 4 & 0 & -\beta & 0 & 0 & & \\ 5 & -\beta & -\beta^2 & 0 & \beta & \beta^2 & \\ 6 & 0 & 0 & 0 & 0 & 0 & 0 \end{array}$$

1      2      3      4      5      6

SYMMETRICAL

(3-28)

Similarly, the strain energy  $U$ , which gives the first order incremental stiffness matrix is

$$U_1 = \frac{AE}{2} \int_0^L (e_x \theta^2 + \theta^3 \beta + e_x \beta^2) dx, \quad (3-29)$$

or, by differentiation,

$$\frac{\partial U_0}{\partial q_i} = \frac{AE}{2} \int (\theta^2 \frac{\partial e_x}{\partial q_i} + 2e_x \theta \frac{\partial \theta}{\partial q_i} + 3\theta^2 \beta \frac{\partial \theta}{\partial q_i} + \beta^2 \frac{\partial e_x}{\partial q_i}) dx, \quad (3-30)$$

where  $i = 1, 6$ . Substitution of Equation (3-23) into partial derivatives gives:

$$\left\{ \frac{\partial U_1}{\partial q_i} \right\} = \frac{AE}{2} \begin{Bmatrix} -\theta^2 - \beta^2 \\ -2e_x \theta - 3\theta^2 \beta \\ 0 \\ \theta^2 + \beta^2 \\ 2e_x \theta + 3\theta^2 \beta \\ 0 \end{Bmatrix} \quad (3-31)$$

Another differentiation and substitution of partial derivatives gives:

$$[N_1] = \frac{\partial U_1}{\partial q_i \partial q_j}$$

$$[N_1] = \frac{AE}{L}$$

1	0	SYMMETRICAL				
2	$\theta$	$e_x + 3\theta\beta$				
3	0	0	0			
4	0	$-\theta$	0	0		
5	$-\theta$	$-e_x - 3\theta\beta$	0	$\theta$	$e_x + 3\theta\beta$	
6	0	0	0	0	0	0
	1	2	3	4	5	6

(3-32)

Similarly, the strain energy  $U_2$  which gives the second order incremental stiffness matrix is:

$$U_2 = \frac{AE}{2} \int_0^L \frac{\theta^4}{4} dx \quad (3-33)$$

or, by differentiation,

$$\frac{\partial U_2}{\partial q_i} = \frac{AE}{2} \int_0^L \left( \theta^3 \frac{\partial \theta}{\partial q_i} \right) dx \quad (3-34)$$

where  $i = 1, 6$ . Substitution of Equation (3-23) into partial derivative gives:

$$\left\{ \frac{\partial U_2}{\partial q_i} \right\} = \frac{AE}{2} \begin{Bmatrix} 0 \\ -\theta^2 \\ 0 \\ 0 \\ \theta^2 \\ 0 \end{Bmatrix} \quad (3-35)$$

Another differentiation and substitution of partial derivatives gives:

$$[N_2] = \frac{\partial U_2}{\partial q_i \partial q_j}$$

$$[N_2] = \frac{AE}{L}$$

1	0	SYMMETRICAL				
2	0					
3	0	0	0			
4	0	0	0			
5	0	$-\frac{3}{2}\theta^2$	0	0	$\frac{3}{2}\theta^2$	
6	0	0	0	0	0	0
	1	2	3	4	5	6

(3-36)

As the so-called geometric stiffness matrix for a beam is given by Equation (3-12), at this stage, it is necessary to correlate the present results with Equation (3-12). If, for the sake of simplicity, we ignore the initial displacements, by using the definition:

$$P = AE\epsilon_x ,$$

or

$$P = AE(e_x + \frac{1}{2}(\theta + \beta)^2 - \frac{1}{2}\beta^2) \quad (3-37)$$

the nonlinear stiffness matrix in Equation (3-24) may be written as:

$$\left[ \frac{\partial^2 U_{NL}}{\partial q_i \partial q_j} \right] = \frac{AE}{L}$$

1	0					
2	$\theta + \beta$	$e_x + 3\theta\beta$ $\beta^2 + \frac{3}{2}\theta^2$	SYMMETRICAL			
3	0	0	0			
4	0	$-\theta - \beta$	0	0		
5	$-\theta - \beta$	$-e_x - 3\theta\beta$ $-\beta^2 - \frac{3}{2}\theta^2$	0	$\theta + \beta$	$e_x + 3\theta\beta$ $\beta^2 + \frac{3}{2}\theta^2$	
6	0	0	0	0	0	0
	1	2	3	4	5	6

(3-38)



or:

$$\left[ \frac{\partial^2 U_{NL}}{\partial q_i \partial q_j} \right] =$$

$\frac{AE}{L}$

1	0	SYMMETRICAL				
2	$\theta + \beta$	$(\theta + \beta)^2$				
3	0	0	0			
4	0	$-\theta - \beta$	0	0		
5	$-\theta - \beta$	$-(\theta + \beta)^2$	0	$\theta + \beta$	$(\theta + \beta)^2$	
6	0	0	0	0	0	0
	1	2	3	4	5	6

+

$\frac{P}{L}$

1	0	SYMMETRICAL				
2	0	1				
3	0	0	0			
4	0	0	0	0		
5	0	-1	0	0	1	
6	0	0	0	0	0	0
	1	2	3	4	5	6

These two matrices may be compared with those presented in Equation (3-12) and Equation (3-14). This procedure is based on the fact that  $(\theta + \beta)$  is restricted to small values and thus  $\cos(\theta + \beta) \approx 1$  and  $\sin(\theta + \beta) \approx (\theta + \beta)$ . For the first matrix on the right hand side of Equation (3-39), the results are similar, when the element stiffness matrix is included. The second matrix on the right hand side is identical to Equation (3-12), which is the geometric stiffness  $[K_G]$  and as usual it accounts for the effect that membrane forces has on lateral displacements.

As Argyris (9) points out, for small additional displacements the element stiffness matrix is the same as the one used in linear theory provided one considers the transformation from deformed to global coordinates. This is shown in Figure (3-4) where the transformation matrix should be based on a transformation from the deformed  $X' - Z'$  coordinates to the global  $X - Z$  coordinates.

For small values of  $\phi$  the transformation matrix from the deformed to the undeformed coordinates is given by Equation (3-14).

Forming the matrix product  $[\lambda]^T [K'] [\lambda]$  yields the first matrix on the right hand side of Equation (3-39) plus the usual element stiffness matrix for a beam element which has been chosen to be separated out and designated as in this formulation. Thus Equation (3-39) has a simple interpretation. The first term is due to a rotation of coordinates from the deformed to the undeformed system.

There has been much debate in the literature about the importance of including the fourth order strain energy expression of Equation (3-9), which was neglected in the moving coordinate system. However, this comparison has shown that the fourth order terms are automatically accounted for in the transformation from deformed to undeformed coordinates and in the definition of the load  $P$ .



### 3.4 PROGRAM DEVELOPMENT

The first stage in the development of a program for pre- and post-buckling analysis is the establishment and testing of a method of dealing with the nonlinearities inherent in such an analysis. In the earlier stages of program development, it is desirable to analyse simple structures, to avoid the complications associated with the manipulation of large matrices. The strut model was used as a simple structure for a buckling analysis, using different approaches such as the incremental or iterative, in the two different coordinate systems, moving and fixed. The simple strut can be modelled with considerable accuracy by means of a small number of simple bending elements, resulting in a relatively small number of degrees of freedom for the structure.

The purpose of the program was to develop an incremental and iterative procedure for geometrically nonlinear problems, the principles of which could be applied to more sophisticated problems such as a plate. Initially, the incremental procedure with consistent geometric stiffness in the moving coordinate system was investigated. As expected, the results were not sufficiently accurate and could only be improved by a load increment refinement, requiring more computer time. The iterative procedure then followed, transforming displacements from global to local coordinates in order to find the local internal load vector. Initially, it was found that for the modified Newton-Raphson procedure, when the applied load reached approximately 60% of the critical load, the solution began to diverge. From these investigations, it was found that correction for the rotation of the elements must be made. This problem arises from the shortening of the element in a given direction due to rotation with respect to the structure. The total shortening in terms of structure coordinates can be considered as a component due to inplane strain, and a component due to rotation. This is true for either compressive or tensile strain provided that the rotational strain is always assumed to be positive. The problem of the existing divergence was overcome, but nevertheless, it must be mentioned that with the modified Newton-Raphson method, there is always the danger of divergence if the load increment size is not carefully chosen.

Since it was intended to develop an efficient program producing reasonably accurate results, the fixed coordinate system was followed. A reduction of computer effort for the fixed coordinate system was anticipated, since it uses the simple geometric stiffness (string stiffness), and it eliminates the need for direct

coordinate transformation. Since there is no direct transformation from global to local coordinates in the iterative procedure, therefore it is not necessary to find the out-of-balance forces in the local coordinate system and to account for the correction of the rotation in the element.

With the availability of numerous standard routines provided by the Cranfield Institute, the NAG (62) inversion routine was used for both the moving and the fixed coordinate programs.

It should be noted that the stiffness matrix of a finite element is not positive definite unless the element has been properly constrained. Positive definiteness of the stiffness matrix means that for any displacement vector  $q^T k q > 0$ . In order to avoid the default of positive definite in the routine, the constraint degrees of freedom in the boundary conditions are multiplied by the large number  $10^{50}$  in the leading diagonal of the assembled stiffness matrices.

For buckling problems, lateral displacements occur with the first load increment provided that initial imperfections are supplied by the input data. The only initial imperfections required to activate the geometrically nonlinear part of the program are the initial lateral displacements.



### 3.5 PROGRAM DESCRIPTION - MOVING COORDINATE SYSTEM - D67A

The process is illustrated by the flow chart in Figure (A-1). The program is to perform either the incremental or the iterative procedure, as the strut deflects under compressive load. The structural stiffness matrix is assembled at the beginning of the first step, according to an assumed initial deflected shape. The load is then used with the stiffness matrix to determine the displacements of the strut. The objective in developing this program was to make it to some extent general so that the user would have a number of options to apply to his own particular problem and procedure. Therefore it was devised so that up to 16 elements can be chosen for the strut and the dimensions and properties of each element can take different values. Any degree of freedom at any node can be restrained and the load can be applied at any of the degrees of freedom at any node. There are four choices of procedure available in the program: purely incremental, incremental with iteration by Newton-Raphson, incremental with iteration by the modified Newton-Raphson process, and incremental with carry over of out-of-balance forces. Any or all of the procedures can be used at different levels of applied load, thus making all options available.

Since, in the geometrically nonlinear problem of an imperfect strut, displacement increments get larger when the load increments are held constant, the purely incremental procedure results in progressively greater drift from the true solution (see Chapter 4), and the modified Newton-Raphson procedure is also in danger of divergence in the solution (see Chapter 4). To correct for these errors, an "approximately constant displacement" option, based on the initial displacement, is incorporated into the program. In the iterative procedure, the number of iterations can be fixed for each increment of load, or can be controlled by the accuracy of the solution obtained.

To account for the reduction in the strut stiffness with increasing axial load, the geometric stiffness matrix is included with the elastic stiffness in the assembled stiffness matrix. The geometric stiffness is in terms of current load in the element.

The assembly of the structural stiffness matrix to conform to the current deflected shape of the strut requires a transformation of the element stiffness matrices from local to global coordinates. This is achieved by means of a transformation matrix. The transformation matrix is a matrix of coefficients obtained by resolving displacements of the structure in the

direction of the local coordinates. In order to obtain these displacements, the load vector must be multiplied by inverted assembled stiffness matrix. The inversion process in the program is using the standard NAG (Ref. 62) routine provided by Cranfield Institute computer facilities.

At the end of each increment, if an equilibrium check is desired, first the nodal forces (and out of balance) forces must be determined. This is achieved by transforming the displacements from global to local coordinates, and then multiplying that by the stiffness matrices. Second, the displacements due to residual forces are found by multiplying the inverted stiffness matrix by these out of balance forces.

A detailed description of the program with a program listing is given in Appendix A.



### 3.6 PROGRAM DESCRIPTION - FIXED COORDINATE SYSTEM - D67B

The main object of using a fixed coordinate system is to eliminate the need for coordinate transformations between the global and local systems. As shown in Section 3.3:2, the nonlinear terms in the strain energy expression can be simplified by assuming an average, constant slope over the whole length of the element, if the element is small in relation to the overall length of the actual strut. This leads to a simplified geometric stiffness (string stiffness) matrix, and without the transformation manipulation will result in less computer effort.

The main process in the solution of the strut problem in the fixed coordinate system, as far as the choices and options available in the program are concerned, is the same as for the moving coordinate system discussed in the previous section. In the fixed coordinate system, the assembled stiffness matrix consists of elastic, zero incremental, first incremental, and second incremental stiffnesses. The zero incremental stiffness matrix is related to the initial deformation of the strut. The corresponding geometric stiffness transformation is obtained from first, and second incremental stiffness. In the iterative procedure, since there is no transformation of global to local coordinates, the displacements obtained from increments are used directly for finding the nodal forces, and subsequently for the residual forces.

This program also uses the standard NAG (Ref. 62) routine for the inversion of the assembled stiffness matrix. The details of the process are shown by the flow chart in Figure (A-1), and Figure (A-3). The detailed description of the program with a program listing is given in Appendix A.

NUMERICAL COMPARISON OF  
TECHNIQUES



## 4.1 USE OF A SIMPLE STRUT AS A MODEL

A strut, because of its simplicity and the relative ease with which accurate finite element calculations can be carried out, is commonly used to represent the non-linear behaviour of more complex structural problems. Since exact solutions are available in suitable cases, the strut is therefore an ideal model on which to base comparisons of performance of the various nonlinear finite element techniques.

The structure modelled in this analysis is a uniform (constant  $EI$ ) pin-ended strut which has an initial imperfection of sinusoidal half-wave shape. The strut is loaded in axial compression at the ends. Since the deformational behaviour of the imperfect strut can be readily predicted by theory and expressed in non-dimensional form, the choice of dimensions and material properties can be made arbitrarily.

The classical (Euler) solution for the critical load of a pinned strut is

$$P_{cr} = \pi^2 EI / L^2 \quad (4-1)$$

where  $EI$  is the flexural rigidity and  $L$  the length of the strut. Assuming the initial imperfection  $W_0$  to be exactly the half-sine wave pattern:

$$w_0 = W_0 \sin(\pi x / L), \quad (4-2)$$

the increase in deflection  $w$  under a compressive load  $P$  (Ref. 63) is

$$w = \frac{W_0 \sin(\pi x / L)}{(P_{cr} / P) - 1} \quad (4-3)$$

Since the maximum deflection occurs at the middle of the strut,  $x = L/2$ , the maximum deflection  $W$  is:

$$W = \frac{W_0}{(P_{cr} / P) - 1} \quad (4-4)$$

The total deflection  $W_T$  is then

$$W_T = W + W_0, \quad (4-5)$$

or

$$\frac{W_T}{W_c} = \frac{1}{1 - (P/P_{cr})} \quad (4-6)$$

Equation (4-4) may be re-arranged as

$$(P_{cr} - P)W = W_0 P \quad (4-7)$$

or, dividing both sides of this Equation by  $P$ ,

$$(P_{cr}) \left(\frac{W}{P}\right) - W = W_0, \quad (4-8)$$

which is a linear equation in  $\frac{W}{P}$  and  $W$ . Thus a plot of  $\frac{W}{P}$  against  $W$  should produce a straight line, the slope of which is  $\frac{1}{P_{cr}}$  and the intercept on the  $W$  axis is  $W_0$ .

This is universally known as the "Southwell Plot," and is used here to determine a theoretical critical load from the computed deflection of the imperfect strut. However, it is the non-dimensional Equation (4-6) which is principally used in this chapter.

Although the computer program devised by the author is a prototype for the more general plate program, its specific function here is to perform finite element calculations for the strut. The program uses a standard matrix inversion routine rather than the frontal solution used subsequently for the plate program, but is in other respects quite similar. It is suitable for a purely incremental solution, as well as for the various iterative techniques.

To find the number of elements necessary for a reasonably accurate solution, the program was run for various numbers of elements. Figure (4-1) shows the accuracy of the strut model for 2, 6, 10, and 14 elements, taking six step loads to reach the critical load. It must be noted that Figure (4-1) is intended only to compare accuracy with various numbers of elements, and being a purely incremental calculation with rather few increments of load, it obviously does not represent an accurate result for a strut.

It is observed that the results for 6, 10, and 14 elements are very close to each other, indicating that increasing the number of elements beyond six does not

substantially improve the accuracy. By using the six element model, the results obtained will be sufficiently accurate and the computer effort consequently less. Therefore the six element strut has been adopted as standard for all subsequent work in this chapter. In addition, it is necessary to analyze only one-half of the strut, because of the symmetry about the mid-height.

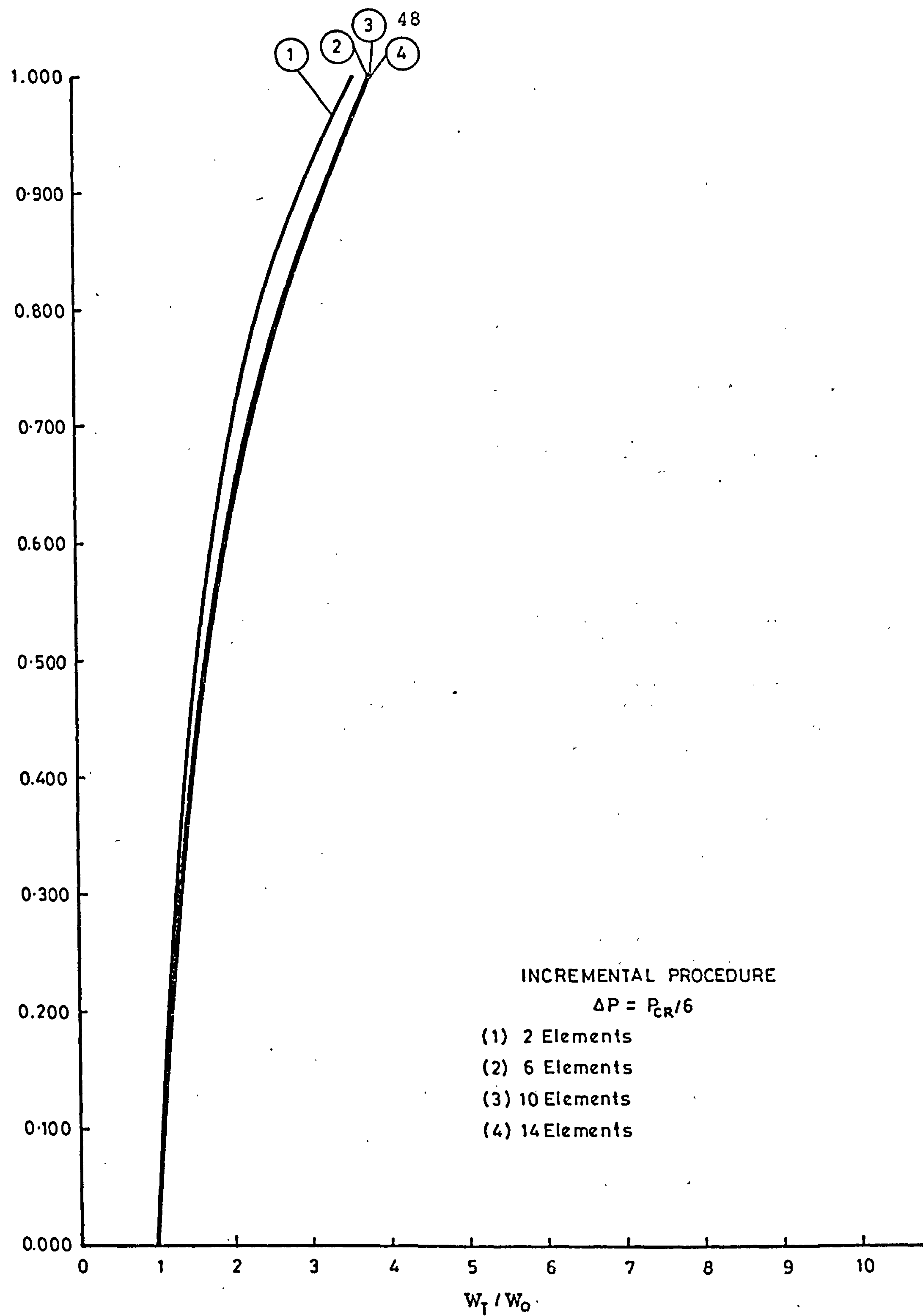


FIGURE 4-1



## 4.2 FINITE ELEMENT REPRESENTATION

The element stiffness, in the deformed position at any stage in the incremental process, may be written in the global coordinate system as

$$[k] = [\lambda]^T [k'] [\lambda] ,$$

where  $[k'] = [k'_G] + [k'_E]$

and  $[\lambda]$  is the displacement transformation matrix arising from the deformation of the structure.

This transformation couples the axial and bending behaviour. The incremental equilibrium equation for the entire structure is in the form of

$$[K] \{\Delta q\} = \{\Delta P\} ,$$

where  $[K]$  is the incremental stiffness matrix obtained by the direct stiffness assembly procedure.

For a given increment of load  $\{\Delta P\}$  the equation is solved for increments of nodal displacements  $\{\Delta q\}$ . These are then added to the previous nodal displacements and, if an iterative solution is being used, element equilibrating forces are evaluated and the difference between the sum of equilibrating forces and the applied loads is considered as the load increment vector for the next iteration. A new stiffness matrix is evaluated for the current state of stress and geometry, and the solution is repeated until the unbalanced nodal forces are arbitrarily small (see Chapter 3).

The two alternative techniques which may be used in the definition of element stiffness at each stage of the process described above are:

- 1) Fixed coordinates
- 2) Moving coordinates

In the moving coordinate system, there are two forms of geometric stiffness matrix, the consistent  $K_G$  matrix and the so-called string stiffness matrix, the latter being a simplified version of the former (see Section 3.3). The fixed coordinate system is necessarily equivalent to the use of the string stiffness.

The apparent simplicity and advantage of the fixed coordinate system, that it avoids the explicit transformation of element stiffness already referred to, has been discussed (Section 3.3:2). A comparison is now made between the use of fixed and moving coordinates, as follows:

- 1) Fixed coordinates,
- 2) Moving coordinates with consistent  $[K_G]$  matrix,
- 3) Moving coordinates with the string stiffness  $[K_G]$  matrix.

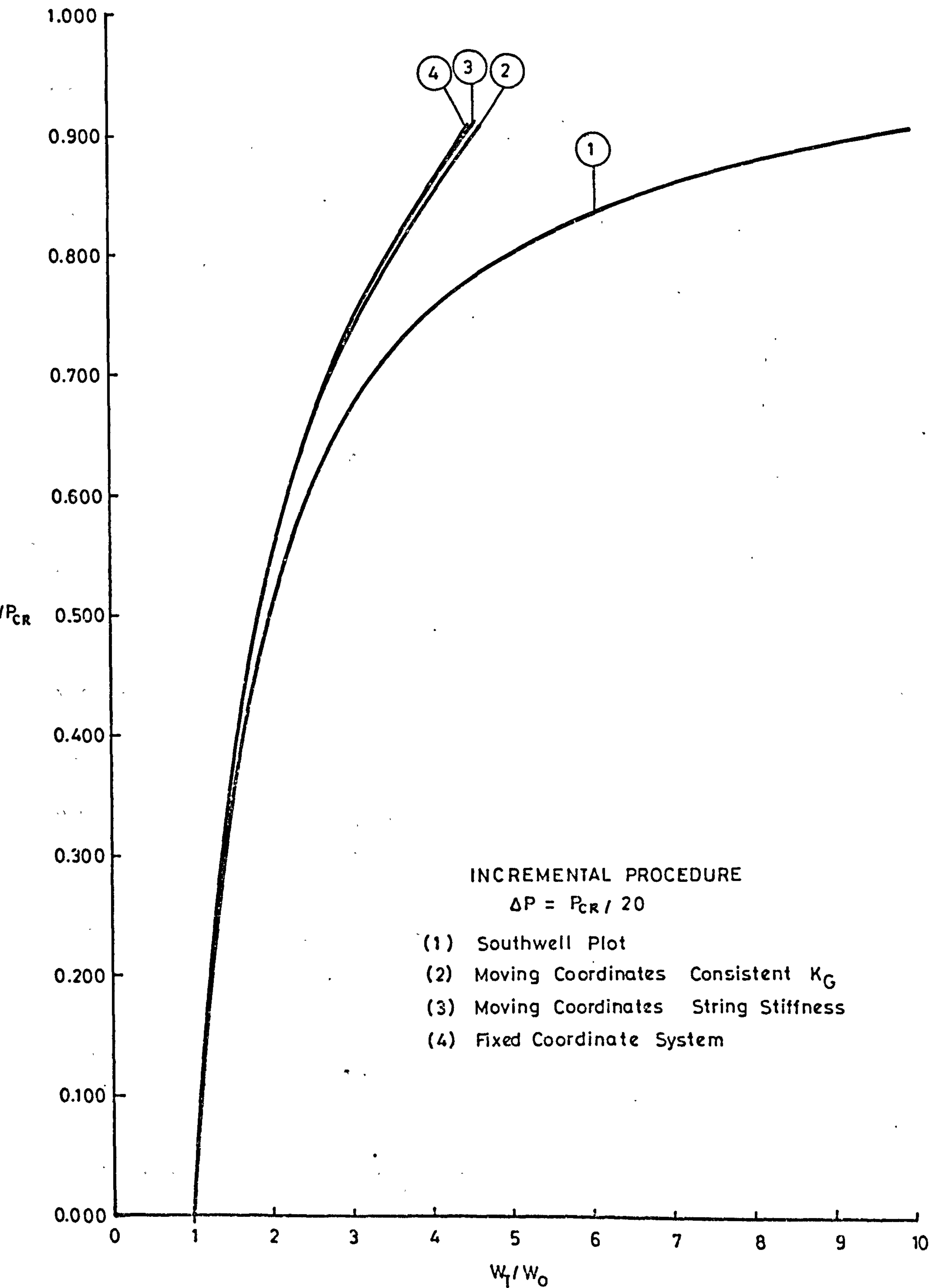
The computer program for the strut model was run using each of these three methods, first for the purely incremental solution and then the incremental solution with modified Newton-Raphson iteration (taking two iterations at each level of load increment). In order to reach the theoretical buckling load with reasonable accuracy, 20 increments of load were used.

Figure (4-2) and Figure (4-3) show that results obtained for the string stiffness in moving coordinates and for the fixed coordinate systems are very similar. These figures are plotted in the non-dimensional form described in Section (4.1), and the curves labelled "Southwell Plot" refer to Equation (4-6). The results for the consistent geometric stiffness matrix are, of course, slightly better, although the difference is not significant.

These results are also plotted as net deflection vs. net deflection/total load (Southwell Plot) in Figures (4-4), (4-5), (4-6), and (4-7). The dimensions chosen for the strut model were such that the critical load obtained from Equation (4-1) is  $P_{cr} = 12600$  lbf. The initial imperfection was taken as 1/100 of the strut length (0.28) in.

The following observations are made from Figures (4-4), (4-5), (4-6), and (4-7):

- 1) The lines plotted are quite straight.
- 2) The prediction of critical load which is obtained from the slope of the lines in each case provides a convenient measure of accuracy, and shows that use of the string stiffness and fixed coordinates both give results within 1 to 2 per cent of that obtained by use of the consistent geometric stiffness matrix.
- 3) The lines in each case intercept the deflection axis at 0.28 in., which is the initial imperfection of the problem.





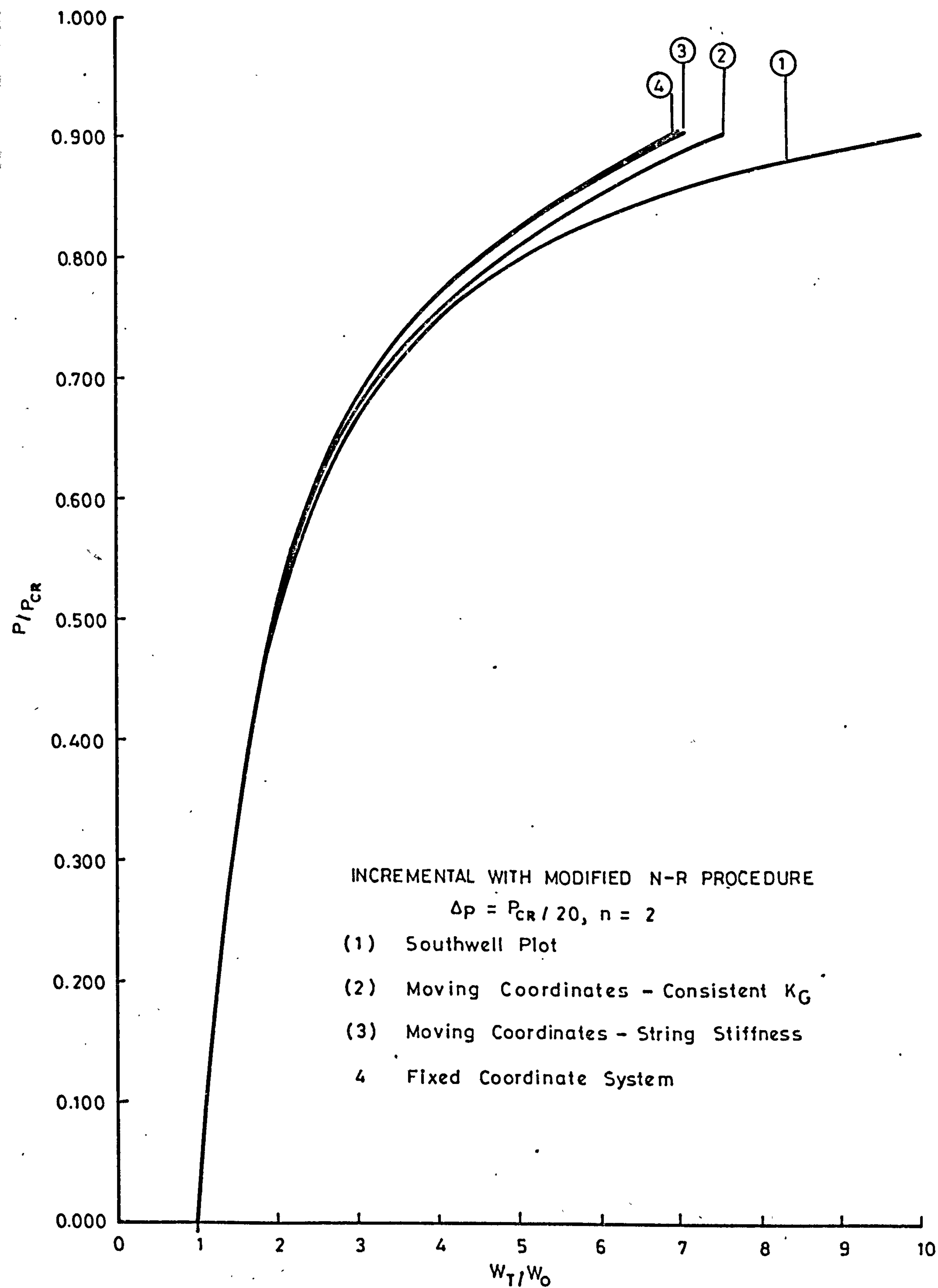
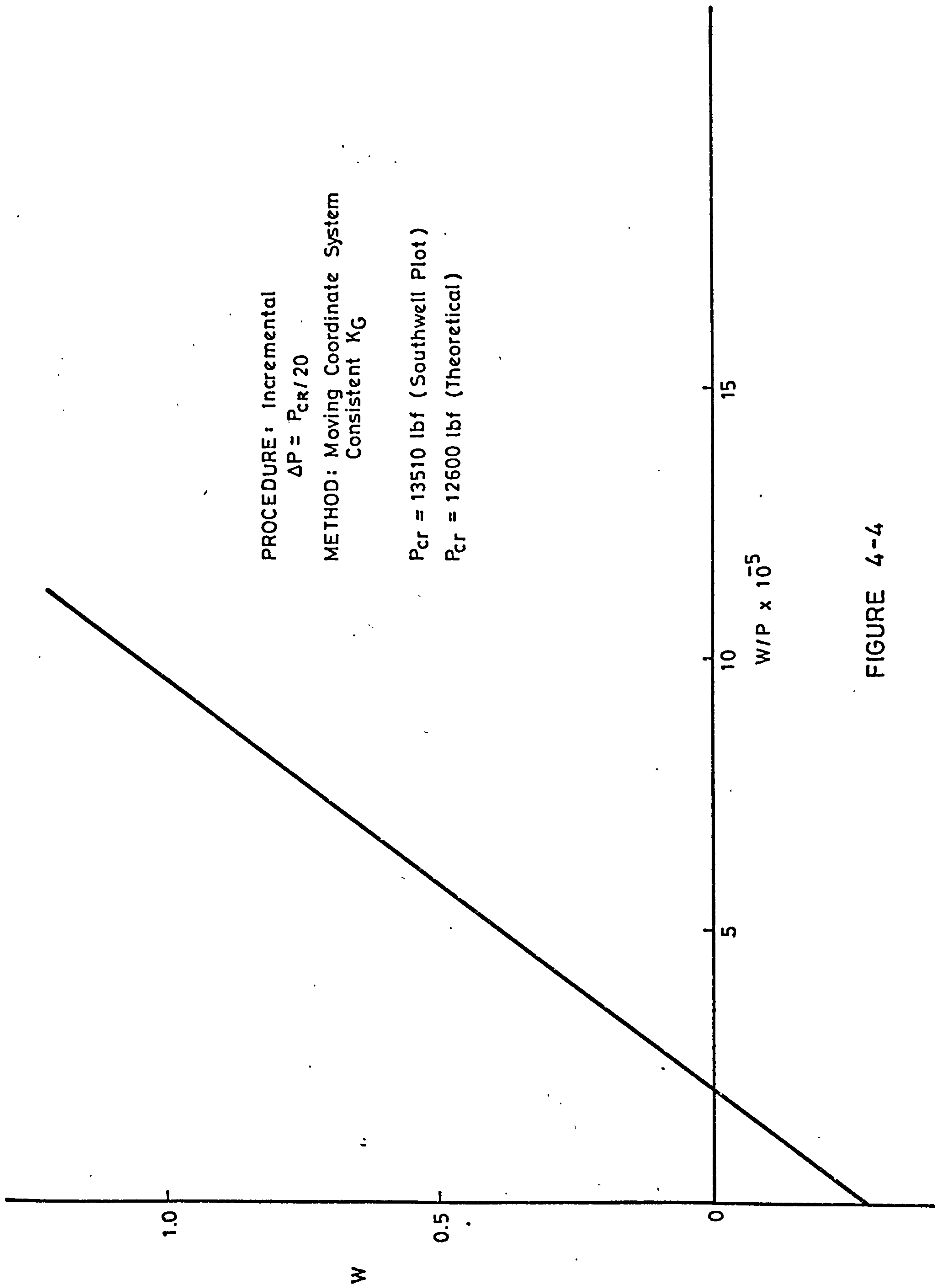


FIGURE 4-3





PROCEDURE: Incremental  
 $\Delta P = P_{CR}/20$

METHOD: Moving Coordinate System  
Consistent  $K_G$

$P_{CR} = 13510$  lbf (Southwell Plot)  
 $P_{CR} = 12600$  lbf (Theoretical)

FIGURE 4-4

PROCEDURE: Incremental with Modified  
Newton Raphson

$$\Delta P = P_{CR} / 20 \quad n = 2$$

METHOD: Moving Coordinate System  
Consistent  $K_G$

$$P_{cr} = 12720 \text{ lbf (Southwell Plot)}$$

$$P_{cr} = 12600 \text{ lbf (Theoretical)}$$

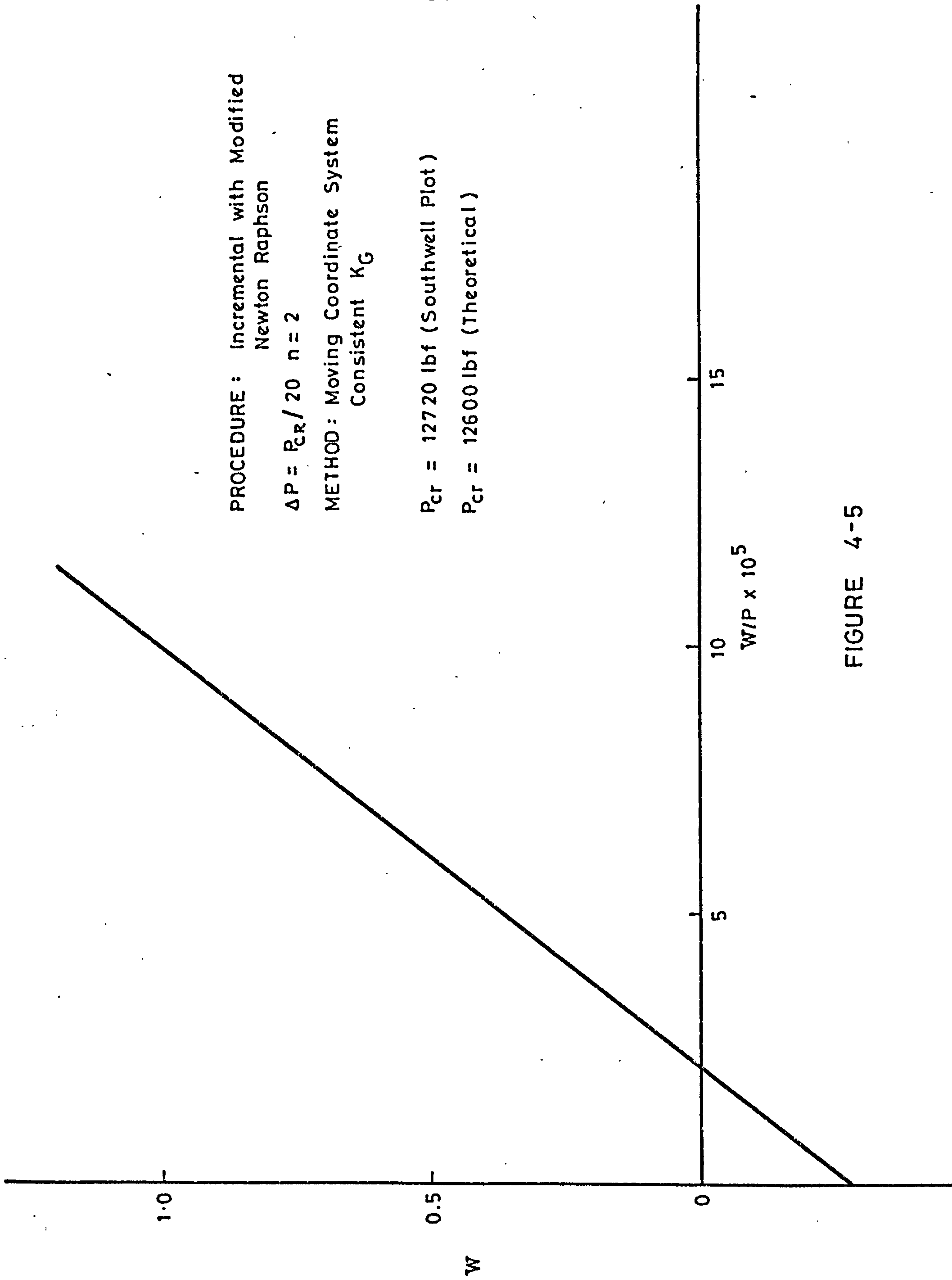
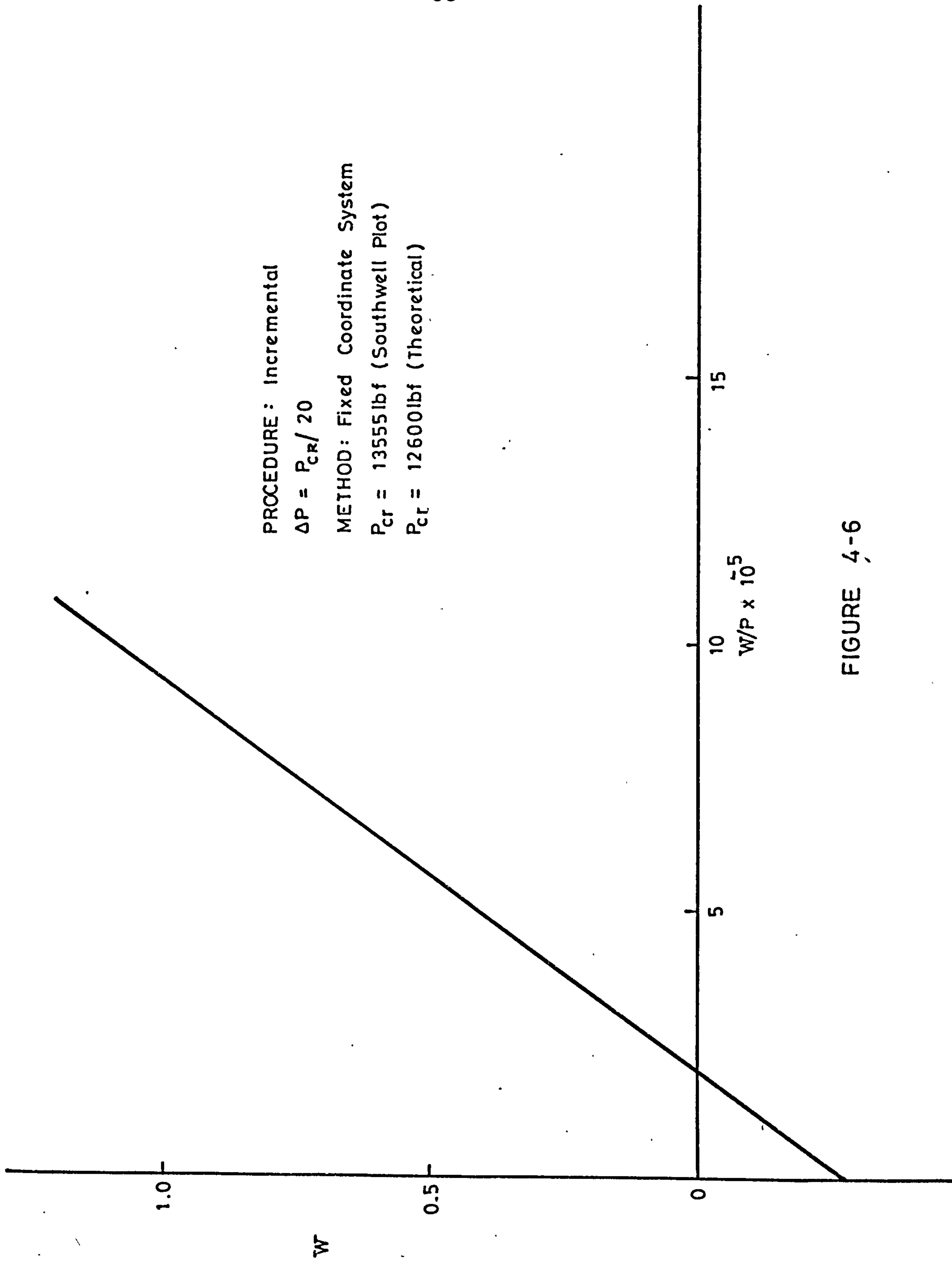


FIGURE 4-5



PROCEDURE: Incremental  
 $\Delta P = P_{cr} / 20$   
METHOD: Fixed Coordinate System  
 $P_{cr} = 13555 \text{ lbf}$  (Southwell Plot)  
 $P_{cr} = 12600 \text{ lbf}$  (Theoretical)

FIGURE 4-6

PROCEDURE: Incremental with Modified  
Newton-Raphson

$$\Delta P = P_{cr} / 20, n = 2$$

METHOD: Fixed-Coordinate System

$$P_{cr} = 12800 \text{ lbf (Southwell Plot)}$$

$$P_{cr} = 12600 \text{ lbf (Theoretical)}$$

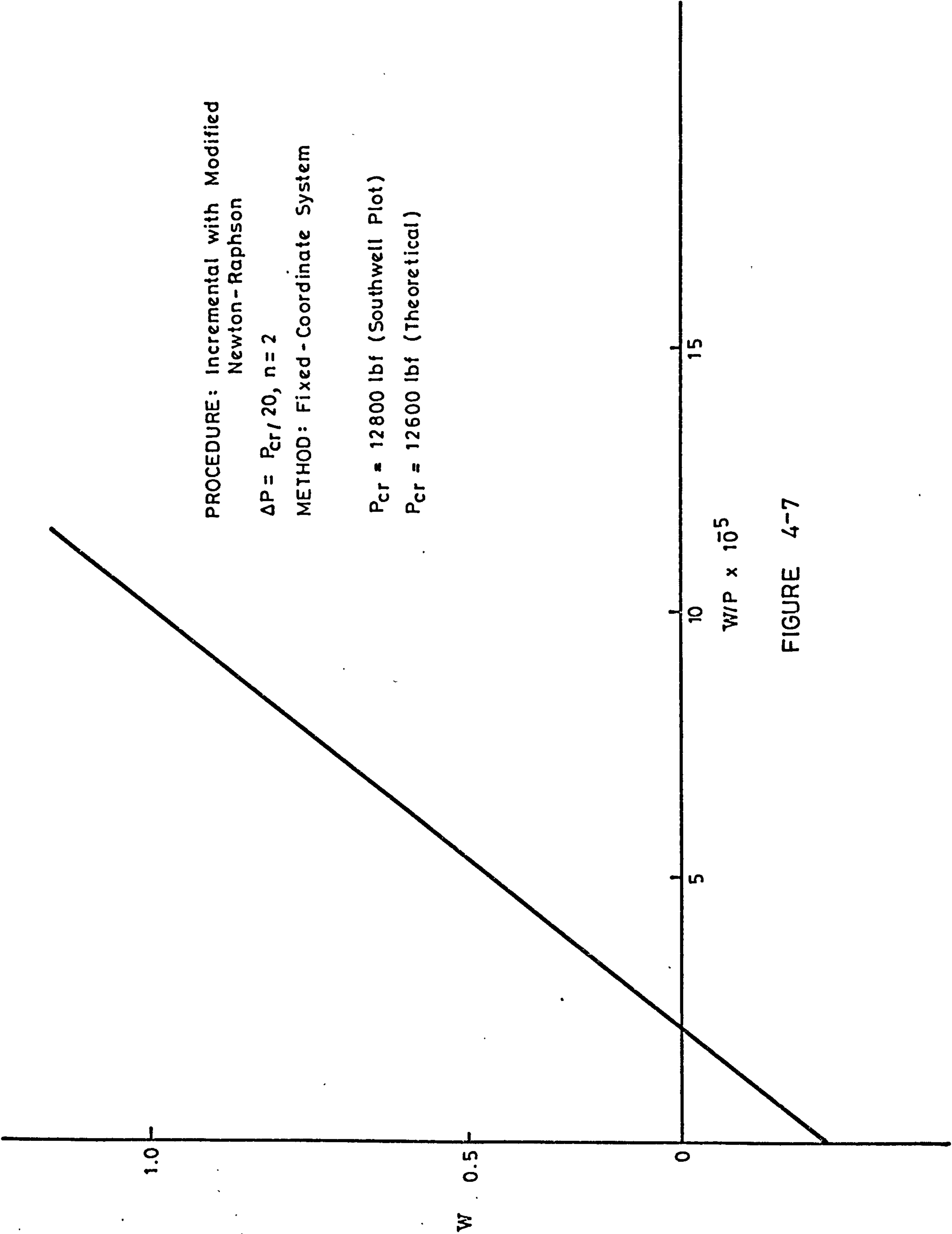


FIGURE 4-7



### 4.3 COMPARISON BETWEEN ITERATIVE AND INCREMENTAL PROCEDURES

In Figures (4-2) and (4-3), already referred to, the accuracy achieved by the purely incremental procedure in moving and fixed coordinates and by the iterative procedure, again in moving and fixed coordinates, can be compared in a representative calculation. The error in critical load obtained by the iterative method is found to be less than 1% of the theoretical buckling load, the actual figure given for the theoretical buckling load being 12600/lbf and the best computer result 12720/lbf.

Figure (4-8) compares further results obtained for the strut by the purely incremental and iterative methods (both Newton-Raphson and modified Newton-Raphson) with the theoretical result (Southwell Plot). The drift of the incremental solution is readily noticeable. The number of increments is arbitrarily chosen to be 20, but in this case, the number of iterations at each load level is controlled by accuracy; that is, when the out-of-balance forces are reduced to 2% (or less) or the load increment, the iteration cycle is terminated.

At this point, the following hypotheses are made:

- 1) Accuracy will be improved by increasing the number of increments used.
- 2) Accuracy will be improved by taking a large number of iterations.

The first hypothesis led us into an investigation of the rate of improvement with increase in the number of increments. Here we were also interested in the additional computer time required by this increase in the number of increments. As the incremental procedure is not self-correcting (see Section 3.1), some drift is expected.

The second hypothesis required a study of the best balance between the number of increments and the number of iterations. Since iteration is a corrective procedure by which as much accuracy as the finite element representation allows can be achieved, a large number of iterations, whatever the number of increments, can be used for the desired accuracy. The necessity of obtaining convergence must be considered, as well as the amount of computer time required for the solution, and it was decided that both the Newton-Raphson and the modified Newton-Raphson methods would be used to demonstrate the validity of this hypothesis.

In the purely incremental procedure (hypothesis 1) no attempt is made to check the equilibrium of the



solution obtained, the accuracy depending on the size of the load increments taken. Figure (4-9) shows the results for the strut taking 10, 20, 40, and 80 increments to reach the critical load. It shows that, as the size of the load increment reduces, the accuracy of the solution increases. These improvements are plotted on Figures (4-10), (4-11), and (4-12), where the percentage error is plotted against the number of increments at 50%, 70%, and 75% of critical load. The points for the incremental method fall in a straight line on the log scale (the uppermost line on Figures (4-10), (4-11), and (4-12) showing that the accuracy improves as a power law approximating to an index  $P = -0.56$ , i.e., the error reduces roughly as the square root of the number of increments. The exact figure for the different levels of critical load are shown on the appropriate graphs.

For the highly nonlinear problems, when convergence is more difficult, the step size may be decreased or the stiffness matrix be updated. When the strut was analyzed for 5, 10, 20, 40, and 80 load increments to reach the critical load, it was found that, using the Modified Newton-Raphson method for five increments with one iteration, convergence failed at about 40% of critical load; for 10 increments with one iteration, it failed at approximately 60%; and for 20 increments with one iteration, convergence failed at about 85% of critical load. Improvements on iteration for the modified Newton-Raphson method is shown on Figures (4-10), (4-11), and (4-12).

As in the incremental procedure, a straight line was obtained for each number of iterations, at the same fractions of critical load. The graphs show the improvement on each of the increment loads using the iterative method and it is readily apparent that the first iteration has proportionately the greatest effect. The improvement obtained by each iteration for the 20, 40, and 80 increments are shown on Figures (4-13), (4-14), and (4-15), where the difference, i.e., the improvement on initial incremental value is plotted against the number of iterations. It is observed that the pattern of improvement in the accuracy obtained for the different number of increments is similar. The values are tabulated in Tables (4-1), (4-2), and (4-3).

Since the results of the iterative procedure are so near to each other, in order to clearly show the accuracy of the different load increments with the various iterations, graph plotting was not used, but the results are tabulated with their corresponding computer mill time in the next section.

The use of the iterative procedure however, requires the user to decide at what load level the matrix should be updated, when the load increments should be changed, and so forth. If precautions are not taken, the procedure may diverge.

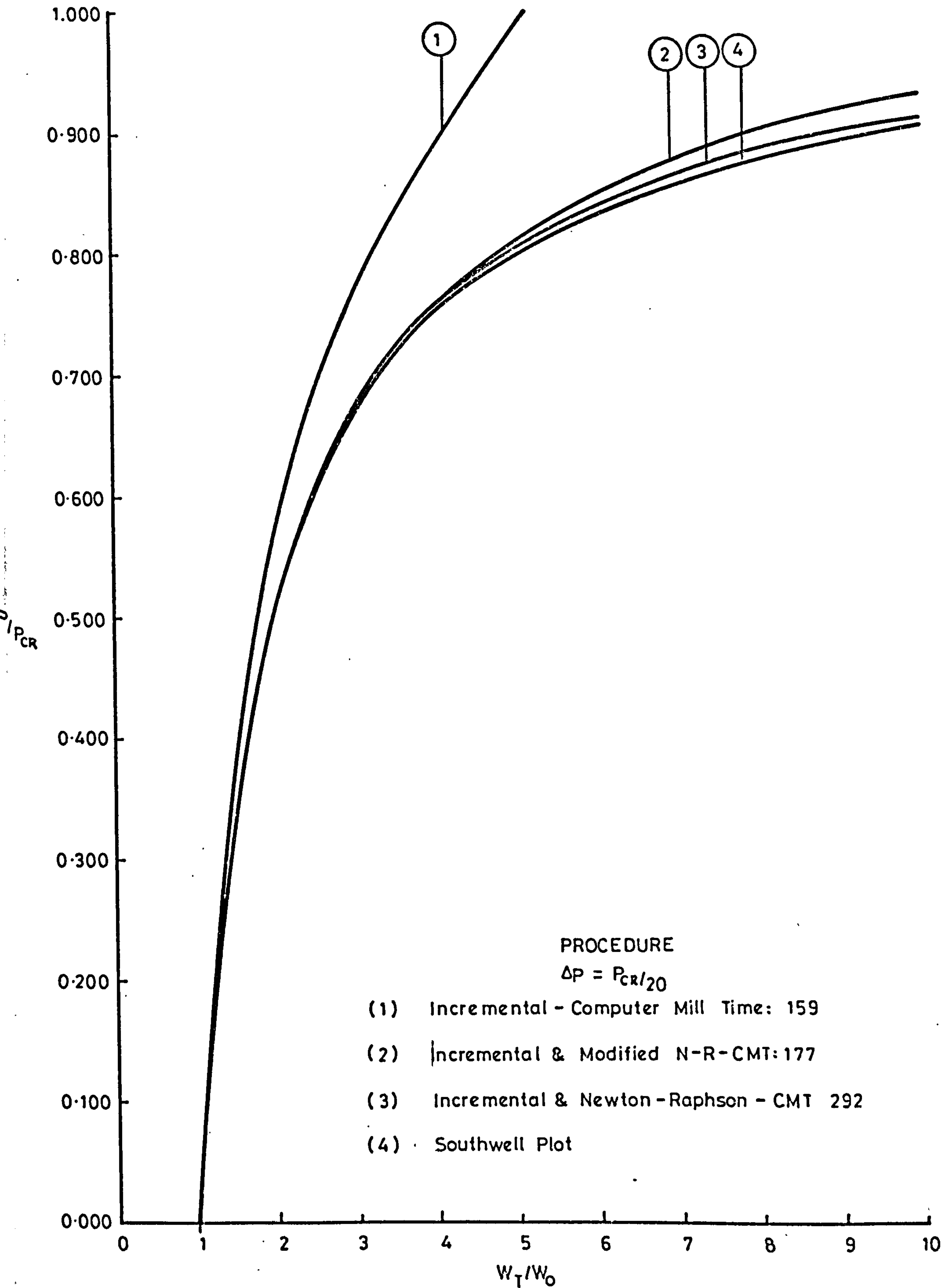


FIGURE 4-8



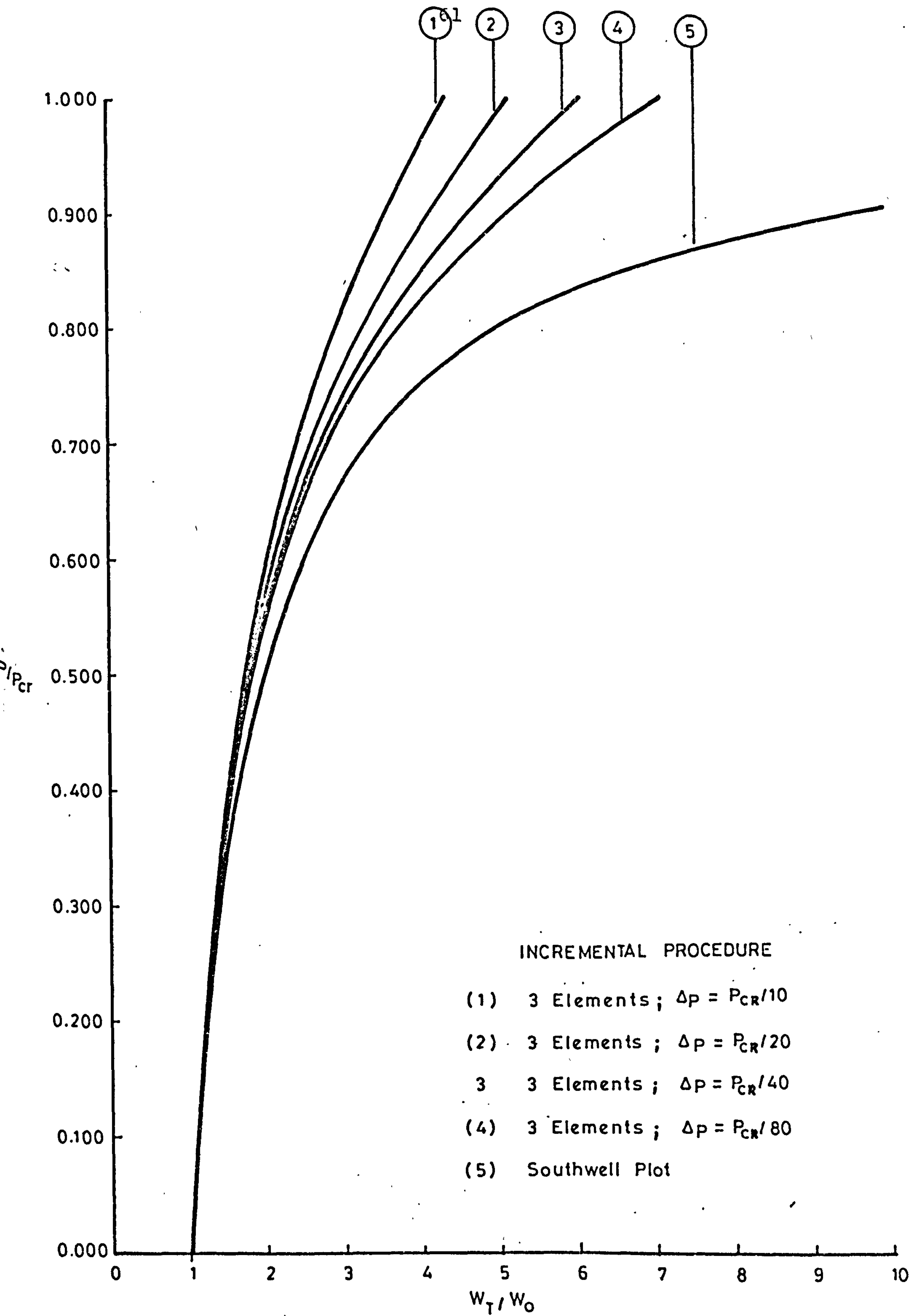


FIGURE 4-9

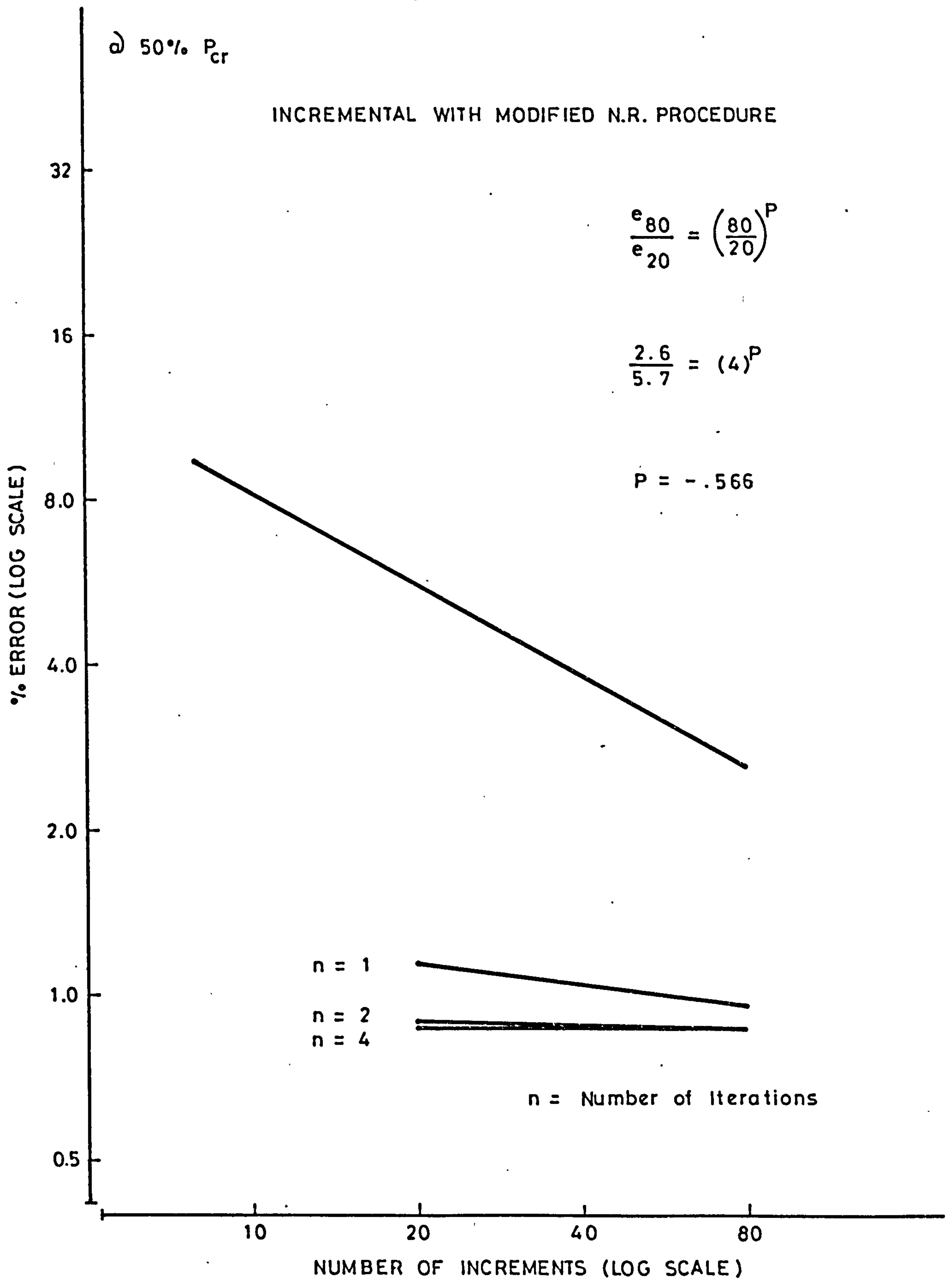


FIGURE 4-10

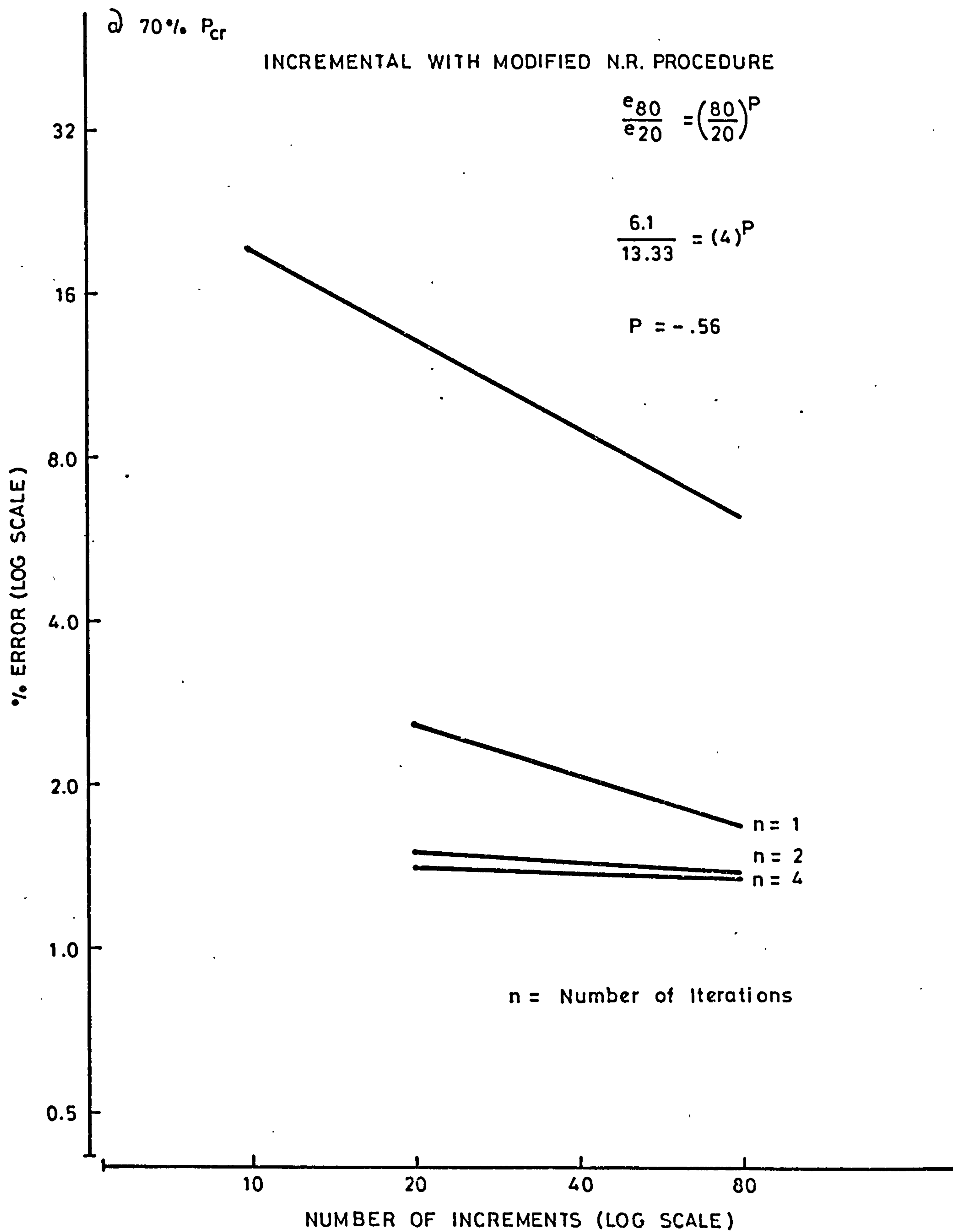


FIGURE 4-11

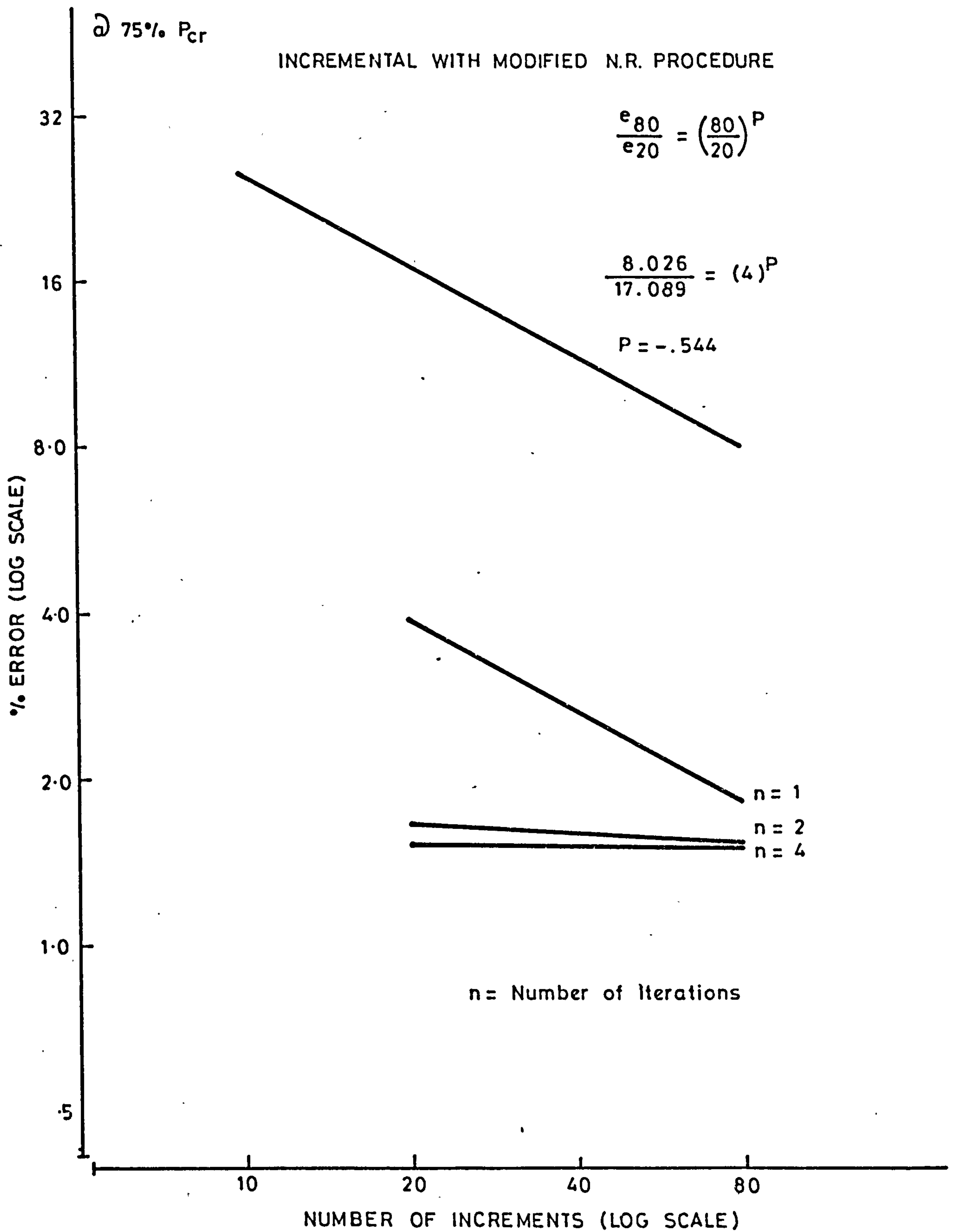


FIGURE 4:12



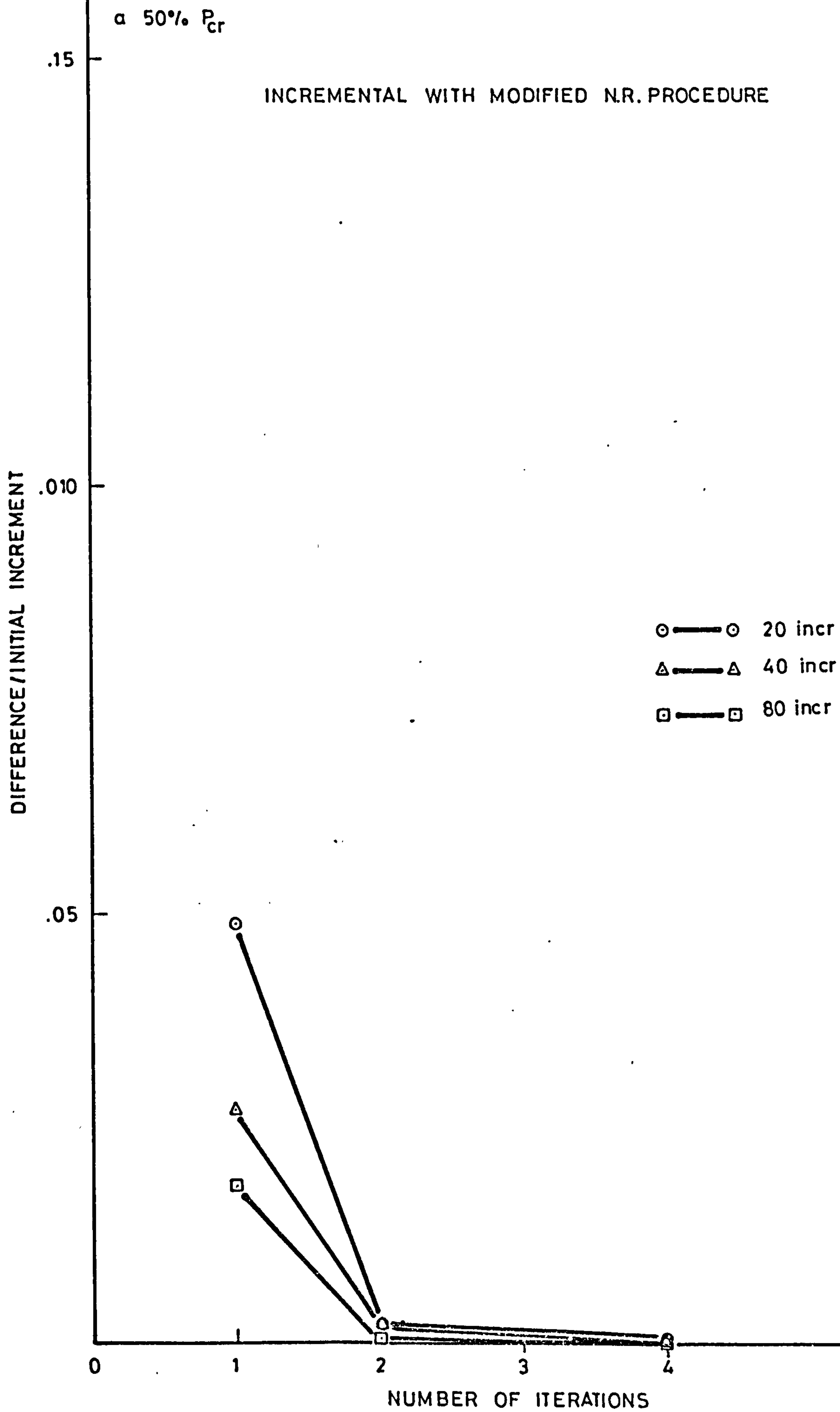


FIGURE 4-13

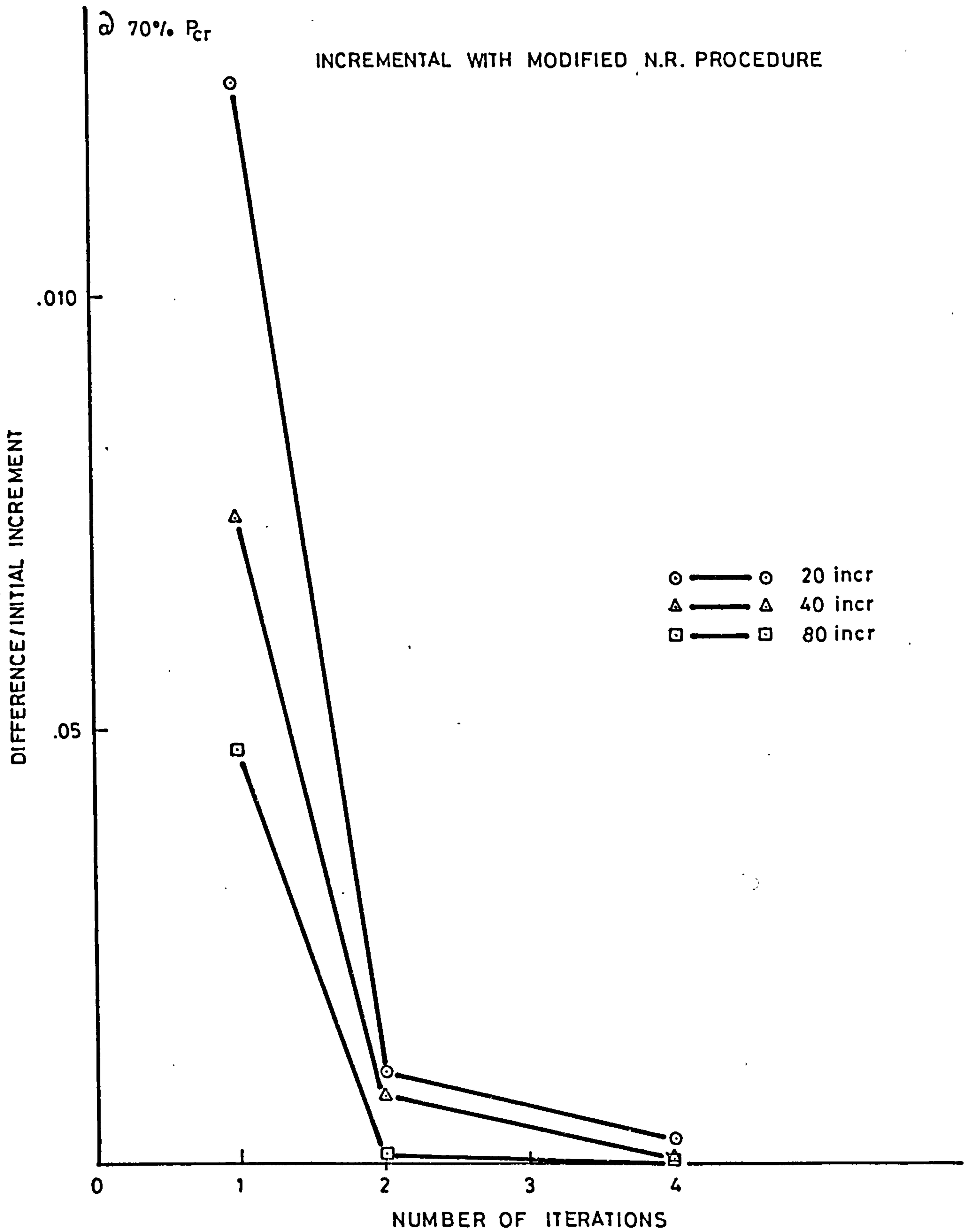


FIGURE 4-14

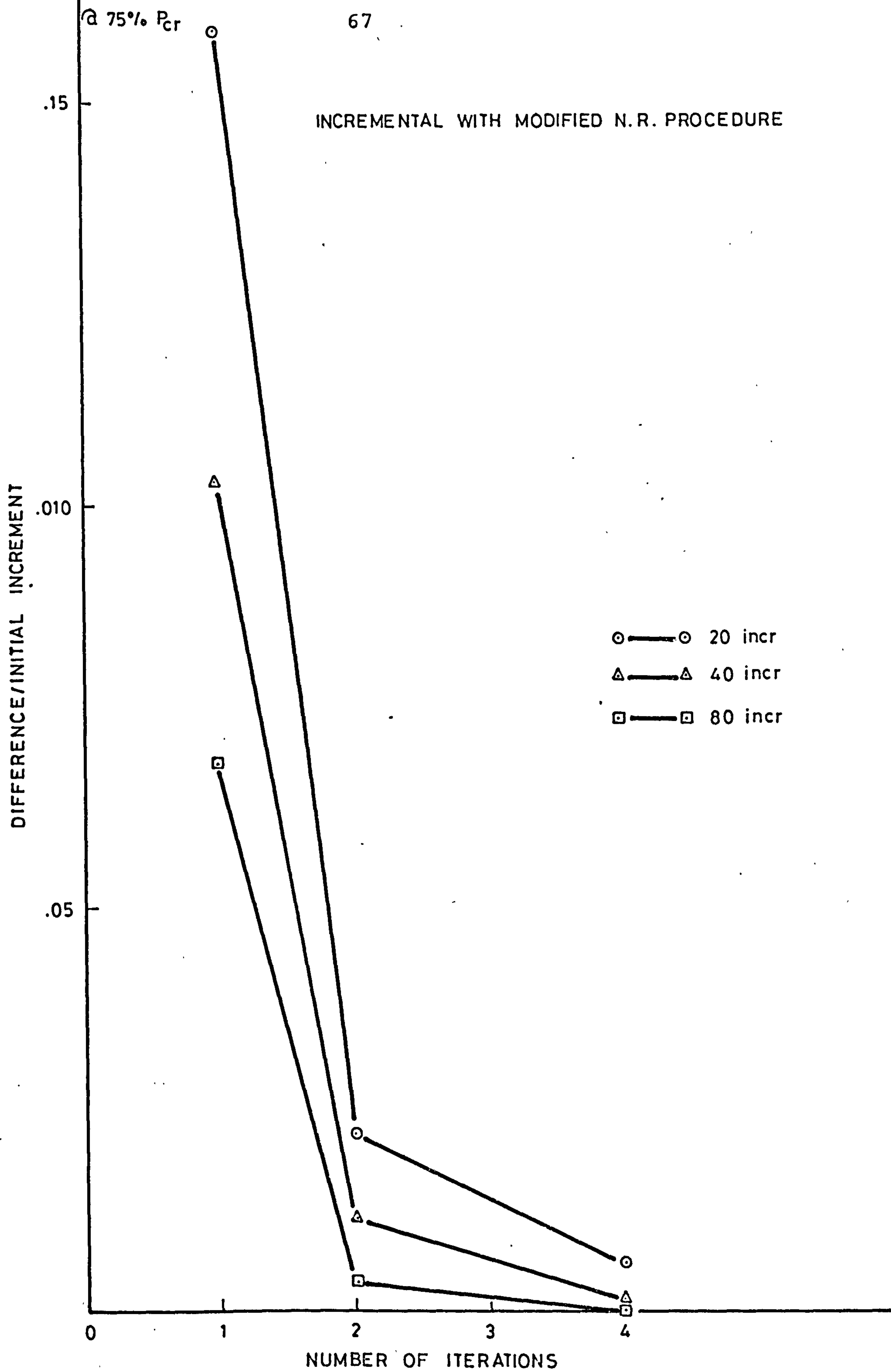


FIGURE 4-15

@ 50%  $P_{cr}$ 20 INCREMENTS

		Difference	Difference/ 1st Inc.	%
INCREMENT	0.5035			
		0.0245	0.049	4.9
1 <sup>st</sup> ITER.	0.528			
		0.001	0.002	0.2
2 <sup>nd</sup> ITER.	0.529			
		0.0003	0.00059	0.059
4 <sup>th</sup> ITER.	0.5293			

40 INCREMENTS

		Difference	Difference/ 1st Inc.	%
INCREMENT	0.514			
		0.0144	0.028	2.8
1 <sup>st</sup> ITER.	0.5284			
		0.0009	0.00175	0.175
2 <sup>nd</sup> ITER.	0.5293			
		0.0	0.0	0.0
4th ITER.	0.5293			

80 INCREMENTS

		Difference	Difference/ 1st Inc.	%
INCREMENT	0.52			
		0.009	0.017	1.7
1 <sup>st</sup> ITER.	0.529			
		0.0003	0.00058	0.058
2 <sup>nd</sup> ITER.	0.5293			
		0.0	0.0	0.0
4 <sup>th</sup> ITER.	0.5293			

TABLE (4-1)



@ 70%  $P_{cr}$ 20 INCREMENTS :

		Difference	Difference/ 1st Inc.	%
INCREMENT	0.728			
		0.09	0.124	12.4
1 <sup>st</sup> ITER.	0.818			
		0.008	0.011	1.1
2 <sup>nd</sup> ITER.	0.826			
		0.002	0.0027	0.27
4 <sup>th</sup> ITER.	0.828			

40 INCREMENTS

		Difference	Difference/ 1st Inc.	%
INCREMENT	0.765			
		0.057	0.0745	7.45
1 <sup>st</sup> ITER.	0.822			
		0.006	0.0078	0.78
2 <sup>nd</sup> ITER.	0.828			
		0.0004	0.00052	0.052
4 <sup>th</sup> ITER.	0.8284			

80 INCREMENTS

		Difference	Difference/ 1st Inc.	%
INCREMENT	0.789			
		0.038	0.048	4.8
1 <sup>st</sup> ITER.	0.827			
		0.0013	0.0016	0.16
2 <sup>nd</sup> ITER.	0.8283			
		0.0001	0.00013	0.013
4 <sup>th</sup> ITER.	0.8284			

TABLE (4-2)

@ 75%  $P_{cr}$

20 INCREMENTS

		Difference	Difference/ 1st Inc.	%
INCREMENT	0.8125			
		0.1295	0.159	15.9
1 <sup>st</sup> ITER.	0.942			
		0.018	0.022	2.2
2 <sup>nd</sup> ITER.	0.96			
		0.005	0.0061	0.61
4 <sup>th</sup> ITER.	0.965			

40 INCREMENTS

		Difference	Difference/ 1st Inc.	%
INCREMENT	0.865			
		0.089	0.103	10.3
1 <sup>st</sup> ITER.	0.954			
		0.01	0.0116	1.16
2 <sup>nd</sup> ITER.	0.964			
		0.001	0.00116	0.116
4 <sup>th</sup> ITER.	0.965			

80 INCREMENTS

		Difference	Difference/ 1st Inc.	%
INCREMENT	0.901			
		0.061	0.068	6.8
1 <sup>st</sup> ITER.	0.962			
		0.003	0.0033	0.33
2 <sup>nd</sup> ITER.	0.965			
		0.00002	0.000022	0.0022
4 <sup>th</sup> ITER.	0.96502			

TABLE (4-3)

## 4.4 COMPUTER TIME AND ACCURACY

A primary concern in structural analysis by computer is the amount of computer time required, the attempt always being made to find a more accurate solution for less computer time. In all the previously described approaches, both incremental and iterative, and with moving and fixed coordinate systems, the relationship between computer time and accuracy must be considered.

Computer mill time as well as accuracy is found to vary considerably among the various solution techniques. To illustrate this point, the total mill time consumed by each method is shown against the appropriate graphs in Figure (4-8), already referred to.

In order to investigate more systematically the computer time taken by various parts of the program, and to obtain an efficient solution technique, the four main stages of the program may be defined as follows:

- 1) Compilation
- 2) Incremental solution
- 3) Iteration (Modified Newton-Raphson)
- or 4) Iteration (Newton-Raphson).

Stage 1 is the compilation of the program which is common to all procedures.

Stage 2 consists of calling various subroutines to perform assembly of the stiffness matrix, transformation of coordinates (in the case of the moving coordinate system), inversion of the stiffness matrix and finally obtaining the incremental displacements by multiplying the inverse matrix by the load vector.

Stage 3 is the iterative procedure, which determines the out-of-balance forces by multiplying the stiffness matrix for each element by the current displacements, and subtracting the result from the load vector. It then determines displacements due to these residual forces, by multiplying the already stored inverse stiffness matrix by the out-of-balance forces.

Stage 4, which is alternative to Stage 3, finds the out-of-balance forces and multiplies the updated inverse stiffness matrix by these residual forces. Obtaining the updated inverse stiffness matrix involves calling subroutines to reassemble the stiffness matrix, to perform the coordinate transformation (in the case of moving coordinates), and to invert the assembled stiffness matrix.



A standard time routine was used to examine the computer time for each stage of the program. This routine is set up to give the mill time to the nearest whole number, and since some subroutines in the program use much less than one unit of mill time, those subroutines were artificially repeated one hundred times, regardless of the actual results of the program.

The results for each stage of the program are shown in the following table:

	Compilation	Incremental Solution	Iterational Mod. N-R.	Iterational N-R.
Computer Mill Time	27	6.60	0.15	6.65

TABLE (4-4)

Relatively, the computer time involved in other operations in the program including input of data and output of results, is small enough to be ignored.

In the previous section (4.3), it was shown that for the purely incremental procedure, as the number of increments increases, the accuracy continuously improves. Figures (4-10), (4-11), and (4-12) show that the error reduces approximately as the square root of the number of increments. Since, according to Table (4-4), each increment takes 6.6 mill time, the desired level of accuracy can be related to the computer time required.

In the incremental procedure with iteration, there are two ways of improving the accuracy; either by increasing the number of load increments, or by increasing the number of iterations. In the Modified Newton-Raphson method, the computer time involved for each iteration is comparatively small. Referring to Table (4-4), it appears by reducing the number of load increments while increasing the number of iterations, considerable computer time can be saved. In this case however, precautions must be taken to prevent divergence. In the Newton-Raphson method, computer time is significantly greater than in the modified Newton-Raphson method because the stiffness matrix is updated and the assembled matrix inverted. Since the Newton-Raphson procedure could be interpreted at each iteration as an incremental procedure with no applied load increment, there is no danger of divergence, and any number



of increments could be chosen. The optimum number of increments and number of iterations with respect to computer time could be deducted from Table (4-4) and Tables (4-5), (4-6), (4-7), (4-8), and (4-9), where the percent error and computer time for the incremental and iterative procedures with one, two and four iterations are tabulated at 50%, 70%, and 75% of  $P_{cr}$ .

To illustrate the relationship between time and accuracy in a specific example, the computer program was run first for the incremental procedure with an arbitrary number of increments, and second for the incremental procedure with iterations, where the number of increments and number of iterations were arranged from Table (4-4) to give the same amount of computer mill time. It must be mentioned that normally, recorded computer mill time fluctuates within one unit of mill time. The computer mill time for the incremental procedure was recorded as 185, and for the iterative method as 184. Figure (4-16), the result of these two procedures requiring computer time, shows that the iterative procedure is more accurate than the incremental method, using the same computer effort.

Briefly, the iterational process consists of two parts, the first of which finds the out-of-balance forces and the second of which finds the displacement due to these residual forces. In an attempt to reduce computer time, the so-called "carry over out of balance forces" method was examined. This method, which performs the initial half of the iteration process, carries the out-of-balance forces to the next step load as applied incremental load without executing any iterations, thereby presumably reducing computer time.

The case was also examined where, after the iterational process, the residual forces in one load step were introduced as a pseudo-load in the next step load in order to gain better accuracy.

However, as the computer time for the initial phase (the out-of-balance forces) requires twice as much computer time as the second phase (displacement due to residual forces), it was found that it is more efficient to use the complete iterational procedure as it requires less computer time.

The displacement error is considered as:

$$\text{error} = \frac{\text{Theoretical (Southwell Plot)} - \text{Computer result}}{(\text{Theoretical result})}$$

The relationship between time and accuracy was also investigated for the fixed and moving coordinate systems. As shown in Section 4.2, the results for the fixed coordinate system are similar to those for the moving coordinate system. However, the fixed coordinate system is a much simpler technique than the moving coordinate system, and it also uses less computer time because there is no coordinate transformation involved. Table (4-10) shows the computer time for different procedures with their respective number of increments and per cent error at 75% of  $P_{cr}$ . It must be observed that the difference in computer mill time for moving and fixed coordinate systems is only for the three element model, and by considering bigger problems with more degrees of freedom, the distinction will obviously be relatively more apparent.

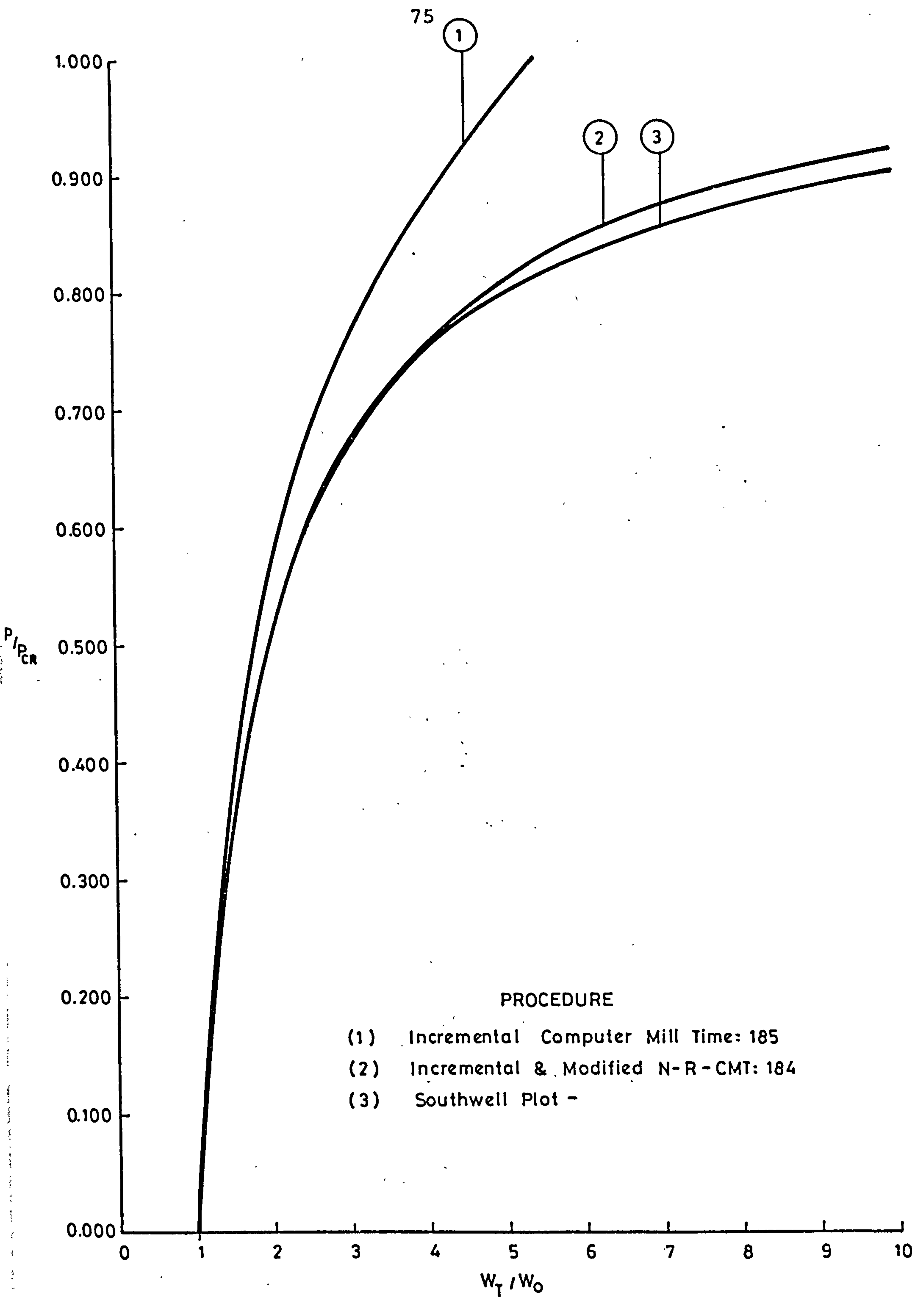


FIGURE 4-16

50%  $P_{cr}$ 

## INCREMENTAL AND MODIFIED NEWTON-RAPHSON

$P_{cr}/\Delta P$		Incremental Procedure	1st Iter.	2nd Iter.	4th Iter.
10	% error	9	3.1	1.65	.95
	Time (CMT)	60	61	62	63
20	% error	5.7	1.14	.91	.88
	Time (CMT)	93	95	96	99
40	% error	3.7	1.04	.883	.88
	Time (CMT)	159	162	165	171
80	% error	2.6	.96	.881	.88
	Time (CMT)	291	297	303	315

TABLE (4-5)

70%  $P_{cr}$ 

## INCREMENTAL AND MODIFIED NEWTON-RAPHSON

$P_{cr}/\Delta P$		Incremental Procedure	1st Iter.	2nd Iter.	4th Iter.
10	% error	19.78			
	Time (CMT)	73			
20	% error	13.33	2.59	1.5	1.42
	Time (CMT)	119	121	123	127
40	% error	8.92	2.1	1.42	1.384
	Time (CMT)	212	216	220	229
80	% error	6.1	1.68	1.39	1.38
	Time (CMT)	397	405	414	431

TABLE (4-6)



75%  $P_{cr}$ 

## INCREMENTAL AND MODIFIED NEWTON-RAPHSON

$P_{cr}/\Delta P$		Incremental Procedure	1st Iter.	2nd Iter.	4th Iter.
20	% error	17.089	3.87	1.65	1.535
	Time (CMT)	126	128	131	136
40	% error	11.714	2.612	1.599	1.532
	Time (CMT)	225	230	235	244
80	% error	8.026	1.82	1.535	1.528
	Time (CMT)	423	433	442	461

TABLE (4-7)

70%  $P_{cr}$ 

## NEWTON-RAPHSON

$P_{cr}/\Delta P$			1st Iter.	2nd Iter.	4th Iter.
10	% error		8.84		
	Time (CMT)		116		

TABLE (4-8)

75%  $P_{cr}$ 

## NEWTON-RAPHSON

$P_{cr}/\Delta P$			1st Iter.	2nd Iter.	4th Iter.
1	% error				1.625
	Time (CMT)				60.2

TABLE (4-9)

85%  $P_{cr}$ 

Type	Procedure	% error	$P_{cr}/P$	Mill Time
Moving (Consistent $K_G$ )	Incremental	22	20	140
Moving (String Stiffness)	Incremental	23	20	138
Fixed	Incremental	23	20	127
Moving (Consistent $K_G$ )	Modified Newton-Raphson	24	20	146
Fixed	Modified Newton-Raphson	26	20	132

TABLE (4-10)

## 4.5 REMARKS AND RECOMMENDATIONS

The purpose of this chapter has been to compare the methods of solution (incremental and iterative) as well as to evaluate the procedure for a geometrically nonlinear problem using a strut as a model. The results are, of course, specific to the model chosen, but it is considered that the following comments on the recommended choice of solution technique apply very generally to the incremental and iterative processes.

By the modified Newton-Raphson method, iteration is shown to be both a very powerful and an economical means of correcting the solution at each increment of load. Since most of the correcting is achieved by the first iteration, and after the second iteration the error in deflection (as a percentage of the deflection in that load increment) appears frequently to be less than 0.1%, there is generally little purpose in proceeding beyond two iterations. At the same time, the computer mill time for each modified Newton-Raphson iteration is only about 2% of that for the incremental stage of the solution. By iteration, therefore, an accurate solution of the nonlinear problem (at least as accurate as the finite element model itself will permit) is readily available.

On the other hand, improving the accuracy simply by decreasing the load increment size is likely to be very expensive in terms of computer time, since to halve the error requires roughly four times the number of load increments and consequently, four times the computer time.

To obtain the most efficient use of computer time, it is recommended that the minimum number of load increments be used; i.e., by taking the minimum number of points necessary to obtain a suitable plot of load against deflection, while insuring that convergence is maintained.

In order to get an accurate result, it is recommended that the option in the computer program for an accuracy test, which stops the iteration cycle when the desired accuracy is obtained at each load increment, be used. However, if the complete curve of load-deflection is not required, or if deflections are needed at one (or only a few) loads, a single increment (or a few increments) of load, with the Newton-Raphson iteration might be more efficient than the modified process.

In view of the relatively small amount of computer time required for modified Newton-Raphson iteration, the policy of carry over of residual forces into the next increment of load without actually completing the iteration is not recommended.



The loss of accuracy involved in the use of the fixed coordinate system is very small compared with the moving coordinate system. Since there is a considerable simplification in the formulation of the element stiffness for the fixed coordinate system, and also less computer effort is necessary because of lack of coordinate transformation, it is recommended that the fixed coordinate system be used.

For bigger problems, such as a plate, which obviously has more elements as well as more degrees of freedom per node, there is a corresponding increase in computer time consumption. However, as the greater part of the computer effort for the incremental method is for the stiffness inversion process, according to the standard inversion routine (NAG Manual, Ref. 62), the time taken for the routine is approximately proportional to  $M^3$ , where  $M$  is the order of assembled stiffness matrix. On the other hand, modified Newton-Raphson iteration is basically a multiplication of a square matrix by a column matrix, in which the computer time roughly follows the square law  $M^2$ , so that the advantage of the modified Newton-Raphson procedure over the purely incremental is likely to become greater with increasing problem size.



FINITE ELEMENT METHOD -  
APPLICATION TO PLATE PROBLEM

## 5.1 PRE- AND POST-BUCKLING ANALYSIS OF PLATES

If the deflection of a plate is of the order of magnitude of its thickness (but is still small compared to its other dimensions) the analysis of the problem must include the strain of the middle plane of the plate. Classical formulation of this problem leads to a set of nonlinear partial differential equations which are characterized by the coupling of the dependent variables describing the membrane and bending behaviour of the plate. These equations are difficult to solve. Several methods have been used to solve the large deflection problems, some of which used the Ritz energy method with polynomials satisfying the boundary conditions, and others employed the double Fourier series to solve the governing equations for rectangular plate by evaluating coefficients.

It is known that Cox (Ref. 64) proposed a very successful energy method for analysis of the geometrically nonlinear problems of elastic plates, whose basic equations were originally derived by von Karman (Ref. 26). Numerical calculation in this method, however, is so laborious that problems of simple plate shapes, boundary conditions, and loading conditions could only be considered after high-speed digital computers became available.

An alternative approach to these problems is available by the use of the finite element method. This method formulates the problem in terms of simple physical concepts and achieves the numerical solutions without directly dealing with the complex differential equations. The analysis of large displacement and stability problems by the use of finite elements has attracted considerable attention in recent years. A variety of analysis methods has been developed, which could be divided into four categories.

The first category is based on formulating the equilibrium equation in linear matrix form and approximating the geometrically nonlinear behaviour by a step-by-step linear incremental approach. In the second category, mathematical iterative techniques are applied to the governing nonlinear equations. The third category involves applying a direct search technique to the potential energy functional. The fourth category employs an approximate incremental stiffness matrix and solves the linearized incremental equilibrium equations by iterative method. The procedure is iterative as well as incremental.

A finite element procedure for predicting large deflection, pre- and post-buckling behaviour of thin elastic plates with initial imperfections is considered here.

The element nonlinear stiffness formulations are derived on the basis of von Karman's assumptions of large deflection of plate and by the use of the minimum potential energy principle. The stiffness matrices thus obtained include the basic linear stiffness matrix and the zero-, first-, and second-order incremental stiffness matrices. Since the incremental stiffness matrices are given in terms of the geometry of the undeformed element, they require no coordinate transformation.

## 5.2 NONLINEAR THEORY

The problem may be presented mathematically as the solution of the von Karman large deflection differential equations:

$$\frac{\partial^4 F}{\partial x^4} + 2 \frac{\partial^4 F}{\partial x^2 \partial y^2} + \frac{\partial^4 F}{\partial y^4} = E \left[ \left( \frac{\partial^2 w}{\partial x \partial y} \right)^2 - \frac{\partial^2 w}{\partial x^2} \frac{\partial^2 w}{\partial y^2} \right] \quad (5-1)$$

$$\begin{aligned} \frac{\partial^4 w}{\partial x^4} + 2 \frac{\partial^4 w}{\partial x^2 \partial y^2} + \frac{\partial^4 w}{\partial y^4} = & \frac{q}{D} + \frac{t}{D} \left( \frac{\partial^2 F}{\partial y^2} \frac{\partial^2 w}{\partial x^2} + \frac{\partial^2 F \partial^2 w}{\partial x^2 \partial y^2} - \right. \\ & \left. 2 \frac{\partial^2 F}{\partial x \partial y} \frac{\partial^2 w}{\partial x \partial y} \right) \end{aligned} \quad (5-2)$$

where  $D$  is flexural rigidity of a plate

$$D = \frac{Et^3}{12(1-\nu^2)} \quad (5-3)$$

If the longitudinal, transverse, and normal displacements at a point in the middle surface of the plane are  $u$ ,  $v$ , and  $w$  ( $w_0$  = initial displacement), it can be shown that the total strain in the  $x$  - direction of the element, taken in the middle plane of the plate is given by:

$$\begin{aligned} \epsilon_x &= \frac{\partial u}{\partial x} + \frac{1}{2} \left[ \frac{\partial (w+w_0)}{\partial x} \right]^2 - \frac{1}{2} \left( \frac{\partial w_0}{\partial x} \right)^2, \\ \epsilon_y &= \frac{\partial v}{\partial y} + \frac{1}{2} \left[ \frac{\partial (w+w_0)}{\partial y} \right]^2 - \frac{1}{2} \left( \frac{\partial w_0}{\partial y} \right)^2, \\ \epsilon_{xy} &= \frac{\partial u}{\partial y} + \frac{\partial v}{\partial x} + \frac{\partial (w+w_0)}{\partial x} \frac{\partial (w+w_0)}{\partial y} - \frac{\partial w_0}{\partial x} \frac{\partial w_0}{\partial y}. \end{aligned} \quad (5-4)$$

The left side of Equation (5-2) is obtained from expressions for bending and twisting moments; and, since the moments depend not on the total displacement, but only on the change in displacement of the plate, the net deflection  $W$ , instead of the total deflection ( $w + w_0$ )



should be used on the left side for plates with initial displacements. The right side of the Equation (5-2) gives the combined effect of the normal load  $q$  and forces in the plane of the plates; and, since the effect of the forces in the plane of the plates depends on the total deflection  $(w + w_0)$ , the right side of Equation (5-2) remains unchanged for plates with initial imperfections.

Therefore, the equations of equilibrium for a plate with initial imperfections becomes

$$\frac{\partial^4 F}{\partial x^4} - 2 \frac{\partial^4 F}{\partial x^2 \partial y^2} + \frac{\partial^4 F}{\partial y^4} = E \left\{ \left[ \frac{\partial^2 (w + w_0)}{\partial x \partial y} \right]^2 - \frac{\partial^2 (w + w_0)}{\partial x^2} \frac{\partial^2 (w + w_0)}{\partial y^2} - \left( \frac{\partial^2 w_0}{\partial x \partial y} \right) - \frac{\partial^2 w_0}{\partial x^2} \frac{\partial^2 w_0}{\partial y^2} \right\} \quad (5-5)$$

$$\frac{\partial^4 w}{\partial x^4} + 2 \frac{\partial^4 w}{\partial x^2 \partial y^2} + \frac{\partial^4 w}{\partial y^4} = \frac{q}{t} + \frac{t}{D} \left[ \frac{\partial^2 F}{\partial y^2} \frac{\partial^2 (w + w_0)}{\partial x^2} + \frac{\partial^2 F}{\partial x^2} \frac{\partial^2 (w + w_0)}{\partial y^2} - 2 \frac{\partial^2 F}{\partial x \partial y} \frac{\partial^2 (w + w_0)}{\partial x \partial y} \right] \quad (5-6)$$

The middle-surface stresses are

$$\sigma_x = \frac{\partial^2 F}{\partial y^2}, \quad \sigma_y = \frac{\partial^2 F}{\partial x^2}, \quad \tau_{xy} = \frac{\partial^2 F}{\partial x \partial y}. \quad (5-7)$$

Subsequently, the middle surface strains can be shown to be

$$\begin{aligned} \epsilon_x &= \frac{1}{E} (\sigma_x - \nu \sigma_y) \\ \epsilon_y &= \frac{1}{E} (\sigma_y - \nu \sigma_x) \\ \epsilon_{xy} &= \frac{2(1+\nu)}{E} \tau_{xy} \end{aligned} \quad (5-8)$$

Equations (5-5) and (5-6) are the basic simultaneous equations governing the elastic behaviour of the plate. Together with the boundary conditions, they can be used to find  $F$  and  $w$ , and the stresses can be found from Equation (5-7). The disadvantage of the basic

equations lies in their being fourth order, nonlinear, and in their being no rigorous solutions available. Because of the difficulty in solving the large deflection equations, the post-buckling behaviour of elastic plates is normally examined by an approximate method, and the energy solution.

To formulate the necessary analysis for pre- and post-buckling of plates, the strain energy of the element during buckling and the potential energy of the applied in-plane load, are now calculated. Finite element procedure is then followed to obtain the elastic and incremental stiffness for the non-conforming shape functions. The post-buckled displacements and stiffness are then obtained for different boundary conditions.

### 5.3 FORMULATION OF INCREMENTAL STIFFNESS EQUATION

The total potential energy  $\Pi$  of a deformed plate with initial deflection of the order of magnitude of thickness and with the same order additional bending deflection is defined as

$$\Pi = U - W \quad (5-9)$$

where  $U$  is the potential energy of deformation and  $W$  is the potential energy of external loading.

The state of equilibrium of a deformed plate can be characterized as that for which the first variation of the total potential energy of the system is equal to zero,

$$\delta\Pi = \delta U - \delta W = 0$$

or

$$\delta U = \delta W \quad (5-10)$$

If the functions for  $U$  and  $W$  are formed, the equation of equilibrium can be obtained by executing the variation as indicated by Equation (5-10).

The potential energy of the external load is

$$W = P_i q_i \quad (5-11)$$

where  $P_i$  is the external load and  $q_i$  is the displacement.

The potential energy of deformation for a plate element with large deflection written in terms of the deflection and the strain of the middle surface (Ref. 65) is:

$$U = \left(\frac{D}{2}\right) \iint \left\{ \left[ (\nabla^2 w)^2 + \left(\frac{12}{t^2}\right) e_1^2 \right] - 2(1-\nu) \left[ \left(\frac{12}{t^2}\right) e_2^2 + \left(\frac{\partial^2 w}{\partial x^2}\right) \left(\frac{\partial^2 w}{\partial y^2}\right) - \left(\frac{\partial^2 w}{\partial x \partial y}\right)^2 \right] \right\} dx dy, \quad (5-12)$$

In which

$$\begin{aligned} e_1 &= \epsilon_x + \epsilon_y, \\ e_2 &= \epsilon_x \epsilon_y - \frac{1}{4} \epsilon_{xy}^2, \end{aligned} \quad (5-13)$$

and  $t$  is the plate thickness.

Upon substitution of strain displacement relations of Equation (5-4) into Equation (5-13), and integration through thickness, the strain energy expression of Equation (5-12) becomes

$$U = U_k + U_0 + U_1 + U_2 \quad (5-14)$$

where

$$\begin{aligned} U_k &= \frac{D}{2} \iint \left\{ (\nabla^2 w)^2 + \frac{12}{t^2} \left( \frac{\partial u}{\partial x} + \frac{\partial v}{\partial y} \right)^2 - 2(1-\nu) \left[ \frac{\partial^2 w}{\partial x^2} \frac{\partial^2 w}{\partial y^2} \right. \right. \\ &\quad \left. \left. - \left( \frac{\partial^2 w}{\partial x \partial y} \right)^2 + \frac{12}{t^2} \frac{\partial u}{\partial x} \frac{\partial v}{\partial y} - \frac{3}{t^2} \left( \frac{\partial u}{\partial y} + \frac{\partial v}{\partial x} \right)^2 \right] \right\} dx dy \end{aligned} \quad (5-15)$$

$$\begin{aligned} U_0 &= -\frac{3D}{2t^2} \iint \left\{ \left( \frac{\partial w_0}{\partial x} \right)^4 + \left( \frac{\partial w_0}{\partial y} \right)^4 - 4 \left( \frac{\partial w}{\partial x} \right)^2 \left( \frac{\partial w_0}{\partial x} \right)^2 - \right. \\ &\quad 4 \left( \frac{\partial w}{\partial y} \right)^2 \left( \frac{\partial w_0}{\partial y} \right)^2 + 2\nu \left( \frac{\partial w}{\partial x} \right)^2 \left( \frac{\partial w_0}{\partial y} \right)^2 + 4\nu \left( \frac{\partial w}{\partial x} \right) \left( \frac{\partial w_0}{\partial x} \right) \left( \frac{\partial w_0}{\partial y} \right)^2 \\ &\quad + 2\nu \left( \frac{\partial w_0}{\partial y} \right)^2 \left( \frac{\partial w_0}{\partial x} \right)^2 + 2\nu \left( \frac{\partial w}{\partial y} \right)^2 \left( \frac{\partial w_0}{\partial x} \right)^2 + 4\nu \left( \frac{\partial w}{\partial y} \right) \left( \frac{\partial w_0}{\partial y} \right) \left( \frac{\partial w_0}{\partial x} \right)^2 \\ &\quad + 2\nu \left( \frac{\partial w_0}{\partial x} \right)^2 \left( \frac{\partial w_0}{\partial x} \right)^2 - 4 \frac{\partial u}{\partial x} \left( \frac{\partial w_0}{\partial x} \right)^2 - 4 \frac{\partial v}{\partial y} \left( \frac{\partial w_0}{\partial y} \right)^2 - \\ &\quad 8 \left( \frac{\partial u}{\partial x} \right) \left( \frac{\partial w}{\partial x} \right) \left( \frac{\partial w_0}{\partial x} \right) - 8 \left( \frac{\partial v}{\partial y} \right) \left( \frac{\partial w}{\partial y} \right) \left( \frac{\partial w_0}{\partial y} \right) - 4\nu \frac{\partial v}{\partial y} \left( \frac{\partial w_0}{\partial x} \right)^2 - \\ &\quad 4\nu \frac{\partial u}{\partial x} \left( \frac{\partial w_0}{\partial y} \right)^2 - 8\nu \frac{\partial v}{\partial y} \left( \frac{\partial w}{\partial x} \right) \left( \frac{\partial w_0}{\partial x} \right) - 8\nu \left( \frac{\partial u}{\partial x} \right) \left( \frac{\partial w}{\partial y} \right) \left( \frac{\partial w_0}{\partial y} \right) - \\ &\quad \left. 4(1-\nu) \left( \frac{\partial u}{\partial y} + \frac{\partial v}{\partial x} \right) \left[ \left( \frac{\partial w}{\partial x} \right) \left( \frac{\partial w_0}{\partial y} \right) + \left( \frac{\partial w}{\partial y} \right) \left( \frac{\partial w_0}{\partial x} \right) + \left( \frac{\partial w_0}{\partial x} \right) \left( \frac{\partial w_0}{\partial y} \right) \right] \right\} \end{aligned}$$

(Cont'd)



$$\begin{aligned}
& - 2 \left( \frac{\partial w}{\partial x} \right)^2 \left( \frac{\partial w_0}{\partial y} \right)^2 - 8 \left( \frac{\partial w}{\partial x} \right) \left( \frac{\partial w}{\partial y} \right) \left( \frac{\partial w_0}{\partial x} \right) \left( \frac{\partial w_0}{\partial y} \right) \\
& - 4 \left( \frac{\partial w}{\partial x} \right) \left( \frac{\partial w_0}{\partial x} \right) \left( \frac{\partial w_0}{\partial y} \right)^2 - 2 \left( \frac{\partial w}{\partial x} \right)^2 \left( \frac{\partial w_0}{\partial y} \right)^2 \\
& - 4 \left( \frac{\partial w}{\partial y} \right) \left( \frac{\partial w_0}{\partial y} \right) \left( \frac{\partial w_0}{\partial x} \right)^2 - 4 \left( \frac{\partial w_0}{\partial x} \right)^2 \left( \frac{\partial w_0}{\partial y} \right)^2 \\
& + 2(1-\nu) \frac{\partial w_0}{\partial x} \frac{\partial w_0}{\partial y} \left( \frac{\partial w}{\partial x} + \frac{\partial w_0}{\partial x} \right) \left( \frac{\partial w}{\partial y} + \frac{\partial w_0}{\partial y} \right) \} \, dx dy
\end{aligned} \tag{5-16}$$

$$\begin{aligned}
U_1 = \frac{6D}{t^2} \iint & \left\{ \left( \frac{\partial u}{\partial x} + \nu \frac{\partial v}{\partial y} \right) \left( \frac{\partial w}{\partial x} \right)^2 + \left( \frac{\partial v}{\partial y} + \nu \frac{\partial u}{\partial x} \right) \left( \frac{\partial w}{\partial y} \right)^2 \right. \\
& + (1-\nu) \left( \frac{\partial u}{\partial y} + \frac{\partial v}{\partial x} \right) \frac{\partial w}{\partial x} \frac{\partial w}{\partial y} + \left( \frac{\partial w}{\partial x} \right)^3 \left( \frac{\partial w_0}{\partial x} \right) \\
& + \left( \frac{\partial w}{\partial y} \right)^3 \left( \frac{\partial w_0}{\partial y} \right) + \left( \frac{\partial w}{\partial x} \right)^2 \left( \frac{\partial w}{\partial y} \right) \left( \frac{\partial w_0}{\partial y} \right) \\
& \left. + \left( \frac{\partial w}{\partial y} \right)^2 \left( \frac{\partial w}{\partial x} \right) \left( \frac{\partial w_0}{\partial x} \right) \right\} \, dx dy
\end{aligned} \tag{5-17}$$

$$U_2 = \frac{3D}{2t^2} \iint \left[ \left( \frac{\partial w}{\partial x} \right)^2 + \left( \frac{\partial w}{\partial y} \right)^2 \right]^2 \, dx dy \tag{5-18}$$

The derivative of initial deflection  $w_0$  (constant slopes) are zero-order terms which do not contribute to the stiffness matrices; therefore, terms such as the following could be neglected from the above energy expression:

$$\frac{1}{4} \left( \frac{\partial w_0}{\partial x} \right)^4, \quad \frac{\partial u}{\partial x} \left( \frac{\partial w_0}{\partial x} \right)^2 \dots \text{etc.}$$

In order to apply the finite element method, shape functions have to be determined both for bending and for in-plane displacements. For bending displacement of the plate element in Figure (5-1) the following shape function is considered:

$$\begin{aligned}
 w = & A_1 + A_2 x + A_3 y + A_4 x^2 + A_5 xy + A_6 y^2 + A_7 x^3 + A_8 x^2 y \\
 & + A_9 xy^2 + A_{10} y^3 + A_{11} x^3 y + A_{12} xy^3
 \end{aligned}
 \quad (5-19)$$

The twelve coefficients  $A_1$  to  $A_{12}$  are determined uniquely by specifying at each node (corner) of the rectangular element the nodal displacement  $w$  and the two rotations  $\frac{\partial w}{\partial x}$ , and  $\frac{\partial w}{\partial y}$ .

Next, for in-plane displacement, the following shape function is assumed:

$$\begin{aligned}
 U &= \alpha_1 + \alpha_2 x + \alpha_3 y + \alpha_4 xy \\
 V &= \alpha_5 + \alpha_6 x + \alpha_7 y + \alpha_8 xy
 \end{aligned}
 \quad (5-20)$$

where  $\alpha_1 \sim \alpha_8$  are arbitrary constants which are determined from the known displacements in the  $x$  and  $y$  directions at the four corners of the rectangle.

The strain energy  $U$  consists of four components  $U_k$ ,  $U_0$ ,  $U_1$ , and  $U_2$ .  $U_k$  results in the so-called "elastic stiffness" which is related to in-plane deformation and linearized plate bending.

$U_0$  results in the zero-order element incremental stiffness matrix, due to initial deformation of the plate.

$U_1$  and  $U_2$  give additional stiffness due to membrane action of the plate.

Note: The geometric stiffness is included in first-order element incremental stiffness matrix  $U_1$ .

The coefficients in each of the above matrices can be obtained by performing the second partial differentiation of the proper component of strain energy with respect to the associated nodal displacements. Generally, an entry in  $i$ th row and  $j$ th column is given by:

$$\begin{aligned}
 K_{ij} &= \frac{\partial^2 U_k}{\partial q_i \partial q_j} \quad (5-21) & N_{0,ij} &= \frac{\partial^2 U_0}{\partial q_i \partial q_j} ; \\
 N_{1,ij} &= \frac{\partial^2 U_1}{\partial q_i \partial q_j} & N_2 &= \frac{\partial^2 U_2}{\partial q_i \partial q_j} \quad (5-22)
 \end{aligned}$$

The potential energy of external loading expressed by Equation (5-11) can now be written in a matrix form.

$$W = [P]\{q\} \quad (5-23)$$

where  $[P]$  is the row vector of external loads.

The element equilibrium equation can be obtained by executing the first variation of Equation (5-21) and (5-23) and following the equilibrium condition defined by Equation (5-10).

$$\{p\} = \left[ [k] + [n_0] + \frac{1}{2}[n_1] + \frac{1}{3}[n_2] \right] \{q\} \quad (5-24)$$

The overall structural stiffness equation of an assemblage of individual finite elements is written by capital letters as

$$\{P\} = \left[ [K] + [N_0] + \frac{1}{2}[N_1] + \frac{1}{3}[N_2] \right] \{Q\} \quad (5-25)$$

This nonlinear stiffness equation is readily applicable to the direct iterative analysis.

The basic incremental stiffness equation follows immediately by applying an incremental operator  $\Delta$  to Equation (5-25). In other words, replacing the displacements  $\{Q\}$  by  $\{Q + \Delta Q\}$  in Equation (5-25), then subtracting the original Equation (5-25) from the replaced equation and neglecting the second and third order terms of incremental degrees of freedom,  $\Delta Q_i \Delta Q_j$ , and  $\Delta Q_i \Delta Q_j \Delta Q_u$ .

$$\{\Delta P\} = \left[ [K] + [N_0] + [N_1] + [N_2] \right] \{\Delta Q\} \quad (5-26)$$

Since the displacement shape can not be assumed, it is not feasible to apply displacement increments  $\{\Delta Q\}$  for solving Equation (5-25). The load increments  $\{\Delta P\}$  are applied instead and an inverse of the stiffness matrices is required for each step.

$$\{\Delta Q\}_i = \left[ [K] + [N_0] + [N_1] + [N_2] \right]_{i-1}^{-1} \{\Delta P\} \quad (5-27)$$

In step  $i$ , the load increment is to be multiplied by the inverse of the sum of four stiffness matrices which is based on the displacement state at the end of step  $i-1$ .

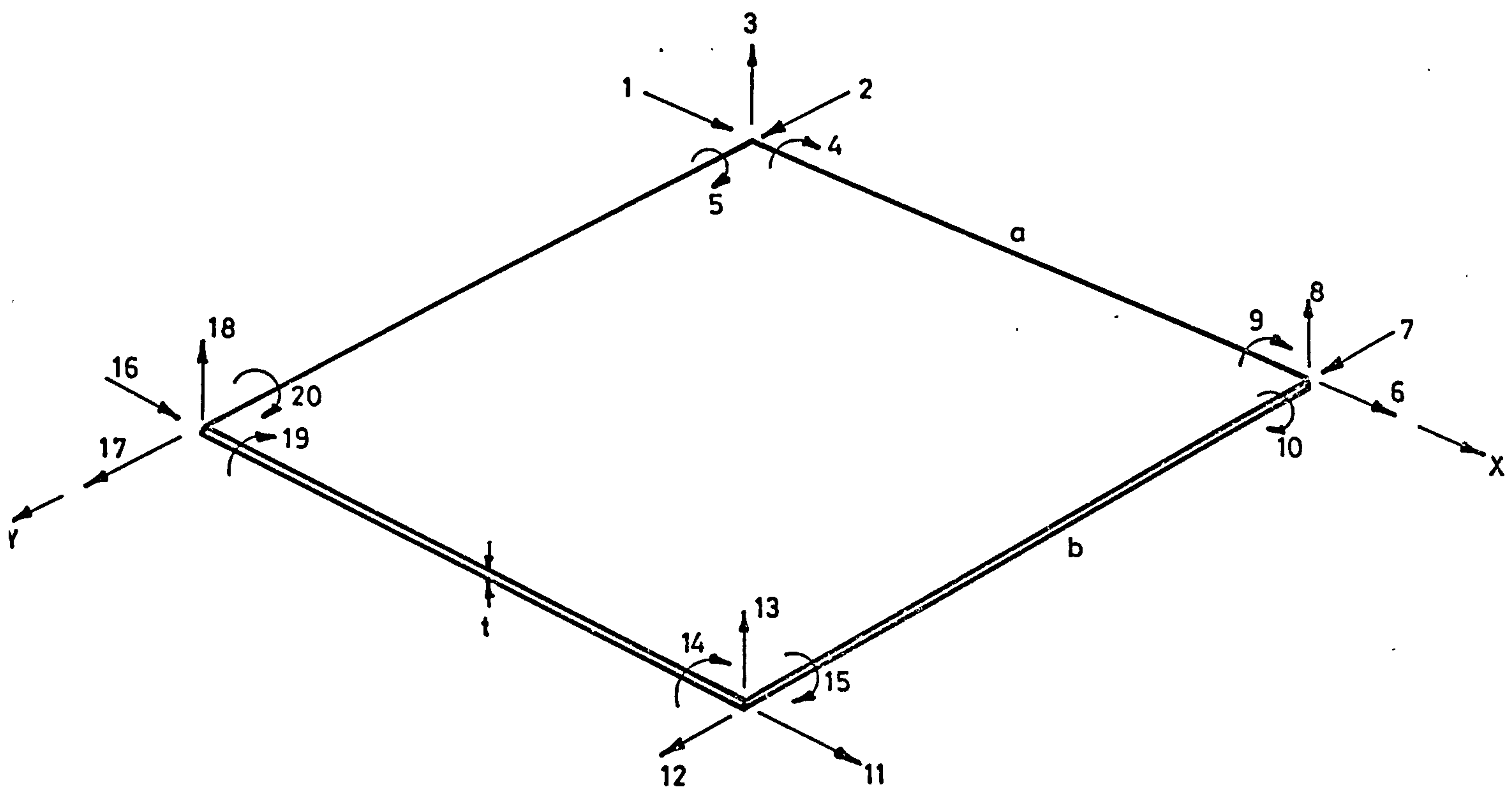


PLATE ELEMENT

FIGURE 5-1



## 5.4 ELASTIC STIFFNESS MATRIX

The calculation necessary for the elastic stiffness  $K$  is carried out in Reference [61]. For simplicity, the in-plane and bending stiffness is given below as a single  $20 \times 20$  matrix.

$$K = \begin{array}{|c|c|} \hline K_{I,I} & \text{Symmetric} \\ \hline K_{II,I} & K_{II,II} \\ \hline \end{array}$$

where the submatrices  $K_{I,I}$ ,  $K_{II,I}$ , and  $K_{II,II}$  are presented separately in the following tables.

Submatrix  $K_{I,I}$

	1	2	3	4	5	6	7	8	9	10
1	$K_1$									
2	$K_2$	$K_3$								
3	O	O	$K_4$							
4	O	O	$K_5$	$K_6$						
5	O	O	$K_7$	$K_8$	$K_9$					
6	$K_{10}$	$K_{11}$	O	O	O	$K_1$				
7	$K_{12}$	$K_{13}$	O	O	O	$K_{14}$	$K_3$			
8	O	O	$K_{15}$	$K_{16}$	$K_{17}$	O	O	$K_4$		
9	O	O	$K_{16}$	$K_{18}$	O	O	O	$K_5$	$K_6$	
10	O	O	$K_{19}$	O	$K_{20}$	O	O	$K_{21}$	$K_{22}$	$K_9$

SYMMETRICAL

(5-28)

	1	2	3	4	5	6	7	8	9	10
11	$K_{23}$	$K_{14}$	O	O	O	$K_{24}$	$K_{11}$	O	O	O
12	$K_{14}$	$K_{25}$	O	O	O	$K_{12}$	$K_{26}$	O	O	O
13	O	O	$K_{27}$	$K_{28}$	$K_{29}$	O	O	$K_{30}$	$K_{31}$	$K_{32}$
14	O	O	$K_{33}$	$K_{34}$	O	O	O	$K_{35}$	$K_{36}$	O
15	O	O	$K_{38}$	O	$K_{39}$	O	O	$K_{32}$	O	$K_{40}$
16	$K_{24}$	O	O	O	O	$K_{23}$	$K_2$	O	O	O
17	$K_{11}$	$K_{26}$	O	O	O	$K_2$	$K_{25}$	O	O	O
18	O	O	$K_{30}$	$K_{41}$	$K_{42}$	O	O	$K_{27}$	$K_{28}$	$K_{38}$
19	O	O	$K_{35}$	$K_{36}$	O	O	O	$K_{33}$	$K_{34}$	O
20	O	O	$K_{42}$	O	$K_{40}$	O	O	$K_{29}$	O	$K_{39}$

Submatrix  $K_{II,I}$

(5-29)

11 12 13 14 15 16 17 18 19 20

11	K <sub>1</sub>	SYMMETRICAL								
12	K <sub>2</sub>	K <sub>3</sub>								
13	O	O	K <sub>4</sub>							
14	O	O	K <sub>3 7</sub>	K <sub>6</sub>						
15	O	O	K <sub>2 1</sub>	K <sub>8</sub>	K <sub>9</sub>					
16	K <sub>1 0</sub>	K <sub>1 2</sub>	O	O	O	K <sub>1</sub>				
17	K <sub>1 2</sub>	K <sub>1 3</sub>	O	O	O	K <sub>1 4</sub>	K <sub>3</sub>			
18	O	O	K <sub>1 5</sub>	K <sub>4 3</sub>	K <sub>1 9</sub>	O	O	K <sub>4</sub>		
19	O	O	K <sub>4 3</sub>	K <sub>1 8</sub>	O	O	O	K <sub>3 7</sub>	K <sub>6</sub>	
20	O	O	K <sub>1 7</sub>	O	K <sub>2 0</sub>	O	O	K <sub>7</sub>	K <sub>2 2</sub>	K <sub>9</sub>

Submatrix K<sub>II,II</sub>

(5-30)

$$S = a/b$$

$$C = Et/12(1-\nu^2)$$

$$B = Et^3/12(1-\nu^2)ab$$

$$K_1 = 4S^{-1}C + 2(1-\nu)SC$$

$$K_2 = 3C/2(1+\nu)$$

$$K_3 = 4SC + 2(1-\nu)S^{-1}C$$

$$K_4 = 4(S^2 + S^{-2})B + 1/15(14-4\nu)B$$

$$K_5 = -2S^2bB + 1/5(1+4\nu)bB$$

$$K_6 = 4/3S^2B + 4/15(1-\nu)b^2B$$

$$K_7 = -2S^{-2}aB - 1/5(1+4\nu)aB$$

$$K_8 = \nu abB$$

$$K_9 = 4/3S^{-2}B + 4/15(1-\nu)a^2B$$

$$K_{10} = -4S^{-1}C + (1-\nu)SC$$

$$K_{11} = 3/2(1-3\nu)C$$

$$K_{12} = -3/2(1-3\nu)C$$

$$K_{13} = 2SC - 2(1-\nu)S^{-1}C$$

$$K_{14} = -3/2(1+\nu)C$$

$$K_{15} = -2(2S^{-2} - S^2)B - 1/5(14-4\nu)B$$

$$K_{16} = -S^2bB + 1/5(1+4\nu)bB$$

$$K_{17} = 2S^{-2}aB + 1/5(1-\nu)aB$$

$$K_{18} = 2/3S^2B - 4/15(1-\nu)b^2B$$

$$K_{19} = -2S^{-2}aB - 1/5(1-\nu)aB$$

$$K_{20} = 2/3S^{-2}a^2B - 1/15(1-\nu)a^2B$$

$$K_{21} = 2S^{-2}aB + 1/5(1+4\nu)aB$$

$$K_{22} = -\nu abB$$

$$K_{23} = -2S^{-1}C - (1-\nu)SC$$

$$K_{24} = 2S^{-1}C - 2(1-\nu)SC$$

$$K_{25} = -2SC - S^{-1}(1-\nu)C$$

$$K_{26} = -4SC + (1-\nu)S^{-1}C$$

$$K_{27} = -2(S^{-2} + S^2)B + 1/15(14-4\nu)B$$

$$K_{28} = S^2bB - 1/5(1-\nu)bB$$

$$K_{29} = S^{-2}aB - 1/5(1-\nu)aB$$

$$K_{30} = 2(S^{-2} - 2S^2)B - 1/5(14-4\nu)B$$

$$K_{31} = 2S^2bB + 1/5(1-\nu)bB$$

$$K_{32} = S^{-2}aB - 1/5(1+4\nu)aB$$

$$K_{33} = -S^2bB + 1/5(1-\nu)bB$$

$$K_{34} = 1/3S^2B + 1/15(1-\nu)b^2B$$

$$K_{35} = -2S^2bB - 1/5(1-\nu)bB$$

$$K_{36} = 2/3S^2B - 1/15(1-\nu)b^2B$$

$$K_{37} = 2S^2bB + 1/5(1+4\nu)bB$$

$$K_{38} = -S^{-2}aB + 1/5(1-\nu)aB$$

$$K_{39} = 1/3S^{-2}Ba^2 + 1/15(1-\nu)a^2B$$

$$K_{40} = 2/3S^{-2}a^2B - 4/15(1-\nu)a^2B$$

$$K_{41} = 2S^2bB + 1/5(1-\nu)bB$$

$$K_{42} = -S^{-2}aB + 1/5(1+4\nu)aB$$

$$K_{43} = S^2bB - 1/5(1+4\nu)bB$$

$$K_{44} = 1/3S^2b^2B + 1/15(1-\nu)b^2B$$



## 5.5 INCREMENTAL STIFFNESS MATRICES

The calculation of the incremental stiffness matrices is carried out in two stages. During the first stage  $\{\partial U/\partial q_i\}$  is calculated, and during the second stage the incremental stiffness  $[\partial U/\partial q_i \partial q_i]$  is determined.

Using Equation (5-16) for evaluating  $U_0$ , it follows:

$$\frac{\partial w}{\partial x} = \theta_x = \frac{q_8 - q_3 + q_{13} - q_{18}}{2a}$$

$$\frac{\partial w}{\partial y} = \theta_y = \frac{q_{18} - q_3 + q_{13} - q_8}{2b}$$

$$\frac{\partial u}{\partial x} = e_x = \frac{q_6 - q_1 + q_{11} - q_{16}}{2a}$$

$$\frac{\partial v}{\partial y} = e_y = \frac{q_{17} - q_2 + q_{12} - q_7}{2b}$$

$$\frac{\partial v}{\partial x} + \frac{\partial u}{\partial y} = e_{xy} = \frac{q_{12} - q_{17} + q_7 - q_2}{2a} + \frac{q_{11} - q_6 + q_{16} - q_1}{2b}$$

$$\frac{\partial w_0}{\partial x} = \beta_x = \frac{q_{08} - q_{03} + q_{013} - q_{018}}{2a}$$

$$\frac{\partial w_0}{\partial y} = \beta_y = \frac{q_{018} - q_{03} + q_{013} - q_{08}}{2b}$$

(5-31)

$$\begin{aligned}
\left\{ \frac{\partial U_0}{\partial q_i} \right\} = & - \frac{3D}{2t^2} \left[ -8\beta_x^2 \theta_x \left( \frac{\partial \theta_x}{\partial q_i} \right) - 8\beta_y^2 \theta_y \left( \frac{\partial \theta_x}{\partial q_i} \right) + 4\nu\beta_y^2 \theta_x \left( \frac{\partial \theta_x}{\partial q_i} \right) \right. \\
& + 4\nu\beta_x \beta_y^2 \left( \frac{\partial \theta_x}{\partial q_i} \right) + 4\nu\beta_x^2 \theta_y \left( \frac{\partial \theta_y}{\partial q_i} \right) + 4\nu^2 \beta_x^2 \beta_y \left( \frac{\partial \theta_y}{\partial q_i} \right) \\
& - 4\beta_x^2 \left( \frac{\partial e_x}{\partial q_i} \right) - 4\beta_y^2 \left( \frac{\partial e_y}{\partial q_i} \right) - 8\theta_x \beta_x \left( \frac{\partial e_x}{\partial q_i} \right) - 8\beta_x e_x \left( \frac{\partial \theta_x}{\partial q_i} \right) \\
& - 8\beta_y \theta_y \left( \frac{\partial e_y}{\partial q_i} \right) - 8\beta_y e_y \left( \frac{\partial \theta_y}{\partial q_i} \right) - 4\nu\beta_x^2 \left( \frac{\partial e_y}{\partial q_i} \right) \\
& - 4\nu\beta_y^2 \left( \frac{\partial e_x}{\partial q_i} \right) - 8\nu\theta_x \beta_x \left( \frac{\partial e_y}{\partial q_i} \right) - 8\nu\beta_x e_y \left( \frac{\partial \theta_x}{\partial q_i} \right) \\
& - 8\nu\beta_y \theta_y \left( \frac{\partial e_x}{\partial q_i} \right) - 8\nu\beta_y e_x \left( \frac{\partial \theta_y}{\partial q_i} \right) - 4(1-\nu)\theta_x \beta_y \left( \frac{\partial e_{xy}}{\partial q_i} \right) \\
& - 4(1-\nu)e_{xy} \beta_y \left( \frac{\partial \theta_x}{\partial q_i} \right) - 4(1-\nu)\theta_y \beta_x \left( \frac{\partial e_{xy}}{\partial q_i} \right) \\
& - 4(1-\nu)e_{xy} \beta_x \left( \frac{\partial \theta_y}{\partial q_i} \right) - 4(1-\nu)\beta_x \beta_y \left( \frac{\partial e_{xy}}{\partial q_i} \right) \\
& - 4\beta_y^2 \theta_x \left( \frac{\partial \theta_x}{\partial q_i} \right) - 8\beta_x \beta_y \theta_y \left( \frac{\partial \theta_x}{\partial q_i} \right) - 8\beta_x \beta_y \theta_x \left( \frac{\partial \theta_y}{\partial q_i} \right) \\
& - 4\beta_x \beta_y^2 \left( \frac{\partial \theta_x}{\partial q_i} \right) - 4\beta_y^2 \theta_y \left( \frac{\partial \theta_y}{\partial q_i} \right) - 4\beta_y \beta_x^2 \left( \frac{\partial \theta_y}{\partial q_i} \right) \\
& + 2(1-\nu)\beta_x \beta_y \theta_y \left( \frac{\partial \theta_x}{\partial q_i} \right) + 2(1-\nu)\beta_x \beta_y \theta_x \left( \frac{\partial \theta_y}{\partial q_i} \right) \\
& \left. + 2(1-\nu)\beta_x \beta_y^2 \left( \frac{\partial \theta_x}{\partial q_i} \right) + 2(1-\nu)\beta_x^2 \beta_y \left( \frac{\partial \theta_y}{\partial q_i} \right) \right] ab
\end{aligned}$$

Where  $i = 1, 2, 3, \dots, 20$ , substitution of  $e_x, e_y, e_{xy}, \theta_x$ , and  $\theta_y$  from Equation (5-31) into partial derivatives yields

$\frac{\partial e_x}{\partial q_1}$ or $\frac{\partial e_x}{\partial q_{16}}$	$\frac{\partial e_x}{\partial q_6}$ or $\frac{\partial e_x}{\partial q_{11}}$	$\frac{\partial e_y}{\partial q_2}$ or $\frac{\partial e_y}{\partial q_{17}}$
$-\frac{1}{2a}$	$\frac{1}{2a}$	$-\frac{1}{2b}$

$\frac{\partial e_y}{\partial q_{17}}$ or $\frac{\partial e_y}{\partial q_{12}}$	$\frac{\partial e_{xy}}{\partial q_{17}}$ or $\frac{\partial e_{xy}}{\partial q_2}$	$\frac{\partial e_{xy}}{\partial q_{12}}$ or $\frac{\partial e_{xy}}{\partial q_7}$
$\frac{1}{2a}$	$-\frac{1}{2a}$	$\frac{1}{2a}$

$\frac{\partial e_{xy}}{\partial q_6}$ or $\frac{\partial e_{xy}}{\partial q_1}$	$\frac{\partial e_{xy}}{\partial q_{11}}$ or $\frac{\partial e_{xy}}{\partial q_{16}}$	$\frac{\partial \theta_x}{\partial q_3}$ or $\frac{\partial \theta_x}{\partial q_{18}}$
$-\frac{1}{2b}$	$\frac{1}{2b}$	$-\frac{1}{2a}$

$\frac{\partial \theta_x}{\partial q_8}$ or $\frac{\partial \theta_x}{\partial q_{13}}$	$\frac{\partial \theta_y}{\partial q_3}$ or $\frac{\partial \theta_y}{\partial q_8}$	$\frac{\partial \theta_y}{\partial q_{18}}$ or $\frac{\partial \theta_y}{\partial q_{13}}$
$\frac{1}{2a}$	$-\frac{1}{2b}$	$\frac{1}{2b}$

TABLE (5-1)

Substituting appropriate terms of Table 5-1 into the partial derivatives, it follows:

1	$  \begin{aligned}  & 2\beta_x^2 b + 4\theta_x \beta_x b + 2v\beta_y^2 b + 4v\beta_y \theta_y b + 2(1-v)\theta_x \beta_y a \\  & + 2(1-v)\theta_y \beta_x a + 2(1-v)\beta_x \beta_y a  \end{aligned}  $
2	$  \begin{aligned}  & 2\beta_y^2 a + 4\beta_y \theta_y a + 2v\beta_x^2 a + 4v\beta_x \theta_y a + 2(1-v)\theta_x \beta_y b \\  & + 2(1-v)\theta_y \beta_x b + 2(1-v)\beta_x \beta_y b  \end{aligned}  $
3	$  \begin{aligned}  & 4\beta_x^2 \theta_x b + 4\beta_y^2 \theta_y a - 2v\beta_y^2 \theta_x b - 2v\beta_x \beta_y^2 b - 2v\beta_x^2 \theta_y a \\  & - 2v\beta_x^2 \beta_y a + 4\beta_x e_x b + 4\beta_y e_y a + 4v\beta_x e_y b + 4v\beta_y e_x a \\  & + 2(1-v)e_{xy} \beta_y b + 2(1-v)e_{xy} \beta_x a + 2\beta_y^2 \theta_x b \\  & + 2\beta_y^2 \theta_y a + 4\beta_x \beta_y \theta_y b + 4\beta_x \beta_y \theta_x a + 2\beta_x \beta_y^2 b + 2\beta_y \beta_x^2 a \\  & - (1-v)\beta_x \beta_y \theta_y b - (1-v)\beta_x \beta_y \theta_x a - (1-v)\beta_x \beta_y^2 b \\  & - (1-v)\beta_x^2 \beta_y a  \end{aligned}  $
4	0
5	0
6	$  \begin{aligned}  & -2\beta_x^2 b - 4\theta_x \beta_x b - 2v\beta_y^2 b - 4v\beta_y \theta_y b + 2(1-v)\theta_x \beta_y a \\  & + 2(1-v)\theta_y \beta_x a + 2(1-v)\beta_x \beta_y a  \end{aligned}  $
7	$  \begin{aligned}  & 2\beta_y^2 a + 4\beta_y \theta_y a + 2v\beta_x^2 a + 4v\beta_x \theta_y a - 2(1-v)\theta_x \beta_y b \\  & - 2(1-v)\theta_y \beta_x b - 2(1-v)\beta_x \beta_y b  \end{aligned}  $



$$\left\{ \frac{\partial U_0}{\partial q_i} \right\} = -\frac{3D}{2t^2} \left\{ \begin{array}{l}
 \begin{array}{l}
 -4\beta_x^2 \theta_x b + 4\beta_y^2 \theta_y a + 2v\beta_y^2 \theta_x b + 2v\beta_x \beta_y^2 b - 2v\beta_x^2 \theta_y a \\
 -2v\beta_x^2 \beta_y a - 4\beta_x e_x b + 4\beta_y e_y a - 4v\beta_x e_y b + 4v\beta_y e_x a \\
 -2(1-v)e_{xy} \beta_y b + 2(1-v)e_{xy} \beta_x a - 2\beta_y^2 \theta_x b + 2\beta_y^2 \theta_y a \\
 -4\beta_x \beta_y \theta_y b + 4\beta_x \beta_y \theta_x a - 2\beta_x \beta_y^2 b + 2\beta_y \beta_x^2 a \\
 + (1-v)\beta_x \beta_y \theta_y b - (1-v)\beta_x \beta_y \theta_x a + (1-v)\beta_x \beta_y^2 b \\
 - (1-v)\beta_x^2 \beta_y a
 \end{array} \\
 0 \\
 0 \\
 \begin{array}{l}
 -2\beta_x^2 b - 4\theta_x \beta_x b - 2v\beta_y^2 b - 4v\beta_y \theta_y b - 2(1-v)\theta_x \beta_y a \\
 -2(1-v)\theta_y \beta_y a - 2(1-v)\beta_x \beta_y a
 \end{array} \\
 \begin{array}{l}
 -2\beta_y^2 a - 4\beta_y \theta_y a - 2v\beta_x^2 a - 4v\beta_x \theta_y a - 2(1-v)\theta_x \beta_y b \\
 -2(1-v)\theta_y \beta_x b
 \end{array} \\
 \begin{array}{l}
 -4\beta_x^2 \theta_x b - 4\beta_y^2 \theta_y a + 2v\beta_y^2 \theta_x b + 2v\beta_x \beta_y^2 b + 2v\beta_x^2 \theta_y a \\
 + 2v\beta_x^2 \beta_y a - 4\beta_x e_x b - 4\beta_y e_y a - 4v\beta_x e_y b - 4v\beta_y e_x a \\
 -2(1-v)e_{xy} \beta_y b - 2(1-v)e_{xy} \beta_x a - 2\beta_y^2 \theta_x b \\
 -2\beta_y^2 \theta_y a - 4\beta_x \beta_y \theta_y b - 4\beta_x \beta_y \theta_x a - 2\beta_x \beta_y^2 b - 2\beta_y \beta_x^2 a
 \end{array}
 \end{array} \right\}$$

	$+(1-\nu)\beta_x\beta_y\theta_y b + (1-\nu)\beta_x\beta_y\theta_x a + (1-\nu)\beta_x\beta_y^2 b$ $+(1-\nu)\beta_x^2\beta_y a$
14	0
15	0
16	$2\beta_x^2 b + 4\theta_x\beta_x b + 2\nu\beta_y^2 b + 4\nu\beta_y\theta_y b - 2(1-\nu)\theta_x\beta_y a$ $- 2(1-\nu)\theta_y\beta_x a - 2(1-\nu)\beta_x\beta_y a$
17	$-2\beta_y^2 a - 4\beta_y\theta_y a - 2\nu\beta_x^2 a - 4\nu\beta_x\theta_y a + 2(1-\nu)\theta_x\beta_y b$ $+ 2(1-\nu)\theta_y\beta_x b + 2(1-\nu)\beta_x\beta_y b$
18	$4\beta_x^2\theta_x b - 4\beta_y^2\theta_y a - 2\nu\beta_y^2\theta_x b - 2\nu\beta_x\beta_y^2 b + 2\nu\beta_x^2\theta_y a$ $+ 2\nu\beta_x^2\beta_y a + 4\beta_x e_x b - 4\beta_y e_y a + 4\nu\beta_x e_y b - 4\nu\beta_y e_x a$ $+ 2(1-\nu)e_{xy}\beta_y b - 2(1-\nu)e_{xy}\beta_x a + 2\beta_y^2\theta_x b$ $- 2\beta_y^2\theta_y a + 4\beta_x\beta_y\theta_y b - 4\beta_x\beta_y\theta_x a + 2\beta_x\beta_y^2 b - 2\beta_y\beta_x^2 a$ $- (1-\nu)\beta_x\beta_y\theta_y b + (1-\nu)\beta_x\beta_y\theta_x a - (1-\nu)\beta_x\beta_y^2 b$ $+ (1-\nu)\beta_x^2\beta_y a$
19	0
20	0

$$\begin{aligned}
\left\{ \frac{\partial^2 U_0}{\partial q_i \partial q_j} \right\} = & - \frac{3D}{2t^2} \left[ - 8\beta_x^2 \left( \frac{\partial^2 \theta_x}{\partial q_i \partial q_j} \right) - 8\beta_y^2 \left( \frac{\partial^2 \theta_y}{\partial q_i \partial q_j} \right) \right. \\
& + 4\nu\beta_y^2 \left( \frac{\partial^2 \theta_x}{\partial q_i \partial q_j} \right) + 4\nu\beta_x^2 \left( \frac{\partial^2 \theta_y}{\partial q_i \partial q_j} \right) \\
& - 8\beta_x \left( \frac{\partial e_x}{\partial q_i} \right) \left( \frac{\partial \theta_x}{\partial q_j} \right) - 8\beta_x \left( \frac{\partial \theta_x}{\partial q_i} \right) \left( \frac{\partial e_x}{\partial q_j} \right) \\
& - 8\beta_y \left( \frac{\partial e_y}{\partial q_i} \right) \left( \frac{\partial \theta_x}{\partial q_j} \right) - 8\beta_y \left( \frac{\partial \theta_y}{\partial q_i} \right) \left( \frac{\partial e_y}{\partial q_j} \right) \\
& - 8\nu\beta_x \left( \frac{\partial e_y}{\partial q_i} \right) \left( \frac{\partial \theta_x}{\partial q_j} \right) - 8\nu\beta_x \left( \frac{\partial \theta_x}{\partial q_i} \right) \left( \frac{\partial e_y}{\partial q_j} \right) \\
& - 8\nu\beta_y \left( \frac{\partial e_x}{\partial q_i} \right) \left( \frac{\partial \theta_y}{\partial q_j} \right) - 8\nu\beta_y \left( \frac{\partial \theta_y}{\partial q_i} \right) \left( \frac{\partial e_x}{\partial q_j} \right) \\
& - 4(1-\nu)\beta_y \left( \frac{\partial e_{xy}}{\partial q_i} \right) \left( \frac{\partial \theta_x}{\partial q_j} \right) \\
& - 4(1-\nu)\beta_y \left( \frac{\partial \theta_x}{\partial q_i} \right) \left( \frac{\partial e_{xy}}{\partial q_j} \right) \\
& - 4(1-\nu)\beta_x \left( \frac{\partial e_{xy}}{\partial q_i} \right) \left( \frac{\partial \theta_y}{\partial q_j} \right) \\
& - 4(1-\nu)\beta_x \left( \frac{\partial \theta_y}{\partial q_i} \right) \left( \frac{\partial e_{xy}}{\partial q_j} \right) \\
& - 4\beta_y^2 \left( \frac{\partial^2 \theta_x}{\partial q_i \partial q_j} \right) - 16\beta_x\beta_y \left( \frac{\partial \theta_x}{\partial q_i} \right) \left( \frac{\partial \theta_y}{\partial q_j} \right) \\
& - 4\beta_y^2 \left( \frac{\partial^2 \theta_y}{\partial q_i \partial q_j} \right) + 2(1-\nu)\beta_x\beta_y \left( \frac{\partial \theta_x}{\partial q_i} \right) \left( \frac{\partial \theta_y}{\partial q_j} \right) \\
& \left. + 2(1-\nu)\beta_x\beta_y \left( \frac{\partial \theta_y}{\partial q_i} \right) \left( \frac{\partial \theta_x}{\partial q_j} \right) \right] \quad ab
\end{aligned}$$

Substituting  $\frac{\partial \theta_x}{\partial q_i}$ ,  $\frac{\partial \theta_x}{\partial q_j}$ ,  $\frac{\partial \theta_y}{\partial q_i}$ ,  $\frac{\partial \theta_y}{\partial q_j}$ ,  $\frac{\partial e_x}{\partial q_i}$ ,  $\frac{\partial e_x}{\partial q_j}$ ,  $\frac{\partial e_y}{\partial q_i}$ ,

$\frac{\partial e_y}{\partial q_j}$ ,  $\frac{\partial e_{xy}}{\partial q_i}$ , and  $\frac{\partial e_{xy}}{\partial q_j}$  into Table (5-1), zero incremental

stiffness is obtained.

$$[N_0] = \begin{bmatrix} L_{I,I} & \text{Sym.} \\ L_{II,I} & L_{II,II} \end{bmatrix}$$

SUBMATRIX  $L_{I,I}$

	1	2	3	4	5	6	7	8	9	10
1	O									
2	O	O								
3	L <sub>1</sub>	L <sub>2</sub>	L <sub>3</sub>							
4	O	O	O	O						
5	O	O	O	O	O					
6	O	O	L <sub>4</sub>	O	O	O				
7	O	O	L <sub>2</sub>	O	O	O	O			
8	L <sub>5</sub>	L <sub>6</sub>	L <sub>7</sub>	O	O	L <sub>8</sub>	L <sub>9</sub>	L <sub>10</sub>		
9	O	O	O	O	O	O	O	O	O	
10	O	O	O	O	O	O	O	O	O	O

SYMMETRICAL



	1	2	3	4	5	6	7	8	9	10
11	O	O	$L_{11}$	O	O	O	O	$L_{12}$	O	O
12	O	O	$L_{13}$	O	O	O	O	$-L_{14}$	O	O
13	$-L_1$	$-L_2$	$-L_3$	O	O	$-L_4$	$-L_2$	$-L_7$	O	O
14	O	O	O	O	O	O	O	O	O	O
15	O	O	O	O	O	O	O	O	O	O
16	O	O	$L_1$	O	O	O	O	$L_6$	O	O
17	O	O	$L_{15}$	O	O	O	O	$L_{16}$	O	O
18	$-L_5$	$-L_6$	$-L_7$	O	O	$-L_8$	$-L_9$	$-L_{10}$	O	O
19	O	O	O	O	O	O	O	O	O	O
20	O	O	O	O	O	O	O	O	O	O

SUBMATRIX  $L_{II, I}$  (5-36)

SUBMATRIX  $L_{II, II}$

	11	12	13	14	15	16	17	18	19	20
11	O									
12	O	O								
13	$-L_{11}$	$-L_{13}$	$L_3$							
14	O	O	O	O						
15	O	O	O	O	O					
16	O	O	$-L_1$	O	O	O				
17	O	O	$-L_{15}$	O	O	O	O			
18	$-L_{12}$	$-L_{14}$	$L_7$	O	O	O	$-L_{16}$	$L_{10}$		
19	O	O	O	O	O	O	O	O	O	
20	O	O	O	O	O	O	O	O	O	O

SYMMETRICAL

(5-37)

$$H = b/a \quad F = a/b \quad A = Et^3/12(1-\nu^2) \quad C = 3A/2t^2$$

$$L_1 = C(2H\beta_x + 2\nu\beta_y)$$

$$L_2 = C(2\nu\beta_x + 2F\beta_y)$$

$$L_3 = C(2H\beta_x^2 + 2F\beta_y^2 - H\nu\beta_y^2 + 4\beta_x\beta_y + H\beta_y^2 + F\beta_x^2 - F\nu\beta_x^2 - 2(1-\nu)\beta_x\beta_y)$$

$$L_4 = C(-2H\beta_x - 2\nu\beta_y + 2(1-\nu)\beta_y + 2F(1-\nu)\beta_x)$$

$$L_5 = C(-2H\beta_x + 2\nu\beta_y)$$

$$L_6 = C(-2\nu\beta_x + 2F\beta_y)$$

$$L_7 = C(-2H\beta_x^2 + H\nu\beta_y^2 + 2F\beta_y^2 + F\beta_x^2 - H\beta_y^2 - F\nu\beta_x^2)$$

$$L_8 = C(2H\beta_x - 2(1-\nu)\beta_y - 2\nu\beta_y + 2F(1-\nu)\beta_x)$$

$$L_9 = C(-2\nu\beta_x + 2F\beta_y)$$

$$L_{10} = C(2H\beta_x^2 - H\nu\beta_y^2 + 2F\beta_y^2 - 4\beta_x\beta_y + H\beta_y^2 + F\beta_x^2 - F\nu\beta_x^2 + 2(1-\nu)\beta_x\beta_y)$$

$$L_{11} = C(-2H\beta_x - 2\nu\beta_y - 2(1-\nu)\beta_y - 2F(1-\nu)\beta_x)$$

$$L_{12} = C(2H\beta_x - 2\nu\beta_y + 2(1-\nu)\beta_y - 2F(1-\nu)\beta_x)$$

$$L_{13} = C(-2\nu\beta_x - 2F\beta_y - 2H(1-\nu)\beta_y - 2(1-\nu)\beta_x)$$

$$L_{14} = C(2\nu\beta_x - 2F\beta_y + 2H(1-\nu)\beta_y - 2(1-\nu)\beta_x)$$

$$L_{15} = C(-2\nu\beta_x - 2F\beta_y + 2H(1-\nu)\beta_y + 2(1-\nu)\beta_x)$$

$$L_{16} = C(2\nu\beta_x - 2F\beta_y - 2H(1-\nu)\beta_y + 2(1-\nu)\beta_x)$$

Using Equation (5-17) for evaluating  $U_1$ , it follows:

$$\begin{aligned}
 \left\{ \frac{\partial U_1}{\partial q_i} \right\} = \frac{6D}{t^2} \left[ \theta_x^2 \left( \frac{\partial e_x}{\partial q_i} \right) + 2\theta_x e_x \left( \frac{\partial \theta_x}{\partial q_i} \right) + \nu \theta_x^2 \left( \frac{\partial e_y}{\partial q_i} \right) + 2\nu \theta_x e_y \left( \frac{\partial \theta_x}{\partial q_i} \right) \right. \\
 + \theta_y^2 \left( \frac{\partial e_y}{\partial q_i} \right) + 2\theta_y e_y \left( \frac{\partial \theta_y}{\partial q_i} \right) + \nu \theta_y^2 \left( \frac{\partial e_x}{\partial q_i} \right) \\
 + 2\nu \theta_y e_x \left( \frac{\partial \theta_y}{\partial q_i} \right) + (1-\nu) e_{xy} \theta_y \left( \frac{\partial \theta_x}{\partial q_i} \right) \\
 + (1-\nu) e_{xy} \theta_x \left( \frac{\partial \theta_y}{\partial q_i} \right) + (1-\nu) \theta_x \theta_y \left( \frac{\partial e_{xy}}{\partial q_i} \right) \\
 + 3\theta_x^2 \beta_x \left( \frac{\partial \theta_x}{\partial q_i} \right) + 3\theta_y^2 \beta_y \left( \frac{\partial \theta_y}{\partial q_i} \right) + 2\theta_x \theta_y \beta_y \left( \frac{\partial \theta_x}{\partial q_i} \right) \\
 \left. + \theta_x^2 \beta_y \left( \frac{\partial \theta_y}{\partial q_i} \right) + 2\theta_y \theta_x \beta_x \left( \frac{\partial \theta_y}{\partial q_i} \right) + \theta_y^2 \beta_x \left( \frac{\partial \theta_x}{\partial q_i} \right) \right] ab
 \end{aligned}$$

(5-38)

Where  $i = 1, 2, \dots, 20$ , substitution of  $e_x$ ,  $e_y$ ,  $e_{xy}$ ,  $\theta_x$

and  $\theta_y$  from Equation (5-31) into partial derivatives yields:

1	$- 1/2\theta_x^2 b - 1/2v\theta_y^2 b - 1/2(1-v)\theta_x\theta_y a$
2	$- 1/2v\theta_x^2 a - 1/2\theta_y^2 a - 1/2(1-v)\theta_x\theta_y b$
3	$- \theta_x e_x b - v\theta_x e_y b - \theta_y e_y a - v\theta_y e_x a$ $- 1/2(1-v)e_{xy}\theta_y b - 1/2(1-v)e_{xy}\theta_x a$ $- 3/2\theta_x^2 \beta_x b - 3/2\theta_y^2 \beta_y a - \theta_x\theta_y \beta_y b$ $- 1/2\theta_x^2 \beta_y a - \theta_y\theta_x \beta_x a - 1/2\theta_y^2 \beta_x a$
4	0
5	0
6	$1/2\theta_x^2 b + 1/2v\theta_y^2 b - 1/2(1-v)\theta_x\theta_y a$
7	$- 1/2v\theta_x^2 a - 1/2\theta_y^2 a + 1/2(1-v)\theta_x\theta_y b$
8	$\theta_x e_x b + v\theta_x e_y b - \theta_y e_y a - v\theta_y e_x a$ $+ 1/2(1-v)e_{xy}\theta_y b - 1/2(1-v)e_{xy}\theta_x a +$ $3/2\theta_x^2 \beta_x b - 3/2\theta_y^2 \beta_y a + \theta_x\theta_y \beta_y b - 1/2\theta_x^2 \beta_y a$ $- \theta_y\theta_x \beta_x a - 1/2\theta_y^2 \beta_x a$
9	0



$$\left\{ \frac{\partial U}{\partial q_i} \right\} = \frac{6D}{2t^2}$$

11

$$1/2\theta_x^2 b + 1/2\nu\theta_y^2 b + 1/2(1-\nu)\theta_x\theta_y a$$

12

$$1/2\nu\theta_x^2 a + 1/2\theta_y^2 a + 1/2(1-\nu)\theta_x\theta_y b$$

13

$$\begin{aligned} & \theta_x e_x b + \nu\theta_x e_y b + \theta_y e_y a + \nu\theta_y e_x a \\ & + 1/2(1-\nu)e_{xy}\theta_y b + 1/2(1-\nu)e_{xy}\theta_x a \\ & + 3/2\theta_x^2 \beta_x b + 3/2\theta_y^2 \beta_y a + \theta_x\theta_y \beta_y b \\ & + 1/2\theta_x^2 \beta_y a + \theta_y\theta_x \beta_x a + 1/2\theta_y^2 \beta_x a \end{aligned}$$

14

0

15

0

16

$$-1/2\theta_x^2 b - 1/2\nu\theta_y^2 b + 1/2(1-\nu)\theta_x\theta_y a$$

17

$$1/2\nu\theta_x^2 a + 1/2\theta_y^2 a - 1/2(1-\nu)\theta_x\theta_y b$$

18

$$\begin{aligned} & -\theta_x e_x b - \nu\theta_x e_y b + \theta_y e_y a + \nu\theta_y e_x a \\ & - 1/2(1-\nu)e_{xy}\theta_y b + 1/2(1-\nu)e_{xy}\theta_x a \\ & - 3/2\theta_x^2 \beta_x b + 3/2\theta_y^2 \beta_y a - \theta_x\theta_y \beta_y b \\ & + 1/2\theta_x^2 \beta_y a + \theta_y\theta_x \beta_x a + 1/2\theta_y^2 \beta_x a \end{aligned}$$

19

0

20

0

$$\begin{aligned}
\left[ \frac{\partial U_1}{\partial q_i \partial q_j} \right] = \frac{6D}{t^2} & \left[ 2\theta_x \left( \frac{\partial e_x}{\partial q_i} \right) \left( \frac{\partial \theta_x}{\partial q_j} \right) + 2e_x \left( \frac{\partial^2 \theta_x}{\partial q_i \partial q_j} \right) + 2\theta_x \left( \frac{\partial \theta_x}{\partial q_i} \right) \left( \frac{\partial e_x}{\partial q_j} \right) \right. \\
& + 2\nu\theta_x \left( \frac{\partial e_y}{\partial q_i} \right) \left( \frac{\partial \theta_x}{\partial q_j} \right) + 2\nu e_y \left( \frac{\partial^2 \theta_x}{\partial q_i \partial q_j} \right) \\
& + 2\nu\theta_x \left( \frac{\partial \theta_x}{\partial q_i} \right) \left( \frac{\partial e_y}{\partial q_j} \right) + 2\theta_y \left( \frac{\partial e_y}{\partial q_i} \right) \left( \frac{\partial \theta_y}{\partial q_j} \right) \\
& + 2e_y \left( \frac{\partial^2 \theta_y}{\partial q_i \partial q_j} \right) + 2\theta_y \left( \frac{\partial \theta_y}{\partial q_i} \right) \left( \frac{\partial e_y}{\partial q_j} \right) \\
& + 2\nu\theta_y \left( \frac{\partial e_x}{\partial q_i} \right) \left( \frac{\partial \theta_y}{\partial q_j} \right) + 2\nu e_x \left( \frac{\partial^2 \theta_y}{\partial q_i \partial q_j} \right) \\
& + 2\nu\theta_y \left( \frac{\partial \theta_y}{\partial q_i} \right) \left( \frac{\partial e_x}{\partial q_j} \right) + 2(1-\nu)e_{xy} \left( \frac{\partial \theta_x}{\partial q_i} \right) \left( \frac{\partial \theta_y}{\partial q_j} \right) \\
& + 2(1-\nu)\theta_y \left( \frac{\partial \theta_x}{\partial q_i} \right) \left( \frac{\partial e_{xy}}{\partial q_j} \right) + 2(1-\nu)\theta_x \left( \frac{\partial \theta_y}{\partial q_i} \right) \left( \frac{\partial e_{xy}}{\partial q_j} \right) \\
& + 6\theta_x \beta_x \left( \frac{\partial^2 \theta_x}{\partial q_i \partial q_j} \right) + 6\theta_y \beta_y \left( \frac{\partial^2 \theta_y}{\partial q_i \partial q_j} \right) \\
& + 2\theta_y \beta_y \left( \frac{\partial^2 \theta_x}{\partial q_i \partial q_j} \right) + 4\theta_x \beta_y \left( \frac{\partial \theta_y}{\partial q_i} \right) \left( \frac{\partial \theta_x}{\partial q_j} \right) \\
& + 2\theta_x \beta_x \left( \frac{\partial^2 \theta_y}{\partial q_i \partial q_j} \right) + 2\theta_y \beta_x \left( \frac{\partial \theta_y}{\partial q_i} \right) \left( \frac{\partial \theta_x}{\partial q_j} \right) \\
& \left. + 2\theta_y \beta_x \left( \frac{\partial^2 \theta_y}{\partial q_i \partial q_j} \right) \right] \quad ab
\end{aligned}$$

(5-40)

Where  $j = 1, 2, 3, \dots, 20$ , substitution of  $\frac{\partial \theta_x}{\partial q_i}, \frac{\partial \theta_x}{\partial q_j},$

$\frac{\partial \theta_y}{\partial q_i}, \frac{\partial \theta_y}{\partial q_j}, \frac{\partial e_x}{\partial q_i}, \frac{\partial e_x}{\partial q_j}, \frac{\partial e_y}{\partial q_i}, \frac{\partial e_y}{\partial q_j}, \frac{\partial e_{xy}}{\partial q_i},$  and  $\frac{\partial e_{xy}}{\partial q_j}$  into

Table (5-1), first incremental stiffness is obtained.

$[N_1]$

$M_{I,I}$	Sym
$M_{I,II}$	$M_{II,II}$

	1	2	3	4	5	6	7	8	9	10
1	O									
2	O	O								
3	M <sub>1</sub>	M <sub>2</sub>	M <sub>3</sub>							
4	O	O	O	O						
5	O	O	O	O	O					
6	O	O	M <sub>4</sub>	O	O	O				
7	O	O	M <sub>2</sub>	O	O	O	O			
8	M <sub>5</sub>	M <sub>6</sub>	M <sub>7</sub>	O	O	M <sub>8</sub>	M <sub>9</sub>	M <sub>10</sub>		
9	O	O	O	O	O	O	O	O	O	
10	O	O	O	O	O	O	O	O	O	O

SYMMETRICAL

SUBMATRIX  $M_{I,I}$

(5-41)

	1	2	3	4	5	6	7	8	9	10
11	O	O	$M_{11}$	O	O	O	O	$M_{12}$	O	O
12	O	O	$M_{13}$	O	O	O	O	$M_{14}$	O	O
13	$-M_1$	$-M_2$	$-M_3$	O	O	$-M_4$	$-M_2$	$-M_7$	O	O
14	O	O	O	O	O	O	O	O	O	O
15	O	O	O	O	O	O	O	O	O	O
16	O	O	$M_1$	O	O	O	O	$M_6$	O	O
17	O	O	$M_{15}$	O	O	O	O	$M_{16}$	O	O
18	$-M_5$	$-M_6$	$-M_7$	O	O	$-M_8$	$-M_9$	$-M_{10}$	O	O
19	O	O	O	O	O	O	O	O	O	O
20	O	O	O	O	O	O	O	O	O	O

SUBMATRIX  $M_{II,I}$  (5-42)

	11	12	13	14	15	16	17	18	19	20
11	O									
12	O	O								
13	$-M_{11}$	$-M_{13}$	$-M_3$							
14	O	O	O	O						
15	O	O	O	O	O					
16	O	O	$-M_1$	O	O	O				
17	O	O	$-M_{15}$	O	O	O	O			
18	$-M_{12}$	$-M_{14}$	$-M_7$	O	O	O	$-M_{16}$	$-M_{10}$		
19	O	O	O	O	O	O	O	O	O	
20	O	O	O	O	O	O	O	O	O	O

SYMMETRICAL

SUBMATRIX  $M_{II,II}$  (5-43)



$$H = b/a \quad F = a/b \quad A = Et^3/12(1-\nu^2) \quad C = 3A/2t^2$$

$$M_1 = C(2H\theta_x + 2\nu\theta_y)$$

$$M_2 = C(2\nu\theta_x + 2F\theta_y)$$

$$M_3 = C(2He_x + 2Hve_y + 2Fe_y + 2Fve_x + 2(1-\nu)e_{xy} + 6H\theta_x\theta_y \\ + 2H\theta_y\beta_y + 4\theta_x\beta_y + 4\theta_y\beta_x + 2F\theta_x\beta_x + 6F\theta_y\beta_y)$$

$$M_4 = C(-2H\theta_x - 2\nu\theta_y + 2(1-\nu)\theta_y + 2F(1-\nu)\theta_x)$$

$$M_5 = C(-2H\theta_x + 2\nu\theta_y)$$

$$M_6 = C(-2\nu\theta_x + 2F\theta_y)$$

$$M_7 = C(-2He_x - 2Hve_y + 2Fe_y + 2Fve_x - 6H\theta_x\beta_x - 2H\theta_y\beta_y \\ + 2F\theta_x\beta_x + 6F\theta_y\beta_y)$$

$$M_8 = C(2H\theta_x - 2(1-\nu)\theta_y - 2\nu\theta_y + 2F(1-\nu)\theta_x)$$

$$M_9 = C(-2\nu\theta_x + 2F\theta_y)$$

$$M_{10} = C(2He_x + 2Hve_y + 2Fe_y + 2Fve_x - 2(1-\nu)e_{xy} + 6H\theta_x\beta_x \\ + 2H\theta_y\beta_y - 4\theta_x\beta_y - 4\theta_y\beta_x + 2F\theta_x\beta_x + 6F\theta_y\beta_y)$$

$$M_{11} = C(-2H\theta_x - 2\nu\theta_y - 2(1-\nu)\theta_y - 2F(1-\nu)\beta_x)$$

$$M_{12} = C(2H\theta_x - 2\nu\theta_y + 2(1-\nu)\theta_y - 2F(1-\nu)\theta_x)$$

$$M_{13} = C(-2\nu\theta_x - 2F\theta_y - 2H(1-\nu)\theta_y - 2(1-\nu)\theta_x)$$

$$M_{14} = C(2\nu\theta_x - 2F\theta_y + 2(1-\nu)\theta_y - 2(1-\nu)\theta_x)$$

$$M_{15} = C(-2\nu\theta_x - 2F\theta_y + 2H(1-\nu)\theta_y + 2(1-\nu)\theta_x)$$

$$M_{16} = C(2\nu\theta_x - 2F\theta_y - 2H(1-\nu)\theta_y + 2(1-\nu)\theta_x)$$

Using Equation (5-18) for evaluating  $U_1$ , it follows:

$$\left\{ \frac{\partial U_2}{\partial q_i} \right\} = \frac{3D}{2t^2} \left[ 4\theta_x^3 \left( \frac{\partial \theta_x}{\partial q_i} \right) + 4\theta_y^3 \left( \frac{\partial \theta_y}{\partial q_i} \right) + 4\theta_x^2 \theta_y \left( \frac{\partial \theta_y}{\partial q_i} \right) + 4\theta_x \theta_y^2 \left( \frac{\partial \theta_x}{\partial q_i} \right) \right] ab$$

Where  $i = 1, 2, 3, \dots, 20$ , substitution of  $\theta_x$  and  $\theta_y$  from Equation (5 - 31) into partial derivatives yields:

$$\left\{ \frac{\partial U_2}{\partial q_i} \right\} = \frac{3D}{2t^2} \left\{ \begin{array}{l} 1 \quad 0 \\ 2 \quad 0 \\ 3 \quad -2\theta_x^3 b - 2\theta_y^3 a - 2\theta_x^2 \theta_y a - 2\theta_x \theta_y^2 b \\ 4 \quad 0 \\ 5 \quad 0 \\ 6 \quad 0 \\ 7 \quad 0 \\ 8 \quad 2\theta_x^3 b - 2\theta_y^3 a - 2\theta_x^2 \theta_y a + 2\theta_x \theta_y^2 b \\ 9 \quad 0 \\ 10 \quad 0 \\ 11 \quad 0 \\ 12 \quad 0 \\ 13 \quad 2\theta_x^3 b + 2\theta_y^3 a + 2\theta_x^2 \theta_y a + 2\theta_x \theta_y^2 b \end{array} \right\}$$

14	0
15	0
16	0
17	0
18	$-2\theta_x^3 b + 2\theta_y^3 a + 2\theta_x^2 \theta_y a - 2\theta_x \theta_y^2 b$
19	0
20	0

(5-44)

$$\left[ \frac{\partial^2 U}{\partial q_i \partial q_j} \right] = \frac{3D}{2t^2} \left[ \begin{aligned} &12\theta_x^2 \left( \frac{\partial^2 \theta_x}{\partial q_i \partial q_j} \right) + 12\theta_y^2 \left( \frac{\partial^2 \theta_y}{\partial q_i \partial q_j} \right) \\ &+ 8\theta_x \theta_y \left( \frac{\partial \theta_y}{\partial q_i} \right) \left( \frac{\partial \theta_y}{\partial q_j} \right) + 4\theta_x \left( \frac{\partial^2 \theta_y}{\partial q_i \partial q_j} \right) \\ &+ 4\theta_y^2 \left( \frac{\partial^2 \theta_x}{\partial q_i \partial q_j} \right) + 8\theta_x \theta_y \left( \frac{\partial \theta_x}{\partial q_i} \right) \left( \frac{\partial \theta_y}{\partial q_j} \right) \end{aligned} \right] \quad ab$$

(5-45)

Where  $j = 1, 2, 3, \dots, 20$ , substitution of  $\frac{\partial \theta_x}{\partial q_i}$ ,  $\frac{\partial \theta_y}{\partial q_j}$ ,

$\frac{\partial \theta_y}{\partial q_i}$ , and  $\frac{\partial \theta_x}{\partial q_j}$  into Table (5-1), second incremental

stiffness is obtained.

$$[N_2] = \begin{bmatrix} N_{I,I} & \text{Sym} \\ N_{I,II} & N_{II,II} \end{bmatrix}$$

	1	2	3	4	5	6	7	8	9	10
1	O									
2	O	O								
3	O	O	N <sub>1</sub>							
4	O	O	O	O						
5	O	O	O	O	O					
6	O	O	O	O	O	O				
7	O	O	O	O	O	O	O			
8	O	O	N <sub>2</sub>	O	O	O	O	N <sub>3</sub>		
9	O	O	O	O	O	O	O	O	O	
10	O	O	O	O	O	O	O	O	O	O

S Y M M E T R I C A L

(5-46)

SUBMATRIX N<sub>I,I</sub>

	1	2	3	4	5	6	7	8	9	10
11	O	O	O	O	O	O	O	O	O	O
12	O	O	O	O	O	O	O	O	O	O
13	O	O	-N <sub>1</sub>	O	O	O	O	-N <sub>2</sub>	O	O
14	O	O	O	O	O	O	O	O	O	O
15	O	O	O	O	O	O	O	O	O	O
16	O	O	O	O	O	O	O	O	O	O
17	O	O	O	O	O	O	O	O	O	O
18	O	O	-N <sub>2</sub>	O	O	O	O	-N <sub>3</sub>	O	O
19	O	O	O	O	O	O	O	O	O	O
20	O	O	O	O	O	O	O	O	O	O

(5-47)

SUBMATRIX N<sub>II,I</sub>



	11	12	13	14	15	16	17	18	19	20
11	O									
12	O	O								
13	O	O	N <sub>1</sub>							
14	O	O	O	O						
15	O	O	O	O	O					
16	O	O	O	O	O	O				
17	O	O	O	O	O	O	O			
18	O	O	N <sub>2</sub>	O	O	O	O	N <sub>3</sub>		
19	O	O	O	O	O	O	O	O	O	
20	O	O	O	O	O	O	O	O	O	O

S Y M M E T R I C A L

(5-48)

$$F = a/b \quad H = b/a \quad A = Et^3/12(1-\nu^2) \quad C = 3A/2t^2$$

$$N_1 = C(3H\theta_x^2 + 3F\theta_y^2 + 4\theta_x\theta_y + H\theta_y^2 + F\theta_x^2)$$

$$N_2 = C(-3H\theta_x^2 + 3F\theta_y^2 - H\theta_y^2 + F\theta_x^2)$$

$$N_3 = C(3H\theta_x^2 + 3F\theta_y^2 - 4\theta_y\theta_x + H\theta_y^2 + F\theta_x^2)$$

## 5.6 THE GAUSS-ELIMINATION SOLUTION

The method for an efficient assembly of element matrices into the global system is considered here. The overall effectiveness of an analysis depends to a large extent on the numerical procedures used in the solution, and the accuracy of the analysis can always be improved by a more refined finite element mesh. Therefore, in practice, an analyst tends to employ larger and larger finite element systems to approximate the actual structure. This means that the success of an analysis depends to a considerable degree on the algorithms available for the solution.

The most effective direct solution techniques currently used are basically applications of Gauss elimination. Although the basic Gauss solution scheme can be applied to almost any set of simultaneous linear equations, the effectiveness in finite element analysis depends on the specific properties of the finite element stiffness matrix, i.e., it is symmetric, positive definite, and banded. The basic procedure of the Gauss elimination solution is to reduce the coefficient matrix of the equations to a lower triangular matrix from which the unknown displacements can be calculated by back substitution.

The reduction of the stiffness matrix  $k$  to lower triangular form can be written,

$$C_{n-1}^{-1} \cdot \cdot C_2^{-1} C_1^{-1} k = T \quad (5-49)$$

where  $T$  is the final lower triangular matrix and the elements  $C$  are the multiplying factors. By reversing the signs of the off diagonal elements in  $C$ , the stiffness matrix is obtained:

$$k = C_1 C_2 \cdot \cdot \cdot C_{n-1} T, \quad (5-50)$$

or

$$k = CT.$$

Since  $T$  is a lower diagonal matrix and the diagonal elements are the pivots in the Gauss eliminations; therefore,

$$k = CGC^T. \quad (5-51)$$

This  $CGC^T$  is a decomposition of  $k$  that can be used effectively to obtain the solution to  $kq = P$  in the following steps;

$$CH = P$$

or

(5-52)

$$H = GC^T q$$

where  $q$  is the displacement and the load vector  $P$  is reduced to obtain  $H$

$$H = C_{n-1}^{-1} \cdot \dots \cdot C^{-1} C^{-1} P \quad (5-53)$$

and from Equation (5-52) the solution  $q$  is obtained by a back substitution

$$C^T q = G^{-1} H . \quad (5-54)$$

In the implementation the vector  $H$  is very effectively calculated at the same time as the matrices  $C^{-1}$  are established.

It must now be mentioned that the matrix multiplication to obtain  $C$  and  $H$  are not formally carried out, but  $C$  and  $H$  are established by directly modifying  $k$  and  $P$ .



## 5.6:1 COMPUTER APPLICATION OF GAUSS ELIMINATION

An important consideration in the computer implementation of the Gauss solution procedure is to minimise the solution time. In addition, the high-speed storage requirements should be kept as small as possible, to avoid the use of back-up storage. Nevertheless, for large systems, it will be necessary to use back-up storage and for this reason it should also be possible to modify the solution algorithm for effective out-of-core solution.

In principle, Gauss elimination assembles the equations in the order of elements. Since the bandwidth is determined by the element numbering system, an effective ordering of the elements is necessary. Owing to the symmetry of the matrix, it is not necessary to store terms above the main diagonal during the triangulation process.

For large systems, instead of assembling the complete structure stiffness matrix, it is possible to assemble and reduce the equations simultaneously, in which case back-up storage for the total unreduced stiffness matrix is not required. A specific solution scheme called the frontal solution (see Section 5.7) method has been used effectively. In the solution procedure only those equations that are actually required for the elimination of a specific degree of freedom are assembled, until the degree of freedom considered is condensed out, and so on.

In principle, the frontal solution uses Gauss elimination, the important aspect of which is the specific computer implementation. The advantage of the frontal solution technique is that at any one time only the equations that are currently needed are assembled in the high-speed storage. However, for large structural analysis, the number of coefficients in the work space becomes very large and may well exceed the storage that is available, in which case additional out-of-core operations are required.

The developed plate program makes use of available disc facilities to store the coefficient matrix as a block of 2000 for the back-substitution process. After completion of forward elimination, the last set of coefficients in the working space are needed immediately in the back-substitution process, and it seems unnecessary to store these on disc. But since the modified Newton-Raphson iterative procedure uses the same matrix coefficients all over again, the whole set of coefficients matrix must in fact be stored.



## 5.7 FRONTAL SOLUTION

The accuracy of the finite element method in structural analysis is based on the type and characteristics of the finite element or elements used, and on the numerical efficiency of the solution routine written for the large number of simultaneous algebraic equations encountered.

When the structure to be analyzed has so many unknown nodal displacements that core storage is exhausted, resort must be had to the use of high-speed peripheral storage such as a drum or a disc, or some other algorithm such as frontal solution (forward partitioning) must be used. This method was proposed by Irons (Ref. 66). It is seen from Figure (5-2) that when a set of banded equations is being reduced by Gaussian elimination, only the triangular portion of the band shaded is influenced by the operation on the row marked  $i$ , and hence this is the only portion needed in the core at that time, thus reducing the storage demand of the program on the computer.

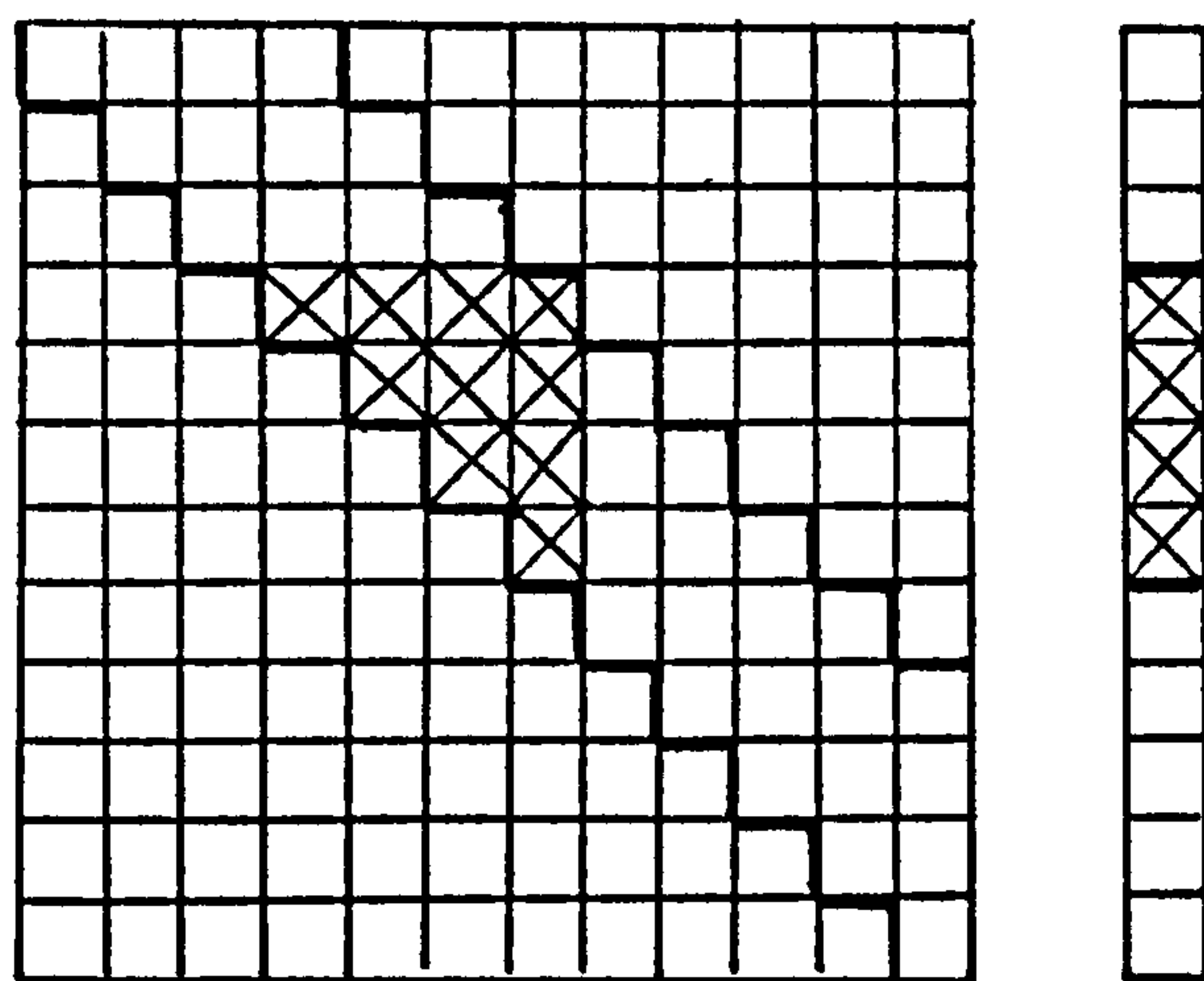


FIGURE (5-2)

Banded Coefficient Matrix  
Stored Portion

Load  
Vector

One of the main factors affecting the efficiency of the solution of large sets of algebraic equations arising in the analysis of complex structures is the method of node numbering. Optimization of node numbering is used to minimize the bandwidth of the algebraic equations. In the special case of plate structures consisting of single continuous components, not necessarily of a regular shape, optimization of the bandwidth can easily be obtained by starting the assembly of the elements at one corner of the structure,

proceeding across its width and repeating the process along the next line of elements across the width until the entire structure is covered.

A suitable procedure to follow in the solution of a system by a direct stiffness method is outlined in the following steps:

- 1) From storage available, and the band width of the  $K$  matrix, determine how many blocks are necessary to fit the band of  $K$  into core. These blocks are shown in Figure (5-3).
- 2) From the member connectivity arrays, determine which members contribute stiffness to each block. Notice that some members will contribute to both blocks I and II and III. It should be clear that the number of rows to a block should be a function of the number of unknowns per joint, so that member  $K$ 's can be loaded by submatrices according to their nodes.
- 3) The blocks I, II, and III are formed in turn from member stiffness matrices. These may have been calculated previously and stored. Modify as necessary for boundary conditions.
- 4) When all blocks have been completed, reduce  $K$  by a Gaussian process that recalls the columns in step 3 to memory.

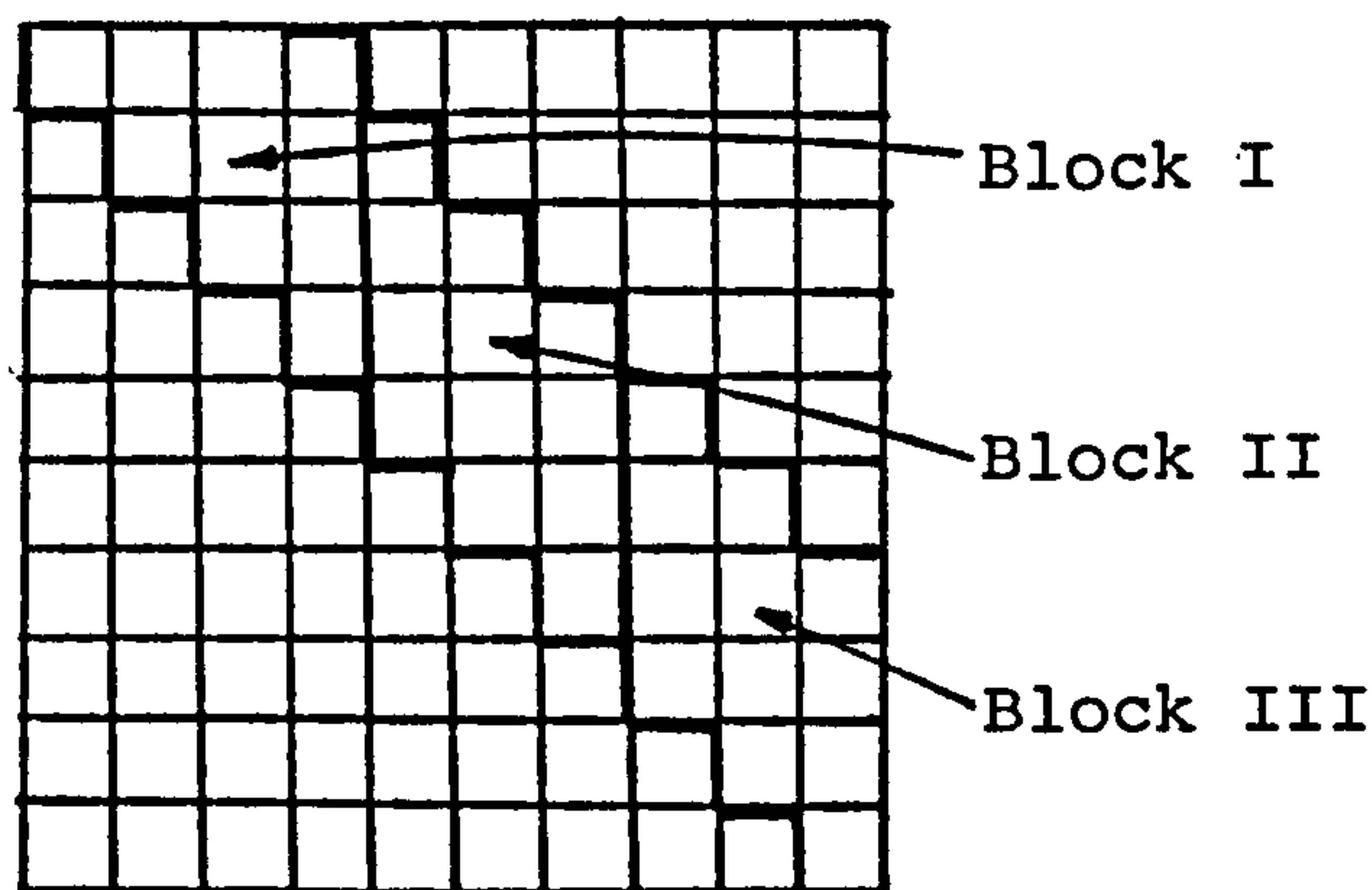


FIGURE (5-3)



## 5.7:1 DESCRIPTION OF FRONTAL SOLUTION

The process of the frontal solution developed in this program is illustrated in Figure (5-4) and has the dual purpose of finding the displacements due to the applied load for the incremental procedure, and of finding the internal load member in the equilibrium check.

Having calculated the element stiffness matrix, assembly into the overall stiffness matrix is carried out by the method mentioned in Appendix A-3 for optimization of the bandwidth. For example, for a structure divided into the 2 x 2 mesh shown in Figure (5-4), if the element stiffness matrix is partitioned in the form shown in Figure (5-5), the overall stiffness matrix becomes as shown in Figure (5-6). This figure can be used to illustrate the main feature of the solution routine.

Initially, the stiffness matrix for the first element is assembled in the appropriate positions in the working space. Since the stiffness matrix is symmetrical, all terms below the diagonal are assembled (Figure 5-6a). After making the appropriate calculations for the first node, the next stage is to reduce the term for the first node to zero and to move the remaining coefficients in Figure (5-6b) up the main diagonal to appear as shown in Figure (5-6c). The stiffness matrix for the second element can now be added and placed in position shown in Figure (5-6d). The process of triangulization, and the following shifting of the terms of the matrix can be repeated to obtain what is shown in Figures (5-6d, 5-6e, and 5-6f). This process is then continued until the triangulization of the entire overall matrix is performed. The program thus requires access only to the triangular area below the rows currently being processed. With certain exceptions, the coefficients of one node at a time are triangularized. The exceptions to this occur at the end of each row of elements, and at the very last element.

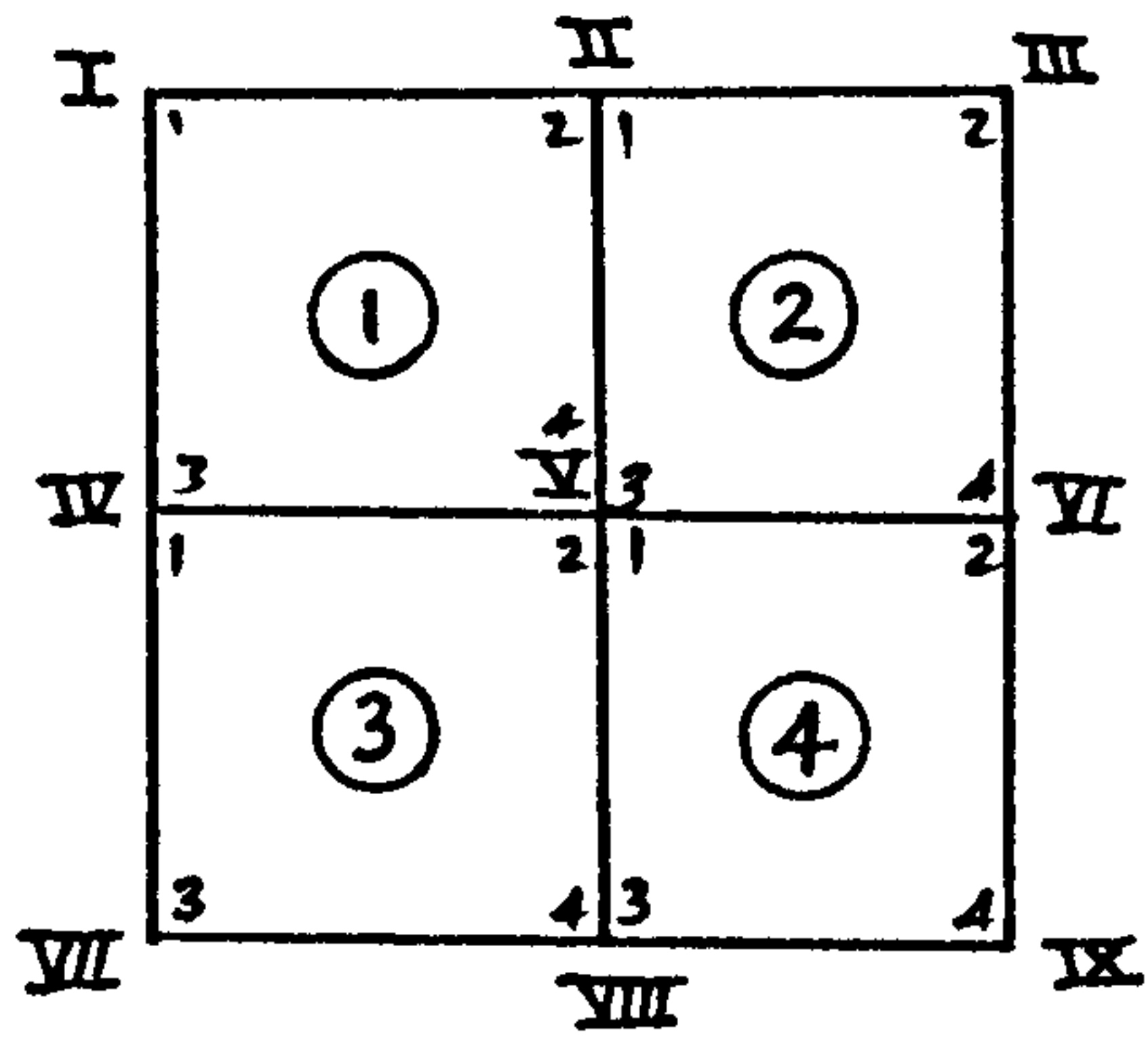


FIGURE (5-4)

Typical 2 x 2 Finite Element mesh

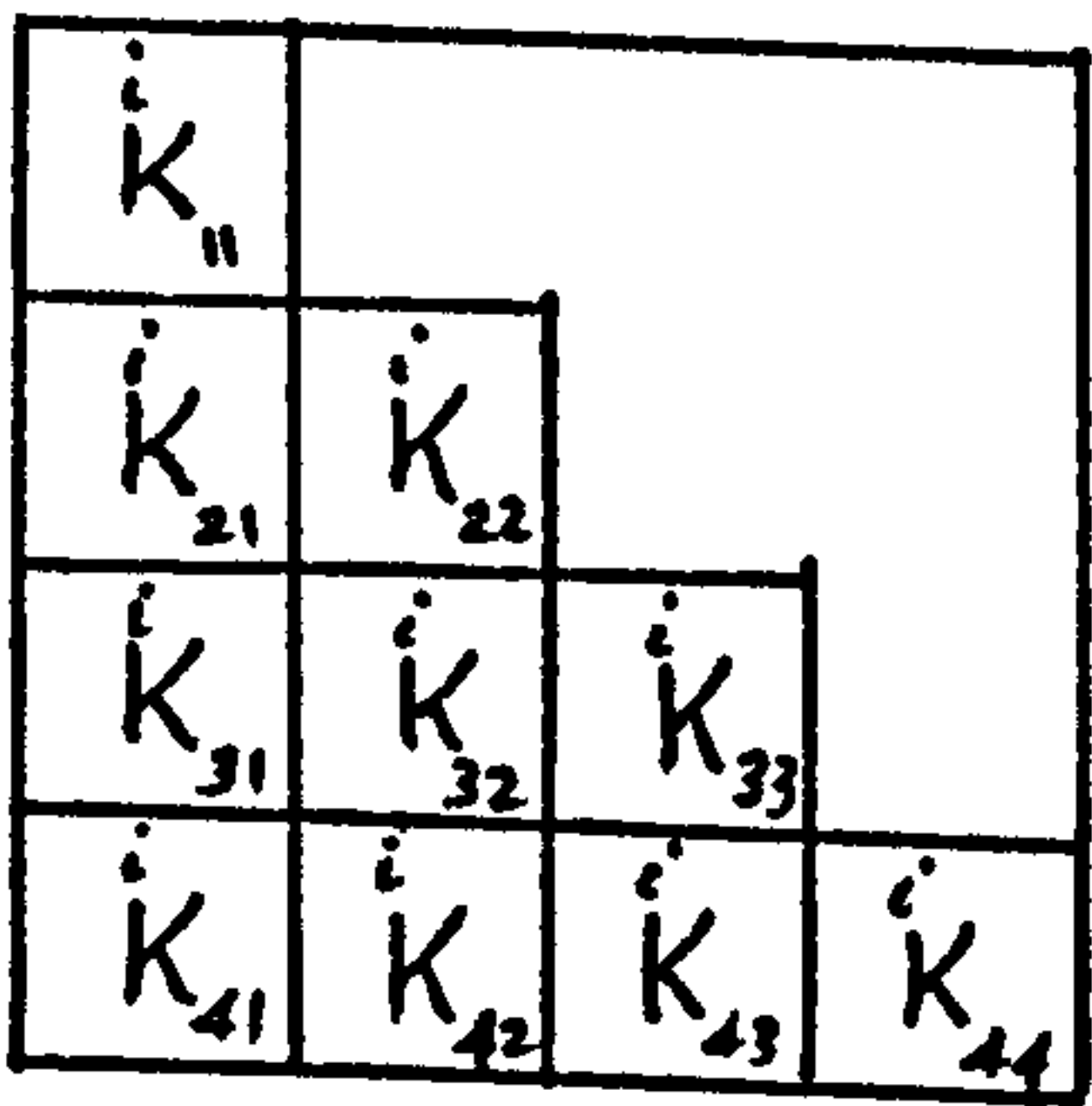
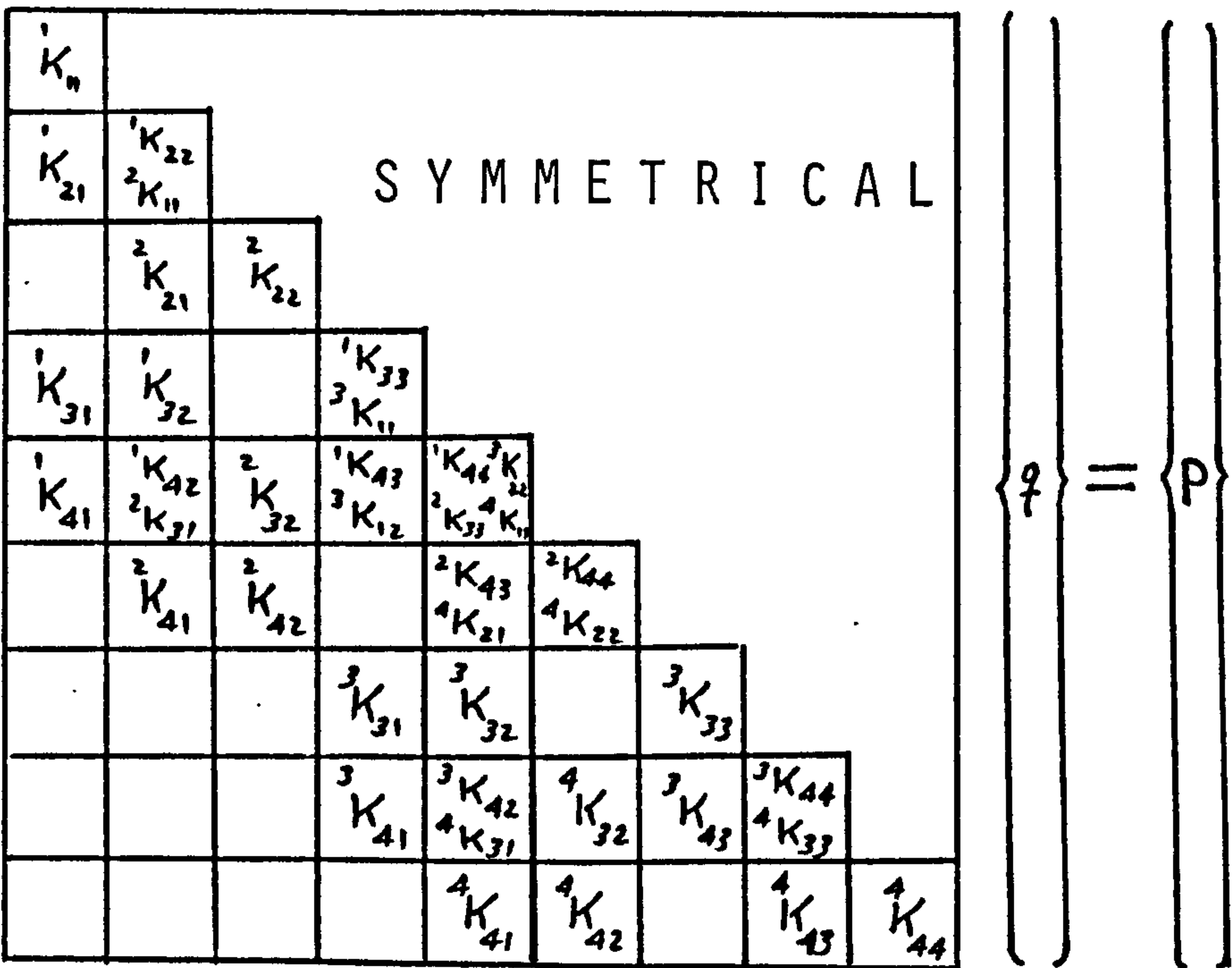


FIGURE (5-5)

Partitioned Matrix for Element i



Assembled Stiffness Matrix

FIGURE (5-6)



## BLOCK SEQUENCE IN WORKING SPACE OF COMPUTER

${}^1K_{11}$				
${}^1K_{21}$	${}^1K_{22}$			
${}^1K_{31}$	${}^1K_{32}$		${}^1K_{33}$	
${}^1K_{41}$	${}^1K_{42}$		${}^1K_{43}$	${}^1K_{44}$

Element 1 Assembled

FIGURE (5-6A)

	${}^1K_{22}$			
	${}^1K_{32}$		${}^1K_{33}$	
	${}^1K_{42}$		${}^1K_{43}$	${}^1K_{44}$

1<sup>st</sup> Stage of Elimination

FIGURE (5-6B)

${}^1K_{22}$				
${}^1K_{32}$		${}^1K_{33}$		
${}^1K_{42}$		${}^1K_{43}$	${}^1K_{44}$	

Triangular Shifting

FIGURE (5-6C)

${}^1K_{22}$ ${}^2K_{11}$				
${}^2K_{21}$	${}^2K_{22}$			
${}^1K_{32}$		${}^1K_{33}$		
${}^1K_{42}$ ${}^2K_{31}$	${}^2K_{32}$	${}^1K_{43}$	${}^2K_{33}$	
${}^2K_{41}$	${}^2K_{42}$		${}^2K_{43}$	${}^2K_{44}$

Element 2 Assembled

FIGURE (5-6D)

	${}^2K_{22}$			
		${}^1K_{33}$		
	${}^2K_{32}$	${}^1K_{43}$	${}^2K_{33}$	
	${}^2K_{42}$		${}^2K_{43}$	${}^2K_{44}$

2<sup>nd</sup> Stage of Elimination

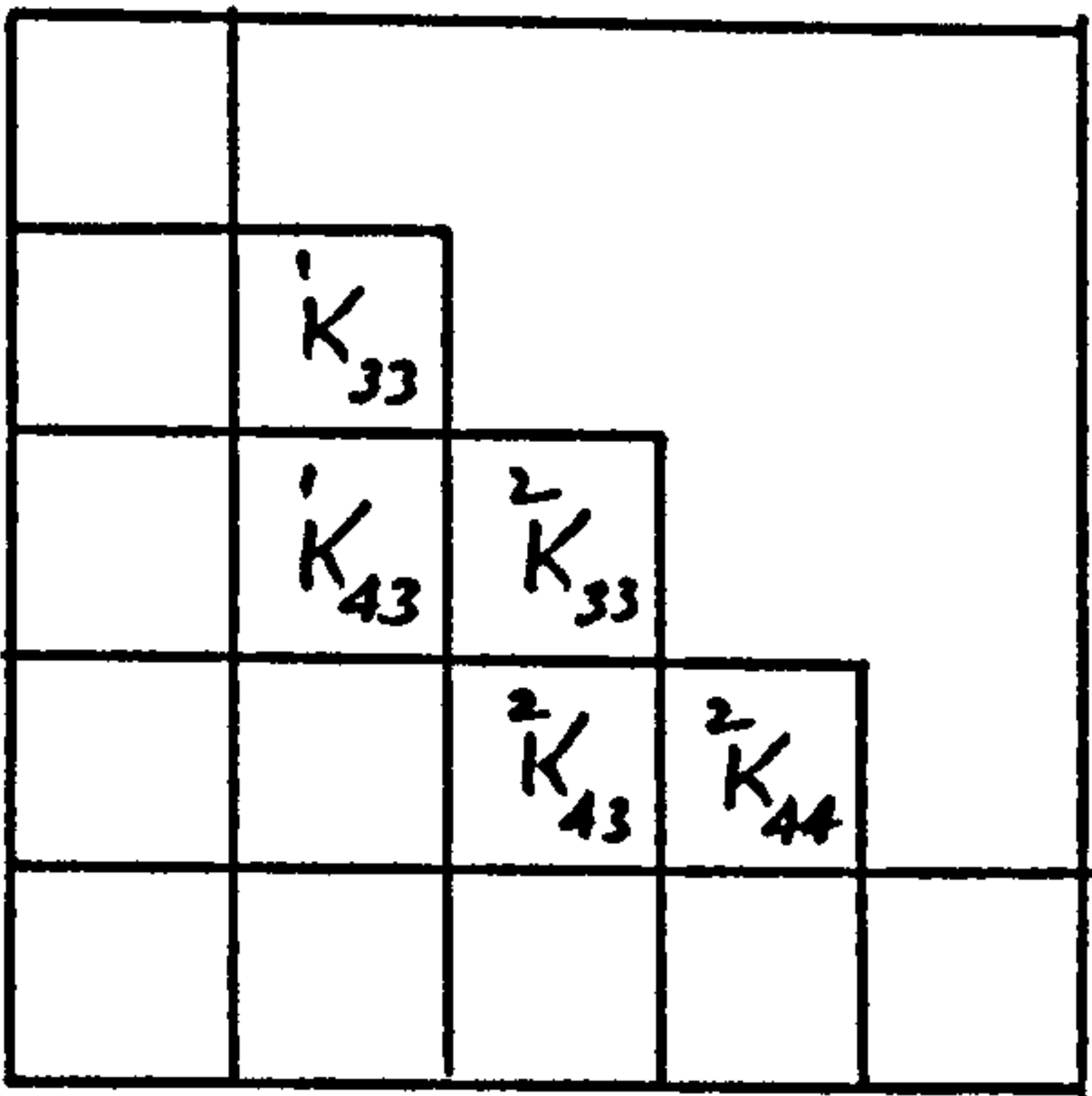
FIGURE (5-6E)

${}^2K_{22}$				
	${}^1K_{33}$			
${}^2K_{32}$	${}^1K_{43}$	${}^2K_{33}$		
${}^2K_{42}$		${}^2K_{43}$	${}^2K_{44}$	

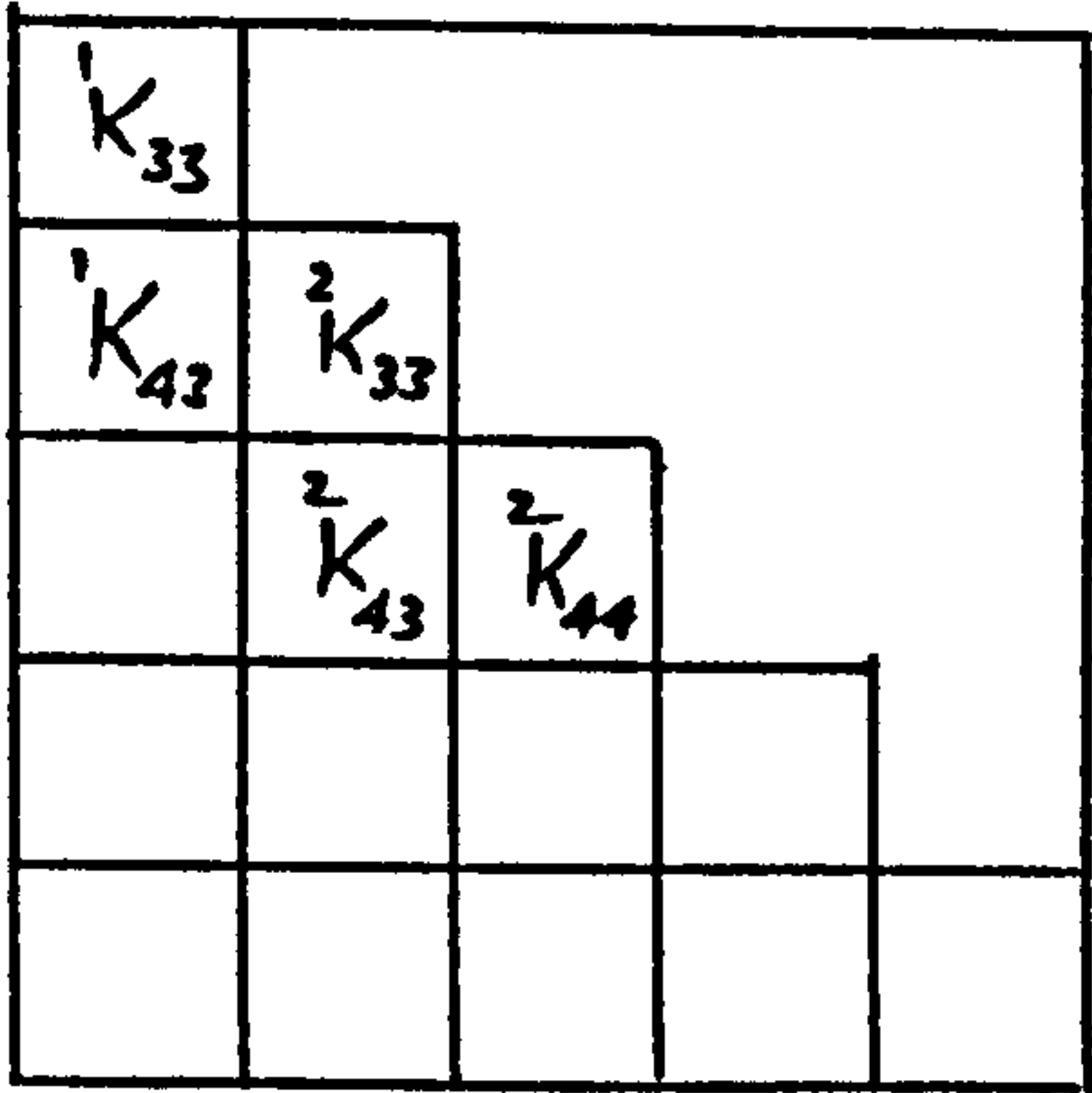
Triangular Shifting

FIGURE (5-6F)

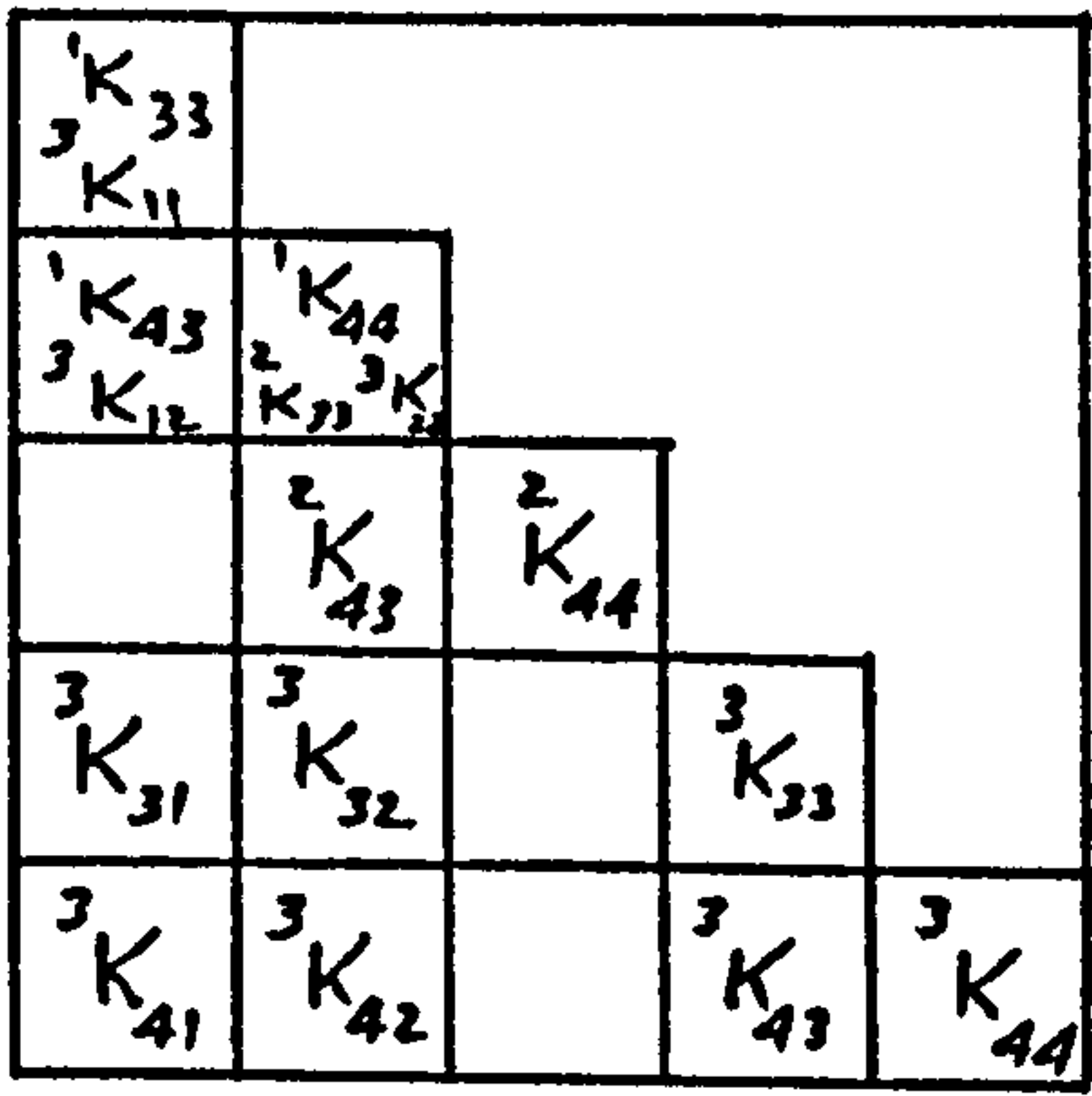
BLOCK SEQUENCE IN WORKING SPACE OF COMPUTER



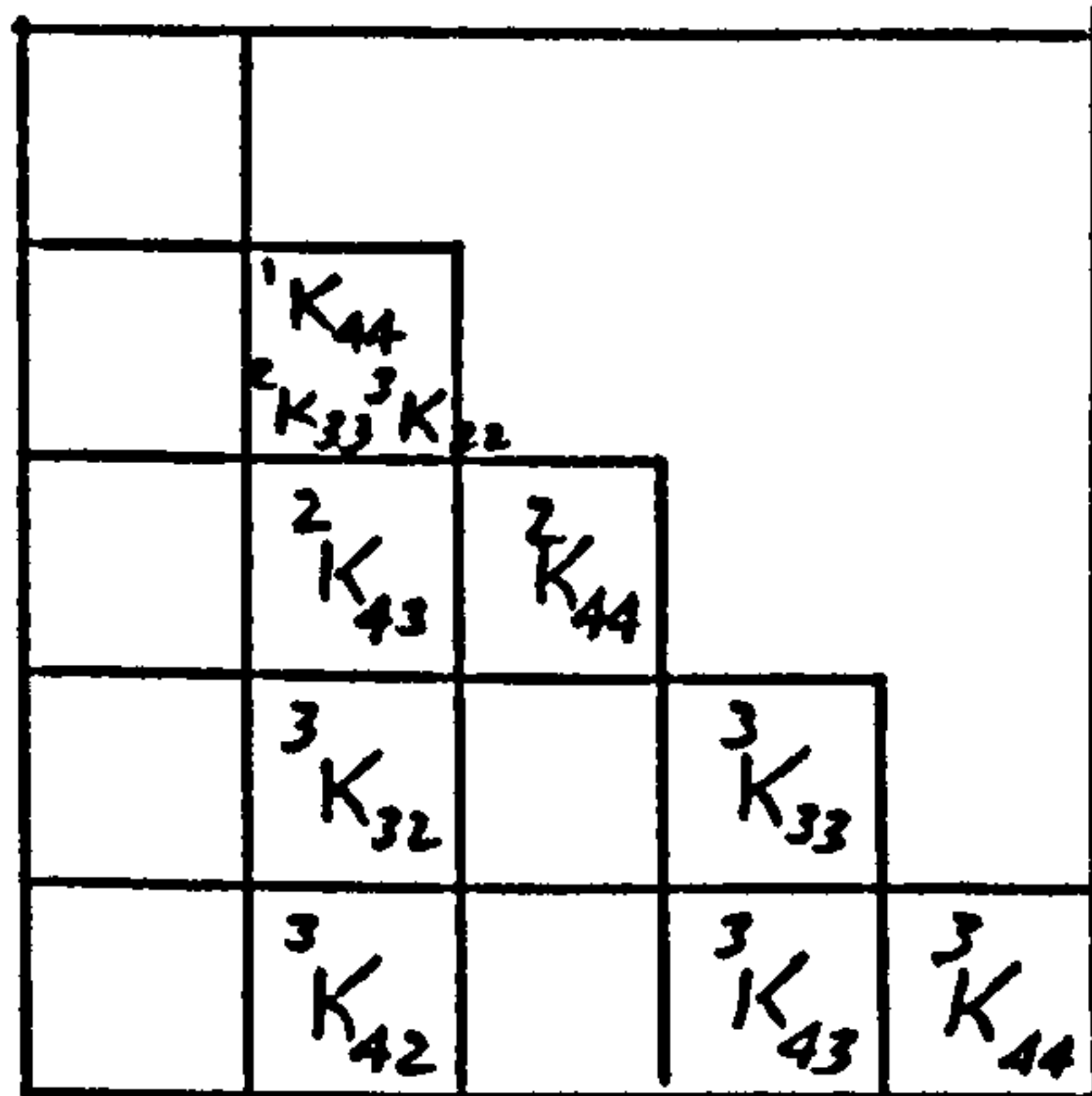
3<sup>rd</sup> Stage of Elimination  
FIGURE (5-6G)



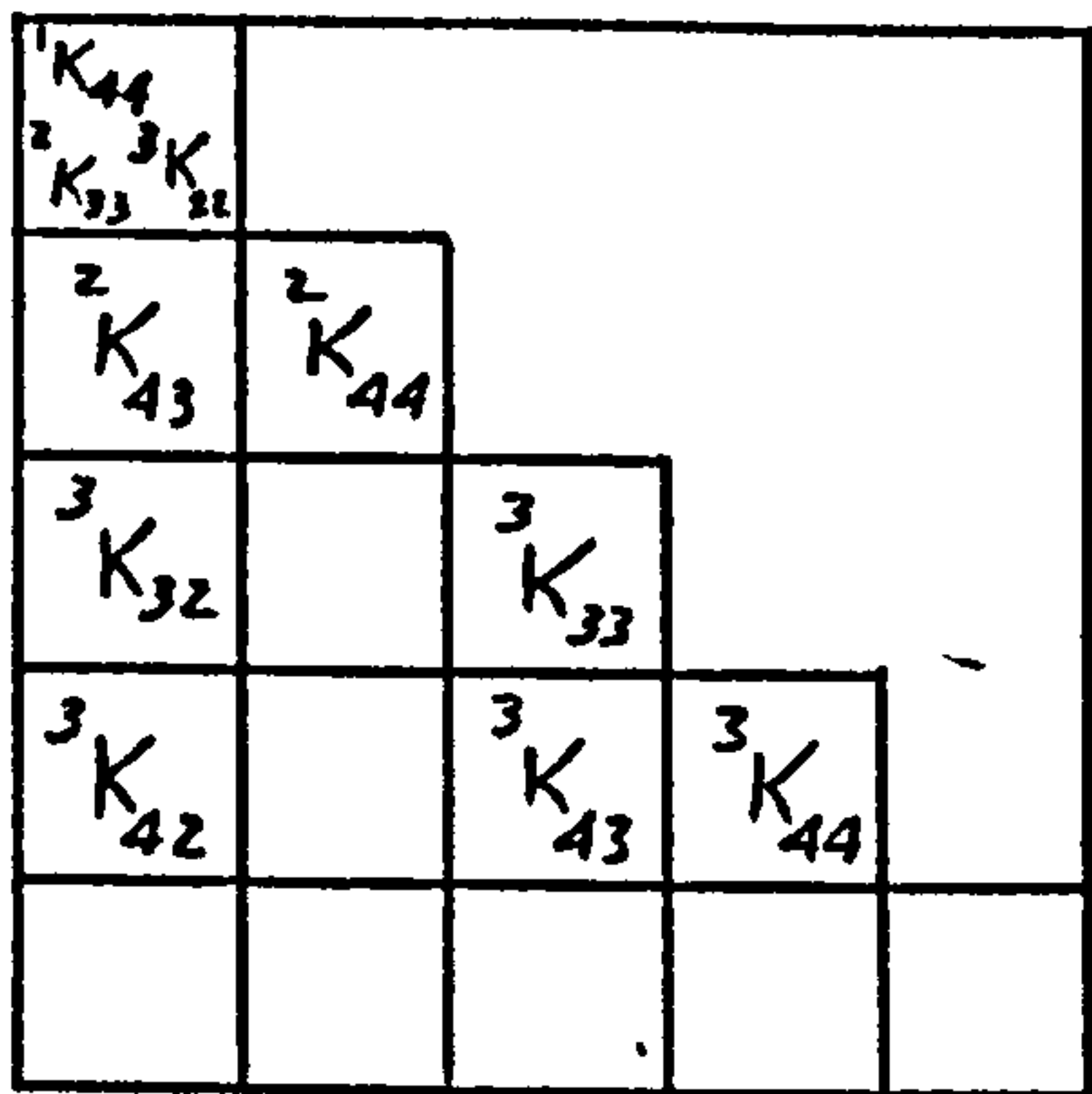
Triangular Shifting  
FIGURE (5-6H)



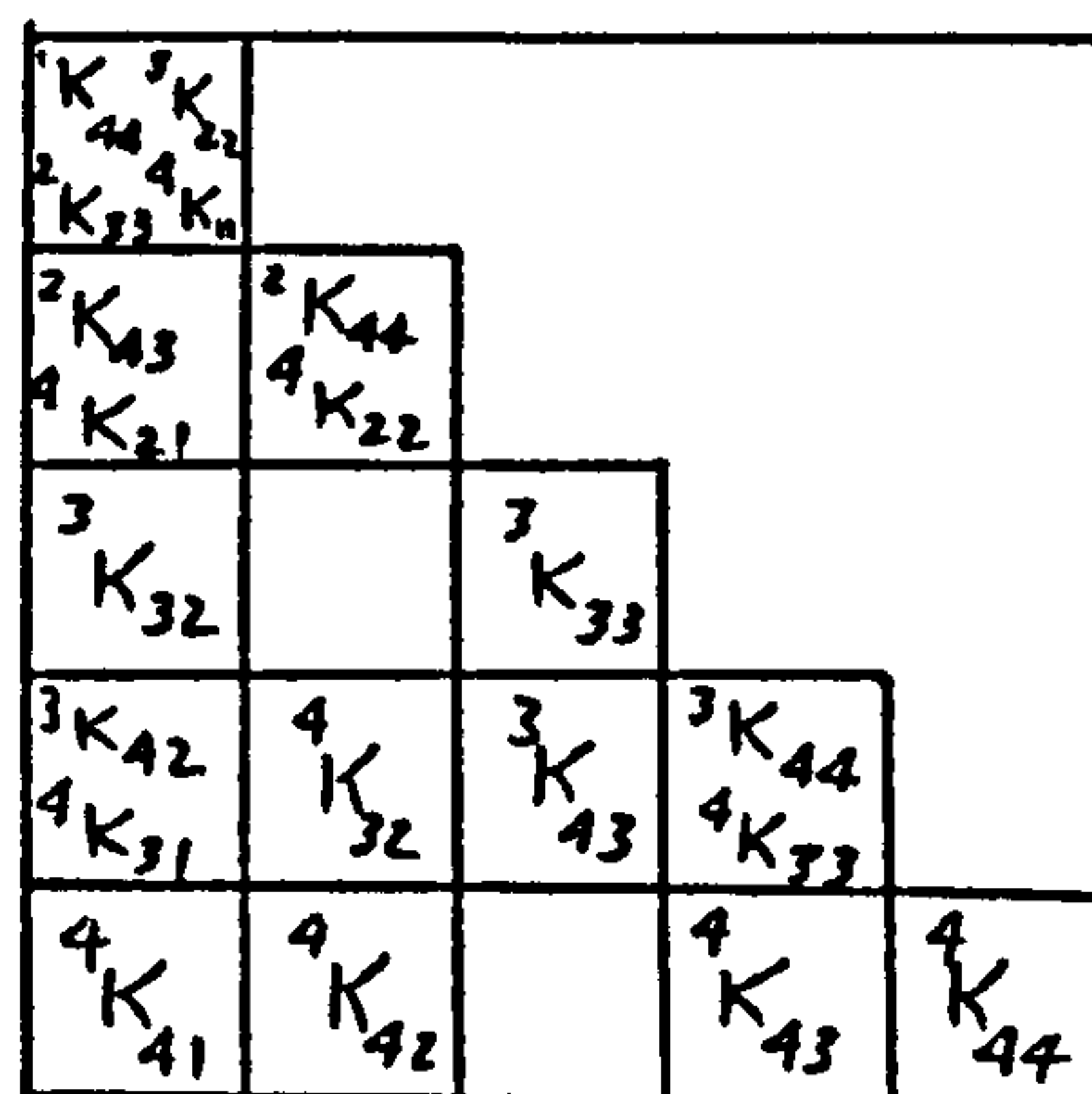
Element 3 Assembled  
FIGURE (5-6I)



4<sup>th</sup> Stage of Elimination  
FIGURE (5-6J)



Triangular Shifting  
FIGURE (5-6K)



Element 4 Assembled  
FIGURE (5-6L)

## BLOCK SEQUENCE IN WORKING SPACE OF COMPUTER

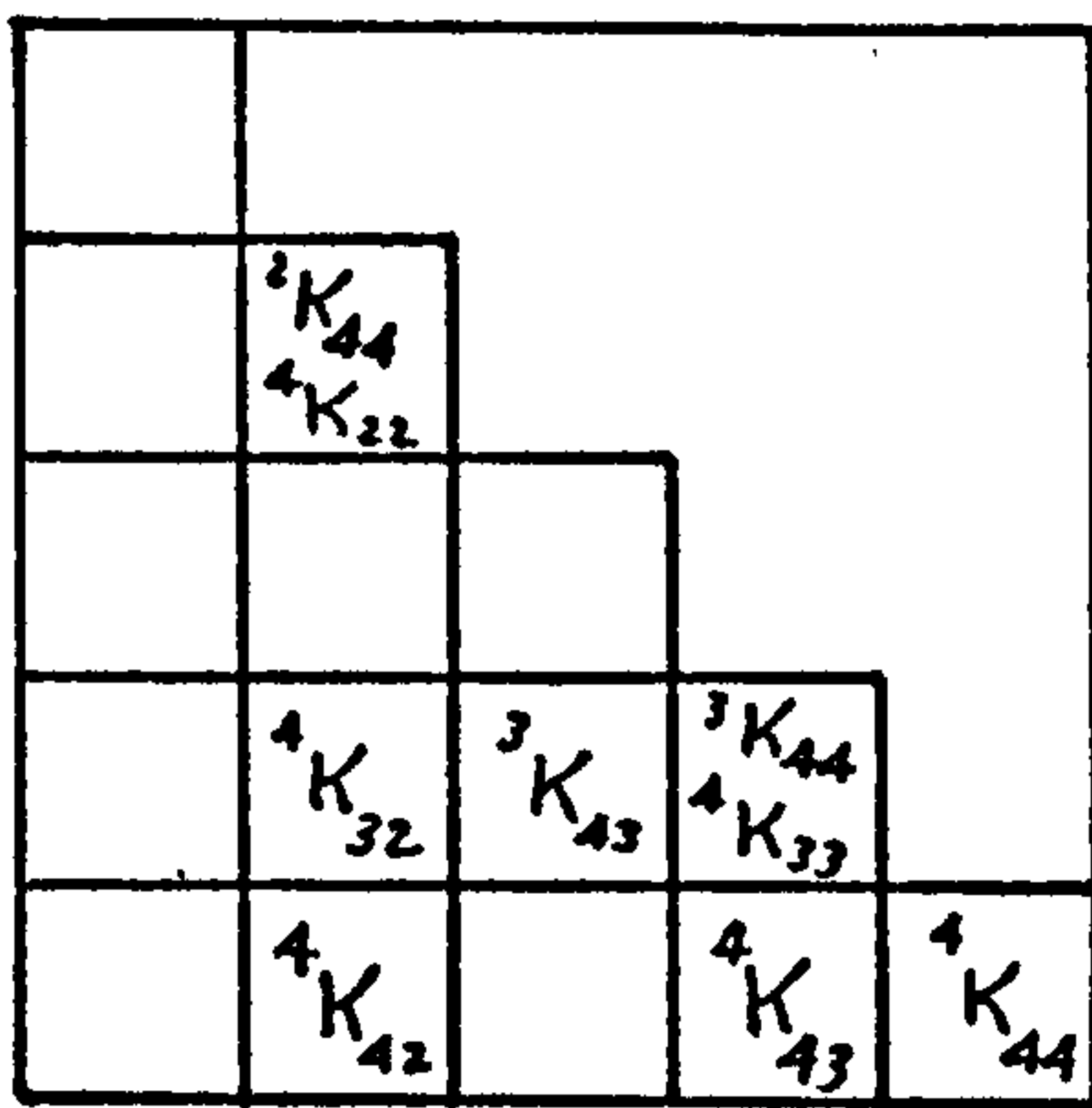
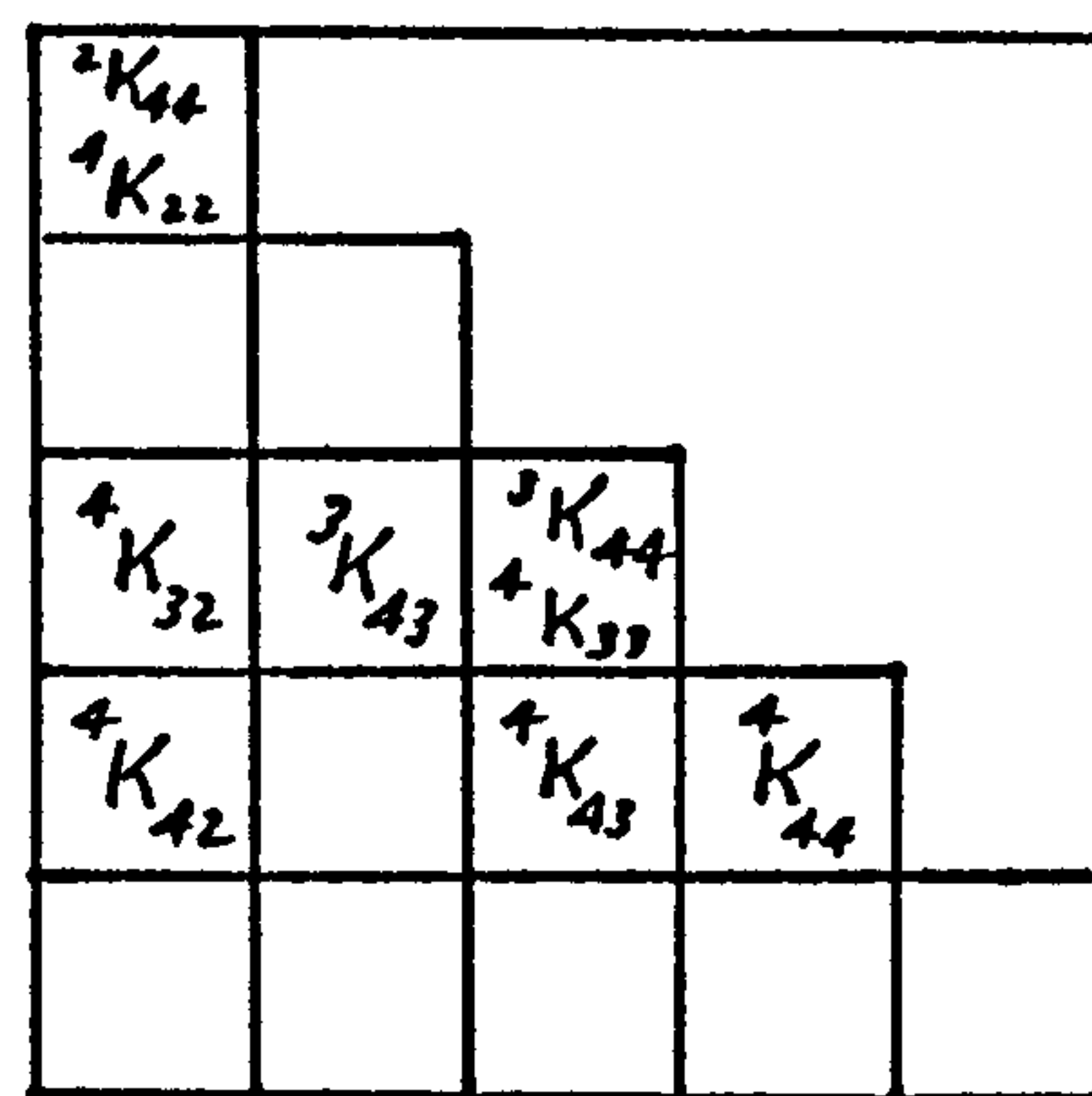
5<sup>th</sup> Stage of Elimination

FIGURE (5-6M)



Triangular Shifting

FIGURE (5-6N)

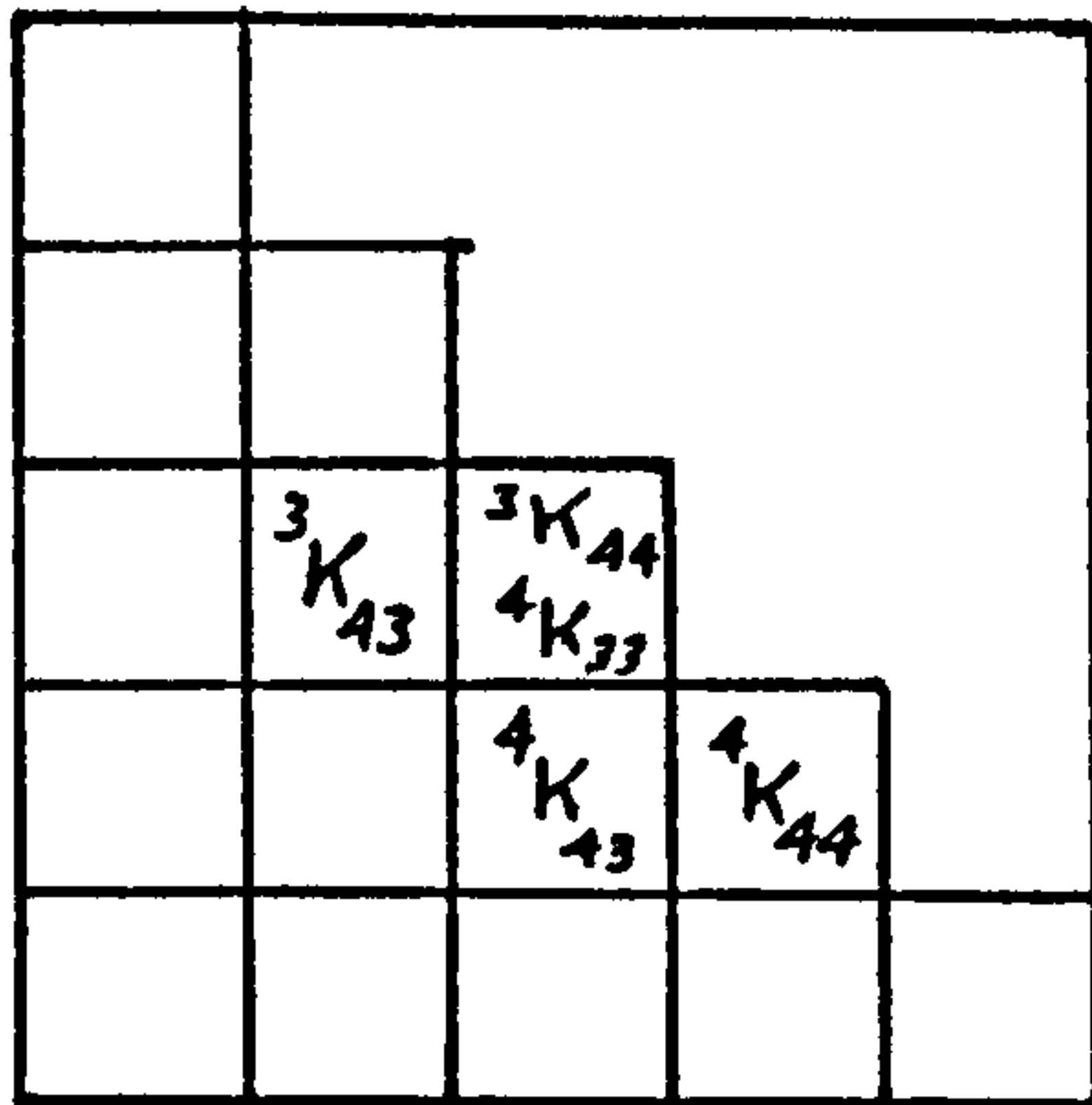
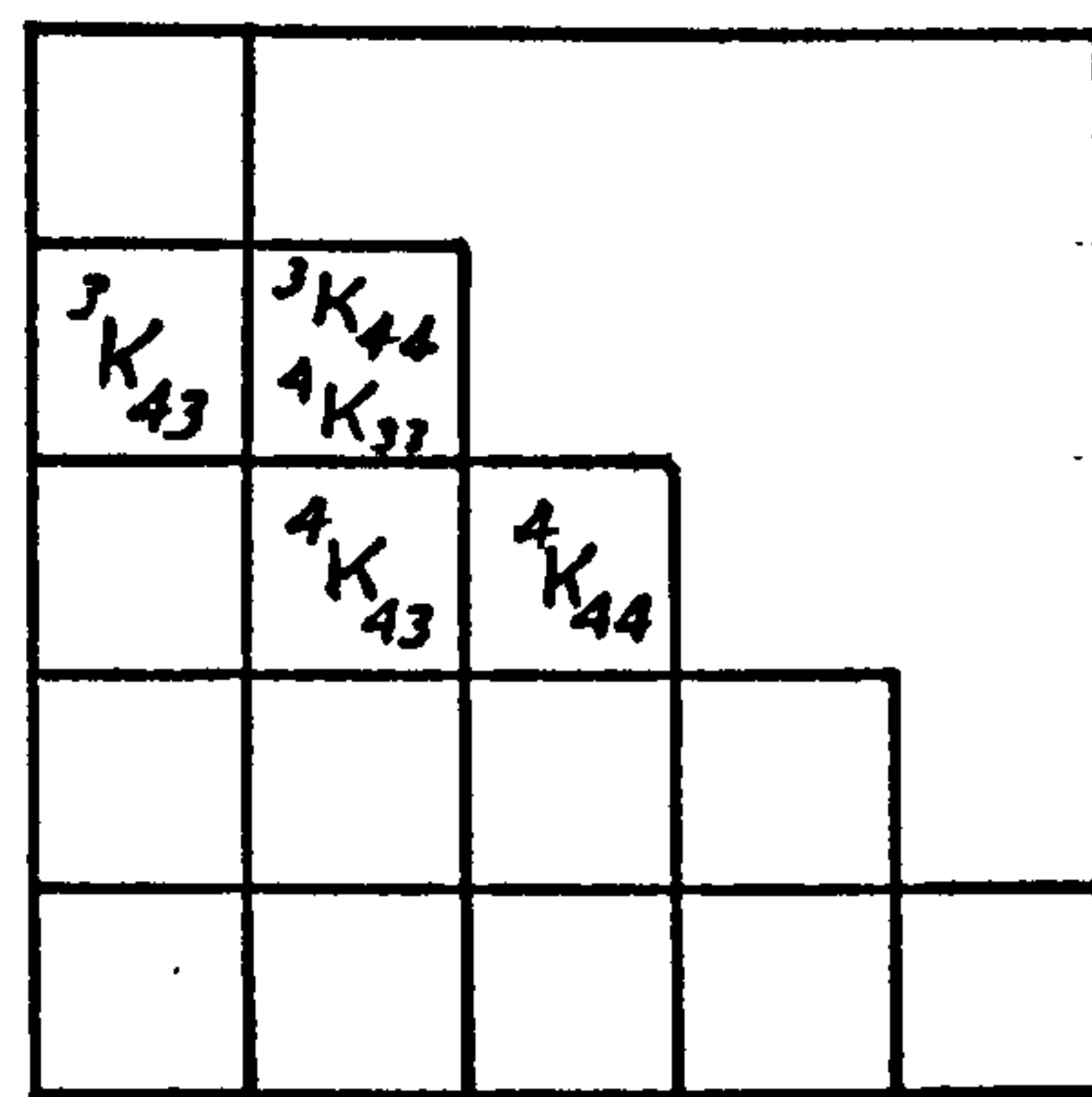
6<sup>th</sup> Stage of Elimination

FIGURE (5-6P)



Triangular Shifting

FIGURE (5-6Q)

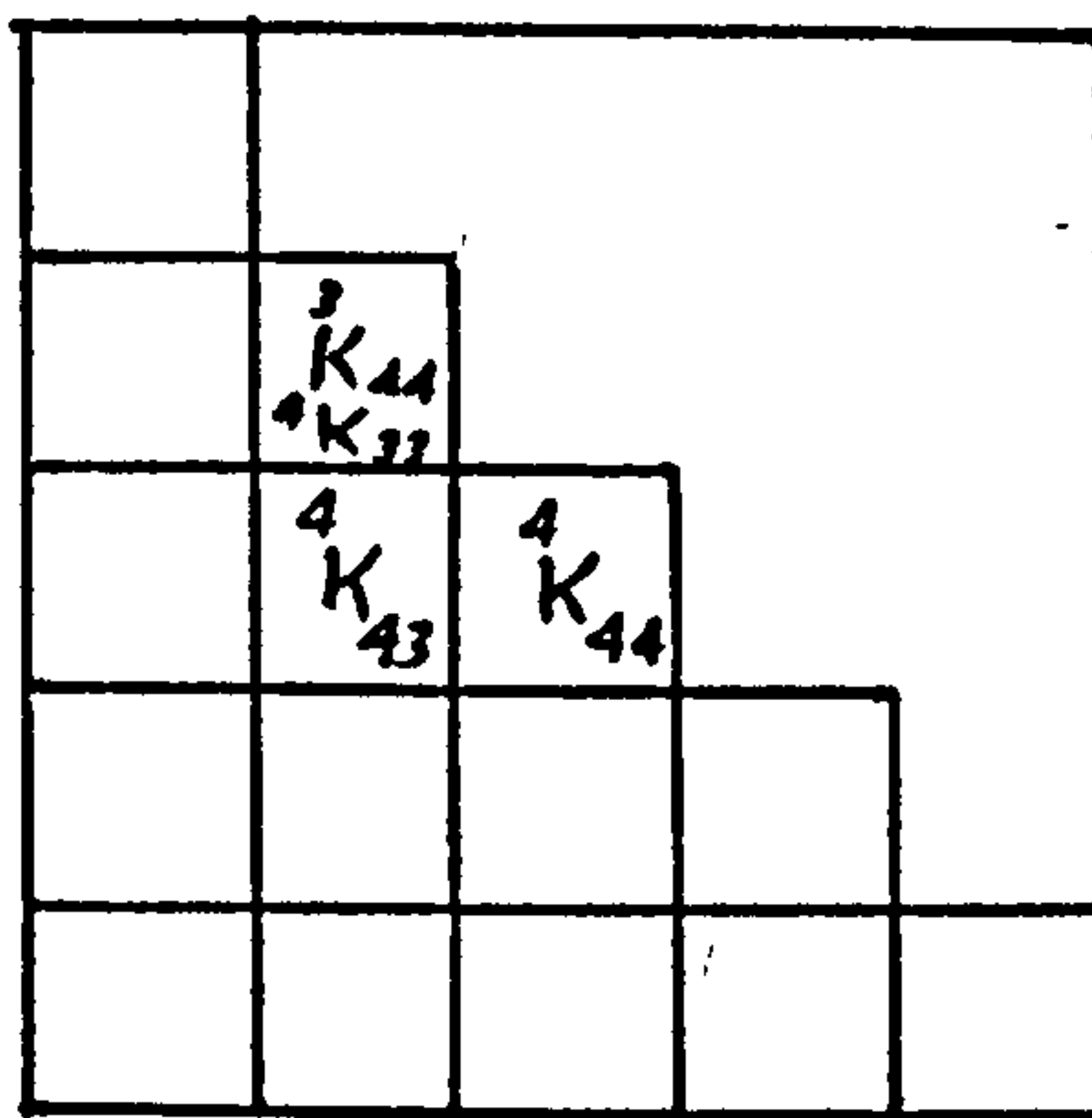
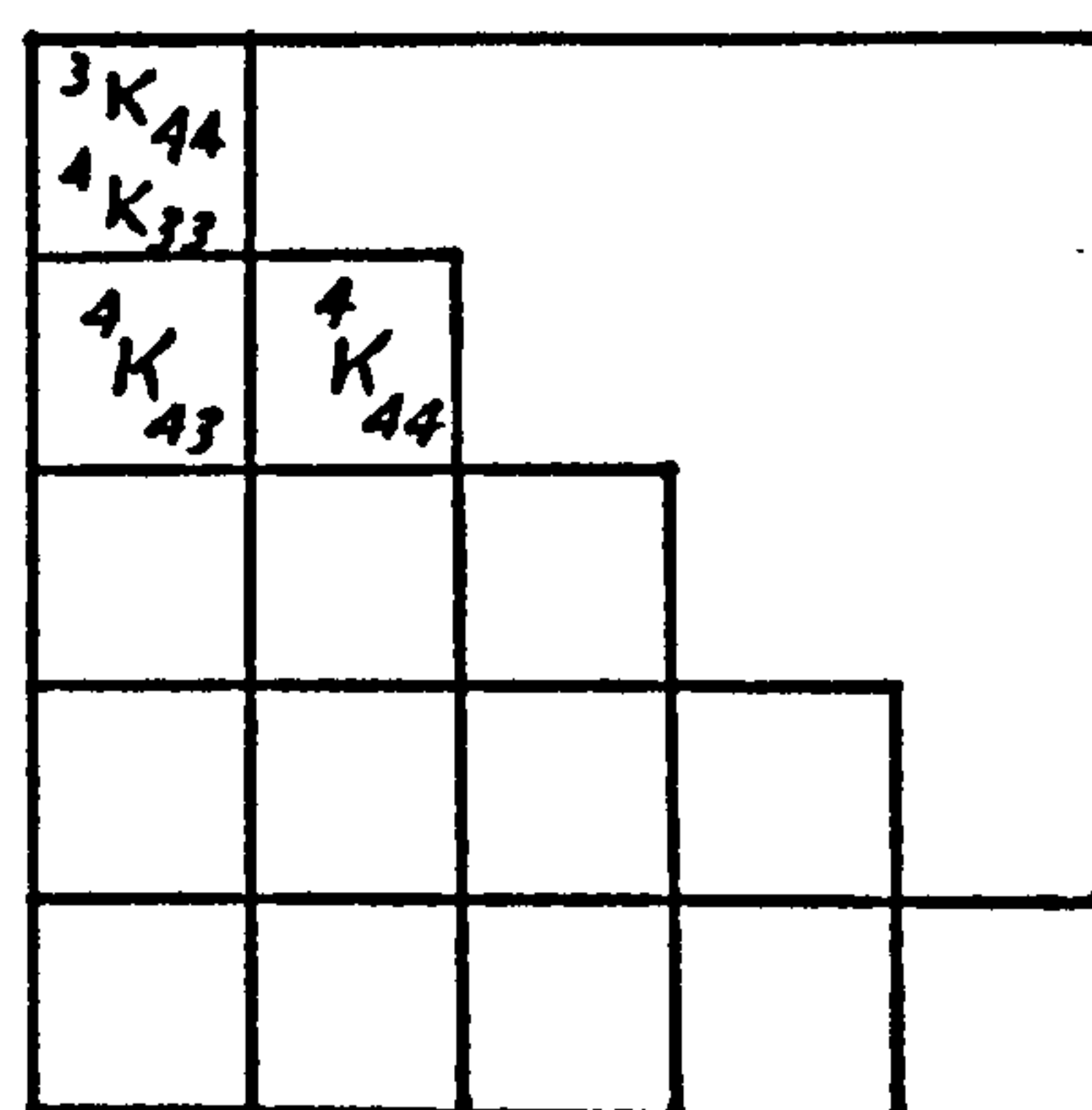
7<sup>th</sup> Stage of Elimination

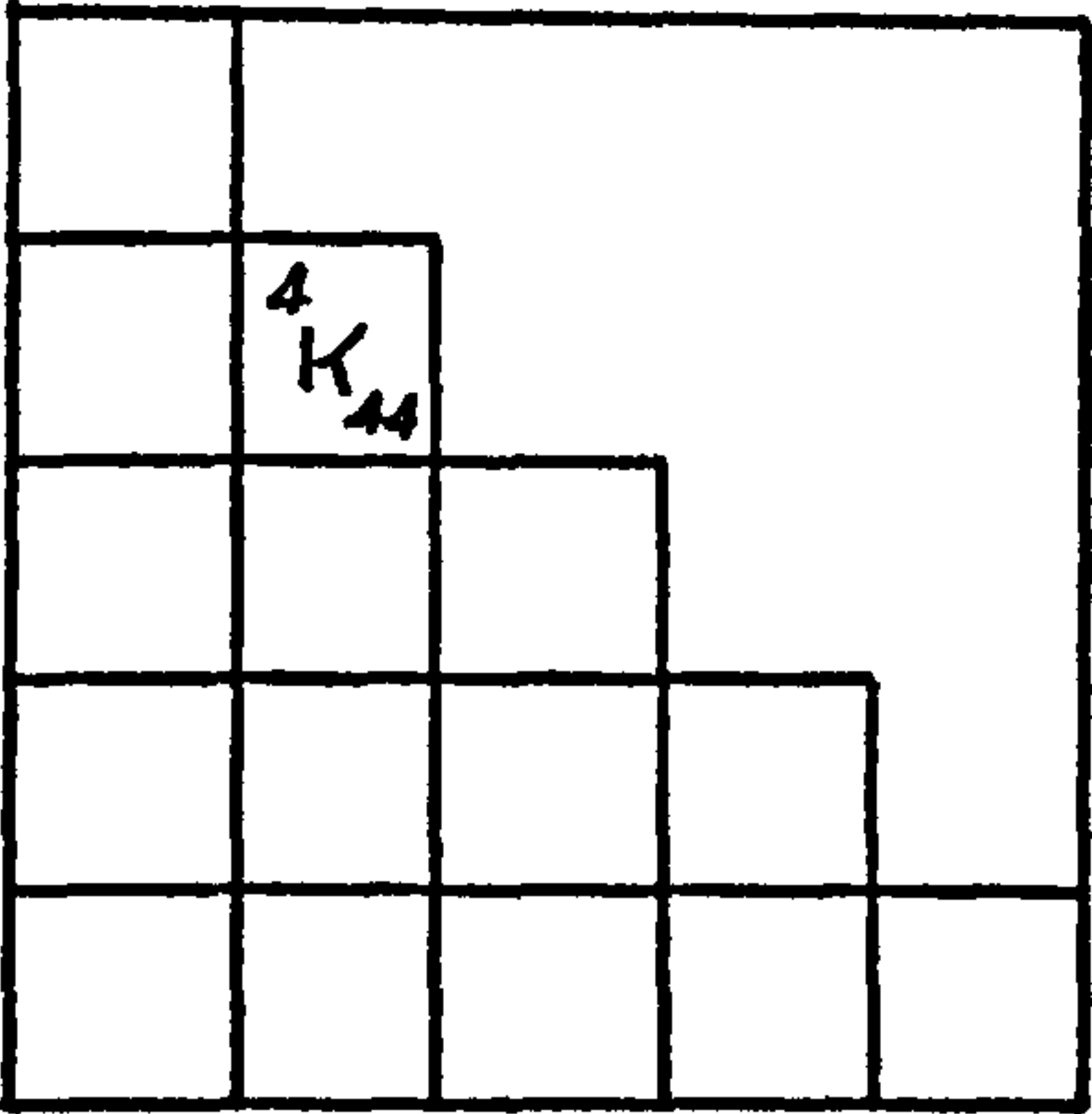
FIGURE (5-6R)



Triangular shifting

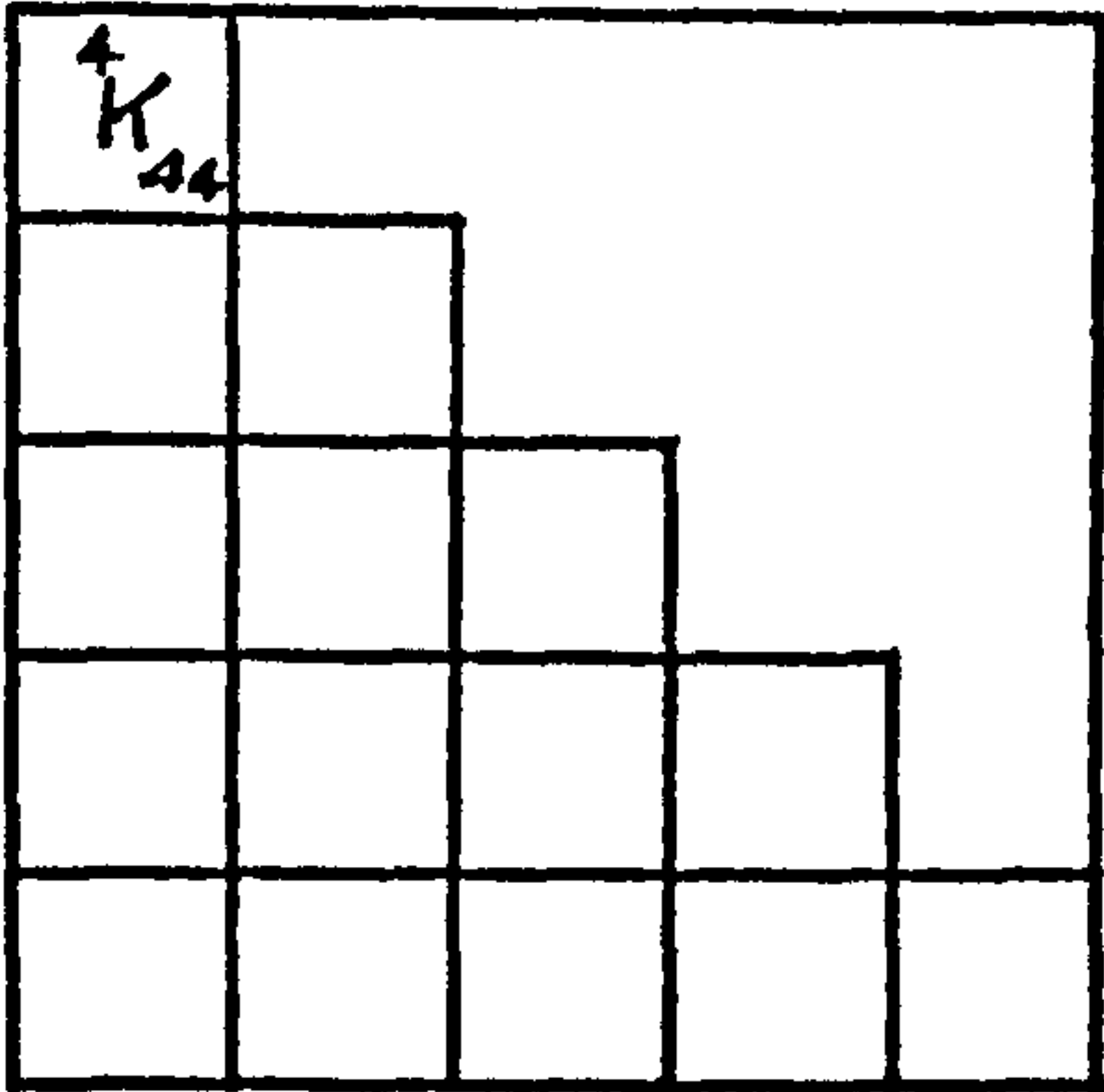
FIGURE (5-6S)

BLOCK SEQUENCE IN WORKING SPACE OF COMPUTER



8<sup>th</sup> Stage of Elimination

FIGURE (5-6T)



Triangular Shifting

FIGURE (5-6U)



## 5.8 PROGRAM DESCRIPTION - PLATE PROGRAM - D67C

This program was originally developed to serve as an all-purpose program for beam and plate structures. Although a four node plate element with five degrees of freedom per node is used in this particular program, the program can be utilized for any type of beam or plate element with replacement of a few subroutines. If a user is interested in any other type of element other than the existing one, the stiffness subroutines in the program must be replaced. In addition, the strain displacement, and the rotation of elements in the subroutine TRANSFM must be adjusted accordingly.

The simplified flow diagram as given in Figures (A-4) through (A-9), illustrates the relationship among subroutines.

The main function of the master segment is to read and print the input data as well as to call appropriate subroutines and to print out the results. The input data can be categorized as two sets of information; one which is considered constant throughout the analysis, and the other which can be varied for different load increments. The first set of input data cards is used to describe the problem, i.e., number of elements in the structure, properties of each element, existence of initial imperfection, etc. The second set of input cards is used to assign applied loads, to select the approximate constant displacement, and to choose the type of procedure. In order to assure that input data cards are read correctly, the input information is all printed out. For detailed description of input information, see input data in Appendix A.

When all of the input data is read, the program calls subroutine SOLV. This routine was developed for dual purposes: first, to find displacements for certain load vectors and second, to assemble stiffness matrix for calculating residual forces. The details of subroutine SOLV is described in the solution routine. If the iterative procedure is desired, the program calls subroutine NODFORCE to find the nodal and out-of-balance forces. Subroutine ITER is then called to perform the iterative cycle. The number of iterations is controlled either by the input information or by accuracy.

After each load increment, displacements and stresses are printed.

A detailed description of the program with a program listing as well as a layout of input data is given in Appendix A.



## 5.8:1 DESCRIPTION OF THE SOLUTION ROUTINE

All data and information required by this subroutine is read from cards by the master segment and is stored in the common storage. The solution routine is used for dual purposes:

1. To implement the incremental procedure, which consists of stiffness matrix assembly, elimination, back substitution, and calculation of incremental displacements.
2. To re-assemble the stiffness matrix to determine nodal forces for the equilibrium check in the iterative procedure.

The subroutine distinguishes between these two options by the signal "MODE." If "MODE" is unity, the routine uses the first option, and if it is greater than unity, it uses the second option. Part of the function of the routine from the beginning to statement "16" is to simultaneously build up the equations and to triangulize them. The bandwidth of the equations depends on NS (the largest node number for the element) and NR (the lowest node number for the element) from which the matrix dimension "MD" is calculated.

The routine starts with the comparison of the first node number of the first element with NR, which being initially zero passes control to a loop which first allocates the smallest value of the node number to NR, and then determines the largest node number and allocates that to NS. Subroutine ASSEMB is then called.

Subroutine ASSEMB first calls another subroutine TRANSFM, which basically determines the elastic stiffness and element orientation to find the zero, first, and second incremental stiffnesses. Subroutine TRANSFM returns with one total element stiffness matrix which depends upon the desired option. If the first option is chosen, the total stiffness matrix is the summation of all the element stiffness matrices, and if the second option is selected, subsequently, the total stiffness matrix consists of the summation of the element stiffness matrices with different multiplying factors. The ASSEMB routine assembles the element stiffness matrix in the appropriate position in the structural stiffness matrix, using a pair of "markers" based on the node numbers of the element. A system of nested loops is used in the assembly routine, a loop to assemble the coefficients for each degree of freedom, and a loop to assemble these by nodes. The outer loop determines the starting position in the structural stiffness matrix for the inner loop to assemble the degree of freedom coefficients. Assembly only takes place below the leading diagonal.



After the element stiffness has been assembled into the structure, the counter for reading the node number and the degree of freedom codes is updated, and subsequently, the subroutine ASSEMB returns.

The first node number for the next element is then compared with NR. If the number is the same as NR, elimination is by-passed and the routine proceeds to the previous procedure by checking the lowest and the highest nodes and calls subroutine ASSEMB. If the new node number is greater than NR, the "IF" statement checks the solution options. If "MODE" is unity, the elimination subroutine "ELIM" is called, and if "MODE" is greater than unity, the nodal force calculation subroutine "NODFORCE" is called.

The procedure used in this program to impose constraints on specified degrees of freedom is by means of an array "M" of length equal to the total number of degrees of freedom. Each element of this vector is made to have a value zero, -1, or a positive number to distinguish between the constraint, a degree of freedom fully constrained, or coupled with another degree of freedom, respectively. Basically, subroutine "ELIM" calculates values of back substitution coefficients. The elimination loop starts by checking the degrees of freedom coded greater than zero as described above. If any degrees of freedom are coupled with another degree of freedom, then subroutine COUPL is called.

Subroutine COUPL uses a process of accumulating the appropriate stiffness matrix and load vectors in order to obtain the same value of displacements. The COUPL routine is used mainly for the practical cases, i.e., a plate loaded in the testing machine where the top edge of the plate remains straight, or unloaded edges kept straight by moving laterally.

Returning from COUPL routine, or finding the degree of freedom less than unity, the elimination loop continues with a limited number of eliminations which are controlled by "markers" based on the node numbers. The number of backsubstitution coefficients stored in "W" which has dimension 2000, and the number of eliminations carried out is recorded by a counter for each degree of freedom. If array "W" is about 2000, the back substitution coefficients are copied on to the auxiliary storage unit (DISC) to be held for the back substitution process. The number of coefficients to be transferred each time is controlled by a factor called NWW, and the total number of coefficients transferred is recorded by NNAA.

The function of the following DO loops (3 and 5) is to overwrite the eliminated coefficients in the structural stiffness matrix by transferring the remaining coefficients diagonally to the top left hand corner of the working space and to fill in with zeros the spaces where coefficients did exist but have now been removed. If a constrained degree of freedom is encountered, the elimination is by-passed, the number of back substitution coefficients stored is nullified, and the number of constrained degrees of freedom are recorded. The number of eliminations and constrained degrees of freedom are taken into account by "markers" describing the limits of elimination. When the elimination process is completed, the routine returns.

The process continues in the same fashion for all elements. When all the degrees of freedom have been completed, a check is made to establish whether the current node number is zero, marking the end of the structure, a dummy element card being included at the end of the node number data for this purpose. With zero node numbers, the back substitution subroutine BCKSUB is called, and the solution of the equations is found.

The back substitution process can be thought of as the reverse of the forward elimination. The subroutine starts by transferring the remaining back substitution coefficients to the auxiliary unit DISC in case, at the same load level, the iterative (modified Newton-Raphson) procedure is needed. In order to use the coefficients stored on DISC, the appropriate coefficients, depending on the number of equations stored in array "MM", are transferred back to array "W". The solution of displacements is then carried out by the Gaussian back substitution process. When the number of coefficients stored on DISC exceeds 2000, transfer of coefficients from DISC to array "W" will take place by checking the unused coefficients with the number of equations at every stage of the solution.

After the back substitution process has been completed, subroutine BCKSUB returns.

In the last part of the subroutine SOLV, increments of displacement are accumulated as both total net displacement in array "UM", and as total plus the initial displacements in array "U".



### 5.8:2 SUBROUTINE TRANSFM

The first part of this subroutine converts the structure displacement numbers into the appropriate element displacement numbers. For this purpose the subroutine makes use of the node numbering system.

Subroutine TRANSFM performs all of the processing of the basic element stiffness matrices before assembling them into the structure stiffness matrix. The processing required is the calculation of the average rotation of the element ( $\theta_x, \theta_y$ ) with respect to the structure coordinates, as well as the calculation of the strain displacement of each element ( $e_x, e_y, e_{xy}$ ). Subroutines STIFFEL, NO, N1, and N2 are then called for the calculation of elastic and incremental stiffnesses. The stiffness matrices are factored by appropriate values if they are used for iterative procedure. These matrices are added and stored in common storage. The subroutine also calls another subroutine STRESS for calculating the stresses in the element.

### 5.8:3 SUBROUTINE NODFORCE

Subroutine NODFORCE is called if only the equilibrium balance is desired. The basic function of this subroutine is to find the nodal forces in each element. The process is the multiplication of the factorized assembled stiffness matrix by the net displacements. But since the assembled stiffness uses the frontal solution method, and only part of the assembled stiffness matrix is available at each stage, the process of finding partial nodal forces, followed by the elimination and shifting of the terms of the matrix must be used. This process is basically similar to the procedure described in Section 5.7:1. The assembled stiffness matrix employed in this subroutine is different than the assembled stiffness matrix used for determining displacements. The incremental stiffness matrices used in this assembled stiffness matrix are first factored, and then added as explained in subroutine TRANSFM.

#### 5.8:4 SUBROUTINE STRESS

The function of the subroutine STRESS is to calculate mean stresses in an element from the strain displacement obtained from the Subroutine TRANSFM. The two dimensional stress-strain relationships are used to obtain the stresses in the element. The stresses obtained by this process are the stresses at the center of the element. Correction of strain to account for the rotation of the element as well as the initial strain effect has been considered in this subroutine.

#### 5.8:5 SUBROUTINE ITER

The purpose of this subroutine is to find displacements due to residual forces. The subroutine is capable of carrying out Newton-Raphson as well as modified Newton-Raphson methods. By using the Newton-Raphson procedure, the subroutine calls another subroutine SOLVE to update the coefficient factors (inverse matrix) in assembled stiffness matrix. Subroutine SOLVE is bypassed if the Modified Newton-Raphson method is chosen.

Obtaining displacements due to out-of-balance forces is very similar to the subroutine BCKSUB except for the factorization of some coefficients in the back substitution process. The final task of this subroutine is to obtain the total displacements by adding the new displacement to the previous results.

USE OF PLATE PROGRAM -  
DEFLECTION



## 6.1 INTRODUCTION

The applicability of the present nonlinear stiffness formulation for a plate finite element to the prediction of large deflection behaviour of plate structures, with or without initial deformation, is demonstrated through various examples. The purpose of these examples is to verify the performance and accuracy of the element stiffness in cases for which an analytical solution is readily available. The cases to be studied are first, a plate under lateral pressure, and second, a plate with different initial imperfections under uniaxial compression.

Generally, when a thin plate is loaded by lateral pressure, if it deflects less than about half of its thickness, this is considered to be a small deflection. In small deflection theory, the bending stiffness of the plate governs its deflection and a plate bending solution may be used. When the deflection is no longer small in comparison with the thickness of the plate, but has reached about half its thickness or more, the plate will develop some membrane action resulting from the stretching of the middle surface. When the plate has a deflection many times its thickness, the resistance of the plate to bending may even be ignored. Figure (6-1) shows the lateral pressure plotted against deflection, characterized by an initial linear solution when the deflection is small, and by nonlinear behaviour when the deflection becomes large.

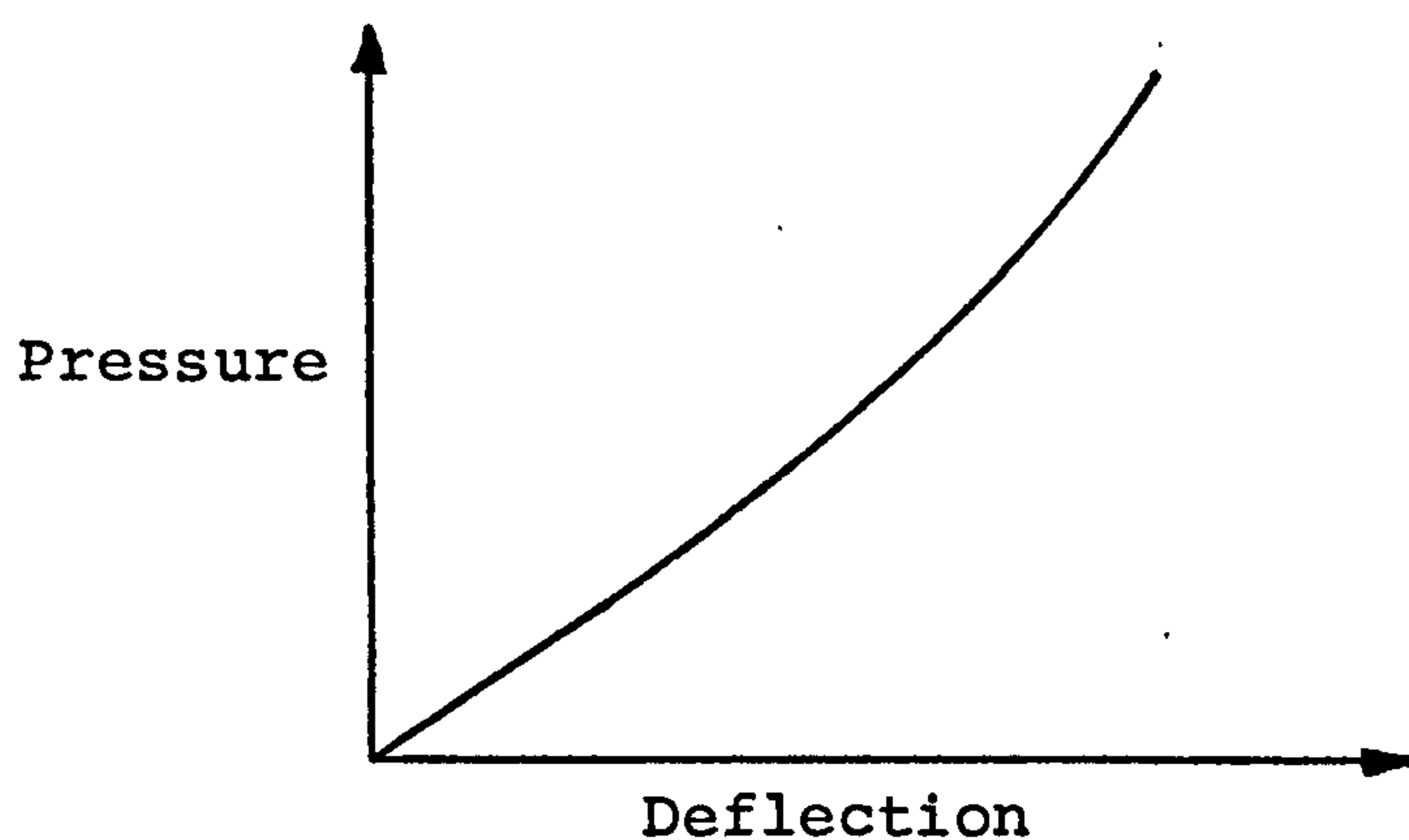


FIGURE (6-1)

A plate loaded in compression and supported along one or both unloaded edges will normally develop additional load capacity after the critical buckling load for the plate has been reached. For a plate with some



initial imperfection, again under compression, buckling deformation may begin at a very small load. If the compressive loading is continued to about four or five times the critical load, the load-deflection curve will be as shown in Figure (6-2). Note that Figure (6-1) and Figure (6-2) are for illustrative purposes only.

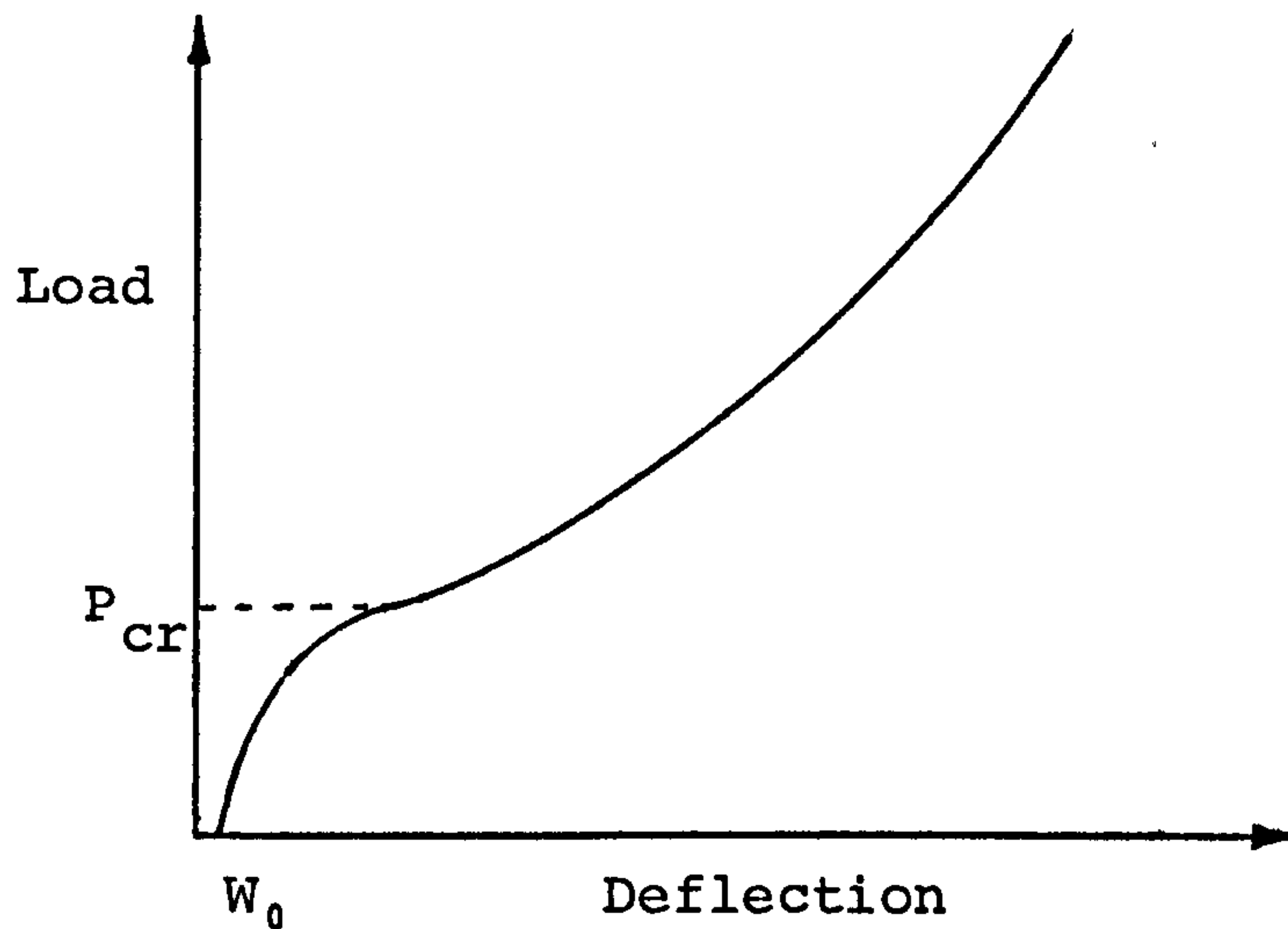


FIGURE (6-2)

Figure (6-2) demonstrates the behaviour of the plate at the pre- and post-buckling stages. The performance in this early stage (to near the critical load) is similar to the strut problem, and could be verified by the Southwell Plot technique, i.e., a straight line is obtained when the deflection  $W$  is plotted against the ratio  $W/P$ , the slope of which gives a value of the critical load. In the latter stage, when buckling occurs, tensile membrane stresses are produced in the plate. These in-plane stresses create extra stiffness in the plate, and make it possible for the plate to carry compressive load beyond buckling. The rate of deflection in this stage decreases as the compression increases.

## 6.2 LARGE DEFORMATIONS OF PLATE UNDER LATERAL PRESSURE

A useful basis for comparison with the computed results is Engineering Sciences Data Unit (ESDU) (Ref. 67). Since the curves in this Data are plotted non-dimensionally, the actual size and properties of the plate are irrelevant and therefore will not be reported.

A square plate which initially is assumed to be perfectly flat, with all edges simply-supported and free to wave in-plane, is under uniformly distributed lateral pressure. Because of the symmetrical nature of the deflected shape, only a quarter of the plate need be analyzed in the present finite element method. The plate is loaded so that the maximum deflection reaches five times the plate thickness. In order to assess the effect of mesh size, four solutions were obtained using the plate program with 2x2, 4x4, 6x6, and 8x8 element meshes respectively. Numerical convergence studies of the stiffness matrix have indicated that it performs adequately. The plate is loaded by a uniformly distributed load and also by a central concentrated load. Table (6-1) gives the numerical factors for the maximum deflection of a square plate, and Figure (6-3) and Figure (6-4) illustrate convergence behaviour of the element. It should be noted that convergence may occur from "above" as well as from "below." This is due to lack of slope continuity along adjacent edges of the plate elements. If the element edges were continuous with respect to both displacements and slopes (not just displacements), then the finite element model would always be stiffer than actual plate, and convergence would always be from "below."

The results obtained are compared with the Timoshenko (Ref. 65) exact solution, where the equations for maximum deflection in the two cases are:

$$w_{\max} = \frac{\alpha q a^4}{D} \quad (\text{Uniformly distributed load}) \quad (6-1)$$

$$w_{\max} = \frac{\gamma P a^2}{D} \quad (\text{Concentrated load}) \quad (6-2)$$

in which  $D$  is the flexural rigidity of a plate. (See Equation (5-3).)

From Table (6-1), it is observed that convergence for uniformly distributed loads is starting from "below" whereas convergence for concentrated loads begins from "above."



Mesh Size	Total No. of Nodes	(Uniformly distributed)	% improvement	(Concentrated load)	% improvement
2x2	9	.003446	12%	.0138	13%
4x4	25	.003940	12%	.0123	2.5%
6x6	36	.004030	2%	.0120	1%
8x8	81	.004034	.09%	.0118	
Exact		.004062		.0116	

TABLE (6-1)

The percentage in Table (6-1), which indicates the convergence of the computed result shows that the effect of increasing the mesh size for 2x2 to 4x4 is approximately twelve times greater than for an increase in mesh size from 6x6 to 8x8. It seems that beyond 8x8 mesh size, improvement in accuracy is very slight, compared to the large computer effort that would be involved.

Figure (6-5) shows the degree of convergence of the deflection for different mesh sizes under normal pressure. The results obtained were not intended for achieving high accuracy, but only for showing the improvement in accuracy for the different number of elements.

In using the normal pressure in the computer program as applied load, the pressure must be converted to concentrated loads and distributed between the nodal points, taking into account that boundary and corner nodes are only carrying a half and a quarter of an internal node load respectively. The system of loading of the plate is shown for the 3x3 mesh size per quarter in Figure (6-6).

$$\text{Total load} = P_T$$

$$\text{Unit load} = P_U$$

$$\text{Nodes} = N$$

$$\text{Total load} = (25N) (P_U) + (20N) \left(\frac{P_U}{2}\right) + (4N) \left(\frac{P_U}{4}\right) = 36N$$

$$P_U = \frac{P_T}{36N}$$

The analysis is initially performed by the incremental procedure to produce an approximate solution. As expected, the results are not satisfactory because of the drift from the true solution previously found in the incremental procedure (Chapter 4). The analysis was then followed by an incremental with modified Newton-Raphson procedure, using two iterations at each load increment. Initially, the question of how to select the load increment was studied. Since the first incremental load is in effect computed on the basis of small deflection theory, where the effect of membrane stress is neglected, the first load increment might be chosen so that it produces the maximum possible deflection subject to the limitations of small deflection theory. From the second incremental load onwards, however, large deflection theory is employed.

For the first computer run, the step size was arbitrarily chosen and it was found that the size of the load increment was sufficiently large to lead to some unexpected inaccuracies.

The total load was divided into 42 unequal load increments. The size of the load increments decreased with increase of applied load because the geometric non-linearity of the plate becomes more severe as the lateral deformation of the plate increases. In order to demonstrate that the result obtained was near the fully converged solution, a special computer run with half size of the previous load increment was performed. The resulting improvement of accuracy was found to be insignificant, confirming that the desired convergence had in fact been obtained with the plate program.

Figure (6-7) shows the result of the computer run for the central deflection of the plate against ESDU (Ref. 67) curves. It is observed that the curves, up to approximately  $W/t = 4$  are very similar, but beyond that, probably when the lateral deformation becomes relatively very large, so that the approximation for angles in the local and global axes does not hold very accurately, an error of approximately 2% exists when the maximum deflection reaches five times the thickness of the plate.

The computer program as developed is primarily intended to produce accurate displacement results. Although the program calculates the stresses in the elements, high accuracy is not expected. The output tensile stress results for the centre of the plate are evaluated by extrapolation and plotted against the ESDU (Ref. 67) result in Figure (6-8). As expected, around  $W/t = 3.5$ , the drift from ESDU results starts. Evidently, this causes the deviation of displacements in Figure (6-7).



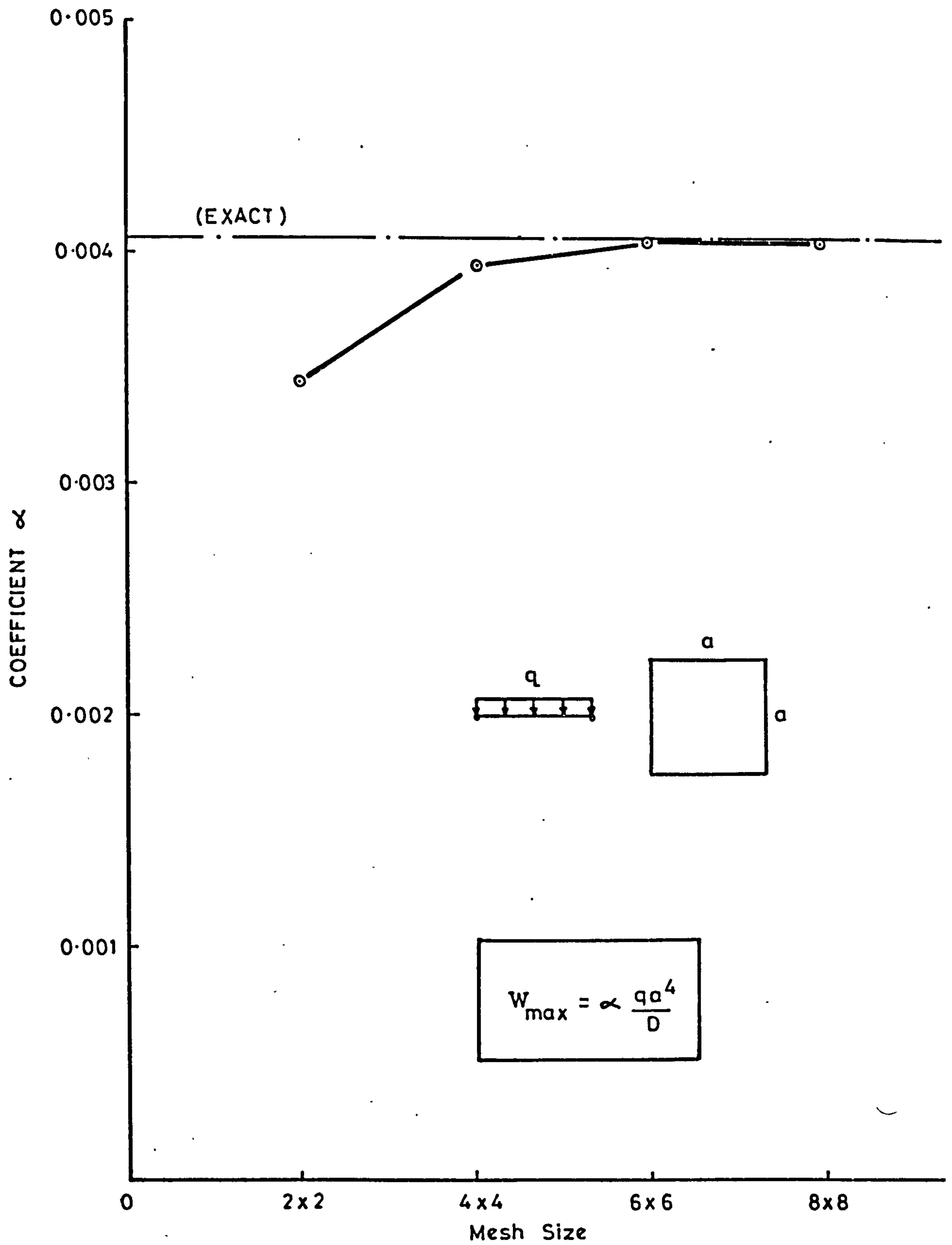


FIGURE 6-3

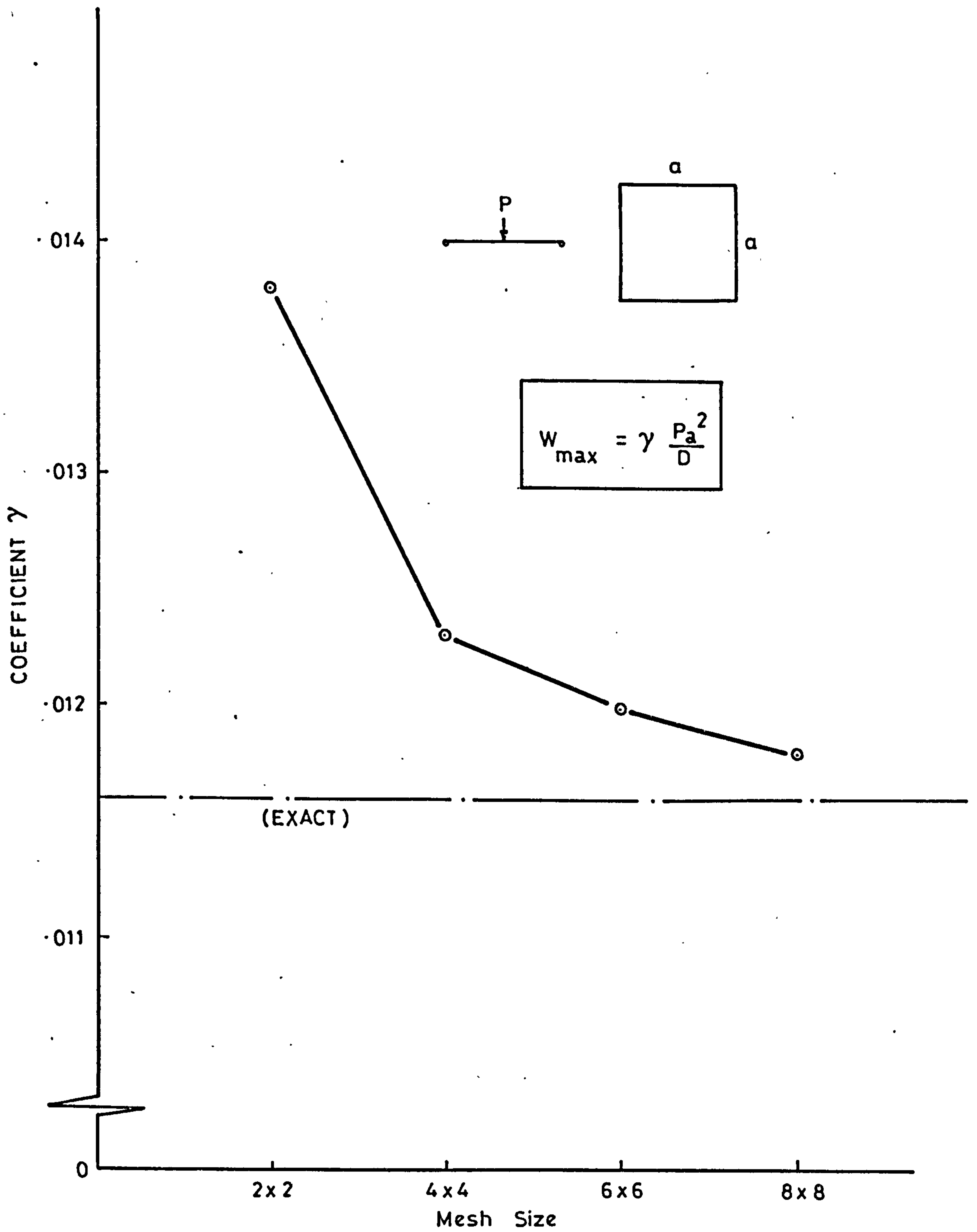


FIGURE 6-4

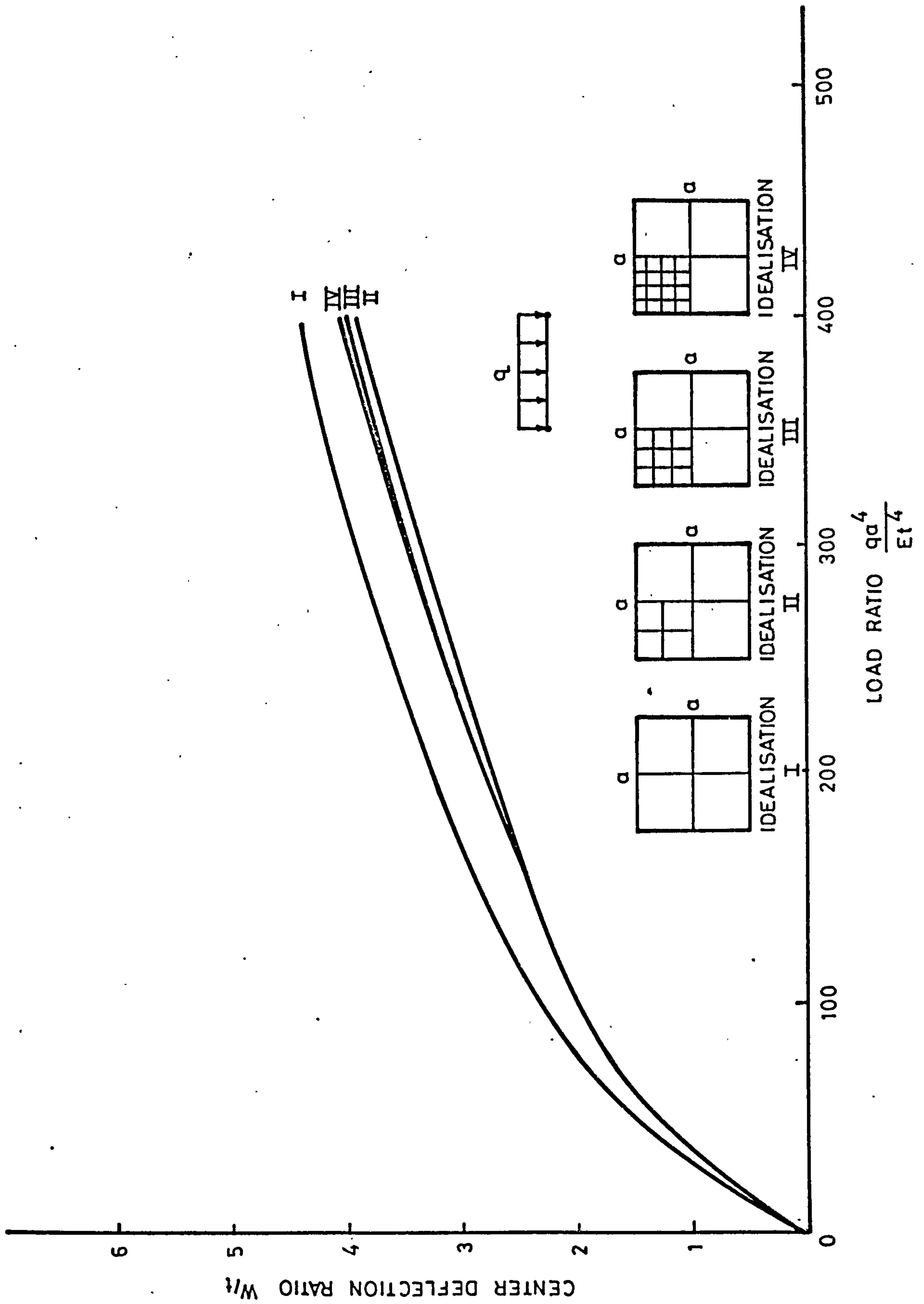
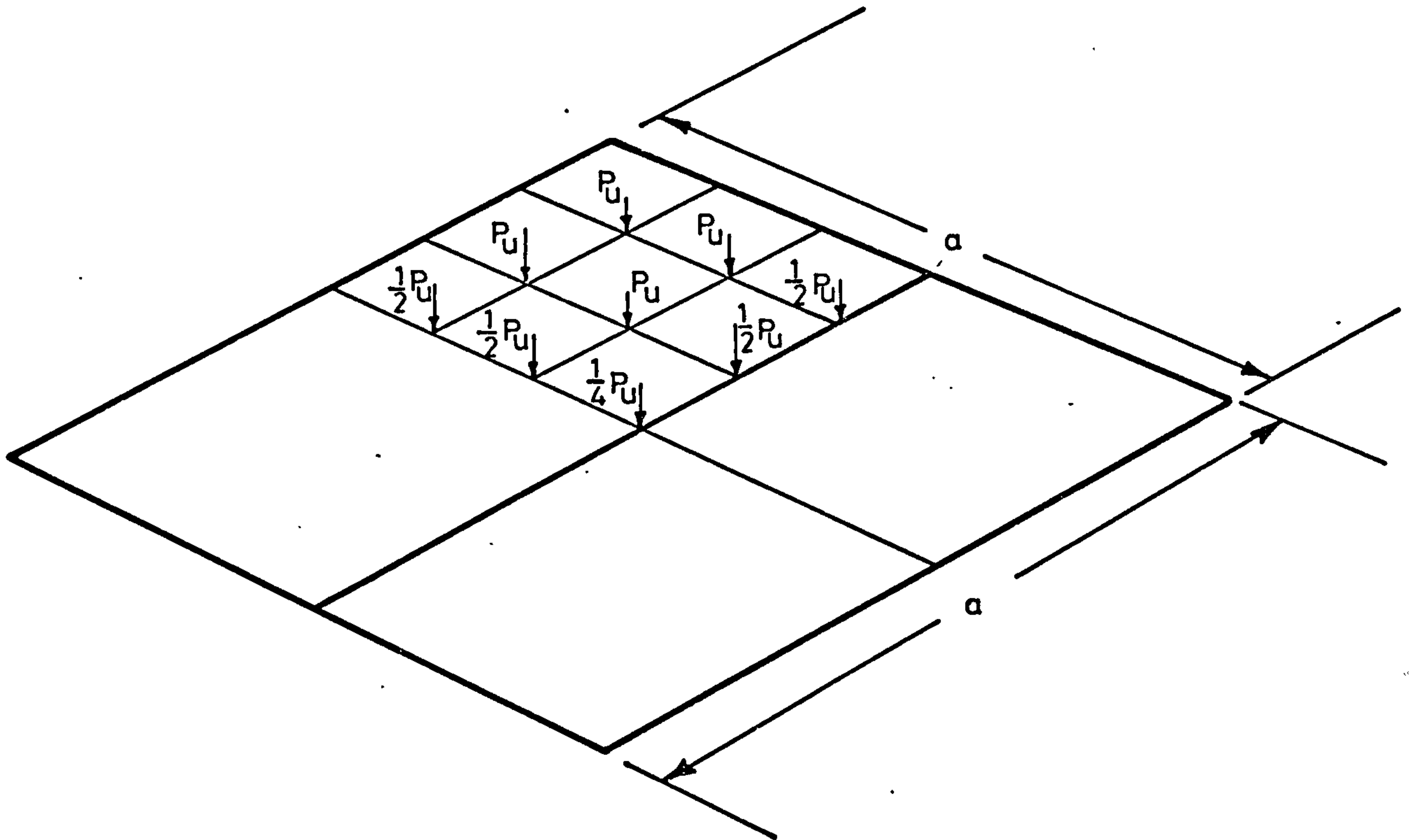


FIGURE 6-5



Normal Pressure Distribution

FIGURE 6-6



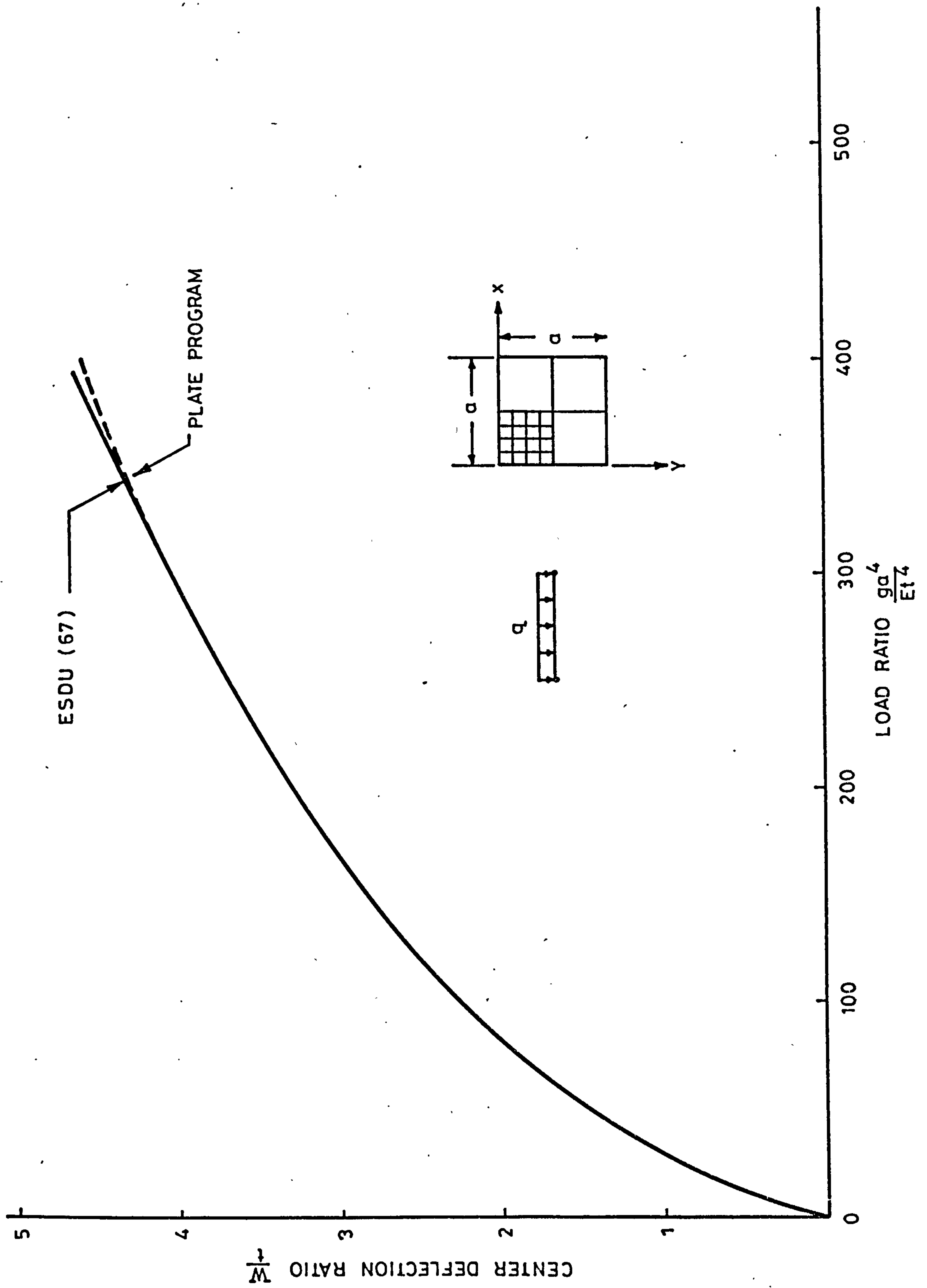


FIGURE 6-7

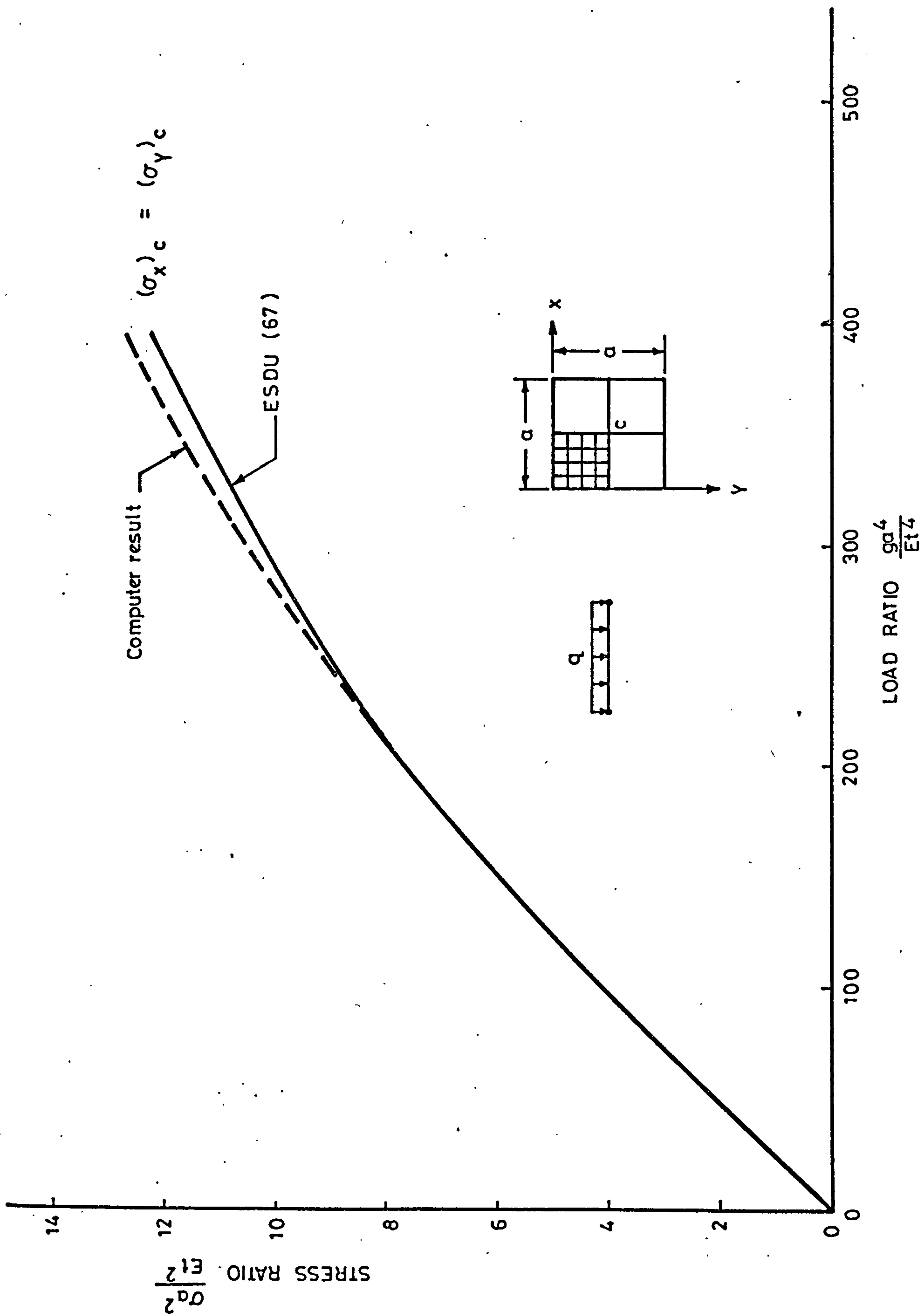


FIGURE 6-8

### 6.3 DEFORMATION OF PLATE IN COMPRESSION

While the previous section gives some check on the accuracy of the large deflection performance of the computer program, a more stringent test is perhaps given by a plate subject to in-plane load. In compression, a plate passes through a stage in which its stiffness reduces, while the plate under lateral load is continuously increasing stiffness. The post-buckling behaviour of plates with initial imperfections subject to uniform compression has been investigated by Coan (Ref. 68), Yamaki (Ref. 69), and Yang (Ref. 70). For plates with initial imperfection, the most accurate of these solutions is that of Yamaki (Ref. 69) who uses a double trigonometric series with four coefficients to solve the fundamental equations.

A plate with various degrees of initial imperfection has been studied for pre- and post-buckling behaviour. The plate is assumed simply-supported, and because of its symmetry, again only one quadrant is to be analyzed. The initial imperfection function is assumed to be

$$w_0 = W_0 \sin(\pi x/a) \sin(\pi y/b) \quad (6-3)$$

Three cases where  $W_0$  has the values  $0.025t$ ,  $0.1t$ , and  $0.4t$  are considered. The compressive load is applied as point loads at the nodes. Since the line across the loaded edges must be kept straight, the appropriate degrees of freedom of the nodes at the end of the plate are coupled together. This facility is already incorporated in the program (by adding the in-plane stiffness and load). Since the applied loads are coupled, the correct ratio of these loads for the different type of nodes (i.e., corner or middle node) is not necessary, and could be considered as either distributed or as total load. The comparison of plate buckling with the above references is based on non-dimensional parameters, so that the particular properties and dimension of the plate are irrelevant, except for examining the prediction of critical load by the Southwell Plot. The value of the theoretical critical load is:

$$P_{cr} \text{ (theoretical)} = 400 \text{ lbf.}$$

Initially, a plate with imperfections of  $W_0/t = 0.1$  is idealized into  $1 \times 1$ ,  $2 \times 2$ ,  $3 \times 3$ , and  $4 \times 4$  mesh size per quarter. The plate is loaded in compression up to three



times the critical load for each idealization. The incremental procedure with twelve increments of loads is chosen in each case. Figure (6-9) is intended to show the improvement in accuracy of the solution, as well as to illustrate the transition from the pre- to the post-buckling range, for different numbers of elements. Because of the purely incremental solution, errors in the actual deflection calculated are expected, and no attempt was made to obtain an accurate solution at this stage.

In order to achieve the most accurate result possible, for comparison with classical results, the plate with an initial imperfection  $W_0/t = 0.1$  was idealized into a 4x4 mesh size per quarter. The total load was taken up to three times the critical load and was incremented by 24 step loads. The procedure chosen was the incremental with modified Newton-Raphson using two iterations at each load level. For this case the unloaded edges are considered free to wave in-plane.

To verify the pre-buckling behaviour and to obtain a prediction of critical load approximate to this finite element idealization, the Southwell Plot technique was again used. Figure (6-10) is the Southwell Plot. (Note that the results do in fact fall in a straight line) giving a critical load of 415 lbf. In order to demonstrate that the results obtained have fully converged and cannot be improved, the size of the load increments were halved, and the results found to be almost identical to the previous one.

Figure (6-11) shows the computed result compared with other investigations. It is seen that the computer result shows a very close agreement with Coan (Ref. 68) and especially with Yamaki's load-deflection curves. Yang's (Ref. 70) curve shows a departure from these two classical solutions. As has already been discussed, Yang's derivation of the incremental stiffness when used in an iterative procedure, was found to be in error. His formulation was investigated and it was found that appropriate terms for the contribution of initial imperfection are not collected in the proper order for the incremental stiffness. Since each order of incremental stiffness matrix is multiplied by different constant (see Equation 5-24) in the iterative procedure, it is essential to collect the appropriate terms for the different orders of incremental stiffness.

The following procedure for different levels of initial imperfection and different conditions of simple support for the unloaded edges was followed. Three initial imperfections  $W_0/t = 0.4$ ,  $W_0/t = 0.1$ , and



$W_0/t = 0.025$  for each of the unloaded edge conditions were studied. The procedure and number of load increments were intended to be similar in all cases. However, for  $W_0/t = 0.025$ , the modified Newton-Raphson method fails around the critical load. This is because the initial imperfection is small and the load-deflection curve behaves somewhat like a perfectly flat plate. Therefore, when the load reaches close to the critical load, it will form a sharp corner and nonlinearity becomes very severe.

Different unloaded edges are considered here. First, those which are free to wave; second, those which are kept straight, but free to move laterally. This condition is performed by coupling the nodes along the unloaded side. Third, those unloaded edges which are straight, but not free to move laterally.

Figure (6-12), Figure (6-13), and Figure (6-14) show the behaviour under these edge conditions, for different initial imperfections. The computer results of stresses are plotted in Figure (6-15) and Figure (6-16) for a square plate with unloaded edges free to wave. These figures show the ratio of stress to average stress for central longitudinal and transverse elements.

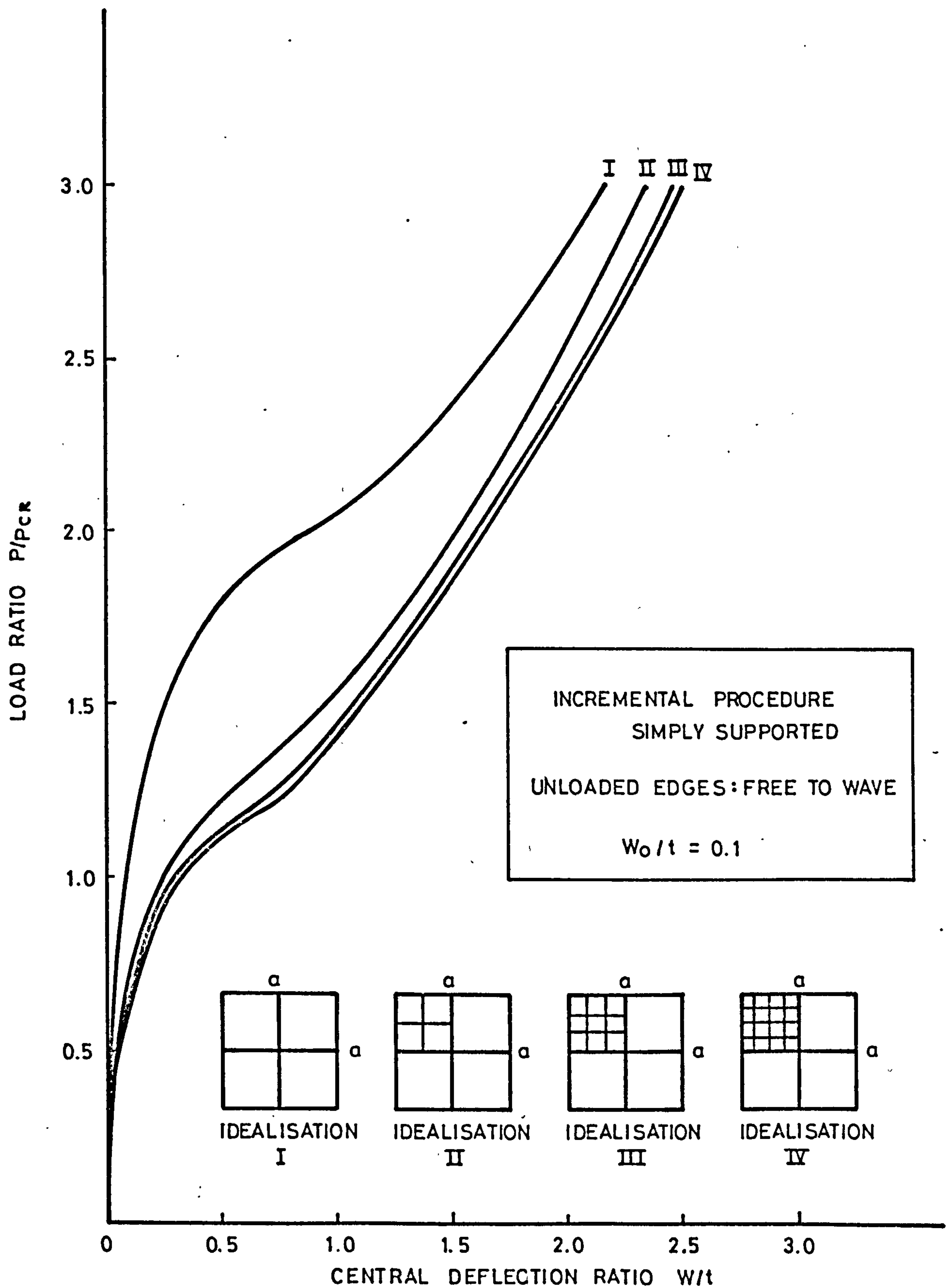


FIGURE 6-9

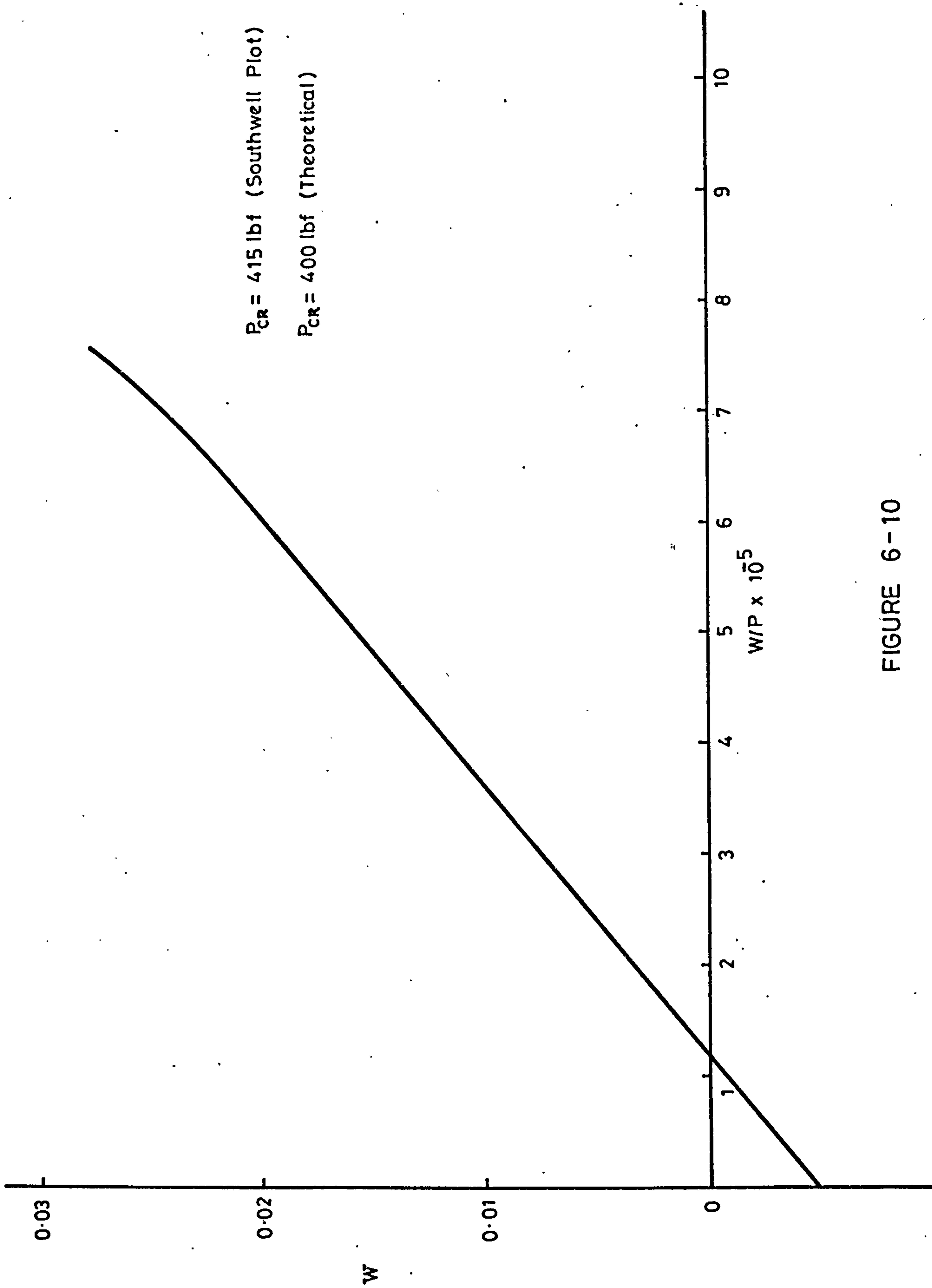


FIGURE 6-10

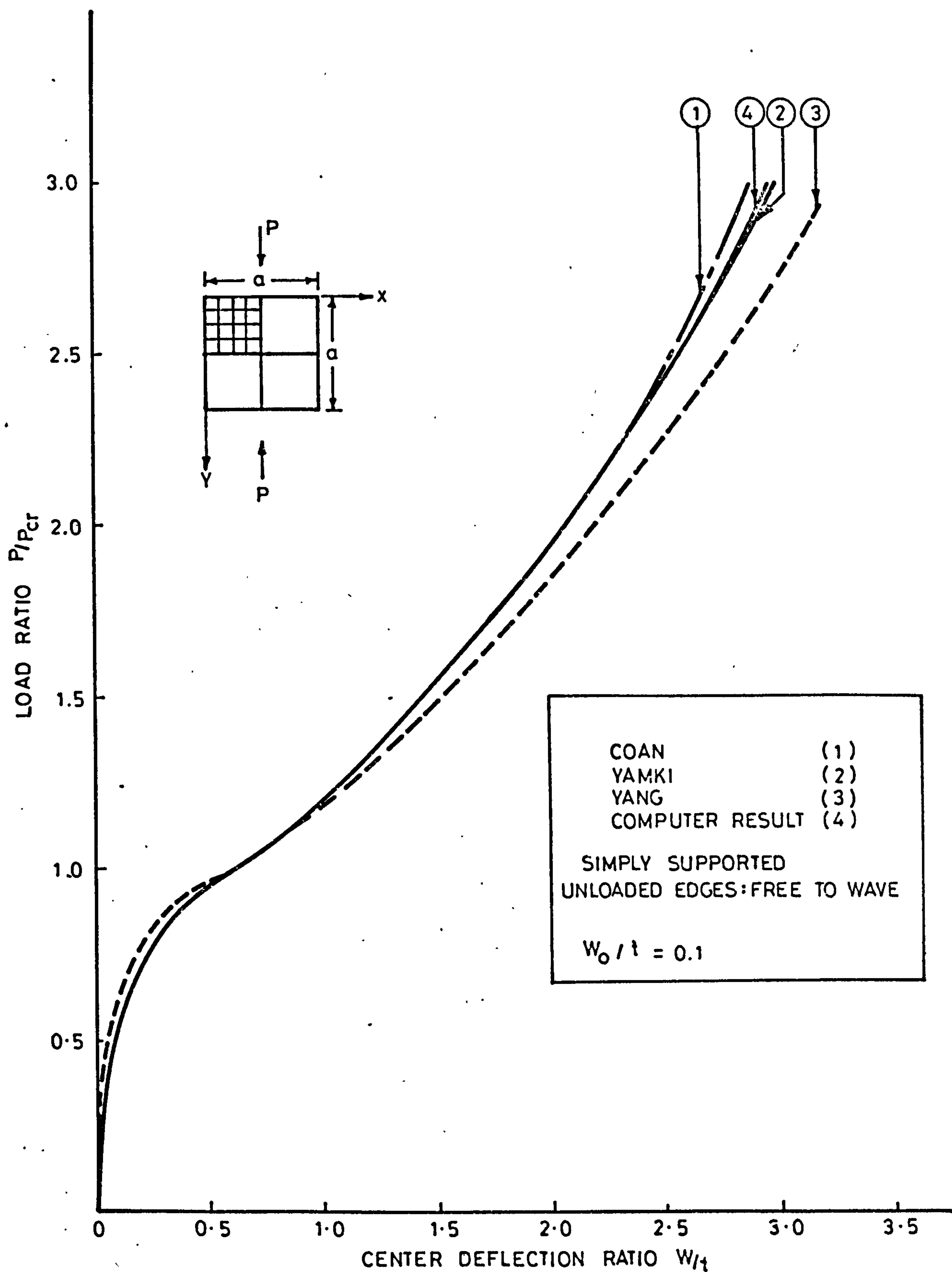


FIGURE 6-11



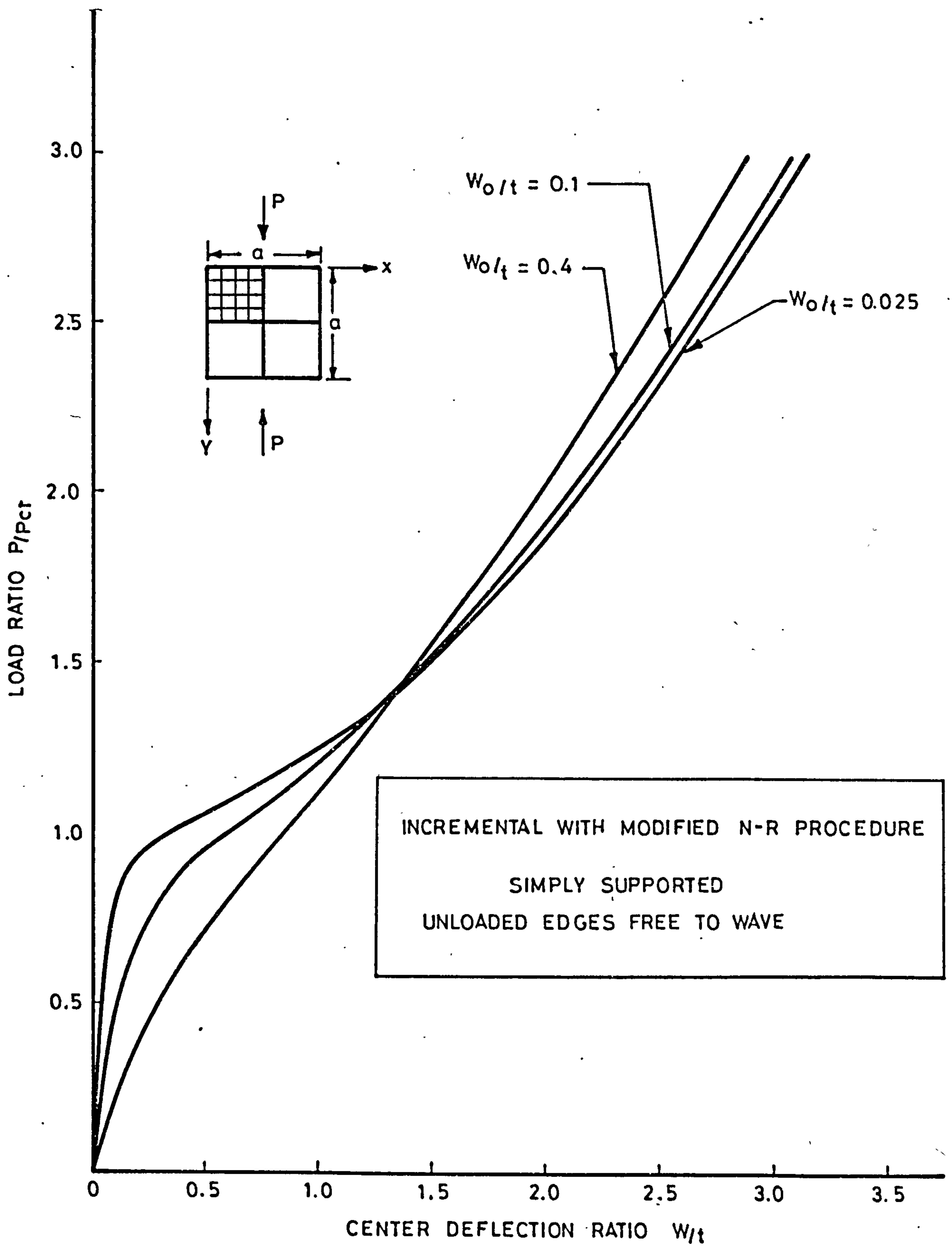


FIGURE 6-12

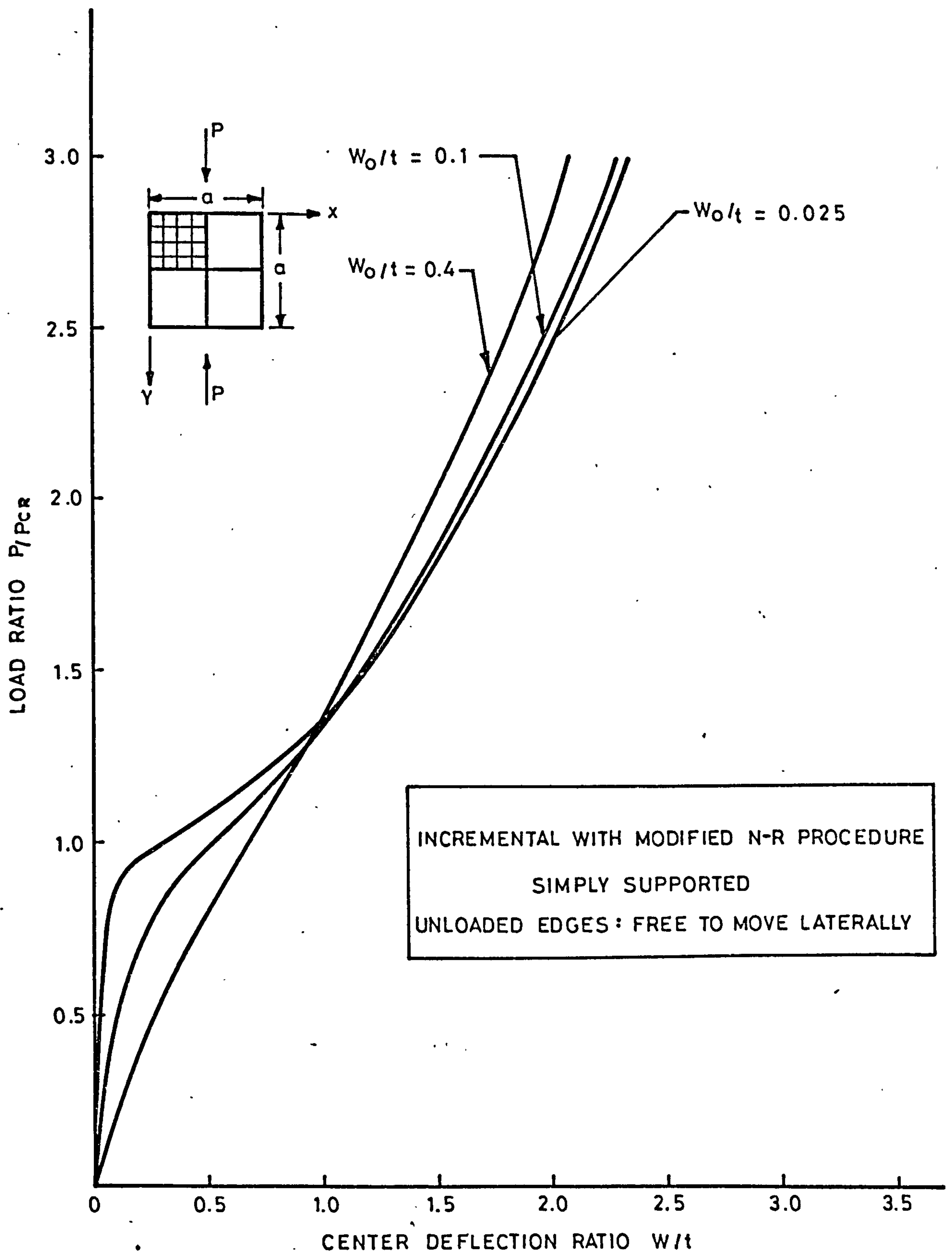


FIGURE 6-13.

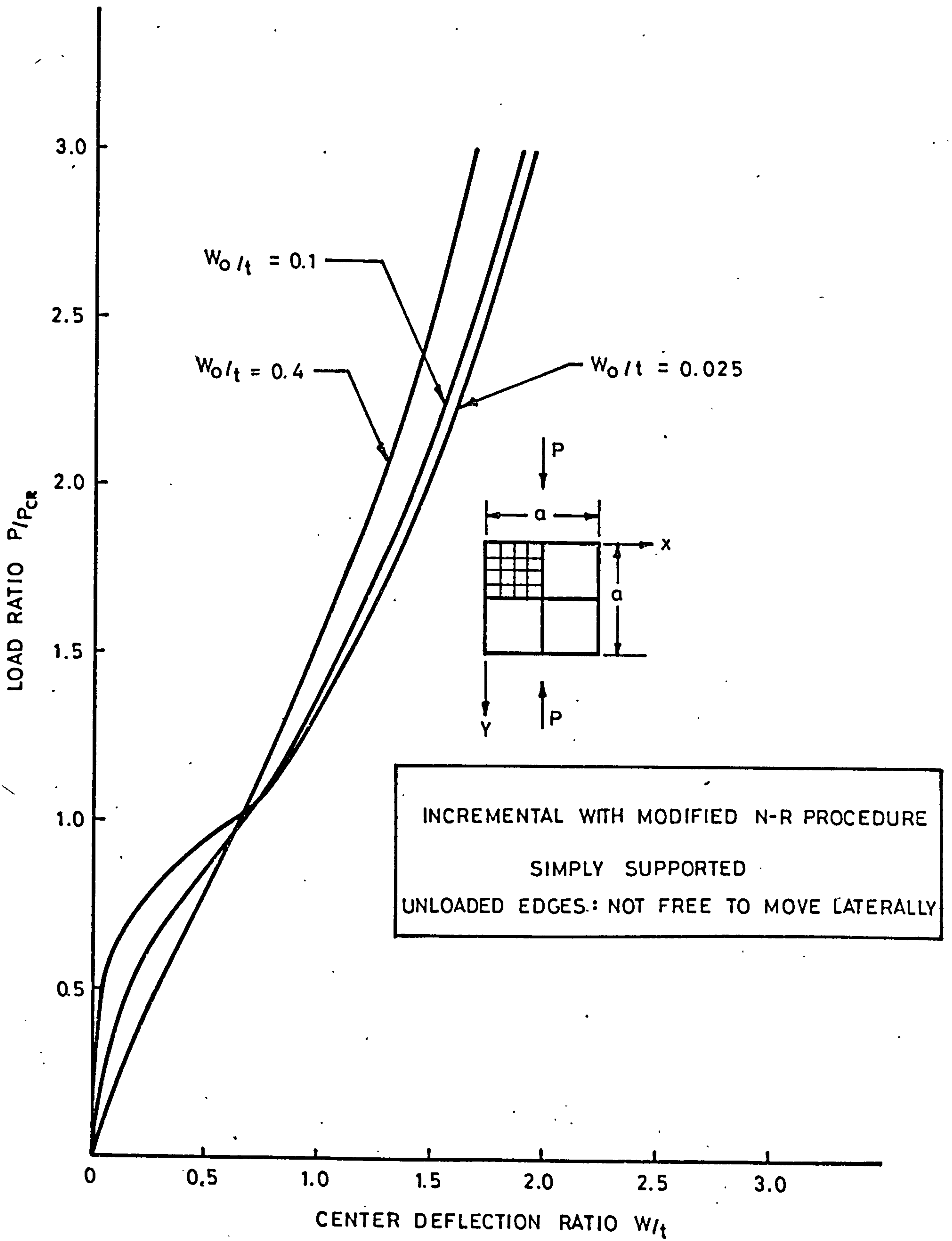


FIGURE 6-14

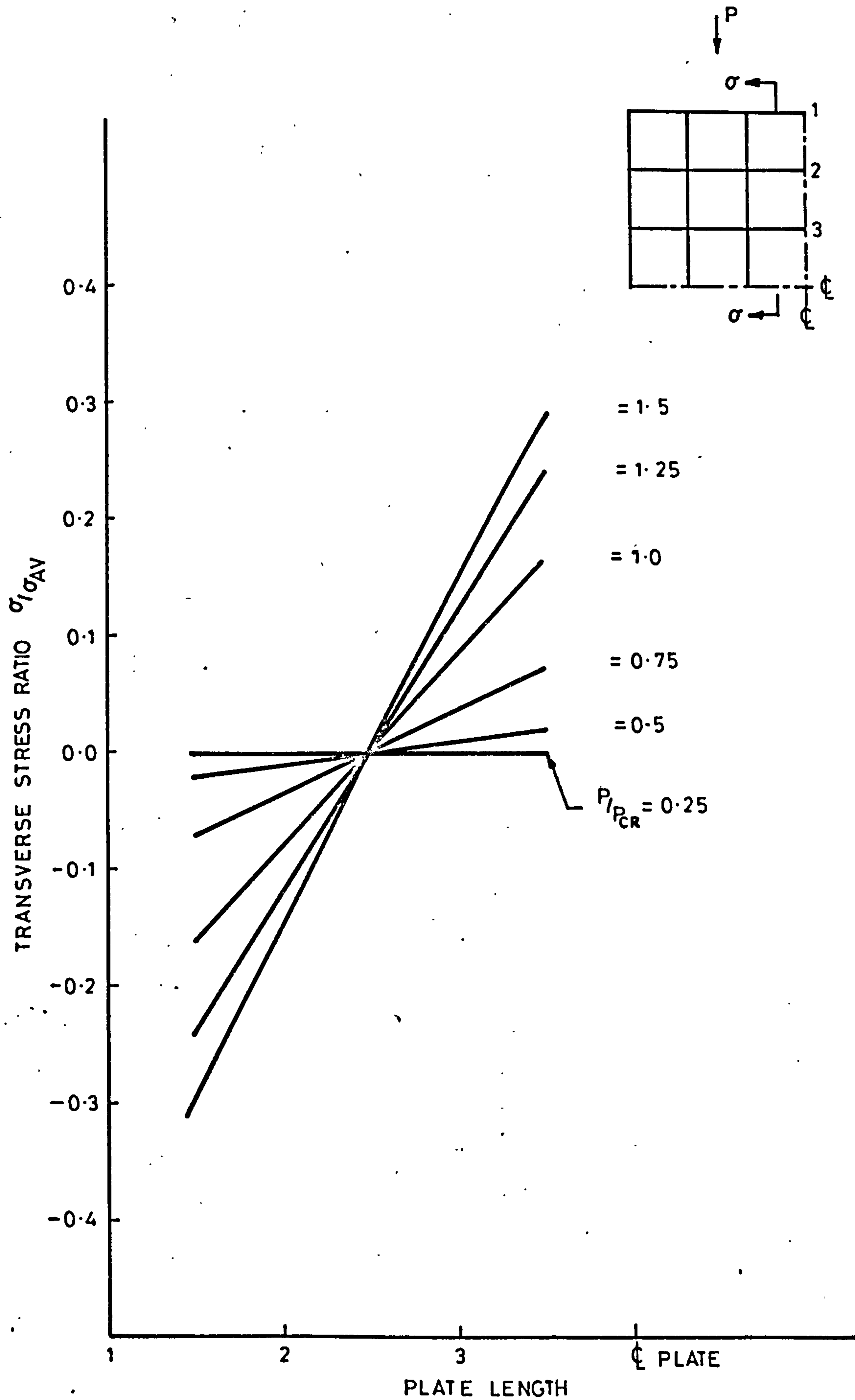


FIGURE 6-15



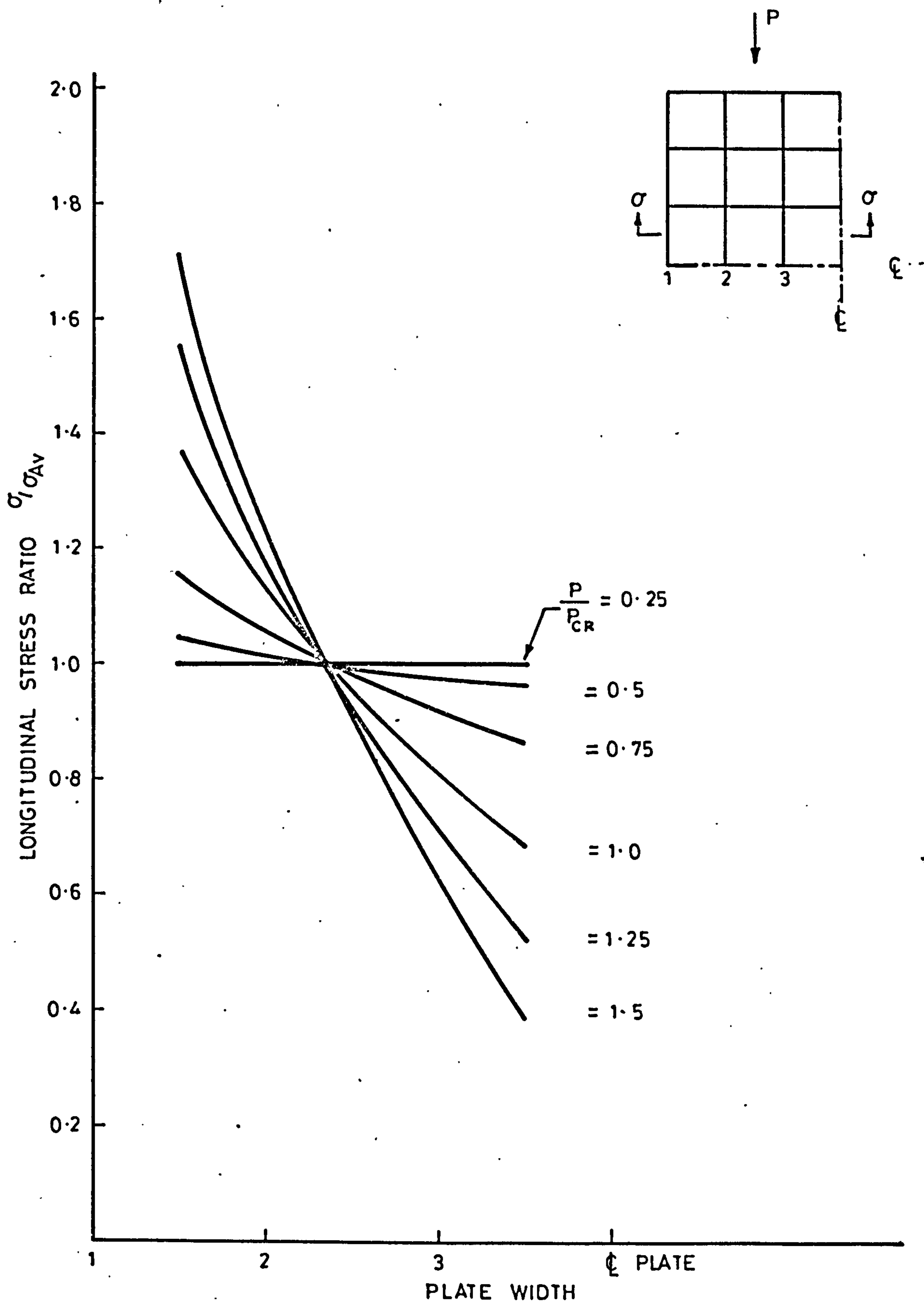


FIGURE 6-16

## 6.4 PERFECTLY FLAT PLATE UNDER COMPRESSION

Unlike an imperfect plate, a perfectly flat plate under increasing compressive loading will remain flat before buckling at the critical load. Nevertheless, the post-buckling behaviour of a perfectly flat plate is very similar to that of a plate with initial imperfection.

Since the in-plane and bending deformations of the plate are not initially coupled, investigation of the post-buckling behaviour of a perfectly flat plate is somewhat cumbersome. In this case, in order to initiate bending stiffnesses in the computer program, a fictitious normal load or a small out-of-plane displacement is required.

For all practical purposes of the computer program, a small normal concentrated load is chosen to start the interaction of the in-plane and bending stiffnesses after the critical load is reached. The concentrated load is removed gradually to avoid upsetting the solution. The value of the concentrated load was found initially by classical plate bending theory, to achieve a maximum deflection equal to the computer result for the maximum displacement of the same plate with an initial imperfection  $W_0/t = 0.025$  at critical load under compression. Since the object is to reduce the fictitious load to the minimum without losing its effect, reduction of this fictitious load was found to be approximately one-quarter of the initial value obtained as described above. However, it was discovered that further reduction of the fictitious load caused the solution to diverge.

The procedure for obtaining post-buckling behaviour of a perfectly flat plate by the computer program is as follows:

- 1) One large increment of the compressive load, equal to the critical load, is applied. The displacement results obtained contain no out-of-plane deformations.
- 2) A small concentrated fictitious load is applied at the centre of the plate. Small out-of-plane displacements are now produced by the concentrated normal load.
- 3) Incremental compressive loads and a gradual reverse of the concentrated load are applied simultaneously.

This method is used for simply-supported plates with unloaded edges which are both free to wave and held straight but free to move laterally. The analysis again

uses one-quarter of the plate because of the symmetry. The application of loads and properties of the plate are the same as in the previous sections.

Because of the initial linear solutions, a purely incremental procedure is chosen for the application of the critical loads for first and second load increments respectively. However, for the remainder of the solution, an incremental method with modified Newton-Raphson procedure using two iterations is selected.

Figure (6-17) and Figure (6-18) show the post-buckling behaviour of the square plate with two different unloaded edges. As expected, the curves are very similar to the post-buckling part of the load-displacement curves of the plates with small initial imperfections ( $W_0/t = 0.025$ ).

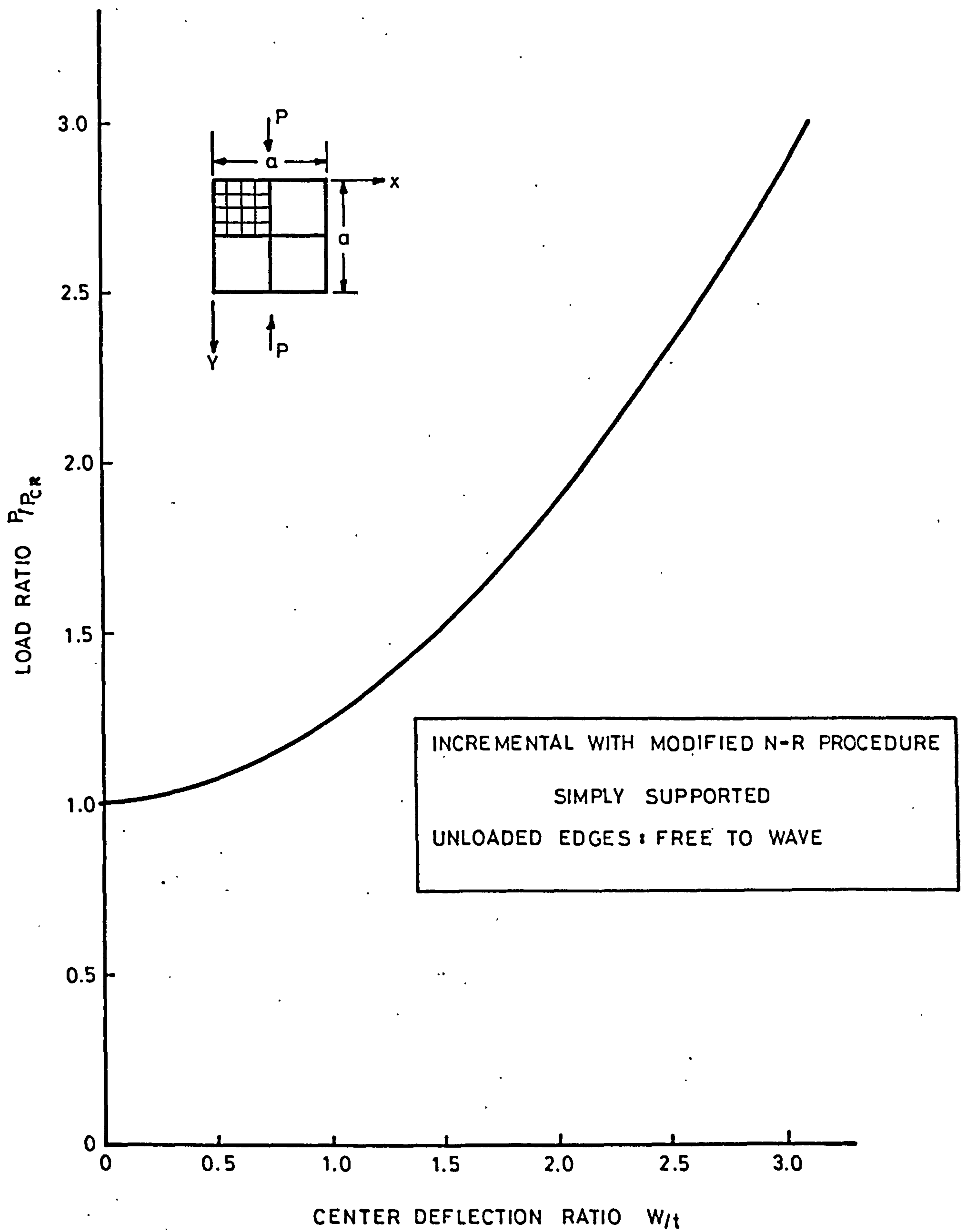


FIGURE 6-17



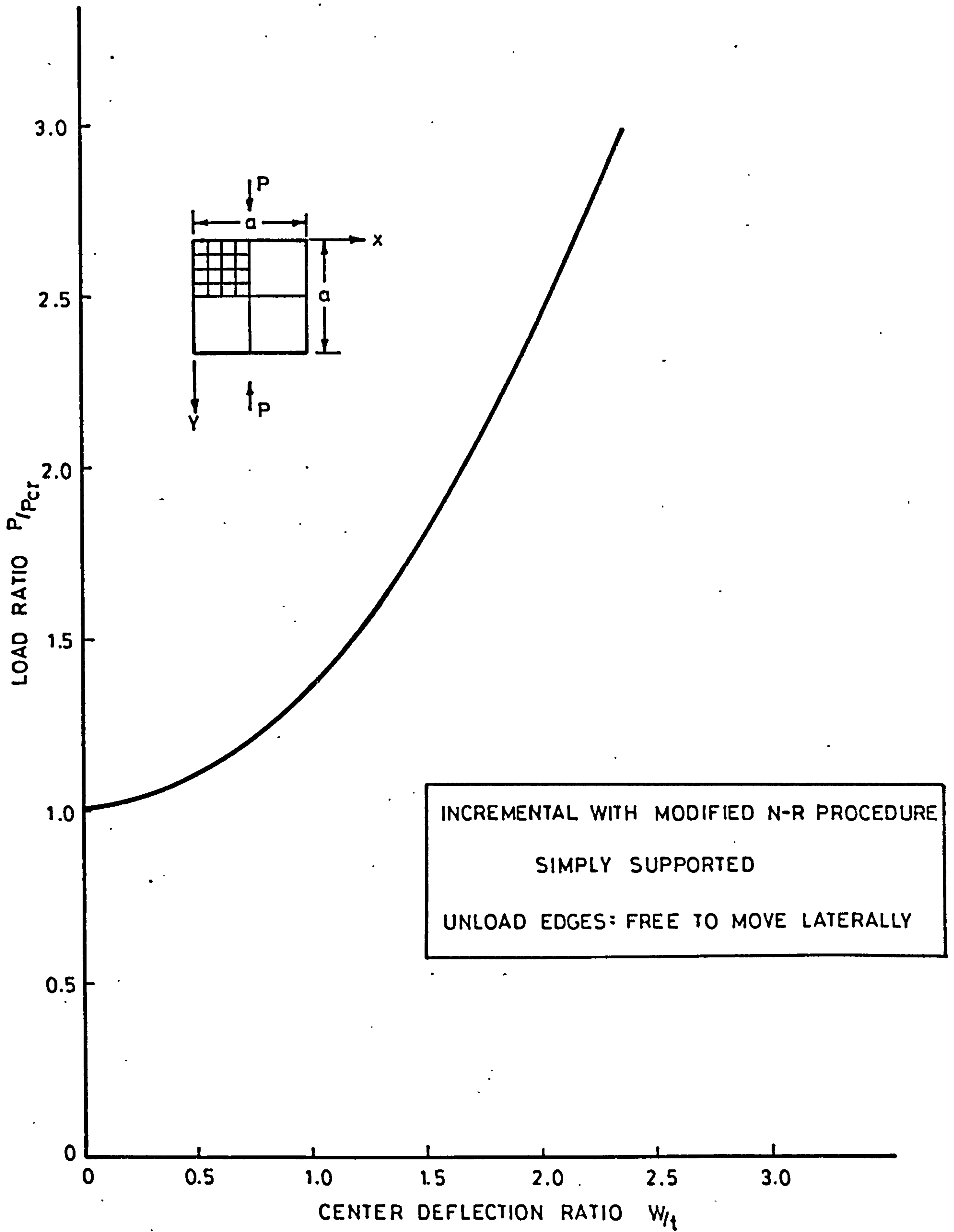


FIGURE 6-18

USE OF PLATE PROGRAM -  
STIFFNESS

## 7.1 POST-BUCKLED STIFFNESS

Post-buckled stiffness can be defined as the ratio of the rate of change of average stress in the plate to the rate of the change of apparent strain, for example in compression:

$$E^* = \frac{\delta \sigma}{\delta \epsilon} \quad (7-1)$$

This is also referred to as the "tangent" stiffness.

After a plate has buckled, a reduction in stiffness will occur due to the non-uniform stress distribution across the plate. The stiffness will remain constant after buckling as long as the form of the buckle pattern remains unchanged. However, when the state of stress is not uniform over the plate, the mode of buckling is likely to change progressively as buckling develops which, in itself, leads to a change of stiffness.

The stiffness of a perfect plate before buckling is constant, with the value equal to that of the material itself (i.e., in case of plate in compression this value is Young's modulus  $E$ ). A useful definition of relative stiffness is the ratio of the post-buckling ( $E^*/E$ ) with a value less than unity. For a plate with imperfection, the reduction in stiffness occurs before the theoretical critical load.

Computer results for pre- and post-buckling displacements were printed out for all degrees of freedom, thus the same output used for the out-of-plane displacements described in Chapter 6 is used to evaluate plate stiffness behaviour in compression. The post-buckled stiffness reduction of a plate with different initial imperfections, including the perfectly flat plate, with two different unloaded edge conditions, is studied here. The self-correcting procedure (incremental with iteration at each load increment) was used to obtain the results. As previously mentioned, since the rate of change of displacement is required to evaluate plate stiffness, a calculation of deformation at different load increments is ideal. By taking a small load increment, the tangent stiffness of the plate is evaluated as the ratio of incremental average stress to incremental strain.

As explained in Chapter 6, the in-plane degrees of freedom of loaded nodes are "coupled" for plates subject to compression. This "coupling," which keeps the loaded edge of the plate straight, makes it possible to obtain uniform contraction during loading.



## 7.2 PURE COMPRESSION

Since the computer results used for the stiffness calculation are the same output as in Chapter 6, detailed information about plate properties, boundary conditions and application of loads may be obtained from that chapter.

In order to deduce the stiffness of the plate, the axial contraction is used to find the apparent strain, and the average stress in the plate is then divided by this results. Since the tangent plate stiffness is being calculated, the deformation is taken at each load increment. The stiffness results are then plotted in a non-dimensional form, as relative stiffness  $E^*/E$  against load ratio  $P/P_{cr}$ .

Figure (7-1) shows the stiffness reduction of a plate having unloaded edges free to wave for different initial imperfections (including no imperfection). The stiffness of the perfectly flat plate or plates with small initial imperfections, e.g.,  $W_0/t \leq 0.1$  starts equal to the value of the material itself ( $E^*/E = 1$ ), whereas the stiffness of a plate with more severe imperfection, e.g.,  $W_0/t \geq 0.4$ , starts somewhat less. This early stiffness reduction of the plate, for an imperfection  $W_0/t = 0.4$ , is 9% of the material stiffness.

The overall characteristics of the curves may be summarized as follows:

- 1) Plates with imperfections show a gradual loss of stiffness before and after buckling.
- 2) The rate of stiffness reduction increases with reducing plate imperfection, above about 75% of the critical load.
- 3) The curves all intersect around  $E^*/E = 0.5$  about 15% above the critical load.
- 4) Beyond the critical load, the curves tend to converge to a value of  $E^*/E = 0.4$ .

These curves, for a square plate in compression, are entirely consistent with the more familiar results for a long plate (see, for example, Ref. 2). It must be mentioned that theoretically, for plates with no imperfection, the compressive stiffness drops at the critical load and then remains constant. However, in the computer program the loading is incremental, therefore the stiffness reduction will not be instantaneous. This phenomenon is demonstrated in the figure.

Figure (7-2) shows the relative stiffness of plates with unloaded edges held straight, but free to move laterally, for different initial imperfections. Plates



with imperfections  $W_0/t \leq 0.1$ , have an initial stiffness equal to that of the material ( $E^*/E = 1$ ), but the plate with an imperfection  $W_0/t = 0.4$ , has an initial stiffness 8% less than the material.

As shown, the curves intersect at about  $E^*/E = 0.6$ , and converge to a value approximately  $E^*/E = 0.5$ .

The classical post-buckled stiffness of a long simply supported rectangular flat plate is  $E^*/E = 0.408$  for sides free to wave, and  $E^*/E = 0.5$  for sides held straight, free to move laterally (Ref. 71).

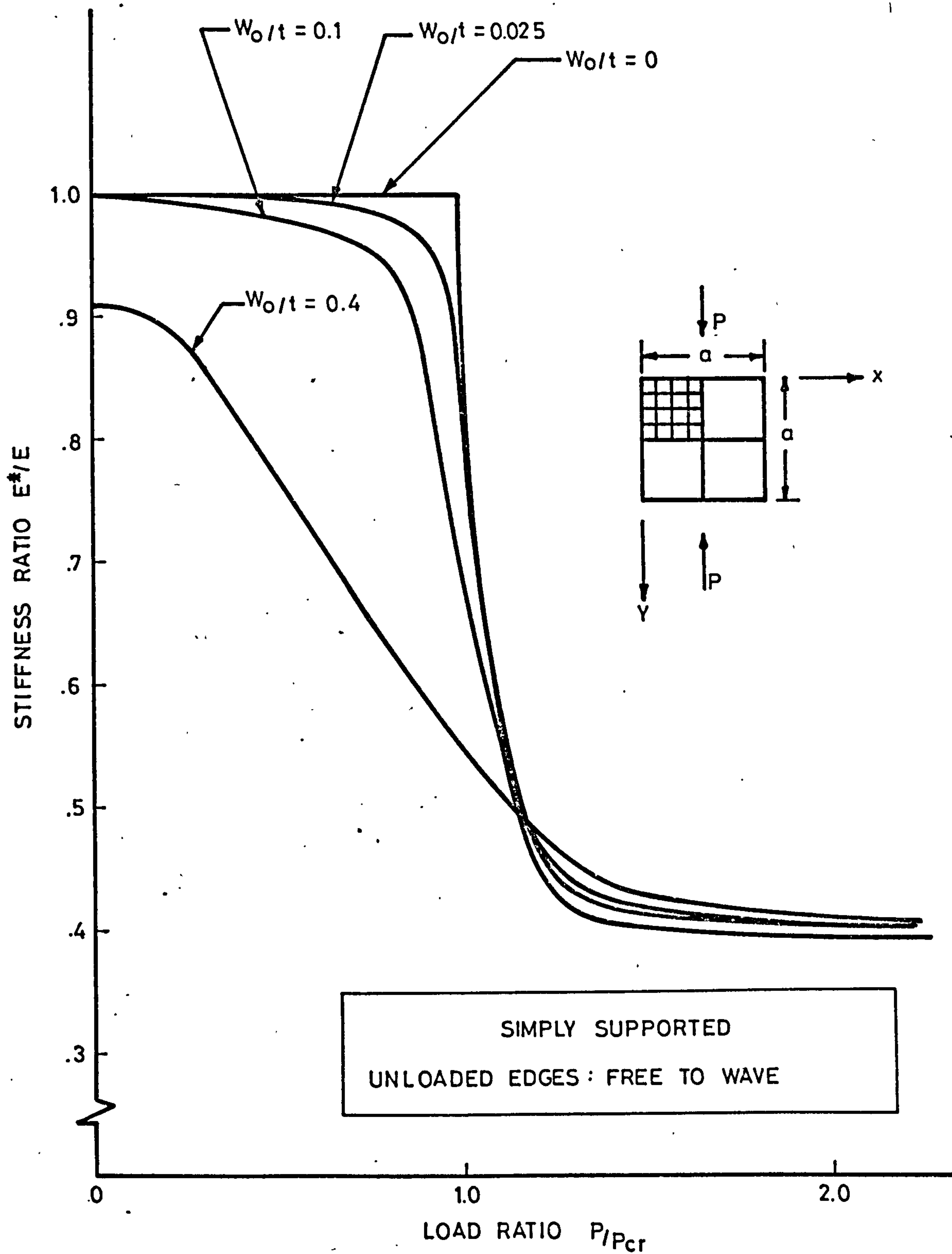


FIGURE 7-1

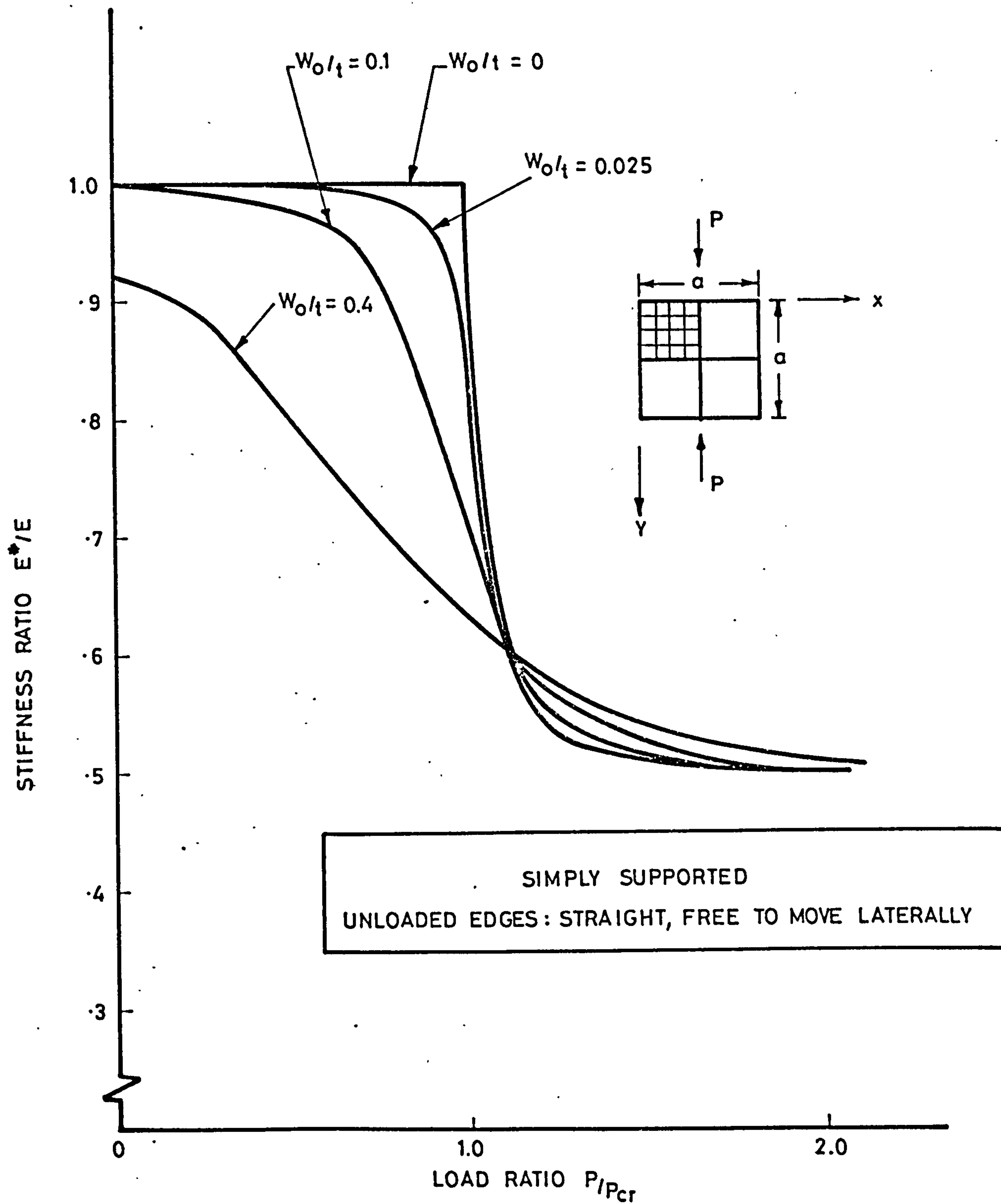


FIGURE 7-2

### 7.3 PURE SHEAR

The nature of the post-buckled shear stiffness of a plate may be considered somewhat different to post-buckled stiffness in compression. The reduction in post-buckled stiffness in shear is gradual, and is known to be less pronounced than the reduction in post-buckled compressive stiffness.

The behaviour of a square plate with and without imperfection, for two different boundary conditions, is investigated. The plate is simply supported along all edges with one pair of opposite sides acting, in effect, as stiffeners. In case (a), these transverse stiffeners are considered to be not sturdy ( $A_s = 0$ ), e.g., a component flat of a corrugated web; whereas, in case (b), the stiffeners are assumed inextensible and very sturdy ( $A_s = \infty$ ), e.g., a shear web with heavy transverse stiffeners. In order to achieve such boundary conditions, the "coupling" technique is used as in Chapter 6. For case (a), the in-plane degrees of freedom for the one pair of opposite sides, in the direction at right angles to these sides, are coupled, in order to keep these sides straight. For case (b), the degrees of freedom are "coupled" to ensure inextensibility along the two sides acting as stiffeners. The boundary conditions for cases (a) and (b) are also illustrated in Figure (7-3). In this figure, the in-plane degrees of freedom with the same number are "coupled" to each other.

Two types of plate are considered for shear stiffness behaviour; a perfectly flat plate and a plate with an initial imperfection  $W_0/t = 0.1$ . The initial mode shape used for this study is explained in Section 7.4. The post-buckled stiffness of the plates is plotted as both tangent and secant stiffness, for both boundary conditions. The tangent shear stiffness is defined as the ratio of the rate of change of average shear stress in the plate to the rate of change of shear strain.

$$G^* = \frac{\delta \tau}{\delta \gamma} \quad (7-2)$$

The secant stiffness is simply the ratio of average shear stress to apparent shear strain. The shear stiffness for a plate with initial imperfection, as well as for a plate with no imperfection, is simply that of the material ( $G^*/G = 1$ ) before buckling. Shear stiffness reduction of the plate with imperfection starts somewhat before the critical load (see Section 7.4) is reached. The shear stiffness reduction for the plate with no

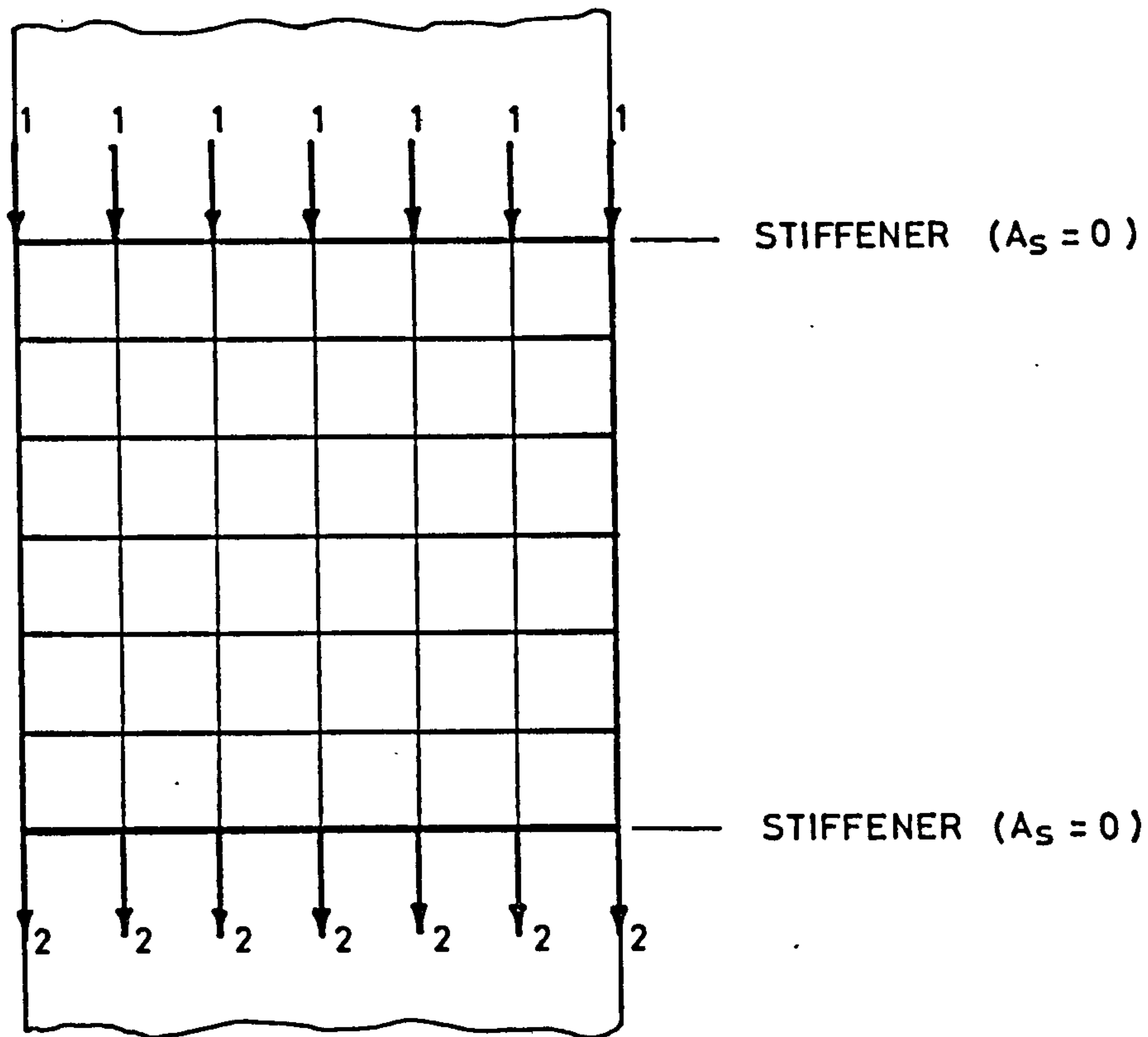


imperfection is gradual after the buckling load is reached, possibly in part because of the incremental load approach.

When the mode of buckling changes, a corresponding change of stiffness is observed. For case (a), a sudden change of stiffness takes place at approximately  $Q/Q_{cr} = 1.6$ ; and for case (b), a sudden change of stiffness occurs at about  $Q/Q_{cr} = 1.7$ . The subsequent stiffness tends to converge to a constant value, as the load is further increased, as shown by dotted lines in Figures (7-4), (7-5), (7-6) and (7-7). Changes in the mode of buckling are examined in Section 7.4.

The relative shear stiffness reduction plotted in ESDU (Ref. 72) is for a long flat panel with various flange and stiffener dimensions, and with boundary conditions quite different to the square plate considered in cases (a) and (b). Nevertheless, as far as the stiffness reduction is concerned, Figures (7-4), (7-5), (7-6), and (7-7) have generally similar characteristics to ESDU (Ref. 72).

CASE (a)



CASE (b)

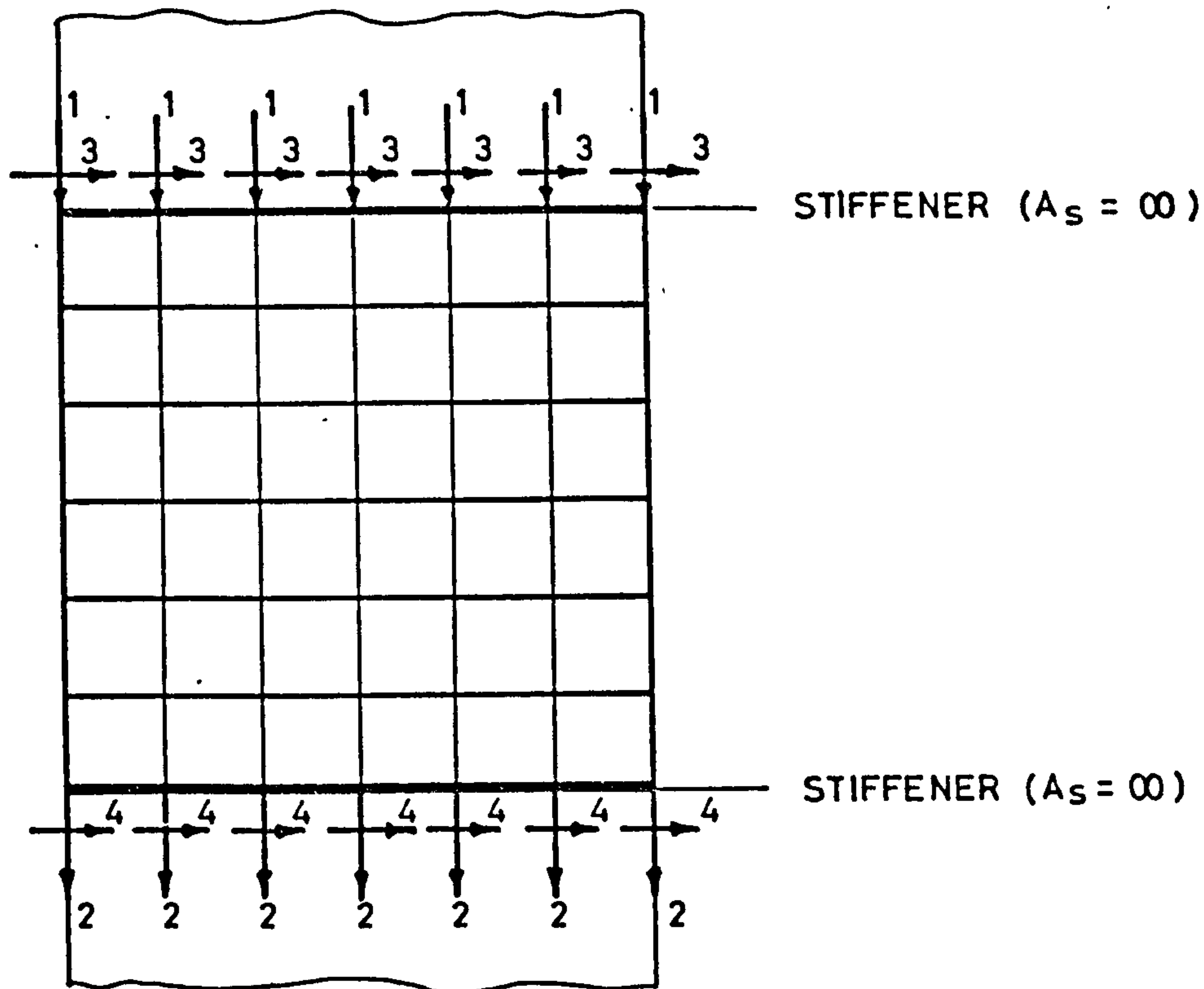


FIGURE 7-3

SIMPLY SUPPORTED  
B.C. - CASE (a)

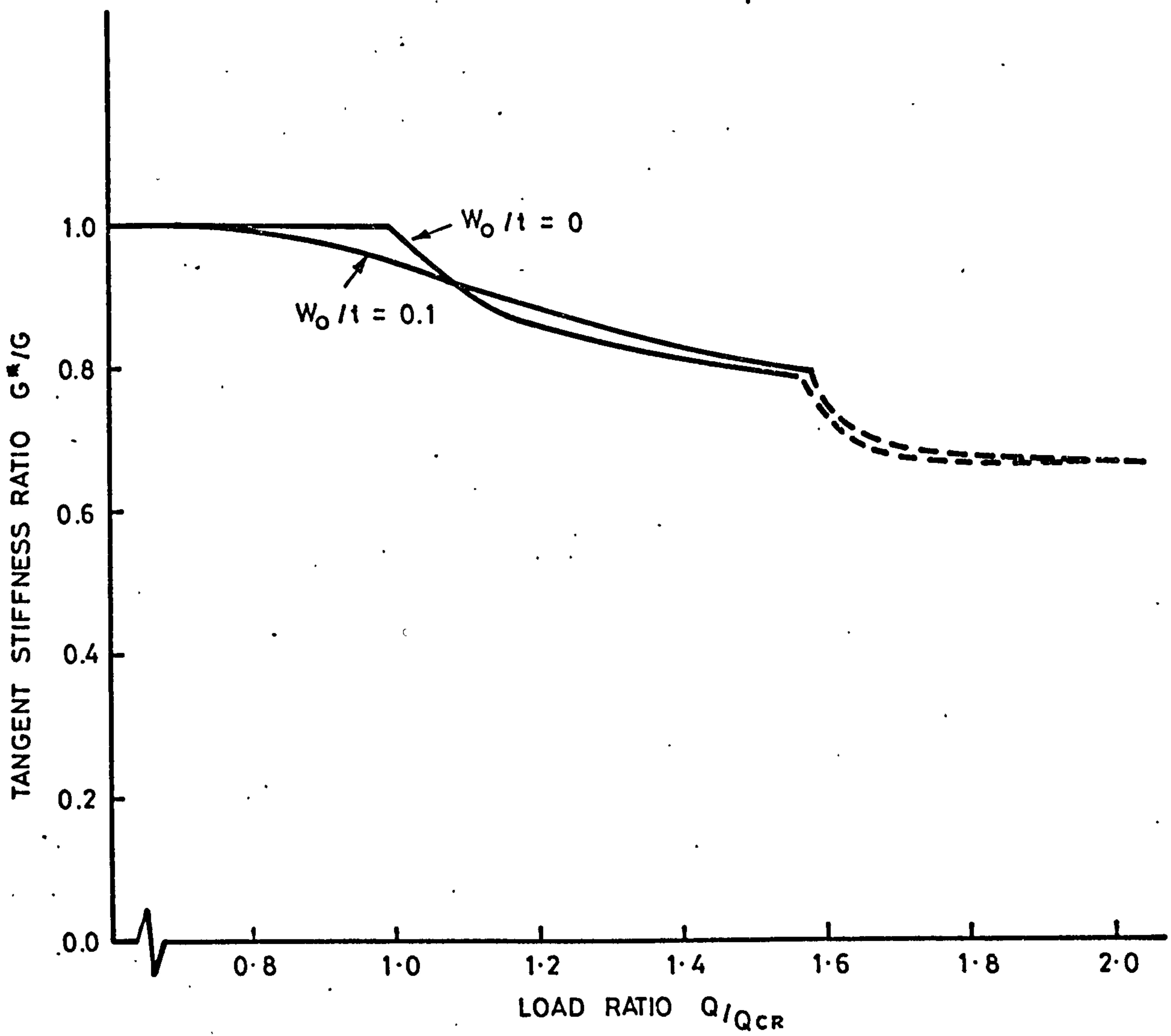
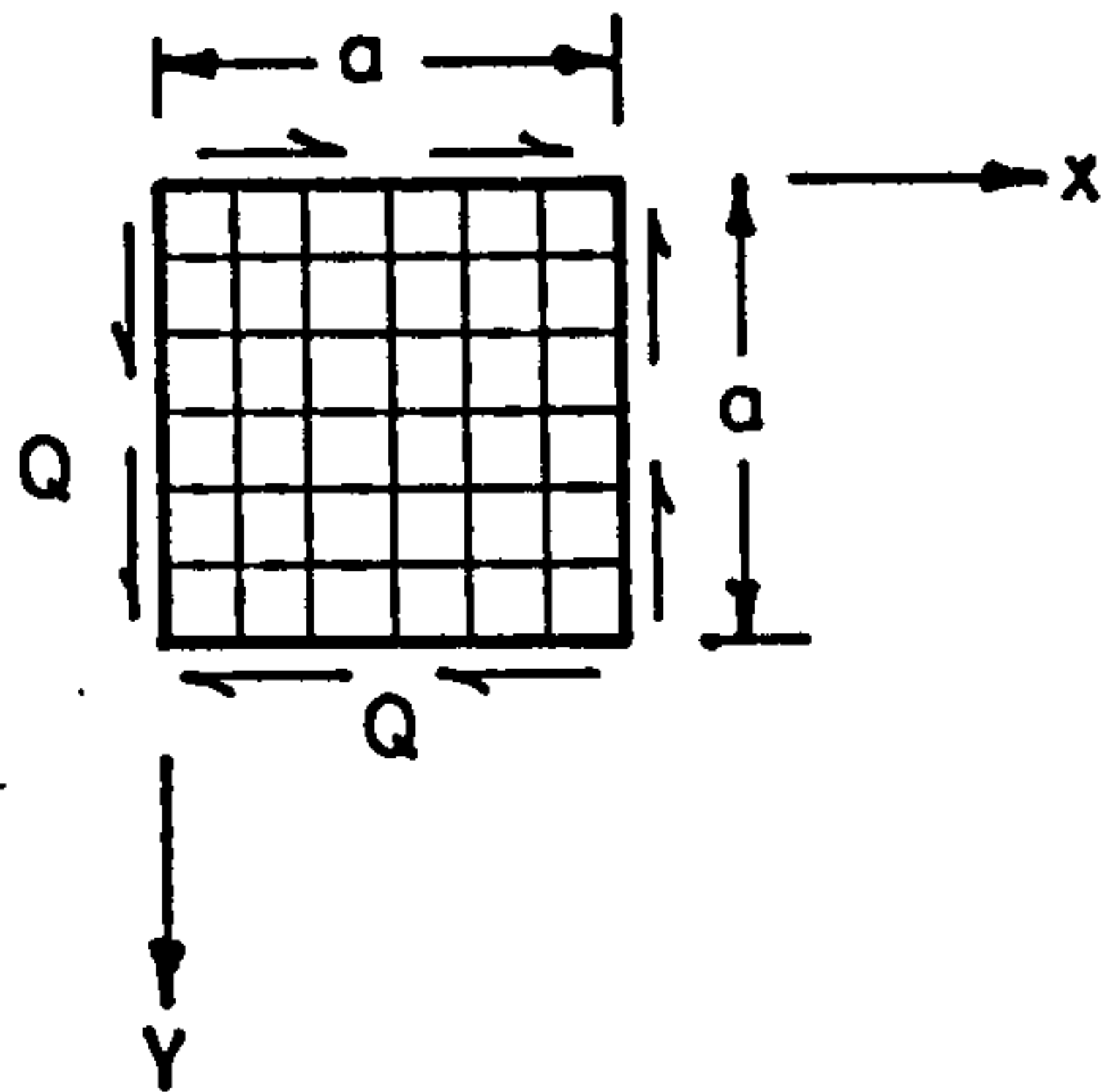


FIGURE 7-4

SIMPLY SUPPORTED  
B.C. - CASE (a)

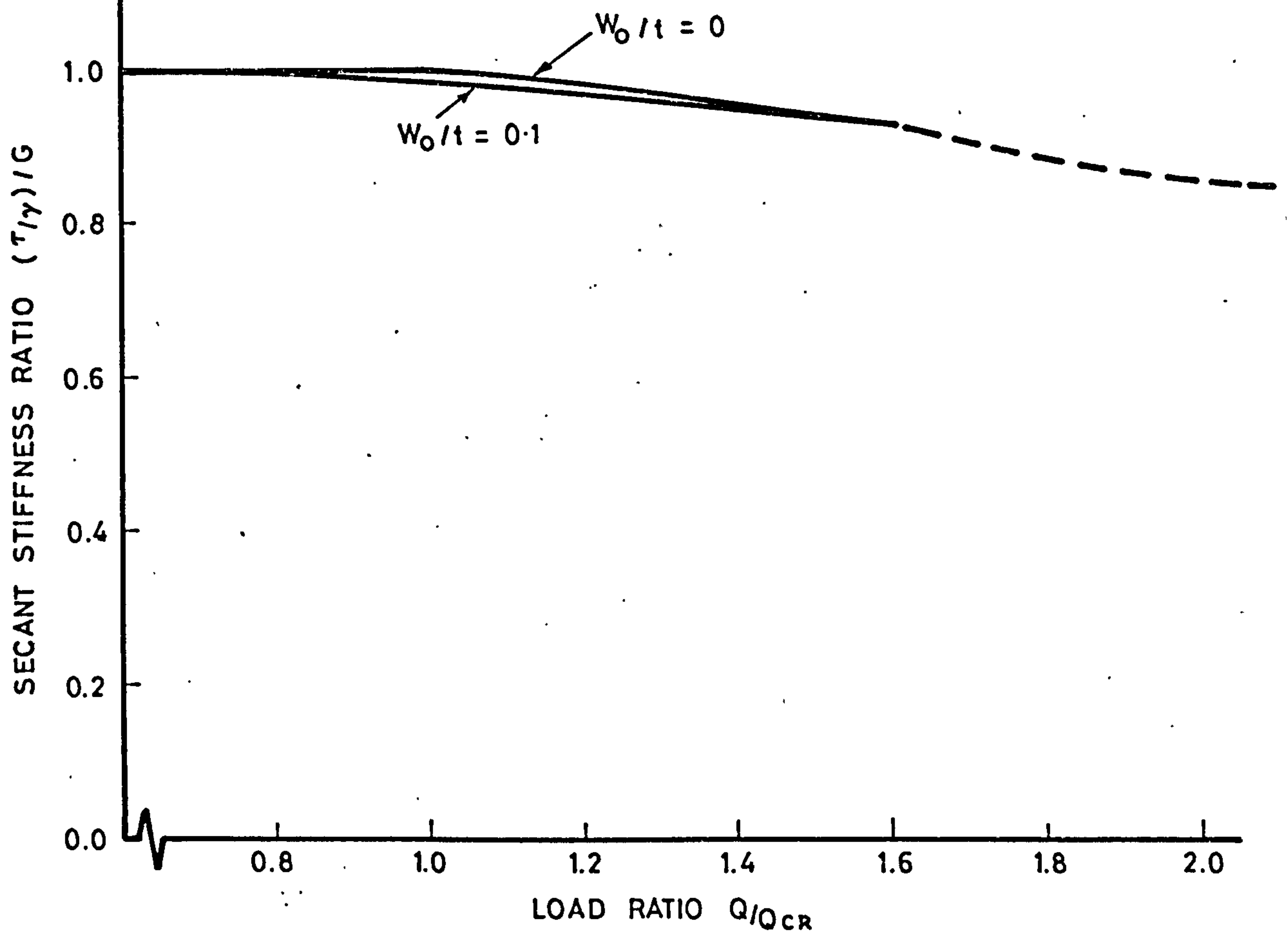
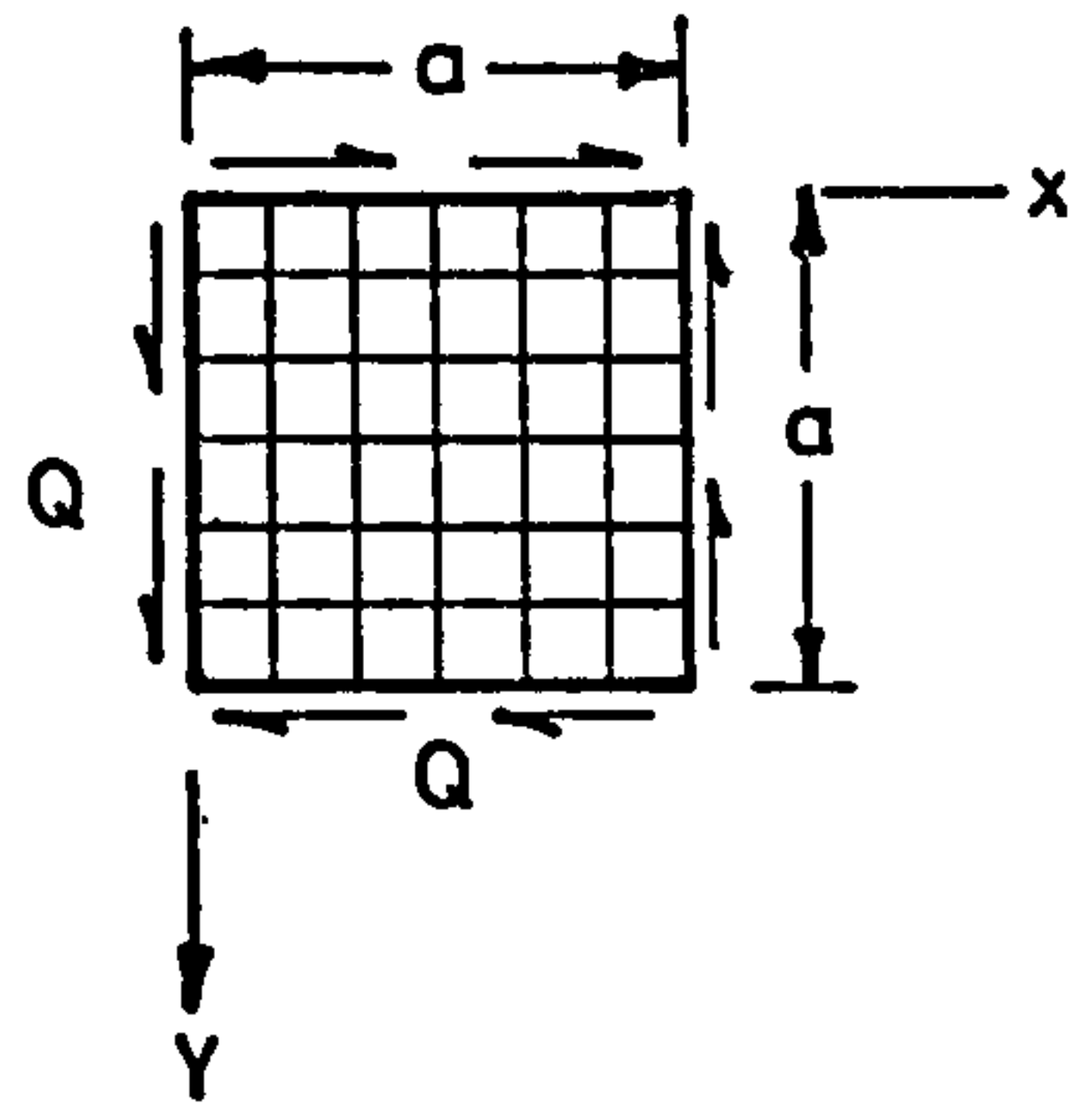


FIGURE 7-5



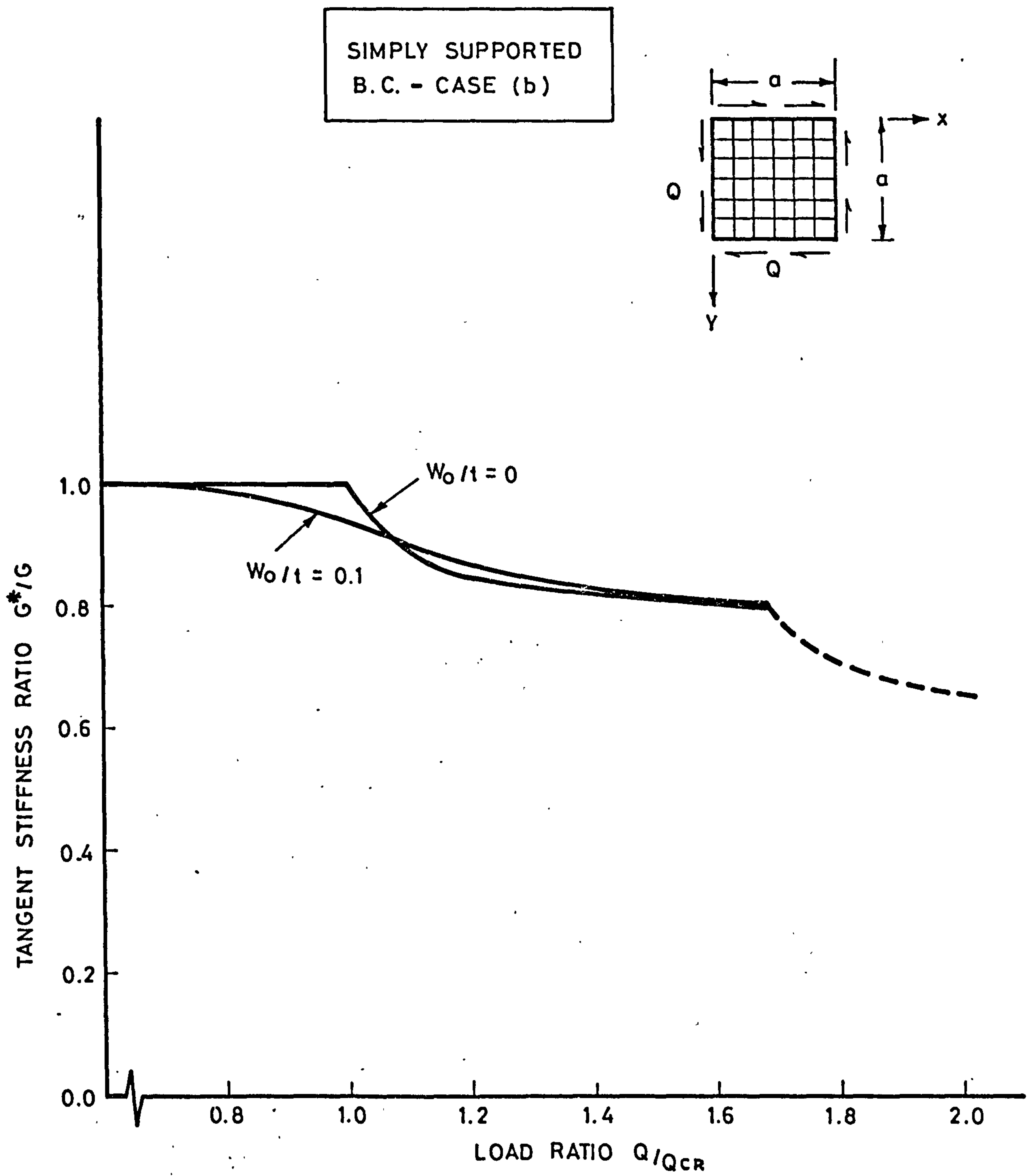


FIGURE 7-6

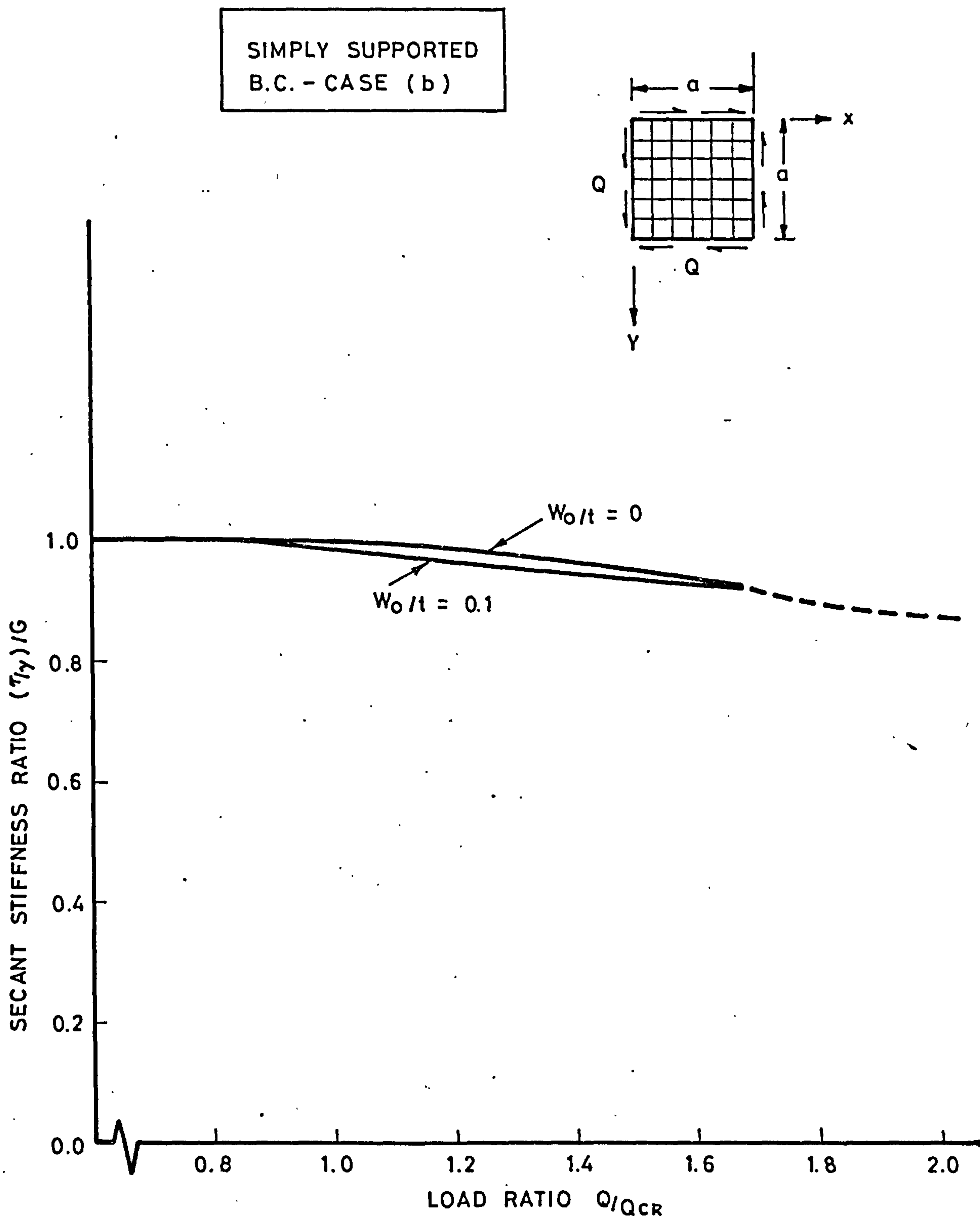


FIGURE 7-7

## 7.4 CHANGE OF MODE SHAPE IN PURE SHEAR

As noted in Section 7.3, the post-buckled shear stiffness of the plate shows a sudden reduction, likely to be due to a change of mode shape. In order to investigate the correlation of shear stiffness and change of mode shape, the lateral displacements of the plate for both boundary conditions are now examined.

Plates, both with and without initial imperfection, are considered for pre- and post-buckling behaviour. For the initial imperfection of the plate, the following expression is used:

$$w = \sum_{m=1}^{m=\infty} \sum_{n=1}^{n=\infty} a_{mn} \sin \frac{m\pi x}{a} \sin \frac{n\pi y}{b} \quad (7-3)$$

Only the terms  $a_{11}$  and  $a_{22}$  of the above expression are taken for an initial approximation of the mode shape. The maximum amplitude is chosen as 10% of the plate thickness. For perfectly flat plates, the system of loading is similar to the plate subject to compression. The plate is initially loaded to the critical shear load, found by the Southwell Plot technique, then a fictitious load (see Chapter 6) is applied at the center of the plate, where the maximum amplitude of the mode shape occurs.

Because of the complicated shape of the actual buckling mode, the whole plate is used for the calculation. To save computer time, the 6x6 mesh is chosen rather than the 8x8 mesh. Before commencing the large deflection analysis, the critical load is calculated by the Southwell Plot technique. A 6x6 mesh gives an answer 16% higher than the classical value (Figure 7-8). It must be mentioned now that the critical shear load referred to in the text or in the graphs is considered to be the calculated computer value (Southwell Plot).

Initially, the incremental procedure with iteration at each load increment was chosen. Iteration failed at approximately  $Q/Q_{cr} = 1.9$ . It was found that, as the mode shape starts to change in the post-buckling range, convergence fails at the point where the maximum displacement starts to reverse. In order to obtain a solution up to about  $Q/Q_{cr} = 3.0$ , the solution was then continued by a purely incremental procedure. This pattern of changing mode shape is demonstrated in the following graphs. Figure (7-9) and Figure (7-10) show the central displacements against the load ratio for cases (a) and (b)

respectively. Figures (7-11), (7-12), and (7-13) show the change of mode shape for different values of  $Q/Q_{cr}$  in the form of amplitude at different sections of the plate, and as a contour plot to show the whole surface of the plate. The contour graphs are executed by computer plotter facilities at the Computer Center (Figures 7-14, 7-15, 7-16, 7-17, and 7-18). Since the number of points available for contour plotting in the computer is small, the contour lines are not smooth curves. The points used for mapping the whole surface are the total number of nodal points available in the finite element mesh.

Comparing the displacement results with the shear stiffness results, it is observed that both have similar characteristics, as far as the effect of mode change is concerned. Also, by observing the stiffness reduction and reversal of centre displacement in the figures, it is noticed that the subsequent stiffness reduction is very sensitive to change of mode shape and occurs before displacement reversal takes place.



SIMPLY SUPPORTED  
B.C. - CASE (a)

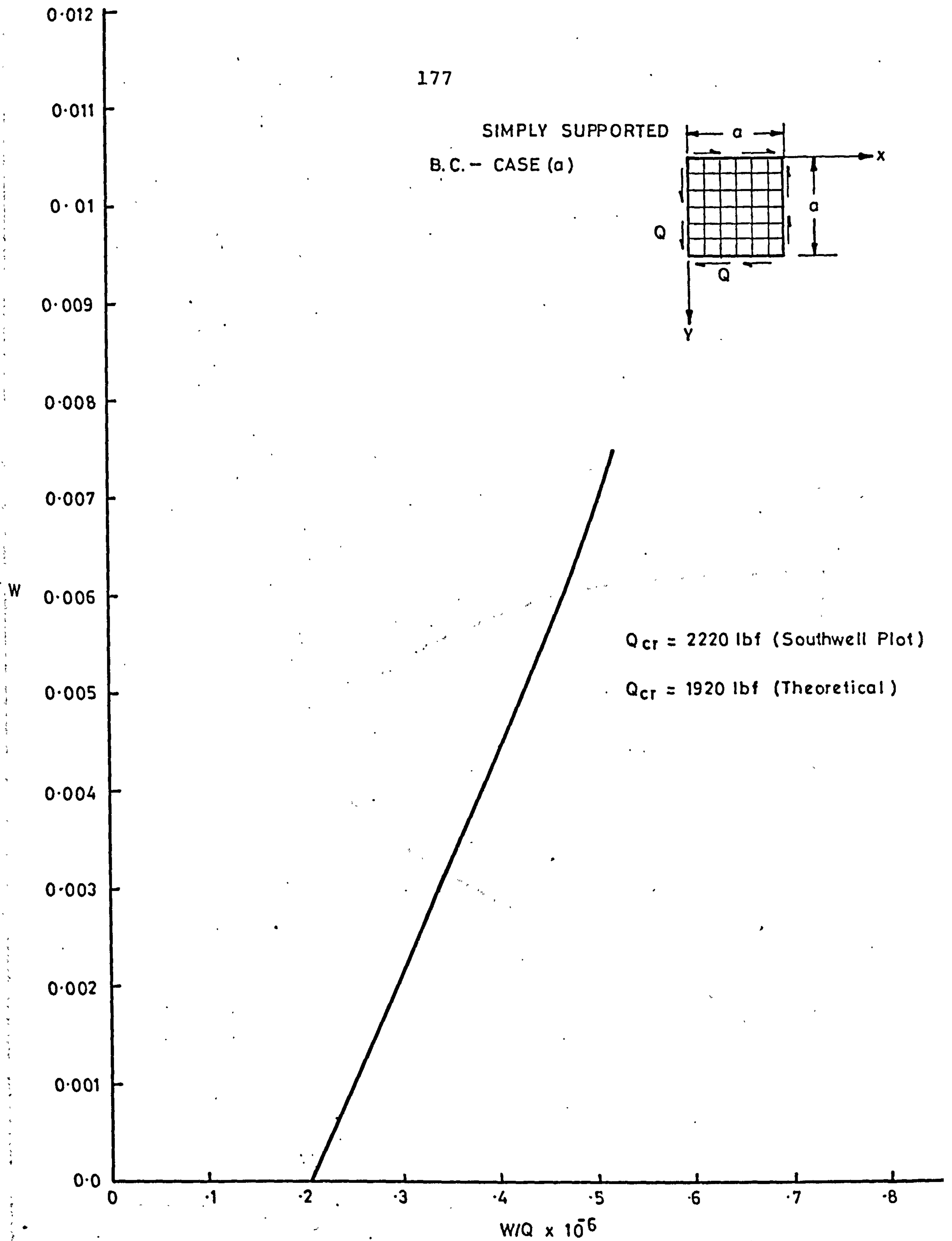
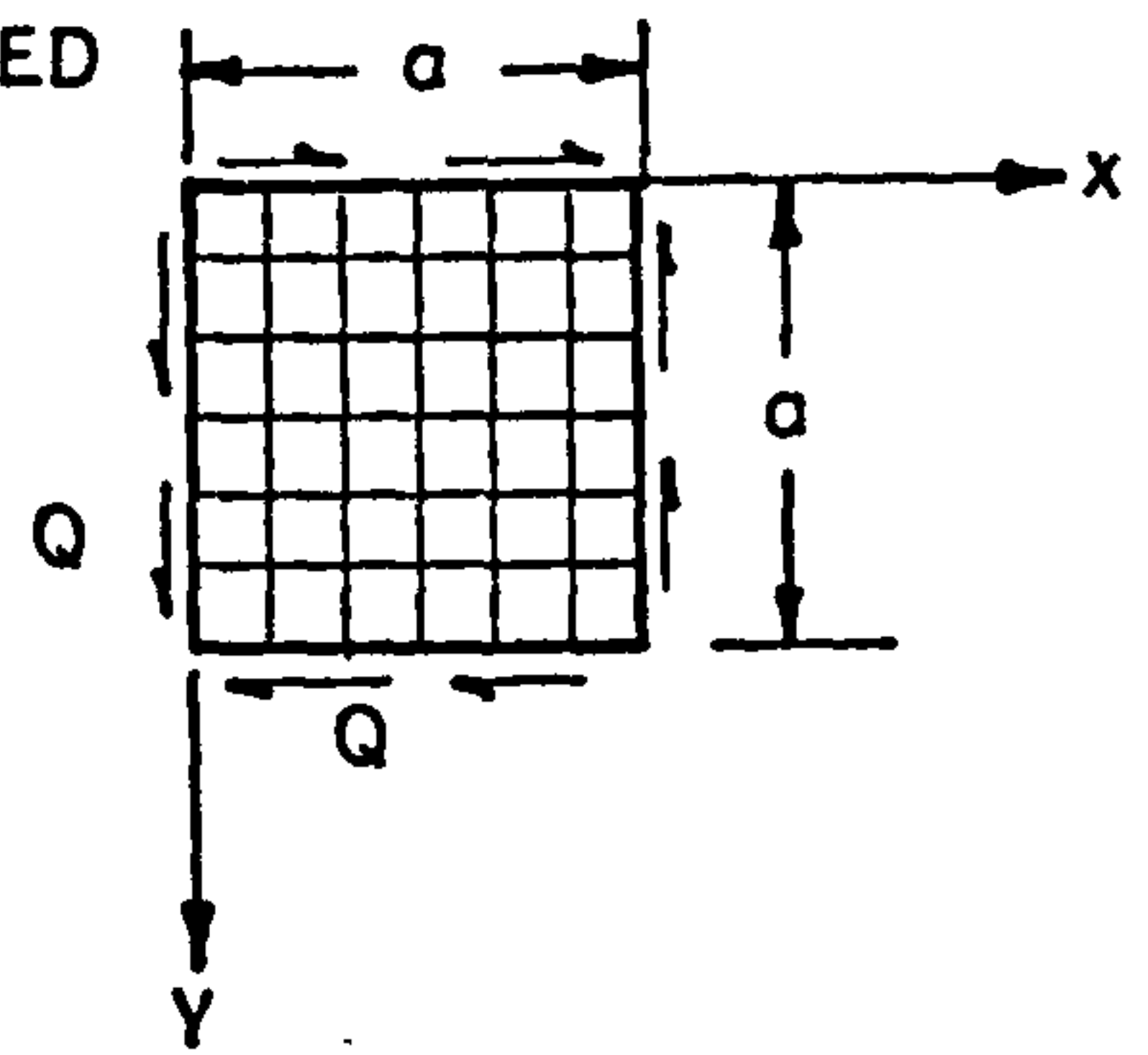
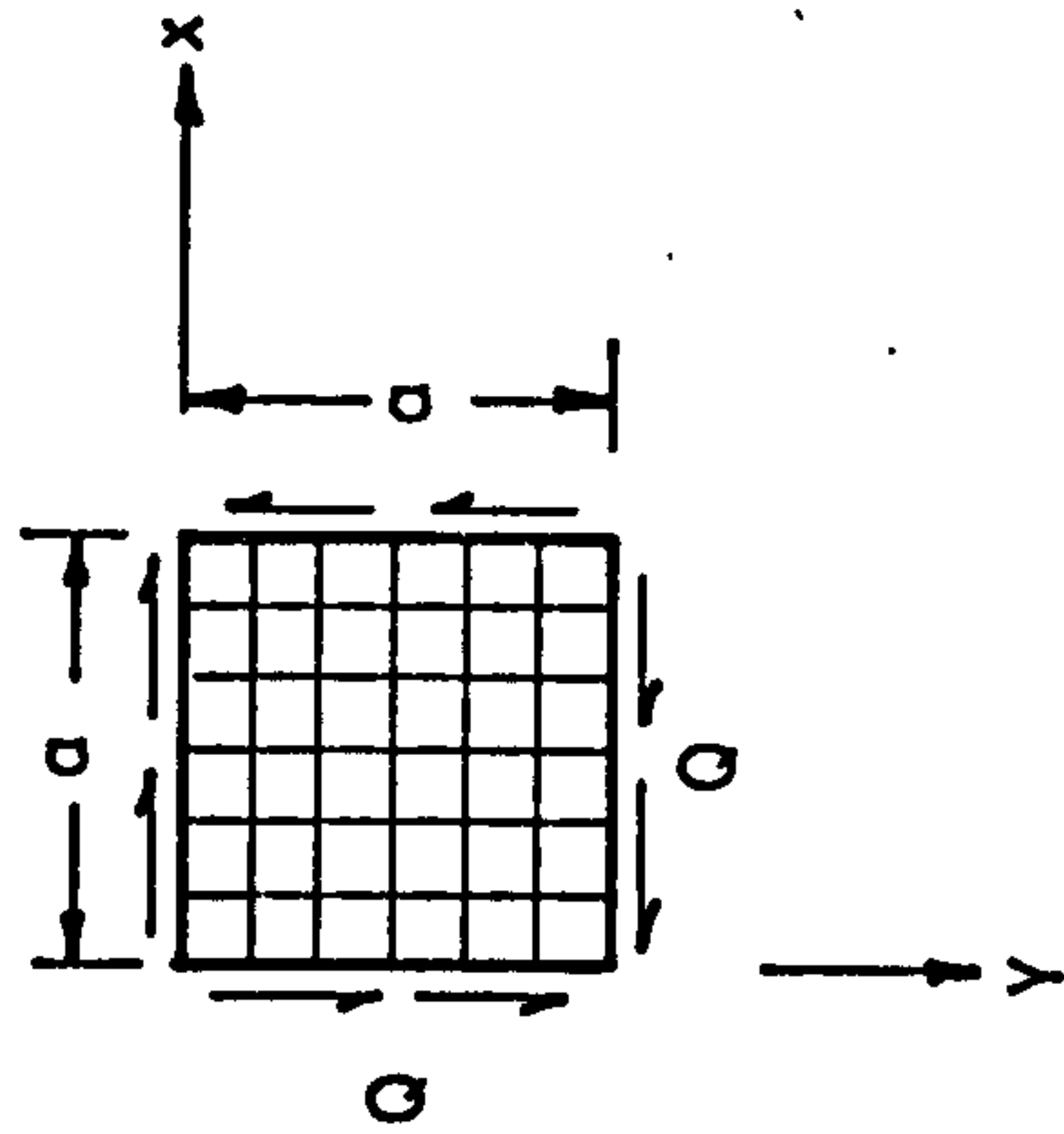
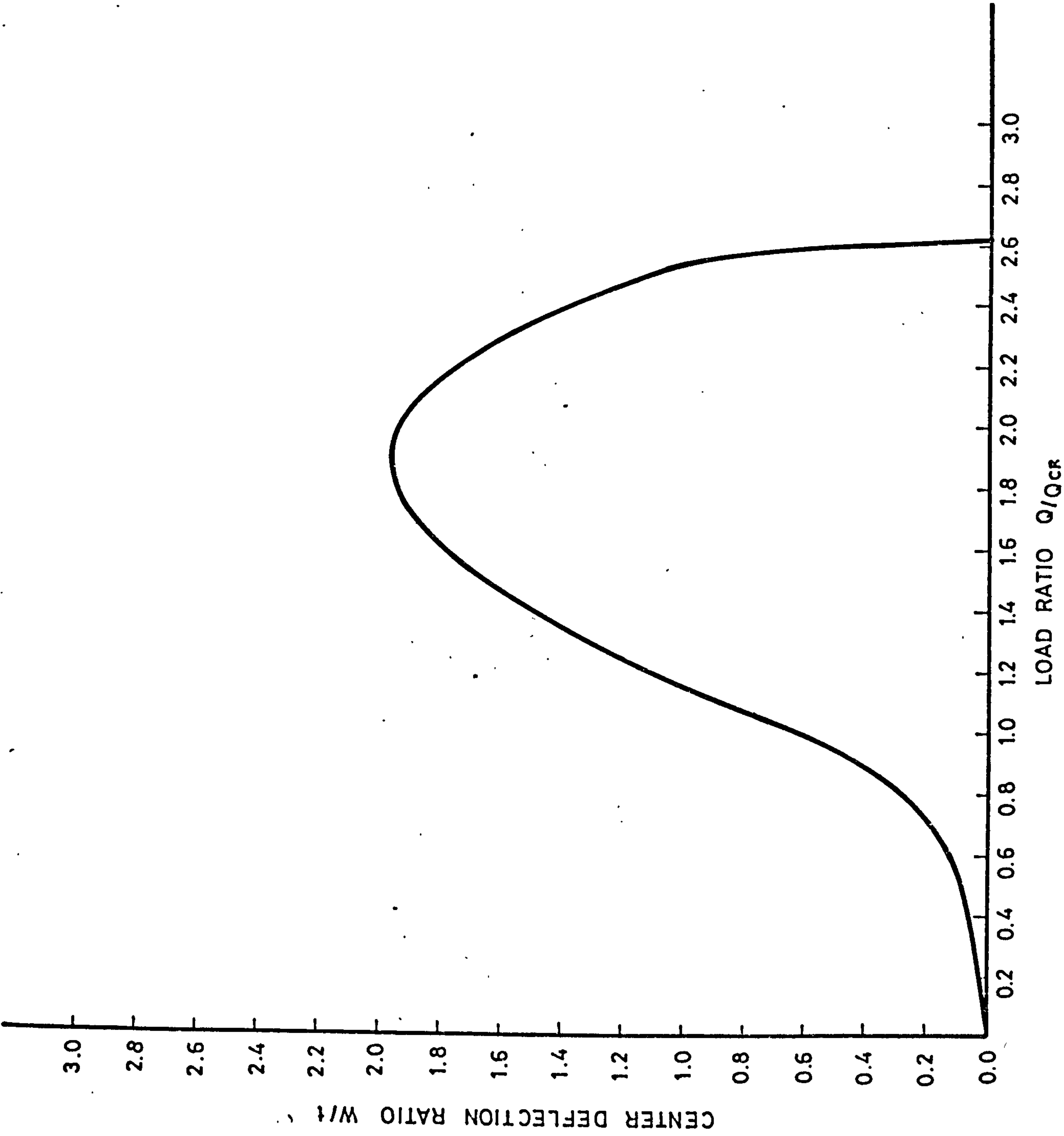
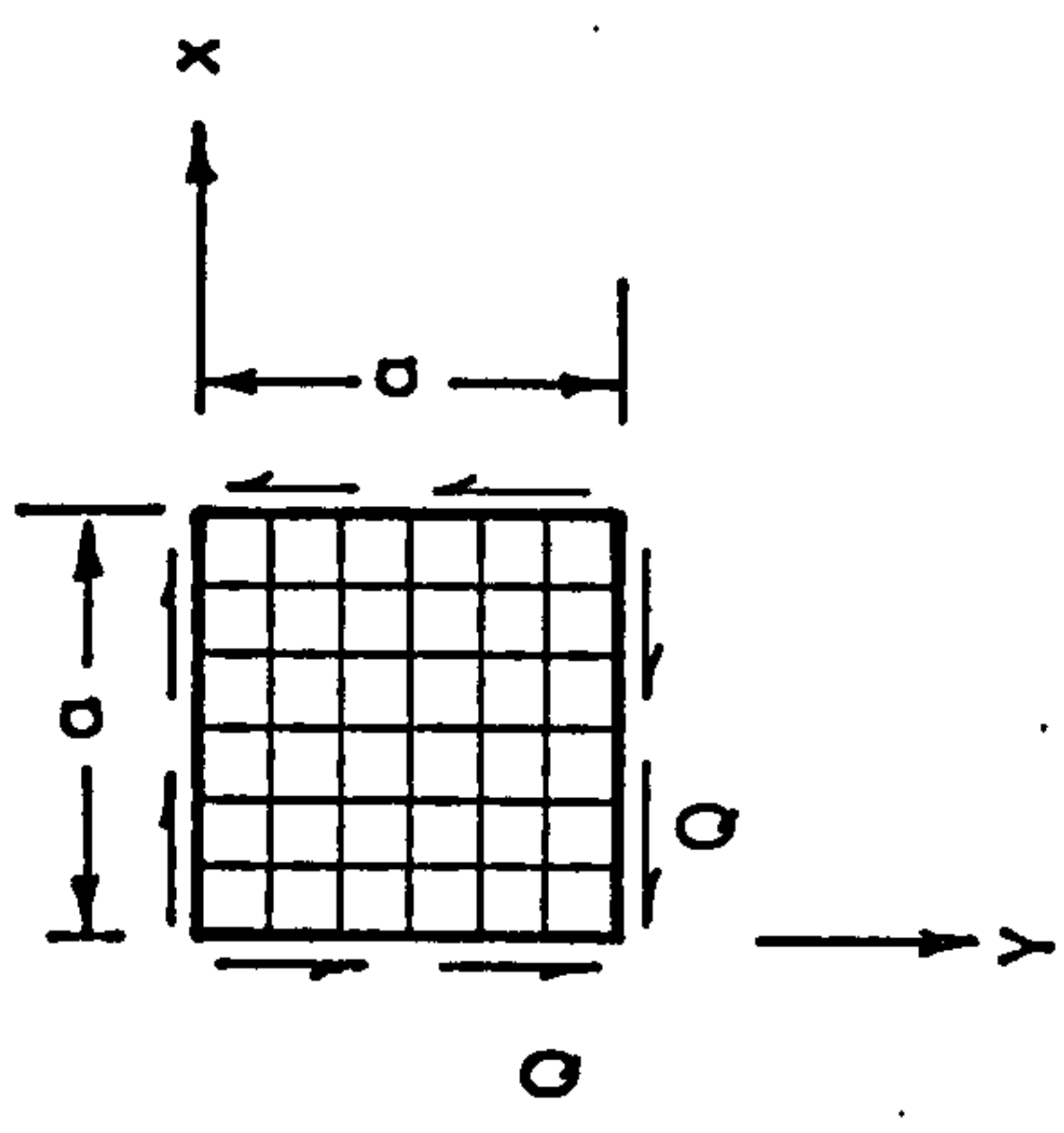
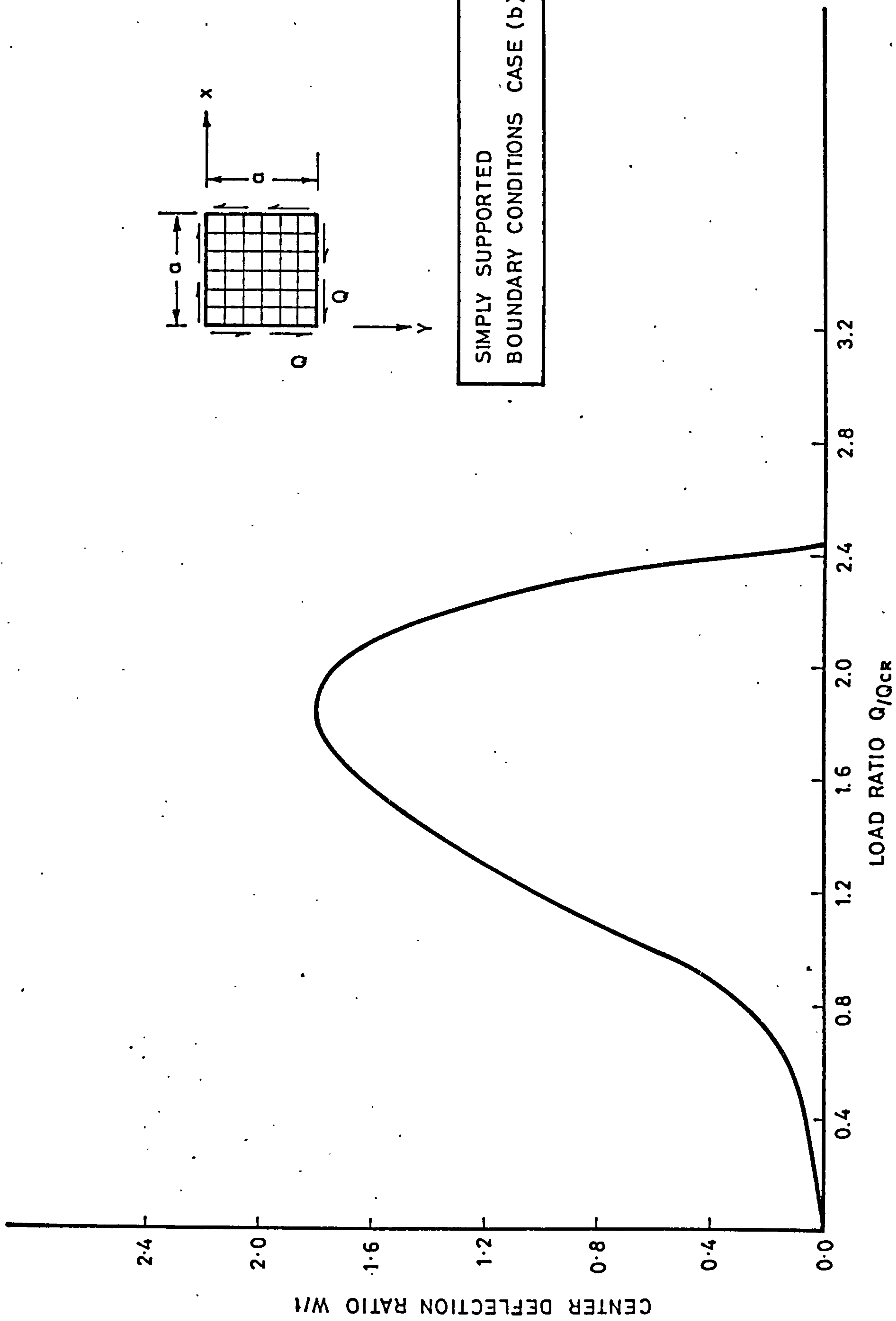


FIGURE 7-8



SIMPLY SUPPORTED  
BOUNDARY CONDITIONS CASE (a)

FIGURE 7-9



SIMPLY SUPPORTED  
BOUNDARY CONDITIONS CASE (b)

FIGURE 7-10

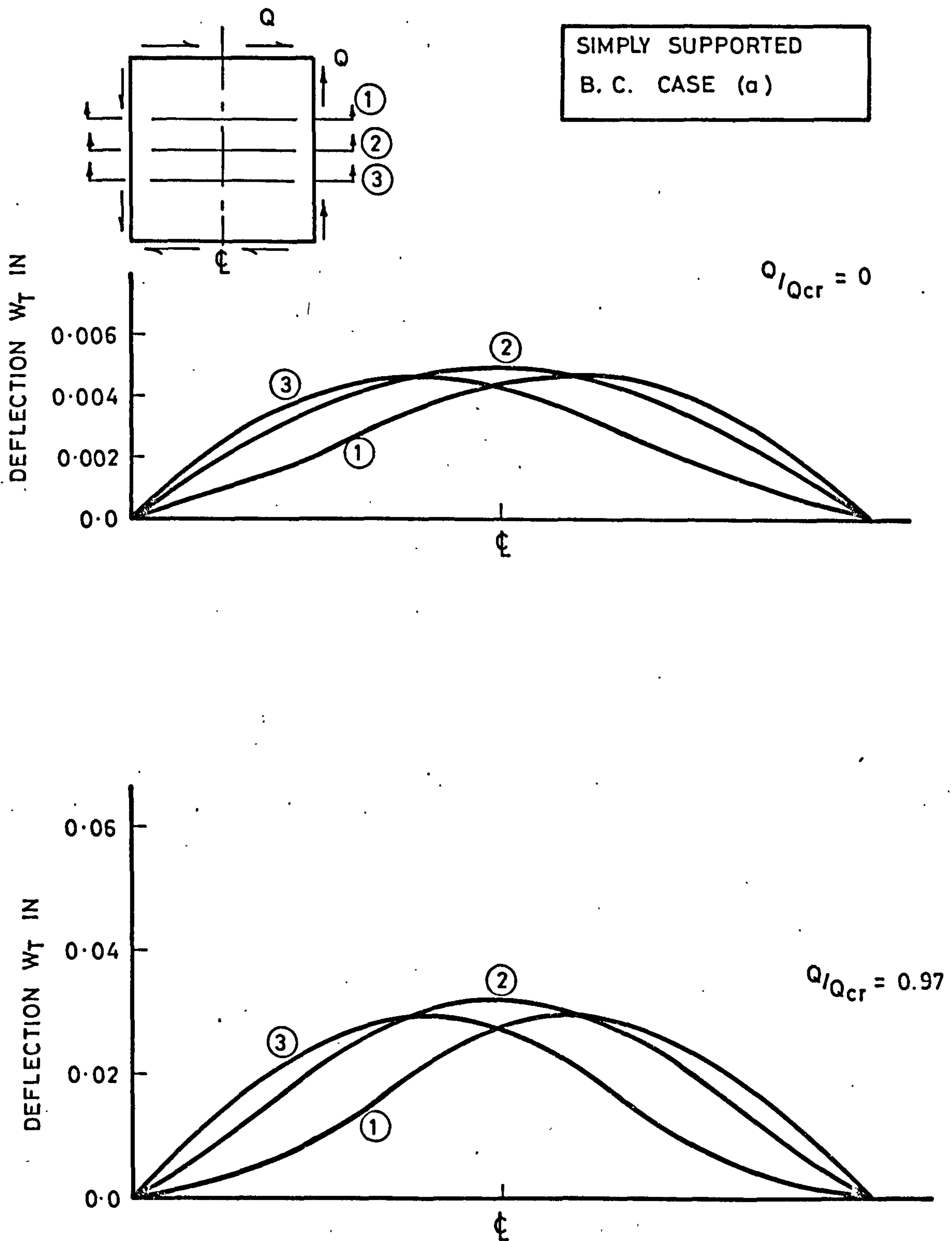


FIGURE 7-11



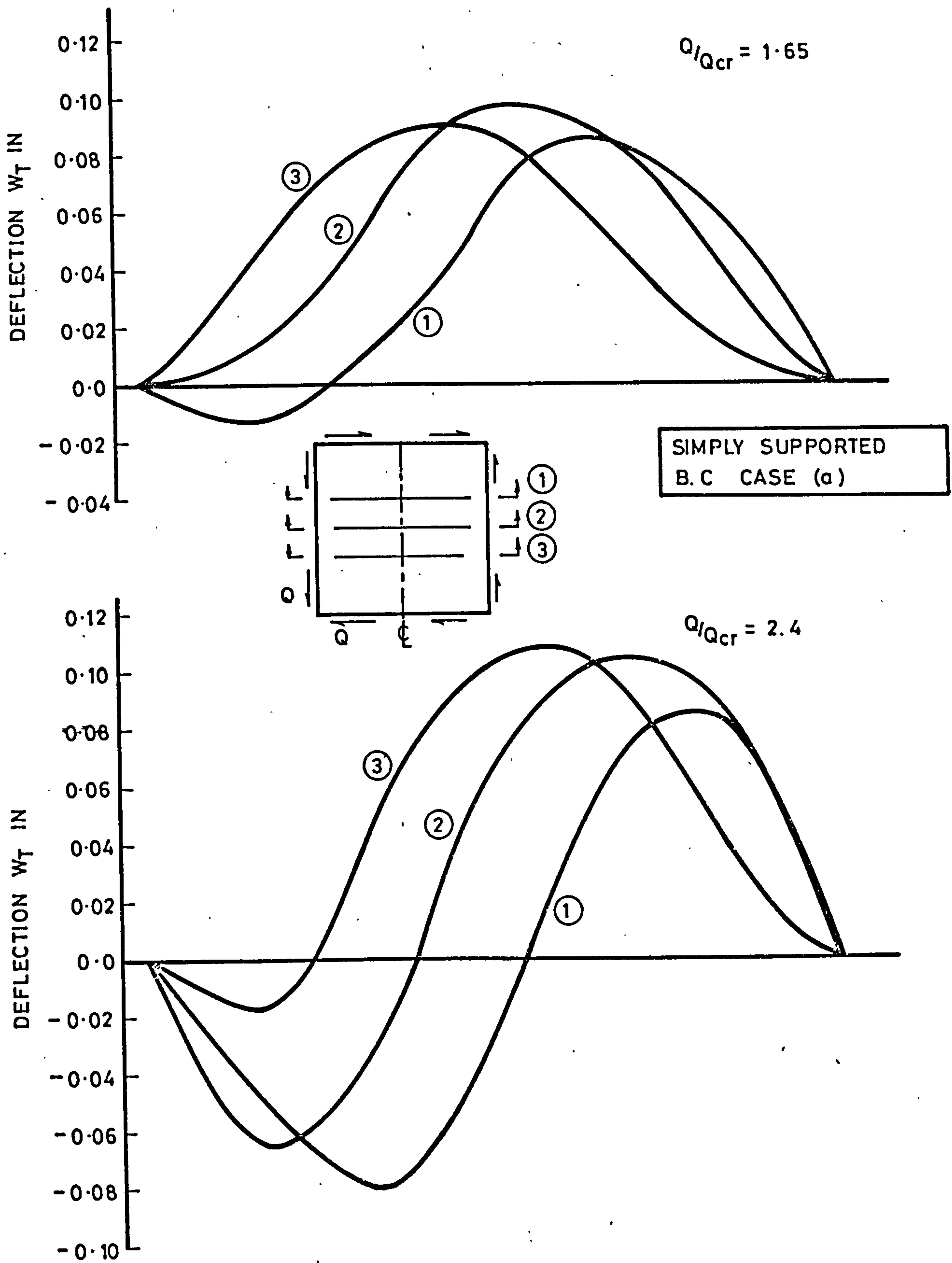


FIGURE 7-12

SIMPLY SUPPORTED  
B.C. CASE (a)

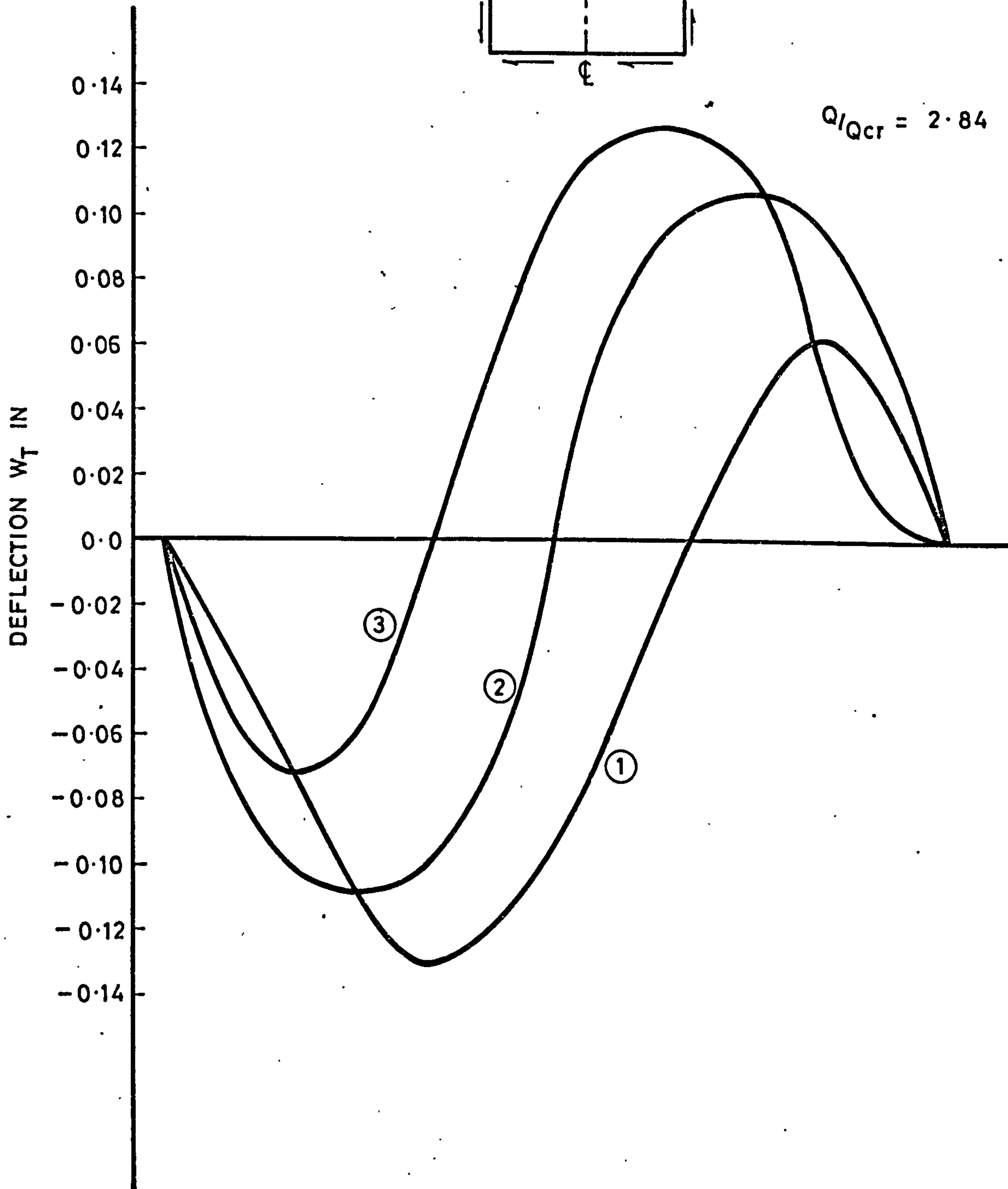
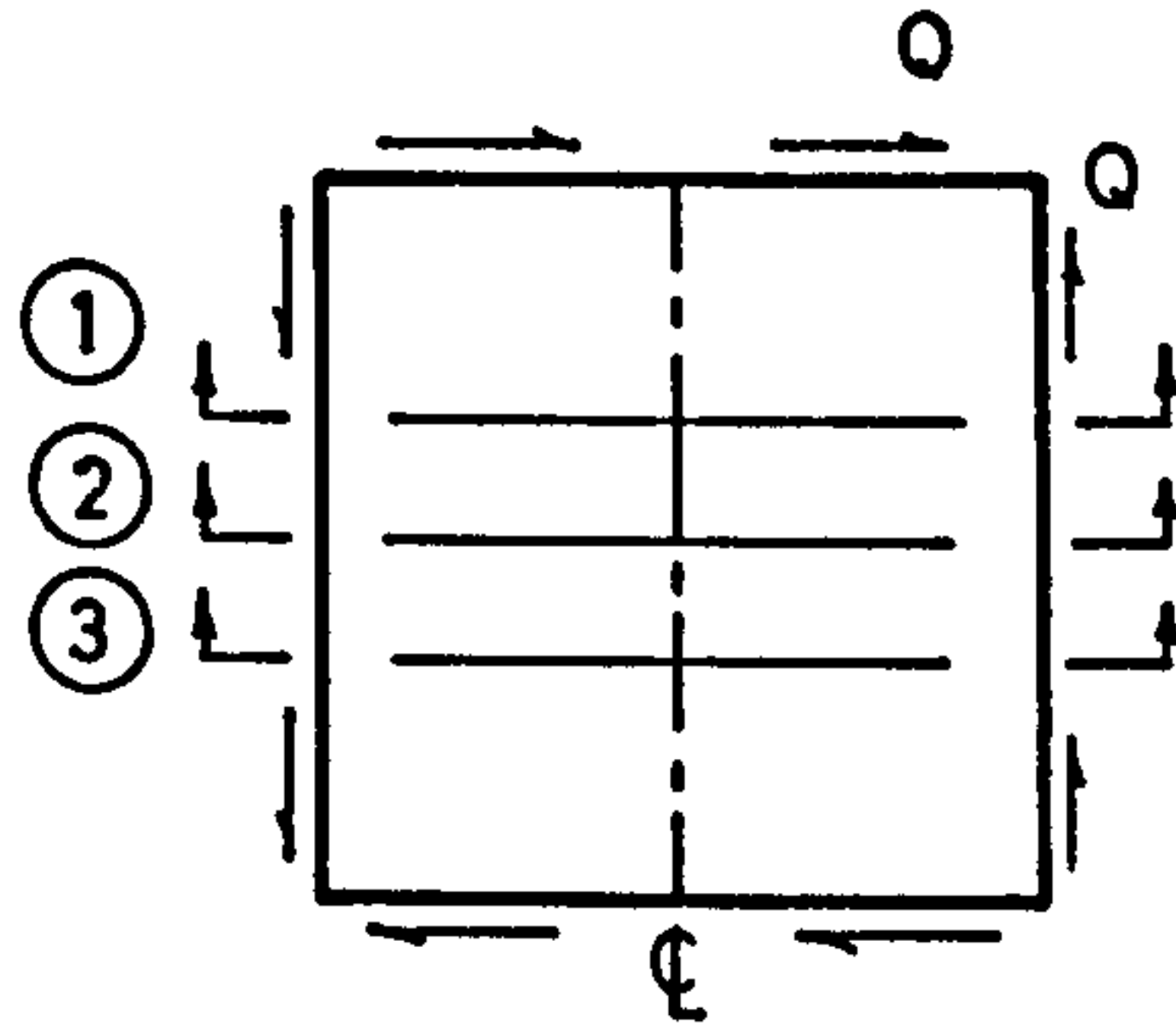
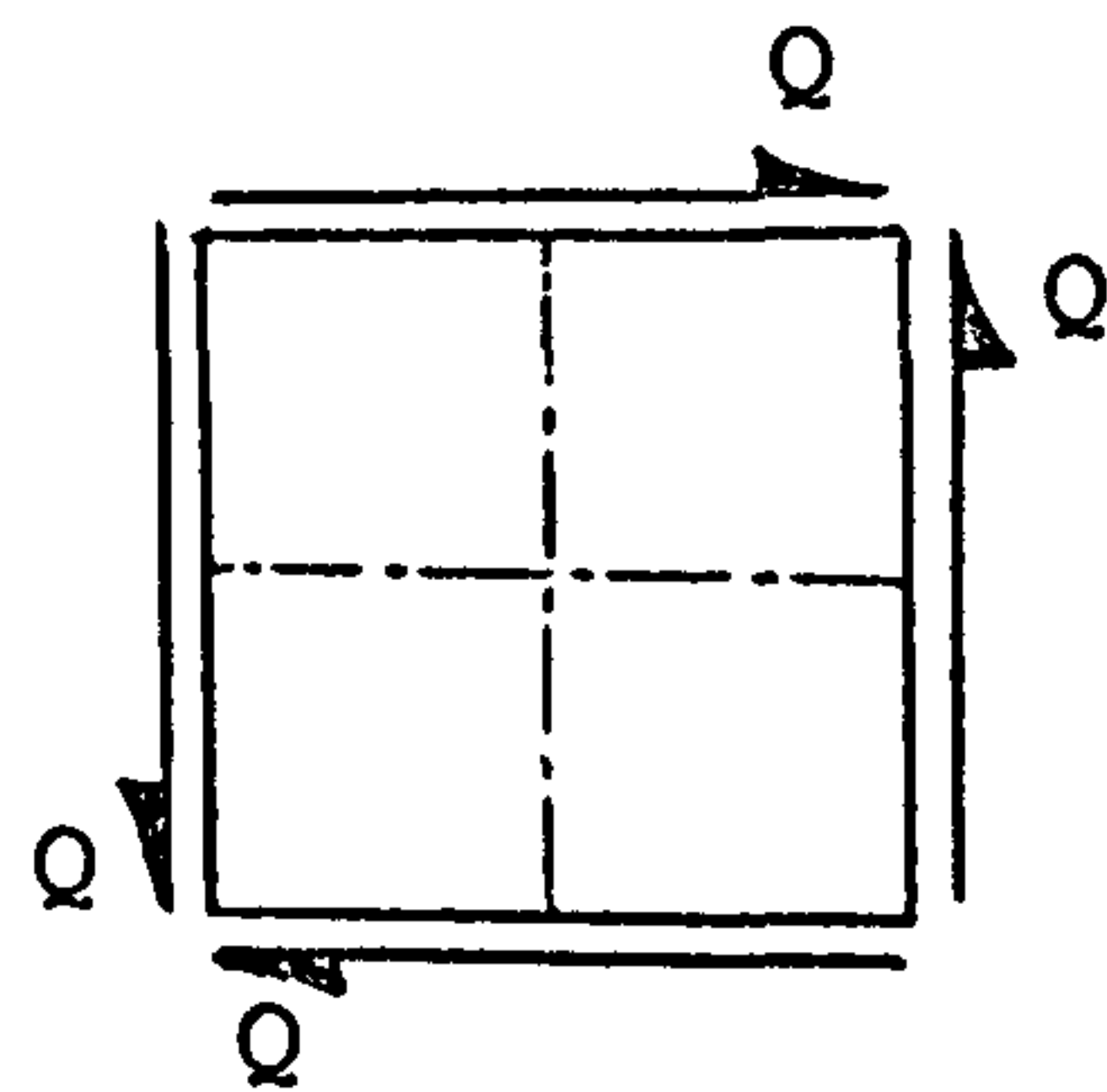


FIGURE 7-13



$$\frac{Q}{Q_{cr}} = 0 \quad ; \quad t = 0.05''$$

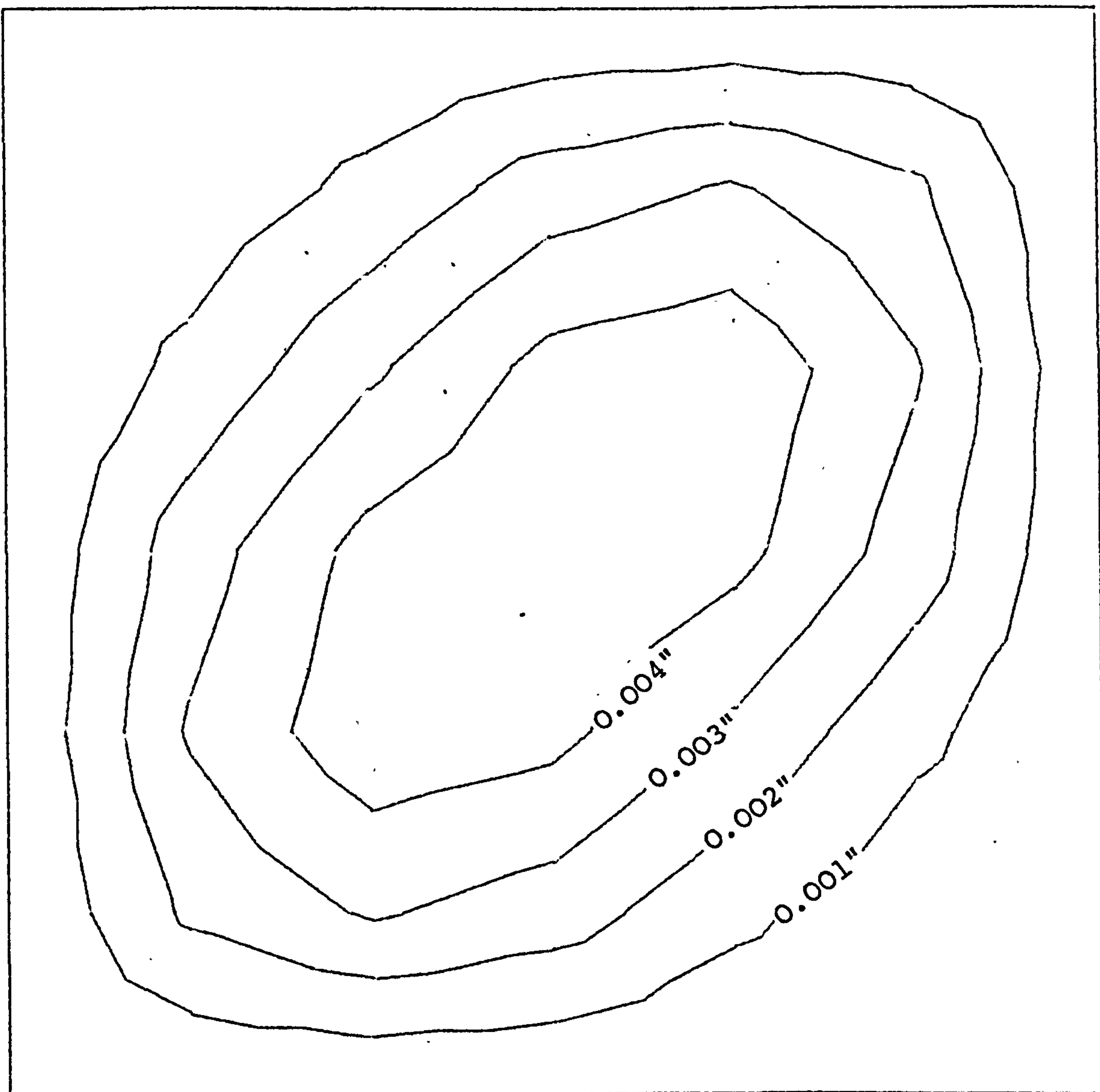


FIGURE (7-14)

$$Q/Q_{cr} = 0.97 \quad ; \quad t = 0.05''$$

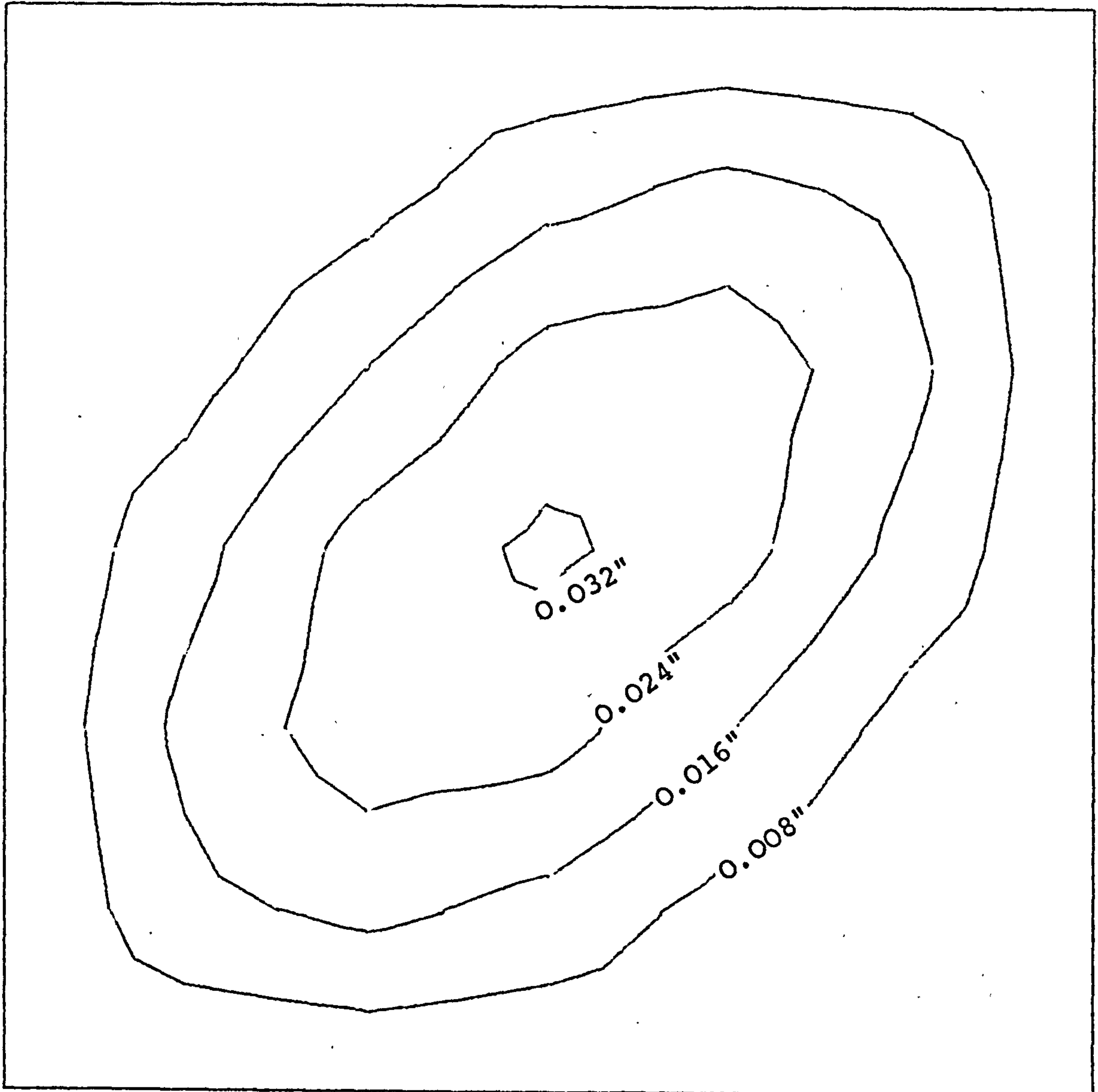
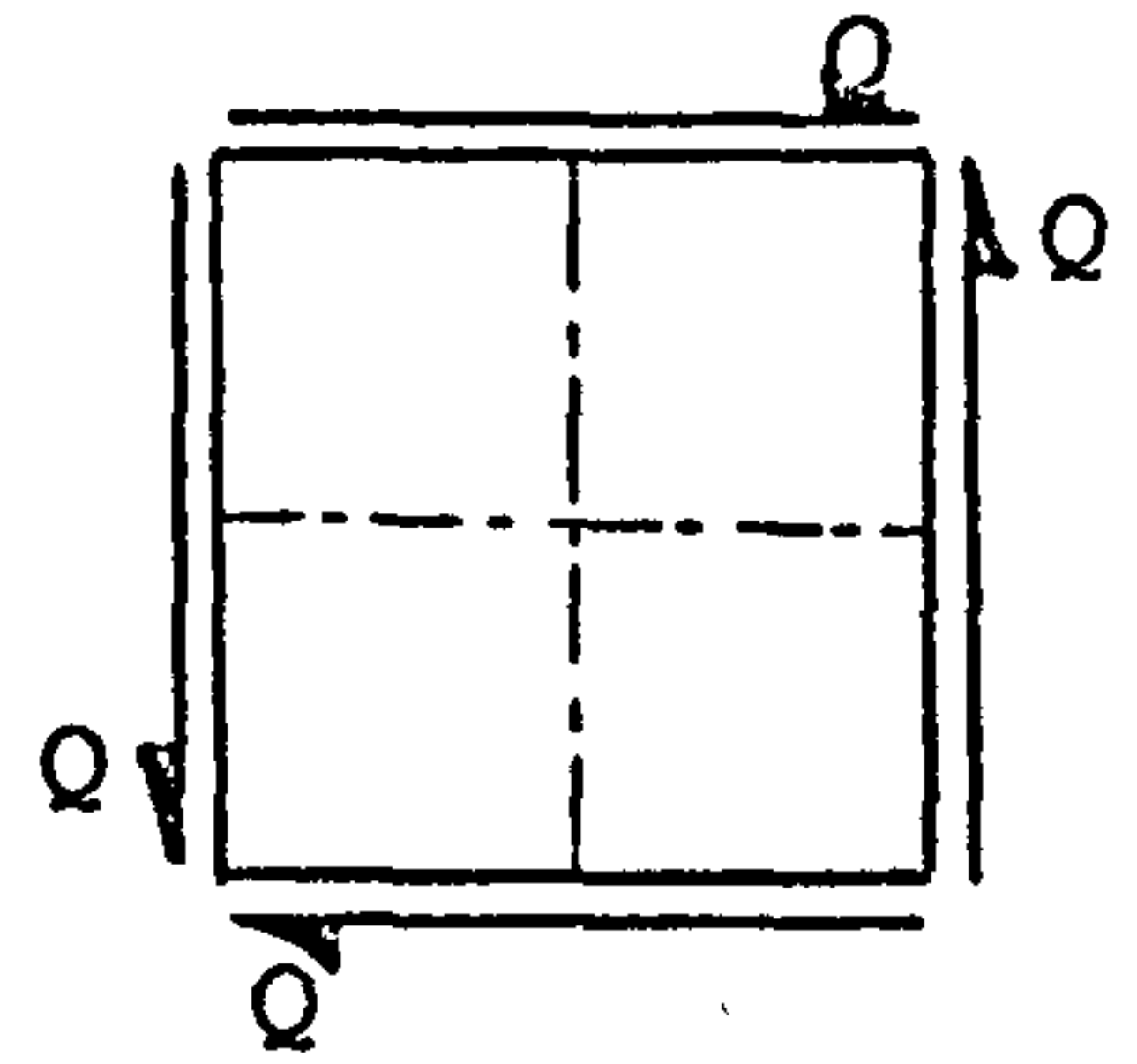


FIGURE (7-15)



$$\frac{Q}{Q_{cr}} = 1.65 ; \quad t = 0.05''$$

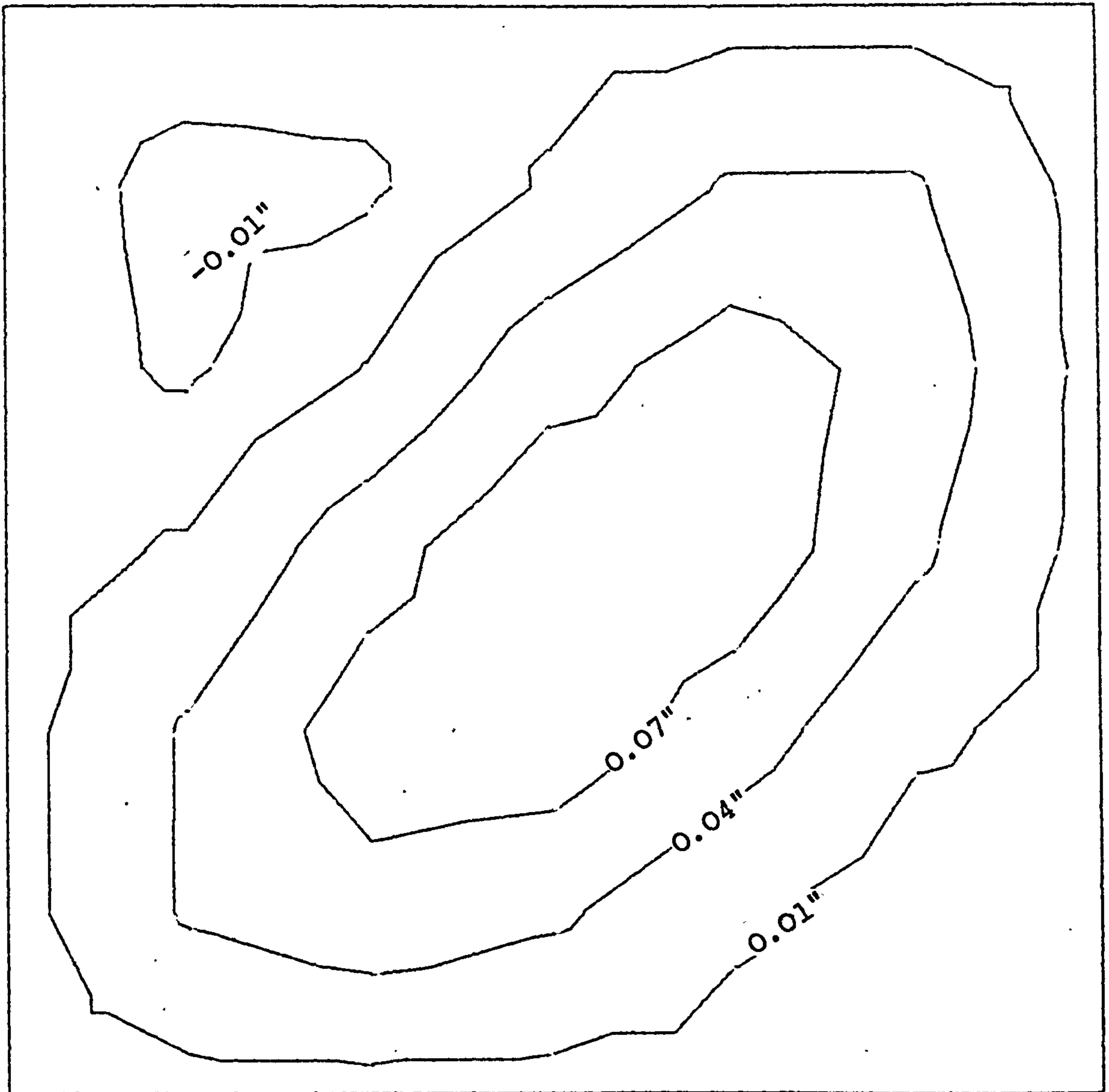
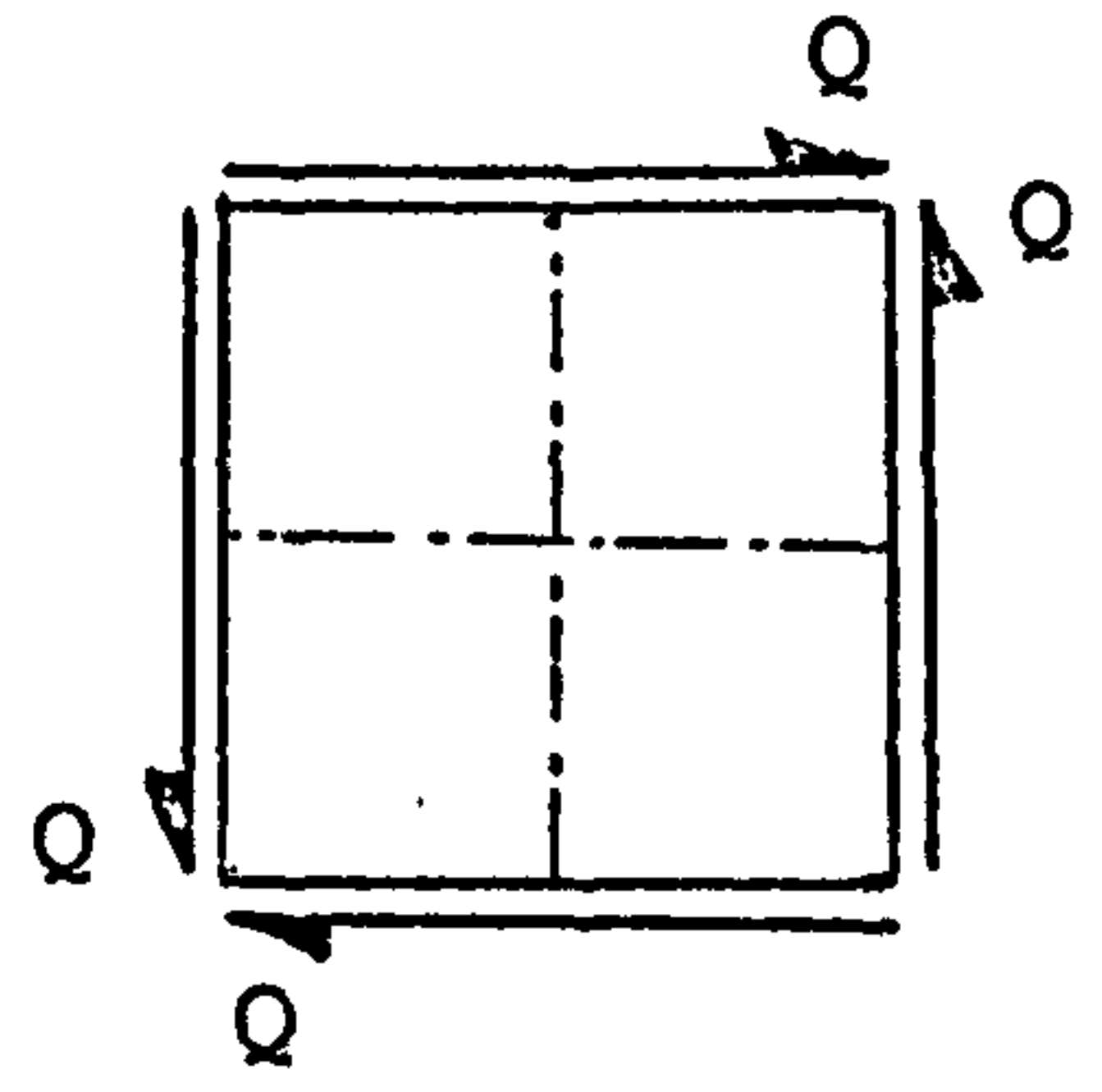


FIGURE (7-16)

$$\frac{Q}{Q_{cr}} = 2.4 \quad ; \quad t = 0.05''$$

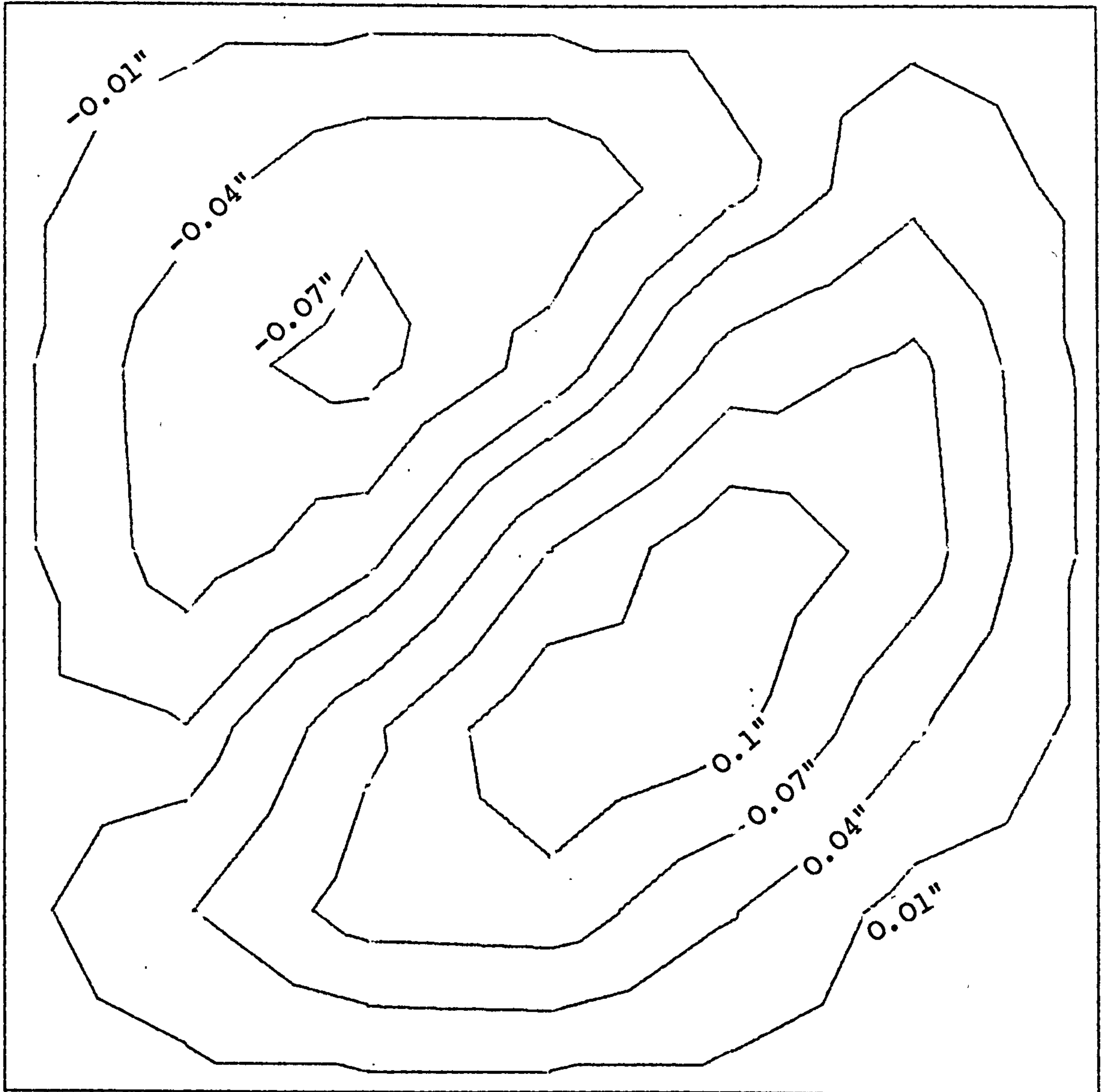
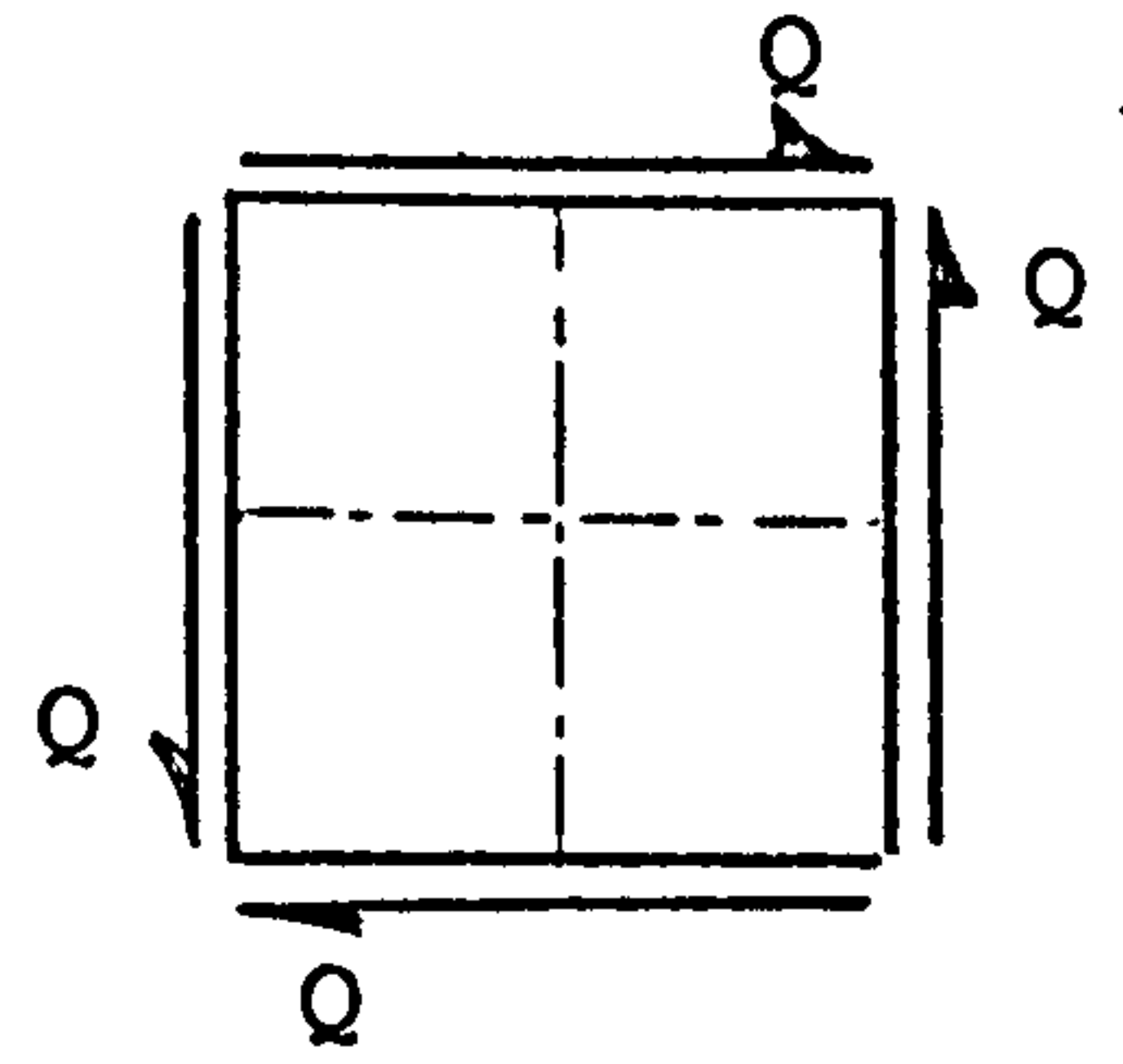


FIGURE (7-17)

$$\frac{Q}{Q_{cr}} = 2.84 \quad ; \quad t = 0.05''$$

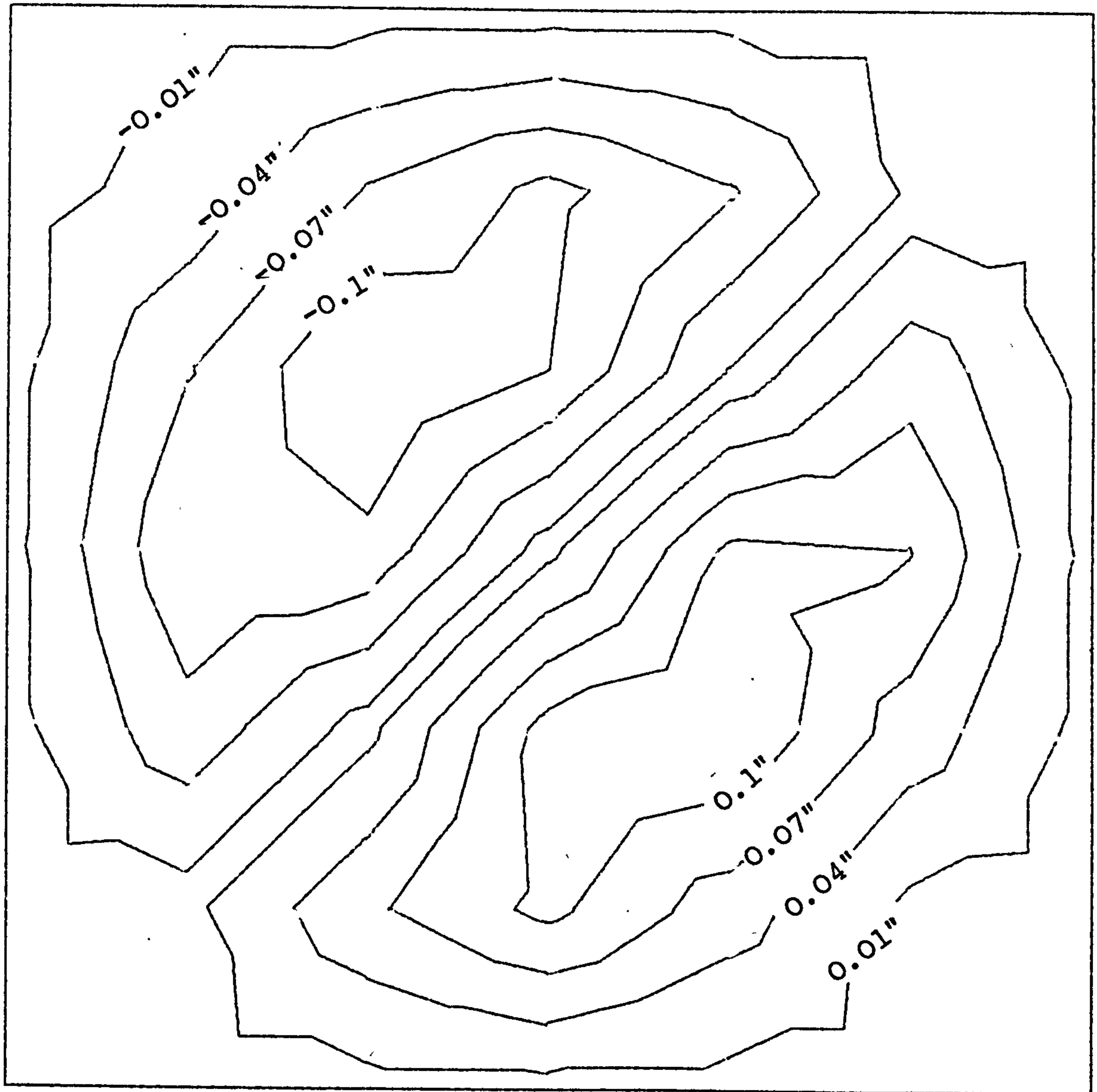
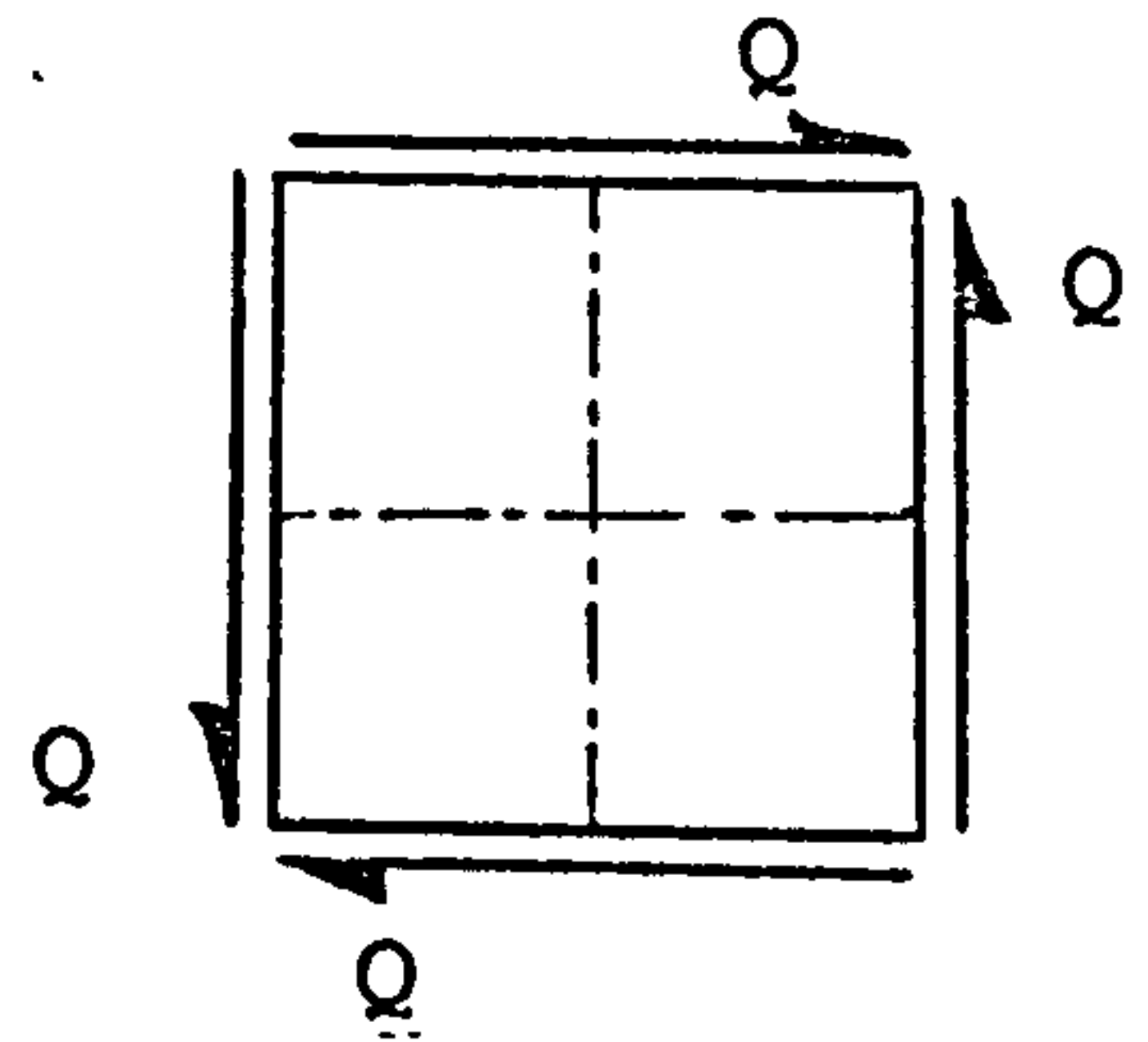


FIGURE (7-18)

## 7.5 EFFECT OF SHEAR BUCKLING ON COMPRESSIVE STIFFNESS

The effect of buckling on the shear stiffness of plates loaded in pure shear has been investigated. When the plate is loaded by a very small compressive load in addition to the shear load, the effect of shear buckling on the compressive stiffness becomes a matter of practical interest. Actually, the small compressive load is introduced here only as a means of detecting this change in stiffness. Compressive stiffness in this case can be defined as

$$E^* = \frac{\delta \sigma}{\delta \epsilon}_{\sigma=0} \quad (7-4)$$

(Note that  $E^*$  now is the compressive stiffness, in the limit as the compressive stress approaches zero, at specified values of  $\tau/\tau_{cr}$ .)

Application of this study can be found in corrugated webs (or any stiffened web for which buckling may occur either in the web between stiffeners or in a mode involving both webs and stiffeners). In a corrugated web (such as shown in cross section in Figure 7-19) in pure shear, local buckling can be defined as buckling within the component flats of the web, which depends on the thickness of the web and the width of the flats. On the other hand, overall buckling is the buckling of the complete web, which may be analyzed as an orthotropic plate. The following equation used in Reference (73) assumes two different flexural rigidities in the perpendicular directions of the web:

$$\tau_{cr} = 4k_s \frac{\sqrt{D_1 D_2^3}}{b^2 t} \quad (7-5)$$



FIGURE (7-19)



where  $K_s$  is the buckling coefficient and  $D_1 = \frac{t}{t'} \cdot \frac{Et^3}{12}$ ,  $D_2 = Et'\rho^2$  are the flexural rigidities of the web about axes parallel and perpendicular to the direction of corrugation respectively. The buckling coefficient  $k$  depends on the rigidity  $D_3$ , which however, is usually<sup>s</sup> negligible for a corrugated web. If there is a loss of compressive stiffness due to local buckling in shear, the effective rigidity of the cross-section (i.e., the  $D_2$  value) will be correspondingly reduced, and premature failure in overall buckling will occur, provided of course that local buckling proceeds overall.

A square plate with simple support, loaded up to and beyond the buckling load in pure shear, is now investigated. The boundary conditions for case (a) (see Section 7.3), are suitable for this problem, because the supports do not act as stiffeners to provide any additional in-plane stiffness, so that the results are applicable to an unstiffened square plate in shear. In order to keep the computer time to a minimum, a 6x6 mesh is employed. Two cases are considered here: one with an initial imperfection  $W_0/t = 0.1$  (see Section 7.3), and another with no imperfection. The method explained in Chapter 6 is used for the interaction of in-plane and out-of-plane stiffnesses for the perfectly flat plate. The solution method used for the plates is incremental with modified Newton-Raphson procedure.

To determine the compressive stiffness of the plate in pure shear, the following steps were taken:

- 1) A shear load is applied up to an arbitrary value of  $Q/Q_{cr}$ .
- 2) A very small compressive load is applied.
- 3) The shear load is increased to the further value of  $Q/Q_{cr}$ , with immediate and simultaneous removal of compressive load.
- 4) The procedure is repeated for desired loads at different levels.

Figure (7-20) shows the change of relative compressive stiffness with the ratio  $Q/Q_{cr}$ . The stiffness variation in the two cases is demonstrated in the figure, and the following observations are made:

- i) There is a severe loss of compressive stiffness for the imperfect plate, with an even more severe loss for a perfectly flat plate.

- ii) The greatest loss of compressive stiffness occurs for the perfectly flat plate at shear loads close to  $Q_{cr}$ , and recovers to some extent as the shear load is increased,
- iii) The maximum compressive stiffness reduction for the perfectly flat plate is shown to be 75% of the material itself, whereas, the maximum compressive stiffness reduction of the plate with an imperfection ( $W_0/t = 0.1$ ) is only 40%.
- iv) Compressive stiffness has an oscillating behaviour, and begins to converge to a value of  $E^*/E = 0.65$  for the plate with imperfection ( $W_0/t = 0.1$ ), but since at about  $Q/Q_{cr} = 1.7$ , a subsequent reduction of compressive stiffness takes place (see Section 7.3 and 7.4), the converged value for a perfectly flat plate is not ascertainable.

From these results, it is seen that the stiffness ratio  $E^*/E$  reduces to as low as 0.25, for the perfectly flat plate previously described. If this reduction is applied to the value of  $D_2$  in Equation (7-5), for the corrugated web, the corresponding loss of buckling strength in the overall mode is 65%. This severe stiffness reduction appears to be located in a narrow band between about  $Q/Q_{cr} = 1$  and  $Q/Q_{cr} = 1.3$ .

However, the loss of buckling strength is in fact less for the web with local imperfections, because of the nature of the stiffness behaviour for the imperfect plate, as shown in Figure (7-20). The stiffness reduction for the imperfect plate becomes significant for  $Q/Q_{cr} > 0.8$ .

On the above basis, suggestions for the design of corrugated webs can be made as follows:

- 1) restrict overall (orthotropic) buckling to be greater than 0.8 x local buckling,
- or
- 2) ensure that overall buckling is sufficiently in excess of local, and take proper account of the loss of stiffeners due to local buckling.

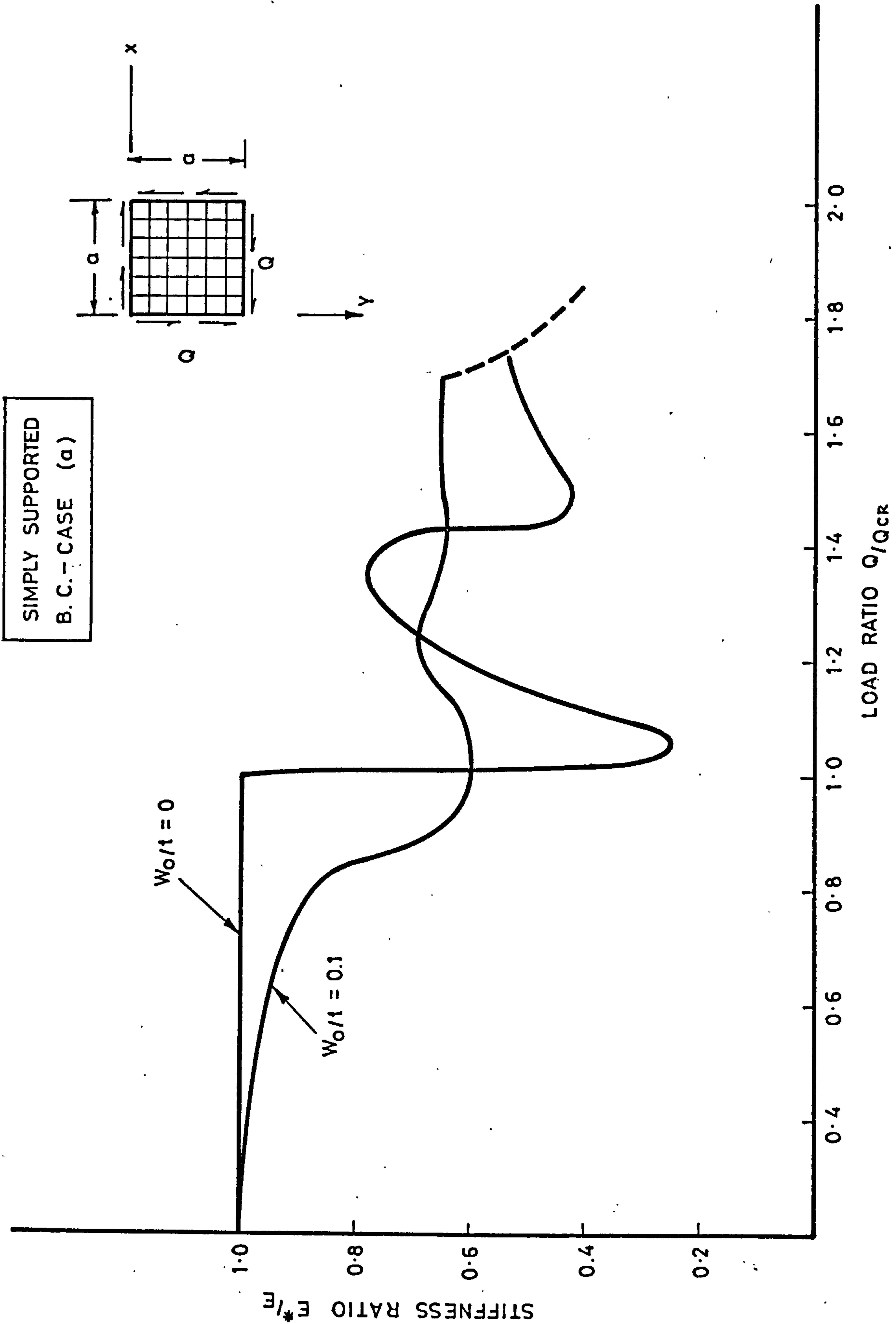


FIGURE 7-20

T H E   E X P E R I M E N T A L   P R O G R A M



## 8.1 PLATE DEVELOPMENT

This section describes experiments carried out on lipped channel section struts. The object of these experiments was to simulate the behaviour of an imperfect simply-supported square plate in compression, in order to illustrate the complexity of pre- and post-buckled deformation, as well as to obtain some experimental results which could be compared with the results of the computer program. The work involves an assessment of the imperfections in the specimen before loading, and the growth of those imperfections during loading. No attempt was made to measure post-buckled stiffness in the experiments.

The choice of test specimen is based on the following considerations:

- 1) An actual square plate would lead to difficulties with the edge attachment.
- 2) A square tube would model a square plate satisfactorily, but would create manufacturing difficulties in fabricating the tube.
- 3) A channel section, with the web representing the plate, would model a simply-supported square plate adequately if it possessed:
  - i) The same elastic buckling stress
  - ii) buckling half wave-length equal to the width of the web
  - iii) no other form of buckling.

The choice of a lipped channel section strut proved suitable, because it has a sufficient number of dimensions which could be varied to meet the above requirements, it is easy to manufacture, and, in addition, access to both sides of the web is very useful.

Dial gauges as well as the mechanical interference between a coarse grid and its shadow are used to define the displacement contours of the plates. The grid shadow method is particularly useful to obtain a pictorial deformation of the whole working area and has the advantage that its implementation is conceptually simple.

## 8.2 TEST SPECIMEN

The lipped channel section for studying pre- and post-buckling behaviour was designed for compression up to at least three times the local buckling load. The design of a lipped channel strut involves consideration of four possible modes - local, flange, torsional-flexural, and flexural. In all modes, displacements vary sinusoidally in the longitudinal direction with a half wave-length of  $\lambda$ . The local mode involves rotation about the junctions between the web and flanges with lateral displacement at the junctions of the flanges and lips. In the torsional-flexural and flexural modes the cross section remains undistorted and either translates while rotating or simply translates.

In order to find the correct dimensions for a lipped channel section to correspond in behaviour to a simply-supported plate, the computer program VIPASA (Ref. 74) was used. In the first computer run, various  $d/c$  ratios were used to locate the correct buckling coefficient  $K = 3.62$ . As shown in Figure (8-1),  $d/c = 5$  gives values both above and below this buckling coefficient. Figure (8-2) illustrates the variation of  $K$  with  $\lambda/b$ , in this case for  $d/c = 2$ . In the second computer run, only the values of  $b$  and  $d$  were altered, with  $d/c = 5$  (Figure 8-3). In this way a test specimen was found with  $K = 3.62$  and  $\lambda/b = 1.0$ . After obtaining suitable cross-section dimensions, the specimen was checked for torsional-flexural buckling using ESDU (Ref. 75).

Two specimens were manufactured; one with its own natural imperfections and the other with a specific geometric defect. The specimens were 21.2 in. long, 24 S.W.G. L70 aluminium alloy. The dimensions are given in Figure (8-4). The specimens are manufactured from sheet material simply by folding the flanges and lips in a folding machine without heat treatment, and casting "cerrobend" end fittings. The "cerrobend" was then machined to  $\frac{1}{2}$  in. to present a flat surface to the testing machine platens.

In order to determine the stress-strain characteristic of the specimens, coupons were cut from the same sheet as the specimen and tested. Stress-strain curves were obtained for compression and tension, for the longitudinal and transverse directions of the parent sheet. The curves are given in Figure (8-5) and Figure (8-6).

The two specimens were checked for deviations from flatness by setting them up on a surface table and taking dial gauge readings at intervals along the web. The readings are recorded for reference in Figures (8-7) and (8-8).



### 8.3 TEST INSTRUMENTATION

Two sets of instrumentation are used for deflection measurements. For the first experiment, deflections were measured by the grid-shadow technique, but in order to verify the correctness of the results, dial gauges were also used on the back of the specimen. The arrangement of the glass grid and the placing of the ball bearings on the face of the web are shown in Figure (8-10). Eight dial gauges were used for finding the body movement of the glass grid, as well as for the web deformation. Figure (8-9a) shows the location of the dial gauges corresponding to the front face of the web.

Dial gauges numbers 1, 2, and 8 are used to find the reference plane movement whereas the rest of the dial gauges are solely used for displacement measurements. The arrangement of dial gauges in the rear view of the specimen is shown in Figure (8-11).

For the second specimen, the first experiment was repeated up to  $P/P_{cr} = 1.5$  to demonstrate the fringe pattern for the more severe initial displacement. Dial gauges were used exclusively on the second specimen after fitting the support attachments. Figure (8-12) shows the support attachment and dial gauge arrangement. Because the support attachments were used, only eight dial gauges could be used. The location of the dial gauges is shown in Figure (8-9b). More dial gauges were used around the area of the defect in order to obtain more detailed results in this area.

## 8.4 THE GRID-SHADOW MOIRE TECHNIQUE

The mechanical interference between a coarse grid and its shadow as cast upon a mat surface by oblique illumination has been applied to the analysis of surface topography. The application of Moire interferometry is demonstrated by a number of investigators. Ref. (76) uses the grid-shadow Moire technique for determining the displacements in a large shear web in place of a large number of dial gauges.

The procedure for employing Moire's technique consists of using a white or monochromatic collimated obliquely incident light beam to illuminate the model surface. A reference grid is attached close to the surface of the model and the interference pattern of this grating and its shadow produced by the oblique light beam is photographed in a position normal to the model. Interference patterns before and after the loading of the specimen allow the determination of isopachics which are the lines of equal thickness.

The basic principle of the method used is presented in Figure (8-13). A small section of a reference grid having a pitch " $e$ " is illuminated by a collimated light source at an angle of incidence  $\theta$ . The light rays collected by the camera are considered to be parallel to each other and normal to the plane of the reference grid. If the shadow plane is coincident with the reference grid plane, the shadow of line A will lie directly under line A. As the shadow plane moves away from the grid plane, the shadow of line A will appear to translate toward line B in the plane of the grid. When the shadow plane moves a distance  $h$ , the shadow of line A is directly under line B and the shadow appears to have moved a distance  $\underline{e}$ , in the plane of the reference grid.

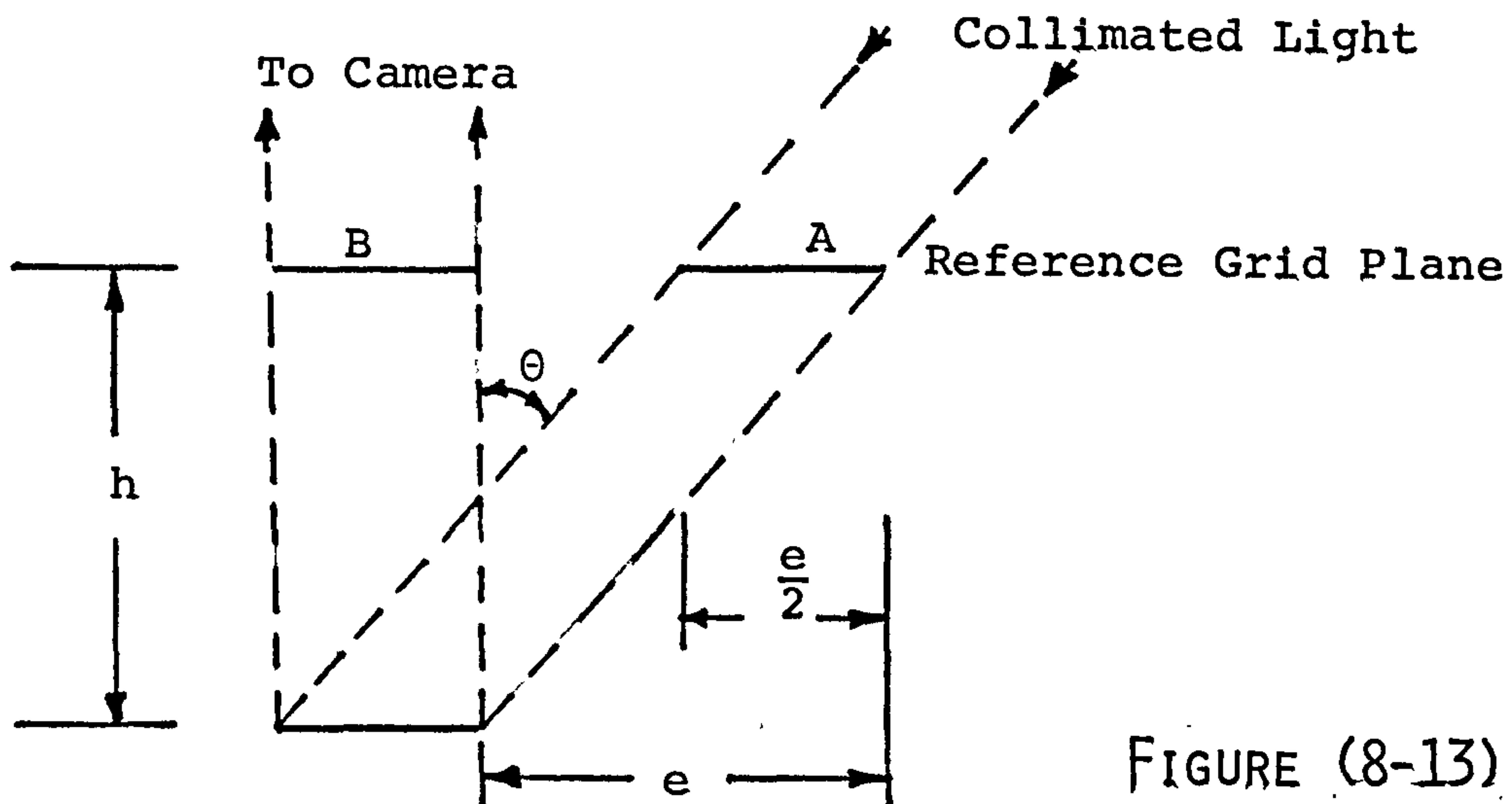


FIGURE (8-13)



The light reaching the camera varies from a maximum to a minimum and back again to a maximum. The shadow plane moves down the distance  $\underline{h}$ , resulting in a shift of one fringe in the pattern. The sensitivity of this system in terms of the out-of-plane displacement of the shadow plane per fringe is:

$$h = \frac{e}{\tan \theta} \quad (8-1)$$

and for the small angles  $\theta$

$$h = \frac{e}{\theta} \quad (8-2)$$

The distance  $\underline{h}$ , expresses the difference in the separation of the grid and the model at the points where two successive fringes occur.

## 8.5 EXPERIMENTAL DESCRIPTION OF THE GRID-SHADOW TECHNIQUE

A simple optical arrangement was devised using a 500 W slide projector as the light source. A suitable reference grid line density, the choice of which depends on the sensitivity desired (the maximum displacement expected to be about three times the specimen thickness) is 65 lines/in. Although a higher line density would result in greater sensitivity, the fringe contrast at large displacements would be unsatisfactory. The grid film was photographed on a special photographic glass in order to obtain a perfect plane surface.

The test surface was prepared by spraying it with a thin and uniform layer of white paint. The side of the grid on which the lines are printed was placed nearest to the test surface. The reference grid glass was suspended parallel to the test surface after the grid was placed against three 1/8" ball bearings on the assumed nodal lines which served as reference points in order to minimize the movement of the grid plane.

Prior to running the experiment, a calibration photograph was obtained, shown in Figure (8-14). A wedge containing known slopes in two opposing directions was positioned on the test surface. The double wedge was used to eliminate errors which might arise in using a single slope wedge on a surface which is not initially flat. The calibration utilized was the average of the values obtained from the two surfaces of the wedge. Since the angle of incidence of light must be regulated to produce the best contrast, tests were made until an angle of  $60^{\circ}$  was found to produce sufficiently dense and sharp patterns. The calibration also eliminated errors in determining the angle of incidence and tended to reduce errors associated with the displacement of the test surface from the reference grid. The nonparallel nature of the fringes in Figure (8-14) is due to a rotation of the surface on which the wedge is placed.



## 8.6 DESCRIPTION AND OBSERVATION OF TESTS

### a) First Specimen (A)

After measuring the initial imperfection of the specimen, the area of interest in the web was painted in order to use the grid-shadow Moire method. The painted area then was marked to correspond to the finite element mesh. Three 1/8" ball bearings were placed on the assumed nodal lines of the web in order that the grid plate would make contact and would produce a plane of reference. (A preliminary test was made to establish the approximate location of the nodal lines, after which the nodal lines were located by measurement, the nodal lines being the width of the web apart.) The grid glass is suspended by the means of a cord from the platens of the testing machine where the axial contraction of the specimen does not interfere with the fringe pattern. As well as using the front side of the web to record the displacements by Moire fringe technique, eight dial gauges are set up on the reverse side to record the deformation simultaneously. After setting up the measurement devices, crosshead drive is engaged, and compression is applied to the specimen. Load increments are chosen as 100 lbf for pre-buckling, and 50 lbf for the post-buckling range. Displacements are photographed, and dial gauge readings are recorded.

During the loading of the specimen, it was noticed that when the load had reached approximately  $P/P_{cr} = 2.4$ , the assumed nodal lines start to move. This behaviour occurred because of the rearrangement of the mode shape forming. This new mode pattern caused the grid glass to make contact with the web, and upset the fringe pattern readings. From this point, only dial gauge readings were used, and the specimen was loaded until it was no longer able to carry the applied load.

### b) Second Specimen (B)

Initially, two tests were planned for the lipped-channel strut. The first with its natural imperfection and the second with a more severe imperfection in the web. Since, in the first experiment, the nodal line movement was found in the post-buckled range, it was decided to use a support attachment in order to provide a better comparison of experimental results with the computer results in the higher post-buckled range. The object of these clamps (see Figure 8-12) is to keep the nodal lines straight and in the same position during

loading. Since the support attachments interfere with the grid glass, two tests were now planned for the specimen, the first using the grid shadow technique without the support attachment, and the second with the support attachment fitted and measuring displacements by dial gauges only.

In order to find the exact nodal line positions, the specimen was first set up in the compression testing machine, and was loaded to initial buckling. After marking the web area to be used in the test, a dent was made in the lower quarter of that area. Measurements of the initial deviation from flatness were then made. The web area was painted and the finite element mesh marked. After setting up the grid glass, and calibrating the light source and camera, the specimen was ready for test. The arrangement of the dial gauges was similar to the previous test. The specimen was to be carefully loaded beyond buckling without damaging it. Load increments were 100 lbf up to buckling, and 50 lbf up to  $P/P_{cr} = 1.6$ . Photographs were taken at each load increment.

During loading, it was observed that with a more severe imperfection, deformation in the web was more apparent than in the previous test. It was also noted that when applied load reached  $P/P_{cr} = 1.7$ , a snap-through occurred (this was both audible and visible in the grid pattern).

For the second test, the support attachments were mounted on the specimen, and eight dial gauges were used (see Figure 8-12). Loading procedures were similar to the previous test, and dial gauge readings were recorded until the specimen was not able to carry an additional load.

In this test, the snap-through did not occur, presumably because of the effect of the support attachments. After local buckling load had been reached, a slight waviness of the lips and flanges was observed. Further increase in load produced more deflection in the web and more waviness in the lips and flanges, as well as widening the distance between the flanges.



## 8.7 EXPERIMENTAL RESULTS

### Specimen A

Two types of results are obtained for this experiment:

- 1) web displacements in terms of fringe patterns up to  $P/P_{cr} = 2.4$ , and
- 2) dial gauge readings of the web up to the failure point of the specimen.

In order to demonstrate the results in a nondimensional form, the applied load is shown as the load ratio  $P/P_{cr}$ .  $P_{cr}$  is the theoretical buckling load for the web which was calculated to be 540 lbf. Figures (8-15) through (8-20) show the fringe patterns at different load levels. In order to evaluate the fringes in each picture, the rigid body movement of the grid glass must be accounted for at each load level. As the loading increases, a new fringe emerges from the centre of the web. The value of zero fringe is assigned to the fringe which passes nearest to the three ball bearings (nodal points), with the subsequent series of concentric fringes inside of the zero fringe numbered consecutively from 1; and those outside of the zero fringe numbered -1, -2, etc. Each fringe is evaluated by the calibration method, and for this case is found to be 0.012 in, per fringe. In order to find any displacement on the area of the web, interpolation of fringes is required. A sample calculation of displacements on the center line by the fringe pattern technique is shown for  $P/P_{cr} = 2.04$ . Rigid body movement is found by taking dial gauge readings of 1, 2, and 8. Linear movement of rigid body can be formulated as

$$W_{rb} = - \frac{.001}{1.76} x + \frac{.031}{2.64} y - 0.017 \quad (8-3)$$

Fringe values are shown in Figure (8-21). Now, if the coordinate points are substituted in Equation (8-3), and the fringe values are evaluated, the net deflection can be found.

### Center Point

Rigid body movement @ x = 0.86 in.;  
@ y = 1.32 in.

$$W_{rb} = - 0.002 \text{ in.}$$

Fringe value is obtained with respect to reference fringe (zero fringe)

$$W = 0.012 (2.1) = 0.0252 \text{ in.}$$

$$\text{Displacement} = 0.0232 \text{ in.}$$

Dial gauge reading of this point is recorded as 0.023 in. The displacement values of the web obtained from these fringe patterns are plotted in Figures (8-22), (8-23), and corresponding dial gauge readings are also shown in the figures. As is demonstrated, the values of displacement obtained by Moire fringe pattern technique were very similar to the dial gauge readings. The advantage of this technique is the observation of mode shape forming in the web. Displacement results from dial gauge readings are plotted in non-dimensional form in Figure (8-24).

#### Specimen B

The effect of a severe local imperfection in the web is demonstrated by Moire fringe patterns in the first specimen. As shown in Figures (8-25) through (8-29), initially the local imperfection is dominating the mode shape, but with increase in load, soon the overall mode takes over. During this test, as described in Section (8-7), a snap-through sound occurred, the result of which is not apparent in the fringe pattern pictures. However, in the dial gauge reading, the snapping is noticeable, and in order to emphasize this effect, web displacements are plotted against load in Figure (8-31). From the figure, it is observed that at approximately  $P/P_{cr} = 1.18$ , a sudden change of displacement takes place. The results from the second experiment on Specimen B with support attachments are plotted as non-dimensional load ratio against displacement.

Since the purpose of the second test is to compare the results with a computer run for the same initial imperfection, dial gauge readings of the initial deviation from flatness were evaluated. From Figure (8-8), for the initial imperfection, an estimate of the overall waviness of the web was obtained as 0.0002 in., (i.e., the first Fourier component). This value was reduced by 20%, to 0.00016 in., in order to make some allowance for the flattening effect of the support attachments. To implement the initial imperfection for the computer program, the edges are assumed to be simply supported with no initial deflection. The overall mode was



considered as a sinusoidal function with a maximum amplitude of 0.00016 in., on to which was then superimposed the defect introduced into the web. It was judged that this could be represented by initial displacements  $-.008$ ,  $-.008$  and  $-.048$  at points 2, 4, and in between respectively (see Figure 8-9 B). Thus the computer analysis uses only the principal characteristics of the imperfect plate.

By running the computer program, it was found that the program is very sensitive to sharp imperfections of the type introduced by the defect. However, the results of the computer program are very similar to the experimental results, considering that the initial imperfections employed in the program could not model precisely the actual imperfection of the web.

From the experimental results, Figure (8-32) and Figure (8-33) show the displacement behaviour for different points of the web. Displacements obtained from the computer results of the corresponding points are plotted in Figure (8-34) and for the sake of comparison of experimental and computer results, the two figures are re-plotted in Figure (8-35).

Note: Because the fringe pattern pictures (Figure 8-15 through Figure 8-30), were printed in an incorrect sequence, they are presented in an inverted position in this thesis.)

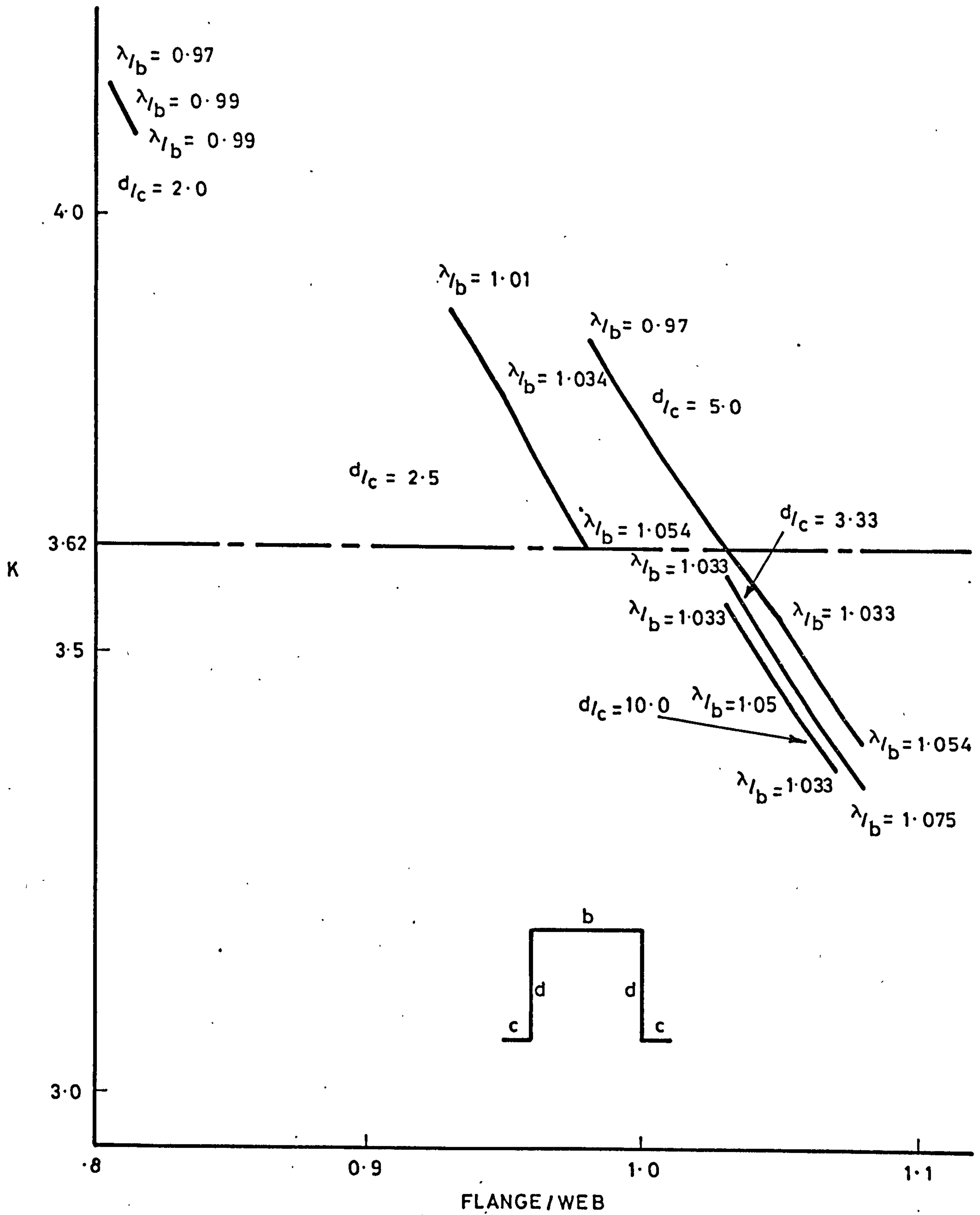


FIGURE 8-1



$$d/c = 2.0$$

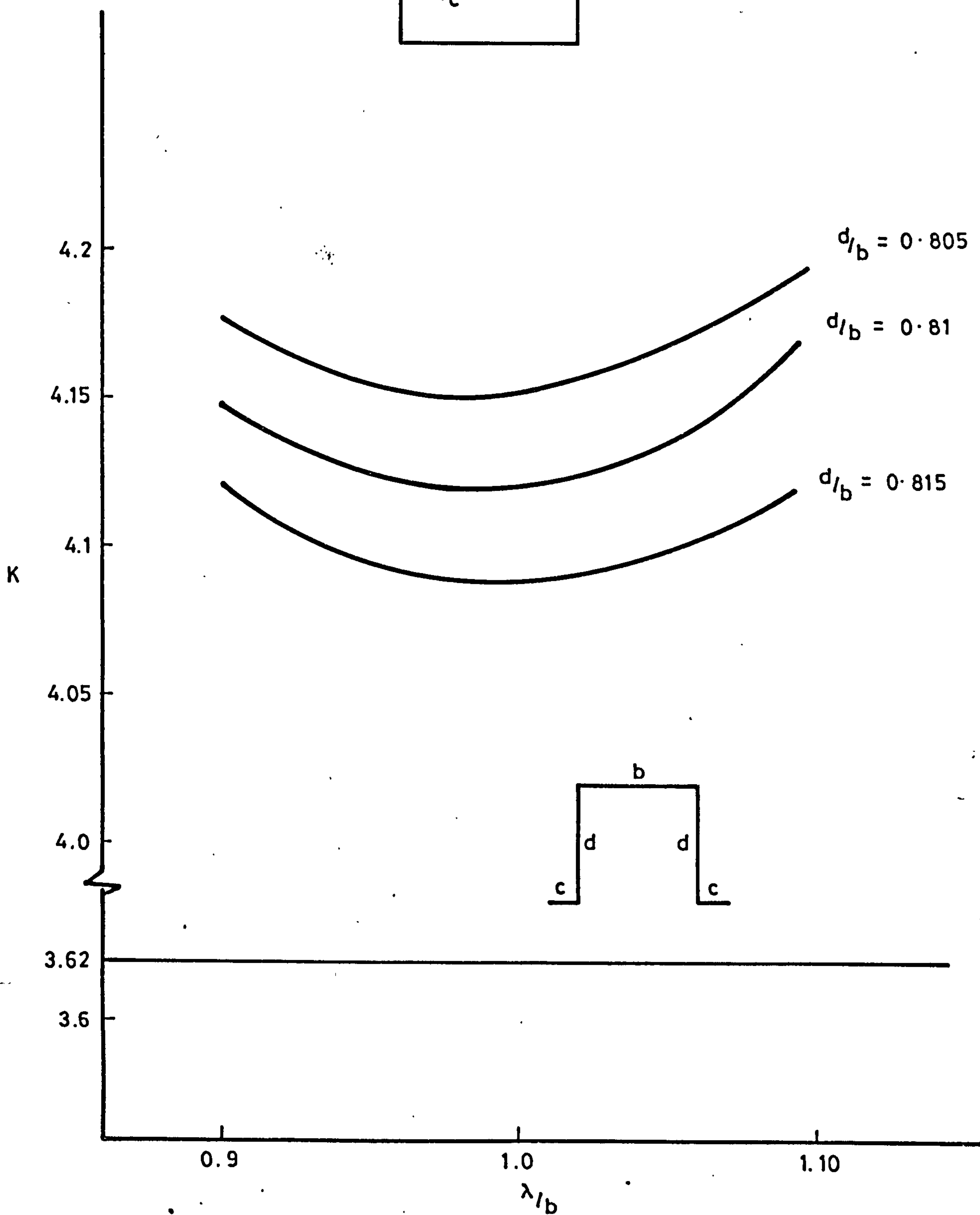


FIGURE 8-2

$$d/c = 5.0$$

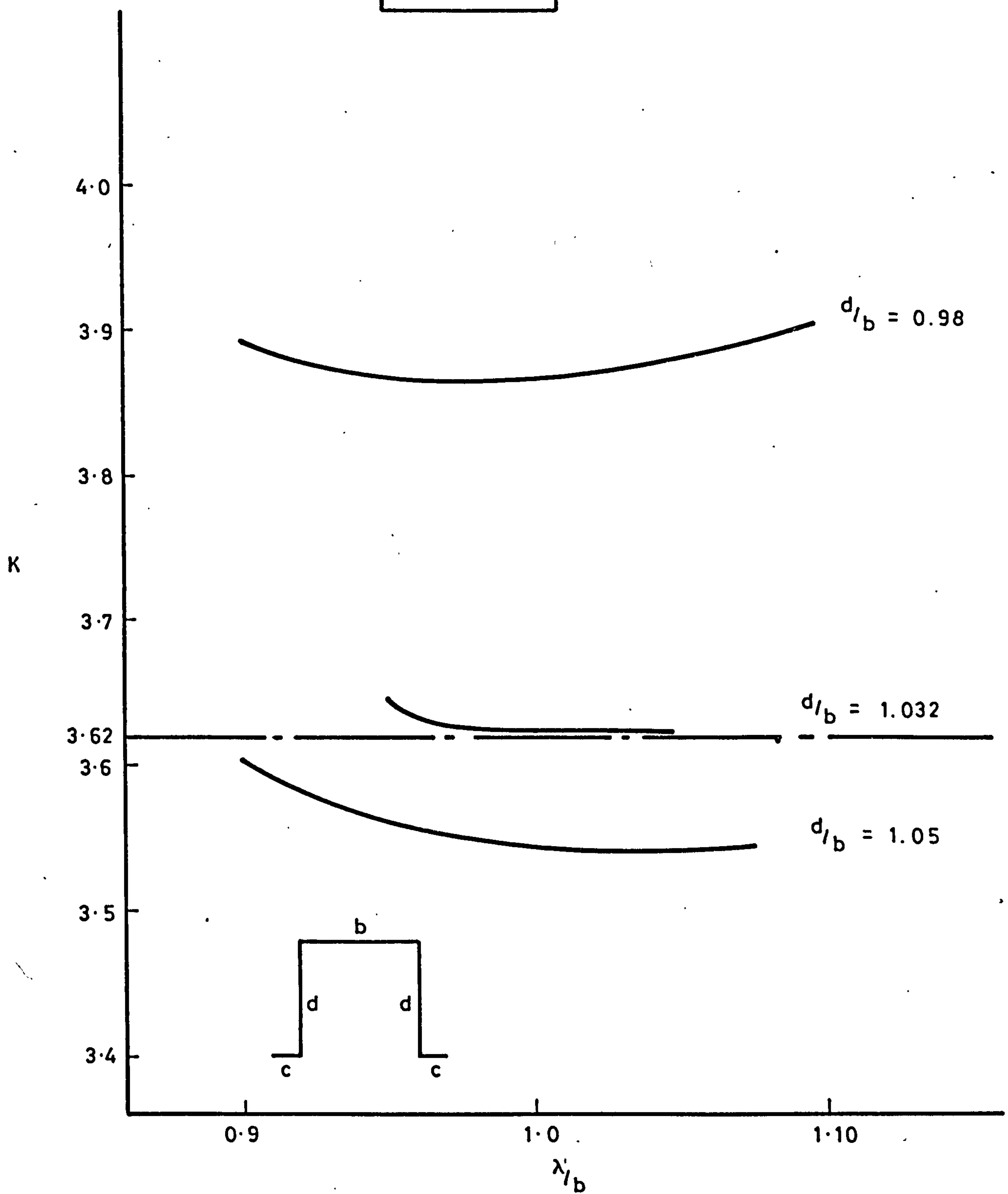


FIGURE 8-3

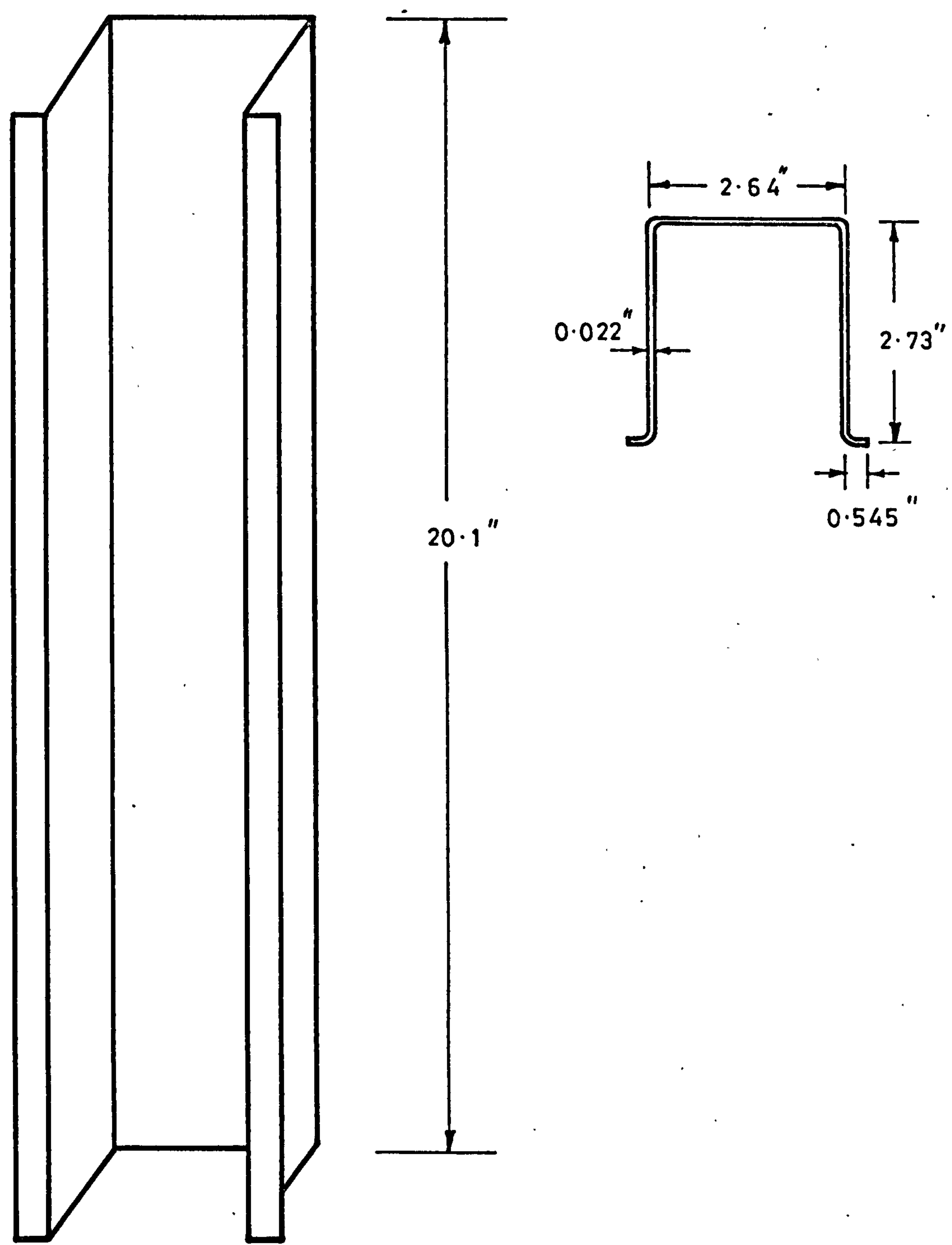


FIGURE 8-4

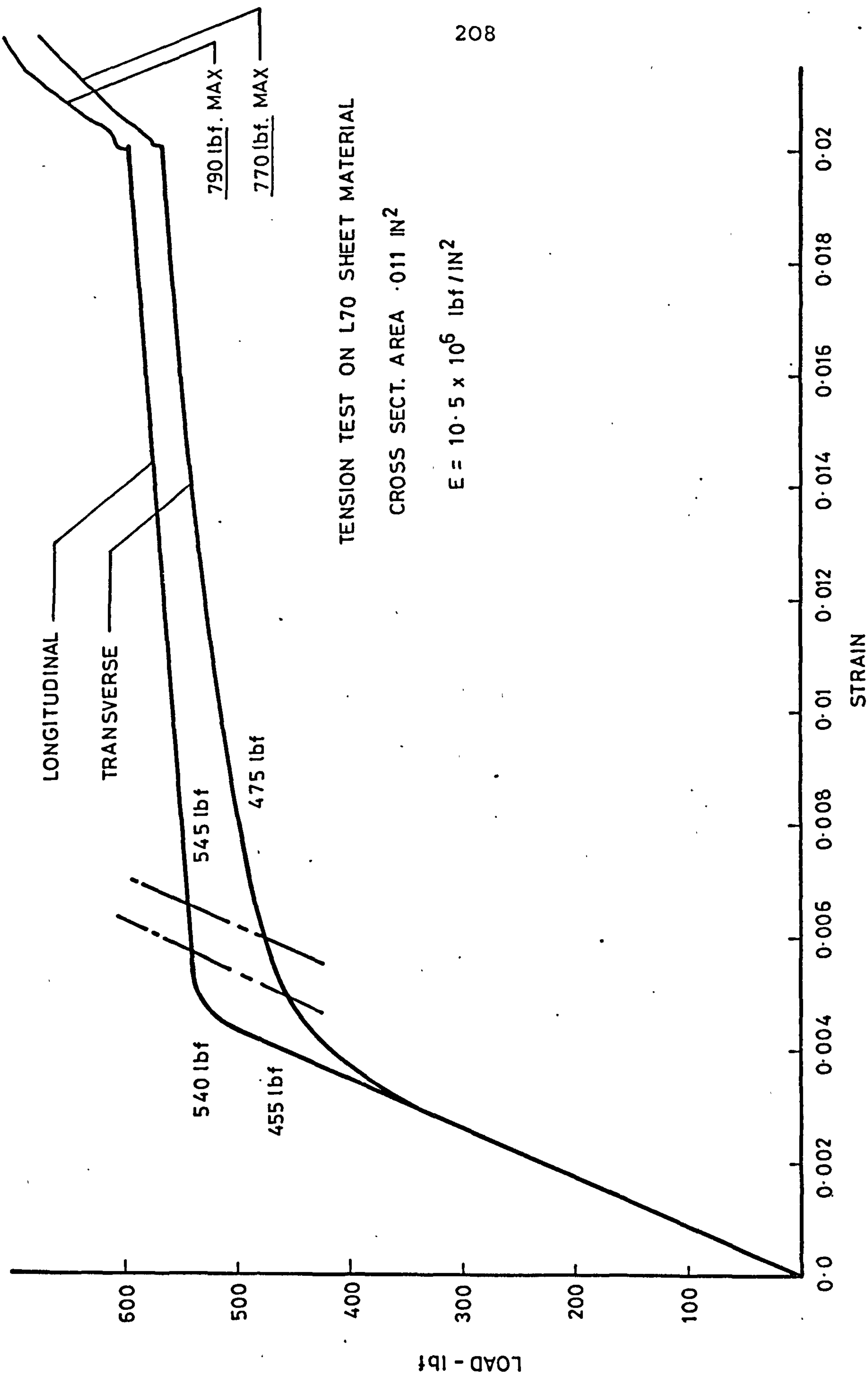


FIGURE 8 - 5



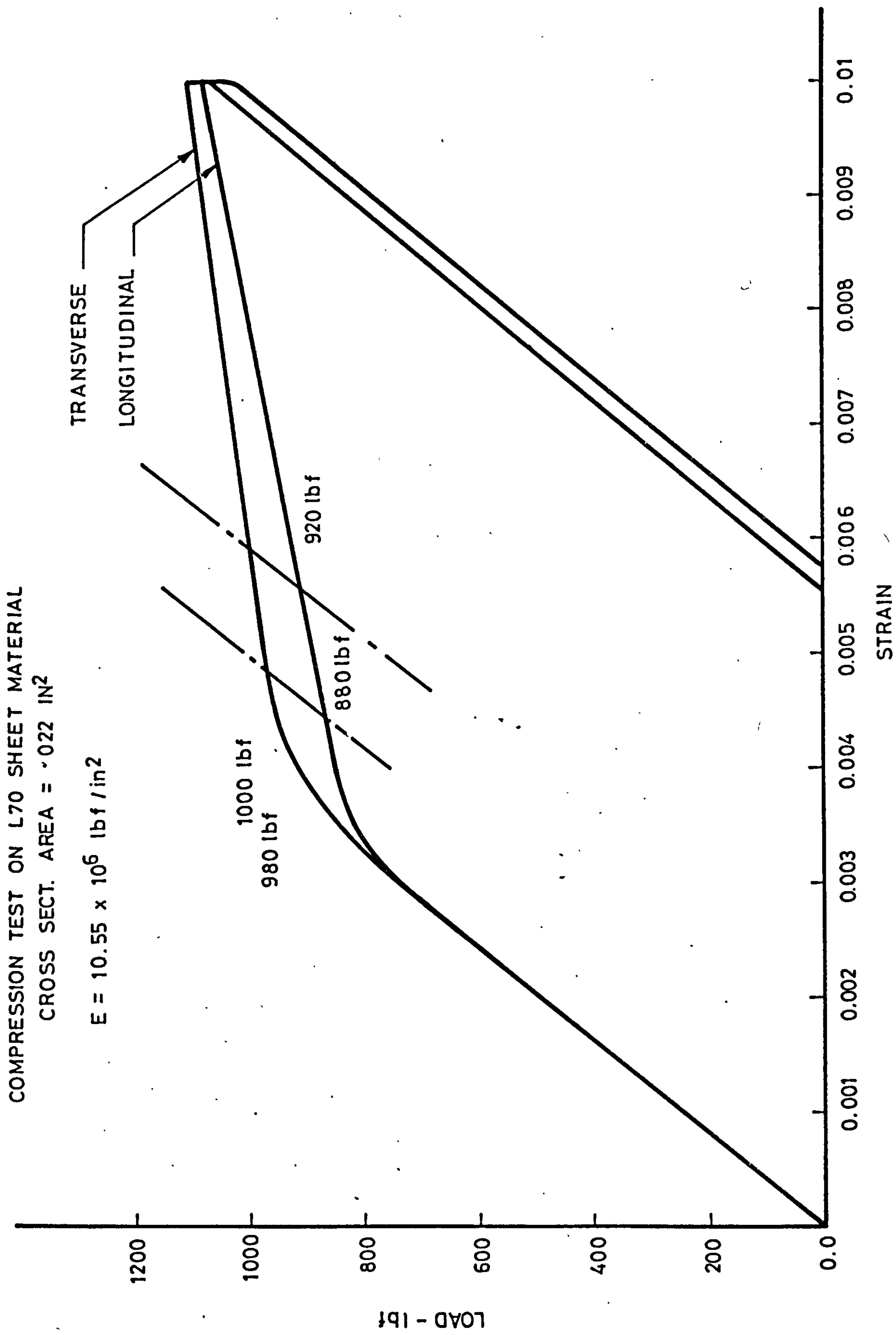


FIGURE 8-6

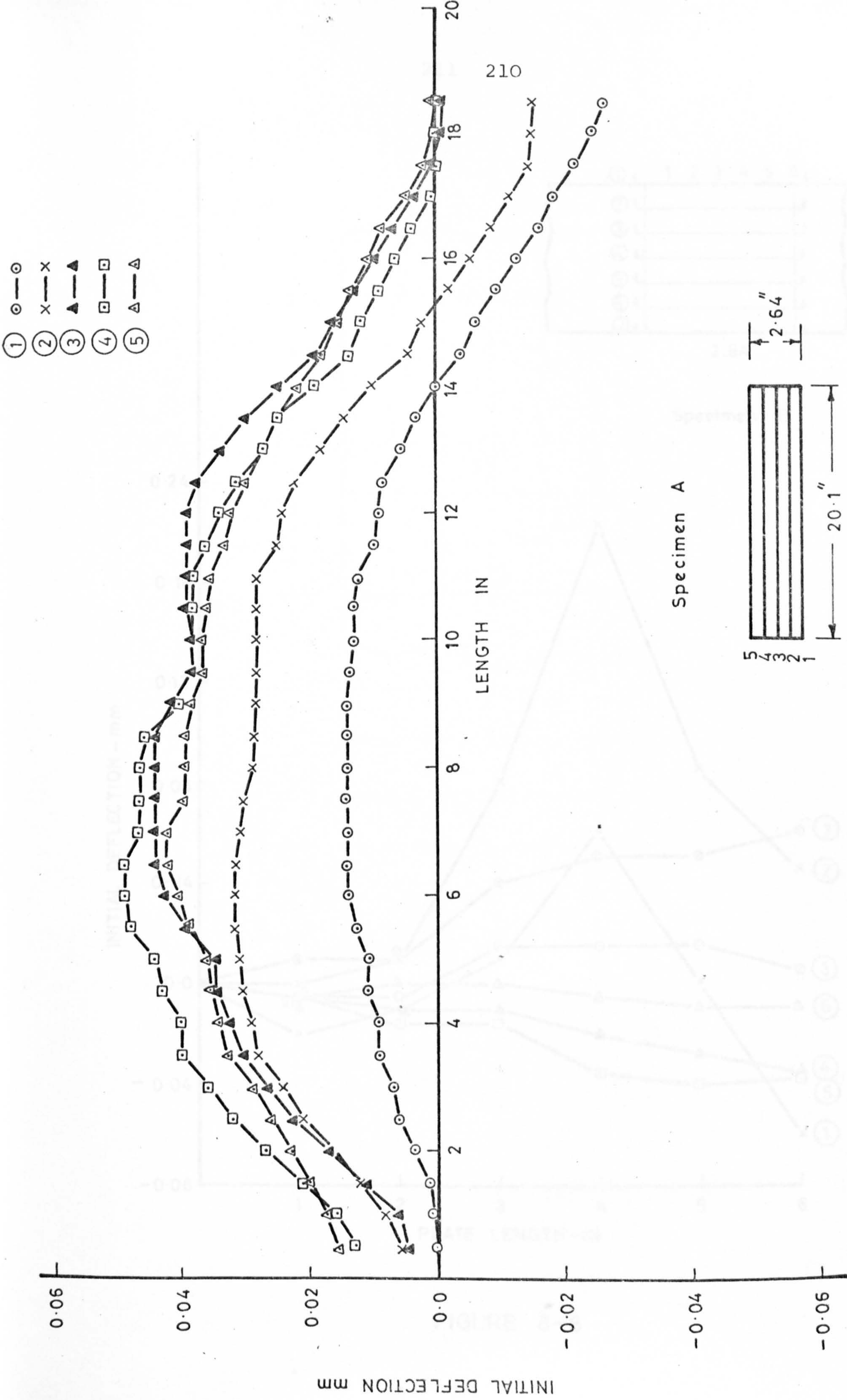


FIGURE 8 - 7

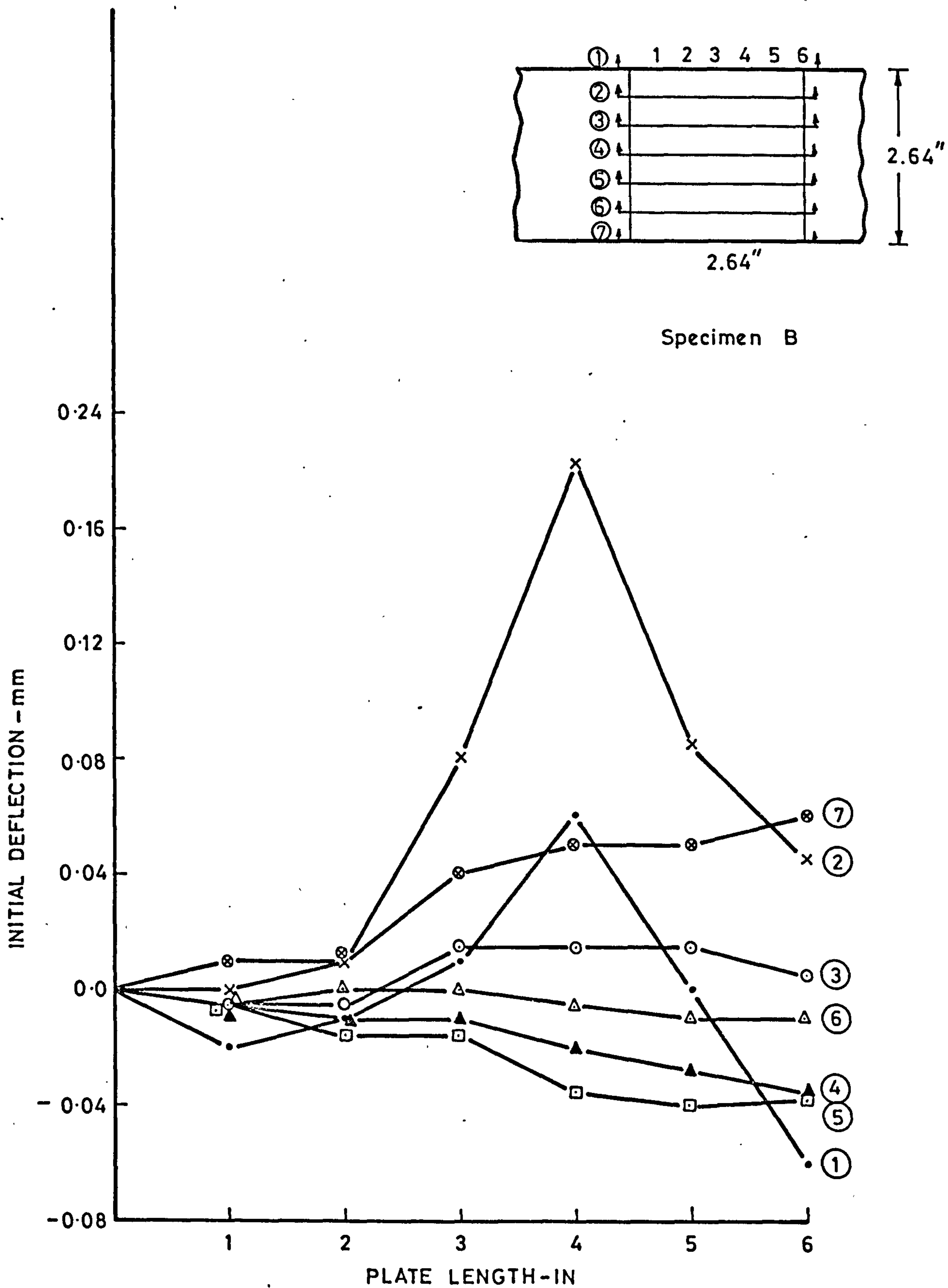
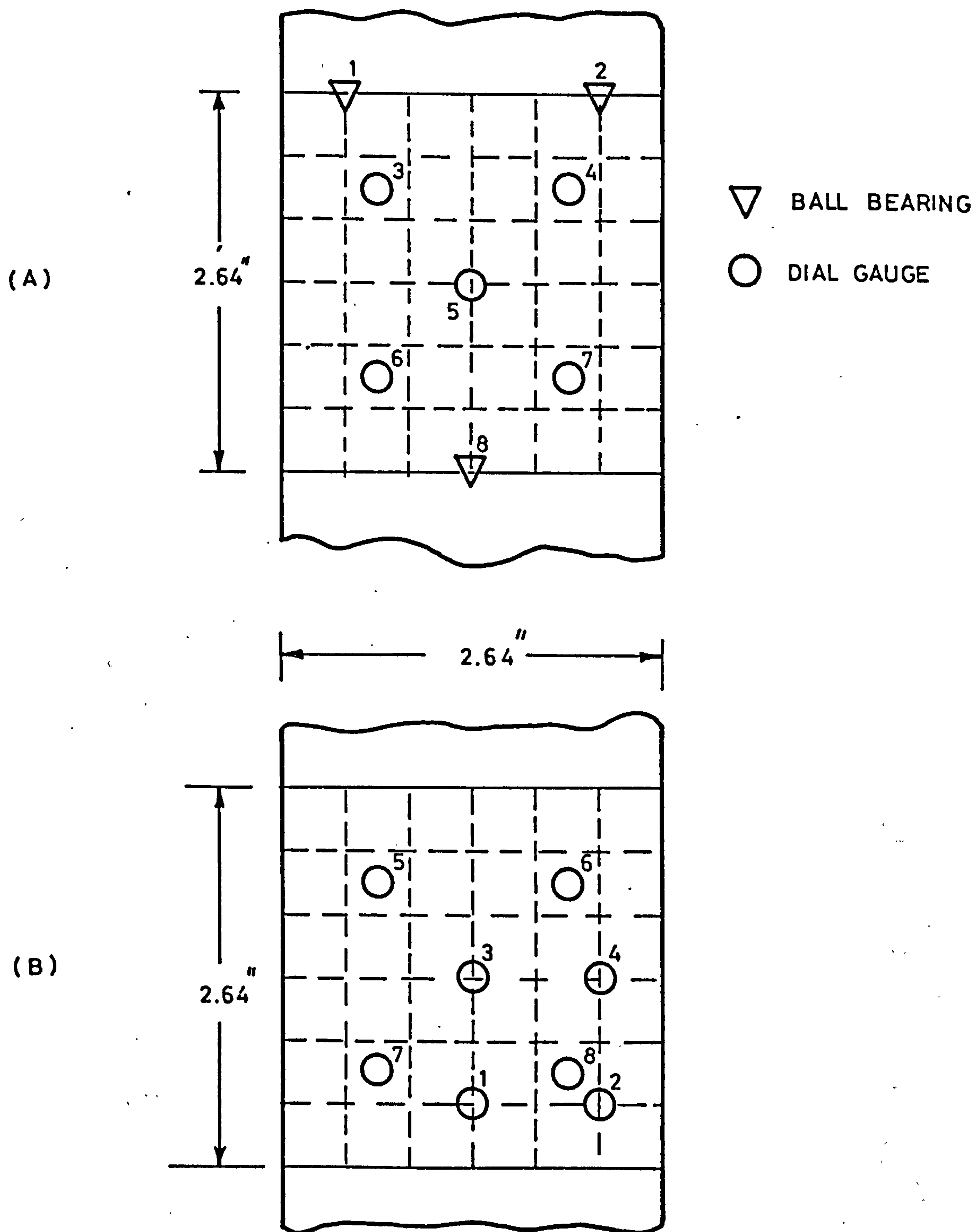


FIGURE 8-8



REFERENCE POINTS IN FINITE ELEMENT MODEL (EQUAL DIMENSIONS)

FIGURE 8-9



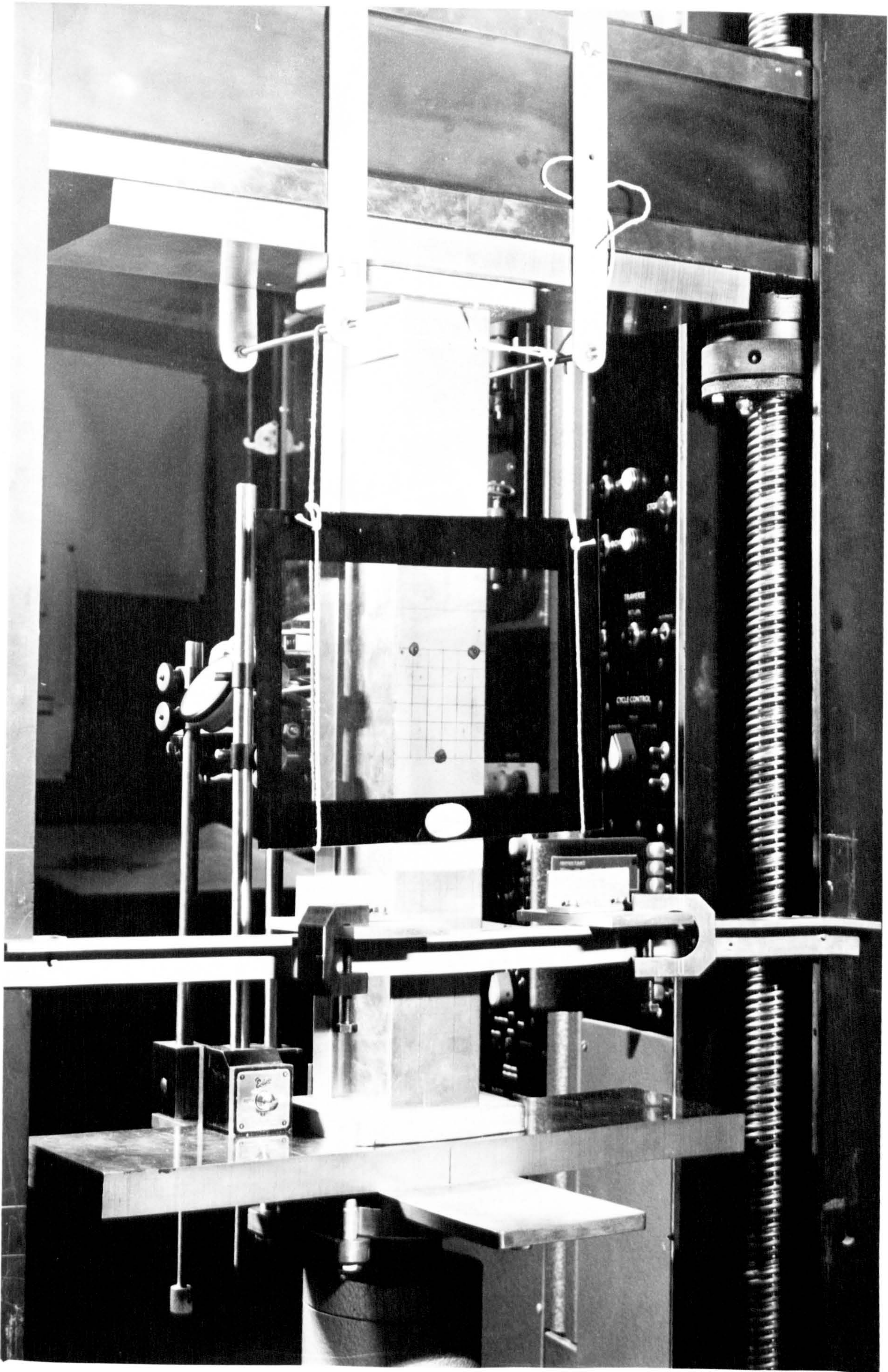


FIGURE (8-10)



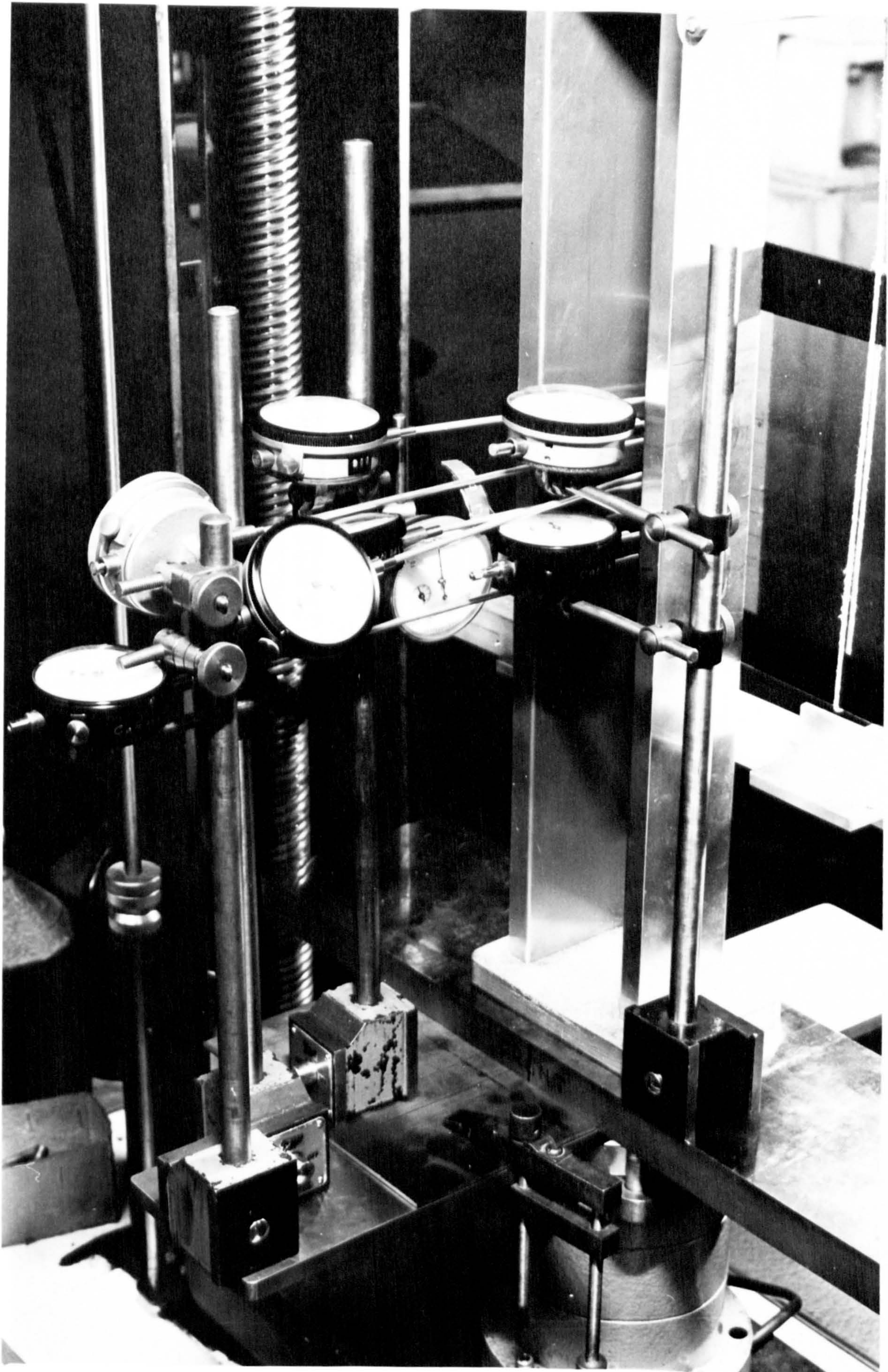


FIGURE (8-11)



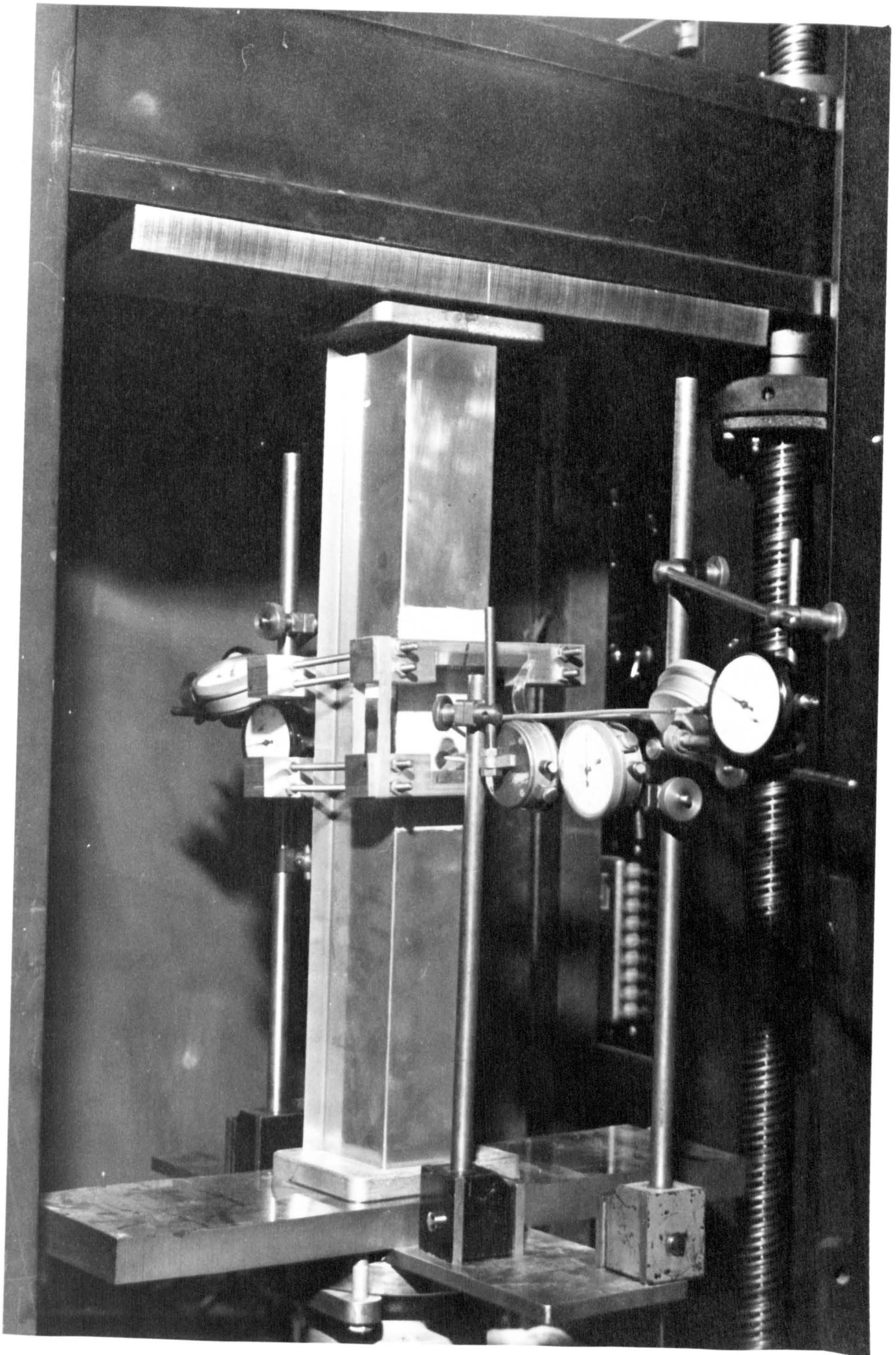


FIGURE (8-12)



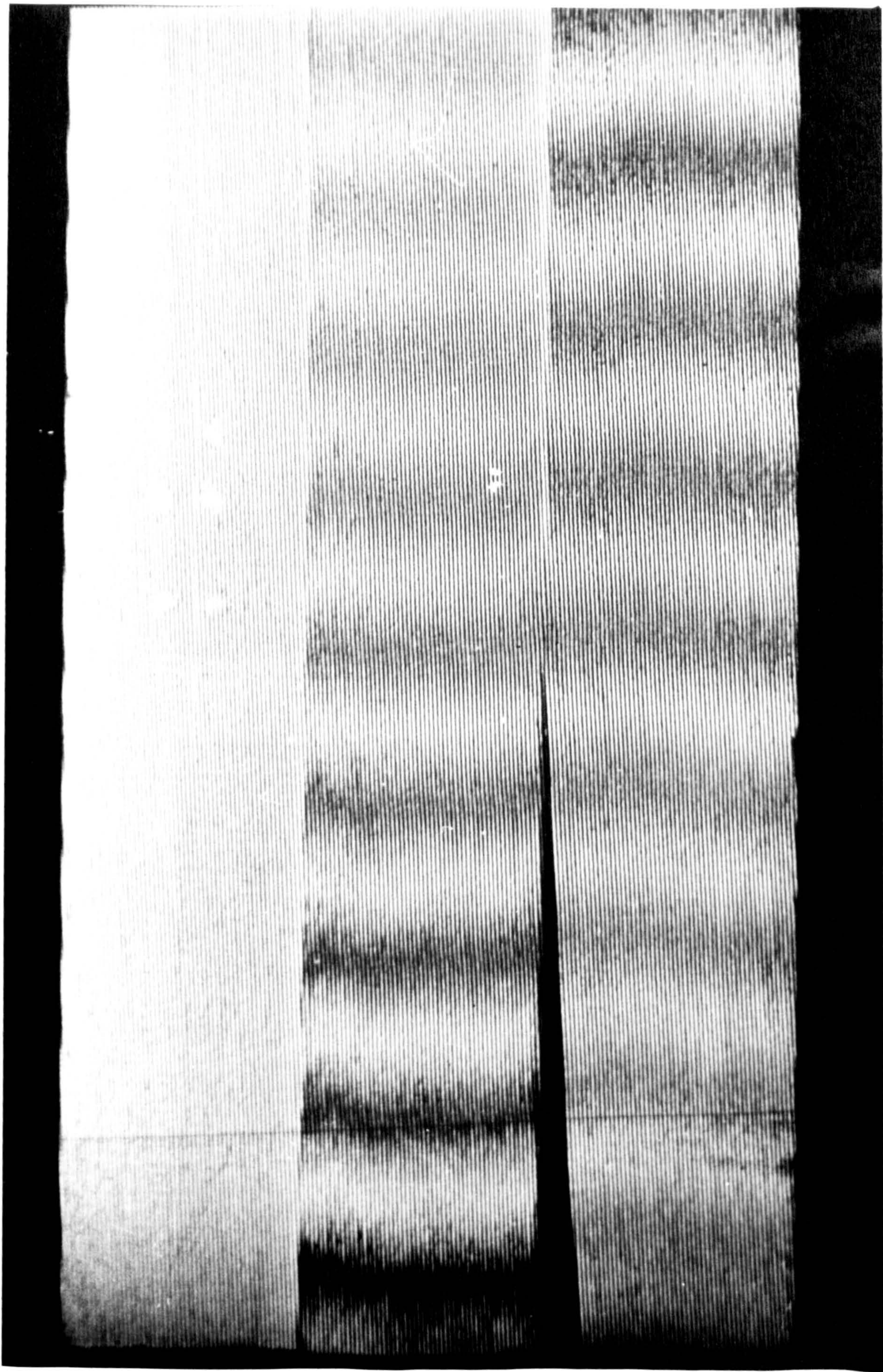
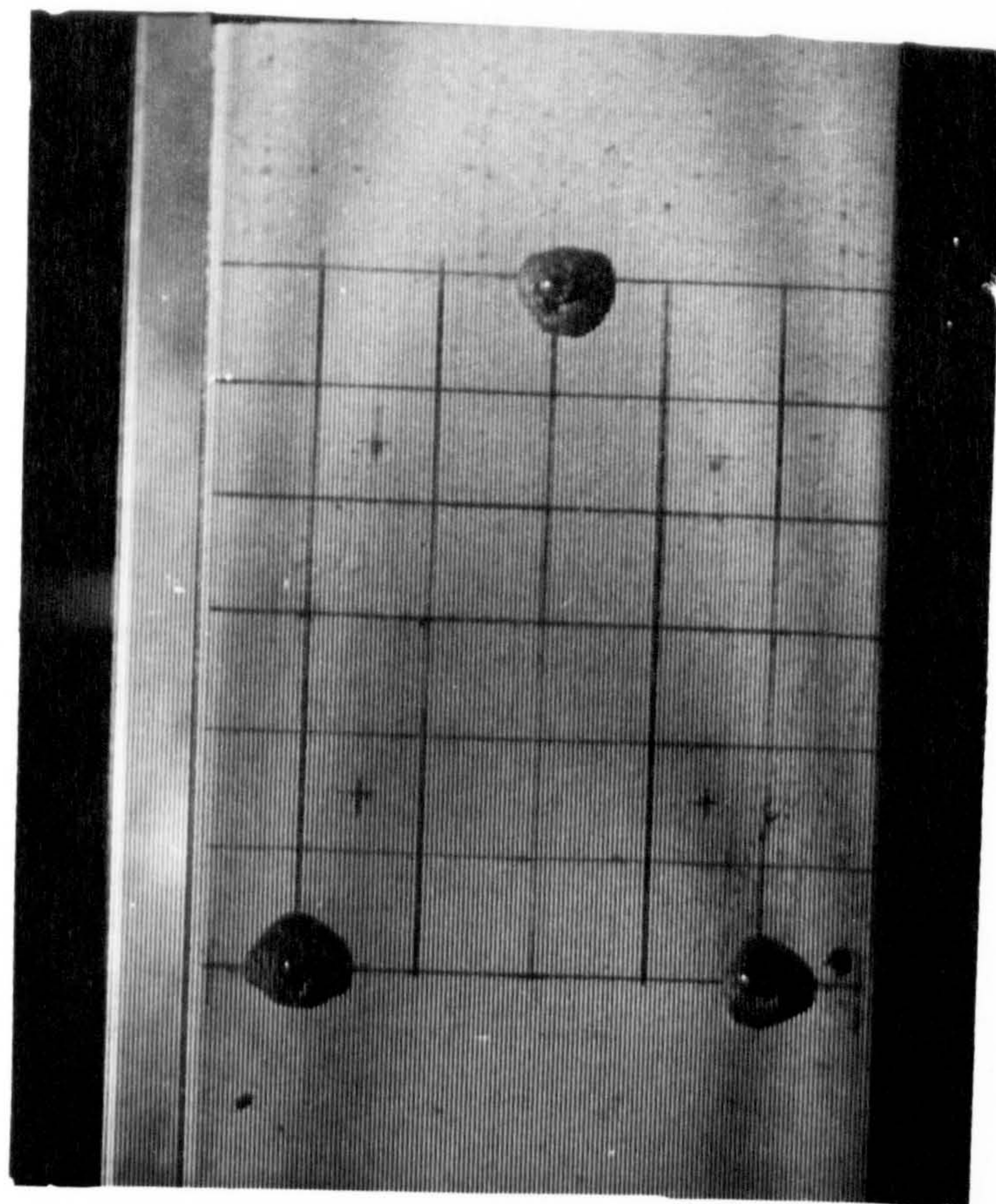


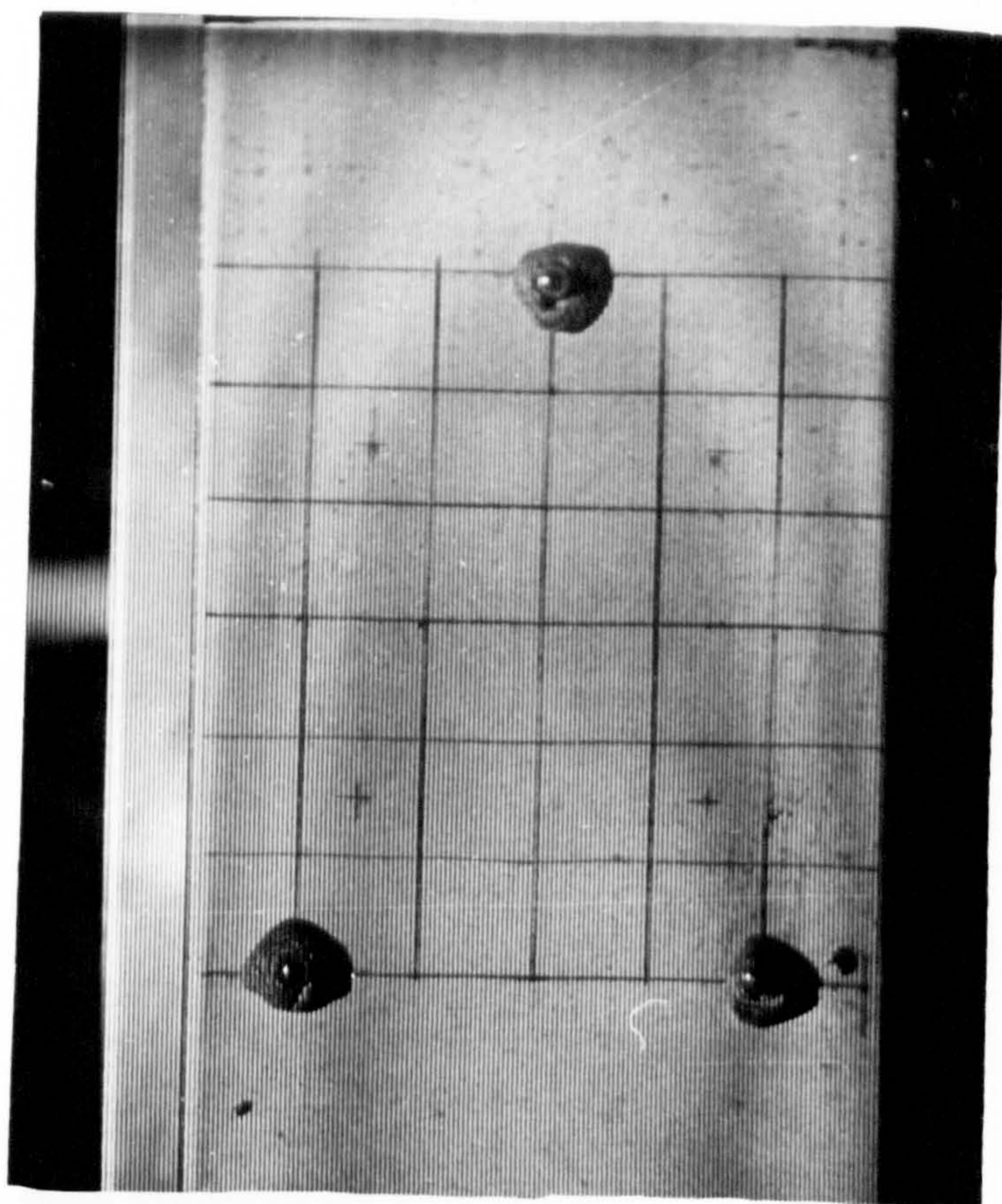
FIGURE (8-14)





$$P/P_{cr} = 0.0$$

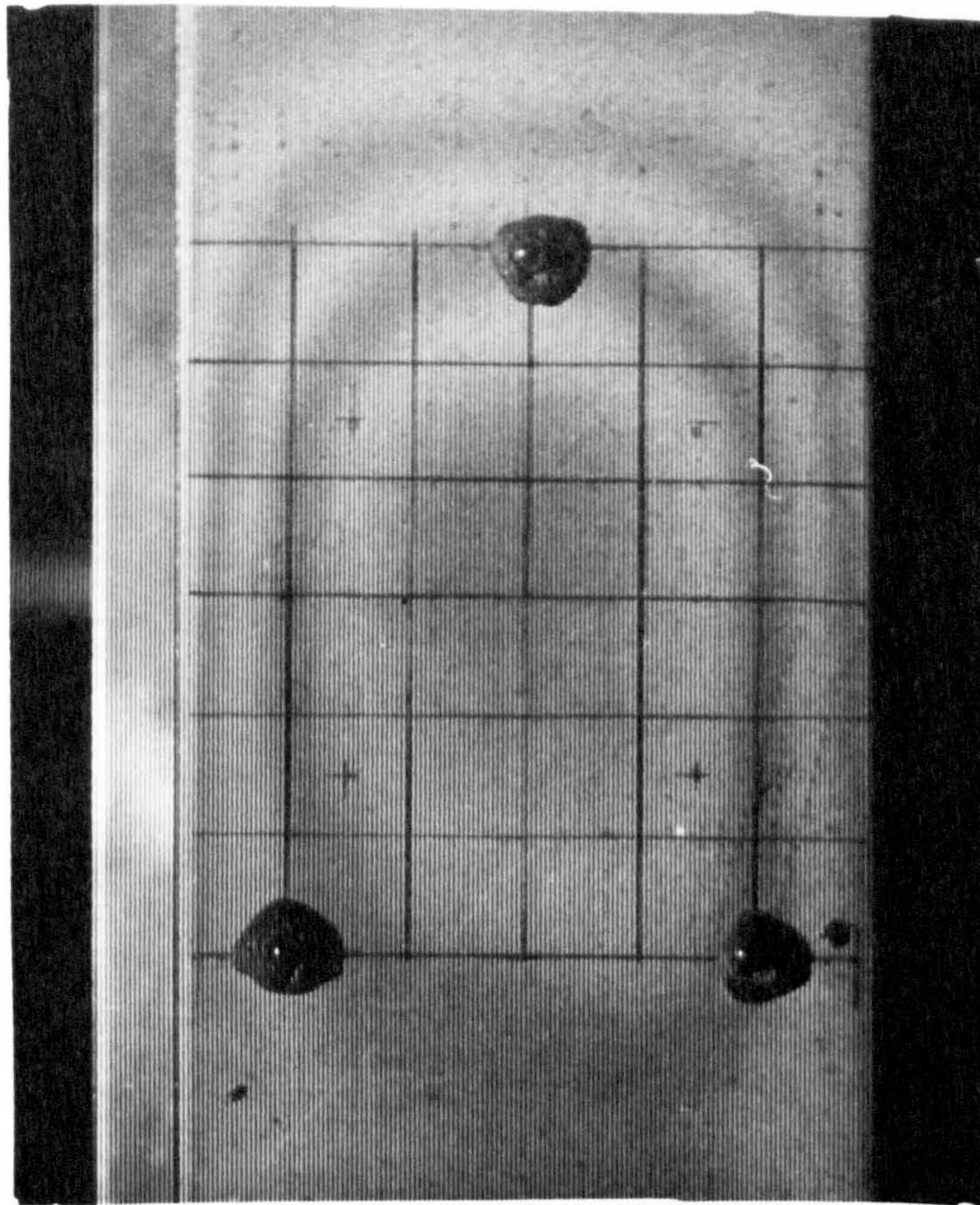
FIGURE (8-15)



$$P/P_{cr} = 0.93$$

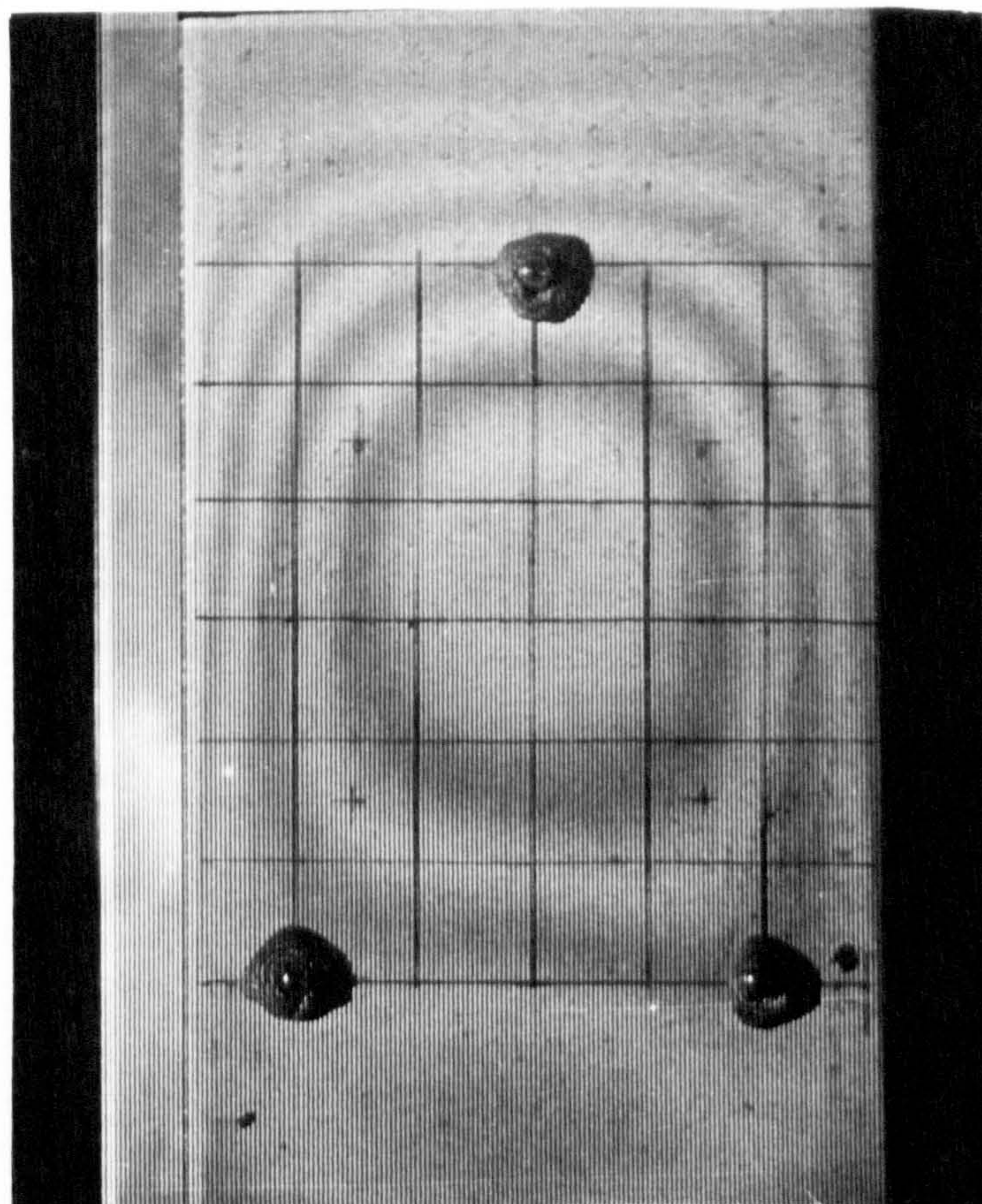
FIGURE (8-16)





$$P/P_{cr} = 1.3$$

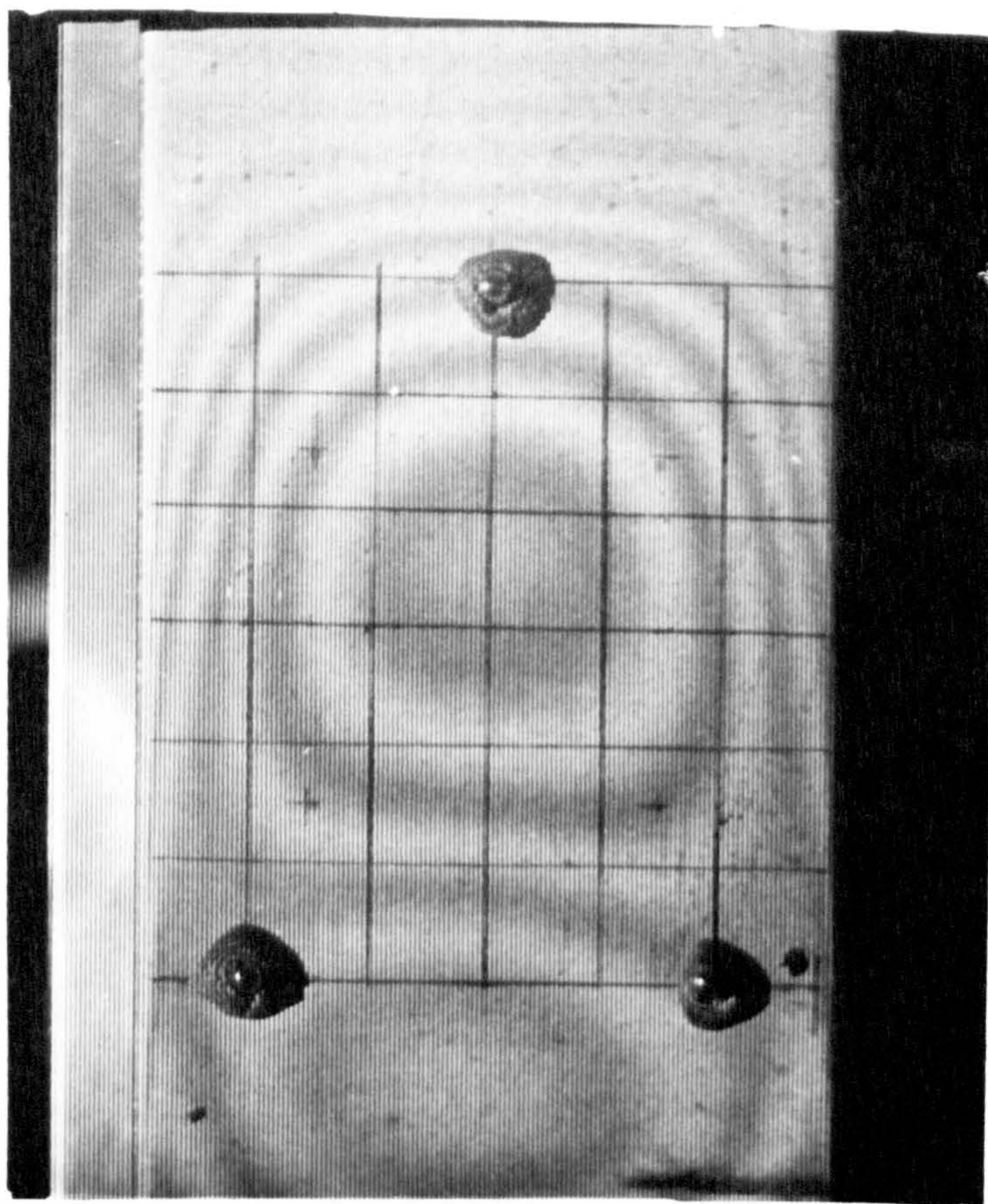
FIGURE (8-17)



$$P/P_{cr} = 1.67$$

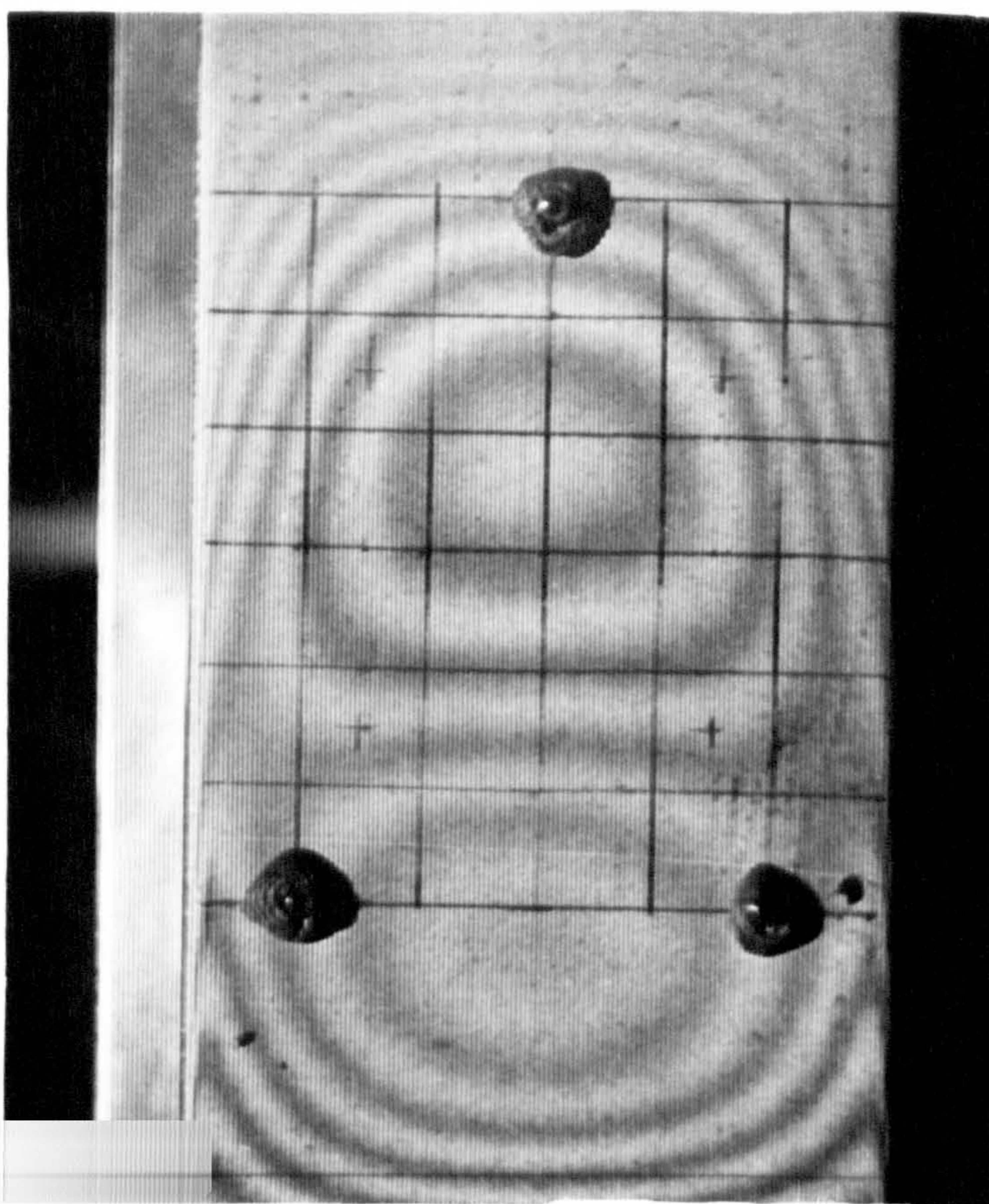
FIGURE (8-18)





$$P/P_{cr} = 2.04$$

FIGURE (8-19)



$$P/P_{cr} = 2.41$$

FIGURE (8-20)



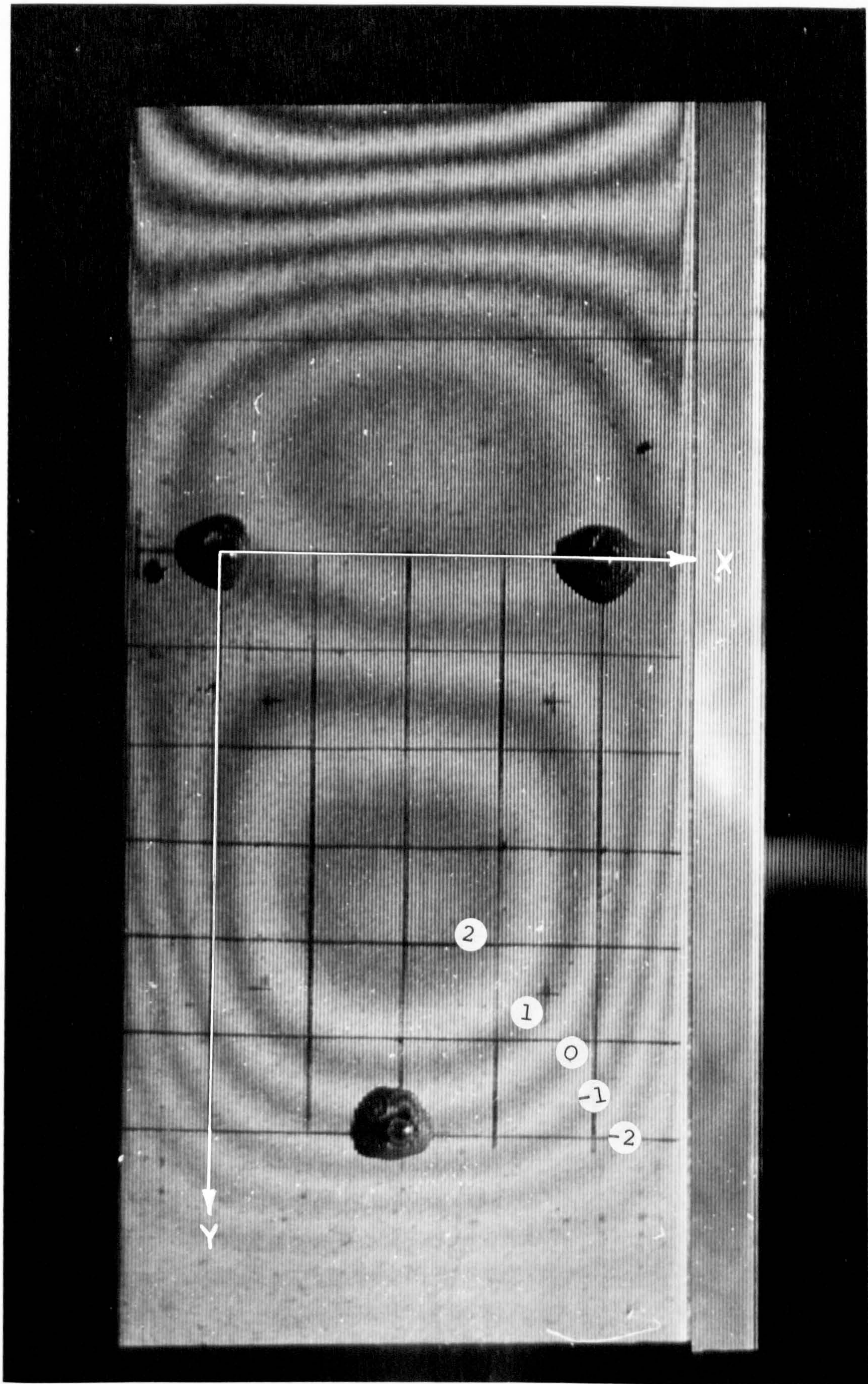


FIGURE (8-21)



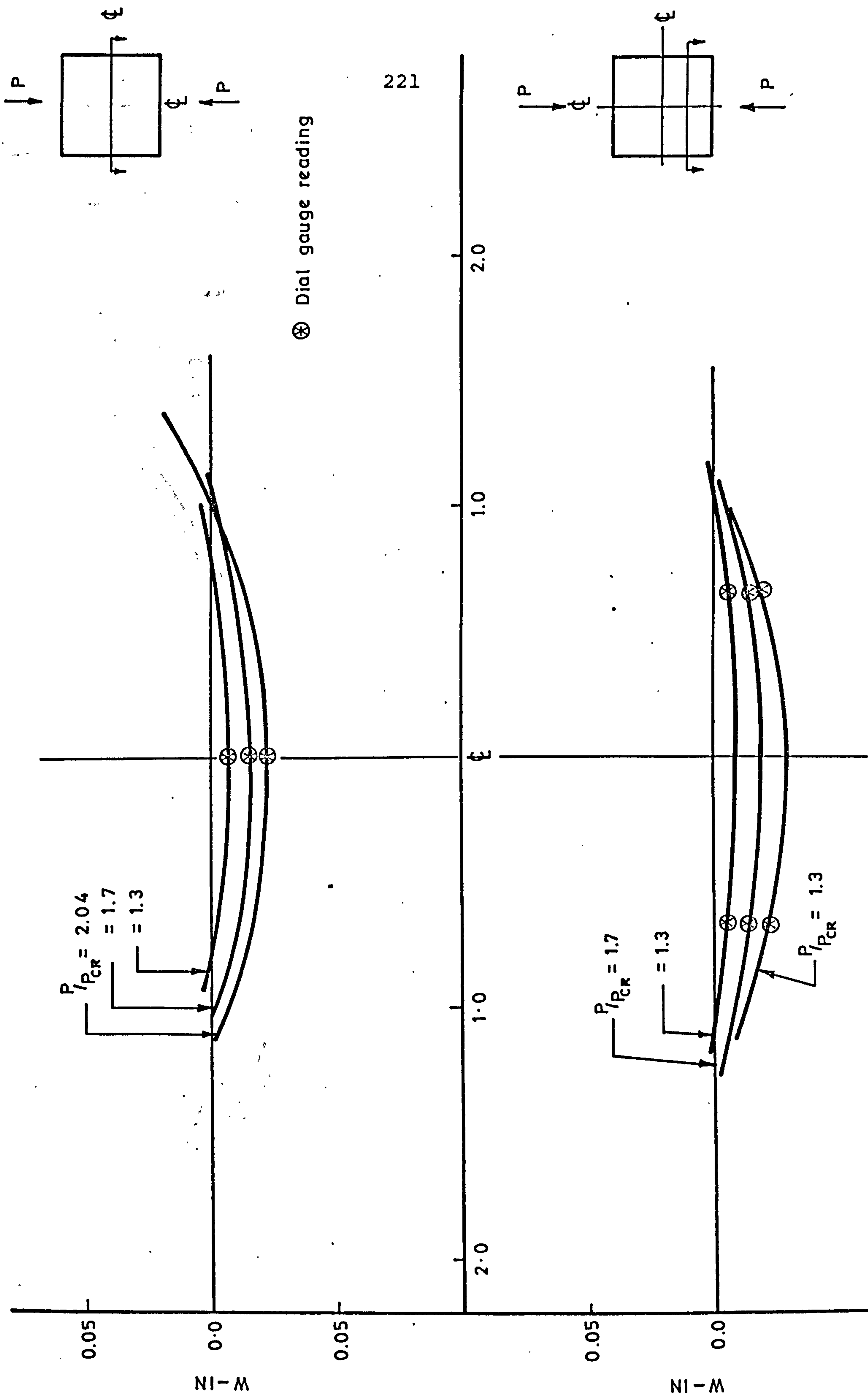


FIGURE 8-22

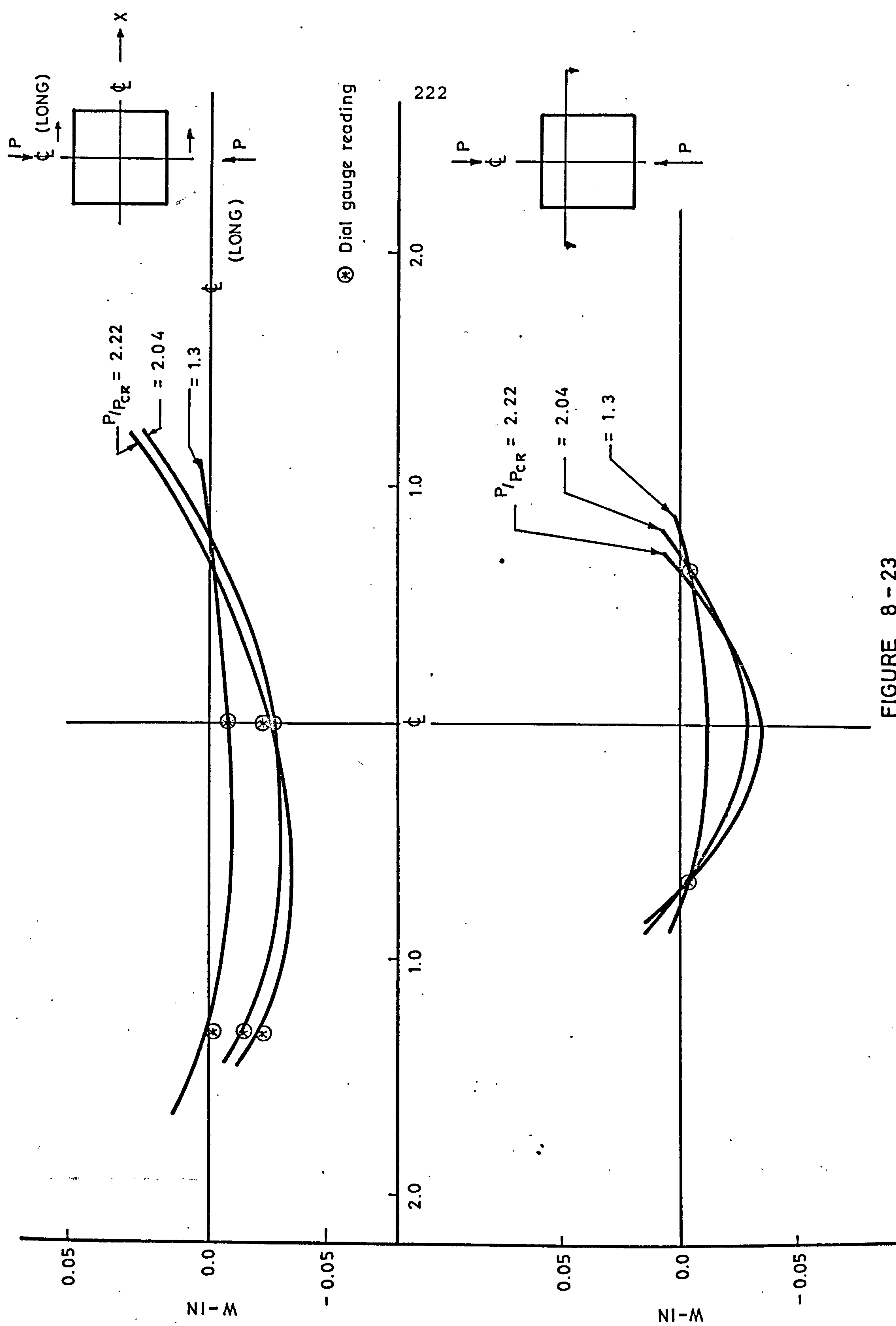


FIGURE 8-23

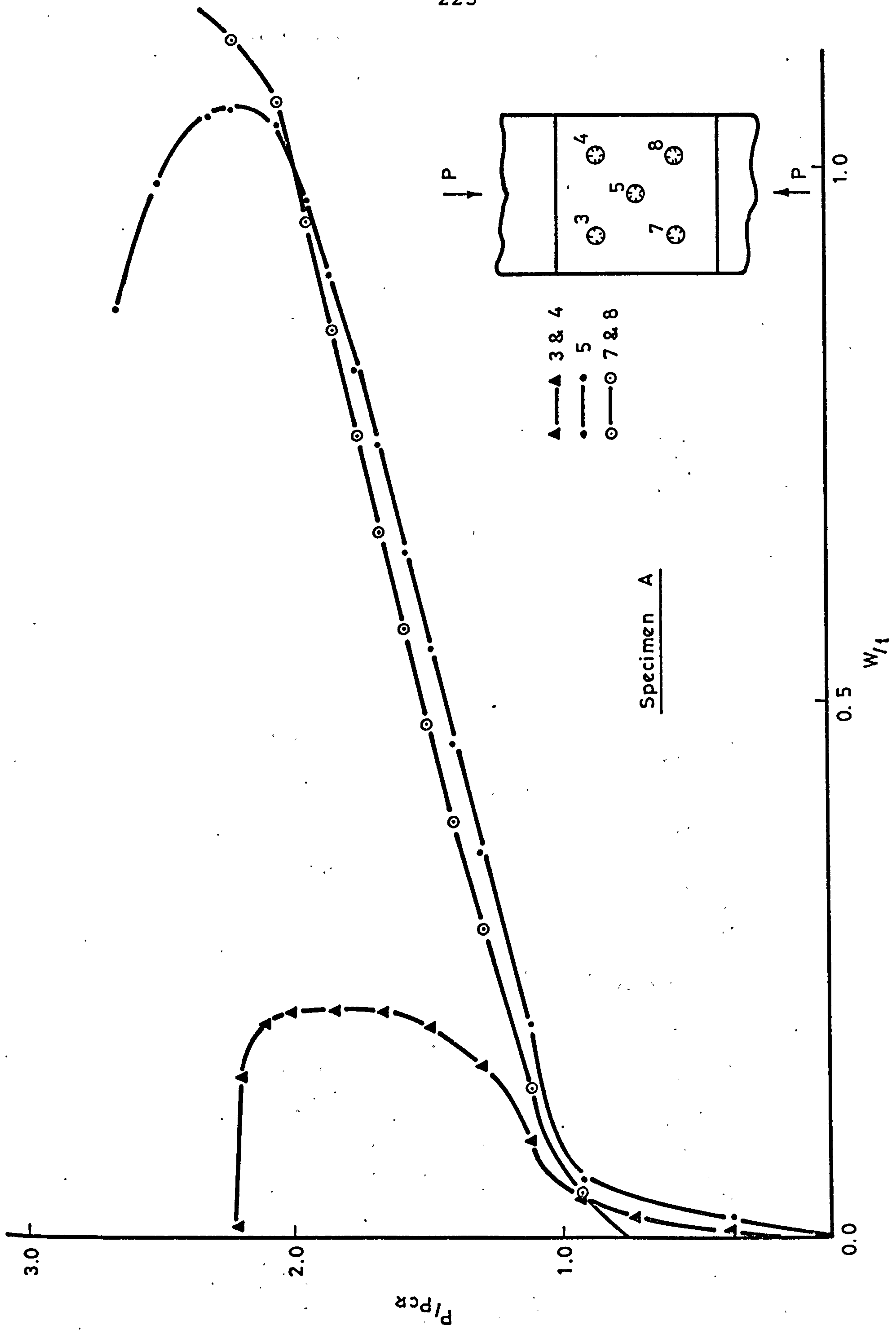
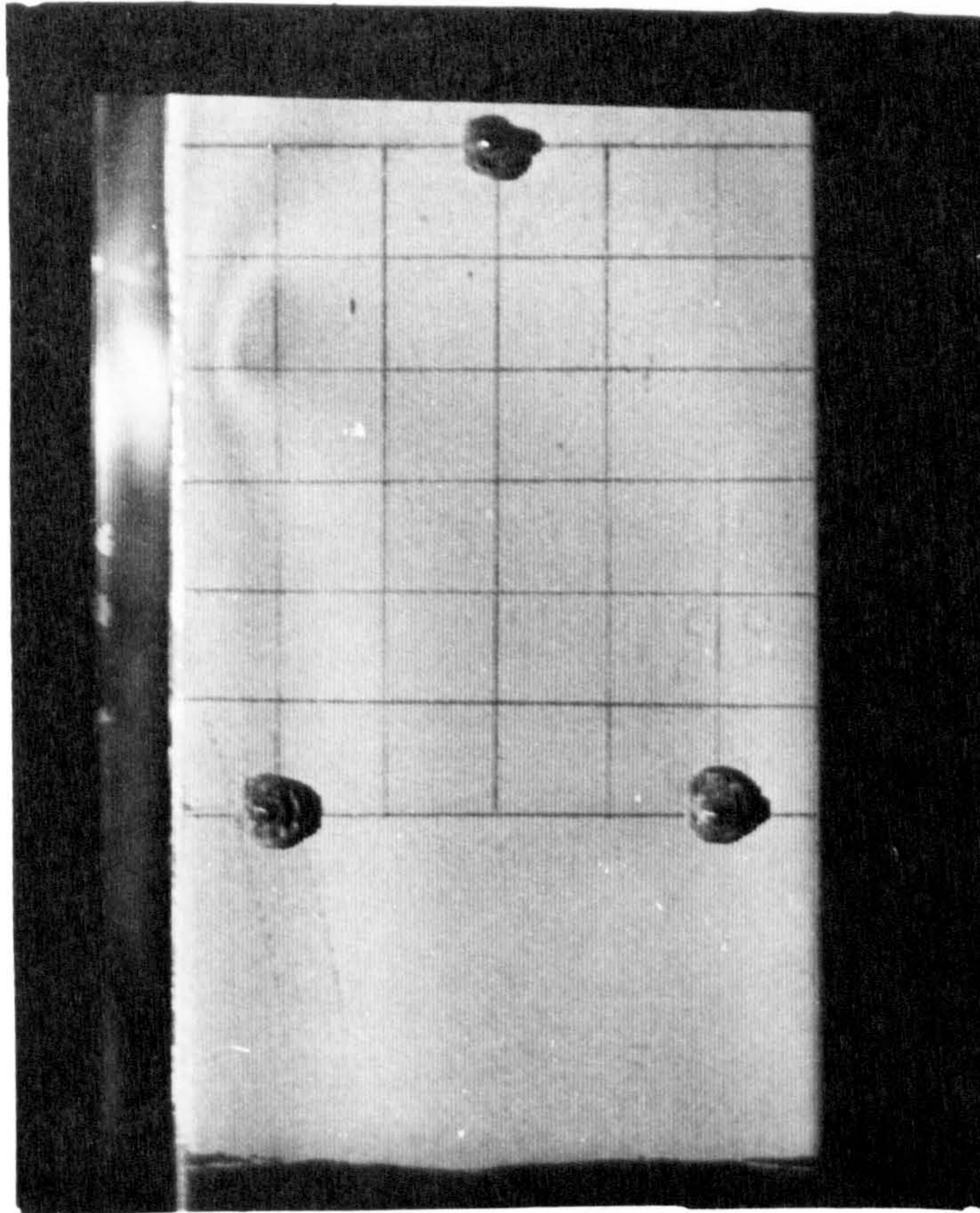


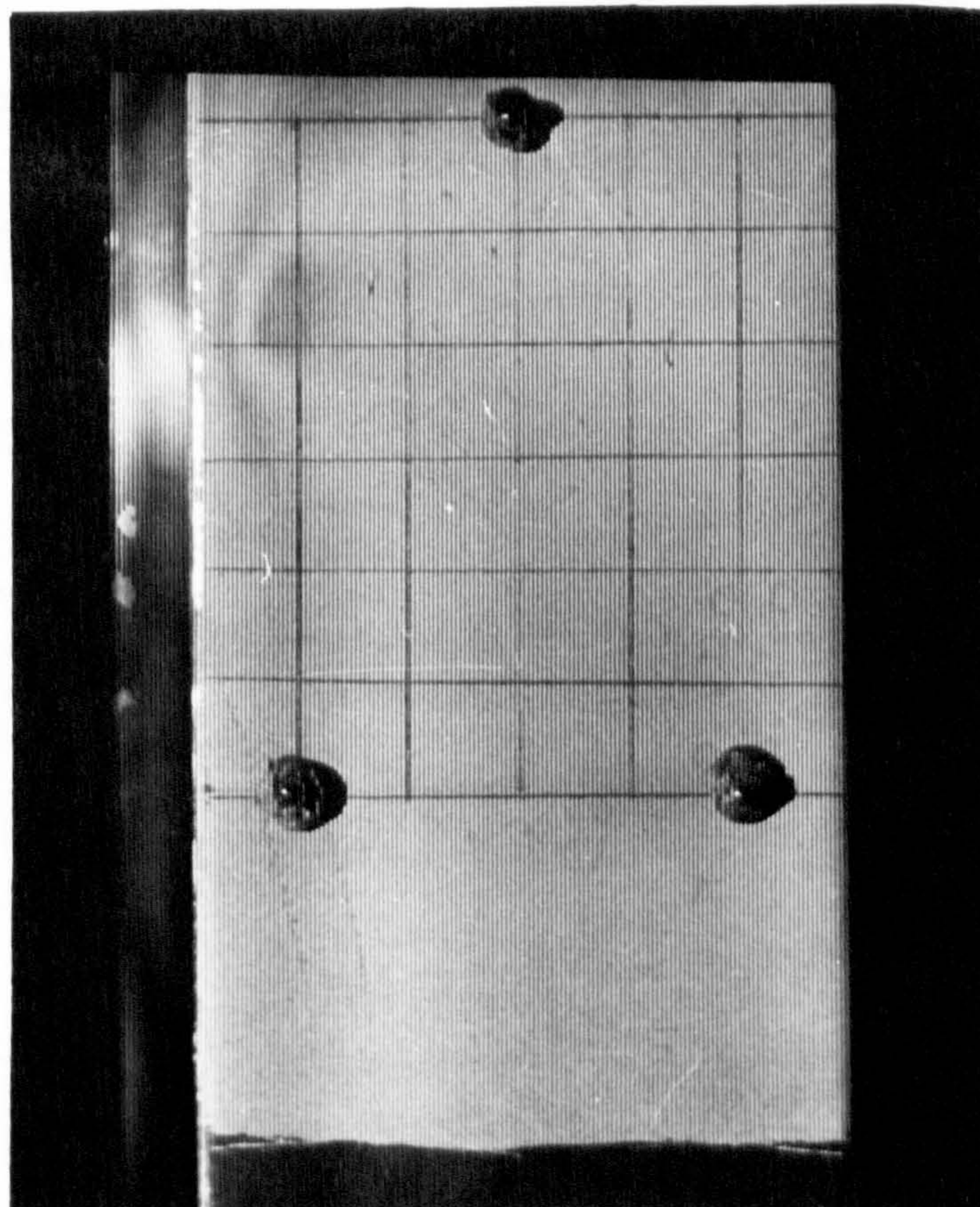
FIGURE 8-24





$$P/P_{cr} = 0$$

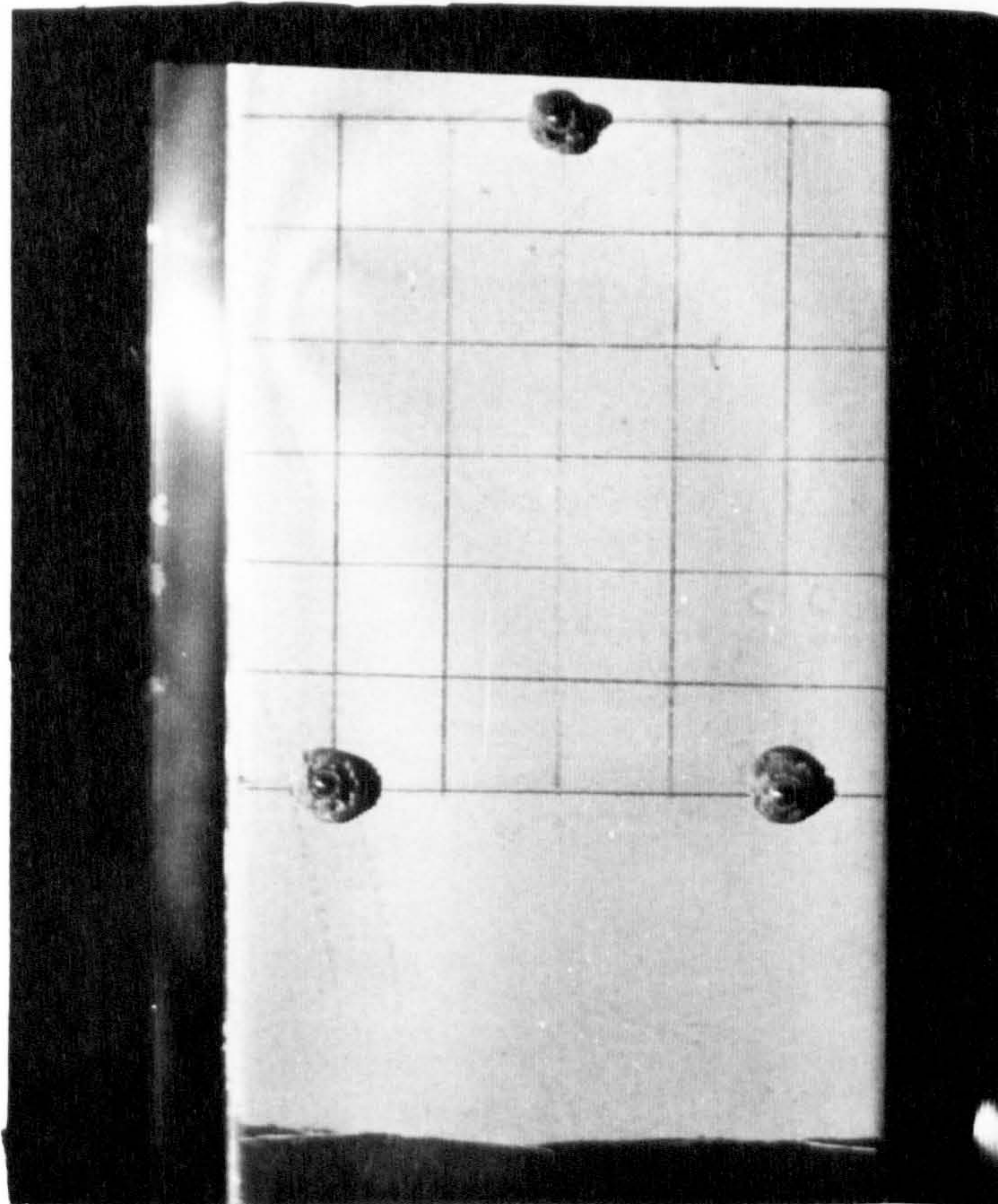
FIGURE (8-25)



$$P/P_{cr} = .56$$

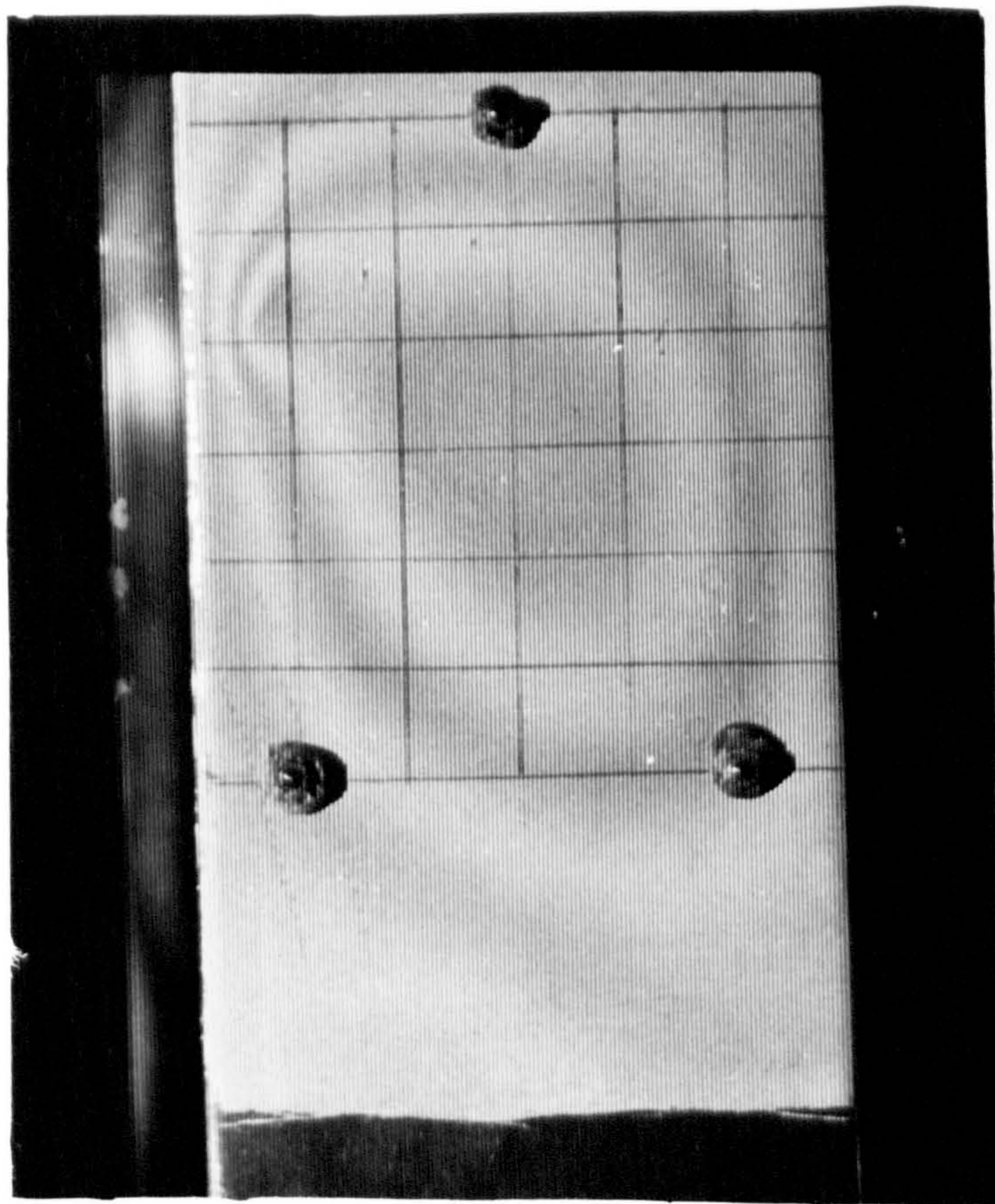
FIGURE (8-26)





$$P/P_{cr} = .92$$

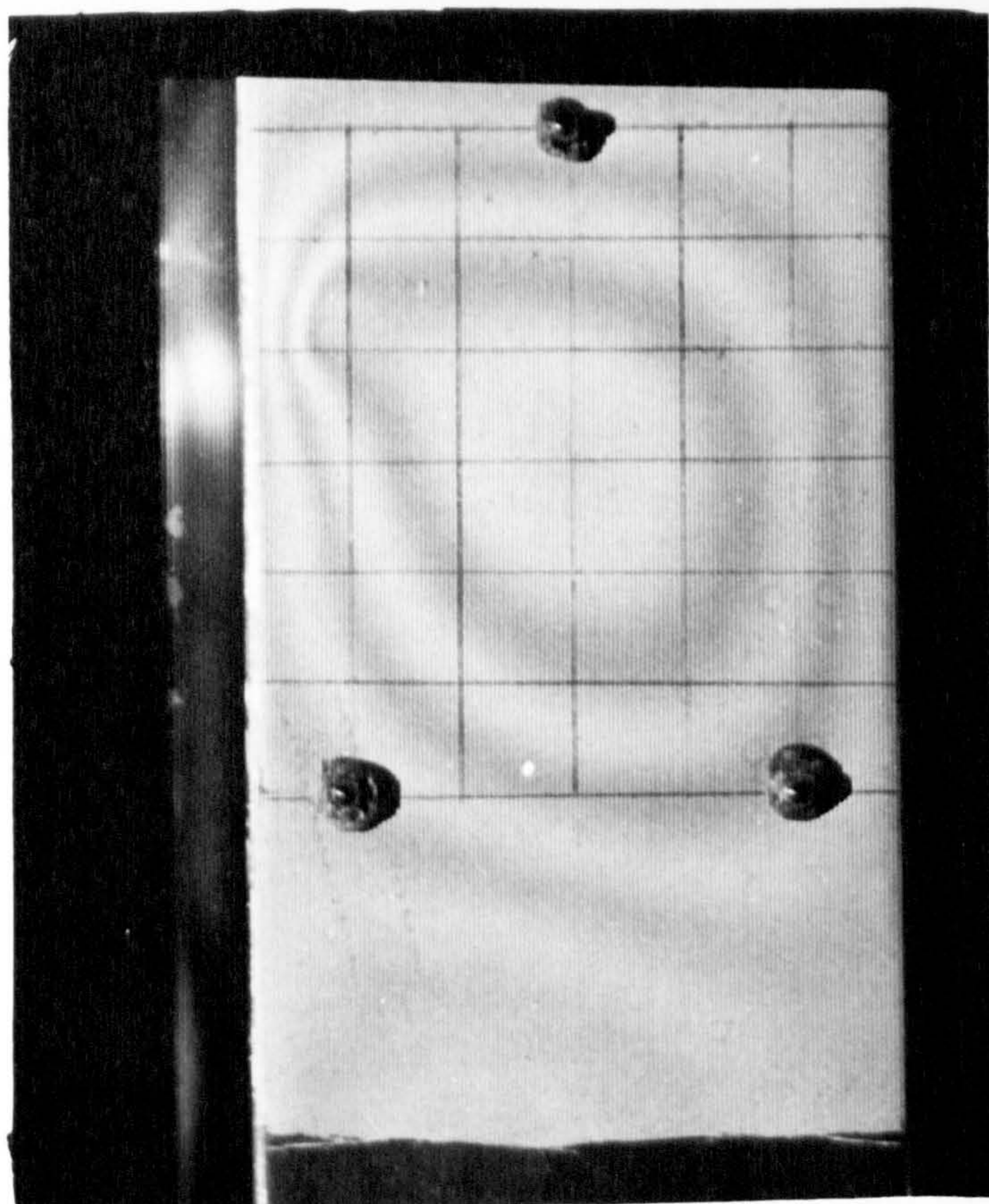
FIGURE (8-27)



$$P/P_{cr} = 1.2$$

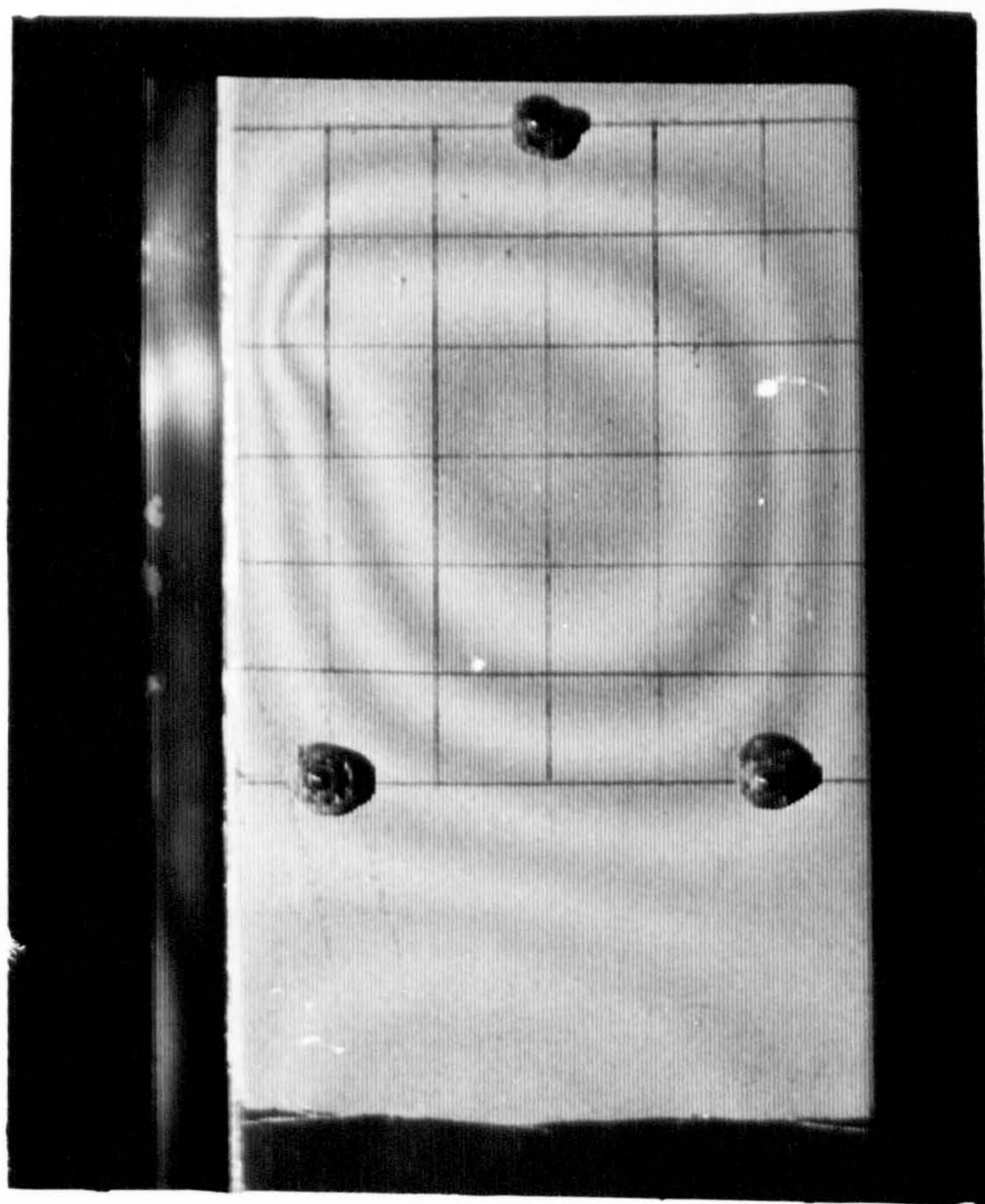
FIGURE (8-28)





$$P/P_{cr} = 1.48$$

FIGURE (8-29)



$$P/P_{cr} = 1.67$$

FIGURE (8-30)



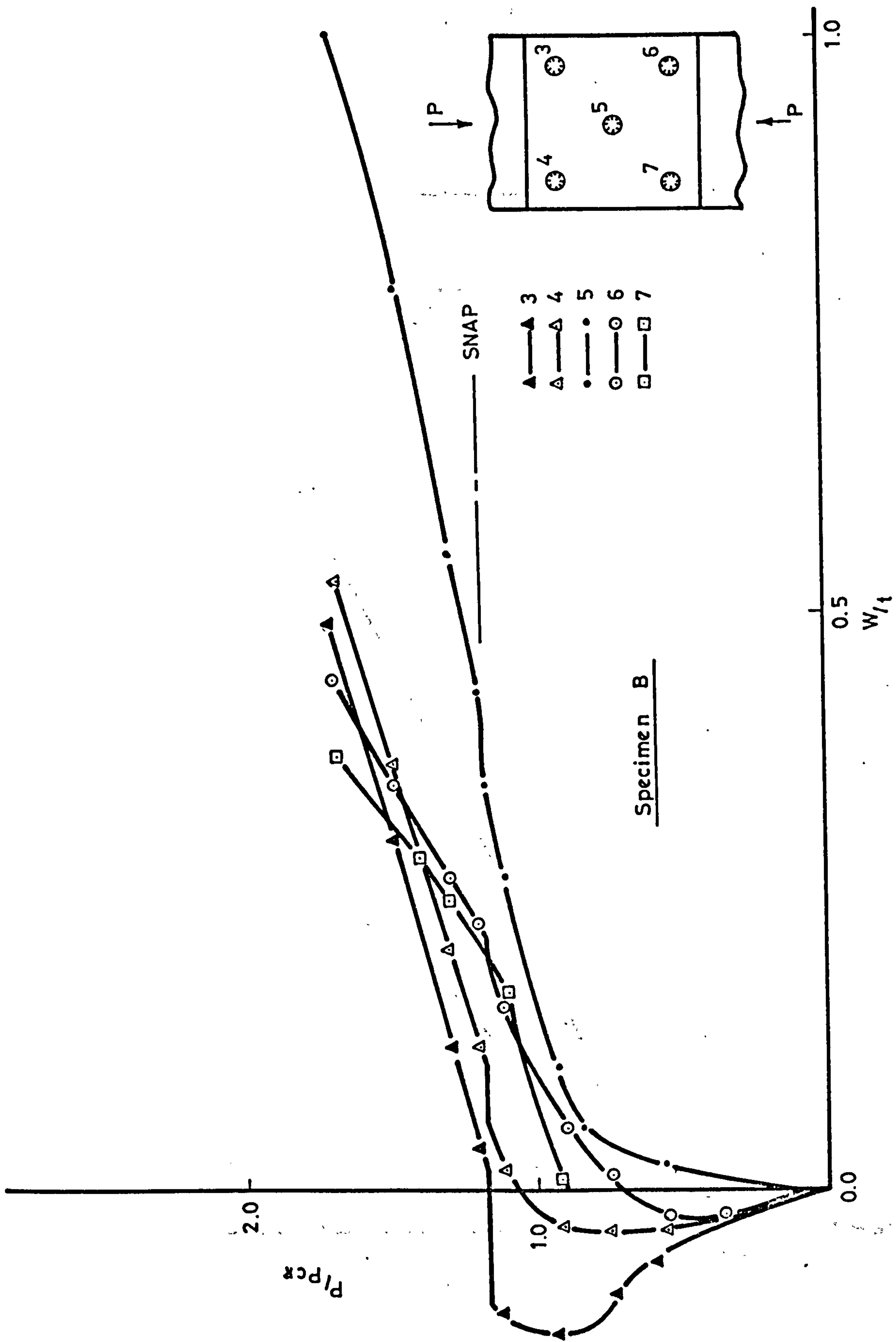


FIGURE 8-31

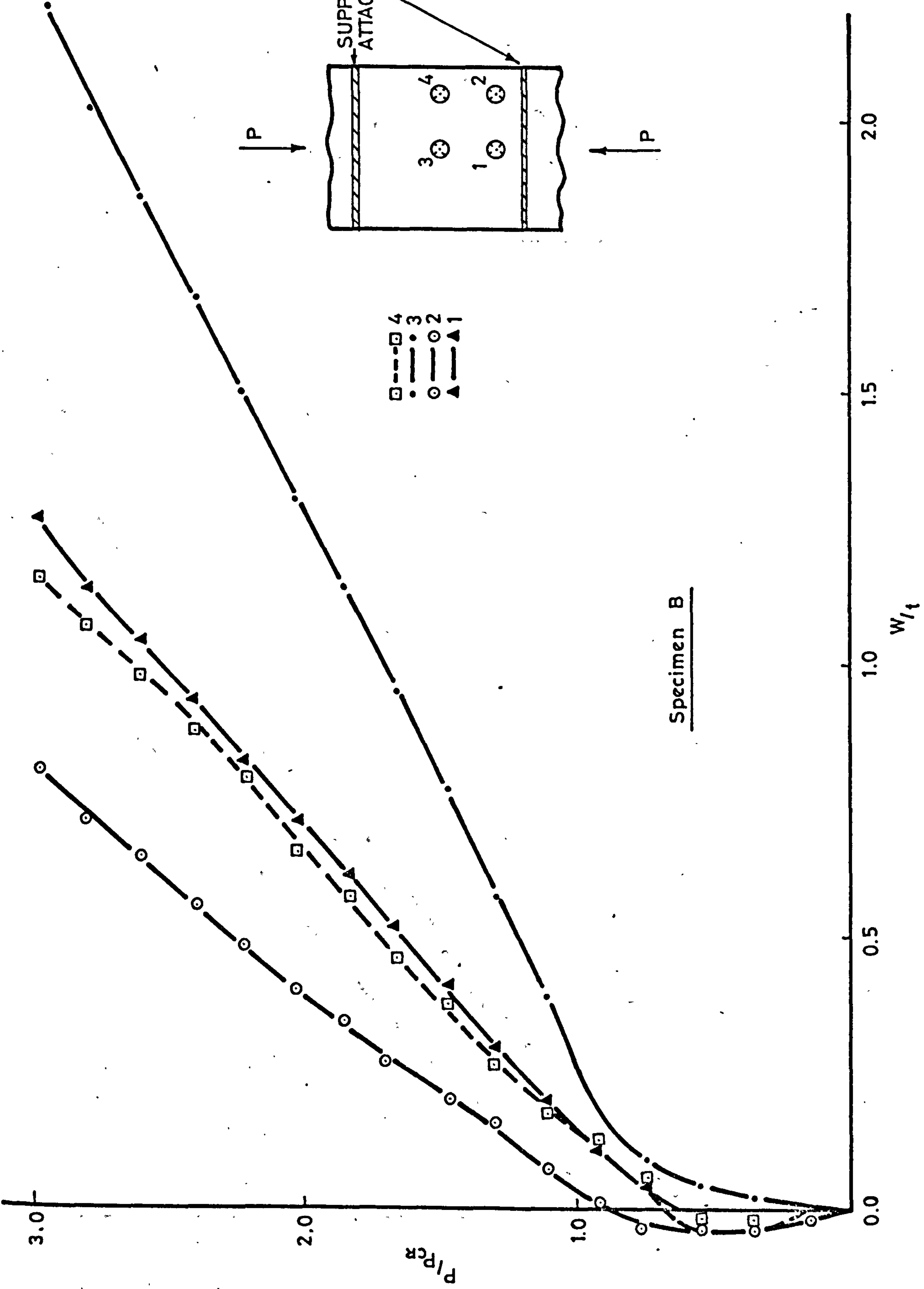


FIGURE 8-32



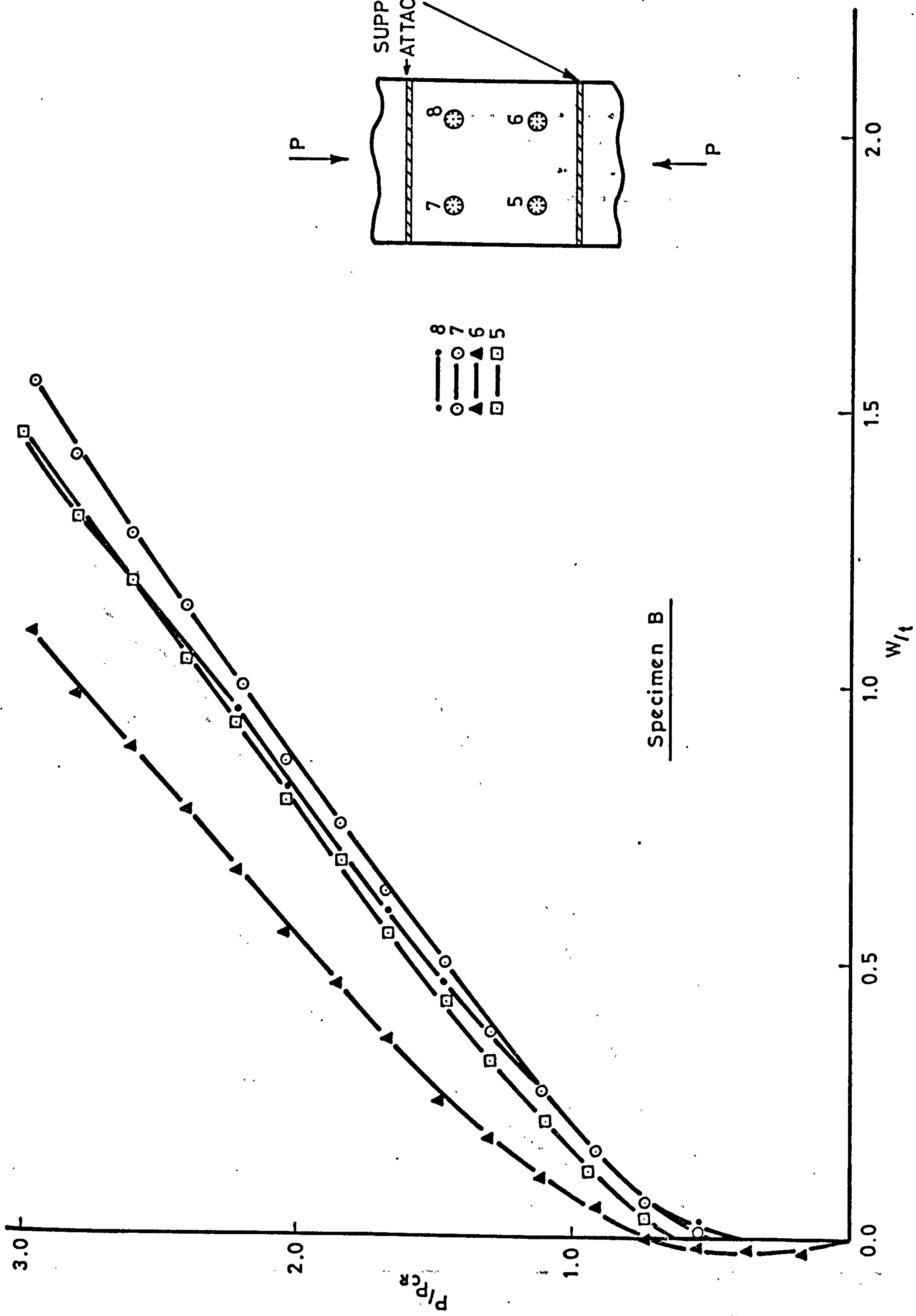


FIGURE 8-33

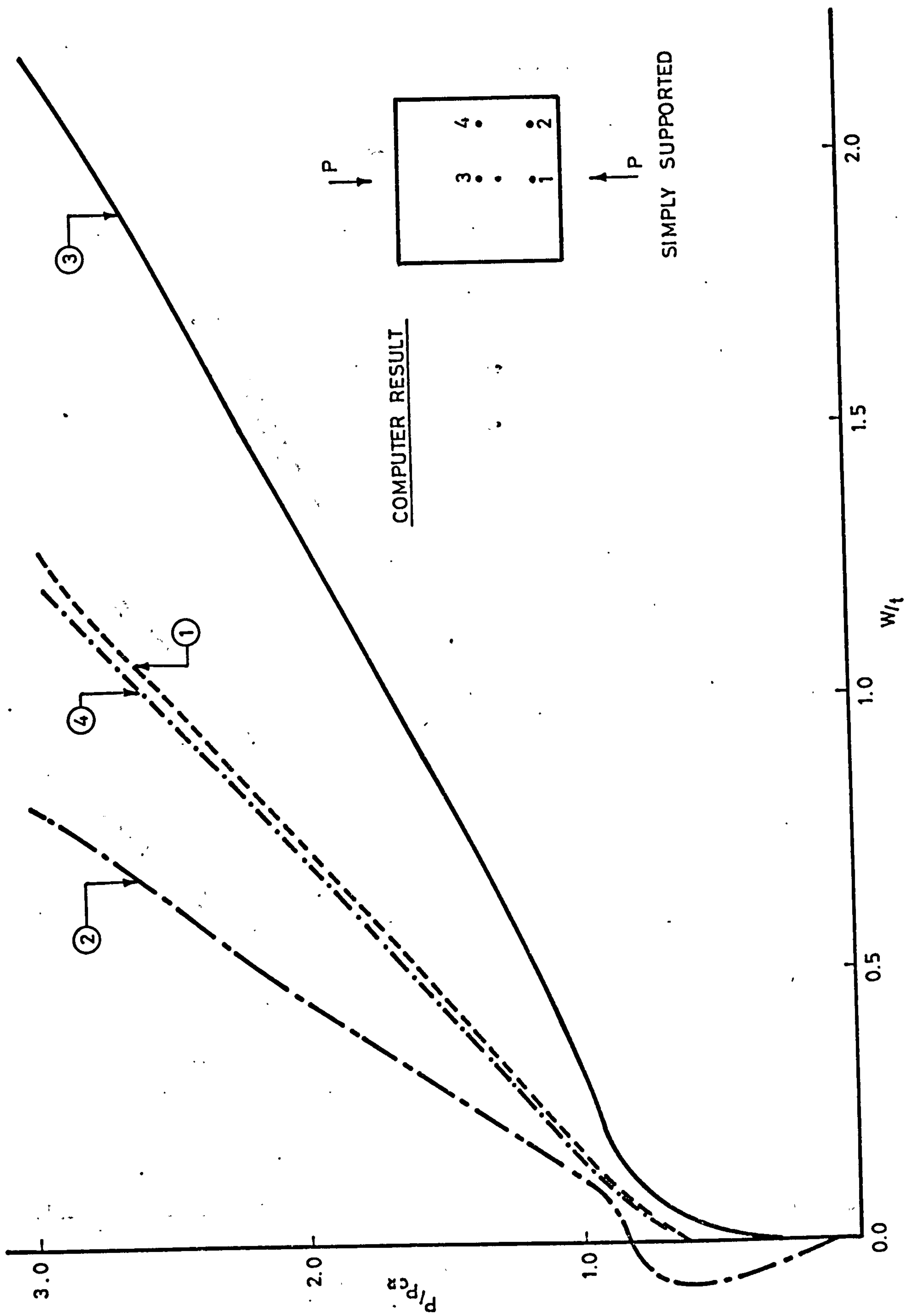


FIGURE 8-34

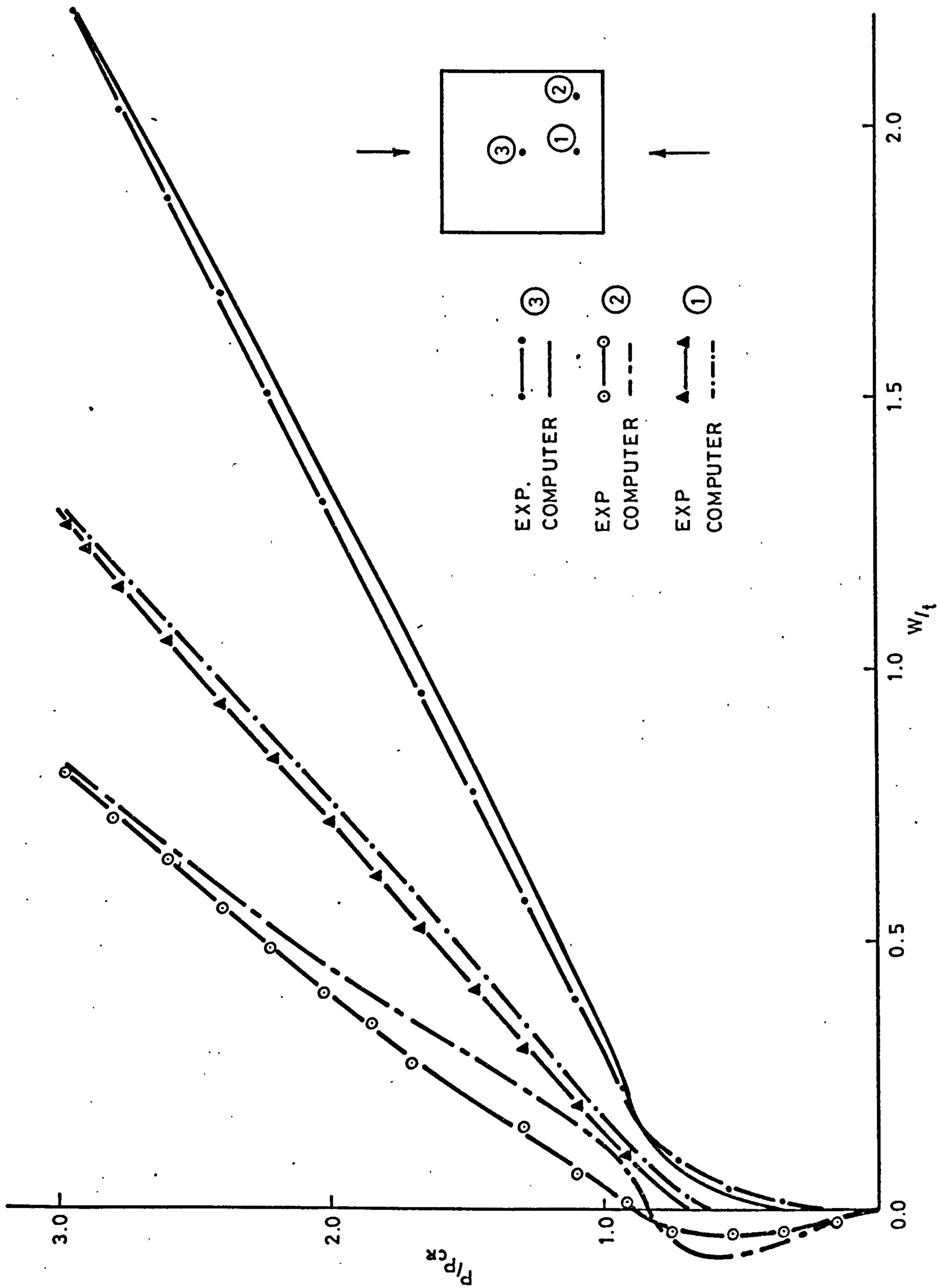


FIGURE 8-35



C O N C L U S I O N   A N D   R E C O M M E N D A T I O N S

## 9.1 CONCLUSION

A general finite element program which is applicable to pre- and post-buckling behaviour has been developed for plates with imperfections. The computer program has been checked against classical solutions for the large deflection behaviour of elastic plates, and good agreement has been found. The program is used to investigate the effect of different levels of imperfection, and various boundary restraints, on the in-plane stiffness behaviour of plates.

A preliminary program for a strut is used as a prototype to examine finite element formulations and to evaluate geometrically nonlinear procedures. The conclusions generally remain valid if the solution techniques are incorporated into a large-scale computer program capable of handling a large number of degrees of freedom.

- 1) For the geometrically nonlinear problem, it appears that the conventional incremental procedure is too prone to drifting from the true solution to be of any real value. Improving the accuracy simply by decreasing the load increment size is likely to be very expensive in terms of computer time.
- 2) The Newton-Raphson method is probably the most accurate method available to date, but unfortunately it is also the most expensive from the standpoint of computer expenditure because of the constant updating and inverting of the coefficient matrix.
- 3) The modified Newton-Raphson is a very accurate method, and iteration is shown to be both a very powerful as well as an economical means of correcting the solution at each load increment. Since most of the correcting is achieved by the first and second iterations, there is generally little purpose in proceeding beyond two iterations.
- 4) Carry over of residual forces into the following increment of load without actually completing the iteration was found to be not beneficial from the point of view of computer time.
- 5) The loss of accuracy involved in the use of the fixed coordinate system is very small compared with the moving coordinate system. On the other hand, there is a considerable

simplification in formulation of the element stiffness for the fixed coordinate system.

Although the incremental stiffness matrices of a rectangular plate element with four nodes and twenty degrees of freedom are generated, by replacement of the stiffness matrices and minor changes in the program, any type of element could easily be incorporated. All programs developed are listed, and user information supplied with a view to further development of these programs.

Investigation of post-buckled stiffness was carried out for a square plate, for which compressive stiffness behaviour was very similar to that of classical long plates. For the square plate subjected to shear load, a change of mode shape was found in the post-buckled range, which caused a sudden drop of stiffness. It was also found that a great loss of compressive stiffness occurs at the critical shear load.

Experimental work on a lipped channel-section strut has been carried out to simulate a simply-supported plate under compression. The Moire fringe technique was used for measuring deflections on both specimens (with its own natural and artificial imperfections) and proved very successful when compared to dial gauge readings. Results show the general behaviour of such plates, and are also compared with generally similar computer results for the developed program.



## 9.2 RECOMMENDATIONS FOR FURTHER WORK

The effect of shear buckling on compressive stiffness was investigated by the finite element method in Section 7.5. A considerable loss of compressive stiffness in the vicinity of the critical shear load, as well as considerable variation in compressive stiffness with respect to  $\tau/\tau_{cr}$ , was found. In order to verify the results obtained, experimental work is now suggested.\*

A suitable test specimen can be considered in the form of a square tube, because shear stress is readily obtained by torsion, and compressive stiffness is also easily measured by application of small axial loads. Preliminary calculation showed that the square tube needs to be rather thin, in order to buckle well before material yielding; thus, an extruded section is unsuitable. Alternatively, to avoid a fabricated joint, a welded section is probably most suitable. In order to achieve a buckling stress not greater than  $1/3$  of the effective yield stress of the tube, and also to obtain a width to thickness ratio  $b/t = 120$ , L70 aluminium is deemed the most suitable choice. This specific aluminium alloy is a reasonable compromise between weldability and mechanical properties. Two types of welded square tubes can be manufactured; first, two right angles, which probably involves less distortion but more residual stress; and second, a channel and plate which probably involves more distortion but less residual stress. Since residual stress must be avoided, the second type of specimen is recommended.

Torsion load is applied through two steel blocks fitted at the ends of the square tube. A very small compressive load is required to measure the axial contraction, while the specimen is loaded in shear (see Figure 9-1). The experiment should then proceed by application of shear load through the torsion machine, checking the compressive stiffness at different shear load levels by applying a very small compressive load through the turn-buckle. Since the axial deformation is extremely small, an electrical measurement device is required to record the measurements accurately.

Appropriate drawings, as well as a design analysis, is available in Appendix C.

---

\*Note: Work based on these recommendations is currently being carried out at Cranfield Institute of Technology. (M.Sc. Thesis to be presented September, 1978.)

236

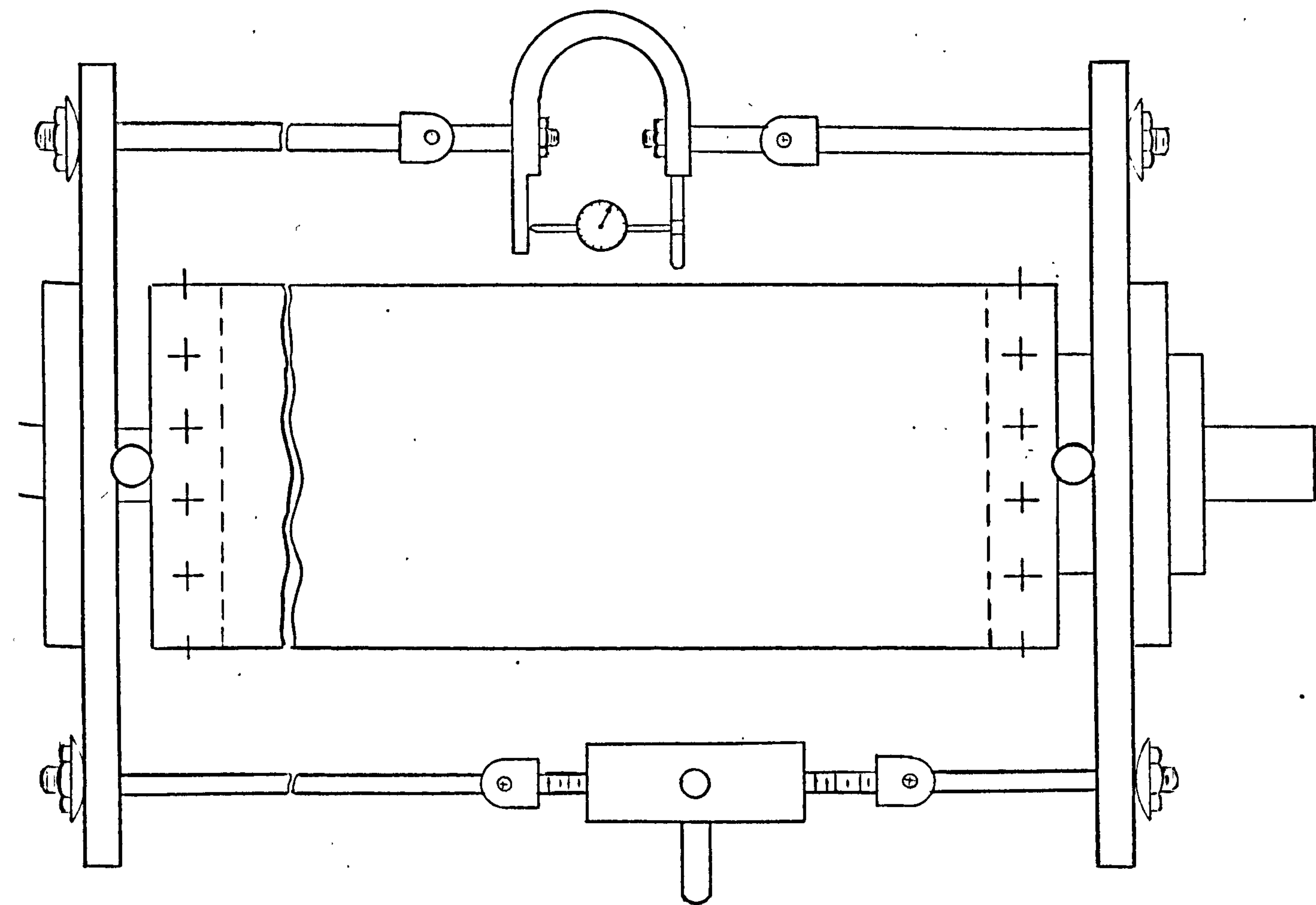
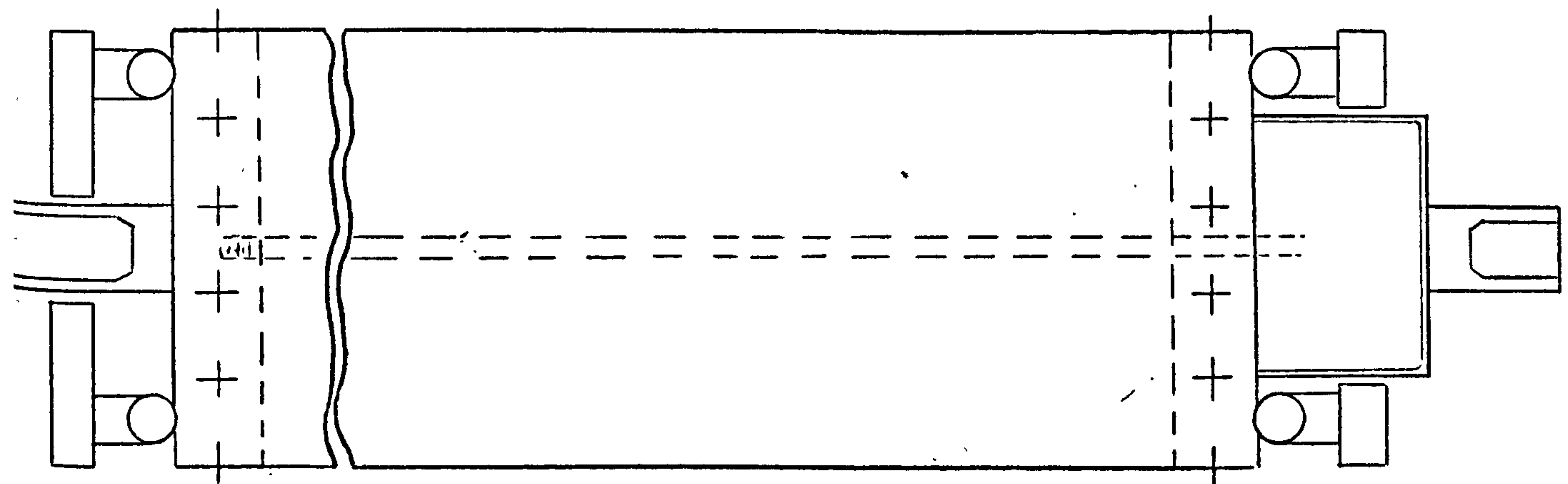


FIGURE 9-1

## REFERENCES

1. ARGYRIS, J. H.      Elasto-plastic Matrix Displacement Analysis of Three-Dimensional Continues.  
Journal of Royal Aeronautical Society, Vol. 69, 1965.
2. VAN DER NEUT, A.    The Interaction of Local Compression Members.  
Proceedings of the Twelfth Applied Mechanics. Stanford University, 1969.
3. VAN DER NEUT, A.    International Journal of Solids Structures, 1973.
4. KOITER, W. T.        The Stability of Elastic Equilibrium. Thesis: Polytechnic Institute of Delft, Amsterdam English Translation. 1945. AFFDL-TR-70-25, 1970. Air Force Flight Dynamics Lab, Wright-Patterson Air Force Base, Ohio.
5. THOMPSON, J. M. T.   Basic Principles in the General Theory of Elastic Stability.  
Journal of Mechanics and Physics of Solids, Vol II, 1963.
6. BUDIANSKY, B.  
HUTCHINSON, J. W.    Dynamic Buckling of Imperfection Sensitivity Structures.  
Proceedings of the XIth International Congress of Applied Mechanics, 1966.
7. MAK, C. K.  
KAO, D. W.            Finite Element Analysis of Buckling and Postbuckling Behaviour of Arches with Geometric Imperfections.  
Computers & Structures, Vol 3, January, 1973.
8. VON KARMAN  
TSIEN, T. S.           The Buckling of Thin Cylindrical Shells under Axial Compression.  
Journal of Aeronautical Science, 1941.
9. VON KARMAN,  
SECHLER, T. E. E.  
DONNEL, L. H.        The Strength of Thin Plates in Compression.  
Trans. ASME, Vol 54, 1932.
10. TURNER, J. J.  
CLOUGH, R. W.  
MARTIN, H. C.  
TOPP, L. J.           Stiffness & Deflection Analysis of Complex Structures.  
Journal of Aero-Science, Vol 23, No. 9, September, 1956, pp. 815-825.



11. TURNER, M. J.  
DILL, E. H.  
MARGIN, H. C.  
MELOSH, R. J.      Large Deflection Analysis of Complex Structures Subjected to Heating and External Loads.  
Journal of Aero-Space Science, Vol. 27, February, 1960.
12. TURNER, J. J.  
MARTIN, H. C.  
WEIKEL, R. C.      Further Development & Application of the Stiffness Method.  
AGARDograph 72, Pergamon Press, 1964. Pp. 202-266.
13. GALLAGHER, R. H.  
PADLOG, J.      Discrete Element Approach to Structural Instability Analysis.  
Journal of the American Institute of Aeronautics and Astronautics, Vol. I, No. 6, June 1963, Pp. 1437-1439.
14. GALLAGHER, R. H.  
PADLOG, J.      Thermal Stress Determination Techniques for Supersonic Transport Aircraft Structures, Part II.  
Technical Documentary Report 63-783, Aeronautical Systems Division, January 1965.
15. ARGYRIS, J. H.      Recent Advances in Matrix Methods of Structural Analysis.  
Progress in Aeronautical Sciences, Pergamon Press, N. Y., 1964.
16. ARGYRIS, J. H.  
KELSEY, S.  
KAMEL, H.      Matrix Methods of Structural Analysis.  
AGARDograph No. 72. Pergamon Press, New York, 1964.
17. MARTIN, H. C.      On the Derivation of Stiffness Matrices for the Analysis of Large Deflections and Stability Problems.  
AFFDL-TR-66-80, December, 1965, Pp. 697 - 716.
18. BROYDEN, C. G.      A Class of Methods for Solving Non-linear Simultaneous Equations.  
Mathematics of Computation, Vol. 19, 1965, Pp. 557 - 593.
19. FLETCHER, R.      Function Minimization Without Evaluating Derivatives - A Review.  
Computer Journal, Vol, 19, 1965. Pp. 557 - 593.
20. MALLET, R. H.  
GALLAGHER, R. H.  
STEBBINS. F. J.      Finite Element Methods in Thin Shell Elastic Stability Analysis.  
Presented at the Structural Stability & Optimization Symposium, Loughborough University of Technology, England, March, 1967.

21. ODEN, J. T. Numerical Formulation of Nonlinear Elasticity Problems.  
Journal of the Structural Division, ASCE, Vol. 93, No. ST3, Proc. Paper 5290, June, 1967, Pp. 235 - 236.
22. STRICKLIN, J. A. Nonlinear Analysis of Shells of  
HAISLER, W. E. Revolution by the Matrix Displace-  
MACDOUGALL, H. R. ment Method.  
STEBBINS, F. J. American Institute of Aeronautics  
& Astronautics, 6th Aerospace Science  
Conference, Paper No. 68-177, Janu-  
ary, 1968.
23. ZIENKIEWICS, O. C. The Finite Element Method in Struc-  
tural & Continuum Mechanics.  
McGraw Hill, Ltd., London, England,  
1967.
24. MALLET, R. H. Automated Method for the Finite  
BERKE, L. Displacement Analysis of Three  
Dimensional Truss & Frame Assem-  
blies.  
AFFDL - TR-102-1966.
25. SCHMIT, L. A., Jr. Finite Deflection Structural Analy-  
BOGNER, F. K. sis Using Plate & Cylindrical Shell  
FOX, R. L. Discrete Elements.  
Proceedings, American Institute of  
Aeronautics & Astronautics; American  
Society of Mechanical Engineers,  
8th Structures, Structural Dynamics  
& Material Conference, 1967.
26. MARCAL, P. V. The Effect of Initial Displacement  
on Problems of Large Deflection and  
Stability.  
Report ARPA E54, November, 1967,  
Brown University, Providence, R.I.
27. PURDY, M. D. Influence of Higher-Order Terms in  
PRZEMIENIECKI, J.S. The Large Deflection Analysis of  
Frameworks.  
Air Force Institute of Technology,  
Wright-Patterson Air Force Base,  
Ohio.
28. WILSON, E. L. Finite Element Analysis of Two-  
Dimensional Structures.  
Ph.D. Dissertation, University of  
California, Berkley, 1963.
29. SWEDLOW, J. L. Stiffness Analysis of Elasto-plastic  
Plates.  
Calcit Report SM 65-10, California  
Institute of Technology, 1965.



30. FELIPPA, C. A. Refined Finite Element Analysis of Linear and Nonlinear Two-Dimensional Ph.D. Dissertation, University of California at Berkley, 1966.
31. REYES, S. E.  
DECRE, D. U. Elasto-plastic Analysis of Underground Opening by the Finite Element Method.  
Proceedings, First International Congress on Rock Mechanics; Vol II, Lisbon, 1966.
32. MARCAL, P. V.  
KING, I. Elastic-Plastic Analysis of Two-Dimensional Stress Systems by the Finite Element Method.  
International Journal of Mechanical Science, Vol. 9, 1967.
33. RICHARD, R. M.  
BLACKLOCK, J. R. Finite Element Analysis of Inelastic Structures.  
AIAA Journal, Vol. 7, 1969.
34. ZIENKIEWICZ, O. C.  
VALLIAPPAN, S.  
KING, I. P. Elasto-plastic Solutions of Engineering Problems, Initial Stress, Finite Element Approach.  
International Journal of Numerical Methods in Engineering, Vol. I, 1969.
35. WITMER, E. A.  
KOTANCHIK, J. J. Progress Report on Discrete Element Elastic and Elastic-Plastic Analysis of Shells of Revolution Subjected to Axisymmetric & Asymmetric Loading.  
Proceeding, Second Conference on Matrix Methods in Structural Mechanics, AFFDL TR-69, Ohio, 1969.
36. ARMER, H., Jr.  
PIFKO, A.  
LEVINE, H. S. Finite Element Method for the Plastic Bending of Structure.  
Proceedings, Second Conference on Matrix Methods in Structural Mechanics, AFFDL TR-69, Ohio, 1969.
37. TURNER, M. J. The Direct Stiffness Method of Structural Analysis.  
Paper Presented at the 10th Meeting of the Structures & Materials Panel, Aachen, Germany, September, 1959.
38. ARGYRIS, J. H. Recent Developments of Matrix Theory of Structures.  
Paper Presented at the 10th Meeting of the Structures and Materials Panel, Aachen, Germany, September, 1969.



39. GREENE, B. C. Buckling Loads for Columns of Variable Section. Structural Analysis Research Memorandum No. 12, The Boeing Company, Aerospace Division, Seattle, June, 1960.
40. ORTEGA, M. A. Application of the Stiffness Method to Large Deflection of Columns with Initial Imperfection. Structural Analysis Research Memorandum No. 17, The Boeing Company, Aerospace Division, Seattle, May, 1960.
41. ARGYRIS, J. H. Matrix Analysis of Three-Dimensional Elastic Media, Small & Large Displacements. AIAA Journal, Vol, 3, No. 1, January, 1965. Pp. 45 - 51.
42. PRZEMIENIECKI, J.S. Stability Analysis of Complex Structures Using Discrete Element Techniques. Symposium on Structural Stability & Optimization, Royal Aeronautical Society & Loughborough University of Technology, England; March, 1967, Pp 23-24.
43. MARTIN, H. C. Large Deflection & Stability Analysis by the Direct Stiffness Method. NASA Technical Report, 32-931, 1966.
44. ODEN, J. T. Calculation of Geometric Stiffness Matrices for Complex Structures. AIAA Journal, Vol. 4, No. 8, 1966. Pp 1480 - 1482.
45. HARTZ, B. J. Matrix Formulation of Structural Stability Problems. Journal of the Structural Division ASCE, Vol. 91, No. ST6, December, 1965.
46. KAPUR, K. K.  
HARTZ, B. J. Stability of Plates Using the Finite Element Method. Journal of the Engineering Mechanics Division, ASCE, Vol. 92, No. EM2, April, 1966.
47. ANDERSON, R. G.  
IRONS, B. M.  
ZIENKIEWICZ, O.C. Vibration and Stability of Plates Using Finite Elements. International Journal of Solids and Structures, Vol. 4, No. 10, October, 1968, Pp. 1031 - 1055.

48. MURRAY, D. W.  
WILSON, E. L. Finite Element Large Deflection Analysis of Plates.  
Journal of the Engineering Mechanics Division. ASCE. Vol. 95, No. EM1, February, 1969, Pp. 143 - 165.
49. MURRAY, D. W.  
WILSON, E. L. Finite Element Postbuckling Analysis of Thin Elastic Plates.  
Proceedings, Second Conference on Matrix Method in Structural Mechanics, AFFDL TR-69, Wright-Patterson Air Force Base, Ohio, Held October, 1968, 1969.
50. THOMPSON, J. M. T.  
WALKER, A. C. The Nonlinear Perturbation Analysis of Discrete Structural Systems.  
International Journal of Solids & Structures, Vol. 4, 1968, Pp 757-768.
51. CONNOR, J.  
MORIN, N. Perturbation Techniques in the Analysis of Geometrically Nonlinear Shells.  
Proceedings, IUTAM Symposium on High Speed Computing of Elastic Structures, Liege, 1970. Pp 683 - 705.
52. LANG, R. E.  
HARTZ, B. J. Finite Element Formulations of Post-Buckling Stability & Imperfection Sensitivity.  
Proceedings IUTAM Symposium on High Speed Computing of Elastic Structures. Liege, 1970, Pp. 727-757.
53. WALKER, A. C. A Nonlinear Finite Element Analysis of Shallow Circular Arches.  
International Journal of Solids and Structures, Vol. 5, 1969, Pp 97-107.
54. Pian, T. H. H.  
TONG, P. Variational Formulation of Finite Displacement Analysis.  
Presented at a Colloquium of International Union of Theoretical & Applied Mechanics, (IUTAM) on High Speed Computing of Elastic Structures, University of Leige, Belgium, August, 1970.
55. FAMILI, J.  
ARCHER, R. R. Finite Asymmetric Deformation of Shallow-Spherical Shells.  
AIAA Journal, Vol, 3, No. 3, March 1965, Pp. 506 - 510.
56. KAWAI, T.  
YOSHIMURA, K. N. Analysis of Large Deflection of Plates by the Finite Element Method.  
International Journal for Numerical Methods in Engineering, Vol. 1, 1969, Pp. 123 - 133.



57. CONNOR, J. J.                      Nonlinear Analysis of Elastic  
LOGCHER, R. D.                      Framed Structures.  
CHAN, S.                                Journal of Structural Division,  
Vol. 94, 1968.
58. STRICKLIN, J. A.                  Self-Correcting Initial Value  
HAISLER, W. E.                      Formulation in Nonlinear Structural  
VON RIESEMANN, W.A.                Mechanics.  
AIAA Journal, Vol. 9, No. 10,  
October, 1971.
59. MASSETT, D. A.                    Self-Correcting Incremental Approach  
STRICKLIN, J. A.                    in Nonlinear Structural Mechanics.  
AIAA Journal, Vol. 9, No. 12,  
December, 1971.
60. ODEN, J. T.                        Numerical Formulation of Nonlinear  
Elasticity Problems.  
Journal of the Structures Division,  
Vol. 93, 1967, Pp. 235 - 236.
61. PRZEMIENIECKI, J.S.                Theory of Matrix Structural Analysis.  
McGraw Hill, 1968.
62. NAG Library Manual                Nottingham Algorithm Group
63. HOFF, N. J.                        The Analysis of Structure.  
New York, J. Wiley & Sons, Inc. 1956.
64. COX, H. L.                        The Buckling of Thin Plate in Com-  
pression.  
Reports and Memoranda, Aeronautical  
Research, No. 1554, 1933.
65. TIMOSHENKO, S. P.                Theory of Plates and Shells.  
WOINOWSKY-KRIEGER, S. McGraw Hill, New York, 1959.
66. IRONS, B. M.                        A Frontal Solution Program for  
Finite Element Analysis.  
International Journal for Numerical  
Methods in Engineering, Vol. 2, 1970.
67. ESDU                                Engineering Science Data Item 70001  
Structures Sub-Series.
68. COAN, J. M.                        Large Deflection Theory for Plates  
With Small Initial Curvature  
Loaded in Edge Compression.  
Journal of Applied Mechanics, June,  
1951, Pp. 143 - 151.



69. YAMAKI, N. Postbuckling Behaviour of Rectangular Plates with Small Initial Curvature Loaded in Edge Compression. Journal of Applied Mechanics, Sept. 1959, Pp. 407 - 414.
70. YANG, T. Y. A Finite Element Procedure for Postbuckling Analysis of Initially Curved Plates. Structures, Structural Dynamics, & Material Conference. AIAA/ASME, 1971.
71. BULSON, P. S. The Stability of Flat Plates. London, Chatto & Windus, 1970.
72. ESDU Engineering Science Data Item No. 77014. Structures Sub-Series.
73. TIMOSHENKO, S. P. Theory of Elastic Stability. McGraw Hill Co., New York, 1961.  
GERE, J. M.
74. VIPASA Vibration and Instability of Plate Assemblies Including Shear and Anisotropy.  
A computer program developed at the University of Birmingham by Dr. F. W. Williams, & Mr. M. E. Anderson. January, 1973.
75. ESDU Engineering Science Data Item No. 01.01.21.  
Structure SubSeries
76. DYKES, B. C. Analysis of Displacements in Large Plates by the Grid-Shadow Moire Technique.  
Conference Proceedings: Experimental Stress Analysis. JBCSA, Cambridge, 1970.

A P P E N D I X    A

## A - 1      NOTATION - PROGRAM D67A AND D67B

LNO	Number of elements
A	Element Area
DL	Element length
DI	Element moment of Inertia
E	Element Modulus of Elasticity
NBO	Number of constraint degrees of freedom
NIN	Number of Initial displacements
U	Total displacements
F	Applied load increment
DP	Total load
INCT	Number of increments
NITER	Number of iterations
NOD	Number of nodes
BETA	Initial element rotation

SUBROUTINE SOLV

W	Load vector
AMA	Incremental displacements
EI	Assembled stiffness matrix
UM	Total net displacements

SUBROUTINE TRANSFOR

ES	Elastic stiffness
EG	Geometric stiffness
TATA	Total element rotation
TM	Transformation matrix

SUBROUTINE NODFORCE

UL	Local displacements
AM	Local element forces
AMA	Global element forces
W	Out-of-balance forces

SUBROUTINE ITER

AMA	Displacements due to residual forces
W	Residual forces
U	Total displacements
UM	Total net displacements



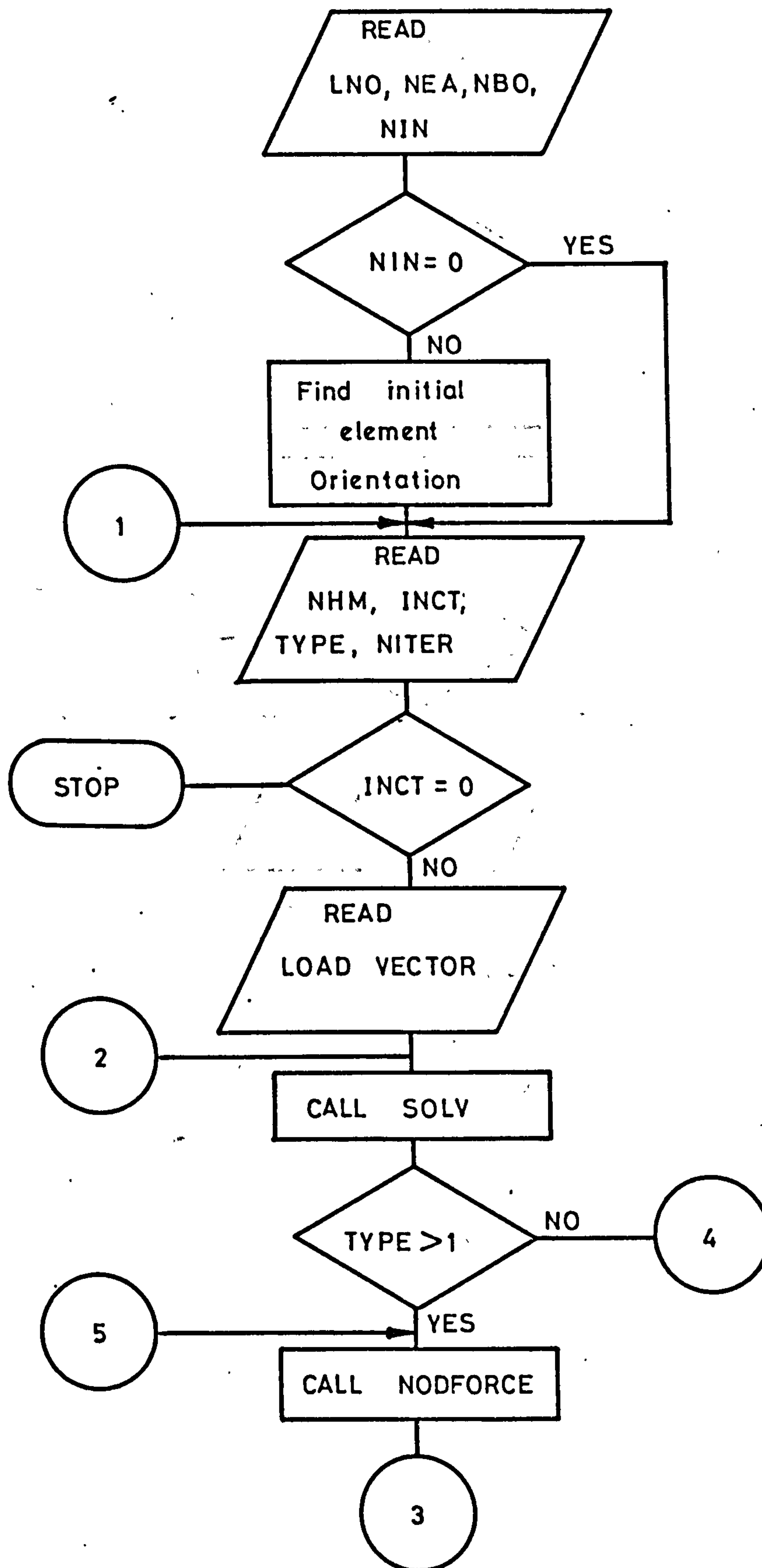
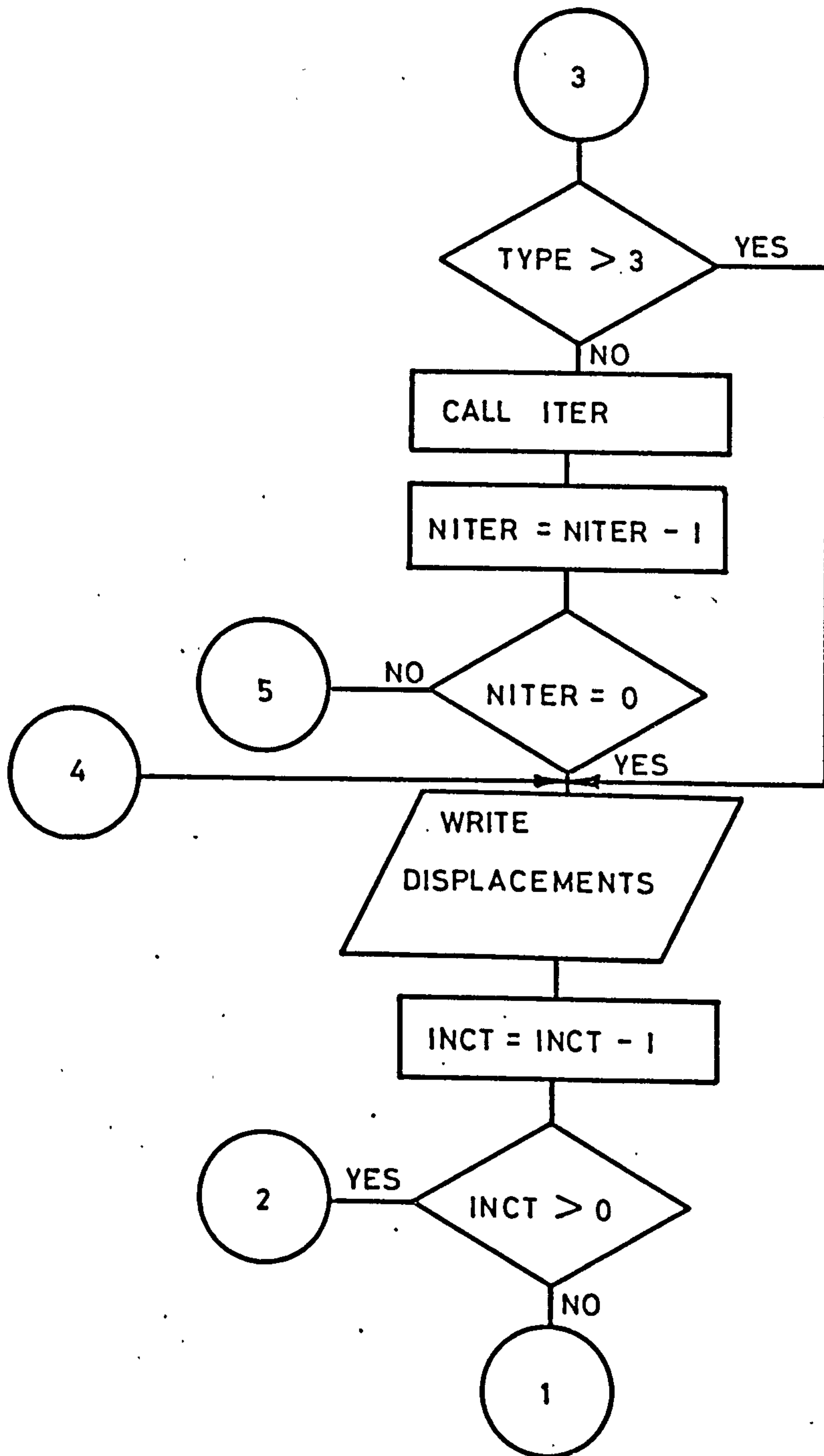
MASTER SEGMENT

FIGURE A-1



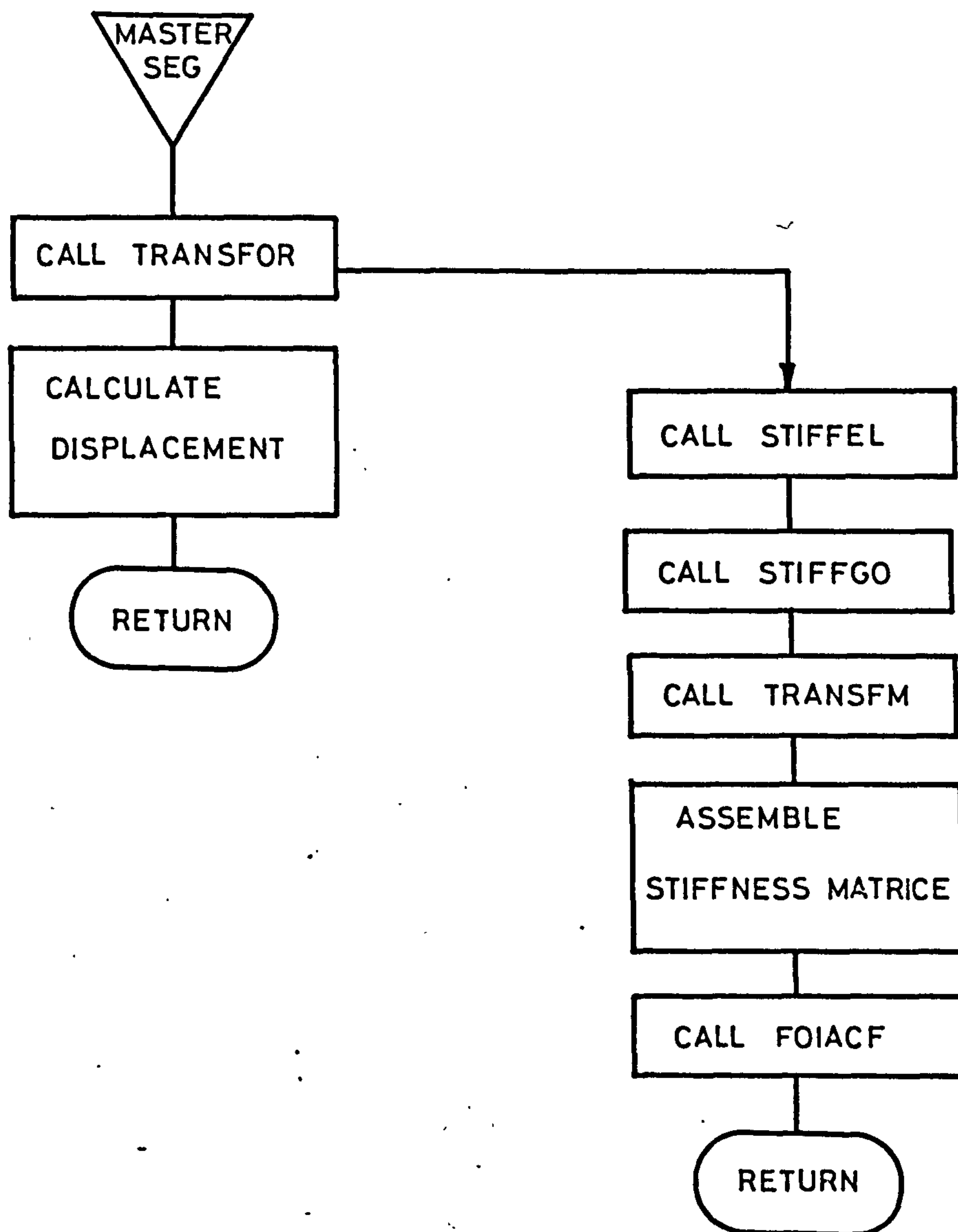
SUBROUTINE SOLV (MOVING COORDINATE SYSTEM)

FIGURE A - 2



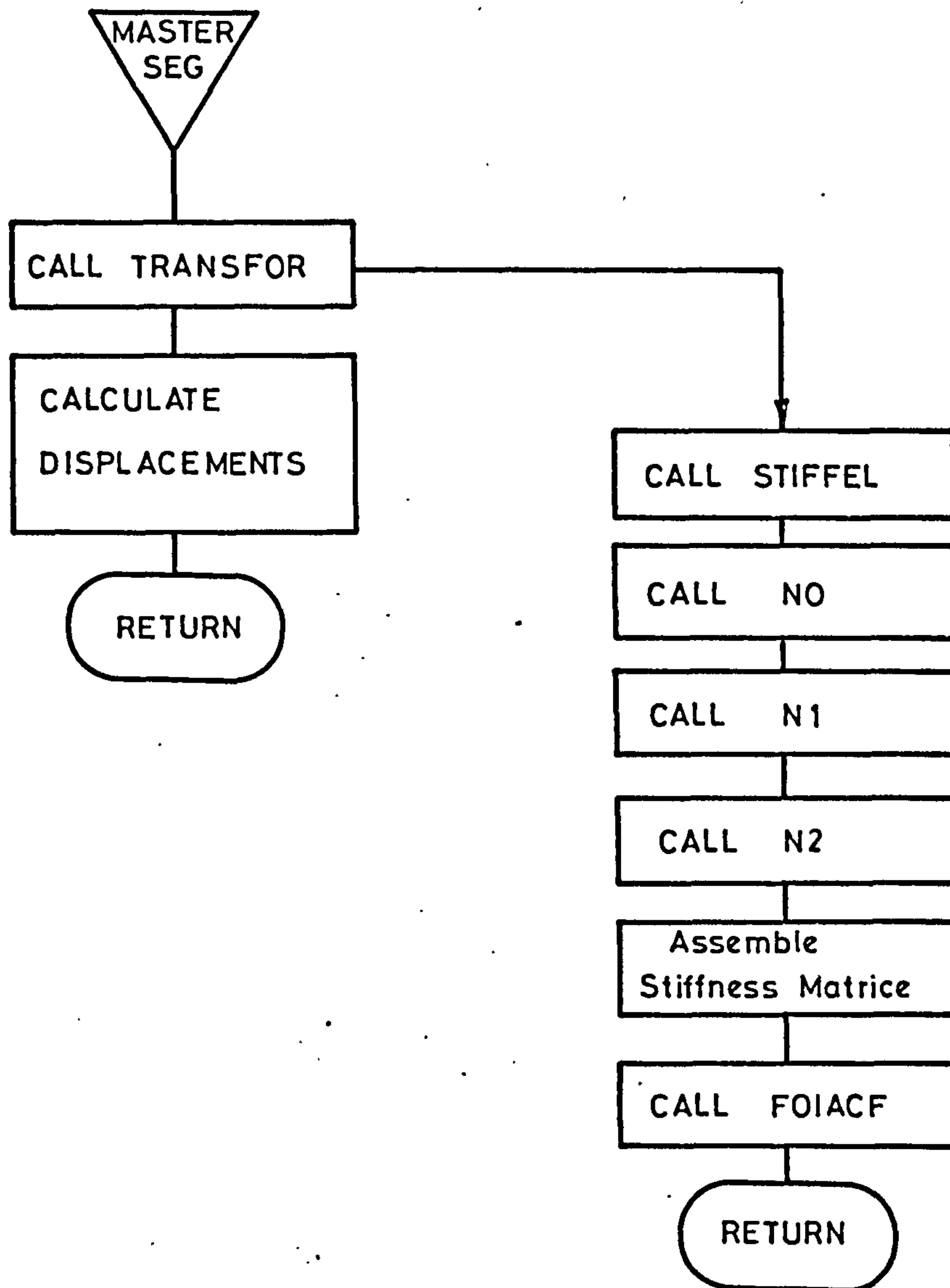
SUBROUTINE SOLV (FIXED COORDINATE SYSTEM)

FIGURE A-3

JOB CA501S,,ALLAHYARI  
 MAXTIME 2000  
 CCFORTRUN D67A,,LIST,2000  
 VOLUME 3000  
 \*\*\*\*

SEND TO(ED,SEMICOMPJOBA)  
 DUMP ON(ED,PROGRAM JOBA)  
 WORK(ED,PROGRAM WRKA(O))  
 LIBRARY (SUBGROUPNAGF)  
 PROGRAM (D67A)  
 INPUT 1=CRO  
 OUTPUT 2=LPO  
 COMPRESS INTEGER AND LOGICAL  
 COMPACT DATA  
 END

C  
C  
C

MASTER SEGMENT

MASTER STRUT  
 DIMENSION U(51),BETA(16)  
 COMMON/PROP/A(16),DL(16),DI(16),E(16)  
 COMMON/S1/ES(6,6),EF(52,52),EE(6,6),EG(6,6)  
 COMMON/S2/B(52,52),Z(52)  
 COMMON/S3/EI(51,51),UM(51)  
 COMMON/S4/SAVE(100),W(51),DP(51),MM(51)  
 COMMON/S5/TM(6,6)  
 COMMON/S6/UL(6),AM(6),AMA(51),P(51),NBC(51),NCC(51)  
 INTEGER TYPE

C  
C  
C  
C  
C

TYPE=1 PURELY INCREMENTAL  
 TYPE=2 INCREMENTAL AND ITERATION BY NEWTON-RAPHSON METHOD  
 TYPE=3 INCREMENTAL AND ITERATION BY MODIFIED NEWTON-RAPHSON METHOD

15 READ(1,15) LNO  
 FORMAT(10)  
 WRITE(2,14) LNO  
 14 FORMAT(1H1,////,52X,15HNO OF ELEMENTS=,15)  
 NJNT=LNO+1  
 NDFT=NJNT\*3  
 READ(1,15) NEA

(CON'T)

```

      IF(NEA) 71,0,400
      NELL=1
      GO TO 401
400  NELL=LNO
401  CONTINUE
      WRITE(2,403)
      DO 404 I=1,NELL
      READ(1,19) NO,A(I),DL(I),DI(I),E(I)
      WRITE(2,405) NO,A(I),DL(I),DI(I),E(I)
404  CONTINUE
19   FORMAT(10,3F0.0,E10.3)
403  FORMAT(/28X,10HELEMENT NO,2X,4HAREA,4X,6HLENGTH
1,2X,17HMOMENT OF INERTIA,2X,21HMODULUS OF ELASTICITY)
405  FORMAT(31X,13,F10.3,F10.3,2X,F10.3,12X,2PE10.3)
      READ(1,15) NBO
      DO 96 I=1,NBO
      READ(1,101) NOD,NUM
      IIA=NOD*3.+NUM-3.
96   MM(I)=IIA
      READ(1,15) NIN
      IF(NIN-1) 1,0,0
      READ(1,17)(U(MX),MX=1,NDF T)
17   FORMAT(3F0.0)
      WRITE(2,18)
18   FORMAT(///,46X,29H****INITIAL DISPLACEMENTS****)
      WRITE(2,300)
302  FORMAT(//44X,36HNODE DEGREES OF FREEDOM TOTAL LOAD)
      DO 27 I=1,NJNT
      JX=I*3-2
      JY=I*3-1
      JXY=I*3
27   WRITE(2,500)(I,U(JX),U(JY),U(JXY))
      DO 50 LL=1,LNO
      KK=KK+3
      IF(NEA) 50,0,406
      LNOO=1
      GO TO 407
406  LNOO=LL
407  CONTINUE
50   BETA(LL)=ATAN((U(KK+2)-U(KK-1))/DL(LNOO))
      KK=0
1    CONTINUE
      READ(1,100) NPO,ACC
100  FORMAT(10,F0.0)
35   READ(1,101) NHM,INCT,TYPE,NITER
101  FORMAT(4I0)
      IF(INCT) 0,71,0

```



(CON'T)

```

GO TO(61,62,63,64) TYPE
61 WRITE(2,21)
21 FORMAT(///,41X,40H***** PURELY INCREMENTAL ***** )
GO TO 24
62 WRITE(2,22)
22 FORMAT(///,29X,62H***** INCREMENTAL AND ITERATION BY NEWTON-RAPHSON
1N METHOD ***** )
GO TO 24
63 WRITE(2,23)
23 FORMAT(///,25X,71H***** INCREMENTAL AND ITERATION BY MODIFIED NEWT
1ON-RAPHSON METHOD ***** )
GO TO 24
64 WRITE(2,25)
25 FORMAT(///32X,48H***** INCREMENTAL PLUS CARRY OVER O.B.FORCES***** )
24 IF(INCT) 0,71,32
READ(1,102) NOD,NUM,F
MMM=NOD*3.+NUM-3.
102 FORMAT(210,F0.0)
TPP=F
GO TO 34
32 CONTINUE
NIHM=0
DO 2 IHM=1,NHM
READ(1,102) NOD,NUM,F
IAA=NOD*3.+NUM-3.
2 P(IAA)=F
301 FORMAT(42X,14,8X,15,10X,F12.5)
INN=INCT
34 CONTINUE
JI=JI+1
DO 94 I=1,NDFT
94 DP(I)=DP(I)+P(I)
WRITE(2,302)
DO 95 I=1,NDFT
INOW=1
IF(DP(I)) 0,95,0
IF(I-3) 0,0,82
NODD=1
NUMM=1
GO TO 83
82 CONTINUE
NOW=I
84 NOW=NOW-3
INOW=INOW+1
IF(NOW-3) 0,0,84
NODD=INOW
NUMM=NOW

```

(CON'T)

```

83  WRITE(2,301)(NODD,NUMM,DP(1))
95  CONTINUE
    CALL SOLV(LNO,NEA,U,NDFT,TYPE,NBO,BETA)
    SAA=AMA(NPO)
    GO TO(31,0,0,33) TYPE
    SA=AMA(NPO)
73  CALL NODFORCE(LNO,NEA,U,BETA,NDFT)
    CALL ITER(LNO,NEA,U,BETA,NDFT,TYPE,NBO)
    NC=NC+1
    SAA=SA+AMA(NPO)
    IF(ABS(SA)-ABS(SAA)) 0,0,80
    IF(NC-NITER) 73,33,0
    IF(ACC-AMA(NPO)/SA) 73,0,0
    GO TO 33
    CALL NODFORCE(LNO,NEA,U,BETA,NDFT)
33  CONTINUE
80  CONTINUE
    WRITE(2,200) NC
    NC=0
31  CONTINUE
    WRITE(2,410)
    WRITE(2,300)
    DO 26 I=1,NJNT
    JX=I*3-2
    JY=I*3-1
    JXY=I*3
26  WRITE(2,500)(I,U(JX),U(JY),U(JXY))
    SAVE(JI)=SAA
    INN=INN-1
    IF(INN) 0,0,34
    IF(INCT) 0,71,35
    FACT=(SAVE(JI)-SAVE(JI-1))/SAVE(JI-1)
    DO 99 I=1,NDFT
99  P(I)=P(I)-FACT*P(I)
    IF(DP(MMM)-TPP) 34,35,35
71  CONTINUE
200  FORMAT(//,45X,15H RESULT FOUND IN,15,11H ITERATIONS)
201  FORMAT(////,50X,11H TOTAL LOAD=,F8.1)
300  FORMAT(/34X,46H  NODE      AXIAL      TRANSVERSE      ROTATION)
500  FORMAT(/34X,15,3X,3(1X,1PE13.6))
410  FORMAT(/46X,29H***** DISPLACEMENTS ***** )
900  FORMAT(5(1X,1PE12.5))
    STOP OK
    END

```

C  
C  
C

ELASTIC STIFFNESS.

SUBROUTINE STIFFEL(L)  
COMMON/PROP/A(16),DL(16),DI(16),E(16)  
COMMON/S1/ES(6,6),EF(52,52),EE(6,6),EG(6,6)  
ES(1,1),ES(4,4)=A(L)\*E(L)/DL(L)  
ES(2,2),ES(5,5)=12.\*E(L)\*DI(L)/DL(L)\*\*3  
ES(3,2),ES(6,2)=6.\*E(L)\*DI(L)/DL(L)\*\*2  
ES(3,3),ES(6,6)=4.\*E(L)\*DI(L)/DL(L)  
ES(4,1)=-ES(1,1)  
ES(5,2)=-ES(2,2)  
ES(5,3),ES(6,5)=-ES(3,2)  
ES(6,3)=2.\*E(L)\*DI(L)/DL(L)  
RETURN  
END

C  
C  
C

GEOMETRIC STIFFNESS

1 SUBROUTINE STIFFGO(TATA,L,BETA,KK,LL)  
DIMENSION U(51),BETA(16)  
COMMON/PROP/A(16),DL(16),DI(16),E(16)  
COMMON/S1/ES(6,6),EF(52,52),EE(6,6),EG(6,6)  
COMMON/S3/EI(51,51),UM(51)  
COMMON/S4/SAVE(100),W(51),DP(51),MM(51)  
DO 1 I=1,6  
DO 1 J=1,1  
EG(I,J)=0.0  
TP=(A(L)\*E(L))\*(((UM(KK+1)-UM(KK-2))-(UM(KK-1)-  
1UM(KK+2))\*TATA)\*(1/DL(L))-0.5\*(TATA-BETA(LL))\*\*2)  
EG(2,2),EG(5,5)=6.\*TP/(5.\*DL(L))  
EG(3,2),EG(6,2)=TP/10.  
EG(3,3),EG(6,6)=2.\*TP\*DL(L)/15.  
EG(6,3)=-2.\*TP\*DL(L)/60.  
EG(5,2)=-EG(2,2)  
EG(5,3),EG(6,5)=-EG(3,2)  
RETURN  
END



## DISPLACEMENT CALCULATION

```

SUBROUTINE SOLV(LNO, NEA, U, NDFT, MOD, NBO, BETA)
DIMENSION U(51), BETA(16)
COMMON/PROP/A(16), DL(16), DI(16), E(16)
COMMON/S3/EI(51, 51), UM(51)
COMMON/S4/SAVE(100), W(51), DP(51), MM(51)
COMMON/S6/UL(6), AM(6), AMA(51), P(51), NBC(51), NCC(51)
CALL TRANSFOR(LNO, NEA, U, NDFT, NBO, BETA)
DO 50 I=1, NDFT
50  W(I)=W(I)+P(I)
DO 1 I=1, NDFT
1   AMA(I)=0.0
DO 6 I=1, NDFT
DO 6 J=1, NDFT
IF(I-J) 0, 0, 8
AMA(I)=EI(J, I)*W(J)+AMA(I)
GO TO 6
8   AMA(I)=EI(I, J)*W(J)+AMA(I)
6   CONTINUE
DO 61 M=1, NDFT
U(M)=U(M)+AMA(M)
61  UM(M)=UM(M)+AMA(M)
DO 78 I=1, NDFT
78  W(I)=0.0
RETURN
END

```

C  
C  
C  
TRANSFORMATION MATRIX

SUBROUTINE TRANSFM(TATA)  
COMMON/S5/TM(6,6)  
TM(1,1),TM(2,2),TM(4,4),TM(5,5)=COS(TATA)  
TM(1,2),TM(4,5)=SIN(TATA)  
TM(2,1),TM(5,4)=-SIN(TATA)  
TM(3,3),TM(6,6)=1.  
RETURN  
END

C  
C  
C  
TRANSFORMATION PROCESS

SUBROUTINE TRANSFOR(LNO,NEA,U,NDFT,NBO,BETA)  
DIMENSION U(51),BETA(16)  
COMMON/PROP/A(16),DL(16),DI(16),E(16)  
COMMON/S1/ES(6,6),EF(52,52),EE(6,6),EG(6,6)  
COMMON/S2/B(52,52),Z(52)  
COMMON/S3/EI(51,51),UM(51)  
COMMON/S4/SAVE(100),W(51),DP(51),MM(51)  
COMMON/S5/TM(6,6)  
DO 3 JM=1,NDFT+1  
DO 3 J=1,JM  
3 EF(J,JM)=0.  
DO 5 IA=1,LNO  
DO 1 I=1,6  
DO 1 J=1,6  
1 EE(I,J)=0.0  
KK=KK+3  
LL=LL+1  
IF(NEA-1) 0,21,21  
LN00=1  
GO TO 22  
21 LN00=IA  
22 CONTINUE  
IF(IA-1) 25,25,0  
IF(LN00-1) 23,23,0  
25 CONTINUE  
CALL STIFFEL(LN00)  
23 CONTINUE  
TATA=ATAN((U(KK+2)-U(KK-1))/DL(LN00))  
CALL STIFFGO(TATA,LN00,BETA,KK,LL)  
DO 10 I=1,6  
DO 10 J=1,1  
10 EG(I,J)=ES(I,J)+EG(I,J)

(CON'T)

```

CALL TRANSFM(TATA)
DO 2 I=1,6
DO 2 J=1,6
DO 2 K=1,6
IF(K-1) 6,0,0
EE(J,I)=TM(K,J)*EG(K,I)+EE(J,I)
GO TO 2
6 EE(J,I)=TM(K,J)*EG(I,K)+EE(J,I)
2 CONTINUE
DO 4 I=1,6
DO 4 J=1,6
DO 4 K=1,6
4 EF(I+KK-3,J+KK-3)=EE(J,K)*TM(K,I)+EF(I+KK-3,J+KK-3)
5 CONTINUE
KK=0
LL=0
DO 50 II=1,NBO
50 EF(MM(II),MM(II))=1.E50
IA=1
ESP=1.E-8
N=NDFT
IEF=52
CALL F01ACF(N,ESP,EF,IEF,B,52,Z,L,IA)
DO 40 II=2,NDFT+1
DO 40 JJ=2,II
40 EI(II-1,JJ-1)=EF(II,JJ-1)
RETURN
END

```



C  
C  
C  
NODAL FORCE CALCULATION

```

SUBROUTINE NODFORCE(LNO, NEA, U, BETA, NDFT)
DIMENSION U(51), BETA(16)
COMMON/PROP/A(16), DL(16), DI(16), E(16)
COMMON/S1/ES(6,6), EF(52,52), EE(6,6), EG(6,6)
COMMON/S3/EI(51,51), UM(51)
COMMON/S4/SAVE(100), W(51), DP(51), MM(51)
COMMON/S5/TM(6,6)
COMMON/S6/UL(6), AM(6), AMA(51), P(51), NBC(51), NCC(51)
DO 9 IB=1, NDFT
9  AMA(IB)=0.0
DO 8 IA=1, LNO
KK=KK+3
LL=LL+1
IF(NEA-1) 0,81,81
LNOO=1
GO TO 82
81  LNOO=IA
82  CONTINUE
TATA=ATAN((U(KK+2)-U(KK-1))/DL(LNOO))
UL(1)=UM(KK-2)*COS(TATA)+.5*(UM(KK+2)-UM(KK-1))*
1  (TATA-BETA(LL))+UM(KK-1)*SIN(TATA)
UL(3)=UM(KK)-(TATA-BETA(LL))
UL(4)=UM(KK+2)*SIN(TATA)+UM(KK+1)*COS(TATA)
UL(6)=UM(KK+3)-(TATA-BETA(LL))
DO 1 I=1,6
1  AM(I)=0.
IF(IA-1) 85,85,0
IF(LNOO-1) 83,83,0
85  CONTINUE
CALL STIFFEL(LNOO)
83  CONTINUE
CALL STIFFGO(TATA, LNOO, BETA, KK, LL)
DO 20 I=1,6
DO 20 J=1,1
20  EG(I,J)=ES(I,J)+EG(I,J)

```

(CON'T)

```

DO 2 I=1,6
DO 2 J=1,6
IF(I-J) 0,0,11
AM(I)=EG(J,I)*UL(J)+AM(I)
GO TO 2
11 AM(I)=EG(I,J)*UL(J)+AM(I)
2  CONTINUE
CALL TRANSFM(TATA)
DO 3 I=1,6
DO 3 J=1,6
3  AMA(I+KK-3)=TM(J,I)*AM(J)+AMA(I+KK-3)
8  CONTINUE
KK=0
LL=0
DO 4 IB=1,NDFT
4  W(IB)=DP(IB)-AMA(IB)
RETURN
END

```

C  
C  
C  
ITERATION BY NEWTON-RAPHSON METHOD

SUBROUTINE ITER(LNO, NEA, U, BETA, NDFT, MOD, NBO)  
 DIMENSION U(51), BETA(16)  
 COMMON/S1/ES(6,6), EF(52,52), EE(6,6), EG(6,6)  
 COMMON/S3/EI(51,51), UM(51)  
 COMMON/S5/TM(6,6)  
 COMMON/S4/SAVE(100), W(51), DP(51), MM(51)  
 COMMON/S6/UL(6), AM(6), AMA(51), P(51), NBC(51), NCC(51)  
 DO 5 IB=1, NDFT  
 5 AMA(IB)=0.0  
 IF(MOD-2) 10, 0, 10  
 CALL TRANSFOR(LNO, NEA, U, NDFT, NBO, BETA)  
 10 CONTINUE  
 DO 6 IB=1, NDFT  
 DO 6 JB=1, NDFT  
 IF(IB-JB) 0, 0, 12  
 AMA(IB)=EI(JB, IB)\*W(JB)+AMA(IB)  
 GO TO 6  
 12 AMA(IB)=EI(IB, JB)\*W(JB)+AMA(IB)  
 6 CONTINUE  
 DO 7 IB=1, NDFT  
 UM(IB)=UM(IB)+AMA(IB)  
 7 U(IB)=U(IB)+AMA(IB)  
 DO 8 I=1, NDFT  
 8 W(I)=0.0  
 RETURN  
 END  
 FINISH



JOB CA501S,,ALLAHYARI  
 MAXTIME 2000  
 CCFORTRUN D67B,,LIST,2000  
 VOLUME 3000  
 \*\*\*\*

SEND TO(ED,SEMICOMPJOB,STORE)  
 DUMP ON(ED,PROGRAM JOBA)  
 WORK(ED,PROGRAM WRKA(O))  
 LIBRARY (SUBGROUPNAGF)  
 PROGRAM (D67B)  
 INPUT 1=CRO  
 OUTPUT 2=LPO  
 COMPRESS INTEGER AND LOGICAL  
 COMPACT DATA  
 TRACE 2  
 END

C  
C  
C

MASTER SEGMENT

MASTER STRUT  
 DIMENSION U(51),BETA(16)  
 COMMON/PROP/A(16),DL(16),DI(16),E(16)  
 COMMON/S1/ES(6,6),EF(52,52)  
 COMMON/S2/B(52,52),Z(52)  
 COMMON/S3/EI(51,51),UM(51)  
 COMMON/S4/SAVE(100),W(51),DP(51),MM(51)  
 COMMON/S6/UL(51),AMA(51),P(51)  
 INTEGER TYPE

C  
C  
C  
C  
C

TYPE=1 PURELY INCREMENTAL  
 TYPE=2 INCREMENTAL AND ITERATION BY NEWTON-RAPHSON METHOD  
 TYPE=3 INCREMENTAL AND ITERATION BY MODIFIED NEWTON-RAPHSON METHOD

15 READ(1,15) LNO  
 FORMAT(10)  
 WRITE(2,14) LNO  
 14 FORMAT(1H1,////,52X,15HNO OF ELEMENTS=,15)  
 NJNT=LNO+1  
 NDFT=NJNT\*3  
 READ(1,15) NEA

(CON'T)

```

IF(NEA) 71,0,763
NELL=1
GO TO 401
763 NELL=LNO
401 CONTINUE
WRITE(2,403)
DO 404 I=1,NELL
READ(1,19) NO,A(I),DL(I),DI(I),E(I)
WRITE(2,405) NO,A(I),DL(I),DI(I),E(I)
404 CONTINUE
19 FORMAT(10,3F0.0,E10.3)
403 FORMAT(/28X,10HELEMENT NO,2X,4HAREA,4X,6HLENGTH
1,2X,17HMOMENT OF INERTIA,2X,21HMODULUS OF ELASTICITY)
405 FORMAT(31X,13,F10.3,F10.3,2X,F10.3,12X,2PE10.3)
READ(1,15) NBO
DO 96 I=1,NBO
READ(1,101) NOD,NUM
IIA=NOD*3.+NUM-3.
96 MM(I)=IIA
READ(1,15) NIN
IF(NIN-1) 1,0,0
READ(1,17)(U(MX),MX=1,NDFT)
17 FORMAT(3F0.0)
WRITE(2,18)
18 FORMAT(///,46X,29H****INITIAL DISPLACEMENTS****)
WRITE(2,300)
302 FORMAT(/44X,36HNODE DEGREES OF FREEDOM TOTAL LOAD)
DO 27 I=1,NJNT
JX=I*3-2
JY=I*3-1
JXY=I*3
27 WRITE(2,500)(I,U(JX),U(JY),U(JXY))
DO 50 LL=1,LNO
KK=KK+3
IF(NEA) 50,0,406
LN00=1
GO TO 407
406 LN00=LL
407 CONTINUE
50 BETA(LL)=ATAN((U(KK+2)-U(KK-1))/DL(LN00))
KK=0
1 CONTINUE
READ(1,100) NPO,ACC
100 FORMAT(10,F0.0)
35 READ(1,101) NHM,INCT,TYPE,NITER
101 FORMAT(410)
IF(INCT) 0,71,0

```

(CON'T)

```

GO TO(61,62,63,64) TYPE
61 WRITE(2,21)
21 FORMAT(///,41X,40H***** PURELY INCREMENTAL ***** )
GO TO 24
62 WRITE(2,22)
22 FORMAT(///,29X,62H***** INCREMENTAL AND ITERATION BY NEWTON-RAPHSON
1N METHOD ***** )
GO TO 24
63 WRITE(2,23)
23 FORMAT(///,25X,71H***** INCREMENTAL AND ITERATION BY MODIFIED NEWT
1ON-RAPHSON METHOD ***** )
GO TO 24
64 WRITE(2,25)
25 FORMAT(///38X,48H*****INCREMENTAL PLUS CARRY OVER O.B.FORCES***** )
24 IF(INCT) 0,71,32
READ(1,102) NOD,NUM,F
MMM=NOD*3.+NUM-3.
102 FORMAT(210,F0.0)
TPP=F
GO TO 34
32 CONTINUE
NIHM=0
DO 2 IHM=1,NHM
READ(1,102) NOD,NUM,F
IAA=NOD*3.+NUM-3.
2 P(IAA)=F
301 FORMAT(42X,i4,8X,i5,10X,F12.5)
INN=INCT
34 CONTINUE
JI=JI+1
DO 94 I=1,NDF T
94 DP(I)=DP(I)+P(I)
WRITE(2,302)
DO 95 I=1,NDF T
INOW=1
IF(DP(I)) 0,95,0
IF(I-3) 0,0,82
NODD=1
NUMM=I
GO TO 83
82 CONTINUE
NOW=I
84 NOW=NOW-3
INOW=INOW+1
IF(NOW-3) 0,0,84
NODD=INOW
NUMM=NOW

```



(CON'T)

```

83  WRITE(2,301)(NODD,NUMM,DP(1))
95  CONTINUE
    CALL SOLV(LNO,NEA,U,NDFT,TYPE,NBO,BETA)
    SAA=AMA(NPO)
    GO TO(31,0,0,33) TYPE
    SA=AMA(NPO)
73  CALL NODFORCE(LNO,NEA,U,BETA,NDFT)
    CALL ITER(LNO,NEA,U,BETA,NDFT,TYPE,NBO)
    NC=NC+1
    SAA=SA+AMA(NPO)
    IF(NC-NITER) 73,33,0
    IF(ABS(SA)-ABS(SAA)) 0,0,80
    IF(ACC-AMA(NPO)/SA) 73,0,0
    GO TO 33
    CALL NODFORCE(LNO,NEA,U,BETA,NDFT)
33  CONTINUE
80  CONTINUE
    WRITE(2,200) NC
    NC=0
31  CONTINUE
    WRITE(2,400)
    WRITE(2,300)
    DO 26 I=1,NJNT
    JX=I*3-2
    JY=I*3-1
    JXY=I*3
26  WRITE(2,500)(I,U(JX),U(JY),U(JXY))
    SAVE(JI)=SAA
    INN=INN-1
    IF(INN) 0,0,34
    IF(INCT) 0,71,35
    FACT=(SAVE(JI)-SAVE(JI-1))/SAVE(JI-1)
    DO 99 I=1,NDFT
99  P(I)=P(I)-FACT*P(I)
    IF(DP(MMM)-TPP) 34,35,35
71  CONTINUE
200  FORMAT(//,45X,15H RESULT FOUND IN,15,11H ITERATIONS)
201  FORMAT(////,50X,11H TOTAL LOAD=,F8.1)
300  FORMAT(/34X,46H  NODE      AXIAL      TRANSVERSE      ROTATION)
500  FORMAT(/34X,15,3X,3(1X,1PE13.6))
400  FORMAT(/46X,29H***** DISPLACEMENTS ***** )
900  FORMAT(5(1X,1PE12.5))
    STOP OK
    END

```

C  
C  
C

ELASTIC STIFFNESS

SUBROUTINE STIFFEL(L)  
COMMON/PROP/A(16),DL(16),DI(16),E(16)  
COMMON/S1/ES(6,6),EF(52,52)  
ES(1,1),ES(4,4)=A(L)\*E(L)/DL(L)  
ES(2,2),ES(5,5)=12.\*E(L)\*DI(L)/DL(L)\*\*3  
ES(3,2),ES(6,2)=6.\*E(L)\*DI(L)/DL(L)\*\*2  
ES(3,3),ES(6,6)=4.\*E(L)\*DI(L)/DL(L)  
ES(4,1)=-ES(1,1)  
ES(5,2)=-ES(2,2)  
ES(5,3),ES(6,5)=-ES(3,2)  
ES(6,3)=2.\*E(L)\*DI(L)/DL(L)  
RETURN  
END

C  
C  
C

ZERO ORDER INCREMENTAL STIFFNESS

SUBROUTINE NO(L,BETA,LL)  
DIMENSION U(51),BETA(16)  
COMMON/PROP/A(16),DL(16),DI(16),E(16)  
COMMON/NODD/ENO(6,6),EN1(6,6),EN2(6,6)  
ENO(2,1),ENO(5,4)=A(L)\*E(L)\*(BETA(LL))/DL(L)  
ENO(2,2),ENO(5,5)=(A(L)\*E(L)/DL(L))\*(BETA(LL))\*\*2  
ENO(4,2),ENO(5,1)=-ENO(2,1)  
ENO(5,2)=-ENO(2,2)  
RETURN  
END

C  
C  
C

FIRST ORDER INCREMENTAL STIFFNESS

SUBROUTINE N1(L,TATA,BETA,LL,KK)  
DIMENSION U(51),BETA(16)  
COMMON/PROP/A(16),DL(16),DI(16),E(16)  
COMMON/S3/EI(51,51),UM(51)  
COMMON/NODD/ENO(6,6),EN1(6,6),EN2(6,6)  
COMMON/S1/ES(6,6),EF(52,52)  
EN1(2,1),EN1(5,4)=A(L)\*E(L)\*(TATA)/DL(L)  
EN1(2,2),EN1(5,5)=-(A(L)\*E(L)/DL(L))\*(UM(KK-2)-UM(KK+1))/DL(L)  
1+3.\*(A(L)\*E(L)/DL(L))\*TATA\*BETA(LL)  
EN1(4,2),EN1(5,1)=-EN1(2,1)  
EN1(5,2)=-EN1(2,2)  
RETURN  
END

C  
C  
C  
SECOND ORDER INCREMENTAL STIFFNESS

SUBROUTINE N2(L,TATA)  
 DIMENSION U(51),BETA(16)  
 COMMON/PROP/A(16),DL(16),DI(16),E(16)  
 COMMON/NODD/ENO(6,6),EN1(6,6),EN2(6,6)  
 EN2(2,2),EN2(5,5)=1.5\*(A(L)\*E(L)/DL(L))\*TATA\*\*2  
 EN2(5,2)=-EN2(2,2)  
 RETURN  
 END

C  
C  
C  
DISPLACEMENT CALCULATION

SUBROUTINE SOLV(LNO,NEA,U,NDFT,MOD,NBO,BETA)  
 DIMENSION U(51),BETA(16)  
 COMMON/PROP/A(16),DL(16),DI(16),E(16)  
 COMMON/S1/ES(6,6),EF(52,52)  
 COMMON/NODD/ENO(6,6),EN1(6,6),EN2(6,6)  
 COMMON/S3/EI(51,51),UM(51)  
 COMMON/S6/UL(51),AMA(51),P(51)  
 COMMON/S4/SAVE(100),W(51),DP(51),MM(51)  
 CALL TRANSFOR(LNO,NEA,U,NDFT,NBO,BETA)  
 DO 50 I=1,NDFT  
 50 W(I)=W(I)+P(I)  
 DO 1 I=1,NDFT  
 1 AMA(I)=0.0  
 DO 6 I=1,NDFT  
 DO 6 J=1,NDFT  
 IF(I-J) 0,0,8  
 AMA(I)=EI(J,I)\*W(J)+AMA(I)  
 GO TO 6  
 8 AMA(I)=EI(I,J)\*W(J)+AMA(I)  
 6 CONTINUE  
 DO 61 M=1,NDFT  
 U(M)=U(M)+AMA(M)  
 61 UM(M)=UM(M)+AMA(M)  
 DO 78 I=1,NDFT  
 78 W(I)=0.0  
 RETURN  
 END



C  
C  
C  
TRANSFORMATION PROCESS

```

SUBROUTINE TRANSFOR(LNO, NEA, U, NDFT, NBO, BETA)
DIMENSION U(51), BETA(16)
COMMON/PROP/A(16), DL(16), DI(16), E(16)
COMMON/S1/ES(6,6), EF(52,52)
COMMON/NODD/ENO(6,6), EN1(6,6), EN2(6,6)
COMMON/S2/B(52,52), Z(52)
COMMON/S3/EI(51,51), UM(51)
COMMON/S4/SAVE(100), W(51), DP(51), MM(51)
DO 3 JM=1, NDFT+1
DO 3 J=1, NDFT+1
3 EF(J, JM)=0.
DO 5 IA=1, LNO
KK=KK+3
LL=LL+1
IF(NEA-1) 0, 21, 21
LN00=1
GO TO 22
21 LN00=IA
22 CONTINUE
IF(IA-1) 25, 25, 0
IF(LN00-1) 23, 23, 0
25 CONTINUE
CALL STIFFEL(LN00)
23 CONTINUE
TATA=ATAN((U(KK+2)-U(KK-1))/DL(LN00))-BETA(LL)
CALL NO(LN00, BETA, LL)
CALL N1(LN00, TATA, BETA, LL, KK)
CALL N2(LN00, TATA)
DO 4 I=1, 6
DO 4 J=1, 1
4 EF(J+KK-3, I+KK-3)=ES(I, J)+ENO(I, J)+EN1(I, J)+EN2(I, J)
1+EF(J+KK-3, I+KK-3)
5 CONTINUE
KK=0
LL=0
DO 50 II=1, NBO
50 EF(MM(II), MM(II))=1.E50
IA=1
ESP=1.E-8
N=NDFT
IEF=52
CALL F01ACF(N, ESP, EF, IEF, B, 52, Z, L, IA)
DO 40 II=2, NDFT+1
DO 40 JJ=2, 11
40 EI(II-1, JJ-1)=EF(II, JJ-1)
RETURN
END

```

C  
C  
C NODAL FORCE CALCULATION

```

SUBROUTINE NODFORCE(LNO,NEA,U,BETA,NDFT)
DIMENSION U(51),BETA(16)
COMMON/PROP/A(16),DL(16),DI(16),E(16)
COMMON/S1/ES(6,6),EF(52,52)
COMMON/S3/EI(51,51),UM(51)
COMMON/S4/SAVE(100),W(51),DP(51),MM(51)
COMMON/S6/UL(51),AMA(51),P(51)
COMMON/NODD/ENO(6,6),EN1(6,6),EN2(6,6)
DO 30 I=1,NDFT
DO 30 J=1,1
30 EF(I,J)=0.0
DO 9 IB=1,NDFT
9 UL(IB)=0.
DO 8 IA=1,LNO
KK=KK+3
LL=LL+1
IF(NEA-1) 0,81,81
LN00=1
GO TO 82
81 LN00=IA
82 CONTINUE
TATA=ATAN((U(KK+2)-U(KK-1))/DL(LN00))-BETA(LL)
CALL NO(LN00,BETA,LL)
CALL N1(LN00,TATA,BETA,LL,KK)
CALL N2(LN00,TATA)
DO 3 I=1,6
DO 3 J=1,1
3 EF(I+KK-3,J+KK-3)=ES(I,J)+ENO(I,J)+.5*EN1(I,J)+(1/3.)*EN2(I,J)
1+EF(I+KK-3,J+KK-3)
8 CONTINUE
DO 22 I=1,NDFT
DO 22 J=1,NDFT
IF(I-J)0,0,21
UL(I)=EF(J,I)*UM(J)+UL(I)
GO TO 22
21 UL(I)=EF(I,J)*UM(J)+UL(I)
22 CONTINUE
KK=0
LL=0
DO 4 IB=1,NDFT
4 W(IB)=DP(IB)-UL(IB)
RETURN
END

```

C  
C  
C  
ITERATION BY NEWTON-RAPHSON METHOD

SUBROUTINE ITER(LNO, NEA, U, BETA, NDFT, MOD, NBO)

DIMENSION U(51), BETA(16)

COMMON/S1/ES(6,6), EF(52,52)

COMMON/S3/EI(51,51), UM(51)

COMMON/S4/SAVE(100), W(51), DP(51), MM(51)

COMMON/S6/UL(51), AMA(51), P(51)

DO 5 IB=1, NDFT

5 AMA(IB)=0.0

IF(MOD-2) 10, 0, 10

CALL TRANSFOR(LNO, NEA, U, NDFT, NBO, BETA)

10 CONTINUE

DO 6 IB=1, NDFT

DO 6 JB=1, NDFT

IF(IB-JB) 0, 0, 12

AMA(IB)=EI(JB, IB)\*W(JB)+AMA(IB)

GO TO 6

12 AMA(IB)=EI(IB, JB)\*W(JB)+AMA(IB)

6 CONTINUE

DO 7 IB=1, NDFT

UM(IB)=UM(IB)+AMA(IB)

7 U(IB)=U(IB)+AMA(IB)

DO 8 I=1, NDFT

8 W(I)=0.0

RETURN

END

FINISH



## INPUT DATA

(Punched on Separate Cards)

DOC DATA-D67A

3

0

1 1. 4.66667 .1 10.0E06

3

1 2

4 1

4 3

1

0. .0 0.

0. .14 0.

0. .2425 0.

0. .28 0.

1 0.

1 2 3 2

1 1 600.

0 0 0 0

272  
SAMPLE OUTPUT

NO OF ELEMENTS= 3

ELEMENT NO	AREA	LENGTH	MOMENT OF INERTIA	MODULUS OF ELASTICITY
1	1.000	4.667	0.100	10.00E 06

\*\*\*\*\*INITIAL DISPLACEMENTS\*\*\*\*\*

NODE	AXIAL	TRANSVERSE	ROTATION
1	0.000000E 00	0.000000E 00	0.000000E 00
2	0.000000E 00	1.400000E-01	0.000000E 00
3	0.000000E 00	2.425000E-01	0.000000E 00
4	0.000000E 00	2.800000E-01	0.000000E 00

\*\*\*\*\* INCREMENTAL AND ITERATION BY MODIFIED NEWTON-RAPHSON METHOD \*\*\*\*\*

NODE	DEGREES OF FREEDOM	TOTAL LOAD
1	1	600.00000

RESULT FOUND IN 2 ITERATIONS

\*\*\*\*\* DISPLACEMENTS \*\*\*\*\*

NODE	AXIAL	TRANSVERSE	ROTATION
1	1.178430E-03	4.288587E-59	1.535320E-03
2	6.878916E-04	1.468512E-01	1.329650E-03
3	2.950980E-04	2.543645E-01	7.676927E-04
4	1.800000E-47	2.936988E-01	5.197331E-48

NODE	DEGREES OF FREEDOM	TOTAL LOAD
1	1	1200.00000

RESULT FOUND IN 2 ITERATIONS

\*\*\*\*\* DISPLACEMENTS \*\*\*\*\*

NODE	AXIAL	TRANSVERSE	ROTATION
1	2.411431E-03	1.467643E-58	3.232610E-03
2	1.396397E-03	1.544256E-01	2.799571E-03
3	5.926286E-04	2.674813E-01	1.616372E-03
4	4.800000E-47	3.088432E-01	1.444773E-47

## A - 2      NOTATION - PROGRAM D67C

SUBROUTINE STIFFEL

A	Element dimension
B	Element dimension
E	Elastic stiffness
V	Element Poisson's ratio
ET	Element modulus of Elasticity
T	Element Thickness

SUBROUTINE TRANSFM

US	Element orientation
N	Node numbering
IKK	Counters for node numbers
TATX	Element rotation 'x' direction
TATY	Element rotation 'y' direction
BETX	Element initial rotation 'x' direction
BETY	Element initial rotation 'y' direction
LNO	Element number
CC	Coefficient factor for incremental stiffness

SUBROUTINE SOLV

NC	Boundary Condition Counter (Constraint B.C.)
NE	Number of Eliminations performed
NR	Lowest node number in an element
NS	Highest node number in an element
NW	Back substitution number
LNO	Element number
NNAA	Disc back-substitution number
KST	Initial Disc number
NWW	Total back-substitution number
MODE	Type of procedure
N	Node number
IKK	Counters for node number
DU	Incremental displacements
U	Total displacements
UM	Total net displacements

SUBROUTINE ELIM

M	Degrees of freedom code (see input data)
NFF	"Coupling" degrees of freedom
NF2	"Coupling" degrees of freedom
EE	Assembled stiffness matrix
ILL	Counters for degrees of freedom number



MM	Number of back-substitution coefficients stored
VI	Inverse diagonal matrix
W	Back-substitution coefficient

SUBROUTINE NODFORCE

F	Element force vector
UM	Total net displacements
EE	Assembled stiffness matrix

275  
MASTER SEGMENT

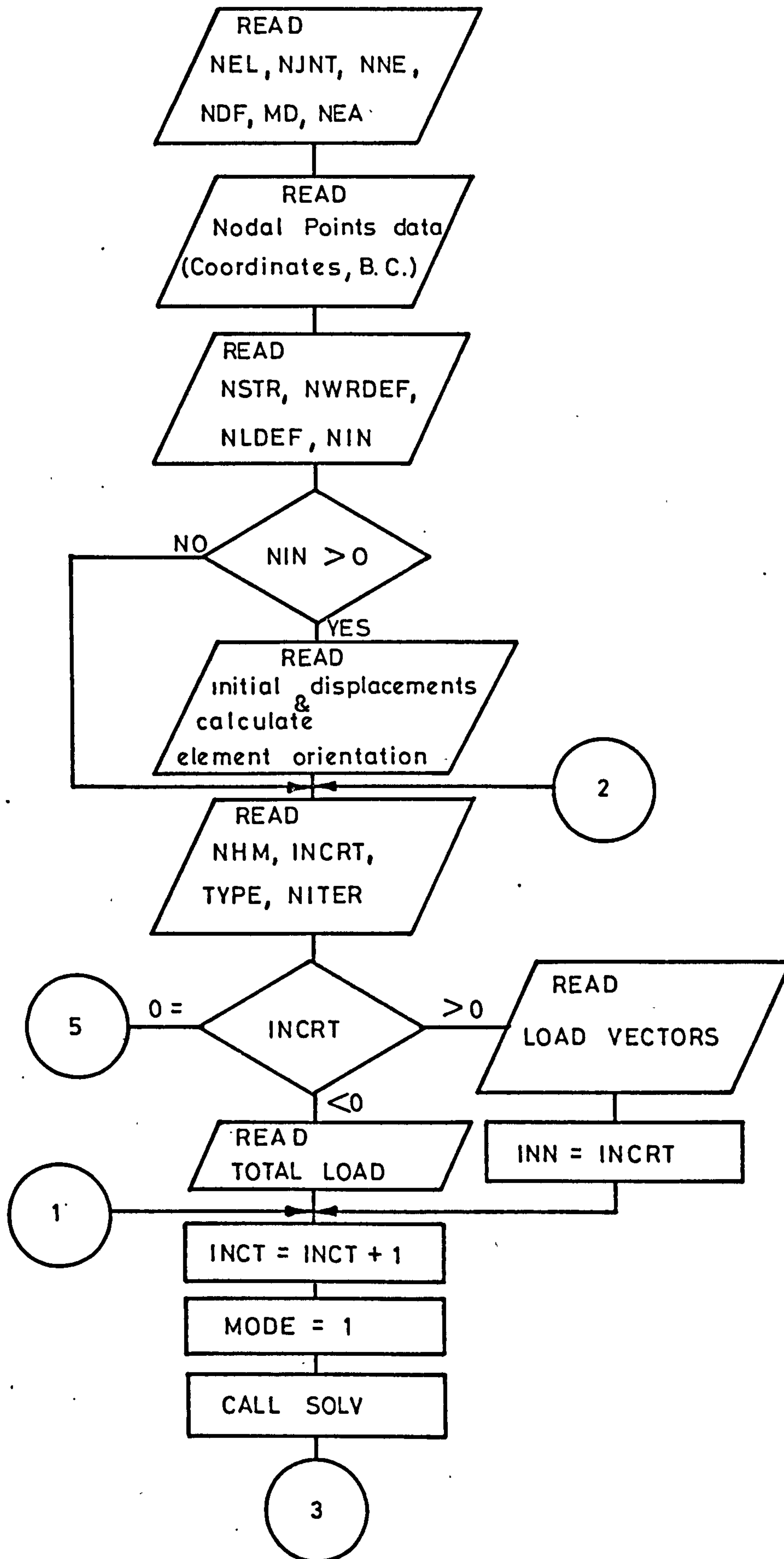
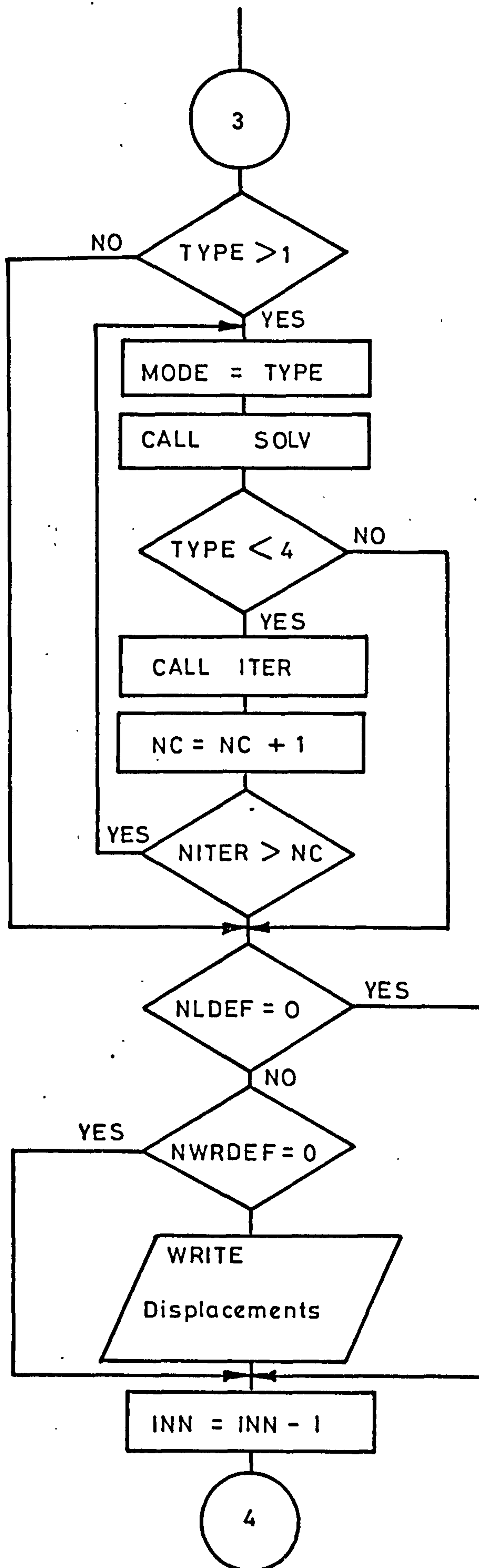
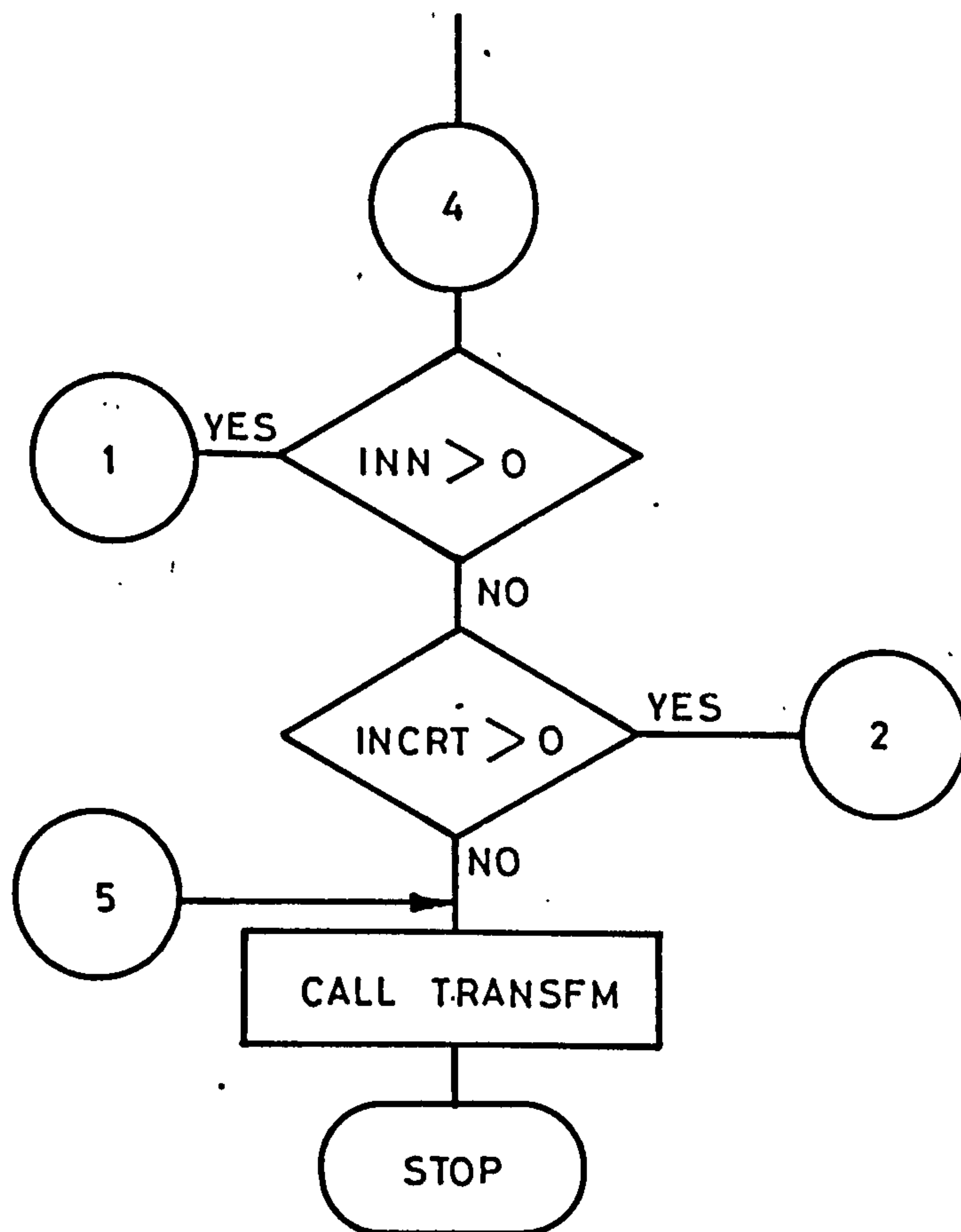


FIGURE A - 4







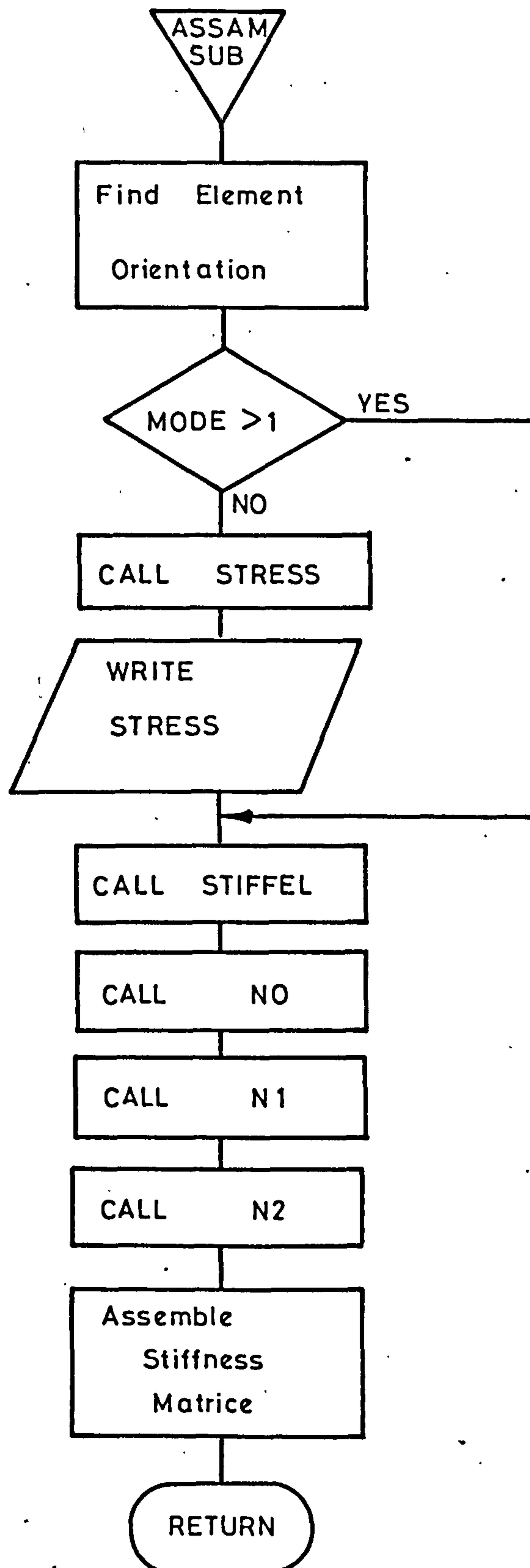
SUBROUTINE TRANSFM

FIGURE A - 5

## SUBROUTINE SOLV

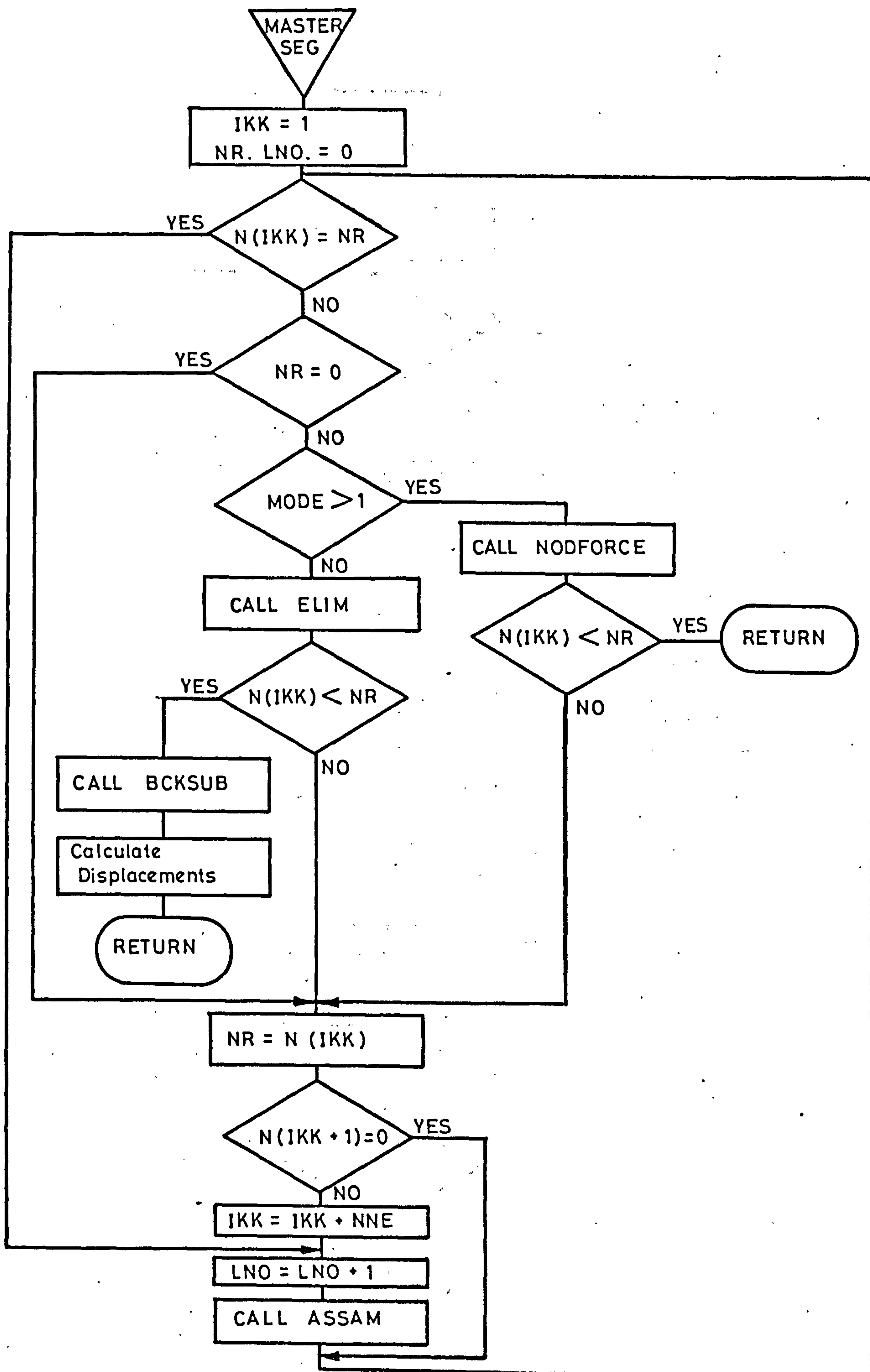


FIGURE A-6



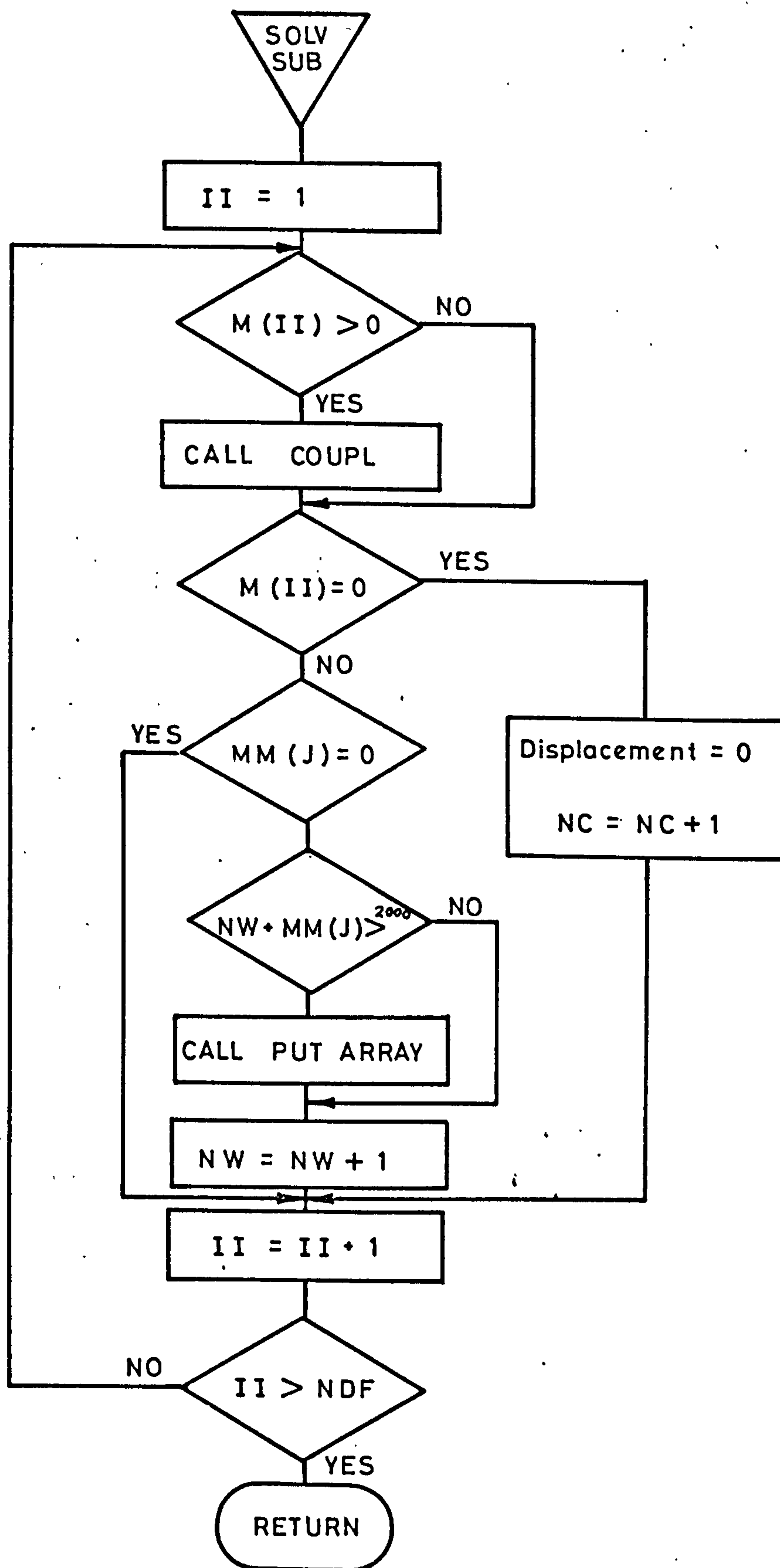
SUBROUTINE ELIM

FIGURE A-7

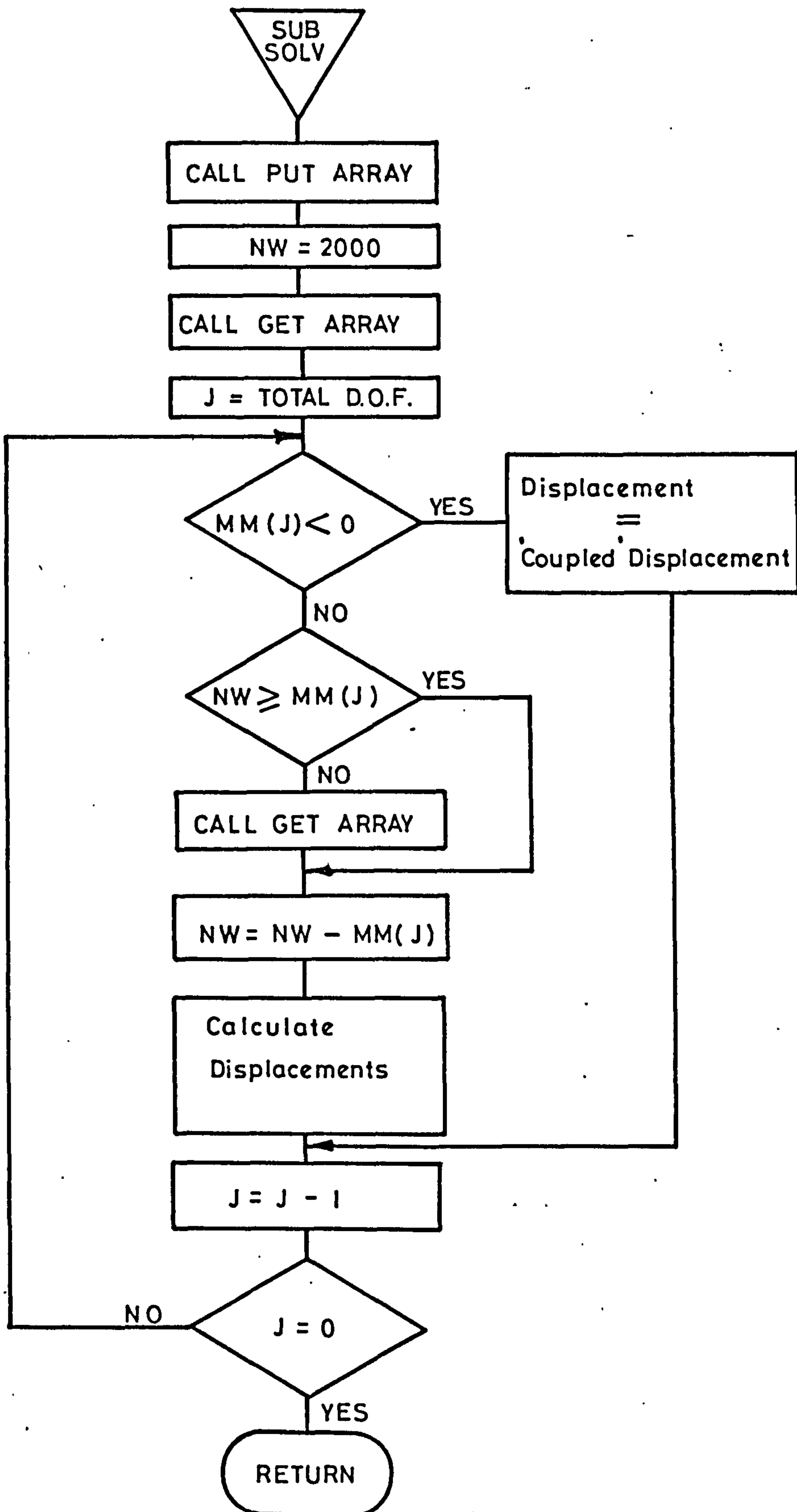
SUBROUTINE BCKSUB

FIGURE A-8

282  
SUBROUTINE ITER

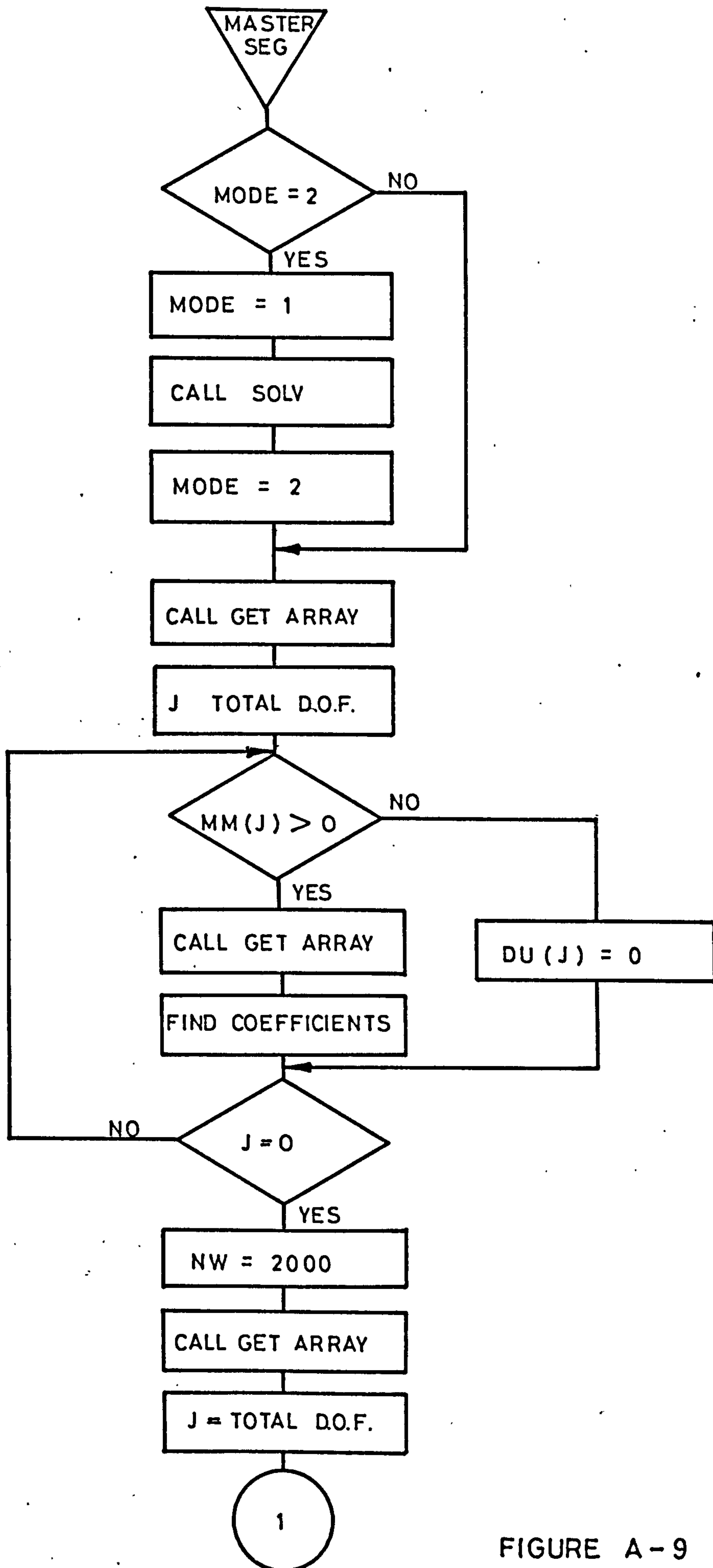
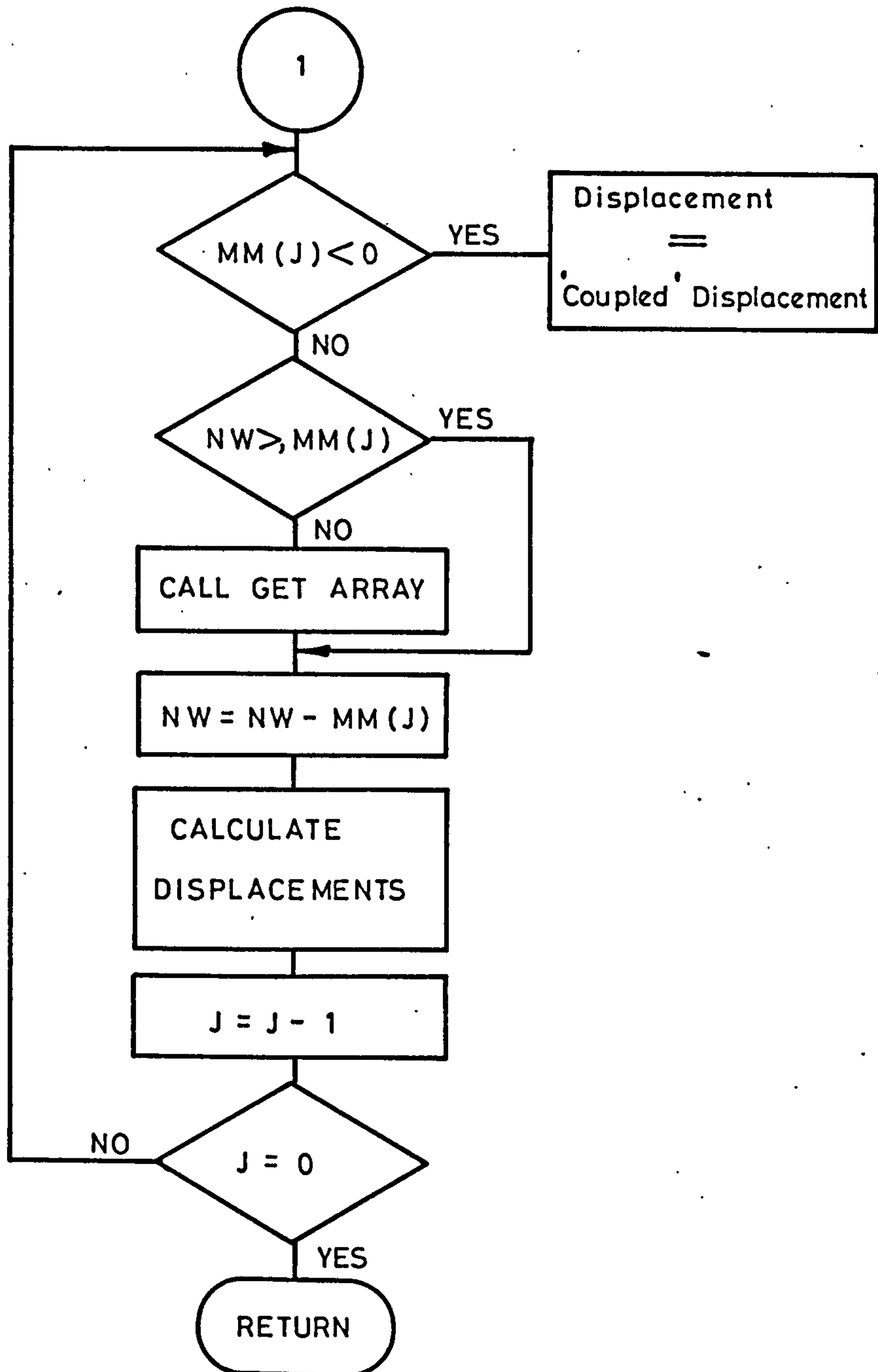


FIGURE A-9





JOB CA501S,,ALLAHYARI  
 MAXTIME 2000  
 CCFORTRUN D67C,,LIST,2000  
 VOLUME 3000  
 \*\*\*\*\*

SEND TO(ED,SEMICOMPJOBA,STORE)  
 DUMP ON(ED,PROGRAM JOBA)  
 WORK(ED,PROGRAM WRKA(0))  
 PROGRAM(D67C)  
 INPUT1 =CRO  
 OUTPUT 2=LP0  
 COMPRESS INTEGER AND LOGICAL  
 END

MASTER SEGMENT

MASTER PLATE BUCKLING  
 COMMON/US/US(20),SAVE(100)  
 COMMON/STIFE/E(20,20),ENO(20,20),EN1(20,20),EN2(20,20)  
 COMMON/ANG/BETX(200),BETY(200)  
 COMMON/PROP/A(200),B(200),T(200),V(200),ET(200)  
 COMMON/BS/W(2000),MM(1210),EE(70,70)  
 COMMON/COEF/VI(1210),DP(1210)  
 COMMON/DISP/U(1210),DU(1210),UM(1280)  
 COMMON/NODE/N(972),M(1210),MMM(7)  
 COMMON/INFRC/F(1210),P(1210),FI(1280)  
 COMMON/STDF/NST(200),NDEF(1210),NLL(100)  
 INTEGER TYPE

TYPE=1 PURELY INCREMENTAL  
 TYPE=2 INCREMENTAL AND ITERATION BY NEWTON-RAPHSON METHOD  
 TYPE=3 INCREMENTAL AND ITERATION BY MODIFIED NEWTON-RAPHSON METHOD

CALL USE FILE(4,2HED,12HDE117ALLAHYA,0,0)  
 READ(1,100) NEL  
 WRITE(2,70) NEL  
 70 FORMAT(1H1,////,48X,16HNO. OF ELEMENTS=,12)  
 READ(1,100) NJNT  
 WRITE(2,72) NJNT  
 72 FORMAT(/48X,13HNO. OF NODES=,13)  
 READ(1,100) NNE  
 WRITE(2,80) NNE  
 80 FORMAT(/48X,25HNO. OF NODES PER ELEMENT=,14)

(CON'T)

```

      READ(1,100) NDF
      WRITE(2,71) NDF
71    FORMAT(/48X,26HNO. OF DEGREES OF FREEDOM=,12)
      READ(1,100) MD
      WRITE(2,669) MD
669   FORMAT(/48X,17HMATRIX DIMENSION=,13)
      READ(1,100) NEA
      IF(NEA) 3,0,888
      NELL=1
      GO TO 999
888   NELL=NEL
999   CONTINUE
      WRITE(2,702)
      DO 701 I=1,NELL
      READ(1,19) NO,A(I),B(I),T(I),V(I),ET(I)
      WRITE(2,703)(NO,A(I),B(I),T(I),V(I),ET(I))
701   CONTINUE
703   FORMAT(23X,13,4X,F9.2,7X,F9.2,2X,F10.3,5X,F10.3,9X,2PE10.3)
702   FORMAT(/18X,10HELEMENT NO,2X,14HELEMENT LENGTH,2X,13HELEMENT . WIDTH
1,2X,9HTHICKNESS,2X,13HPOISSON RATIO,2X,21HMODULUS OF ELASTICITY)
19    FORMAT(10,4F0.0,E10.3)
      NDFT=NJNT*NDF
      DO 865 I=1,NJNT+1
      READ(1,100)(N(NKE+INK),INK=1,NNE)
865   NKE=NKE+NNE
      WRITE(2,73)
73    FORMAT(/44X,30H***ELEMENT NUMBERING SYSTEM***/)
      DO 866 I=1,NJNT+1
      WRITE(2,200)(N(NKK+NCS),NCS=1,NNE)
866   NKK=NKK+NNE
      READ(1,100) NNBC
      WRITE(2,74)
      DO 666 IKI=1,NNBC
      READ(1,100) (MMM(IR),IR=1,NDF+1)
      WRITE(2,201)(MMM(IR),IR=1,NDF+1)
      DO 667 I=1,NDF
      ICU=NDF*MMM(1)-NDF+1
667   M(ICU)=MMM(I+1)
666   CONTINUE
74    FORMAT(/48X,25H***BOUNDARY CONDITIONS***/
1      45X,4HNODE,8X,11HD . O . F ./)
      READ(1,100) NSTR
      IF(NSTR) 401,401,0
      DO 402 I=1,NSTR
      READ(1,100) NSTRR
402   NST(NSTRR)=1
401   CONTINUE
      READ(1,100) NWRDEF

```



(CON'T)

```

      IF(NWRDEF) 416,416,0
      DO 403 I=1,NWRDEF
      READ(1,100) NODDEF
403  NDEF(NODDEF)=1
416  CONTINUE
      READ(1,100) NLDEF
      IF(NLDEF) 405,405,0
      DO 404 IL=1,NLDEF
      READ(1,90) NOD,NUM,TLOAD
      NDLD=NOD*NDF-NDF+NUM
404  NLL(IL)=TLOAD
      ICC=1
405  CONTINUE
      READ(1,100) NIN
      IF(NIN-1) 1,0,0
      DO 91 IIN=1,NIN
      READ(1,90) NOD,NUM,DEF
90  FORMAT(210,F0.0)
      IAA=NOD*NDF+NUM-NDF
      U(IAA)=DEF
91  CONTINUE
      WRITE(2,18)
18  FORMAT(/,,/,46X,29H*****INITIAL DISPLACEMENTS*****/)
      WRITE(2,77)
77  FORMAT(/24X,69HNODE          U          V          W          X-ROT
1ATION  Y-ROTATION/)
      DO 27 I=1,NJNT
      WRITE(2,500) I,(U(IGL+IR),IR=1,NDF)
27  IGL=IGL+NDF
500  FORMAT(22X,15,2X,5(1X,1PE12.5))
      DO 1 I=1,NEL
      IF(N(NN+2)) 0,0,777
      NN=NN+NNE
777  CONTINUE
      US(3)=U(N(NN+1)*NDF-2)
      US(8)=U(N(NN+2)*NDF-2)
      US(13)=U(N(NN+3)*NDF-2)
      US(18)=U(N(NN+4)*NDF-2)
      IF(NEA-1) 0,496,496
      LN00=1
      GO TO 497
496  LN00=1
497  CONTINUE
      BETX(1)=(US(8)-US(3)+US(13)-US(18))/(2.*A(LN00))
      BETY(1)=(US(18)-US(3)+US(13)-US(8))/(2.*B(LN00))
      NN=NN+NNE
1  CONTINUE
      READ(1,90) NOD,NUM,ACC

```

(CON'T)

```

NPO=NOD*NDF-NDF+NUM
300 FORMAT(/44X,36HNODE DEGREES OF FREEDOM TOTAL LOAD)
96 READ(1,100) NHM, INCRT, TYPE, NITER
DO 711 I=1, NDFT
711 P(I)=0.0
    IF(INCRT) 0,3,0
    IF(LONG-1) 0,51,51
    GO TO(61,62,63,64) TYPE
61 WRITE(2,21)
21 FORMAT(/,42X,40H***** PURELY INCREMENTAL ***** )
    GO TO 24
62 WRITE(2,22)
22 FORMAT(/,29X,62H***** INCREMENTAL AND ITERATION BY NEWTON-RAPHSON
1N METHOD ***** )
    GO TO 24
63 WRITE(2,23)
23 FORMAT(/,25X,71H***** INCREMENTAL AND ITERATION BY MODIFIED NEWT
1ON-RAPHSON METHOD ***** )
    GO TO 24
64 WRITE(2,25)
25 FORMAT(/,38X,48H***** INCREMENTAL PLUS CARRY OVER O.B.FORCES***** )
24 IF(LONG-1) 0,52,52
51 CONTINUE
    IF(INCRT) 0,3,93
    READ(1,90) NOD, NUM, ALOAD
    MMI=NOD*NDF-NDF+NUM
    TPP=ALOAD
    GO TO 40
93 CONTINUE
    NIHM=0
    DO 2 IHM=1, NHM
    READ(1,90) NOD, NUM, ALOAD
    IAA=NOD*NDF+NUM-NDF
2 P(IAA)=ALOAD
    INN=INCRT
40 CONTINUE
    INCT=INCT+1
    DO 94 I=1, NDFT
    DU(I)=P(I)+F(I)
94 DP(I)=DP(I)+P(I)
    IF(LONG-1) 0,55,55
    WRITE(2,300)
    DO 41 I=1, NDFT
    INOW=1
    IF(DP(I)) 0,41,0
    IF(I-NDF) 0,0,86
    NODD=1
    NUMM=1

```

(CON'T)

```

      GO TO 88
86  CONTINUE
      NOW=1
87  NOW=NOW+NDF
      INOW=INOW+1
      IF(NOW-NDF) 0,0,87
      NODD=INOW
      NUMM=NOW
88  WRITE(2,301)(NODD,NUMM,DP(1))
41  CONTINUE
55  CONTINUE
301  FORMAT(43X,14,8X,15,8X,F12.5)
      MODE=1
      CALL SOLV(NEA,MD,NDF,MODE,NSS,NEL,NDFT,NNE,IGN,INCT,NSTR,MI,NLDEF)
      MI=0
      SAA=DU(NPO)
      IF(TYPE-2) 26,0,0
      SA=DU(NPO)
      SAG=1.E50
97  CONTINUE
      F(1)=0.0
      CALL FMOVE(F(1),F(2),(NDFT-1))
      FI(1)=0.0
      CALL FHOVE(FI(1),FI(2),(NDFT+MD-1))
      MODE=TYPE
      CALL SOLV(NEA,MD,NDF,MODE,NSS,NEL,NDFT,NNE,IGN,INCT,NSTR,MI,NLDEF)
      DO 98 I=1,NJNT
      DO 926 J=1,NDF
      IF(M(J+ILL)) 926,926,0
      NMM=M(J+ILL)*NDF-NDF+J
      F(NMM)=F(NMM)+F(ILL+J)
926 CONTINUE
      ILL=ILL+NDF
98  CONTINUE
      ILL=0
      DO 50 I=1,NDFT
50  F(I)=DP(I)-F(I)
      IF(TYPE-3) 0,0,33
      CALL ITER(NEA,MD,NDF,MODE,NSS,NEL,NDFT,NNE,IGN,INCT,NSTR,MI,NLDEF)
      NC=NC+1
      SAA=SA+DU(NPO)
      IF(NC-NITER) 97,33,0
      IF(ACC) 0,33,0
      IF(ABS(DU(NPO))-SAG) 0,0,85
      SAG=ABS(DU(NPO))
      SAGG=SAG/ABS(SA)
      IF(ACC-SAGG) 97,0,0

```



(CON'T)

```

IF(ACC-DU(NPO)/SA) 97,0,0
33 CONTINUE
85 CONTINUE
WRITE(2,207) NC
NC=0
26 CONTINUE
IF(LONG-1) 56,0,0
GO TO(61,62,63,64) TYPE
52 CONTINUE
WRITE(2,300)
DO 57 I=1,NDF T
INOW=1
IF(DP(I)) 0,57,0
IF(I-NDF) 0,0,89
NODD=1
NUMM=1
GO TO 600
89 CONTINUE
NOW=1
601 NOW=NOW-NDF
INOW=INOW+1
IF(NOW-NDF) 0,0,601
NODD=INOW
NUMM=NOW
600 WRITE(2,301)(NODD,NUMM,DP(I))
57 CONTINUE
56 CONTINUE
LONG=1
IF(NLDEF) 407,406,0
IF(DP(NDLN)-NLL(ICC)) 406,0,0
ICC=ICC+1
MI=1
407 CONTINUE
IF(NWRDEF) 0,406,0
WRITE(2,204)
WRITE(2,77)
DO 76 I=1,NJNT
IF(NWRDEF) 408,76,0
IF(NDEF(I)) 0,411,0
408 CONTINUE
WRITE(2,500) I,(U(ICL+IR),IR=1,NDF)
411 ICL=ICL+NDF
76 CONTINUE
406 CONTINUE
ICL=0
SAVE(INCT)=SAA
INN=INN-1

```

(CON'T)

```

IF(INN) 0,0,40
IF(INCRT) 0,3,96
FACT=(SAVE(INCT)-SAVE(INCT-1))/SAVE(INCT-1)
DO 99 I=1,NDFT
99 P(I)=P(I)-FACT*P(I)
IF(DP(MMI)-TPP) 40,96,96
3 CONTINUE
LSTR=1
LNO=0
IKK=1
DO 555 I=1,NEL
LNO=LNO+1
IF(N(IKK+1)) 0,0,556
IKK=IKK+NNE
556 CONTINUE
CALL TRANSFM(NEA,NDF,MODE,LNO,IGN,INCT,NSTR,IKK,MI,NLDEF,LSTR)
IKK=IKK+NNE
555 CONTINUE
CALL FREEFILE(4)
100 FORMAT(1310)
101 FORMAT(110,510)
200 FORMAT(47X,1315)
201 FORMAT(45X,13,715)
203 FORMAT(5(1X,1PE13.6))
204 FORMAT(/45X,35H***** DISPLACEMENTS *****/)
207 FORMAT(/,45X,15H RESULT FOUND IN,15,11H ITERATIONS)
STOP OK
END

```

## ELASTIC STIFFNESS

```

SUBROUTINE STIFFEL(LO)
COMMON/PROP/A(200),B(200),T(200),V(200),ET(200)
COMMON/STIFE/E(20,20),ENO(20,20),EN1(20,20),EN2(20,20)
C=(B(LO)/A(LO))**2
D=(A(LO)/B(LO))**2
E1=B(LO)/A(LO)
F=A(LO)/B(LO)
AA=(ET(LO)*T(LO))/(12*(1-(V(LO)**2)))
BB=ET(LO)*(T(LO)**3)/(12*(1-(V(LO)**2))*A(LO)*B(LO))
E(1,1),E(6,6),E(11,11),E(16,16)=(((4*E1)+(2*(1-V(LO))*F))*AA)
E(2,2),E(7,7),E(12,12),E(17,17)=((4*F)+(2*(1-V(LO))*E1))*AA
E(3,3),E(8,8),E(13,13),E(18,18)=(4*(C+D)+1./5*(14-(4*V(LO))))*BB
E(4,4),E(9,9),E(14,14),E(19,19)=(4./3*D+4./15*(1-V(LO)))
1*(B(LO)**2)*BB
E(5,5),E(10,10),E(15,15),E(20,20)=(4./3*C+4./15*(1-V(LO)))
1*(A(LO)**2)*BB
E(2,1),E(16,7),E(12,11),E(17,6)=(3./2*(1+V(LO)))*AA
E(4,3),E(9,8)=-(2*D+1./5*(1+(4*V(LO))))*B(LO)*BB
E(5,3),E(20,18)=-(2*C+1./5*(1+(4*V(LO))))*A(LO)*BB
E(5,4),E(15,14)=V(LO)*A(LO)*B(LO)*BB
E(6,1),E(16,11)=((-4*E1)+(1-V(LO))*F)*AA
E(7,2),E(17,12)=((2*F)-(2*(1-V(LO))*E1))*AA
E(7,6),E(11,2),E(12,1),E(17,16)=(-3./2*(1+V(LO)))*AA
E(8,3),E(18,13)=(-2*((2*C)-D)-1./5*(14-(4*V(LO))))*BB
E(8,4),E(9,3)=(-D+1./5*(1+(4*V(LO))))*B(LO)*BB
E(8,5),E(20,13)=(2*C+1./5*(1-V(LO)))*A(LO)*BB
E(9,4),E(19,14)=(2./3*D-4./15*(1-V(LO)))*(B(LO)**2)*BB
E(10,5),E(20,15)=(2./3*C-1./15*(1-V(LO)))*(A(LO)**2)*BB
E(10,8),E(15,13)=(2*C+1./5*(1+(4*V(LO))))*A(LO)*BB
E(10,9),E(20,19)=-V(LO)*A(LO)*B(LO)*BB
E(11,6),E(16,1)=((2*E1)-(2*(1-V(LO))*F))*AA
E(11,7),E(6,2),E(17,1),E(16,12)=(3./2*(1-(3*V(LO))))*AA
E(12,6),E(7,1),E(17,11),E(16,2)=(-3./2*(1-(3*V(LO))))*AA
E(12,7),E(17,2)=((-4*F)+(1-V(LO))*E1)*AA
E(13,3),E(18,8)=(-2*(C+D)+1./5*(14-(4*V(LO))))*BB
E(13,4),E(18,9)=(D-1./5*(1-V(LO)))*B(LO)*BB
E(13,5),E(20,8)=(C-1./5*(1-V(LO)))*A(LO)*BB
E(13,9)=(2*D+1./5*(1-V(LO)))*B(LO)*BB
E(14,3),E(19,8)=(-D+1./5*(1-V(LO)))*B(LO)*BB
E(14,4)=(1./3*D+1./15*(1-V(LO)))*(B(LO)**2)*BB
E(14,9),E(19,4)=(2./3*D-1./15*(1-V(LO)))*(B(LO)**2)*BB
E(15,8),E(13,10)=(C-1./5*(1+(4*V(LO))))*A(LO)*BB
E(15,3),E(18,10)=(-C+1./5*(1-V(LO)))*A(LO)*BB
E(15,5),E(20,10)=(1./3*C+1./15*(1-V(LO)))*(A(LO)**2)*BB

```



(CON'T)

```

E(18,3),E(13,8)=(2*(C-(2*D))-1./5*(14-(4*V(LO))))*BB
E(17,7),E(12,2)=((-2*F)-(E1*(1-V(LO))))*AA
E(16,6),E(11,1)=((-2*E1)-((1-V(LO))*F))*AA
E(18,15),E(10,3)=- (2*C+1./5*(1-V(LO)))*A(LO)*BB
E(14,13),E(19,18)=(2*D+1./5*(1+(4*V(LO))))*B(LO)*BB
E(19,3),E(14,8)=(-2*D-1./5*(1-V(LO)))*B(LO)*BB
E(19,9)=(1./3*D+1./15*(1-V(LO)))*(B(LO)**2)*BB
E(20,5),E(15,10)=(2./3*C-4./15*(1-V(LO)))*(A(LO)**2)*BB
E(18,4)=(2*D+1./5*(1-V(LO)))*B(LO)*BB
E(19,13),E(18,14)=(D-1./5*(1+(4*V(LO))))*B(LO)*BB
E(20,3),E(18,5)=(-C+1./5*(1+(4*V(LO))))*A(LO)*BB
RETURN
END

```

C  
C  
C

ZERO ORDER INCREMENTAL STIFFNESS

```

SUBROUTINE NO(LO,L,CC)
COMMON/PROP/A(200),B(200),T(200),V(200),ET(200)
COMMON/STIFE/E(20,20),ENO(20,20),EN1(20,20),EN2(20,20)
COMMON/ANG/BETX(200),BETY(200)
D=B(LO)/A(LO)
F=A(LO)/B(LO)
ENO(1,1)=0.0
CALL FMOVE(ENO(1,1),ENO(2,1),399)
ENO(3,1)=CC*(2.*D*BETX(L)+2.*V(LO)*BETY(L))
ENO(3,2)=CC*(2.*V(LO)*BETX(L)+2.*F*BETY(L))
ENO(3,3)=CC*(2.*D*BETX(L)**2+2.*F*BETY(L)**2-V(LO)*D*BETY(L)**2
1+4.*BETX(L)*BETY(L)+D*BETY(L)**2+F*BETX(L)**2-V(LO)*F*BETX(L)**2
2-2.*(1-V(LO))*BETX(L)*BETY(L))
ENO(6,3)=CC*(-2.*D*BETX(L)-2.*V(LO)*BETY(L)+2.*(1-V(LO))
1*BETY(L)+2.*(1-V(LO))*F*BETX(L))
ENO(7,3)=ENO(3,2)
ENO(8,1)=CC*(-2.*D*BETX(L)+2.*V(LO)*BETY(L))
ENO(8,2)=CC*(-2.*V(LO)*BETX(L)+2.*F*BETY(L))
ENO(8,3)=CC*(-2.*D*BETX(L)**2+D*V(LO)*BETY(L)**2+2.*F*BETY(L)**2
1+F*BETX(L)**2-D*BETY(L)**2-F*V(LO)*BETX(L)**2)
ENO(8,6)=CC*(2.*D*BETX(L)-2.*(1-V(LO))*BETY(L)-2.*V(LO)*BETY(L)
1+2.*(1-V(LO))*F*BETX(L))
ENO(8,7)=CC*(-2.*V(LO)*BETX(L)+2.*F*BETY(L))
ENO(8,8)=CC*(2.*D*BETX(L)**2-V(LO)*D*BETY(L)**2+2.*F*BETY(L)**2
1-4.*BETX(L)*BETY(L)+D*BETY(L)**2+F*BETX(L)**2-V(LO)*F*BETX(L)**2
2+2.*(1-V(LO))*BETX(L)*BETY(L))
ENO(11,3)=CC*(-2.*D*BETX(L)-2.*V(LO)*BETY(L)-2.*(1-V(LO))*BETY(L)
1-2.*F*(1-V(LO))*BETX(L))
ENO(11,8)=CC*(2.*D*BETX(L)-2.*V(LO)*BETY(L)+2.*(1-V(LO))
1*BETY(L)-2.*F*(1-V(LO))*BETX(L))
ENO(12,3)=CC*(-2.*V(LO)*BETX(L)-2.*F*BETY(L)-2.*D*(1-V(LO))*
1BETY(L)-2.*(1-V(LO))*BETX(L))
ENO(12,8)=CC*(2.*V(LO)*BETX(L)-2.*F*BETY(L)+2.*(1-V(LO))*D*
1BETY(L)-2.*(1-V(LO))*BETX(L))
ENO(13,1)=-ENO(3,1)
ENO(13,2)=-ENO(3,2)
ENO(13,3)=-ENO(3,3)
ENO(13,6)=-ENO(6,3)
ENO(13,7)=-ENO(3,2)
ENO(13,8)=-ENO(8,3)
ENO(13,11)=-ENO(11,3)
ENO(13,12)=-ENO(12,3)
ENO(13,13)=ENO(3,3)
ENO(16,3)=ENO(3,1)

```

(CON'T)

```

      ENO(16,8)=ENO(8,1)
      ENO(16,13)=-ENO(3,1)
      ENO(17,3)=CC*(-2.*V(LO)*BETX(L)-2.*F*BETY(L)+2.*(1-V(LO))*D
1*BETY(L)+2.*(1-V(LO))*BETX(L))
      ENO(17,8)=CC*(2.*V(LO)*BETX(L)-2.*F*BETY(L)-2.*(1-V(LO))*D
1*BETY(L)+2.*(1-V(LO))*BETX(L))
      ENO(17,13)=-ENO(17,3)
      ENO(18,1)=-ENO(8,1)
      ENO(18,2)=-ENO(8,2)
      ENO(18,3)=-ENO(8,3)
      ENO(18,6)=-ENO(8,6)
      ENO(18,7)=-ENO(8,7)
      ENO(18,8)=-ENO(8,8)
      ENO(18,11)=-ENO(11,8)
      ENO(18,12)=-ENO(12,8)
      ENO(18,13)=ENO(8,3)
      ENO(18,16)=ENO(18,1)
      ENO(18,17)=-ENO(17,8)
      ENO(18,18)=ENO(8,8)
      RETURN
      END

```



## FIRST ORDER INCREMENTAL STIFFNESS

```

SUBROUTINE N1(LO, TATX, TATY, L, EX, EY, EXY, CC)
COMMON/PROP/A(200), B(200), T(200), V(200), ET(200)
COMMON/STIFE/E(20, 20), ENO(20, 20), EN1(20, 20), EN2(20, 20)
COMMON/ANG/BETX(200), BETY(200)
D=B(LO)/A(LO)
F=A(LO)/B(LO)
EN1(3, 1)=CC*(2.*D*TATX+2.*V(LO)*TATY)
EN1(3, 2)=CC*(2.*V(LO)*TATX+2.*F*TATY)
EN1(3, 3)=CC*(2.*D*EX+2.*V(LO)*D*EY+2.*F*EY+2.*V(LO)*F*EX+2.*
1(1-V(LO))*EXY+6.*D*TATX*BETX(L)+2.*TATY*BETY(L)*D+4.*TATX*BET Y(L)
2+4.*BETX(L)*TATY+2.*TATX*BETX(L)*F+6.*F*BETY(L)*TATY)
EN1(6, 3)=CC*(-2.*D*TATX-2.*V(LO)*TATY+2.*
1(1-V(LO))*TATY+2.*(1-V(LO))*TATX*F)
EN1(7, 3)=EN1(3, 2)
EN1(8, 2)=CC*(-2.*V(LO)*TATX+2.*F*TATY)
EN1(8, 1)=CC*(-2.*D*TATX+2.*V(LO)*TATY)
EN1(8, 3)=CC*(-2.*D*EX-2.*V(LO)*D*EY+2.*F*EY+2.*V(LO)*F*EX-6.*
1D*TATX*BETX(L)-2.*TATY*BETY(L)*D+2.*TATX*BETX(L)*F+6.*F*BET Y(L)
2*TATY)
EN1(8, 6)=CC*(2.*D*TATX-2.*(1-V(LO))*TATY
1-2.*V(LO)*TATY+2.*(1-V(LO))*F*TATX)
EN1(8, 7)=CC*(-2.*V(LO)*TATX+2.*F*TATY)
EN1(8, 8)=CC*(2.*D*EX+2.*V(LO)*D*EY+2.*F*EY+2.*V(LO)*F*EX-2.*(1-
1V(LO))*EXY+6.*D*TATX*BETX(L)+2.*TATY*BETY(L)*D-4.*TATX*BET Y(L)-
24.*BETX(L)*TATY+2.*TATX*BETX(L)*F+6.*F*TATY*BETY(L))
EN1(11, 3)=CC*(-2.*D*TATX-2.*V(LO)*TATY-2.*
1(1-V(LO))*TATY-2.*(1-V(LO))*F*TATX)
EN1(11, 8)=CC*(2.*D*TATX-2.*V(LO)*TATY+2.*
1(1-V(LO))*TATY-2.*(1-V(LO))*F*TATX)
EN1(12, 3)=CC*(-2.*V(LO)*TATX-2.*F*TATY-2.*
1*(1-V(LO))*D*TATY-2.*(1-V(LO))*TATX)
EN1(12, 8)=CC*(2.*V(LO)*TATX-2.*F*TATY+2.*
1*(1-V(LO))*TATY-2.*(1-V(LO))*TATX)
EN1(13, 1)=-EN1(3, 1)
EN1(13, 2)=-EN1(3, 2)
EN1(13, 3)=-EN1(3, 3)
EN1(13, 6)=-EN1(6, 3)
EN1(13, 7)=-EN1(3, 2)
EN1(13, 8)=-EN1(8, 3)
EN1(13, 11)=-EN1(11, 3)
EN1(13, 12)=-EN1(12, 3)
EN1(13, 13)=EN1(3, 3)
EN1(16, 3)=EN1(3, 1)
EN1(16, 8)=EN1(8, 1)

```

(CON'T)

```

EN1(16,13)=-EN1(3,1)
EN1(17,3)=CC*(-2.*V(LO)*TATX-2.*F*TATY+2.
1*(1-V(LO))*D*TATY+2.*(1-V(LO))*TATX)
EN1(17,8)=CC*(2.*V(LO)*TATX-2.*F*TATY-2.*(1
1-V(LO))*D*TATY+2.*(1-V(LO))*TATX)
EN1(17,13)=-EN1(17,3)
EN1(18,1)=-EN1(8,1)
EN1(18,2)=-EN1(8,2)
EN1(18,3)=-EN1(8,3)
EN1(18,6)=-EN1(8,6)
EN1(18,7)=-EN1(8,7)
EN1(18,8)=-EN1(8,8)
EN1(18,11)=-EN1(11,8)
EN1(18,12)=-EN1(12,8)
EN1(18,13)=EN1(8,3)
EN1(18,16)=EN1(18,1)
EN1(18,17)=-EN1(17,8)
EN1(18,18)=-EN1(18,8)
RETURN
END

```

## SECOND ORDER INCREMENTAL STIFFNESS

```

SUBROUTINE N2(LO, TATX, TATY, CC)
COMMON/PROP/A(200), B(200), T(200), V(200), ET(200)
COMMON/STIFE/E(20, 20), ENO(20, 20), EN1(20, 20), EN2(20, 20)
F=A(LO)/B(LO)
D=B(LO)/A(LO)
EN2(3, 3)=CC*(3.*D*TATX**2
1+3.*F*TATY**2+4.*TATX*TATY+D*TATY**2+F*TATX**2)
EN2(8, 3)=CC*(-3.*D*TATX**2+3.*F*TATY**2
1-D*TATY**2+F*TATX**2)
EN2(8, 8)=CC*(3.*D*TATX**2
1+3.*F*TATY**2-4.*TATY*TATX+D*TATY**2+F*TATX**2)
EN2(13, 3)=-EN2(3, 3)
EN2(13, 8)=-EN2(8, 3)
EN2(13, 13)=EN2(3, 3)
EN2(18, 3)=-EN2(8, 3)
EN2(18, 8)=-EN2(8, 8)
EN2(18, 13)=EN2(8, 3)
EN2(18, 18)=EN2(8, 8)
RETURN
END

```



C  
C  
C  
TRANSFORMATION PROCESS

SUBROUTINE TRANSFM(NEA,NDF,MODE,LNO,IGN,INCT,NSTR,IKK,MI,NLDEF,  
1LSTR)

COMMON/US/US(20),SAVE(100)

COMMON/STIFE/E(20,20),ENO(20,20),EN1(20,20),EN2(20,20)

COMMON/PROP/A(200),B(200),T(200),V(200),ET(200)

COMMON/ANG/BETX(200),BETY(200)

COMMON/DISP/U(1210),DU(1210),UM(1280)

COMMON/NODE/N(972),M(1210),MMM(7)

COMMON/STDF/NST(200),NDEF(1210),NLL(100)

US(1)=U(N(1KK)\*NDF-4)

US(2)=U(N(1KK)\*NDF-3)

US(3)=U(N(1KK)\*NDF-2)

US(6)=U(N(1KK+1)\*NDF-4)

US(7)=U(N(1KK+1)\*NDF-3)

US(8)=U(N(1KK+1)\*NDF-2)

US(11)=U(N(1KK+2)\*NDF-4)

US(12)=U(N(1KK+2)\*NDF-3)

US(13)=U(N(1KK+2)\*NDF-2)

US(16)=U(N(1KK+3)\*NDF-4)

US(17)=U(N(1KK+3)\*NDF-3)

US(18)=U(N(1KK+3)\*NDF-2)

IF(NEA-1) 0,21,21

LN00=1

GO TO 22

21 LN00=LNO

22 CONTINUE

TATX=(US(8)-US(3)+US(13)-US(18))/(2.\*A(LN00))

TATY=(US(18)-US(3)+US(13)-US(8))/(2.\*B(LN00))

EX=(US(6)-US(1)+US(11)-US(16))/(2.\*A(LN00))

EY=(US(17)-US(2)+US(12)-US(7))/(2.\*B(LN00))

EXY=((US(11)-US(6)+US(16)-US(1))/(2.\*B(LN00))+(US(12)-US(17)  
1+US(7)-US(2))/(2.\*A(LN00)))

IF(NSTR) 0,10,0

IF(NLDEF) 30,2,0

IF(NST(LNO)) 10,10,0

IF(MI) 0,10,0

30 CONTINUE

IF(LSTR-1) 0,20,0

IF(MODE-1) 0,0,10

IF(INCT-1) 10,10,0

IF(IGN-1) 0,10,0

20 CALL STRESS(LN00,TATX,TATY,LNO,EX,EY,EXY)

(CON'T)

```

10 IF(LSTR-1) 0,2,0
   CONTINUE
   TATX=TATX-BETX(LNO)
   TATY=TATY-BETY(LNO)
   IF(KKK-1) 0,26,26
   IF(LNO-1) 25,25,0
26 CONTINUE
   IF(LNOO-1) 23,23,0
25 CONTINUE
   CALL STIFFEL(LNOO)
   PP=ET(LNOO)*((T(LNOO))**3)/(12*(1-(V(LNOO))**2))
   CC=3.*PP/(2.*(T(LNOO)**2))
   KKK=1
23 CONTINUE
   CALL NO(LNOO,LNO,CC)
   CALL N1(LNOO,TATX,TATY,LNO,EX,EY,EXY,CC)
   CALL N2(LNOO,TATX,TATY,CC)
   IF(MODE-1) 0,0,1
   DO 12 I=1,20
   DO 12 J=1,1
12 ENO(I,J)=E(I,J)+ENO(I,J)+EN1(I,J)+EN2(I,J)
   GO TO 2
1 CONTINUE
   DO 13 I=1,20
   DO 13 J=1,1
13 ENO(I,J)=E(I,J)+ENO(I,J)+.5*EN1(I,J)+(1/3.)*EN2(I,J)
2 CONTINUE
   RETURN
   END

```

C  
C  
C  
COUPLING PROCESS

```
SUBROUTINE COUPL(L,NE,NFF,NF2)
COMMON/BS/W(2000),MM(1210),EE(70,70)
COMMON/COEF/VI(1210),DP(1210)
COMMON/DISP/U(1210),DU(1210),UM(1280)
NF1=NFF-NE
EE(NF2,NF2)=EE(NF2,NF2)+EE(NF1,NF1)+2*EE(NF2,NF1)
DO 1 I=1,NF1
1  EE(NF2,I)=EE(NF2,I)+EE(NF1,I)
DO 2 I=NF1+1,NF2-1
2  EE(NF2,I)=EE(NF2,I)+EE(I,NF1)
DO 3 I=NF2+1,L
3  EE(I,NF2)=EE(I,NF2)+EE(I,NF1)
DO 4 I=1,NF1
4  EE(NF1,I)=0.
DO 5 I=NF1,L
5  EE(I,NF1)=0.
DU(NF2+NE)=DU(NF2+NE)+DU(NFF)
DP(NF2+NE)=DP(NF2+NE)+DP(NFF)
DU(NFF),DP(NFF)=0.0
RETURN
END
```



C  
C  
C

## SOLUTION ROUTINE

```

SUBROUTINE SOLV(NEA,MD,NDF,MODE,NSS,NEL,NDFT,NNE,IGN,INCT,
1NSTR,MI,NLDEF)
COMMON/STIFE/E(20,20),ENO(20,20),EN1(20,20),EN2(20,20)
COMMON/BS/W(2000),MM(1210),EE(70,70)
COMMON/NODE/N(972),M(1210),MMM(7)
COMMON/DISP/U(1210),DU(1210),UM(1280)
COMMON/COEF/VI(1210),DP(1210)
COMMON/INFRC/F(1210),P(1210),FI(1280)
NC,NE,NR,NS,NW,LNO=0
NWW,KST=2
NNAA,IKK=1
ILL=-NDF
NOO=MD/NDF
EE(1,1)=0.0
CALL FMOVE(EE(1,1),EE(2,1),(MD*MD-1))
1 IF(N(IKK)-NR) 0,9,0
  IF(NR) 0,3,0
  IF(MODE-1) 0,0,4
  CALL ELIM(NDF,NC,NS,NE,ILL,NR,NNAA,NW,NWW,KST)
  GO TO 8
4 CALL NODFORCE(MD,NDF,NE,NOO)
  IF(N(IKK)-NR) 7,3,3
8 IF(N(IKK)-NR) 16,0,0
3 NR=N(IKK)
  IF(N(IKK+1)) 2,0,2
  IKK=IKK+NNE
  ILL=ILL+NDF
  GO TO 1
9 CONTINUE
  ILL=ILL-NDF
2 CONTINUE
  IF(MODE-1) 0,0,10
  DO 15 I=1+IKK,NNE+IKK-1
    IF(N(I)-NS) 15,15,14
14 NS=N(I)
15 CONTINUE
10 CONTINUE
  LNO=LNO+1

```

(CON'T)

CALL ASSMB(NEA,NDF,MODE,LNO,IGN,INCT,NSTR,IKK,MI,NLDEF,NNE  
1,NE,ILL)

GO TO 1

16 CALL BCKSUB(KST,NW,NNAA,NDF,NS)

NSS=NS

DO 5 I=1,NDF T

5 UM(1)=DU(1)+UM(1)

DO 6 I=1,NDF T

6 U(1)=U(1)+DU(1)

7 CONTINUE

RETURN

END

C  
C  
C  
ELIMINATION PROCESS

```

SUBROUTINE ELIM(NDF,NC,NS,NE,ILL,NR,NNA,NW,NWW,KST)
COMMON/NODE/N(972),M(1210),MMM(7)
COMMON/DISP/U(1210),DU(1210),UM(1280)
COMMON/BS/W(2000),MM(1210),EE(70,70)
COMMON/COEF/VI(1210),DP(1210)
DO 2 II=1,NDF
K=1+NC
L=NS*NDF-NE
IF(M(II+ILL)) 1,1,0
NFF=II+ILL
NF2=M(II+ILL)*NDF-NDF+II-NE
CALL COUPL(L,NE,NFF,NF2)
1 CONTINUE
J,JJ=(NR-1)*NDF+II
IF(M(II+ILL))4,0,4
EE(K,K)=1.0/EE(K,K)
VI(J)=EE(K,K)
DU(J)=DU(J)*EE(K,K)
MM(J)=L-K
IF(MM(J))0,6,0
NNA=NNA+MM(J)
IF(NW+MM(J)-2000) 9,9,0
CALL PUT ARRAY(4,KST,W)
NWW=NW+MM(J)
KST=NWW
DO 7 IA=1,NW
7 W(IA)=0.
NW=0
9 CONTINUE
DO 8 I=K+1,L
NW=NW+1
JJ=JJ+1
DU(JJ)=DU(JJ)-DU(J)*EE(I,K)
8 W(NW)=EE(I,K)*EE(K,K)
DO 3 I=K+1,L
DO 3 J=K+1,I
3 EE(I-K,J-K)=EE(I,J)-EE(I,K)*W(NW+J-L)
DO 5 I=L-K+1,L
DO 5 J=1,I
5 EE(I,J)=0.
6 NE=NE+NC+1

```



(CON'T)

NC=0

GO TO 2

4 DU(J)=0.

MM(J)=0.

IF(M(11+ILL).GE.1) MM(J)=- (M(11+ILL)\*NDF-NDF+11)

NC=NC+1

2 CONTINUE

RETURN

END

C  
C  
C BACKSUBSTITUTION PROCESS

```

SUBROUTINE BCKSUB(KST,NW,NNAA,NDF,NS)
COMMON/BS/W(2000),MM(1210),EE(70,70)
COMMON/DISP/U(1210),DU(1210),UM(1280)
CALL PUT ARRAY(4,KST,W)
NW=2000
NNAA=NNAA-2000
IF(NNAA) 0,2,2
NW=1999+NNAA
KST=2
GO TO 3
2 CONTINUE
KST=NNAA+1
3 CALL GET ARRAY(4,KST,W)
J,JJ=NS*NDF
DO 4 I=1,JJ
IF(MM(J)) 5,5,0
IF(NW-MM(J)) 0,6,6
NNAA=NNAA-2000+NW
IF(NNAA-2) 0,8,8
NW=1999+NNAA
KST=2
CALL GET ARRAY(4,KST,W)
GO TO 6
8 CONTINUE
KST=NNAA+1
CALL GET ARRAY(4,KST,W)
NW=2000
6 CONTINUE
NW=NW-MM(J)
DO 10 I=1,MM(J)
10 DU(J)=DU(J)-DU(J+I)*W(NW+I)
GO TO 4
5 NFIX=-MM(J)
IF(MM(J).LT.-1) DU(J)=DU(NFIX)
4 J=J-1
RETURN
END

```

C  
C  
C

STIFFNESS ASSEMBLY

```

SUBROUTINE ASSMB(NEA,NDF,MODE,LNO,IGN,INCT,NSTR,IKK,MI,NLDEF
1,NNE,NE,ILL)
COMMON/NODE/N(972),M(1210),MMM(7)
COMMON/BS/W(2000),MM(1210),EE(70,70)
COMMON/STIFE/E(20,20),ENO(20,20),EN1(20,20),EN2(20,20)
CALL TRANSFM(NEA,NDF,MODE,LNO,IGN,INCT,NSTR,IKK,MI,NLDEF)
DO 1 JJ=1,NNE
LL=(N(JJ+IKK-1)-1)*NDF-NE
KKK=1
LLL=0
DO 1 II=JJ,NNE
KK=(N(II-1+IKK)-1)*NDF-NE
DO 2 J=1,NDF
L=LL+J
JL=(JJ-1)*NDF+J
JJJ=KKK*J+LLL
DO 2 I=JJJ,NDF
K=KK+I
IF(LL-KK)3,3,4
4 L=KK+I
K=LL+J
3 IK=(II-1)*NDF+I
2 EE(K,L)=EE(K,L)+ENO(IK,JL)
KKK=0
1 LLL=1
IKK=IKK+NNE
ILL=ILL+NDF
RETURN
END

```



C  
C  
C

NODAL FORCE CALCULATION

```

SUBROUTINE NODFORCE(MD,NDF,NE,NOO)
COMMON/BS/W(2000),MM(1210),EE(70,70)
COMMON/INFRC/F(1210),P(1210),FI(1280)
COMMON/DISP/U(1210),DU(1210),UM(1280)
DO 2 I=1,NDF
DO 3 J=1,I
F(I+NE)=EE(I,J)*UM(J+NE)+F(I+NE)
IF(I-J) 3,0,3
DO 4 J=I+1,MD
4 F(I+NE)=EE(J,I)*UM(J+NE)+F(I+NE)
F(I+NE)=F(I+NE)+FI(I+NE)
GO TO 2
3 CONTINUE
2 CONTINUE
NE=NE+NDF
DO 7 I=1+NDF,MD
DO 7 J=1,NDF
7 FI(I-NDF+NE)=EE(I,J)*UM(J-NDF+NE)+FI(I-NDF+NE)
NT=0
DO 700 II=1,NOO-1
DO 701 I=1,MD-NT
DO 701 J=1,NDF
701 EE(I+NT,J+NT)=0.0
DO 5 I=1,MD-NDF-NT
DO 5 J=1,NDF
5 EE(I+NT,J+NT)=EE(I+NDF+NT,J+NDF+NT)
NT=NT+NDF
700 CONTINUE
DO 702 I=1,MD-NT
DO 702 J=1,NDF
702 EE(I+NT,J+NT)=0.0
RETURN
END

```

C  
C  
C  
ITERATIONAL PROCESS

```

SUBROUTINE ITER(NEA, MD, NDF, MODE, NSS, NEL, NDFT, NNE, I GN, INCT, NSTR, MI
1, NLDEF)
COMMON/BS/W(2000), MM(1210), EE(70, 70)
COMMON/NODE/N(972), M(1210), MMM(7)
COMMON/DISP/U(1210), DU(1210), UM(1280)
COMMON/COEF/VI(1210), DP(1210)
COMMON/INFRC/F(1210), P(1210), FI(1280)
NW=0
KST=2
NWW=2
NNAA=1
DO 4 J=1, NDFT
4 DU(J)=F(J)
IF(MODE-2) 10, 0, 10
MODE=1
IGN=1
CALL SOLV(NEA, MD, NDF, MODE, NSS, NEL, NDFT, NNE, I GN, INCT, NSTR, MI, NLDEF)
IGN=0
MODE=2
GO TO 2
10 CONTINUE
CALL GET ARRAY(4, KST, W)
DO 37 J=1, NSS*NDF
JJ=J
IF(MM(J)) 36, 36, 0
NNAA=NNAA+MM(J)
DU(J)=DU(J)*VI(J)
IF(NW+MM(J)-2000) 666, 666, 0
NWW=NWW+NW
KST=NWW
CALL GET ARRAY(4, KST, W)
NW=0
666 CONTINUE
DO 31 I=1, MM(J)
NW=NW+1
JJ=JJ+1
31 DU(JJ)=DU(JJ)-DU(J)*W(NW)/VI(J)
GO TO 37
36 DU(J)=0.0
37 CONTINUE
NW=2000
NNAA=NNAA-2000
IF(NNAA) 0, 700, 700

```

(CON'T)

```

NW=1999+NNAA
KST=2
GO TO 701
700 CONTINUE
KST=NNAA+1
701 CALL GET ARRAY(4,KST,W)
J,JJ=NSS*NDF
DO 42 I=1,JJ
IF(MM(J)) 43,43,0
IF(NW-MM(J)) 0,667,667
NNAA=NNAA-2000+NW
IF(NNAA-2) 0,668,668
669 CONTINUE
NW=1999+NNAA
KST=2
CALL GET ARRAY(4,KST,W)
GO TO 667
668 CONTINUE
KST=NNAA+1
CALL GET ARRAY(4,KST,W)
NW=2000
667 CONTINUE
NW=NW-MM(J)
DO 41 I=1,MM(J)
41 DU(J)=DU(J)-DU(J+1)*W(NW+1)
GO TO 42
43 NFIX=-MM(J)
IF(MM(J).LT.-1) DU(J)=DU(NFIX)
42 J=J-1
2 CONTINUE
DO 5 I=1,NDF T
5 UM(I)=DU(I)+UM(I)
DO 6 J=1,NDF T
6 U(J)=U(J)+DU(J)
F(1)=0.0
CALL FMOVE(F(1),F(2),(NDF T-1))
RETURN
END

```



C  
C  
C

## STRESS CALCULATION

```

SUBROUTINE STRESS(LNOO, TATX, TATY, LNO, EX, EY, EXY)
COMMON/PROP/A(200), B(200), T(200), V(200), ET(200)
COMMON/ANG/BETX(200), BETY(200)
X2=EX+.5*(TATX)**2-.5*(BETX(LNO)**2)
Y2=EY+.5*(TATY)**2-.5*(BETY(LNO)**2)
X=(ET(LNOO)/(1-V(LNOO)**2))*(X2+V(LNOO)*Y2)
Y=(ET(LNOO)/(1-V(LNOO)**2))*(Y2+V(LNOO)*X2)
XY=(ET(LNOO)/(2.*(1+V(LNOO))))*(EXY+TATX*TATY-BETX(LNO)*BETY(LNO))
WRITE(2,100) LNO
100  FORMAT(/,56X,10HELEMENT NO,15)
WRITE(2,101)
101  FORMAT(60X,6HSTRESS/50X,26HAXIAL    TRANSVERSE    SHEAR)
WRITE(2,102) Y,X,XY
102  FORMAT(44X,3F10.0)
RETURN
END
FINISH

```

# SAMPLE OUTPUT

NO. OF ELEMENTS= 4

NO. OF NODES= 9

NO. OF NODES PER ELEMENT= 4

NO. OF DEGREES OF FREEDOM= 5

MATRIX DIMENSION= 30

ELEMENT NO	ELEMENT LENGTH	ELEMENT WIDTH	THICKNESS	POISSON RATIO	MODULUS OF ELASTICITY
1	1.00	1.00	0.050	0.300	10.00E 06

## \*\*\*ELEMENT NUMBRING SYSTEM\*\*\*

1	2	5	4
2	3	6	5
3	0	0	0
4	5	8	7
5	6	9	8
6	0	0	0
7	0	0	0
8	0	0	0
9	0	0	0
0	0	0	0

## \*\*\*BOUNDARY CONDITIONS\*\*\*

NODE	D . O . F .			
1	0	2	-1	-1
2	0	3	-1	-1
3	-1	0	-1	-1
4	0	0	-1	0
6	-1	0	0	-1
7	0	-1	-1	0
8	0	-1	0	0
9	-1	-1	-1	-1

\*\*\*INITIAL DISPLACEMENTS\*\*\*

NODE	U	V	W	X-ROTATION	Y-ROTATION
1	0.0000E 00	0.0000E 00	0.0000E 00	0.0000E 00	0.0000E 00
2	0.0000E 00	0.0000E 00	0.0000E 00	0.0000E 00	0.0000E 00
3	0.0000E 00	0.0000E 00	0.0000E 00	0.0000E 00	0.0000E 00
4	0.0000E 00	0.0000E 00	0.0000E 00	0.0000E 00	0.0000E 00
5	0.0000E 00	0.0000E 00	2.5000E-03	0.0000E 00	0.0000E 00
6	0.0000E 00	0.0000E 00	3.5350E-03	0.0000E 00	0.0000E 00
7	0.0000E 00	0.0000E 00	0.0000E 00	0.0000E 00	0.0000E 00
8	0.0000E 00	0.0000E 00	3.5350E-03	0.0000E 00	0.0000E 00
9	0.0000E 00	0.0000E 00	5.0000E-03	0.0000E 00	0.0000E 00

\*\*\*\*\* PURELY INCREMENTAL \*\*\*\*\*

NODE DEGREES OF FREEDOM TOTAL LOAD  
3 2 100.00000

\*\*\*\*\* DISPLACEMENTS \*\*\*\*\*

NODE	U	V	W	X-ROTATION	Y-ROTATION
1	-5.96910E-05	2.00956E-04	0.0000E 00	0.0000E 00	0.0000E 00
4	-5.9144E-05	1.00746E-04	0.0000E 00	0.0000E 00	-4.22463E-04
6	0.0000E 00	9.97811E-05	4.07561E-03	-4.22110E-04	0.0000E 00
9	0.0000E 00	0.0000E 00	5.76436E-03	0.0000E 00	0.0000E 00

ELEMENT NO 1  
STRESS  
AXIAL TRANSVERSE SHEAR  
-1003. -1. 2.

ELEMENT NO 4  
STRESS  
AXIAL TRANSVERSE SHEAR  
-996. 2. 1.



### A - 3 INPUT DATA PREPARATION

The developed program is intended to be quite general in its application to the solution of plate and beam problems. Although the program listed in A - 2 uses a four node rectangular element with five degrees of freedom, any type of element could easily be incorporated in the program by replacing the few appropriate subroutines (see Section 5.8). Since all the results obtained for plate problems use the listed elements from A - 2, the example problems demonstrated in the input data preparation are also based on the same element.

The input formats quoted in the data preparation have standard FORTRAN meanings. The program makes use of free format, because of its simplicity and accuracy.

## LAYOUT OF INPUT DATA FOR PLATE

The input data can be classified in eleven groups of cards, as in the table below:

Group	Number of Cards	Purpose
A	5	Details of element and finite element mesh
B	*	Element properties
C	*	Node numbering system
D	*	Details of boundary conditions
E	*	Specifies the extent of stress calculation
F	*	Controls the output displacements
G	*	Controls the output load levels
H	*	Details of initial displacements
I	1	Specifies the accuracy of solution desired, for iterational procedure
J	†	Specifies the number of loads, the choice of constant displacements, the type of procedure, the number of iterations, and the magnitude and location of applied loads.
K	1	Terminates the computer execution

\* Depends on the number of elements

† Depends on the procedure used

TABLE (A-1)

Group A

## First Card

Reads the total number of elements.

NEL  
(IO)

## Second Card

Reads the total number of nodes.

NJNT  
(IO)

## Third Card

Reads the number of nodes per element.

NNE  
(IO)

## Fourth Card

Reads the number of degrees of freedom per node.

NDF  
(IO)

## Fifth Card

Reads the maximum dimension of the stiffness matrix during assembly and elimination. This maximum dimension basically depends on the bandwidth, using the greatest difference between the highest and lowest node numbers for any element.

$$MD = \left\{ \left[ (\text{Highest no.}) - (\text{Lowest no.}) \right] + 2 \right\} (NDF) \quad (A-1)$$

MD  
(IO)

Note: The value of MD suggested in Equation (A-1) is only for economizing computer time and core size, thus a greater value of MD will have no effect on the results. See also the further requirements under Group D.



GROUP BFirst Card

Reads the number of elements for which data follows.

NEA  
(IO)

Warning: If all elements are identical, NEA must be zero; otherwise NEA = NEL.

Following Cards

Reads the properties of each element (one card per element.) If NEA = 0, then only one card is required.

NO A B T V ET  
(IO, 4F0.0, E10.3)

NO is the element reference number  
A, B are the element dimensions (see Figure 5-1).  
T is the plate thickness  
V is the value of Poisson's ratio  
ET is the modulus of elasticity

GROUP C

This group defines the node numbering system in the finite element mesh. In general, to minimise the bandwidth, the node numbering must start at one corner of the structure, proceed across its width and repeat the process along the next line of elements across the width, until the entire structure is covered.

Each card reads element node numbers in the order defined in Figure (5-1). Each card must contain the same number of integers as the number of nodes per element NNE. For the last node number on each line of elements, an extra "dummy" card must be prepared to indicate the end of a row or column. Since each card contains NNE integers, the first number on the dummy card must be the last node number of the line, and the rest must be set to zero. The organization of the cards in Group C must be such that the initial number on each card is in ascending order, and this initial number must be less than any other node number on the card. At the end of this group, an extra card with NNE zeroes must follow.

(IO, IO, ....)

GROUP D

Boundary conditions and other constraints are introduced by this group. If there is a constraint of any degree of freedom at a node, then information about all the degrees of freedom for that node, whether constrained or free, must be read. In order to indicate that a degree of freedom is constrained or free, -1 or 0 respectively, must be used. If any of the degrees of freedom of a node is "coupled" to the corresponding degree of freedom of another (higher numbered) node, then the node number of the latter must be entered as constraint data. The term "coupled" implies displacements (or rotations) at two or more nodes are required to be equal.

Warning: The higher node must be within the band width, or otherwise the value of MD must be suitably adjusted.

The value of MD is then given in the difference between the coupled node numbers, as follows:

$$MD = \{ [\text{difference between nodes}] + 2 \} (NDF)$$

It is desirable therefore, when more than two nodes are coupled to each other, to couple each node in turn to the next highest.

#### First Card

Reads the total number of nodes which have any degree of freedom constrained or which are coupled to any other node.

(IO)

#### Following Cards

Each card reads first the node number and then constraint data for all degrees of freedom at that node.

(IO, IO, ....)

GROUP E

This group specifies the extent of stress calculation.

## First Card

NSTR  
(IO)

- 1 indicates that a stress calculation is required for all elements.
- 0 indicates that no stress calculation is required.
- >0 is the total number of elements for which a stress calculation is required.

If NSTR is either -1 or 0, the following instruction in this group is not applicable and must be ignored.

## Following Cards

Each card reads the element number for which a stress calculation is required.

NSTRR  
(IO)

GROUP F

This group controls the nodes at which output of displacements is obtained.

## First Card

NWRDEF  
(IO)

- 1 indicates that output of displacements is required at all nodes.
- 0 indicates that no output of displacements is required.
- >0 is the total number of nodes for which output of displacements is required.

If NWRDEF is either -1 or 0, the following instruction is not applicable and must be ignored.

## Following Cards

Each card reads the node number for which output of displacements is required.

NODDEF  
(IO)



GROUP G

This group controls the load levels at which output of stresses and displacements is obtained.

## First Card

NLDEF

- 1 indicates that output of stresses and displacements for all load increments is required.
- >1 is the total number of load levels for which output of stresses and displacements is required.

## Following Cards

Each card reads the node number at which the load level for output of stresses and displacements is defined.

NOD      NUM      TLOAD  
(210, F0.0)

- NOD is the node number
- NUM is the degrees of freedom at that node.
- TLOAD is the total load level at node NOD at which output of stresses and displacements is required.

GROUP H

Reads the initial displacements (and rotations)

## First Card

NIN  
(10)

- 0 indicates that there are no initial displacements.
- >0 is the total number of initial displacements.

If NIN = 0, the following instruction is not applicable, and must be ignored.

## Following Cards

Each card gives the initial displacement for a single degree of freedom.

- NOD is the node number.
- NUM is the degree of freedom at that node.
- DEF is the value of initial displacement (or rotation) at that node.

GROUP I

To use the iterative procedure with a fixed accuracy, the following information should be on a single card.

NOD      NUM      ACC  
(2IO,FO.0)

NOD    is the node number at which the accuracy check is made.

NUM    is the degree of freedom number at that node.

ACC    is the required percentage accuracy (iteration continues until the change in displacement is brought down to a pre-determined percentage of the displacement in that increment).

Warning:    If fixed accuracy is not used, a single card with the following information must be used

1      1      0

GROUP J

This group is used to control the application of loads (forces or moments) in the program. If various load increments (for example, initially a series of large increments followed by smaller increments) or different approaches (for example, initially purely incremental followed by an iterative procedure) are required, this group may be repeated as many times as necessary, provided the proper sequence is preserved.

The group starts with a single card, to give, in order,

NHM      INCRT      TYPE      NITER  
(4IO)

NHM    is the number of loads to be read for each increment of load.

INCRT

-1      approximately constant displacement is required

0      terminates the computer run

>0      is the number of load increments

Warning:    First load increment must start with INCRT >0.

TYPE There are four procedural options, indicated by the value of TYPE, as follows:

- 1 Purely incremental
- 2 Incremental with Newton-Raphson method
- 3 Incremental with Modified Newton-Raphson method
- 4 Incremental with carry-over of out-of-balance forces

NITER is the number of iterations required

Warning: If the number of iterations are controlled by accuracy, then NITER must be set to zero.

The following cards define the location and magnitude of loads. For each concentrated load applied, one card must be supplied. All loads must be acting into the global X, Y, or Z direction (or moments about these axes).

NOD      NUM      ALOAD  
(2IO,FO.O)

NOD is the node number at which a load is applied.

NUM is the degree of freedom number at that node.

ALOAD depends on previous information about INCRT.

If INCRT >0, ALOAD is the magnitude of the load increment.

If INCRT <0, ALOAD is the total load to be reached by (approximately) constant displacements.

Group J therefore contains (NHM + 1) cards and, as previously states, this group may be repeated as many times as necessary.

#### GROUP K

In order to terminate the computer execution, a single card is required:

0      0      0      0



The following examples are intended to make use of the facilities of all groups in Table (A-1).

### Example I

This example demonstrates how the program can be used to calculate the pre- and post-buckling behaviour of a plate.

A square plate with simple support along the four sides and unloaded edges free to wave in plane is uniformly compressed in the 'y' direction (see Figure A-1). The properties of the plate are as follows:

Length:	4 in.
Thickness:	0.05 in.
Poisson's Ratio	0.3
Modulus of elasticity:	$10 \times 10^6$ lbf/in <sup>2</sup>

The plate is symmetrical, so only a quarter of the plate need be analyzed. The number of elements chosen is four and the numbering of nodes is shown in Figure (A-1). The plate has an initial imperfection  $W_0/t = 0.1$ , and by using the function

$$w = W_0 \sin \frac{\pi x}{a} \sin \frac{\pi y}{b}$$

the corresponding initial displacements at nodes 5, 6, 7 and 9 are 0.0025, 0.003535, 0.003535, and 0.005 in., respectively.

Since the problem is nonlinear, loads are applied in increments. The total compressive load is to reach 2000 lbf. but since only a quarter of the plate is taken into account, the total load is considered as 1000 lbf.

The procedure chosen is as follows:

- 1) Purely incremental procedure is used up to 300 lbf. compressive load, in increments of 100 lbf.
- 2) Incremental with modified Newton-Raphson method is used up to 700 lbf. compressive load, in increments of 50 lbf., with two iterations at each load increment.
- 3) Fixed accuracy of 10% with the Newton-Raphson method is used up to 1000 lbf., in increments of 100 lbf.

Output display is obtained at every 100 lbf. Displacements are printed for nodes numbers 1, 4, 6, and 9. Stresses are output for element numbers 1 and 4.

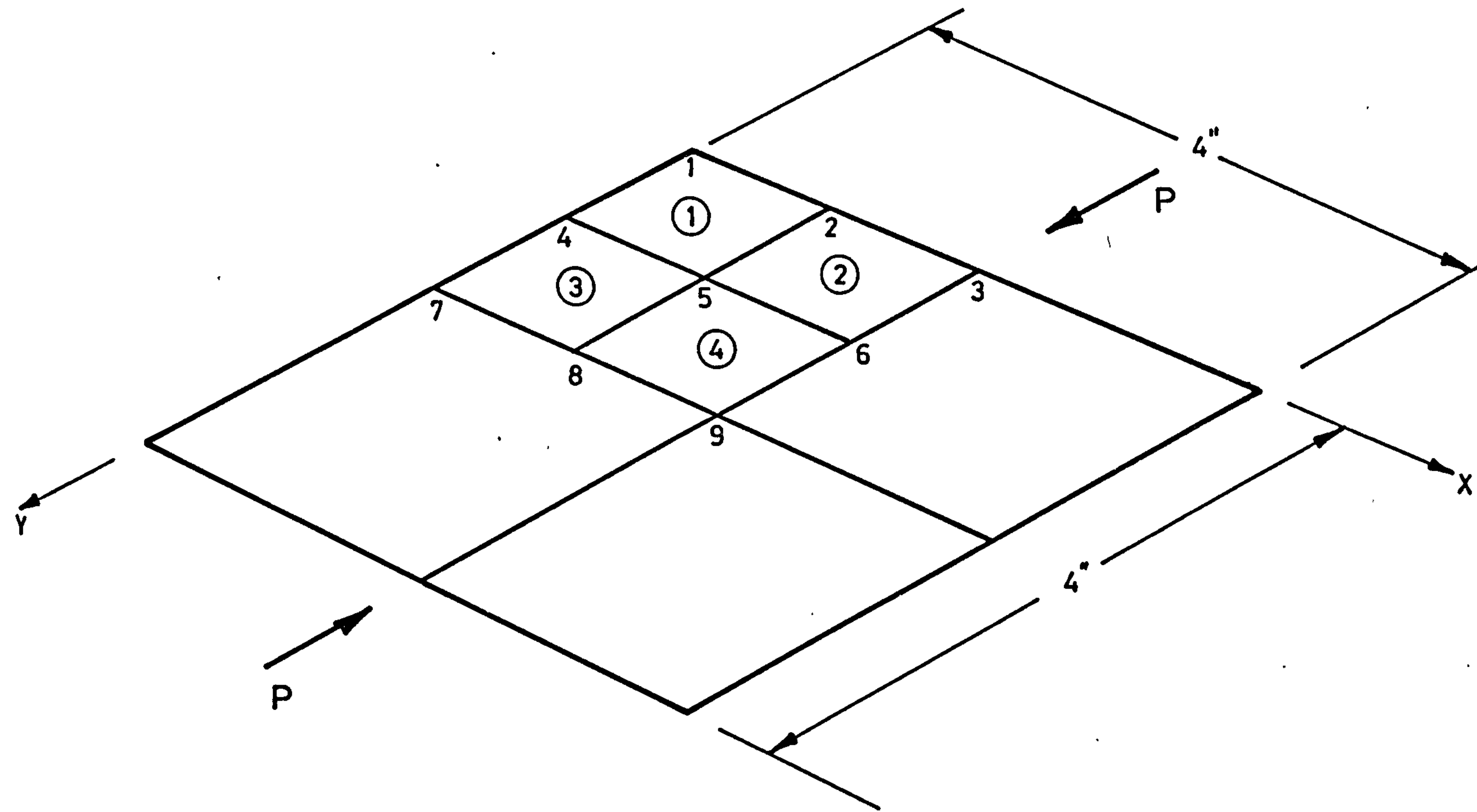


FIGURE A-10

## DATA PREPARATION

Each line represents a data card.

4
9
4
5
30

Group A

			0		
1	1.	1.	.05	.3	10.E06

Group B

1	2	5	4
2	3	6	5
3	0	0	0
4	5	8	7
5	6	9	8
6	0	0	0
7	0	0	0
8	0	0	0
9	0	0	0
0	0	0	0

Group C

		8			
1	0	2	-1	-1	-1
2	0	3	-1	0	-1
3	-1	0	-1	0	-1
4	0	0	-1	-1	0
6	-1	0	0	0	-1
7	0	-1	-1	-1	0
8	0	-1	0	-1	0
9	-1	-1	0	-1	-1

Group D

2
1
4

Group E



4
1
4
6
9

Group F

	0	
3	2	100.
3	2	200.
3	2	300.
3	2	400.
3	2	500.
3	2	600.
3	2	700.
3	2	800.
3	2	900.
3	2	1000.

Group G

	4	
5	3	.0025
6	3	.003535
8	3	.003535
9	3	.005

Group H

9	3	.01
---	---	-----

Group I

1		3	1	0	
	3			2	100
1		8	3	2	
	3			2	50
1		3	2	0	
	3			2	100

Group J

0	0	0	0
---	---	---	---

Group K

EXAMPLE II

This example illustrates how the program is used to obtain elastic stresses and deflections for a flat plate under uniformly distributed normal pressure.

A square plate with the following dimensions and properties is chosen:

Length:	6 in.
Thickness:	0.022 in.
Poisson's ratio:	0.3
Modulus of elasticity:	$10.5 \times 10^6$ lbf/in <sup>2</sup> .

The sides are simply supported, but held straight and free to move in plane.

The applied loading is a uniform normal pressure of 10psi. In order to apply this loading in the program, it must be converted into concentrated loads. The total load must be applied incrementally, because of the nonlinearity of the problem.

The plate is symmetrical and only a quarter of the plate need be analyzed. Four elements are chosen for the quarter plate and the numbering of the nodes is shown in Figure (A-11).

The distribution of concentrated loads is explained in Section 6.2. The concentrated loads for 1 psi pressure are

$$P = 36\text{in}^2 \times 1 \text{ psi} = 36 \text{ lbf.}$$

$$P_u = \frac{36}{16} = 2.25 \text{ lbf.}$$

The procedure is as follows:

1) Incremental with modified Newton-Raphson method with two iterations at each load increment is used until the normal pressure reaches 7 psi., in increments of 2.25 lbf.

2) Fixed accuracy of 5% with the Newton-Raphson method is used up to 10 psi normal pressure. Increments are controlled to give approximately constant changes of displacement. The printout of results will contain displacements at nodes 1 and 4, and stresses for element 4. Output is obtained for every 2 psi normal pressure.

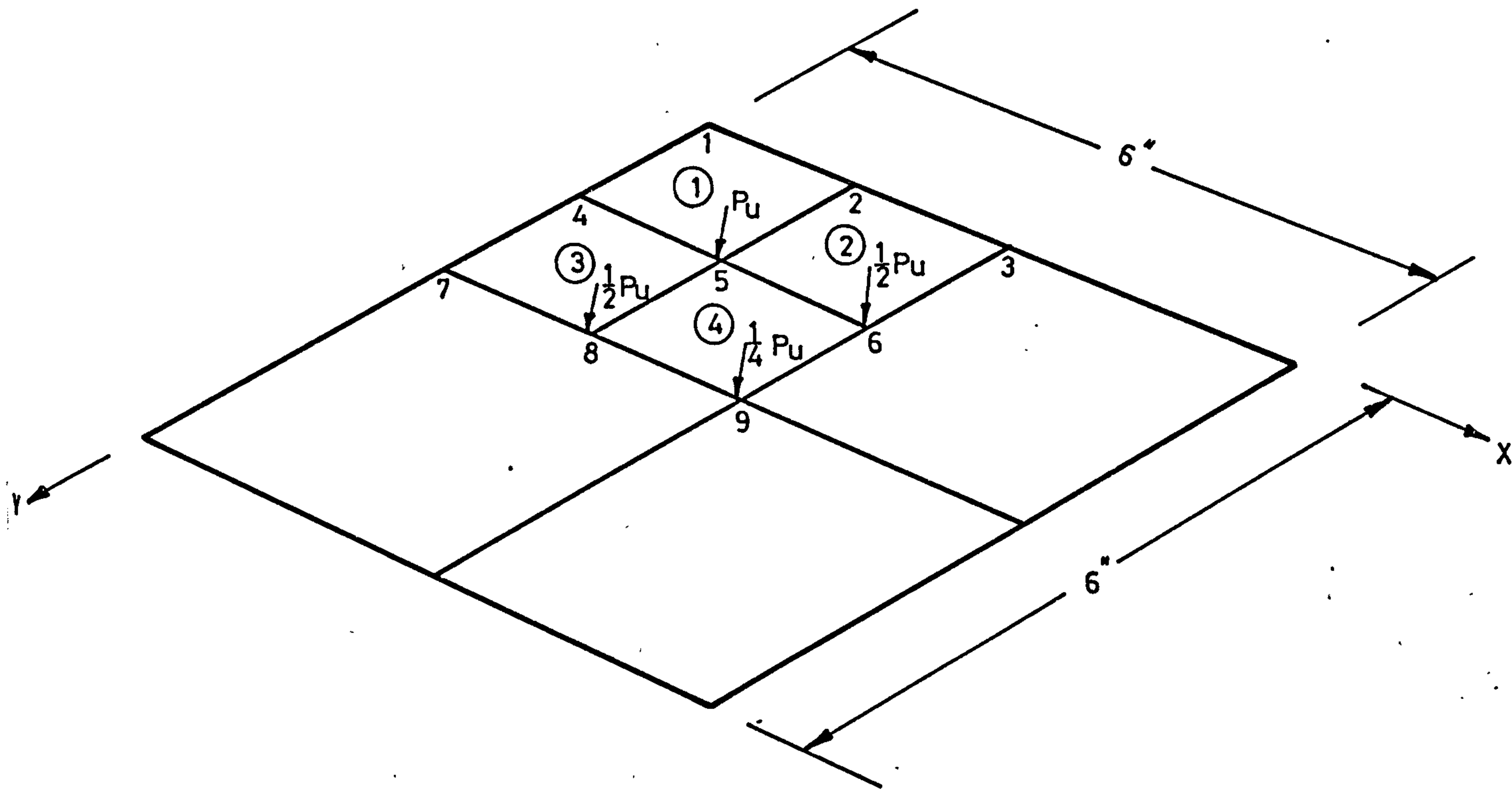


FIGURE A-11



DATA PREPARATION

Each line represents a data card.

4
9
4
5
30

Group A

0				
1	1.5	1.5	.022	10.5E06

Group B

1	2	5	4
2	3	6	5
3	0	0	0
4	5	8	7
5	6	9	8
6	0	0	0
7	0	0	0
8	0	0	0
9	0	0	0
0	0	0	0

Group C

8					
1	4	2	-1	-1	-1
2	0	3	-1	0	-1
3	-1	0	-1	0	-1
4	7	0	-1	-1	0
6	-1	0	0	0	-1
7	0	-1	-1	-1	0
8	0	-1	0	-1	0
9	-1	-1	0	-1	-1

Group D

1
4

Group E

2
1
4

Group F

	5	
5	3	4.5
5	3	9.0
5	3	13.5
5	3	18.0
5	3	22.5

Group G

0

Group H

9	3	.05
---	---	-----

Group I

4		7	3		2
	5		3	2.25	
	6		3	1.125	
	8		3	1.125	
	9		3	.5625	
1		-1	2		0
	5		3	22.5	

Group J

0	0	0	0
---	---	---	---

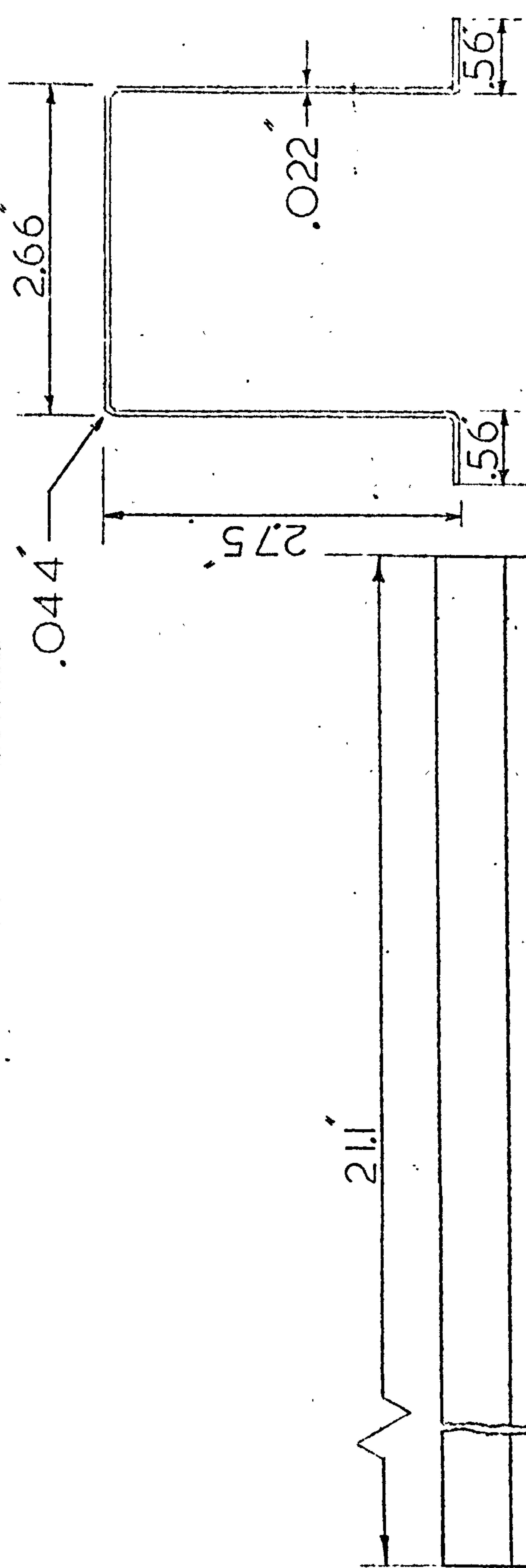
Group K

A P P E N D I X   B



~~ALL DIMENSIONS IN MILLIMETRES UNLESS OTHERWISE STATED.~~

ISSUE	MODIFICATION



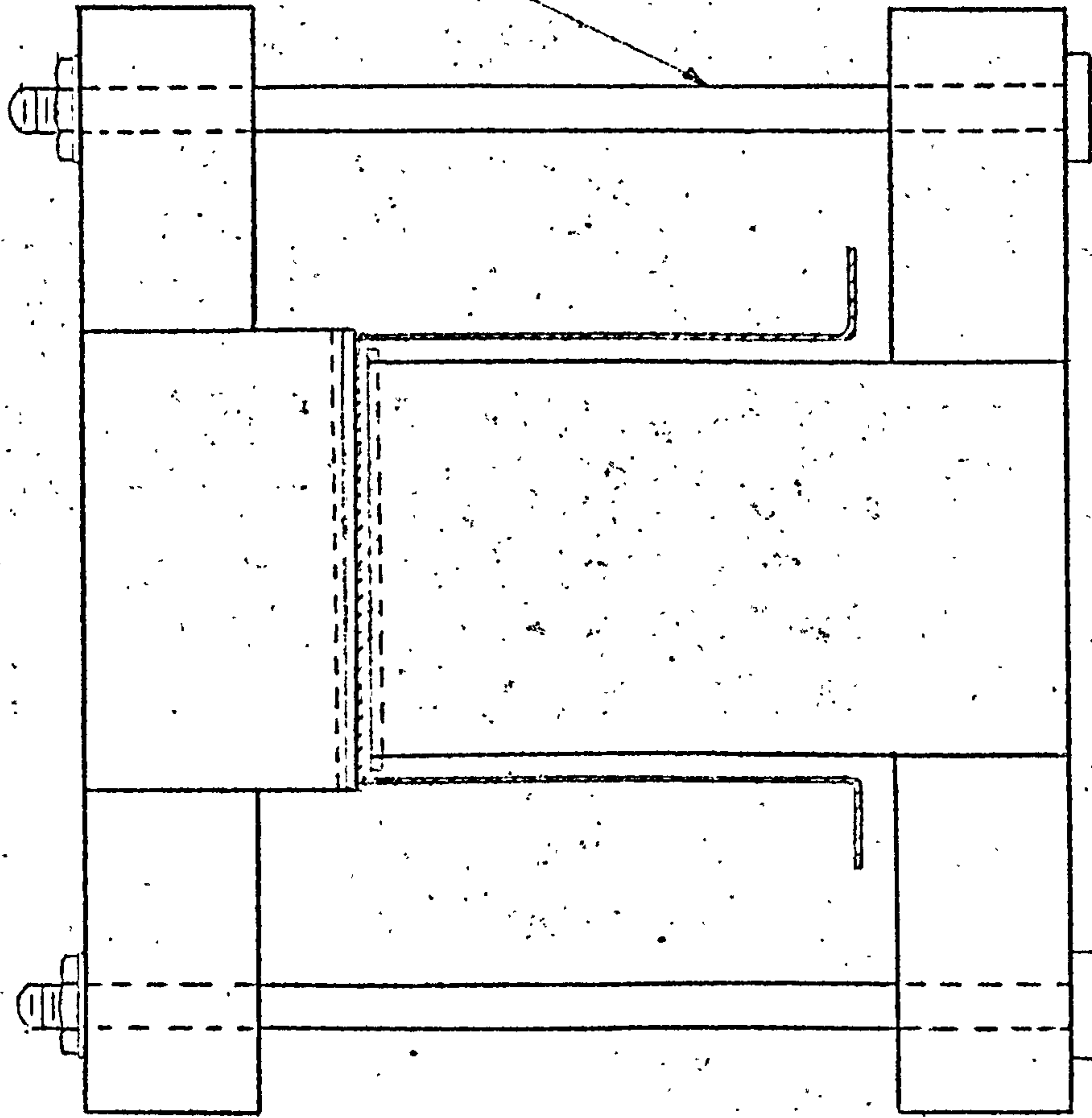
331

CEROBEND END FITTINGS 1/2 DEEP

THIRD ANGLE PROJECTION										SHEET SIZE A 3		CHANNEL STRUT		2		AL ALLOY		L-70																	
GENERAL TOLERANCE ON DIMENSIONS MACHINED UNMACHINED OTHER DIMENSIONS AS STATED										JOB No.		No. OF SETS REQ'D		SCALE		FULL		DRAWN		CHK'D		APPV'D		STRESS APPVD		DESCRIPTION		No. OFF		MAT'L		SPEC.		REMARKS	
										WELD WHERE SHOWN THUS		L		FINISH		ISSUED BY		DRAWING No.		DT 268/1-		SHT. 1		OF 3		SHEETS									
										MACHINE WHERE SHOWN THUS		✓		USED ON DRG.		CRANFIELD INSTITUTE OF TECHNOLOGY		CRANFIELD.																	

**DRAWING NO.**

ISSUE	MODIFICATION



2BA-1/4  
SCREWED ROD

332

FIGURE (B-2)

THIRD ANGLE PROJECTION										SHEET SIZE A 3																																																																					
GENERAL TOLERANCE ON DIMENSIONS MACHINED				JOB No.		No. OF SETS REQ'D		SCALE FULL		DRAWN		CHK'D AYZ		APP'VD [Signature]		STRESS APPROV'D		DESCRIPTION		PART No.		No. OFF		MAT'L		SPEC.		REMARKS																																																			
UNMACHINED																																																																															
OTHER DIMENSIONS AS STATED																																																																															
WELD WHERE SHOWN THUS																																																																															
MACHINE WHERE SHOWN THUS																																																																															
FINISH										ISSUED BY										DRAWING No. DT 268/3																																																											
CRANFIELD INSTITUTE OF TECHNOLOGY										CRANFIELD INSTITUTE OF TECHNOLOGY										SHT. 2 OF 3 SHEETS																																																											
CRANFIELD.										CRANFIELD.										SHT. 2 OF 3 SHEETS																																																											
1										2										3										4										5										6										7										8									



ALL DIMENSIONS IN MILLIMETRES UNLESS OTHERWISE STATED.

ISSUE	MODIFICATION

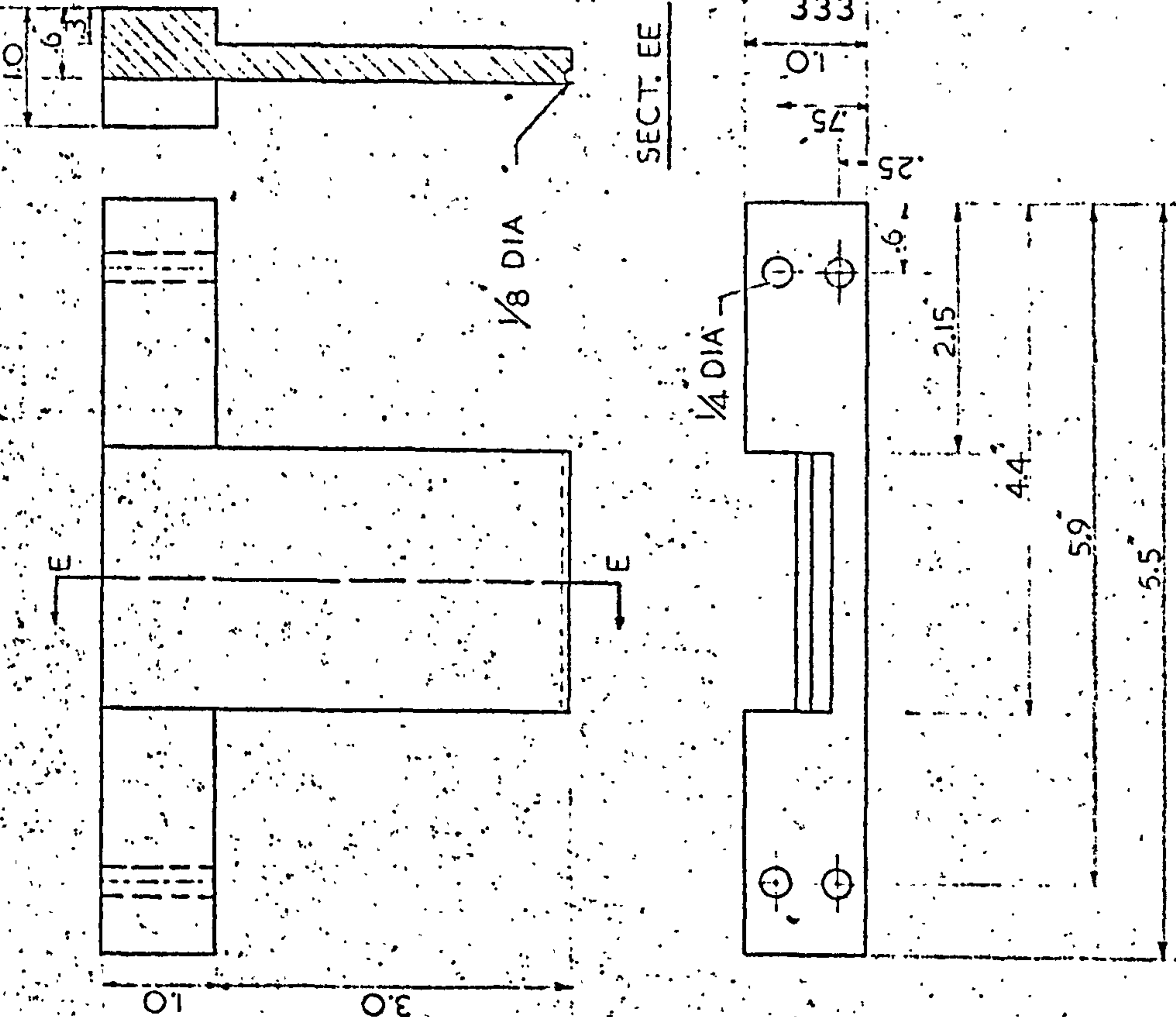
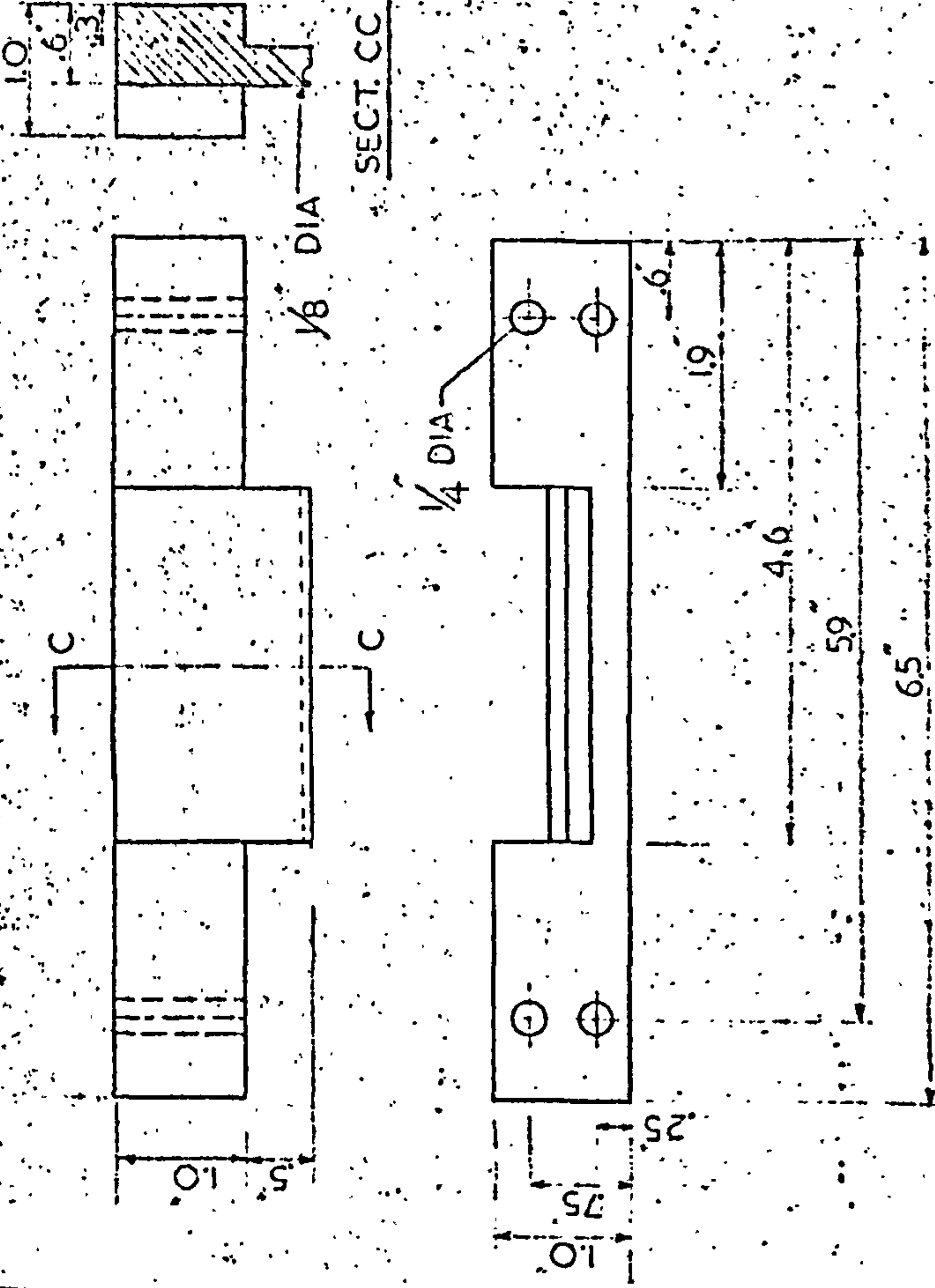


FIGURE (B-3)

THIRD ANGLE PROJECTION		SHEET SIZE		ITEM		PART No.		DESCRIPTION		No. OFF		SPEC.		REMARKS	
A 2		A 2		DRAWN		CHKD		APPRD		STRESS		APPRD		DETAIL	
GENERAL TOLERANCE ON DIMENSIONS		SCALE		FULL		FINISH		ISSUED BY		DRAWING No.		DT 268/2		SHT. 3 OF 3	
MACHINED		No. OF		SETS REQD		JOB No.		USED ON DRG.		CRANFIELD INSTITUTE OF TECHNOLOGY		CRANFIELD.		SHT. 3 OF 3	
UNMACHINED		OTHER DIMENSIONS AS STATED		WELD WHERE SHOWN THUS		MACHINE WHERE SHOWN THUS		USED ON DRG.		CRANFIELD INSTITUTE OF TECHNOLOGY		CRANFIELD.		SHT. 3 OF 3	
MACHINE WHERE SHOWN THUS		USED ON DRG.		WELD WHERE SHOWN THUS		MACHINE WHERE SHOWN THUS		USED ON DRG.		CRANFIELD INSTITUTE OF TECHNOLOGY		CRANFIELD.		SHT. 3 OF 3	



## DIAL GAUGE READINGS (MM)

Dial Gauge Numbers

Load lbf.	1	2	3	4	5	6	7	8
0	4.50	14.49	8.51	7.08	5.10	8.22	6.80	6.54
200	4.50	14.49	8.50	7.07	5.10	8.22	6.80	6.54
400	4.50	14.51	8.50	7.07	5.11	8.22	6.79	6.54
500	4.52	14.53	8.49	7.07	5.07	8.20	6.75	6.54
600	4.54	14.54	8.46	7.04	4.99	8.14	6.69	6.54
700	4.55	14.57	8.42	7.02	4.90	8.05	6.60	6.52
750	4.57	14.59	8.41	7.01	4.84	8.00	6.55	6.48
800	4.60	14.62	8.40	7.00	4.79	7.95	6.50	6.45
850	4.63	14.66	8.39	6.99	4.74	7.90	6.44	6.41
900	4.69	14.73	8.39	6.99	4.68	7.85	6.39	6.34
950	4.71	14.75	8.39	6.99	4.64	7.80	6.34	6.30
1000	4.77	14.81	8.39	6.99	4.60	7.74	6.28	6.23
1050	4.81	14.85	8.39	6.99	4.56	7.69	6.23	6.18
1100	4.87	14.92	8.39	7.00	4.52	7.64	6.18	6.12
1150	4.91	14.96	8.40	7.01	4.50	7.59	6.13	6.07
1200	5.01	15.06	8.50	7.12	4.51	7.55	6.08	5.97
1250	5.06	15.12	8.53	7.16	4.51	7.50	6.04	5.91
1300	5.13	15.19	8.61	7.24	4.52	7.46	5.99	5.84
1350	5.20	15.27	8.71	7.35	4.56	7.42	5.95	5.76
1400	5.30	15.40	8.97	7.63	4.79	7.41	5.96	5.64
1450	5.39	15.49	9.19	7.88	5.00	7.40	5.95	5.55
1500	5.42	15.52	9.20	7.89	5.00	7.38	5.92	5.52
1550	5.46	15.56	9.26	7.96	5.02	7.35	5.89	5.47
1600	5.52	15.62	9.40	8.11	5.14	7.34	5.89	5.42
1650	5.58	15.68	9.54	8.26	5.29	7.34	5.89	5.40
1700	5.67	15.80	9.69	8.43	5.47	7.36	5.92	5.54

Maximum Load = 1860 lbf.

TABLE (B-1)



## DIAL GAUGE READINGS (MM)

## Dial Gauge Numbers

Load lbf.	1	2	3	4	5	6	7	8
0	6.83	1.88	5.05	5.69	2.09	6.61	5.14	3.22
100	6.86	1.89	5.05	5.69	2.07	6.61	5.14	3.21
200	6.88	1.91	5.06	5.69	2.07	6.62	5.14	3.21
300	6.92	1.93	5.09	5.71	2.07	6.62	5.14	3.22
400	6.95	1.95	5.10	5.71	2.06	6.60	5.14	3.22
500	6.99	1.95	5.12	5.71	2.03	6.58	5.13	3.22
600	7.05	1.97	5.11	5.68	1.94	6.52	5.04	3.20
650	7.04	1.96	5.03	5.62	1.85	6.48	5.00	3.25
700	7.03	1.94	4.98	5.57	1.78	6.45	4.98	3.29
750	7.03	1.93	4.95	5.54	1.73	6.44	4.96	3.35
800	7.01	1.91	4.88	5.48	1.65	6.04	4.95	3.41
850	6.99	1.88	4.83	5.43	1.59	6.38	4.94	3.48
900	6.97	1.86	4.78	5.39	1.53	6.36	4.93	3.53

Snap-through at 635 lbf.

TABLE (B-2)

## DIAL GAUGE READINGS (MM)

Dial Gauge Numbers

Load lbf.	1	2	3	4	5	6	7	8
0	7.40	5.80	4.53	5.03	5.07	5.28	5.92	5.85
100	7.40	5.79	4.53	5.03	5.07	5.29	5.92	5.85
200	7.40	5.78	4.54	5.02	5.07	5.29	5.92	5.85
300	7.40	5.78	4.55	5.02	5.07	5.29	5.91	5.83
400	7.42	5.78	4.58	5.05	5.05	5.28	5.88	5.81
500	7.46	5.81	4.66	5.09	5.00	5.25	5.83	5.76
600	7.51	5.84	4.75	5.13	4.95	5.22	5.77	5.70
650	7.54	5.85	4.79	5.15	4.92	5.20	5.74	5.68
700	7.57	5.88	4.85	5.18	4.89	5.18	5.71	5.65
750	7.60	5.89	4.90	5.21	4.86	5.15	5.67	5.62
800	7.63	5.91	4.96	5.24	4.83	5.14	5.64	5.59
850	7.65	5.92	5.01	5.26	4.79	5.11	5.61	5.56
900	7.69	5.95	5.06	5.29	4.76	5.08	5.57	5.52
950	7.71	5.97	5.11	5.32	4.73	5.05	5.54	5.49
1000	7.74	5.99	5.17	5.35	4.69	5.02	5.50	5.46
1050	7.77	6.00	5.21	5.38	4.66	5.00	5.47	5.43
1100	7.80	6.02	5.26	5.40	4.63	4.97	5.44	5.40
1150	7.83	6.04	5.31	5.44	4.59	4.94	5.40	5.36
1200	7.86	6.08	5.37	5.47	4.55	4.91	5.36	5.32
1250	7.89	6.09	5.42	5.50	4.51	4.88	5.32	5.29
1300	7.92	6.11	5.47	5.52	4.48	4.85	5.28	5.26
1350	7.95	6.13	5.52	5.55	4.45	4.82	5.25	5.23
1400	7.98	6.16	5.57	5.58	4.41	4.79	5.21	5.19
1450	8.00	6.18	5.61	5.61	4.37	4.76	5.17	5.16
1500	8.04	6.20	5.66	5.63	4.34	4.73	5.13	5.13
1550	8.08	6.23	5.71	5.66	4.29	4.70	5.09	5.08
1600	8.11	6.26	5.77	5.68	4.26	4.67	5.05	5.04
1650	8.15	6.29	5.82	5.71	4.21	4.64	5.00	5.01
1700	8.20	6.33	5.88	5.73	4.16	4.61	4.95	4.96
1750	8.28	6.37	5.96	5.74	4.09	4.57	4.87	4.90
1800	8.37	6.44	6.07	5.75	3.99	4.55	4.78	4.82
1850	8.48	6.52	6.20	5.75	3.94	4.53	4.66	4.73

TABLE (B-3)

## APPENDIX C



t	.036 in.
b	4.32 in
b/t	120
L	20.0 in
E	$10.6 \times 10^6$ psi
G	$4 \times 10^6$ psi
$\sigma_y$	36,000 psi
$\tau_b$	3,550 psi
$\tau_y^*$	12,000 psi
Torque Required at buckling	5,300 in-lb
Torque Required at Yield	16,200 in-lb
$\sigma_{cr}$	2,660 psi
$P_{cr}$	1,660 lb
Shear Angle **	$.342^\circ$
Axial Contraction ***	.0015 in

\*Nominal shear stress at yield is taken as  $1/3 \times \sigma_y$ , due to buckling and possible development of diagonal tension.

\*\*At maximum torque taking  $G_{\text{effective}} = \frac{G}{2}$

\*\*\*Pre-buckling range - axial load = 30% of  $P_{cr}$   
 Post-buckling range - axial load = 10% of  $P_{cr}$  and  
 taking  $E_{\text{effective}} = 1/3 E$ .

TABLE (C-1)

DRAWING No.

MODIFICATION

ISSUE

ALL DIMENSIONS IN MILLIMETRES UNLESS OTHERWISE STATED.

R=040

A

B

C

D

E

A

B

C

D

E

436

436

036

339

22.3

FIGURE (C-1)

THIRD ANGLE PROJECTION

SHEET SIZE

A 3

WELDED SQUARE TUBE

2

ALLOY

L-70

REMARKS


GENERAL TOLERANCE ON DIMENSIONS

MACHINED

UNMACHINED

OTHER DIMENSIONS AS STATED

WELD WHERE SHOWN THUS 

MACHINE WHERE SHOWN THUS 

NO. OF SETS REQD

JOB No.

USED ON DRG.

TITLE:-

TEST SPECIMEN

DESCRIPTION

STRESS APPVD

APPROV

CHKD

DRAWN

ITEM

PART No.

NO. OFF

MATL

SPEC.

ISSUED BY

DRAWING No.

CRANFIELD INSTITUTE OF TECHNOLOGY

CRANFIELD.

DT 26311

SHT. 1 OF 2 SHEETS

6880

2

3

4

5

6

7

8

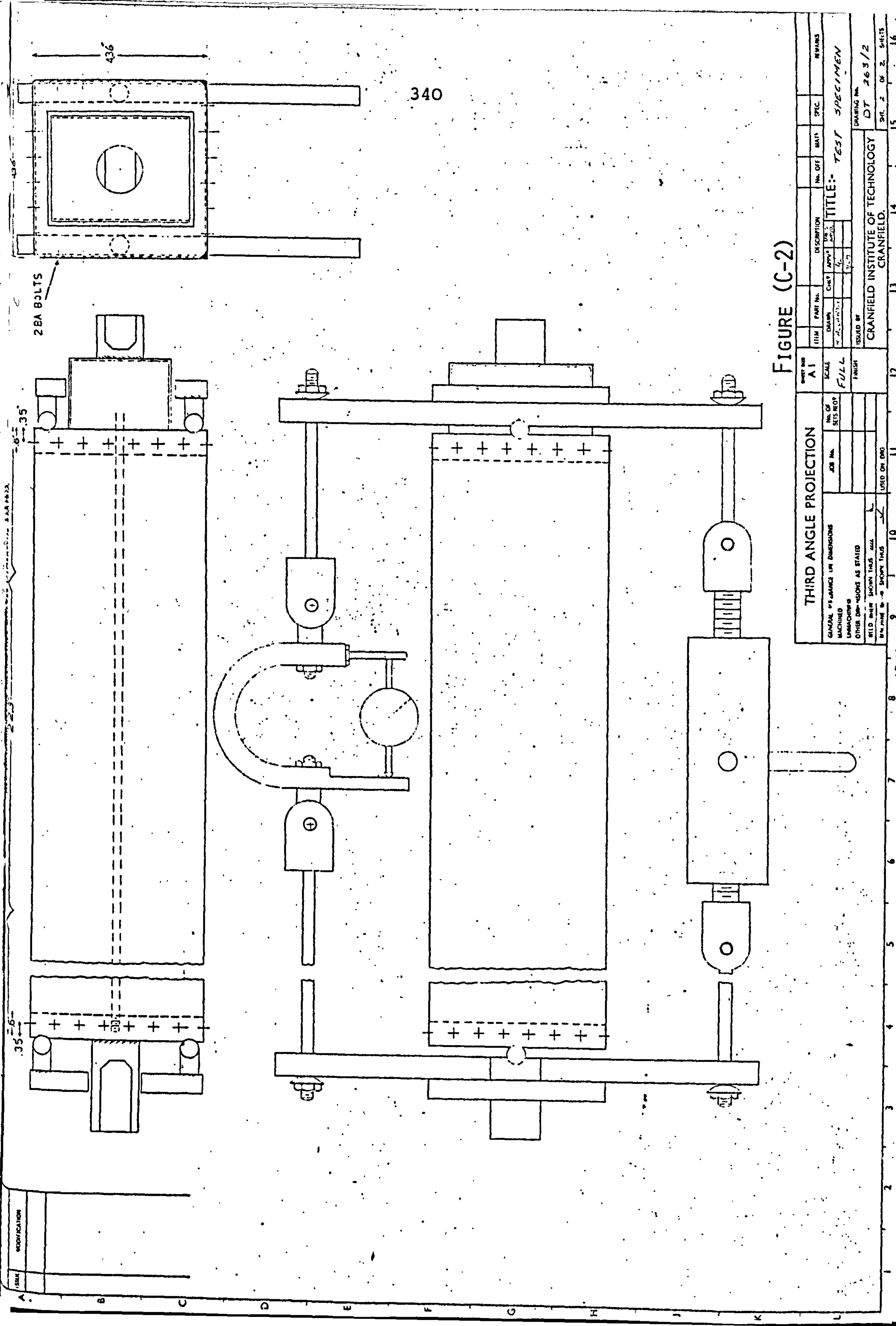


FIGURE (C-2)

THIRD ANGLE PROJECTION		PART NO.		DESCRIPTION		NO. OFF.		SPEC.		REMARKS	
GENERAL DIMENSIONS IN DIMENSIONS		SCALE		CHECKED BY		APPROVED BY		TITLE: TEST SPECIMEN		DRAWING NO.	
MACHINED		FULL		7/10/71		7/10/71		DT 263/2		SHEET 2 OF 2 SHEETS	
OTHER DIMENSIONS AS STATED		FINISH		ISSUED BY		CRANFIELD INSTITUTE OF TECHNOLOGY		CRANFIELD		SHEET 2 OF 2 SHEETS	
WELD SHOWN THIS WAY		USED ON DRG		10		11		12		13	